NASA/TP-97-206257

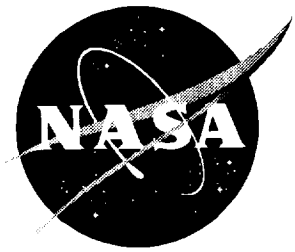

The Characteristics of Fatigue Damage in the Fuselage Riveted Lap Splice Joint

Robert S. Piascik
Langley Research Center, Hampton, Virginia

Scott A. Willard
Lockheed Martin Engineering & Sciences Company, Hampton, Virginia

National Aeronautics and
Space Administration

Langley Research Center
Hampton, Virginia 23681-2199

November 1997

Available from the following:

NASA Center for AeroSpace Information (CASI)
800 Elkridge Landing Road
Linthicum Heights, MD 21090-2934
(301) 621-0390

National Technical Information Service (NTIS)
5285 Port Royal Road
Springfield, VA 22161-2171
(703) 487-4650

Contents

Nomenclature

a	crack length
b	regression coefficient
bay	region of lap splice joint boarded by tear straps
AFT	a direction towards the rear of the aircraft
clad	a corrosion protection surface layer of 1230 aluminum, nominally 50 μm
counter bore	refer to Figure 2.2
counter sink	refer to Figure 2.2
crack link-up	the joining of two adjacent cracks
EC	eddy current inspection
FA	fretting average, refer to Figure 13.4
faying surface	lap splice joint mating surface (refer to Figure 2.2)
fretting	an abrasion caused by the rubbing between two adjacent (faying) surfaces
FWD	a direction (forward) towards the front of the aircraft
horizontal stiffener	inboard structure oriented horizontally to the lap splice joint
IC	inner corner
inboard	refer to Figure 2.2
inner skin (IS)	refer to Figure 2.2
IS	inner skin
K	crack-tip stress intensity factor
ΔK	cyclic crack-tip stress intensity factor
K_T	stress concentration factor
MSD	multiple site damage
N	pressure (load) cycle
NDE	nondestructive examination
outboard	refer to Figure 2.2
outer skin (OS)	refer to Figure 2.2
pillowing	outboard protrusion of the lap splice outer skin
r	correlation factor
RT	X-ray radiographic inspection
SEM	scanning electron microscopy
shank	refer to Figure 2.2
tear strap (TS)	vertical inboard structure that boarders each lap splice bay to assist preventing crack extension into adjacent bays
UT	ultrasound inspection
vertical stiffener	inboard structure oriented vertical to the horizontal lap splice joint
WFD	widespread fatigue damage

Abstract

An extensive data base has been developed to form the physical basis for new analytical methodology to predict the onset of widespread fatigue damage in the fuselage lap splice joint. The results of detailed destructive examinations have been cataloged to describe the physical nature of MSD in the lap splice joint. The catalog includes a detailed description, e.g., crack initiation, growth rates, size, location, and fracture morphology, of fatigue damage in the fuselage lap splice joint structure.

Detailed examinations were conducted on a lap splice joint panel removed from a full scale fuselage test article after completing a 60,000 cycle pressure test. The panel contained a four bay region that exhibited visible outer skin cracks and regions of crack link-up along the upper rivet row. Destructive examinations revealed undetected fatigue damage in the outer skin, inner skin, and tear strap regions. Outer skin fatigue cracks were found to initiate by fretting damage along the faying surface. The cracks grew along the faying surface to a length equivalent to two to three skin thicknesses before penetrating the outboard surface of the outer skin. Analysis of fracture surface marker bands produced during full scale testing revealed that all upper rivet row fatigue cracks contained in a three bay region grow at similar rates; this important result suggests that fracture mechanics based methods can be used to predict the growth of outer skin fatigue cracks in lap splice structure. Results are presented showing the affects of MSD and out-of-plane pressure loads on outer skin crack link-up.

Acknowledgment

The authors gratefully acknowledge Mr. Robert F. Berry, Jr., of the LaRC Fabrication Division, for his comprehensive nondestructive examination of the lap splice panel. The authors also recognize Dr. Charles E. Harris, Dr. James C. Newman, Jr., and Dr. David S. Dawicke of the LaRC Materials Division for providing numerous technical contributions during this exhaustive study.

1. Introduction

Considerable attention has been given to the structural integrity and damage tolerance of aging aircraft in recent years (See refs. 1–3). Based on this work, the potential threat to aging airframe residual strength has been defined in terms of a widespread fatigue damage (WFD) phenomenon (See ref. 4). The WFD phenomenon is defined as the simultaneous presence of cracks at multiple structural details that are of sufficient size and density whereby the structure will no longer meet residual strength requirements. Aircraft structural damage is also defined in terms of multiple site damage (MSD) which is a type of WFD. MSD is characterized by the simultaneous presence of fatigue cracks in the same structural element (e.g., fatigue cracks that may coalesce with or without other damage leading to a loss of required residual strength). The goal of current research is to develop the analytical methodology to predict onset of WFD. To accomplish this goal, an airframe MSD data base must be developed to form the physical basis for new analytical methodology to predict the onset of widespread fatigue damage in airframe structure. The aim of this work is to create an extensive data base that will establish the characteristics of multiple site fatigue damage contained in fuselage riveted lap splice structure. The detailed destructive examinations identify: (1) the damage mechanism(s) contributing to fatigue crack initiation in riveted structure, (2) the physical behavior of fatigue crack propagation from rivet holes, and (3) the characteristics of fatigue crack link-up in the lap splice joint.

2. Background

The incidence of airframe fatigue damage increases as airplanes are operated past their economic design objective. Because high cycle aircraft have reduced durability, the commercial aircraft industry has instituted elaborate inspection and maintenance requirements to ensure continued airworthiness of aging airplanes. To ensure safe and economical operation of aging commercial aircraft, pressure testing of full scale fuselage structure is conducted (See refs. 5-8). Detailed nondestructive examinations of fuselage structure during the full pressurization tests often lead to design improvements and practical inspection programs for the commercial fleet. As part of this commitment towards continued aircraft airworthiness, the airframe industry has entered into a cooperative aging aircraft program with the National Aeronautical and Space Administration (NASA) Langley Research Center (LaRC) to resolve durability issues associated with the aging commercial airplane fleet. Here, LaRC has performed detailed examinations of a commercial aircraft fuselage structure that has been subjected to a long term pressure test in order to develop a MSD data base and better understand important fatigue damage mechanisms associated with the aging fleet.

Figure 2.1 is a schematic of a panel containing a riveted lap splice joint removed from a full size fuselage test article that received a total of 60,000 load cycles (pressurizations). The panel consists of four full bays (bays 2, 3, 4, and 5) and two partial bays (bays 1 and 6). The bay numbering system shown in Figure 2.1 will be used throughout this report. Each bay is separated by a tear strap bonded and riveted to the inner surface of the fuselage skin. The tear strap regions are identified by the vertical dashed lines in Figure 2.1. The lap splice joint is formed by overlapping and joining two sections of fuselage skin (Alclad 2024-T3) using a four row riveted construction. All rivets are a counter bore design as shown in Figure 2.2. A sealant was applied to the mating (faying) surface of the lap splice to prevent internal pressure loss during flight and to prevent the ingress of moisture that may lead to joint corrosion. The bonded tear strap acts as a fail safe load path and a crack arrest feature between bays. A horizontal frame, not depicted in Figure 2.1, is riveted (third row from the top) along the length of the lap splice joint inner surface.

The small arrows in Figure 2.1 mark the locations of visible rivet hole cracks detected during *in situ* visual examinations conducted during the full-scale fuselage pressure test. Summarized is the chronology of cracking from first detection of cracking in bay 5 at 33,750 cycles, to the total link-up of bay 2 cracks at 60,000 pressurizations. It should be noted that all visible rivet hole cracking detected within this 6 bay region was limited to the upper rivet row. After the initial 20,000 pressure cycles, *in situ* outer skin surface visual inspections were conducted at intervals of about 1700 cycles.[1] The first evidence of lap splice outer skin fatigue cracking was observed along the upper rivet row near the middle of bay 5 after accumulating 33,570 pressurizations. Visible cracks were observed in bays 4 and 2 after 35,000 and 38,333 cycles, respectively. No further visible cracking was noted until after 50,000 cycles. The first evidence of fatigue crack link-up was detected in bay 2 at 58,200 cycles. An additional 300 pressurization cycles were performed, totaling 58,500 cycles, before cracks at all upper rivet row locations in bay 2 had grown together (link-up), forming a single long crack. The long crack measured 18.85 inches (47.9 cm) in length and extended along the entire upper row of rivets in bay 2 and terminated at the tear straps. At 59,900 cycles, bay 4 exhibited crack link-up between two upper rivet row rivet hole locations. Upon completing the full scale fuselage fatigue test at 60,000 cycles, 33 of the total 60 upper rivet row hole locations in bays 2, 3, 4 and 5 exhibited visible cracks along the outer surface of the fuselage skin. No visible cracks were detected along other rivet rows. The six bay panel of lap splice joint containing visible MSD was removed from the fuselage test article for a detailed teardown inspection at LaRC. Reported herein is a detailed description of the results of all examinations conducted on the six bay panel at LaRC.

[1] More frequent visual inspections were performed in local regions that exhibited evidence of cracking.

2.1 References:

1. *Proc. of the Intn'l. Workshop on Structural Integrity of Aging Airplanes*, Atluri, S.N., Harris, C.E., Hoggard, A., Miller, M., and Sampath, S.G., eds., Atlanta Technology Publications, P.O. Box 77032, Atlanta, GA (1992).

2 *Proc. of Intn'l. Symposium on Advanced Structural Integrity Methods for Airframe Durability and Damage Tolerance*, Harris, C.E., ed., NASA Conf. Pub. 3274, Langley Research Center, Hampton, VA (1994).

3. *FAA-NASA Symposium on Continued Airworthiness of Aircraft Structures*, Bigelow, C.A., ed., Atlanta, GA (1996).

4. Swift, T., "Widespread Fatigue Damage Monitoring - Issues and Concerns", *Proc. of Intn'l. Symposium on Advanced Structural Integrity Methods for Airframe Durability and Damage Tolerance*, Harris, C.E., ed., NASA Conf. Pub. 3274, Langley Research Center, Hampton, VA, pp. 829-870 (1994).

5. Gopinath, K.V., "Structural Airworthiness of Aging Boeing Jet Transports - 747 Fuselage Test Program", *1992 Aerospace Design Conference*, AIAA 92-1128, American Institute of Aeronautics and Astronautics, 370 L'Enfant Promenade, S.W., Washington, D.C.

6. Goranson, U.G., and Miller, M., , "Aging Jet Transport Structural Evaluation Programs", *Structural Integrity of Aging Airplanes*, Atlanta, GA, March 1990, Atluri, S.N., Sampath, S.G., and Tong, P., eds., Spinger-Verlag, Berlin, 1991, pp. 131-140.

7. Hoggard, A.W.,"Fuselage Longitudinal Splice Design", *Structural Integrity of Aging Airplanes*, Atlanta, GA, March 1990, Atluri, S.N., Sampath, S.G., and Tong, P., eds., Spinger-Verlag, Berlin, 1991, pp. 167-181.

8. Roll, R., van Dalan, A., and Jongebreur, A.A., "Results of Review of Fokker F28 Fellowship Maintenance Program", *Structural Integrity of Aging Airplanes*, Atlanta, GA, March 1990 S.N. Atluri, S.G. Sampath, and P. Tong, eds., Spinger-Verlag, Berlin, 1991, pp. 309-320.

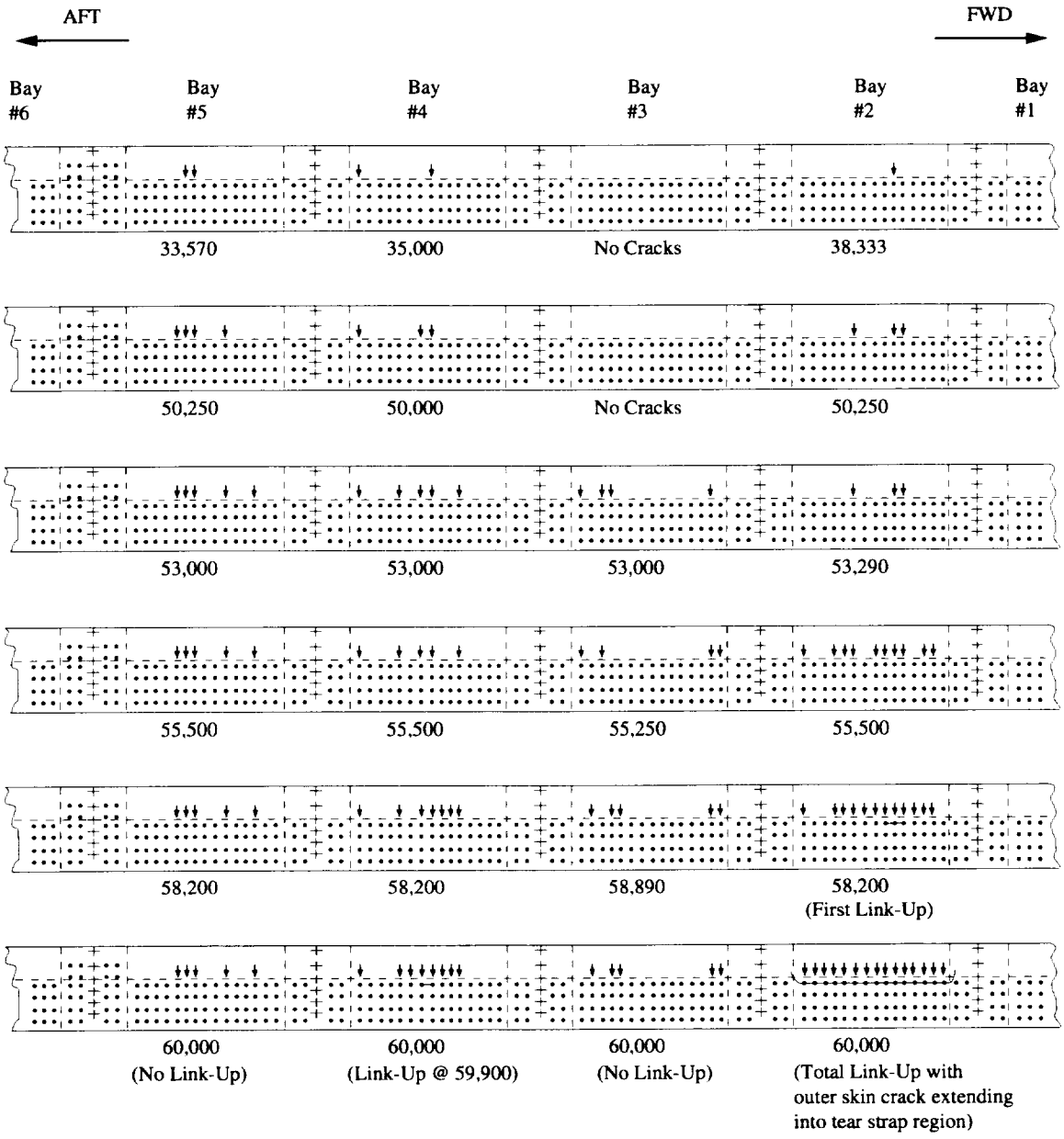

Figure 2.1 The schematics show the results of the *in situ* inspection. Arrows indicate rivet hole locations that contain visible fatigue cracks. Cycle counts associated with the visual observations are located below each schematic. Crack link-up occurred in bay 2 and bay 4.

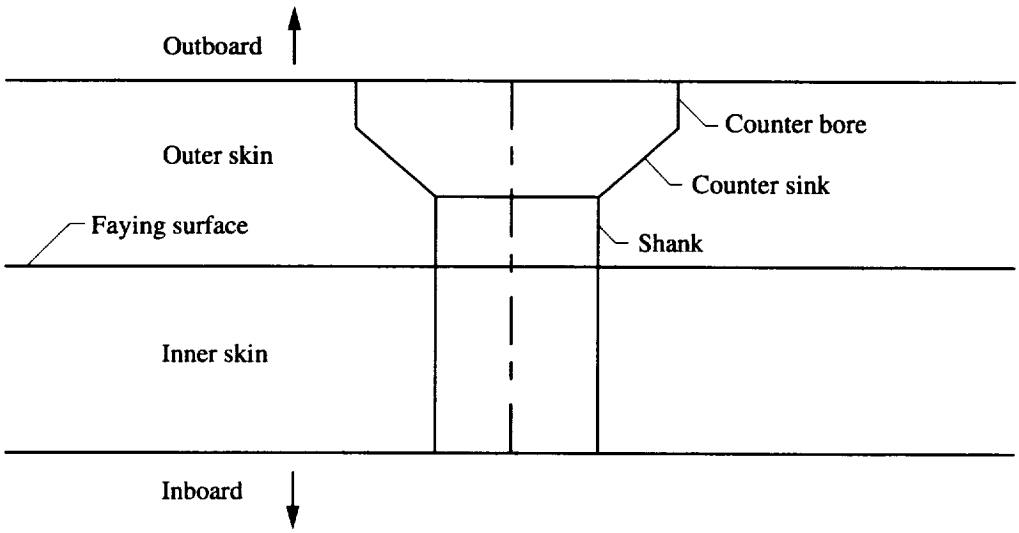

Figure 2.2 The schematic shows the cross section view of the counter-bore lap splice rivet hole region.

3. Visual Examination

A complete visual examination of the outer and inner surfaces was performed upon receipt of the six bay panel at NASA LaRC. As part of these examinations, detailed macro photographs were taken of the inboard and outboard surfaces of the panel. The panel was received in good condition with little evidence of corrosion. Some pitting and corrosion products were noted within the open rivet holes.[2] Subsequent destructive examinations of holes containing rivets showed no evidence of corrosion, suggesting that corrosion within open holes occurred after rivet removal and exposure to outdoor environment. It should be noted that the pressure test was conducted out-of-doors and the test article outside surface was exposed to all elements of weather. The following paragraphs document the structural features and the visible fatigue damage identified in each lap splice bay.

3.1 Bays 1 and 2:

Figure 3.1 shows a schematic of bay 2 detailing the locations of the lap splice rivet holes, the tear straps and the 18.85 inch (47.9 cm) upper rivet row crack. It should be noted that the schematics shown in this section are used to show general features; the drawings (not drawn to scale) show the approximate rivet hole locations. More accurate drawings of the rivet hole spacings are found in Sections 6.0 through 11.0. As fatigue cracks were visually observed during the pressurization test, the sequence of outer skin fatigue cracking was identified alphabetically. The letters A through Z shown in Figure 3.1 therefore identify the chronology of fatigue cracking within the bay. Figures 3.2 and 3.3 are photographs showing the appearance of the outboard skin surface of bays 1 and 2, respectively. Open holes remain where rivets were removed after pressure testing and prior to receipt of the panel. The numbers located above each of the upper rivet holes are used to identify specific rivet locations within each bay. The large crack is easily visible along the entire upper rivet row in bay 2 and extending into both tear straps. Figures 3.4, 3.5 and 3.6 are more detailed photographs of the large upper rivet row crack observed in bay 2. Each fatigue crack segment is identified per the chronological code (A through V) shown in Figure 3.1.[3] From Figures 3.4, 3.5 and 3.6, the following observations are made.

1. All visible fatigue cracking was contained in the upper rivet row.
2. Each fatigue crack initiated at or above the mid plane (centerline) of the rivet hole.
3. The region of fatigue cracking between rivet holes 5, 6, and 7 in Figure 3.5 was the first region of crack link-up in bay 2, refer to Figure 2.1. These fatigue cracks exhibit a characteristic curved crack path that resulted in an oblong shaped crack link-up configuration. Cracking at other bay 2 rivet hole locations exhibited a straighter crack path.
4. The upper portion of the rivet head contained in holes 2, 4, 5, 8, 10, 11, 12, and 14 were severed during pressure testing. As the crack link-up process proceeded from holes 5, 6, and 7, increased out-of-plane loads resulted in the fracture of the upper portion to the rivet head, allowing out-of-plane loading (Mode III). Presumably, Mode III loading increased as subsequent crack link-up had occurred. The outer skin below the long crack was captured by the rivet head and showed no evidence of outward deformation (pillowing).
5. As the long fatigue crack grew into the tear strap region, the growing crack tended to be deflected upward.

---

[2] All top row rivets and some second row rivets were remove during *in situ* examinations to facilitate inspections after pressure testing was completed and prior to panel shipment to LaRC. The open rivet holes were exposed to an outdoor environment and are likely regions for entrapped moisture.

[3] The letters designate the order each fatigue crack was observed during *in situ* visual inspection; crack A was observed first followed by B, C, D, etc.

3.2 Bay 3:

Figures 3.7 and 3.8 show the configuration and overall condition of bay 3 outer surface. Note that all top row and six second row rivets were removed prior to receipt of the panel. Figure 3.9 shows the outer skin surface region that contain visible fatigue cracks adjacent to upper rivet holes 1 through 4 and 12 through 15. Visible fatigue cracks were observed at locations J, K, L, M, O, R, and T. No crack link-up was visible in bay 3. Figure 3.10 is a photograph of the tear strap region that separates bays 3 and 4. No visible evidence of outer skin cracking was observed with the bay 3/4 tear strap.

3.3 Bay 4:

The schematic in Figure 3.11 and the photograph in Figure 3.12 show the location of fourteen fatigue cracks contained in nine upper rivet row holes. Crack link-up occurred in the middle of the bay between upper rivet row locations 8 and 9. Figures 3.13 and 3.14 are photographs of the outer surface showing the visible fatigue cracks along the upper rivet row. Figure 3.13b details the region of crack link-up, cracks F and C. Crack C propagated within a plane slightly elevated with respect to crack F. Link-up occurred at a point located nearly mid-distance between the rivet holes 8 and 9. Final link-up occurred by the failure of the small ligament located between the two fatigue cracks C and F, producing a crack at an angle nearly 30° from vertical.

3.4 Bays 5 and 6:

Figure 3.15 shows the rivet hole configuration for bay 5. Here, seven upper rivet holes contained a total of twelve visible fatigue cracks. No visible fatigue crack link-up was observed in bay 5. The photographs in Figures 3.16 and 3.17 shows the outboard surface of bays 4 and 5 and the tear strap regions bordering bays 5 and 6, respectively. Figures 3.18 and 3.19 are photographs detailing the visible cracks found in bay 5 upper rivet row. Figure 3.19 shows the crack path between upper rivet holes 7, 8, 9, and 10. All fatigue cracks that propagated in the forward direction exhibited a curved crack path slanted upwards and fatigue cracks that grew in the aft direction curved downwards. Many of the fatigue cracks shown in Figure 3.19 extend close to the adjacent rivet hole without crack link-up. A number of the aft fatigue cracks, i.e., crack C in hole 10, initiated below the mid plane of the rivet holes. This crack path configuration differs from that observed in bays 2, 3, and 4 and suggest the possible influence of complex loading created by nearby structure.

3.5 Interior surface of Bays 1, 2, 3, 4, 5, and 6:

Figures 3.20 through 3.25 document the condition to the inboard surface of the panel. Each photograph details the location of the interior structure, i.e., vertical stiffener, horizontal stiffener, lap splice, and tear strap. Visual inspection of the inboard surfaces revealed no evidence of fatigue cracking.

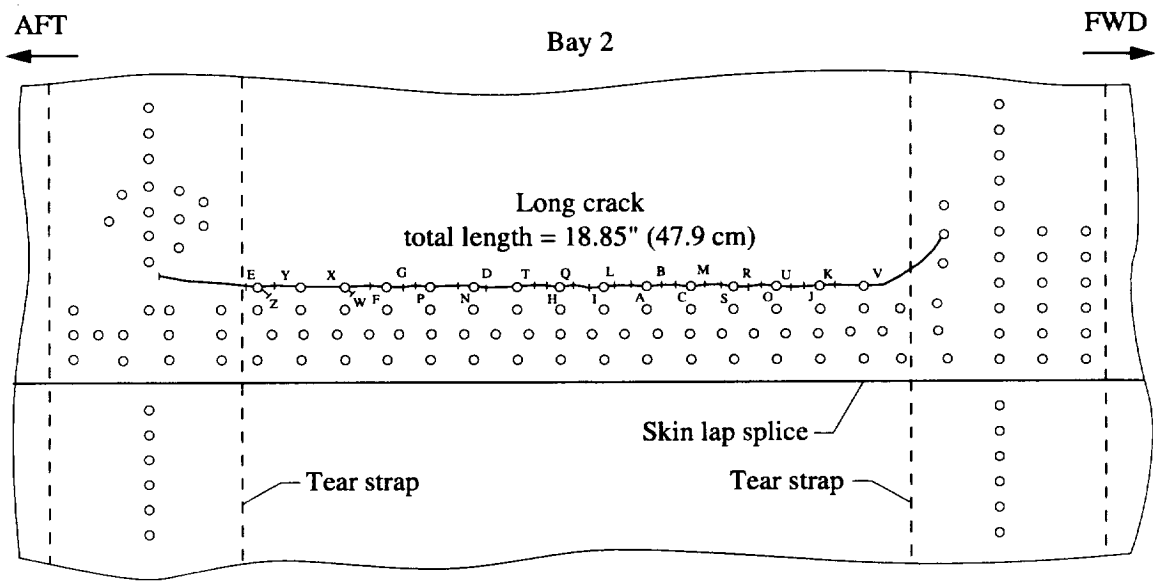

Figure 3.1 The schematic shows bay 2 and two adjacent tear strap regions. Dashed lines mark the location of the tear straps. The "tic" marks locate the approximate location for fatigue cracks A through Z prior to link-up. The long crack is shown along the upper rivet row.

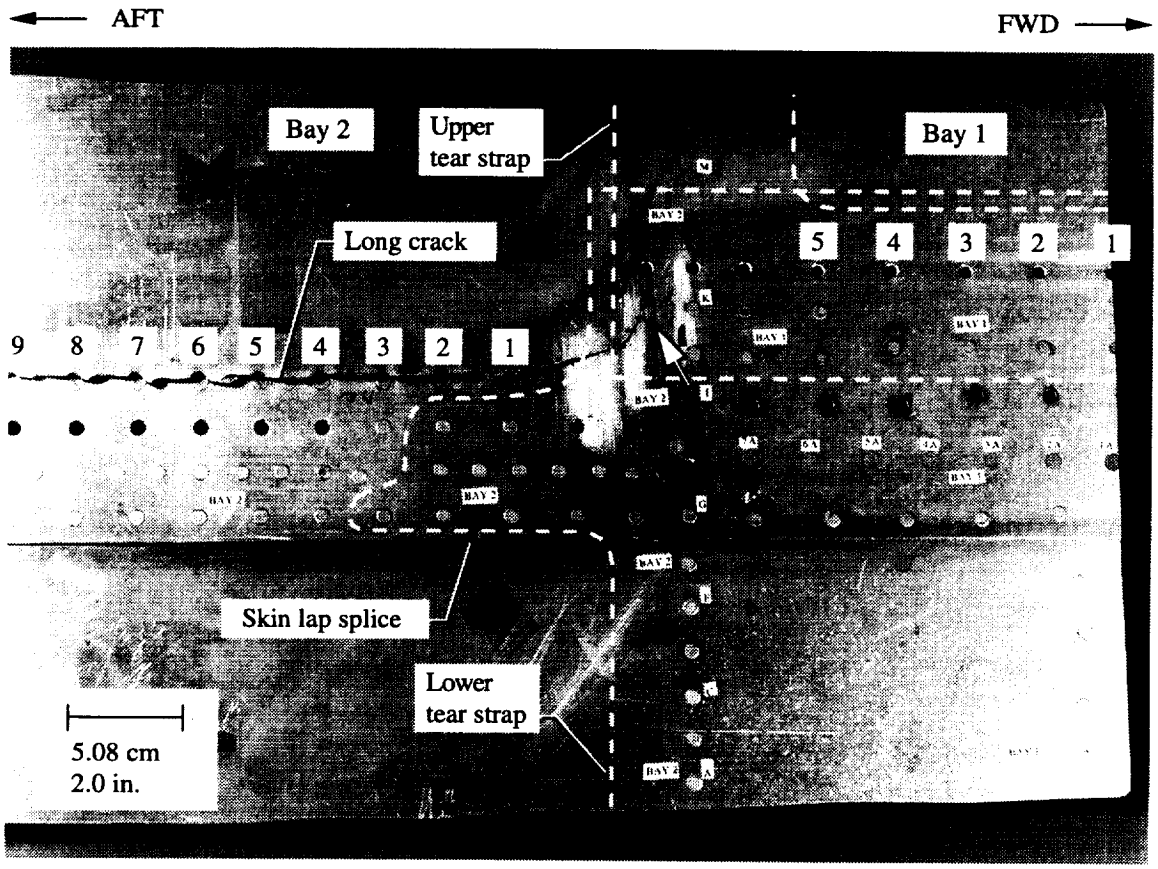

Figure 3.2 The photograph shows the bay 1 tear strap region and a portion of bay 2. The complex shape of the bay 1 tear strap is shown by the dotted lines. The bay 2 long crack is clearly visible along the upper rivet row of the midbay section. Growth of the forward portion of the bay 2 crack terminated at a rivet hole in the bay 1 tear strap region (arrow). Rivet rows are labeled with letters (bottom to top) and rivet holes are numbered from forward to aft (right to left). Note: A number of rivets were removed for visual and within hole eddy current inspection prior to receipt of the panel.

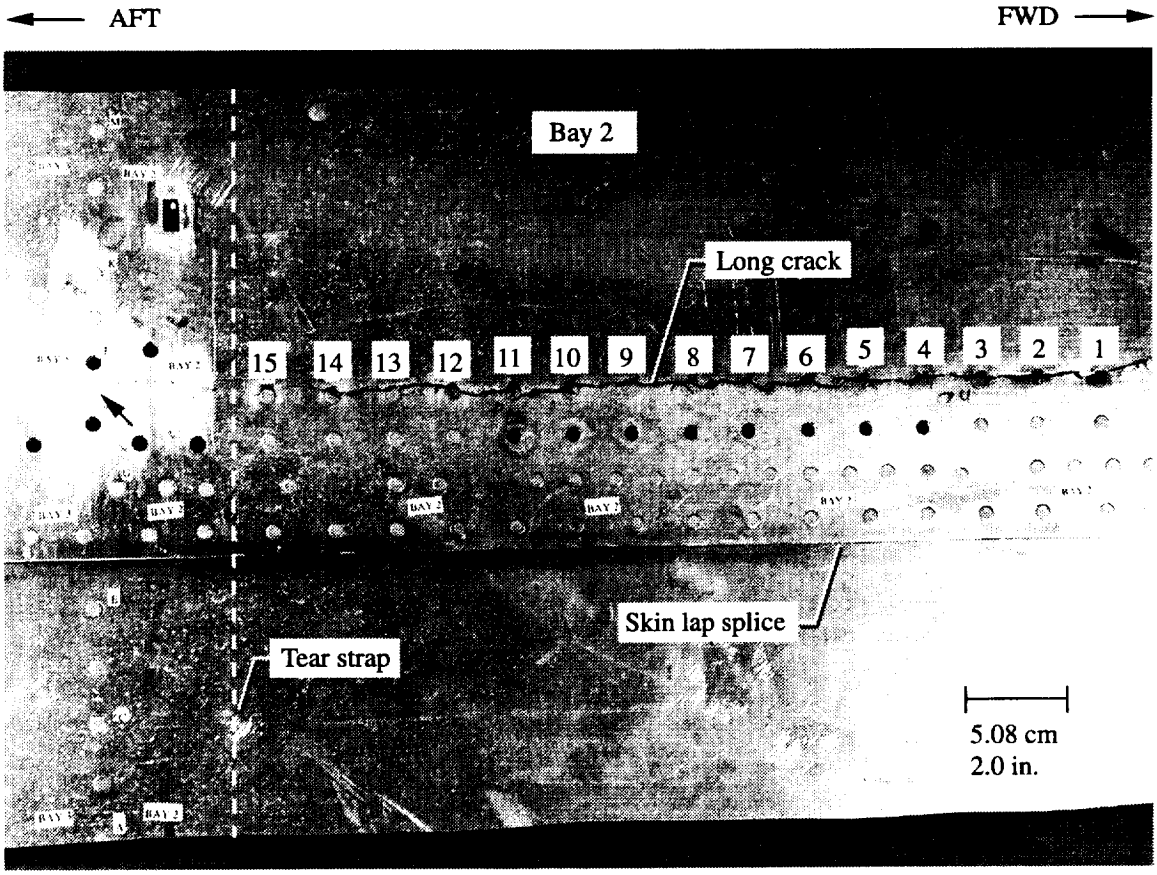

Figure 3.3 The photograph shows bay 2 and the bay 2/3 tear strap region (left of the dotted line). The long bay 2 crack is visible along the upper rivet row. Growth of the aft portion of the bay 2 crack terminated in the 2/3 tear strap region. Rivet rows are labeled with letters (bottom to top) and rivet holes are numbered from forward to aft (right to left). Note: A number of rivets were removed for visual and within hole eddy current inspection prior to receipt of the panel.

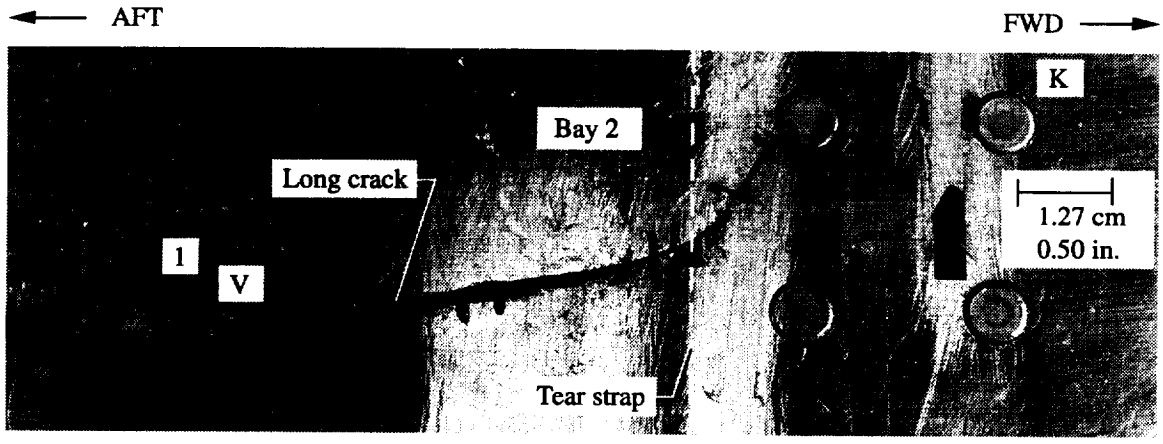

a)

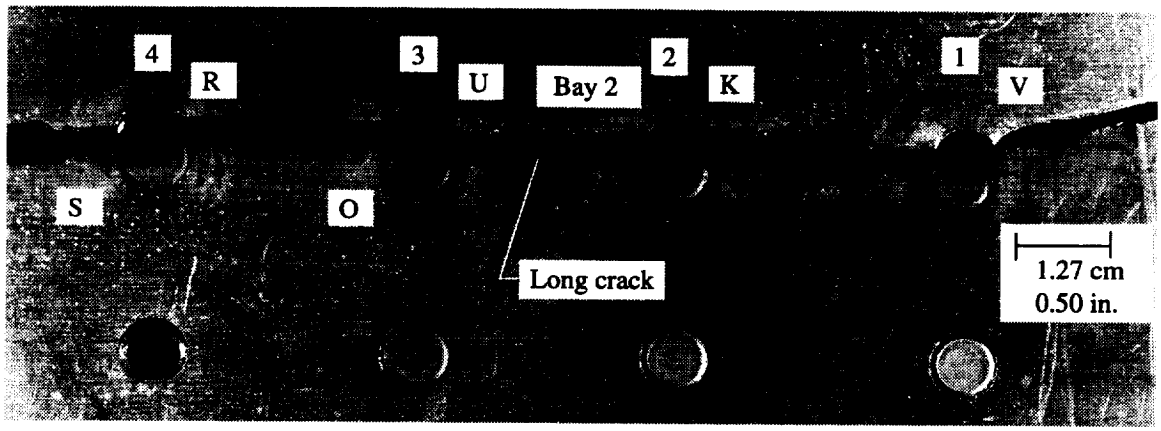

b)

Figure 3.4 a) The photograph shows the forward end of the long bay 2 crack. Growth of the forward end of the crack terminated in a row K rivet hole contained in the bay 1 tear strap region (dashed line). The position of the fatigue crack front, detected by *in situ* visual observation, is noted by the arrow at position V. b) The photograph shows upper rivet holes 1 through 4 and a portion of the long bay 2 crack. Arrows mark the position of fatigue crack fronts detected by *in situ* visual observations at positions S, R, O, U, K, and V.

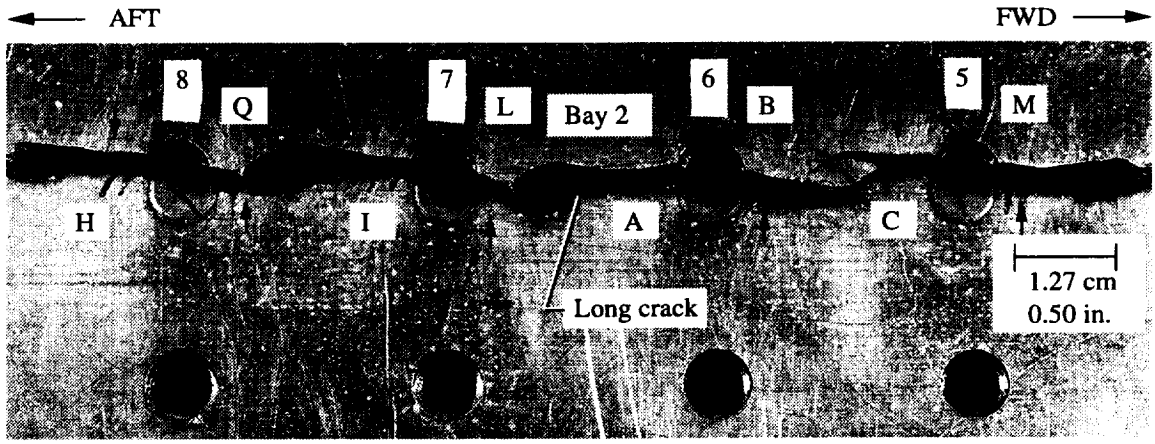

(a)

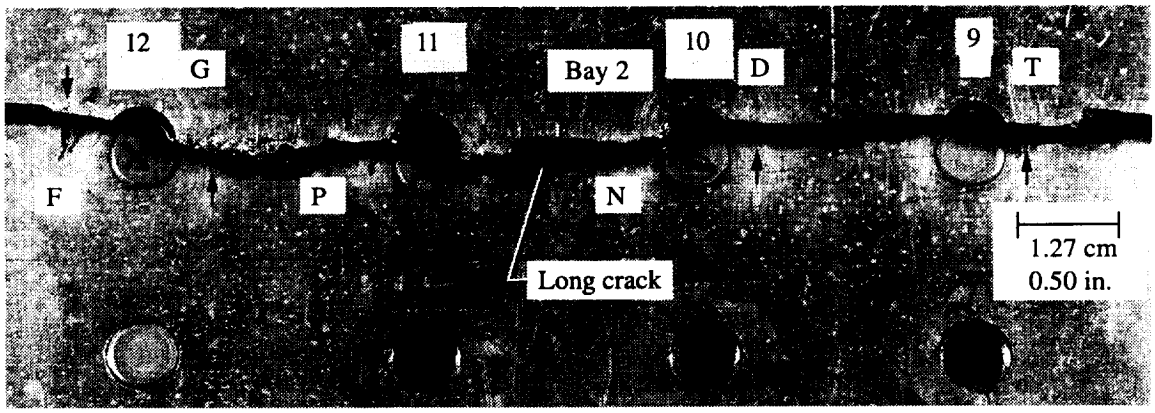

(b)

Figure 3.5 a) The photograph shows upper rivet row holes 5 through 8 and a portion of the long bay 2 crack. The position of fatigue crack fronts, detected by *in situ* visual observations, are noted by arrows at positions H, Q, I, L, A, B, C, and M. b) The photograph shows upper rivet holes 9 through 12 and a portion of the long bay 2 crack. The position of fatigue crack fronts, detected by *in situ* visual observations, are noted by arrows at positions F, G, P, N, D, and T.

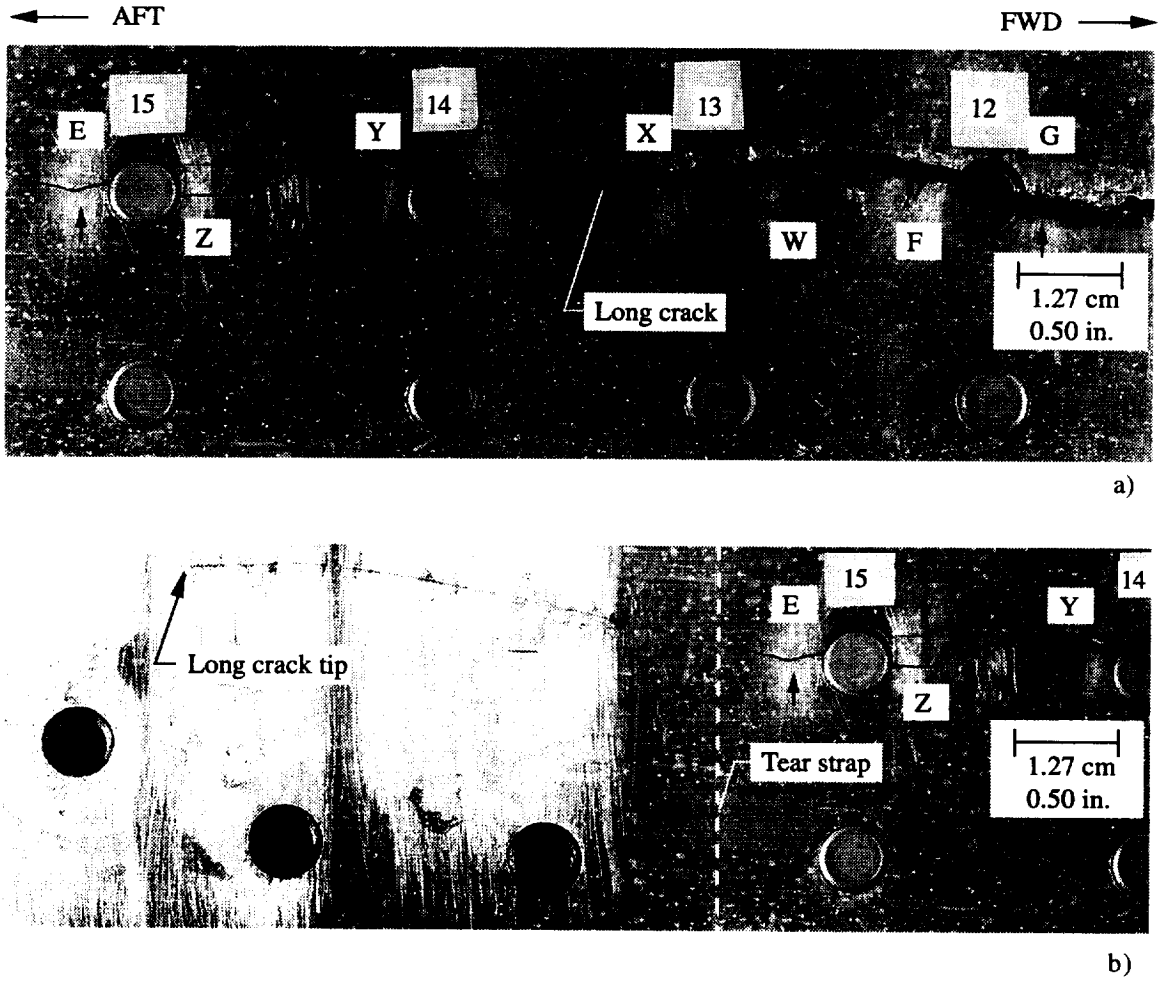

Figure 3.6 a) The photograph shows upper rivet holes 12 through 15 and a portion of the long bay 2 crack. The position of fatigue crack fronts, detected by *in situ* visual observations, are noted by arrows at positions E, Z, Y, X, W, F, and G. Secondary cracks can be seen at locations Z and W. b) The photograph shows upper rivet holes 14 and 15 and a portion of the long bay 2 crack. Growth of the aft end of the crack terminated in the center of the bay 2/3 tear strap (to the left of the dashed line). The position of fatigue crack fronts, detected by *in situ* visual observations, are noted by arrows at positions E, Z and Y.

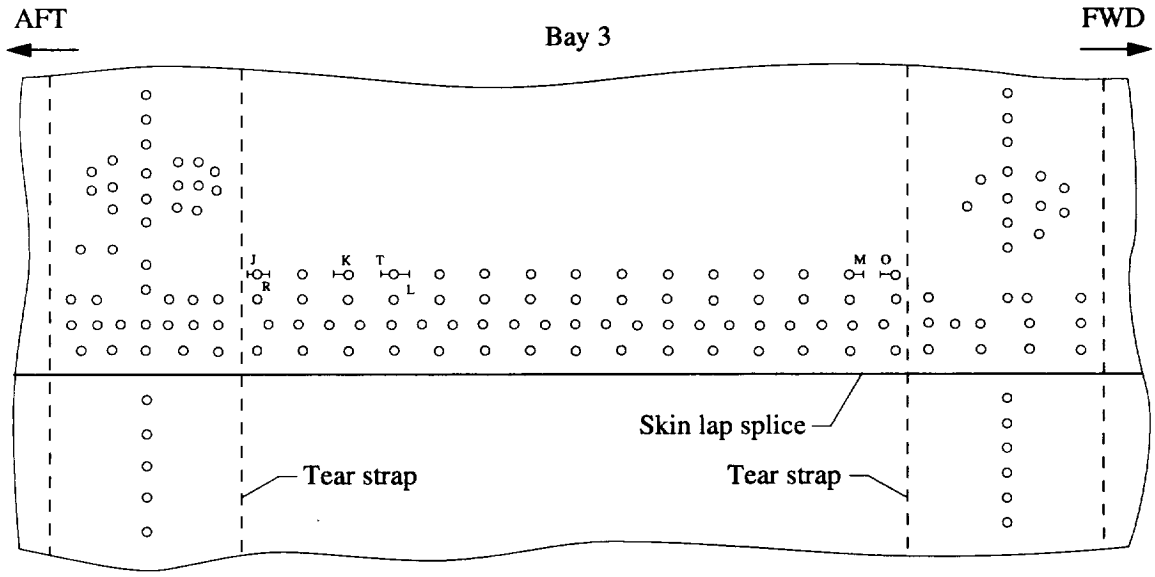

Figure 3.7 The schematic shows bay 3 and the two adjacent tear strap regions. Dashed lines show the location of the tear straps. Shown are the locations of fatigue cracks, J, K, L, M, O, R, and T.

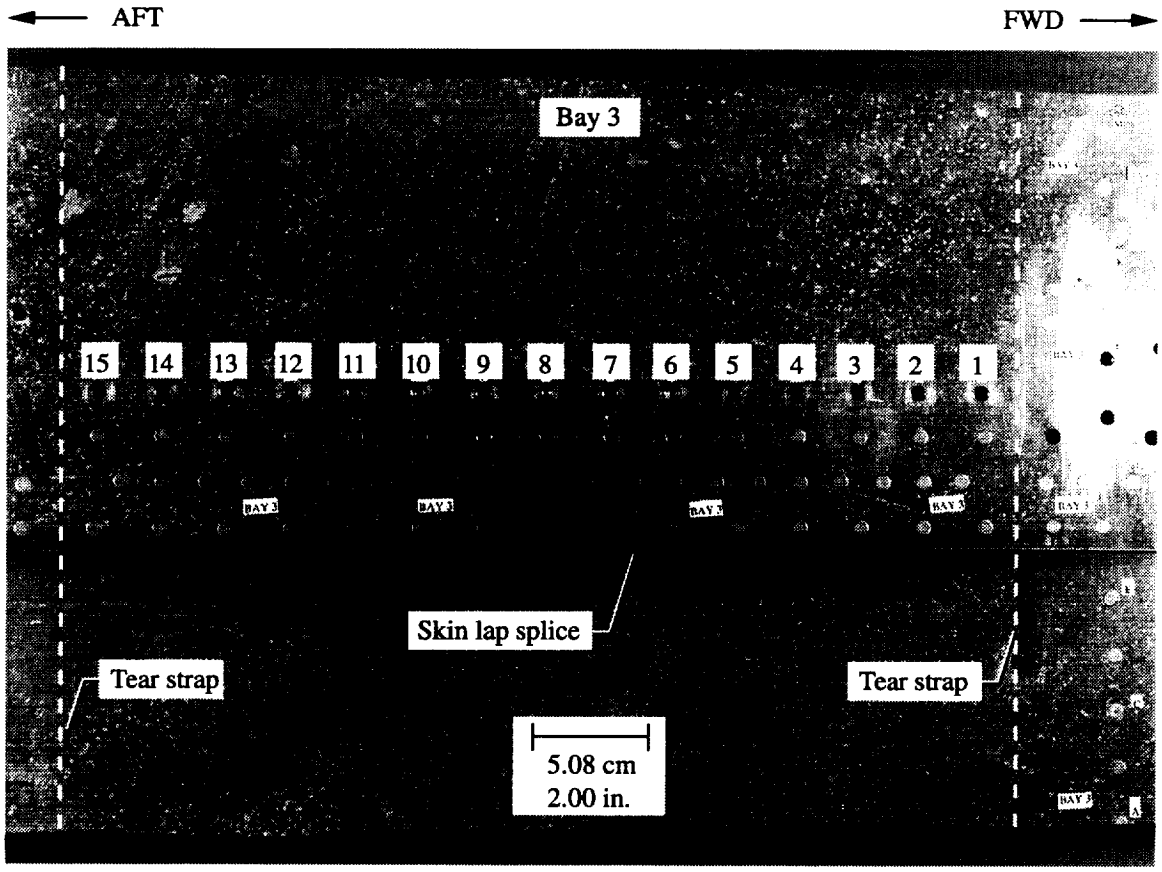

Figure 3.8 The photograph shows bay 3 and portions of the bay 3/4 and bay 2/3 tear strap regions (marked by dashed lines) to the left and right of the photograph, respectively. Rivet rows are labeled with letters (right) from bottom to top (A through M) and rivet holes are numbered from forward to aft (right to left).

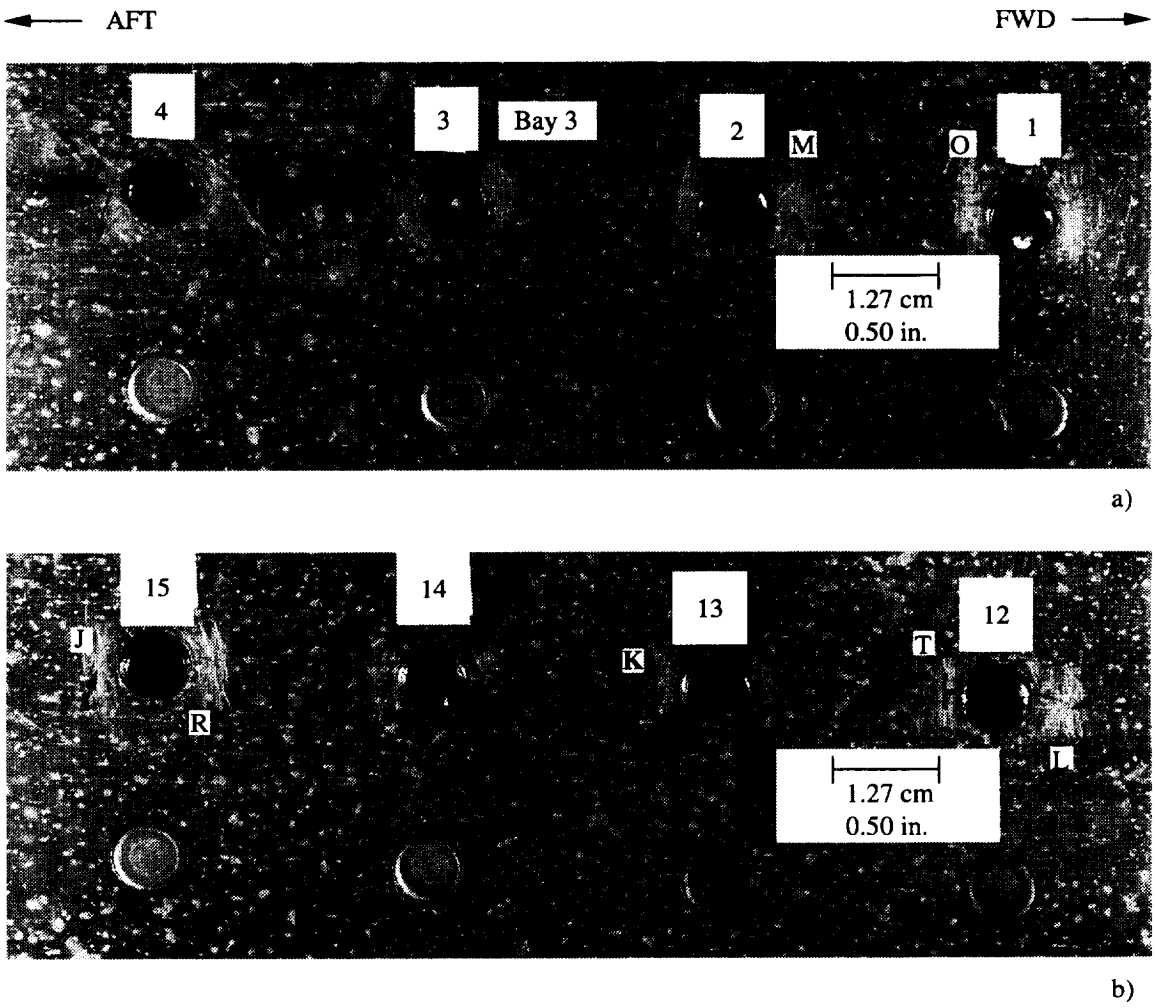

Figure 3.9 a) The photograph shows bay 3 upper rivet row holes 1 through 4. The position of fatigue crack fronts, detected by *in situ* visual observations, are noted by arrows at positions M and O. b) The photograph shows bay 3 upper rivet row holes 12 through 15. The position of fatigue crack fronts, detected by *in situ* visual observations, are noted by arrows at positions J, R, K, T and L.

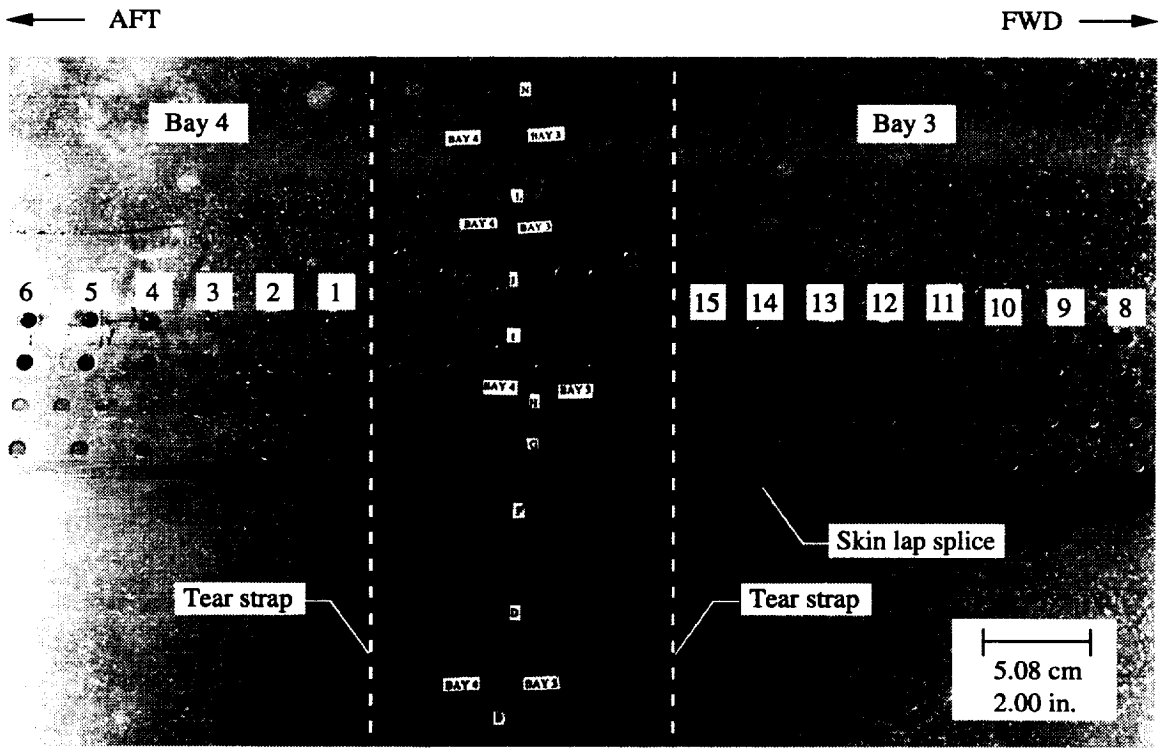

Figure 3.10 The photograph shows part of bay 4, the bay 3/4 tear strap (dashed lines), and part of bay 3. Rivet rows are labeled with letters from bottom to top while rivet holes are numbered from forward to aft (right to left).

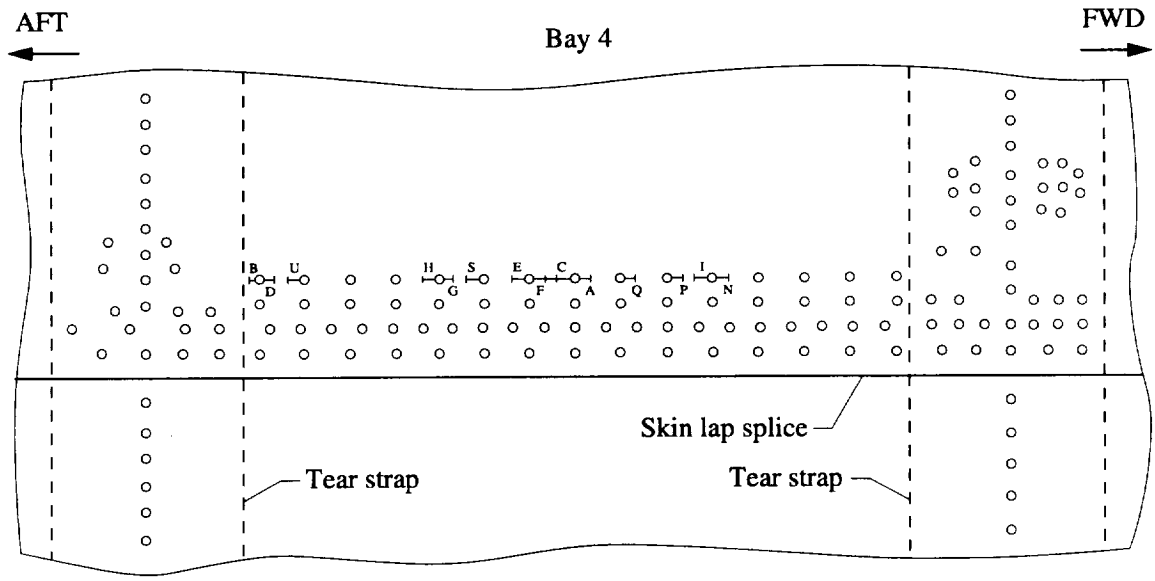

Figure 3.11 The schematic shows bay 4 and two adjacent tear strap regions. Dashed lines show the location of the tear straps. The location of thirteen fatigue cracks are noted at A, B, C, D, E, G, H, I, N, P, Q, S, and U. Crack link-up occurred between fatigue cracks C and F.

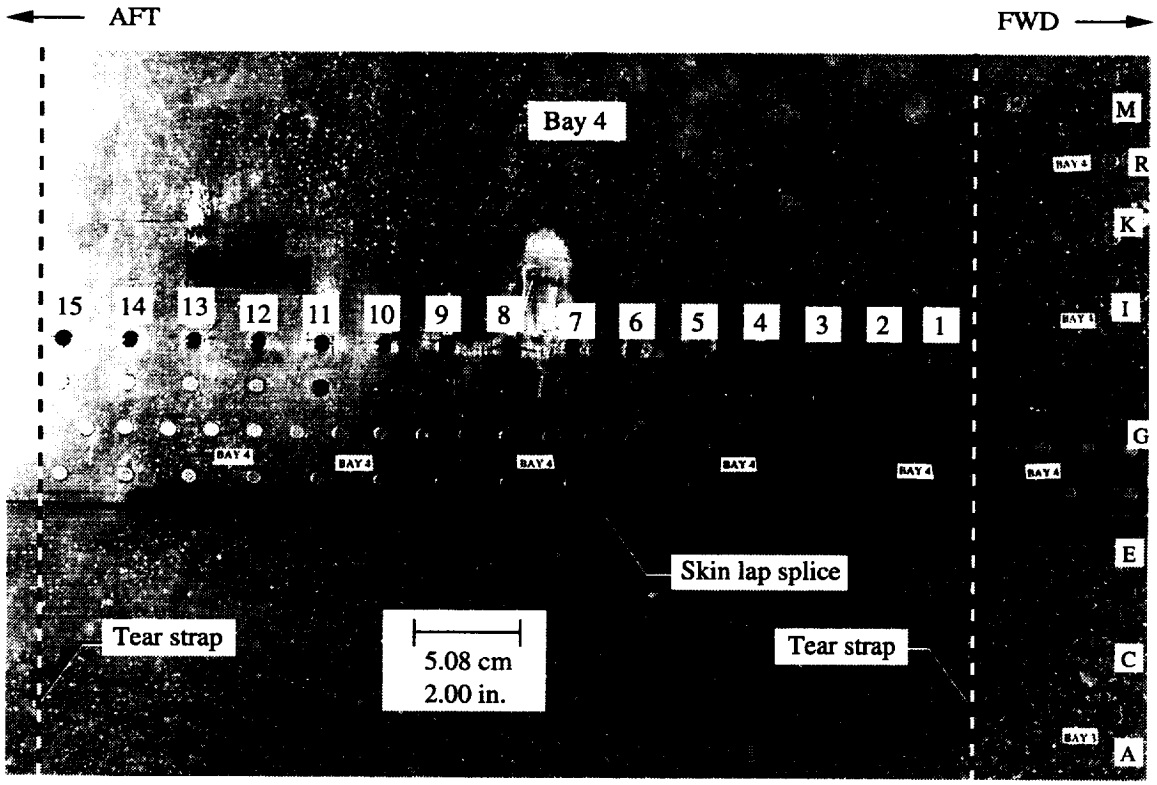

Figure 3.12 The photograph shows bay 4 and portions of the bay 4/5 and bay 3/4 tear strap regions (dashed lines) that are visible to the left and right of the photograph, respectively. Rivet rows are labeled with letters (right) from bottom to top (A through P) and rivet holes are numbered from forward to aft (right to left).

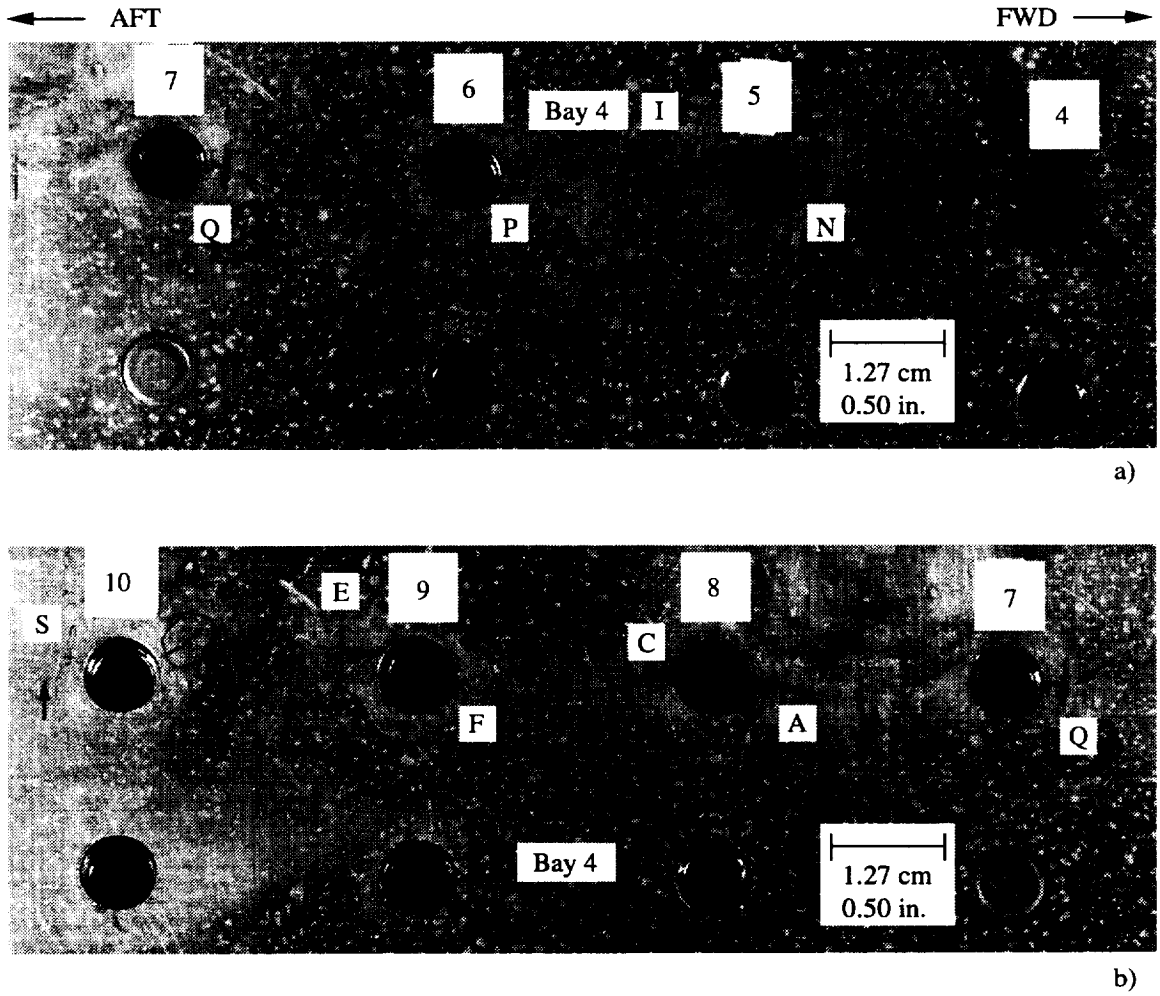

Figure 3.13 a) The photograph shows bay 4 upper rivet row holes 4 through 7. The position of fatigue crack fronts, detected by *in situ* visual observations, are noted by arrows at positions Q, P, I, and N. b) The photograph shows bay 4 upper rivet row holes 7 through 10. The position of fatigue crack fronts, detected by *in situ* visual observations, are noted by arrows at positions S, E, F, C, A, and Q. The cracks between rivet holes 8 and 9 have linked-up.

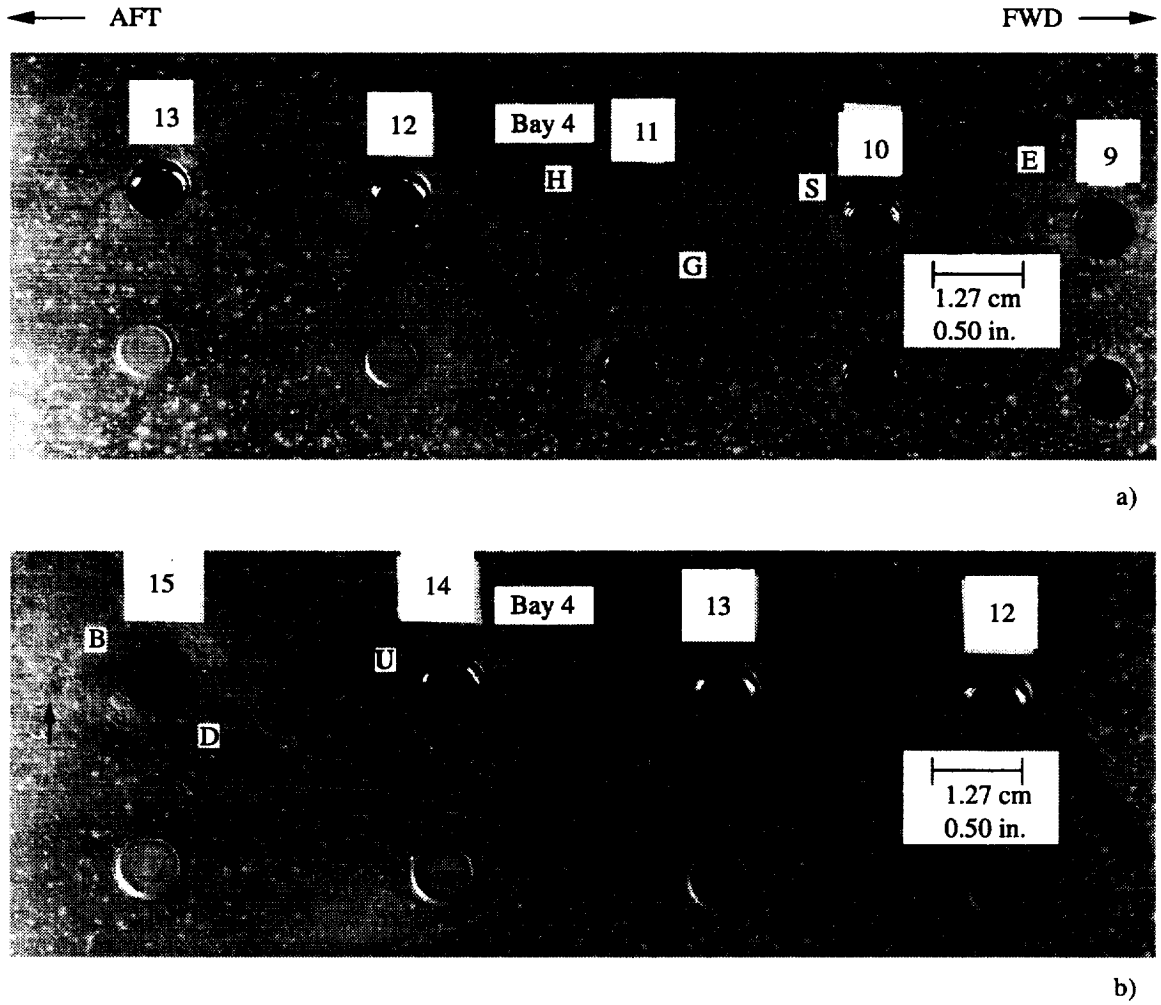

Figure 3.14 a) The photograph shows bay 4 upper rivet row holes 9 through 13. The position of fatigue crack fronts, detected by *in situ* visual observations, are noted by arrows at positions H, G, S, and E. b) The photograph shows bay 4 upper rivet row holes 12 through 15. The position of fatigue crack fronts, detected by *in situ* visual observations, are noted by arrows at positions B, D, and U.

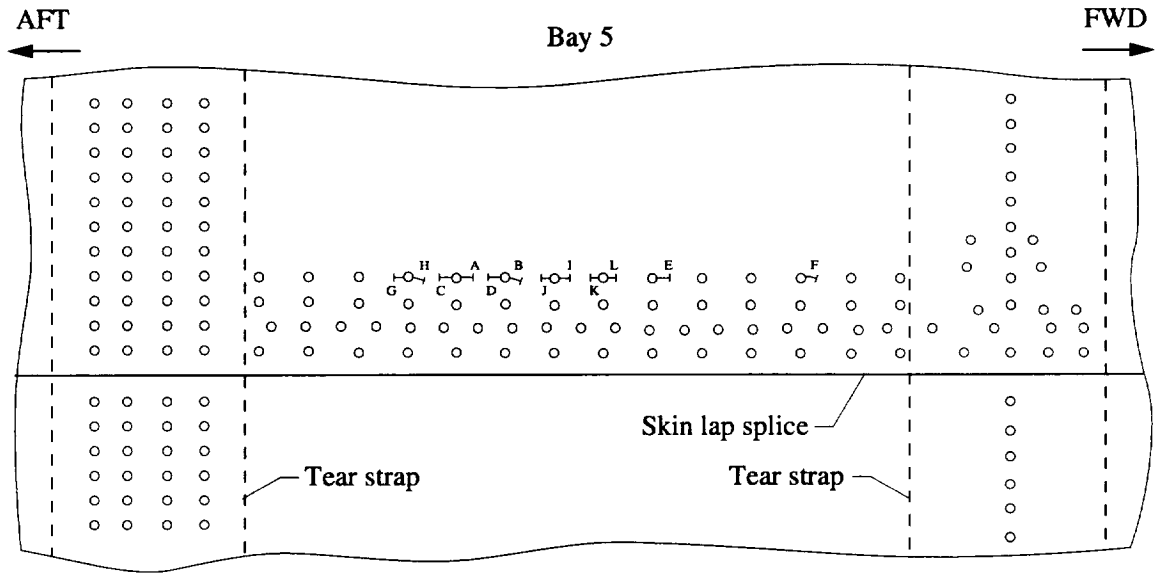

Figure 3.15 The schematic shows bay 5 and two adjacent tear strap regions. Dashed lines highlight the location of the tear straps. Shown are the locations of fatigue cracks A through L.

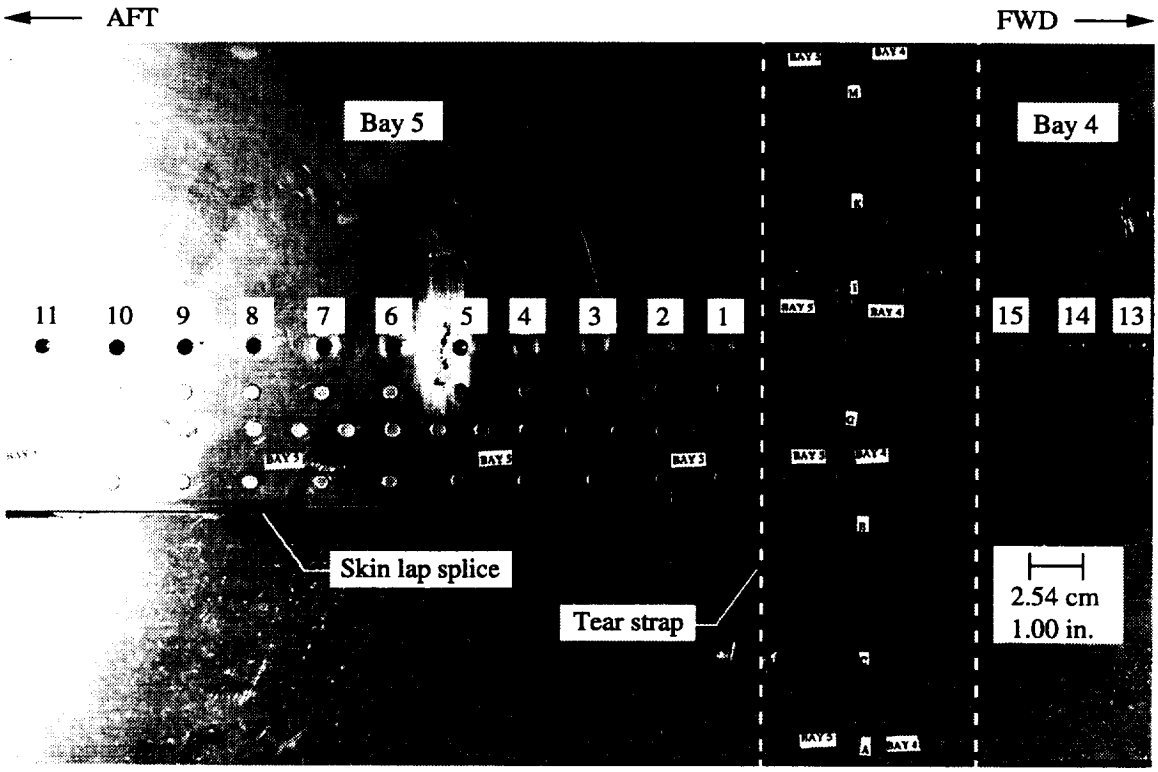

Figure 3.16 The photograph shows most of bay 5, the bay 4/5 tear strap region (marked by dashed lines), and a small portion of bay 4. Rivet rows are labeled with letters (right) from bottom to top (A through P) and rivet holes are numbered from forward to aft (right to left).

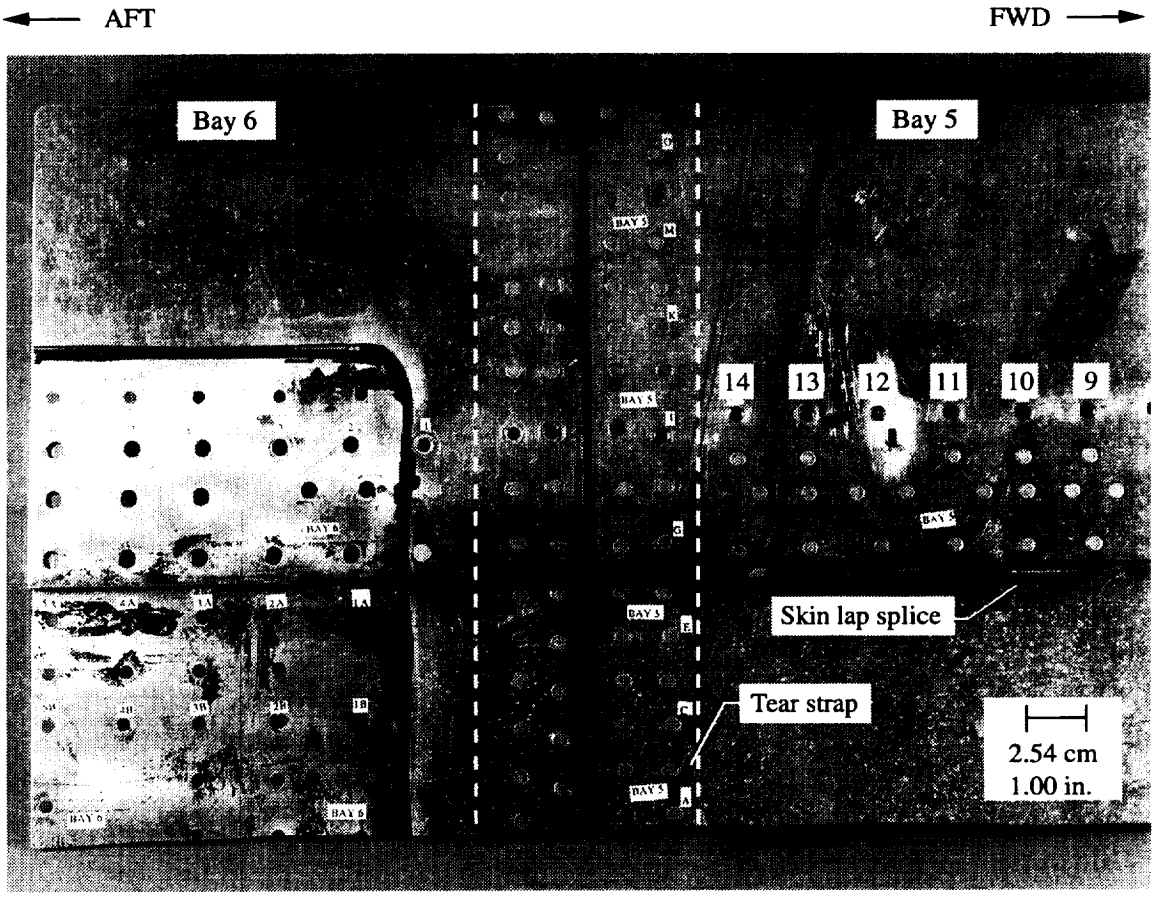

Figure 3.17 The photograph shows bay 6, the 5/6 tear strap region (marked with dashed lines), and a portion of bay 5. Rivet rows are labeled with letters (center) from bottom to top (A through P) and rivet holes are numbered from forward to aft (right to left).

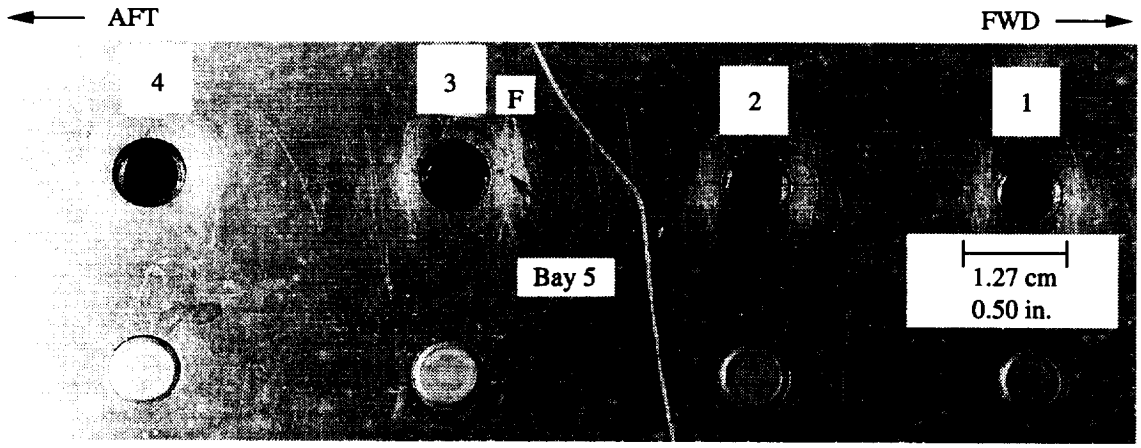

a)

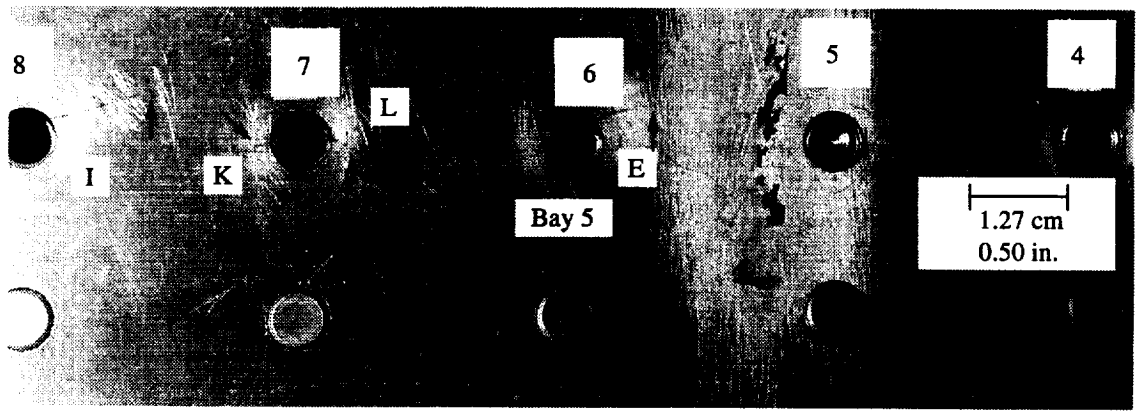

b)

Figure 3.18 a) The photograph shows bay 5 upper rivet row holes 1 through 4. The position of the fatigue crack front, detected by *in situ* visual observation, is noted by an arrow at position F. b) The photograph shows bay 5 upper rivet row holes 4 through 8. The position of fatigue crack fronts, detected by *in situ* visual observations, are noted by arrows at positions I, K, L, and E.

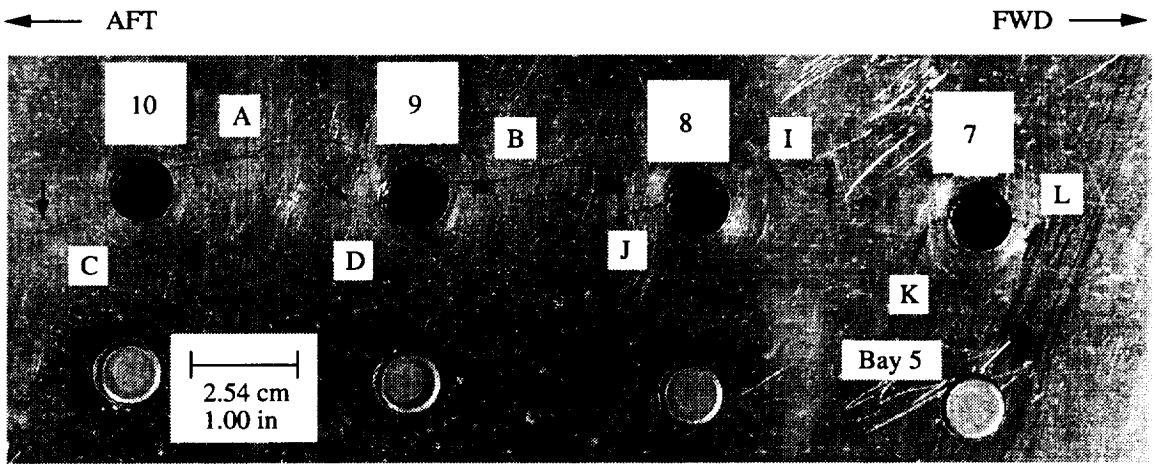

a)

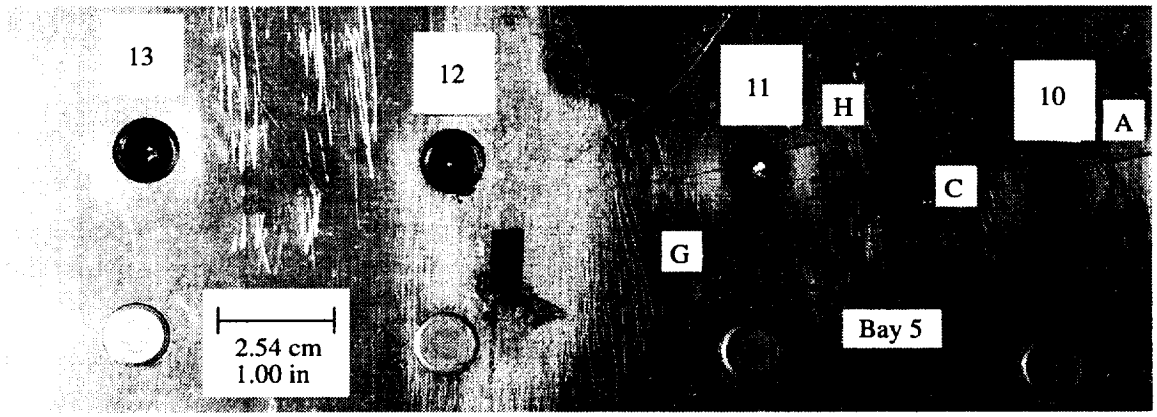

b)

Figure 3.19 a) The photograph shows bay 5 upper rivet row holes 7 through 10. The position of fatigue crack fronts, detected by *in situ* visual observations, are noted by arrows at positions C, A, D, B, J, I, K, and L. b) The photograph shows bay 5 upper rivet row holes 10 through 13. The position of fatigue crack fronts, detected by *in situ* visual observations, are by arrows noted at positions G, H, C, and A.

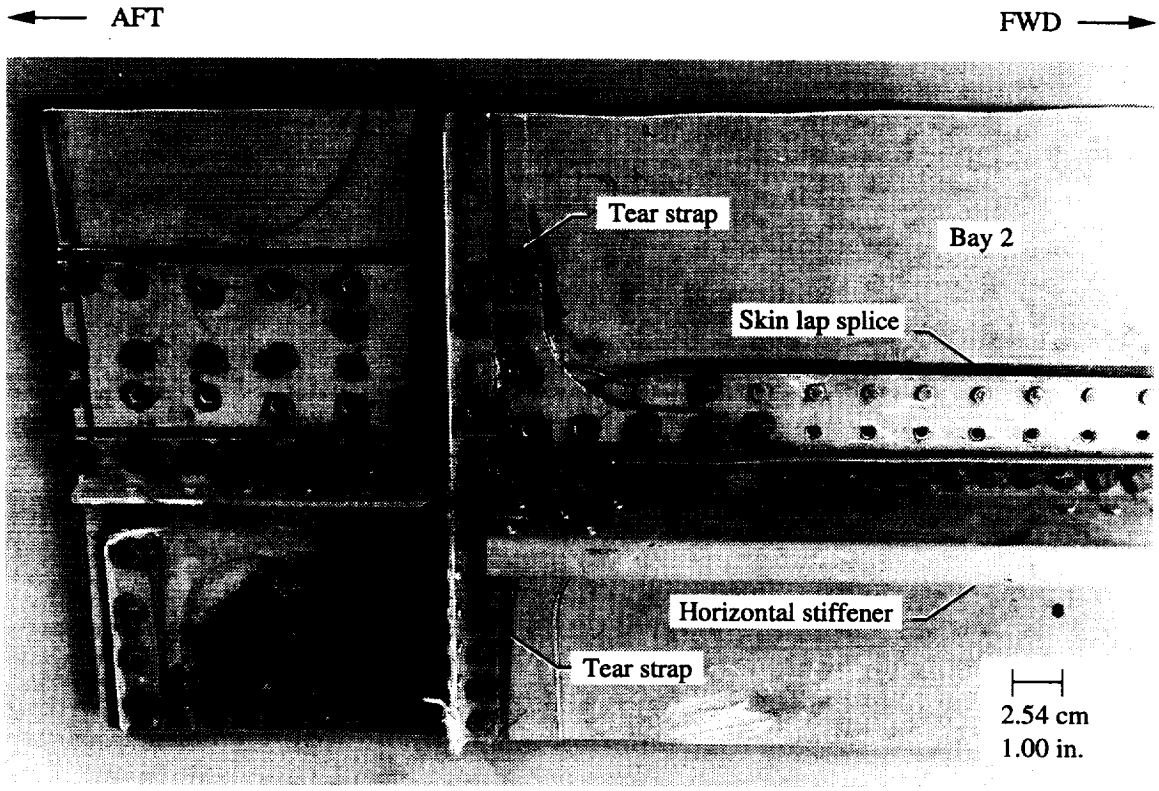

Figure 3.20 The photograph shows the inboard surface of the bay 1 tear strap region and a portion of bay 2. Structural features such as the tear strap, skin lap splice, and horizontal stiffener are visible.

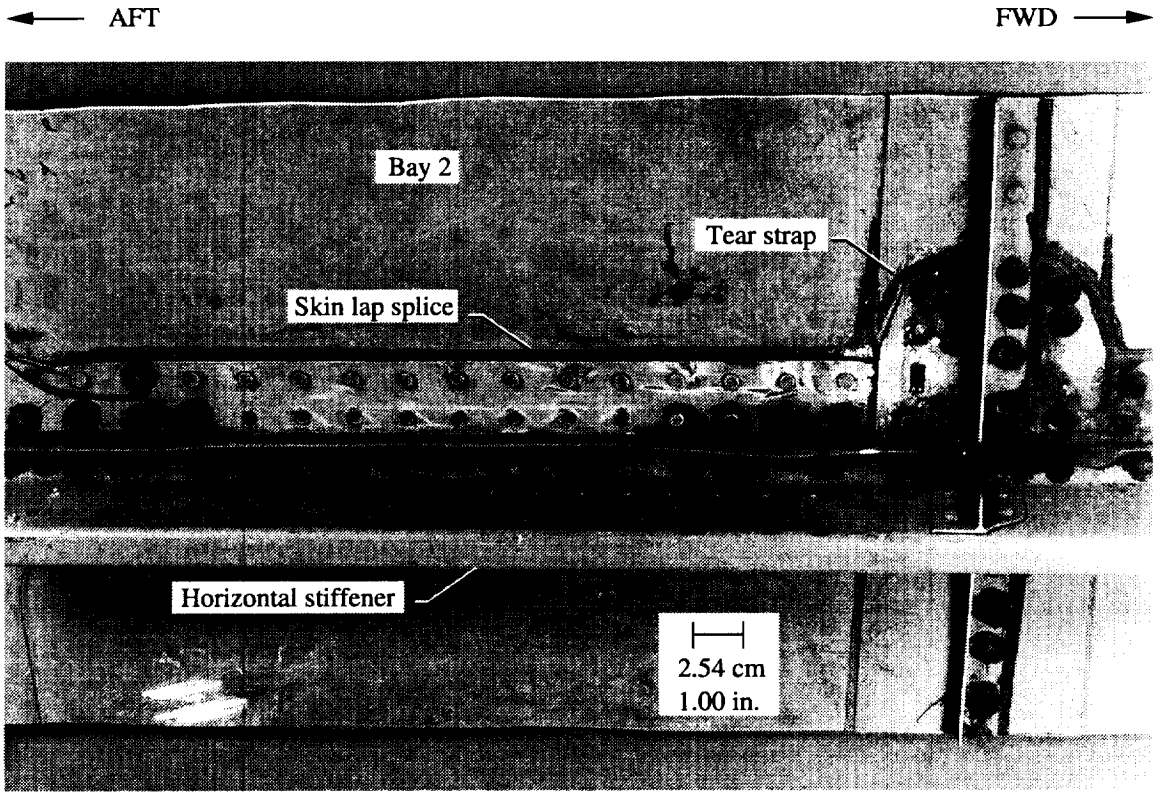

Figure 3.21 The photograph shows the inboard surface the bay 2 and bay 2/3 tear strap regions. Structural features such as the tear strap, skin lap splice, and horizontal stiffener are all visible.

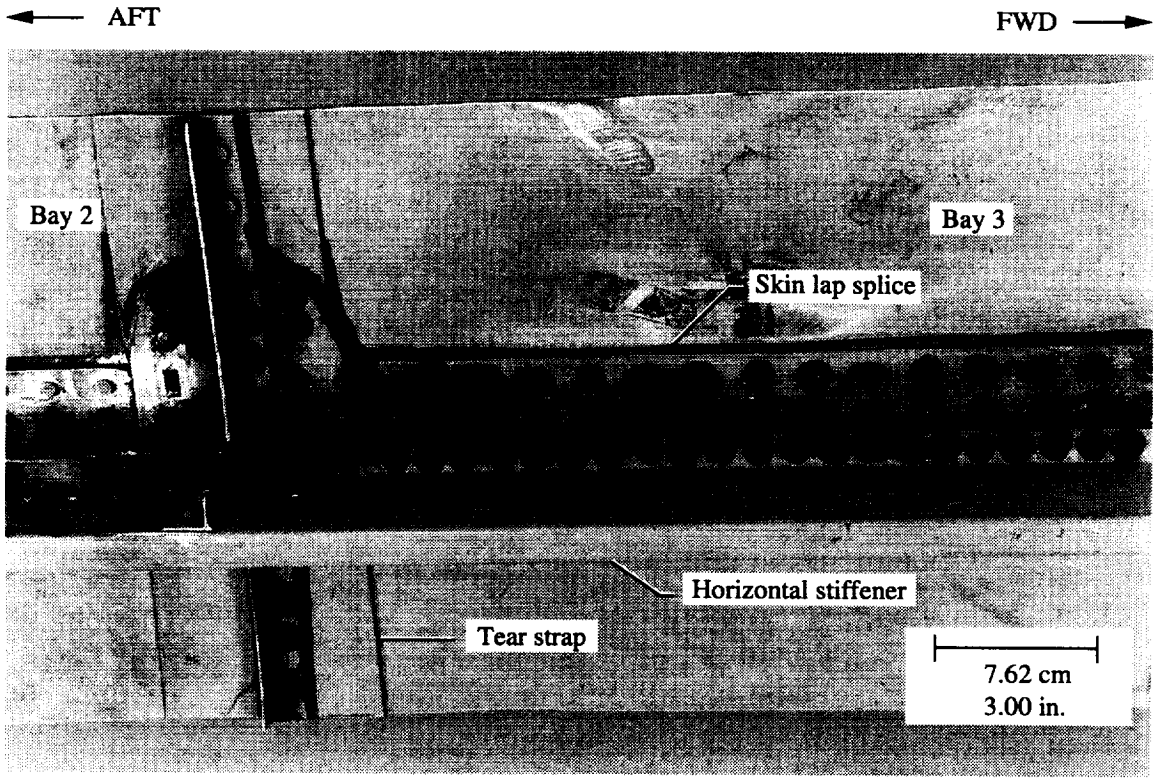

Figure 3.22 The photograph shows the inboard surface of the panel. The bay 2, bay 2/3 tear strap, and bay 3 regions are shown. Structural features such as the tear strap, skin lap splice, and horizontal stiffener are all visible.

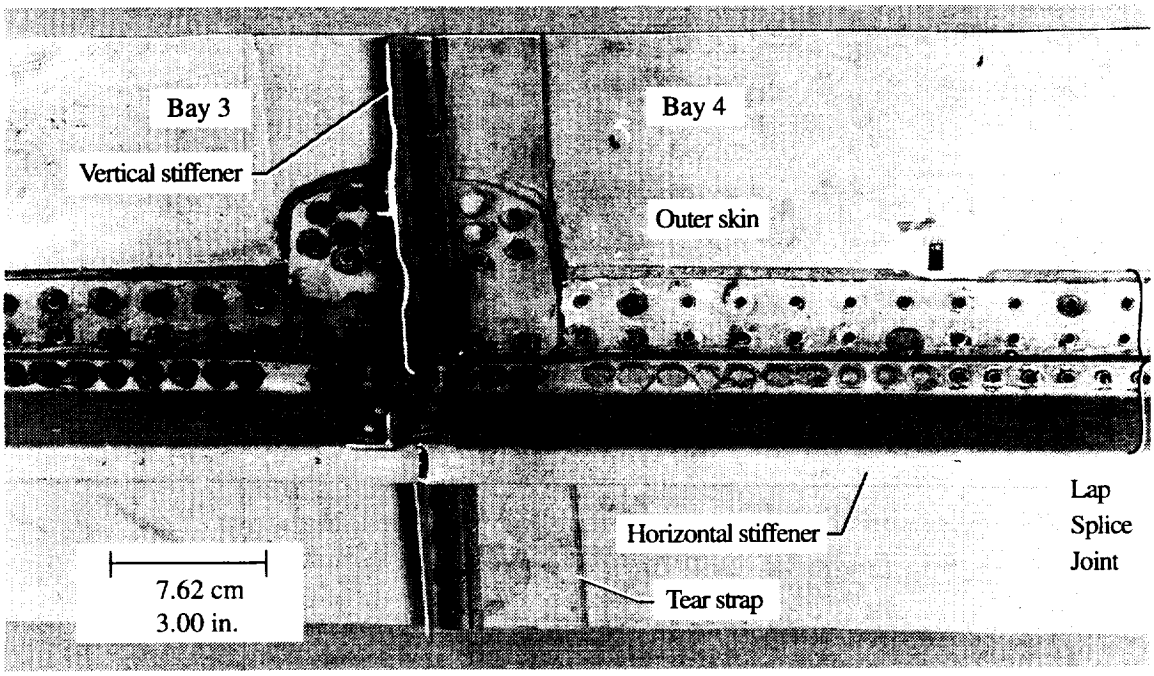

Figure 3.23 The photograph shows the inboard surface of the bay 2, bay 3/4 tear strap, and bay 4 regions. Structural features such as the tear strap, skin lap splice, vertical stiffener, and horizontal stiffener, are all visible.

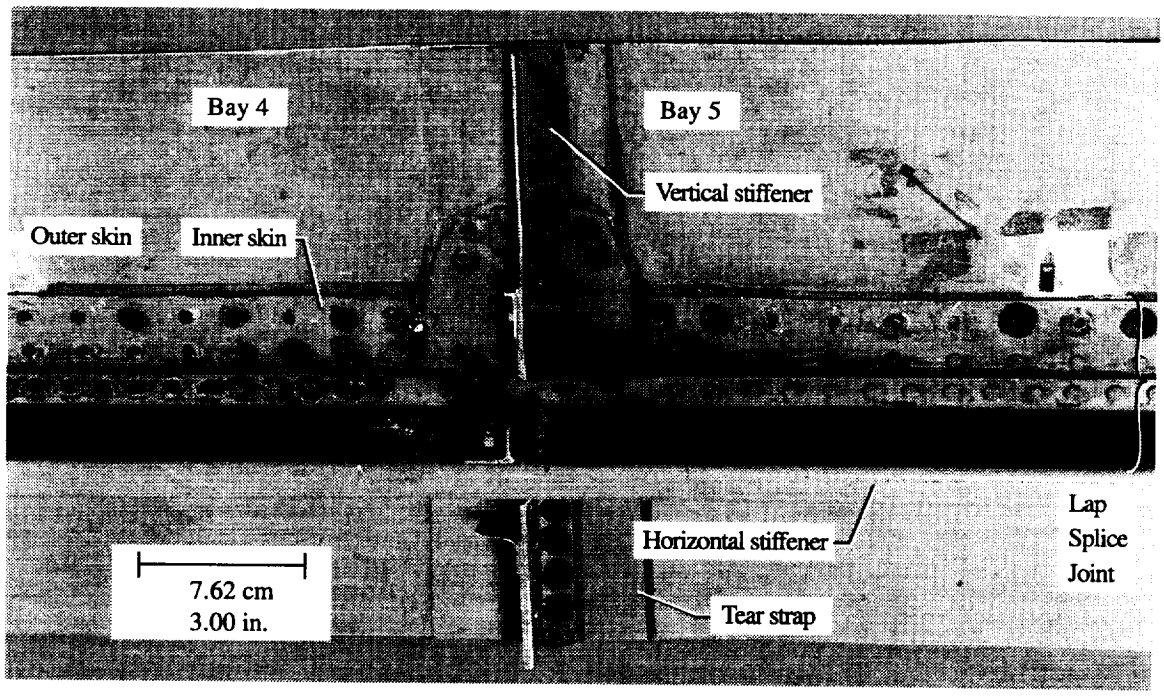

Figure 3.24 The photograph shows the inboard surface of the bay 4, bay 4/5 tear strap, and bay 5 regions. Structural features such as the tear strap, skin lap splice, vertical stiffener, and horizontal stiffener are all visible.

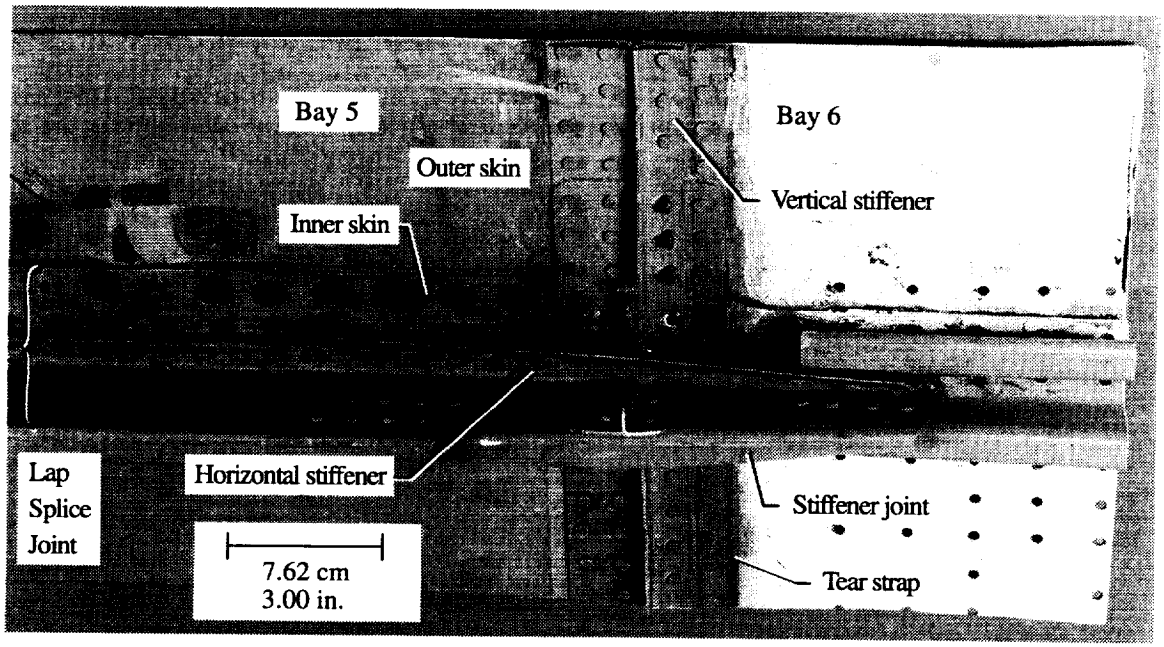

Figure 3.25 The photograph shows the inboard surface of the bay 5, bay 5/6 tear strap, and bay 6 regions. Structural features such as the tear strap, skin lap splice, vertical stiffener, stiffener joint, and horizontal stiffener are all visible.

4. Non-Destructive Examinations (NDE)

Prior to destructive examination, the entire panel was examined using a variety of standard NDE techniques summarized in Table 4.1. Great care was taken not to affect (contaminate or bend) the panel during handling or NDE testing.

Table 4.1 NDE Techniques

NDE Technique	Comments
visual (8X)	Chart all visible flaws.
eddy current (EC)	Rivet hole regions were inspected using the outboard surface sliding probe or template method. For open rivet holes, a hole EC probe was employed with a crack detection limit of 1.27 mm (0.050 inch).
ultrasound (UT)	All joints were inspected using acoustic impedance to detect tear strap disbonds, lap splice sealant voids and corrosion of areas greater (6.35 mm (0.25 inch) diameter).
radiography (RT)	X-ray inspections were used to detect internal and external flaws equal to or greater than 0.76 mm (0.03 inch).

4.1 Eddy Current Inspection:

The primary focus of the EC inspections was to identify cracks emanating from fastener holes. Three techniques were used depending on the specific configuration of the fastener hole: 1) Vacant rivet holes (countersink and outer skin) were inspected with a NDT Products Engineering Type CSM100-12, 3/16 inch diameter countersink probe operated at 200 Khz, 2) Vacant fastener holes (all layers) were inspected with a GK Engineering Type 1 HC-3/16-12, 3/16 inch diameter bolt hole probe operated at 300 KHz, and 3) Rivet locations, containing in-place rivets, were inspected with a ZETEC Inc., Type LTW1004-2, sliding probe operated at 30 KHz.

The EC inspections revealed a total of 49 defects categorized as follows:

Type A - Cracks in the outer skin, originated at the counter bore, and radiate away from the rivet hole. In no instance were these cracks found to extend to the outer surface. The EC technique listed above was used to identify these cracks. Of the 42 Type A cracks, 20 were identified using RT and visual inspections.

Type B - Cracks identified using EC technique #2 were found to be located in the inner skin and emanating from the vacant rivet hole. Four Type B cracks were found. (Note: The type B crack in bay 4 was a "false call".

Type C - Cracks similar to Type B cracks were observed in the third layer or tear strap layer. Four Type C cracks were found.

Type D - Holes containing rivets exhibited slightly different reactions to ET sliding probe technique #3. Despite attempts to correlate the cause of this anomalous reaction with visual and RT inspections, the exact nature of the difference is unknown. Four rivets exhibited this reaction.

A summary of all EC results is shown in Table 4-2 and Figures 4.1, 4.2, 4.3, and 4.4. Each EC flaw listed in Table 4-2 is identified by bay number, row number, rivet number, and type of flaw (A, B, or C).

Table 4-2 Eddy Current Inspection Results

Bay #	Row #	Rivet #	Type
1	L	3AFT	B
1	L	5AFT	B
1	L	6AFT	B
1	I	5FWD	A
1	I	6AFT	A
1	I	6FWD	A
1	I	8AFT	A
1	I	9FWD	A
2/3	T.S.	10FWD	C
2/3	T.S.	12AFT	C
3	J	1	D
3	J	1FWD	A
3	J	2AFT	A
3	J	3AFT	A
3	J	3FWD	A
3	J	4FWD	A
3	J	4AFT	A
3	J	5AFT	A
3	J	5FWD	A
3	J	6FWD	A
3	J	7AFT	A
3	J	7FWD	A
3	J	8AFT	A
3	J	9AFT	A
3	J	9FWD	A
3	J	10AFT	A
3	J	10FWD	A
3	J	11FWD	A
3	J	13AFT	A
3	J	13FWD	A
3/4	T.S.	19AFT	C
4	J	1AFT	A
4	J	1FWD	A
4	J	2AFT	A
4	J	2FWD	A
4	J	4AFT	A
4	J	4FWD	A
4	J	6AFT	A
4	J	10FWD	A
4	I	11AFT	B
4	J	12AFT	A
4	J	12FWD	A
4	J	13AFT	A
4	J	13FWD	A
4	J	14FWD	A
4/5	T.S.	8AFT	B
4/5	T.S.	1	D
5	J	2AFT	A
5	J	2FWD	A
5	J	3AFT	A
5	J	6AFT	A
5/6 T.S.	L	1	D
5/6 T.S.	E	4	D

4.2 Radiographic Inspection Results:

The X-ray radiographic inspection parameters are summarized in Table 4-3.

Table 4-3 RT Parameters

X-ray source energy	75 KVP
X-ray source current	7 mamp
Exposure time	60 seconds
Source-to-film distance	90 inches
Film type	Eastman Kodak M2
Focal spot size	3.5 mm × 3.5 mm

The resulting radiographic images were interpreted using up to 8X magnification. In addition to the cracks previously identified by *in situ* examinations performed during and immediately after the fuselage test article pressure test, the RT examinations identified 22 locations containing small cracks. Information regarding the 22 additional cracks are summarized in Table 4-4. Listed are bay and rivet hole location, crack length, and whether the flaw was detected by visual inspection. All outer skin cracks, cracks numbered 2 through 22 in Table 4-4, originated at the countersink inboard edge and were, with four exceptions, visibly verified on the rivet hole interior surface. None of these cracks were observed on the skin exterior surface. Figures 4.5, 4.6, and 4.7 describe the location of the cracks listed in Table 4-4.

4.3 Ultrasonic Inspection Results:

The sealant in the lap splice and the bond in the tear strap joints were inspected from the exterior surface using the ultrasonic inspection technique using a NDT Instruments Bondascope 2100, an L1 probe at 164.6 Khz transducer, and Sonotech Soundclear normal viscosity acoustic couplant under a specific acoustic impedance mode of operation. The UT technique was used to detect regions along the inner surface of the joints that were not completely sealed or bonded. A map of the UT inspection results summarized in Figures 4.8, 4.9, 4.10, and 4.11 reveal that extensive regions in the lap splice joint were not completely sealed (shaded regions) and only small islands were sealed. All tear strap regions were found to be well bonded with the exception of the lower ends of the upper straps, immediately adjacent to the lap. These ends were found to be partially unbonded.

4.4 Summary:

A summary of bay 3 and bay 4 NDE results are compared with destructive examination data in Tables 4-5 and 4-6, respectively. Destructive, visual, EC (within hole technique) and RT examinations were performed at all rivet locations in bays 3 and 4. Listed in tables 4-5 and 4-6 are destructive examination results for only those rivet locations where NDI found indications of cracking. These data reveal that NDI detected cracking only in the upper rivet rows[4] . The destructive examination crack length data were measured from the hole inside diameter (shank region) to the crack tip. Table 4-5 shows that six visible cracks were detected by visual examinations showing that most upper rivet row fatigue cracks propagated below the outer surface a substantial distance before becoming through-thickness cracks. Refer to section 9.0 for bay 3 destructive examination results. A comparison of open hole EC examinations with destructive examination data shows that within hole EC examination reliably detected subsurface upper rivet hole cracking. It should be noted that little success was achieved using standard surface EC techniques. EC examinations were conducted with rivet heads placed into the open holes having known cracks revealing that

[4] Surface EC inspection did indicate cracking at one second row location, 11- AFT, in bay 4. Destructive examination of that rivet hole revealed no cracking. The EC result was therefore deemed a "false call".

Table 4-4 Radiographic Inspection Results.

Bay #	Row #	Rivet #	Crack Length mm (in.) RT/Destructive	Comments
2	J	Tear Strap	3.175(.125)/1.19(.047)*	Inner Skin, Visible
3	J	2	2.286(.090)/2.300(.091)	Outer Skin, Not Vis.
3	J	3	1.524(.060)/1.625(.064)	Outer Skin, Visible
3	J	10	2.540(.100)/0.307(.012)	Outer Skin, Visible
3	J	10	2.540(.100)/0.905(.012)	Outer Skin, Visible
3	J	11	3.175(.125)/4.16(.164)*	Outer Skin, Visible
3	J	13	2.540(.100)/2.500(.098)	Outer Skin, Visible
3	J	13	2.540(.100)/2.030(.080)	Outer Skin, Visible
3	J	14	3.175(.125)/FC	Outer Skin, Not Vis.
3	J	14	2.540(.100)/FC	Outer Skin, Not Vis.
4	J	1	3.175(.125)/0.769(.030)	Outer Skin, Visible
4	J	1	3.175(.125)/2.893(.114)	Outer Skin, Not Vis.
4	J	2	2.286(.090)/2.814(.111)	Outer Skin, Visible
4	J	2	2.286(.090)/0.905(.036)	Outer Skin, Visible
4	J	3	3.175(.125)/2.427(.096)	Outer Skin, Visible
4	J	4	2.286(.090)/2.700(.106)	Outer Skin, Visible
4	J	4	3.175(.125)/2.497(.098)	Outer Skin, Visible
4	J	12	3.175(.125)/2.460(.097)	Outer Skin, Visible
4	J	12	3.175(.125)/1.874(.074)	Outer Skin, Visible
4	J	13	1.524(.060)/1.102(.043)	Outer Skin, Visible
4	J	13	1.524(.060)/1.835(.072)	Outer Skin, Visible
4	J	14	1.524(.060)/2.810(.111)	Outer Skin, Visible

* - The actual crack orientation was opposite to that detected by radiography.
ND - No crack was observed during destructive examination.
FC - False Call: No crack was found by destructive examination.

subsurface cracking could not be detected using standard EC inspection techniques. Comparison of X-ray radiography results with destructive examination results shows that RT exhibits limited crack detection capability. From a total of nineteen locations containing non-visible cracks, only six were detected by RT.

The comparisons of bay 4 destructive examination and NDE results shown in Table 4-6 are similar to that observed for bay 3 (Table 4-5). In bay 4, EC (within hole) examinations detected all nonvisible fatigue cracks. RT examinations also detected all nonvisible fatigue cracks. Here, the upper rivet row fatigue cracks contained in bay 4 are longer compared than those observed in bay 3. A comparison of RT results for bay 3 and 4 suggest that fatigue cracks less than 0.25 mm (0.1 inch) were not reliably detected by RT.

Table 4-5 A Comparison of NDE and Destructive Examination Results for Bay #3

Top Row Location	Destructive Exam. Results Length mm (in.)	NDE Visual in situ	NDE EC Open Hole	NDE RT
1-AFT	4.724(0.186)	X	*	*
1-FWD	2.540(0.100)	NI	X	NI
2-AFT	2. 311(0.091)	NI	X	X
2-FWD	4.216(0.166)	X	*	*
3-AFT	1.626(0.064)	NI	X	X
3-FWD	1.067(0.042)	NI	X	NI
4-AFT	1.829 (0.072)	NI	X	NI
4-FWD	2.337 (0.092)	NI	X	NI
5-FWD	1.727 (0.068)	NI	X	NI
6-FWD	0.660(0.026)	NI	X	NI
7-AFT	1.422(0.056)	NI	X	NI
7-FWD	2.489(0.098)	NI	X	NI
8-AFT	0.737 (0.029)	NI	X	NI
9-AFT	1.727(0.068)	NI	X	NI
9-FWD	1.118(0.044)	NI	X	NI
10-AFT	0.914(0.036)	NI	X	X
10-FWD	0.305(0.012)	NI	X	X
11-FWD	4.166(0.164)	NI	X	NI
12-AFT	3.226(0.127)	X	*	*
12-FWD	4.877(0.192)	X	*	*
13-AFT	2.032(0.080)	NI	X	X
13-FWD	2.489(0.098)	NI	X	X
14-AFT	No Cracks	NI	NI	X
14-AFT	No Cracks	NI	NI	X
15-AFT	3.048(0.120)	X	*	*
15-FWD	2.921(0.115)	X	*	*

X - Flaw observed

* - EC and RT testing were not conducted on rivet holes containing visible cracks.

NI - No indication of flaw.

Table 4-6 A Comparison of NDE and Destructive Examination Results for Bay #4

Top Row Location	Destructive Exam. Results Length mm (in.)	NDE Visual in situ	NDE EC Open Hole	NDE RT
1-AFT	2.893(0.114)	No Indication(NI)	X	X
1-FWD	0.769(0.030)	NI	X	X
2-AFT	0.905(0.036)	NI	X	X
2-FWD	2.814(0.111)	NI	X	X
3-FWD	2.427(0.096)	NI	X	X
4-AFT	2.497 (0.098)	NI	X	X
4-FWD	2.700 (0.106)	NI	X	X
5-AFT	5.334(0.210)	X	NI	NI
5-FWD	5.279 (0.207)	X	*	*
6-AFT	2.714(0.107)	NI	X	*
6-FWD	3.848(0.152)	X	*	NI
7-AFT	1.113(0.044)	NI	NI	NI
7-FWD	3.310(0.130)	X	*	*
8-AFT	Link-up/9-FWD	X	*	*
8-FWD	12.954(0.510)	X	*	*
9-AFT	8.265(0.325)	X	*	*
9-FWD	Link-up/8-AFT	X	*	*
10-AFT	4.194(0.165)	X	*	*
10-FWD	3.042(0.120)	NI	X	NI
11-AFT	5.397(0.212)	X	*	*
11-FWD	5.675(0.223)	X	*	*
12-AFT	1.874(0.074)	NI	X	X
12-FWD	2.460(0.097)	NI	X	X
13-AFT	1.835(0.072)	NI	X	X
13-FWD	1.102(0.043)	NI	X	X
14-AFT	2.995(0.118)	X	*	*
14-FWD	2.810(0.111)	NI	X	X
15-AFT	8.559(0.337)	X	*	*
15-FWD	6.959(0.274)	X	*	*
**11-AFT	No Crack	NI	X (filled hole)	NI

X - Flaw observed.

NI - No indication of flaw.

* - EC and RT testing were not conducted on rivet holes containing visible cracks.

** - This is a second row rivet hole location. No crack was found by destructive examination. EC examination was performed by the surface technique.

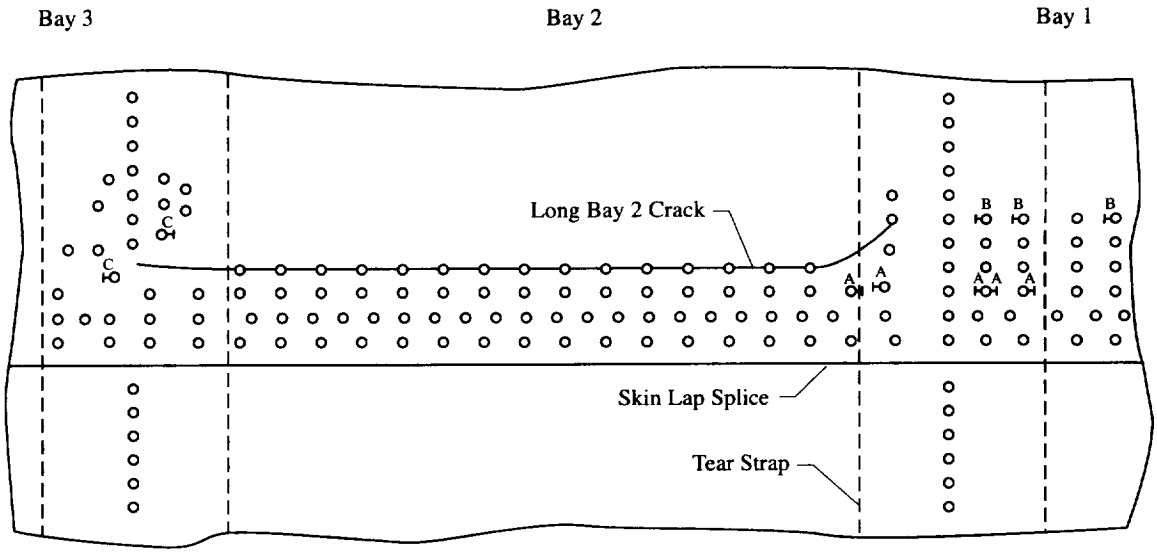

Figure 4.1 The schematic shows the location of possible cracks as detected by the eddy current inspection for the bay 2/3 T.S., bay 2 and the bay 1 T.S. regions. Dashed lines mark the tear strap regions. The long bay 2 crack (solid line) is shown in the upper rivet row of bay 2.

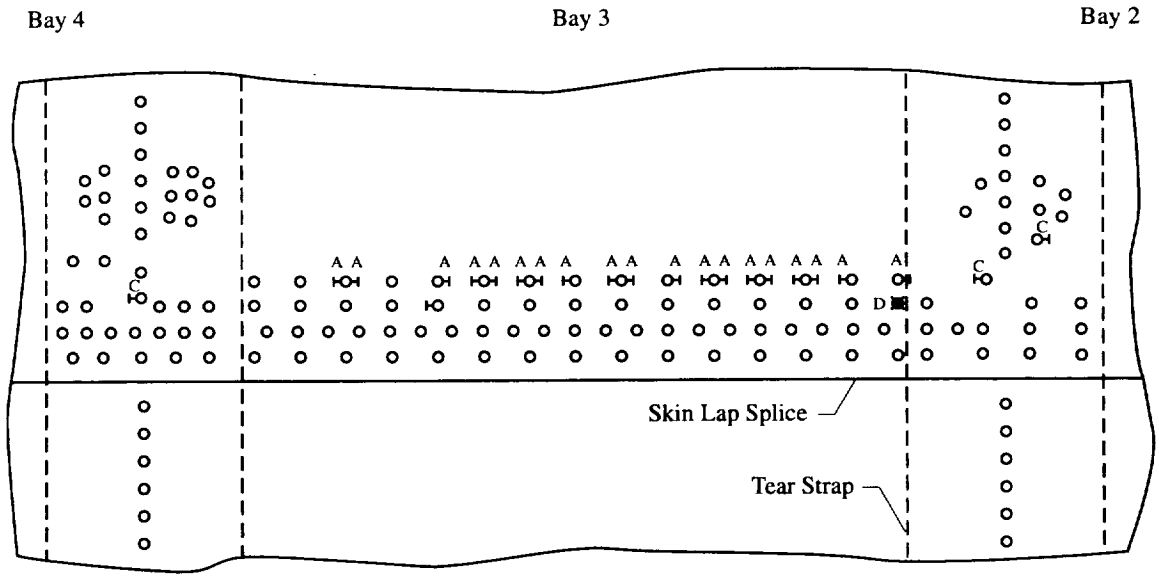

Figure 4.2 The schematic shows the location of possible cracks as detected by the eddy current inspection for the bay 3/4 T.S., bay 3 and the bay 2/3 T.S. regions. Dashed lines mark the tear strap regions.

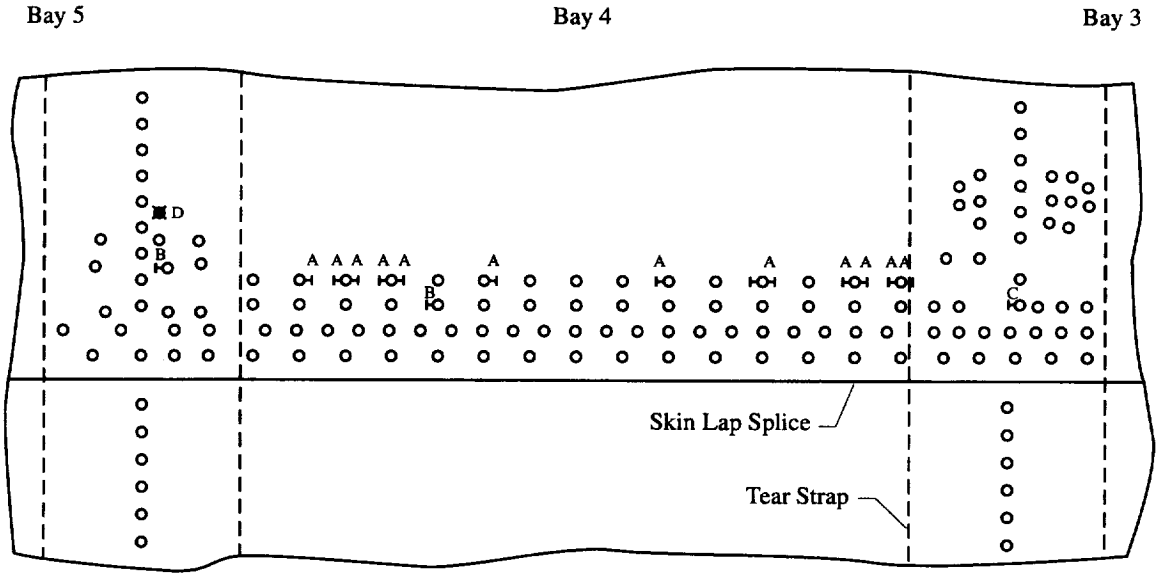

Figure 4.3 The schematic shows the location of possible cracks as detected by the eddy current inspection for the bay 4/5 T.S., bay 4 and the bay 3/4 T.S. regions. Dashed lines mark the tear strap regions. NDE was not performed on visible fatigue cracks.

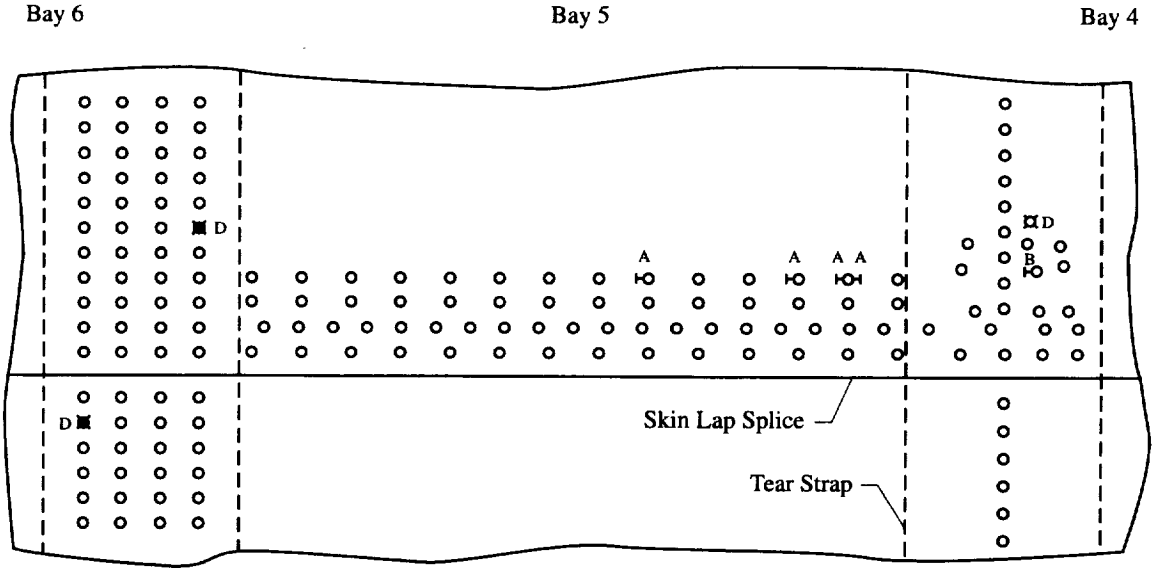

Figure 4.4 The schematic shows the location of possible cracks as detected by the eddy current inspection for the bay 6 T.S., bay 5 and the bay 4/5 T.S. regions. Dashed lines mark the tear strap regions.

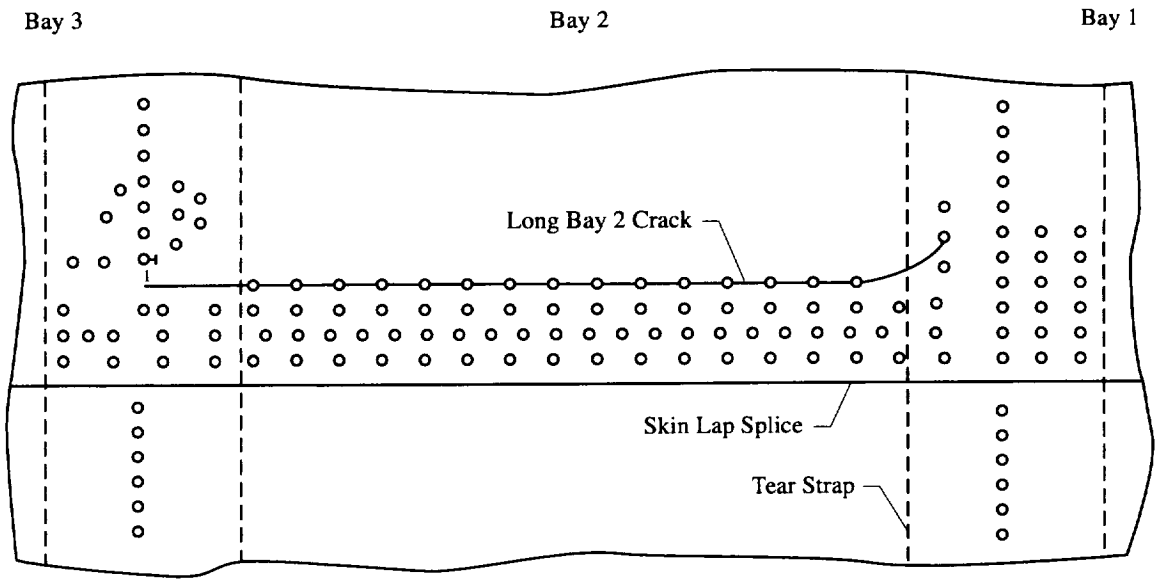

Figure 4.5 The schematic shows the location of possible cracks as detected by the X-ray inspection for the bay 2/3 T.S., bay 2 and the bay 1 T.S. regions. Crack indication #1 was found in the bay 2/3 T.S. The long bay 2 crack (solid line) is shown in the upper row of bay 2. Dashed lines mark the tear strap regions.

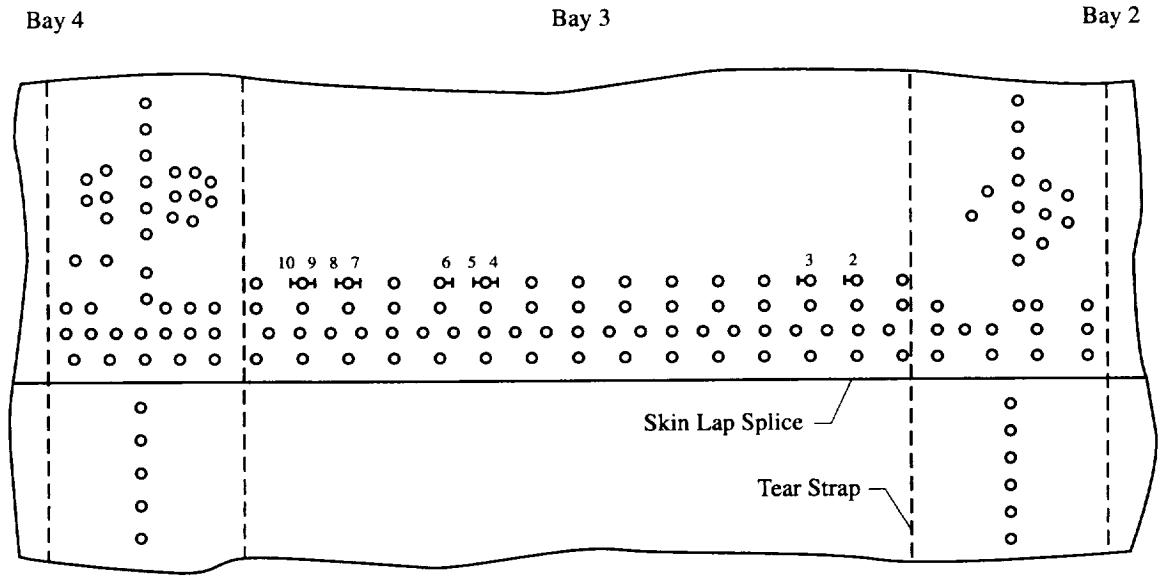

Figure 4.6 The schematic shows the location of possible cracks as detected by the X-ray inspection for the bay 3/4 T.S., bay 3 and the bay 2/3 T.S. regions. Cracks indications #4–10 were found in the upper rivet row of bay 3. Dashed lines mark the tear strap regions.

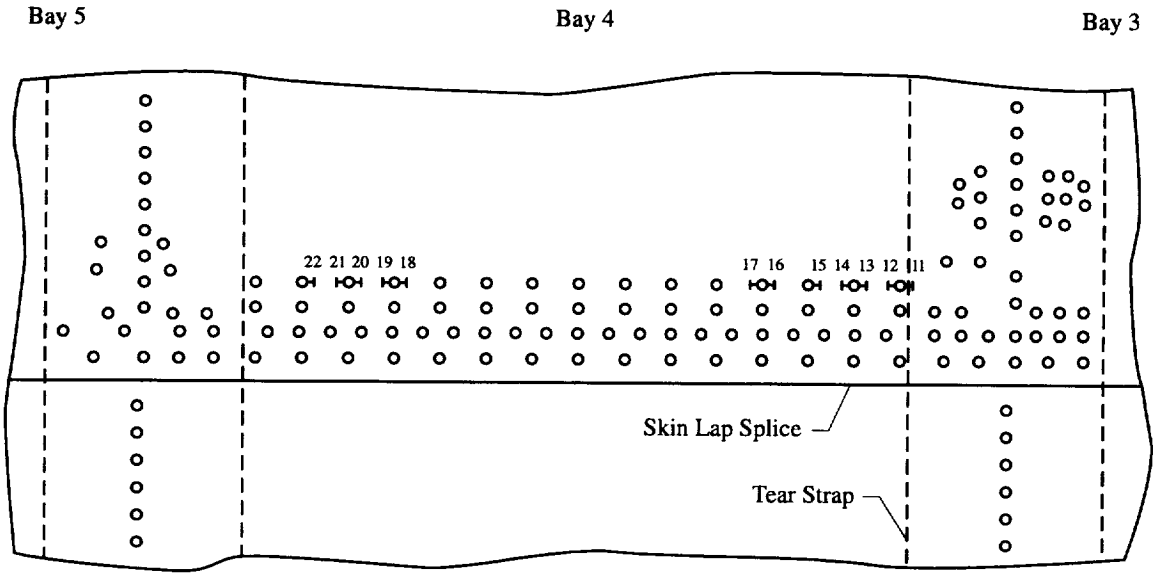

Figure 4.7 The schematic shows the location of possible cracks as detected by the X-ray inspection for the bay 4/5 T.S., bay 4 and the bay 3/4 T.S. regions. Crack indications #11–22 were found in the upper rivet row of bay 4. Dashed lines mark the tear strap regions.

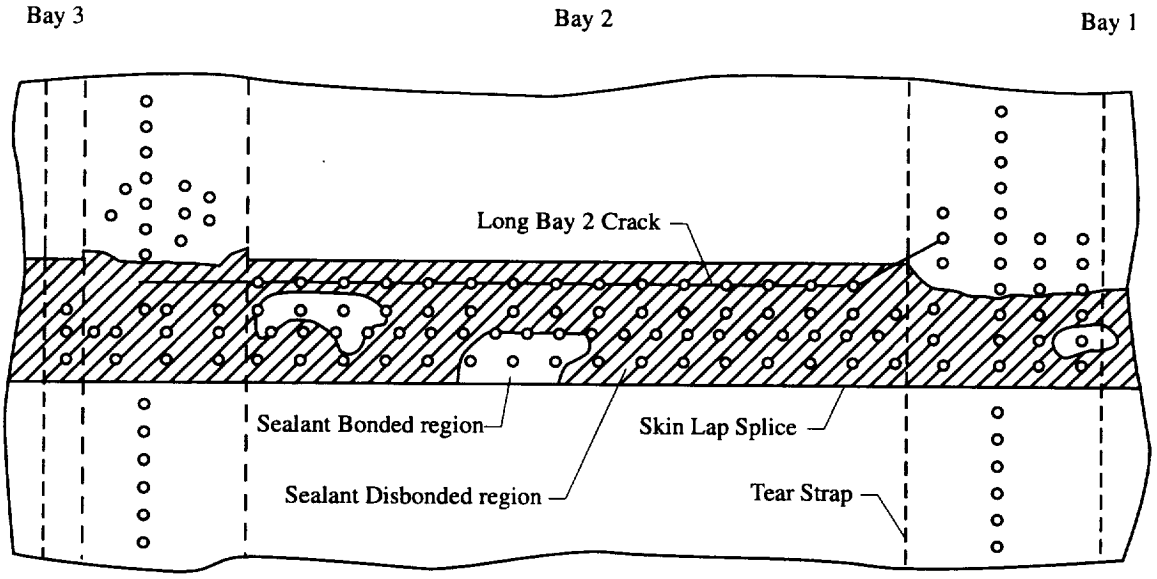

Figure 4.8 The schematic shows the result of the ultrasonic disbond detection technique for bay 2/3 T.S., bay 2 and the bay 1 T.S. lap splice joint region. The shaded regions represent the area that is no longer sealed between the inner and outer skin. Dashed lines mark the tear strap regions. Some minor disbonding occurred in the tear strap region in the upper portion of the lap splice joints. A solid line along the upper rivet row depicts the long outer skin crack in bay 2.

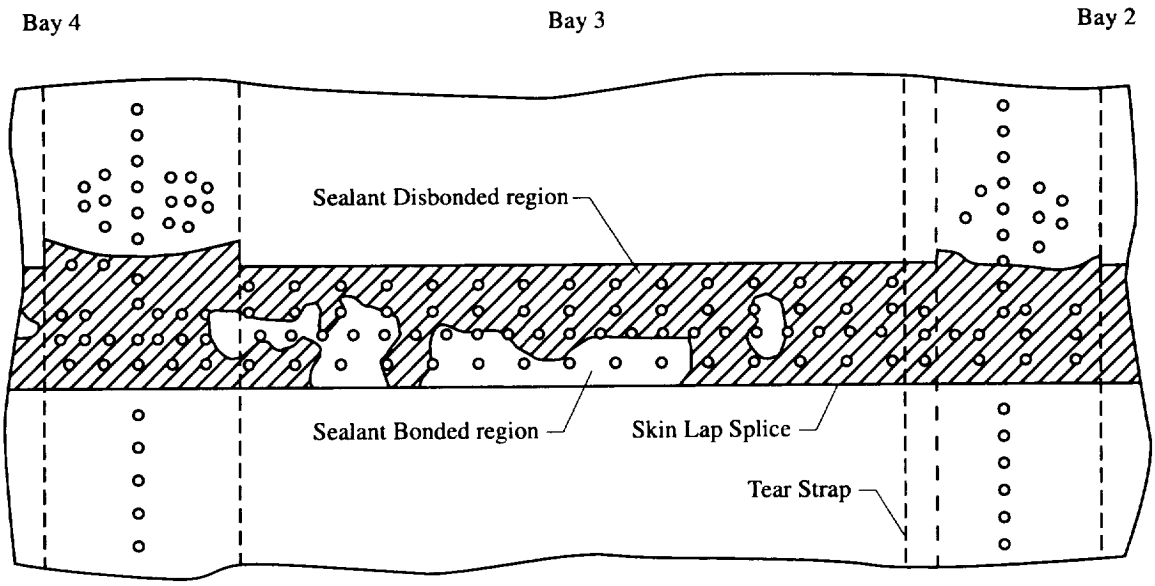

Figure 4.9 The schematic shows the results of the ultrasonic disbond detection technique for bay 3/4 T.S., bay 3 and the bay 2/3 T.S. lap splice joint region. The shaded regions represent the area that is no longer sealed between the inner and outer skin. Dashed lines mark the tear strap regions. Some minor disbonding occurred in the tear strap region in the upper portion of the lap splice joints.

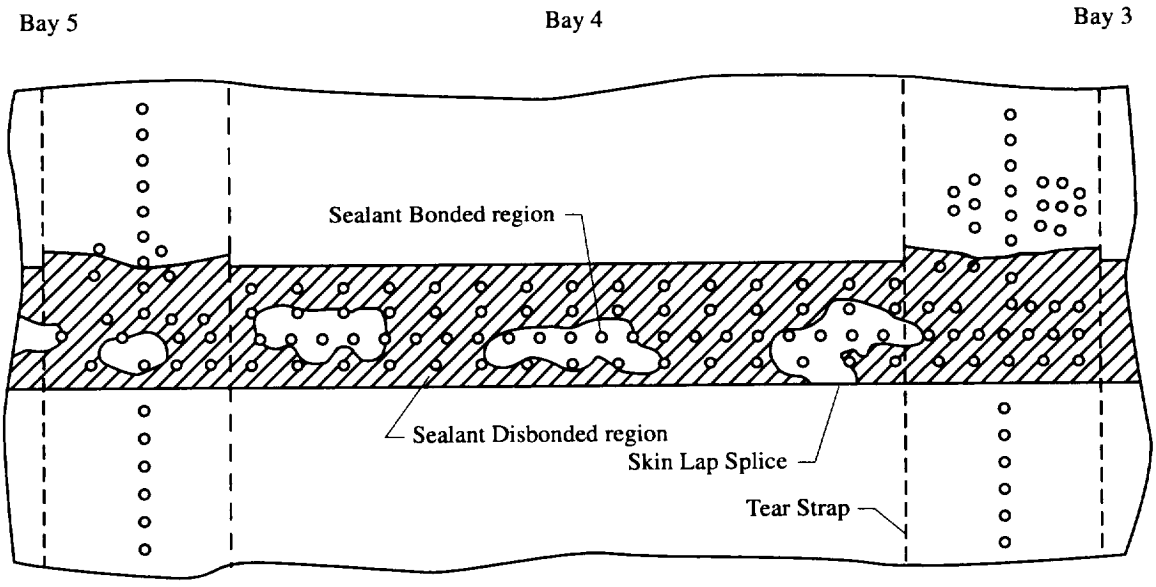

Figure 4.10 The schematic shows the results of the ultrasonic disbond detection technique for bay 4/5 T.S., bay 4 and the bay 3/4 T.S. lap splice joint region. The shaded regions represent the area that is no longer sealed between the inner and outer skin. Dashed lines mark the tear strap regions.

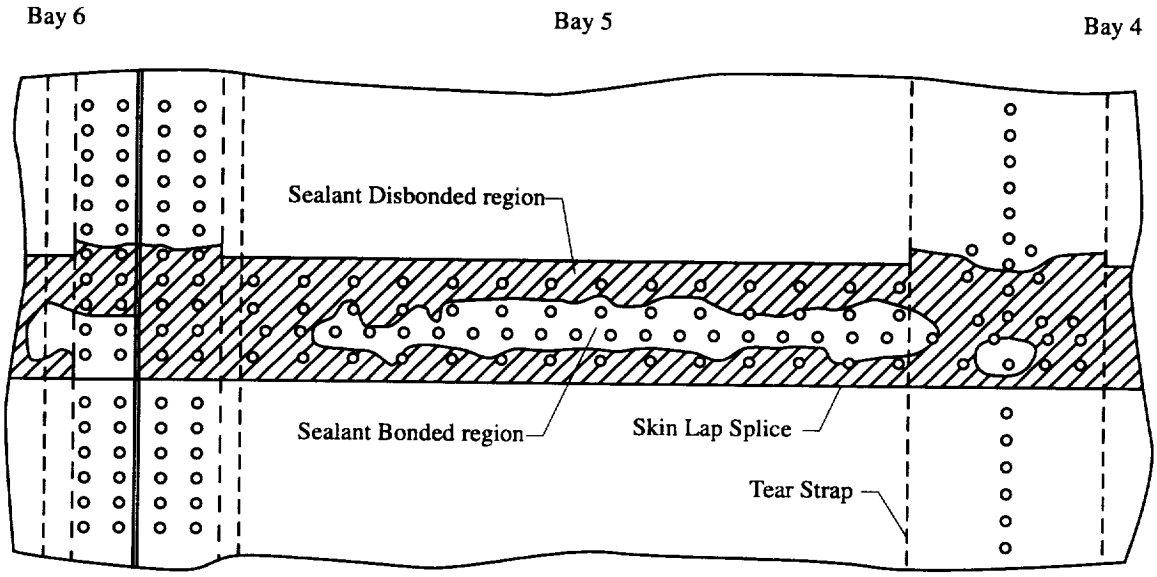

Figure 4.11 The schematic shows the results of the ultrasonic disbond detection technique for bay 5/6 T.S., bay 5 and the bay 4/5 T.S. lap splice joint region. The shaded regions represent the area that is no longer sealed between the inner and outer skin. Dashed lines mark the tear strap regions.

5. Destructive Examination Procedure

Detailed destructive examinations were conducted after all nondestructive examinations were completed. The primary focus of the destructive examination was to fully characterize all cracks in the lap splice joint contained in bays 1, 2, 3, 4, and adjoining tear strap regions. The following is a description of the panel teardown procedures. Using these procedures, a detailed destructive examination was performed resulting in a complete catalog of fatigue cracking in the fuselage lap splice. The results of the destructive examinations are detailed in Sections 6.0 through 11.0.

5.1. Procedure:

Destructive examination procedures were developed for the careful dismantling of the six bay lap splice joint panel. After considering a number of elaborate cutting methods, the band saw was found to be the most appropriate tool for dismantling the panel without contaminating fracture surfaces or excessively bending sections of the panel. To eliminate panel bending during the cutting operation, the panel was braced at critical points along the length of the lap splice. Slow cutting speeds were used during the band saw operations to limit local bending and vibration. Each bay was first separated from the panel by a single cut, typically, a single cut was made adjacent and parallel to the tear strap region and along the tear strap/bay interface. The bay was further sectioned into smaller and more manageable configurations. Great care was taken to cut each rivet location from the bay. To insure specimen traceability, each rivet location was marked for identification and orientation prior to removal.

Figure 5.1 depicts the procedure for rivet hole specimen preparation. The band saw operation was used to cut out each rivet hole location which resulted in a square piece similar to that shown in Figure 5.1a. Each specimen was sectioned precisely, Figure 5.1b, using a slow speed diamond saw. To prevent cutting into the region that most likely contained fatigue cracks, all rivet holes were sectioned normal to the horizontal aft (A) / forward (B) orientation. Each specimen half was marked to identify it by bay number, row, rivet number and orientation. For example, 3J12B is the specimen from bay 3, row J (upper rivet row), rivet hole 12, forward orientation. The rivet specimens were carefully strained open, as shown in Figures 5.1c, 5.1d, and 5.1e, using a three point bend fixture. This operation allowed careful removal of the sectioned rivet head without disturbing the inside surface of the hole. Once the rivet head was removed, the bending process was performed incrementally. After each strain increment, the inside surface of the hole was examined for incipient fatigue cracks using optical and scanning electron microscopy (SEM). Once the specimen was completely separated into two pieces, each fracture surface (identified by hole number, aft-top and bottom, forward-top and bottom) was examined optically and by SEM. All layers of structure were examined. For example, in the lap splice region, the outer and inner skin were examined. In the tear strap region, the four or five layers of structure were examined for cracks. Each fatigue fracture surface was examined for the following attributes.

1. Crack initiation site - The initiation site was related to either high K_T regions (corners, burrs, surface discontinuities, etc.) or faying surface damage (fretting).
2. Evidence of fatigue marker bands - During full scale fuselage pressurization, underload pressure cycles were used to mark the fatigue fracture surface. A coded sequence of reduced pressure cycles was used to register the cycle number after every 10,000 pressurizations. Crack growth during the reduced pressurization cycles resulted in a marked change in fracture surface morphology that was observed using optical microscopy at 400X to 600X. By noting each marker band the fatigue crack length (a) versus load cycle (N) history can be developed.
3. Crack front shape versus crack length - The crack front shape of each fatigue crack is charted as a function of crack length.
4. Fatigue crack/stable tearing transition crack length - The transition from fatigue crack growth to stable tearing corresponds to a change in fracture morphology from transgranular cracking to a dominance of ductile fracture, respectively.

5. slant fracture morphology - Flat to slant fracture occurs at a characteristic level of ΔK. This observation can be used to approximation the level of ΔK for fatigue crack growth.

6. evidence of corrosion - All evidence of corrosion (pitting, intergranular cracking, etc.) and corrosion products are noted.

Scanning electron microscopy was performed to document the degree of fatigue cracking within the lap splice joint. Photomicrographs of all fatigue crack are shown detailing fracture morphology and the location of crack initiation. Fractography was normally performed without cleaning the fracture surface; when oxide debris obscured the fracture surface, the fracture surface was cleaned ultrasonically in acetone. To enhance SEM resolution and reduce charging due to oxide debris, some fracture surfaces were gold sputtered. After all SEM studies were completed, surfaces were further cleaned prior to marker band determinations.

5.2 Fatigue Cracking - Detailed Description

Sections 6.0 through 11.0 present a detailed description of all fatigue cracks (location and fracture morphology) observed in bays 1, 2, 3, and 4 and associated tear strap regions. Each section is organized in a similar manner.

1. A series of schematic drawings are presented showing the regions of interest. The first schematic summarizes all information, i.e., exact rivet hole location, the location of the rivet holes examined (filled hole), the location of all fatigue cracks observed during the destructive examination, the location of substructure and the rivet row identification (L,K,....G). A series of schematics show the location of fatigue cracks found in each structural layer, starting with the outer skin (first layer) and followed by the second and third layers.

2. Through-thickness schematics are given for each rivet row showing the location of fatigue crack initiation and crack shape. A tabular summary is also presented listing the location, length, type and initiation site of all fatigue cracks.

3. A detailed fractographic summary is presented for each fatigue crack. The fractographic summary includes detailed SEM micrographs and within hole locations of the fatigue crack. This complete characterization allows the reader to visualize the fatigue crack surface morphology and the exact location of each crack relative to structure.

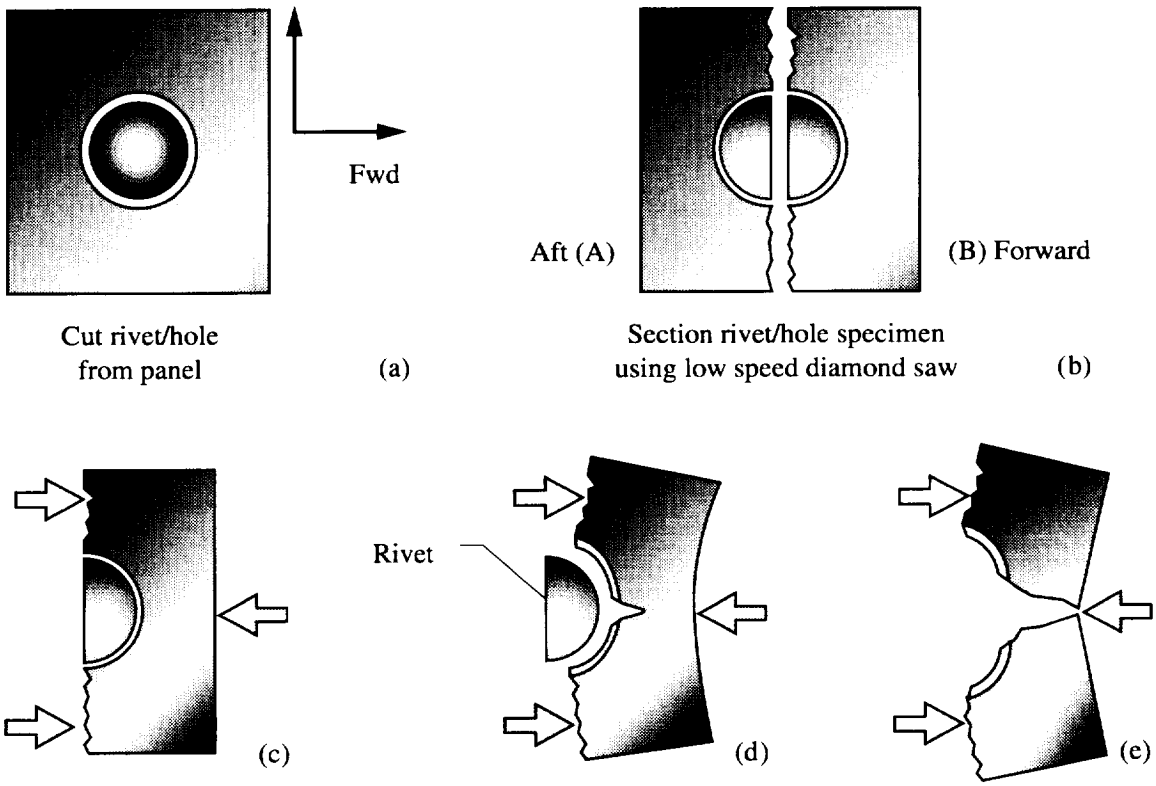

Figure 5.1 Schematic illustrating the rivet hole destructive examination procedure.

6. Destructive Examination of Bay #1 Tear Strap Region

A total of twenty-five rivet hole locations in the bay 1 tear strap region (identified by the filled hole symbols in Figure 6.1), were destructively examined. Seventeen fatigue cracks were found in eleven rivet holes located in rivet rows L, J, and I. Figures 6.2, 6.3 and 6.4 show the location of the fatigue cracks found in the first layer (outer skin), the second layer (upper tear strap) and third layer (lower tear strap), respectively. The through-thickness crack orientation is summarized for rivet rows L, J, and I in Figures 6.5, 6.6 and 6.7, respectively. The following is a description of the fatigue damage in the bay 1 tear strap region for rivet rows I, J, and L.

6.1 Fatigue Cracks Contained in Row I:

Figures 6.8 through 6.12 describe the fatigue crack morphology in row I.

6.2 Fatigue Cracks Contained in Row L:

Figures 6.13 through 6.19 describe the fatigue crack morphology in row L.

6.3 Fatigue Cracks Contained in Row J:

Figures 6.20 through 6.23 describe the fatigue crack morphology in row J.

6.4 Bay #1 Summary

Table 6-1 summarizes the bay 1 tear strap region fatigue crack data for rivet rows L, J, and I. The range of fatigue crack lengths summarized in Table 6-1 were determined based on fractography and show that cracks ranged from 0.060 mm (0.002 inch) to 1.03 mm (0.041 inch) in length. A review of the fractographic data for bay 1 shows that the fatigue cracks initiated at high stress concentration (high K_T) regions. The crack initiation data (small arrows) in Figures 6.5, 6.6, and 6.7 reveal that most fatigue cracks initiated at either the corner of the rivet hole (examples are shown in Figures 6.9.c and 6.11.c) or within a rough surface region (examples are shown in Figures 6.14.d and 6.20.d) within the rivet hole inside diameter. The following observations were made as a result of fractographic examinations of bay 1.

6.4.1 ***Crack initiation site(s):*** Row L: Fatigue cracking was contained in the upper tear strap. Crack initiation occurred within the rivet hole surface or at a hole corner burr.

Row J: Fatigue cracking was contained to the upper and lower tear strap. Crack initiation occurred within the rivet hole surface or at the hole corner.

Row I: Fatigue cracking was limited to the outer skin. Crack initiation occurred at the rivet hole shank region.

6.4.2 ***Crack front shape as a function of crack length:*** Bay 1 contained only small cracks and no crack front shape correlations were made.

6.4.3 ***Fatigue crack/stable tearing transition crack length:*** No evidence of stable tearing was observed.

6.4.4 ***Slant fracture morphology:*** No slant fracture morphology was observed.

6.4.5 ***Evidence of corrosion:*** No evidence of corrosion was observed.

Table 6-1 Bay #1 Fatigue Crack Summary

Rivet Row	No. of Cracks (Holes)	Location	Crack Length mm (in.)	Comment
L	7 (5)	Upper Tear Strap	$0.060(0.002) \leq a \leq 0.650(0.026)$	High K_T
J	4 (2)	Lower Tear Strap	$0.210(0.008) \leq a \leq 0.425(0.017)$	High K_T
I	5 (4)	Outer Skin	$0.150(0.006) \leq a \leq 1.03(0.041)$	High K_T

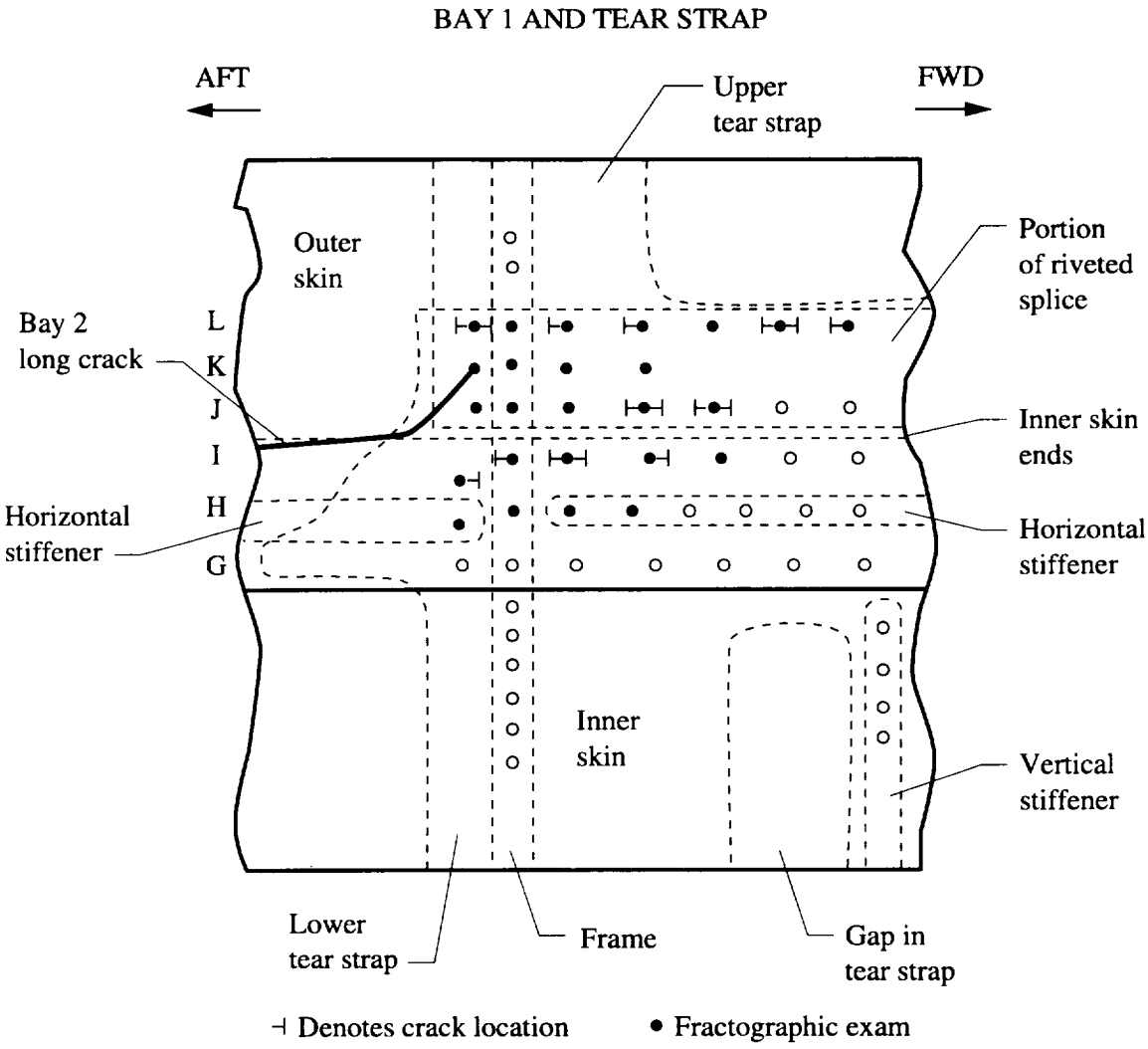

Figure 6.1 The schematic shows the location of all fatigue cracks found in the bay 1 tear strap and lap splice joint regions by destructive examination. Fractographic examinations were performed on the hole locations marked by the solid circles. Note the dark solid line that marks the location of the long crack extending from bay 2.

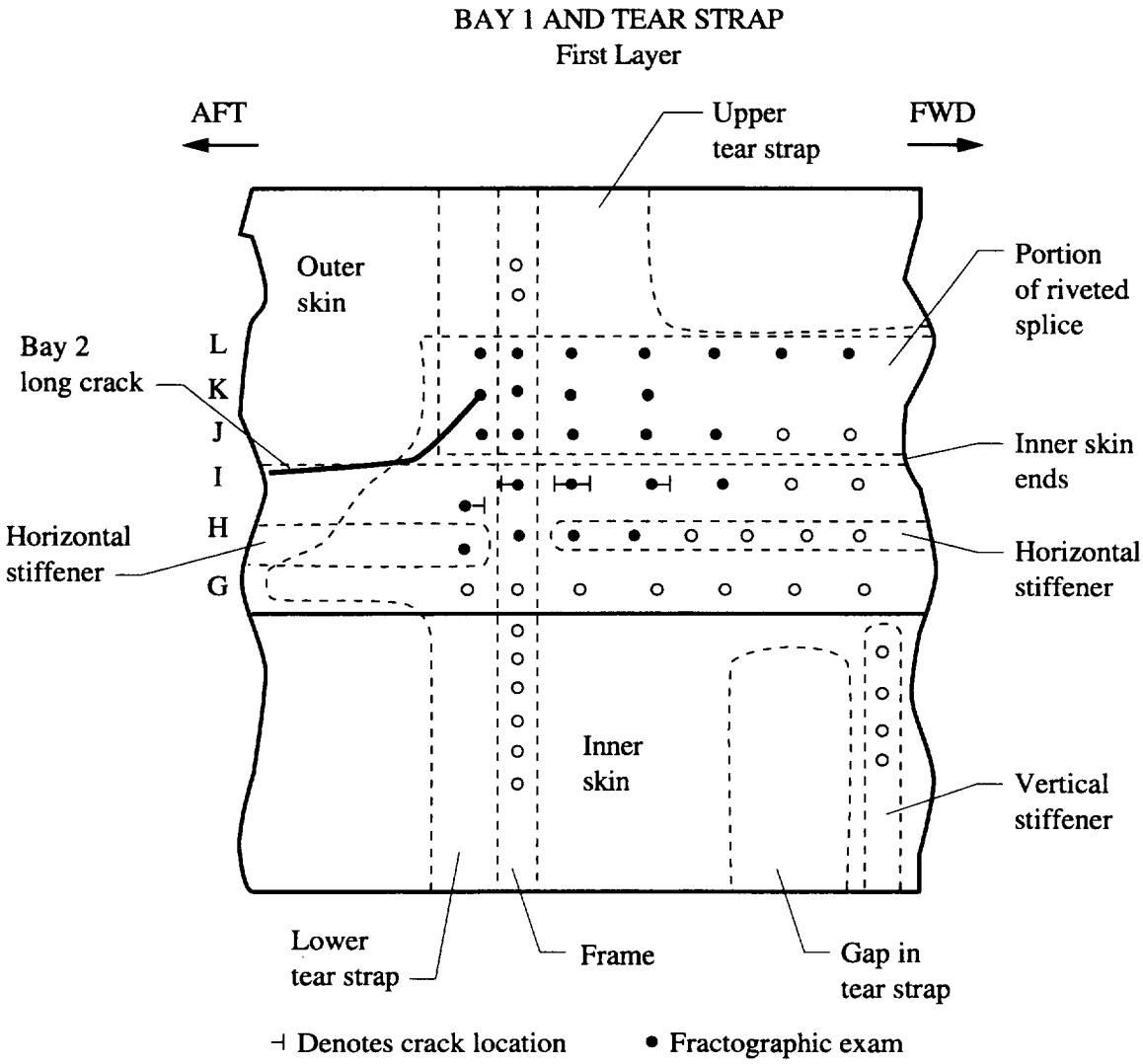

Figure 6.2 The schematic shows the location of fatigue cracks found in the first layer (outer skin) of the bay 1 tear strap and lap splice joint regions by destructive examination. One end of the long bay 2 fatigue crack (dark solid line) extended into this region.

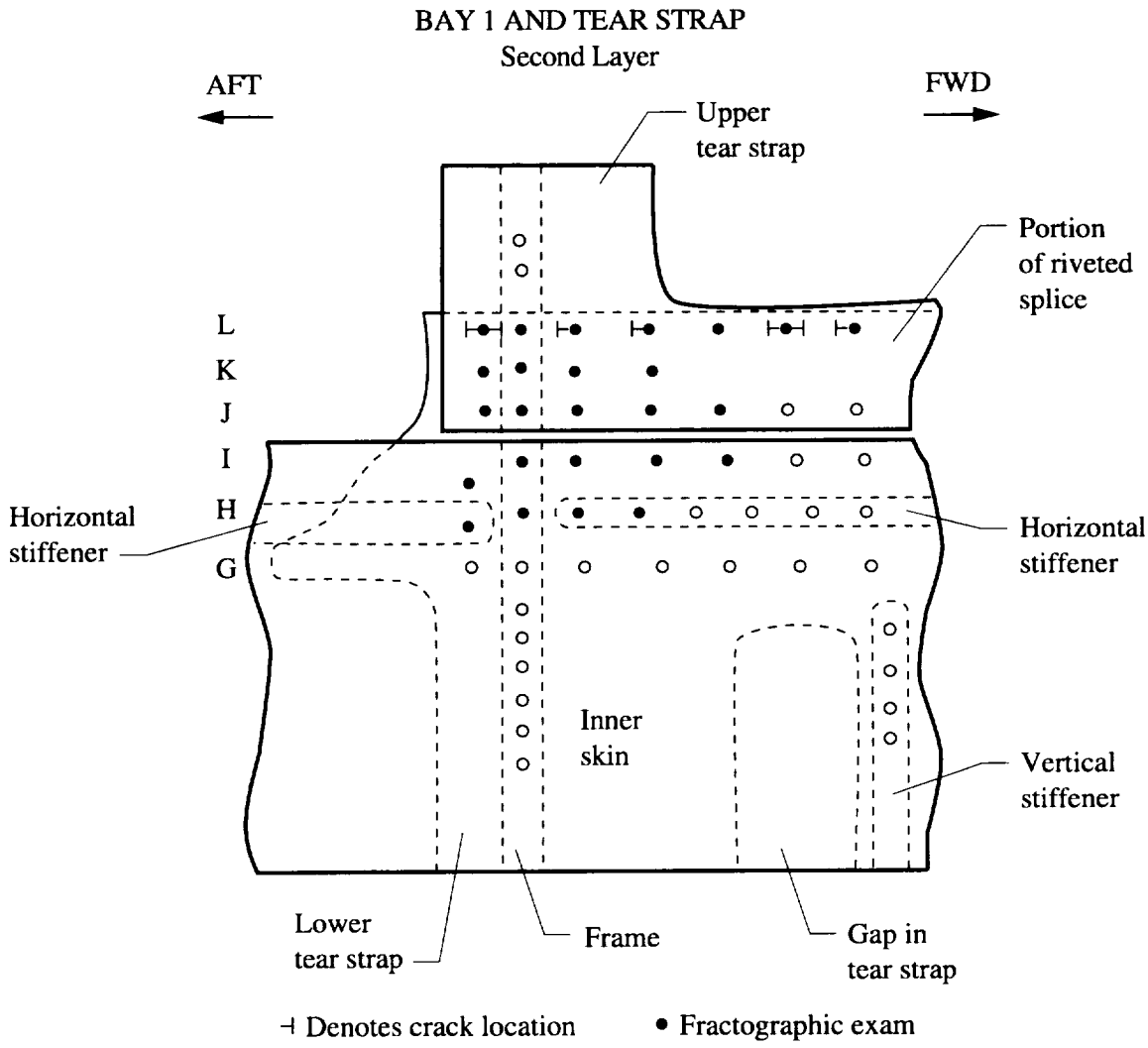

Figure 6.3 The schematic shows the location of fatigue cracks found in the second layer (upper tear strap and inner skin) of the bay 1 tear strap and lap splice joint regions by destructive examination.

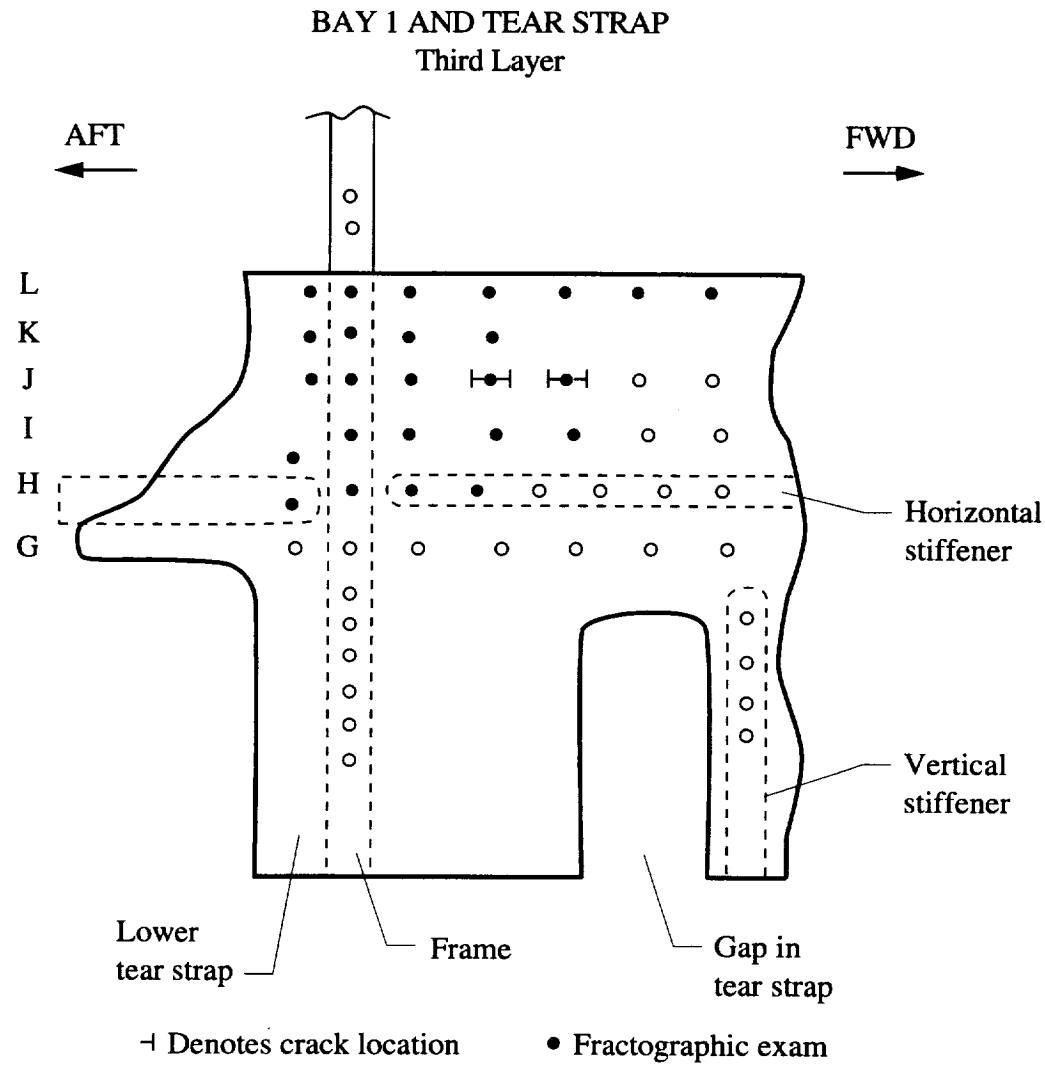

Figure 6.4 The schematic shows the location of fatigue cracks found in the third layer (lower tear strap) of the bay 1 tear strap and lap splice joint regions by destructive examination.

BAY 1 ROW L

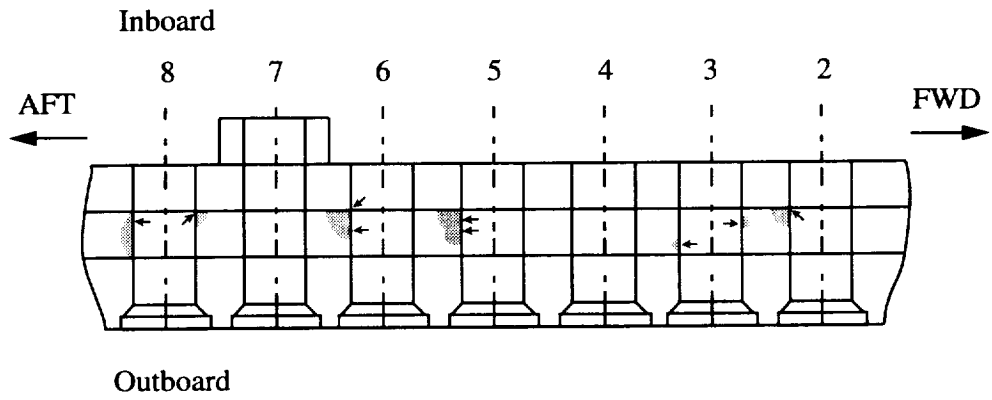

Hole #	Location	Length mm (in)	Type	Initiation site
2 (AFT)	U. tear strap	0.230 (0.009)	Corner	Inboard corner (I.C.)
3 (FWD)	U. tear strap	0.060 (0.002)	Multiple surface	Multiple center
3 (AFT)	U. tear strap	0.230 (0.009)	Multiple surface	Outboard side of center
5 (AFT)	U. tear strap	0.650 (0.026)	Multiple surface & corner	Surface and I.C.
6 (AFT)	U. tear strap	0.590 (0.023)	Multiple surface & corner	Multiple surface
8 (FWD)	U. tear strap	0.250 (0.010)	Corner	I.C.
8 (AFT)	U. tear strap	0.380 (0.015)	Corner	Inboard side of surface

Figure 6.5 The through thickness schematic shows the location and initiation site (small arrows) of fatigue cracks found in rivet row L from the bay 1 tear strap/lap splice joint region. The table summarizes crack location, crack length, crack type, and initiation site for each fatigue crack shown.

BAY 1 ROW J

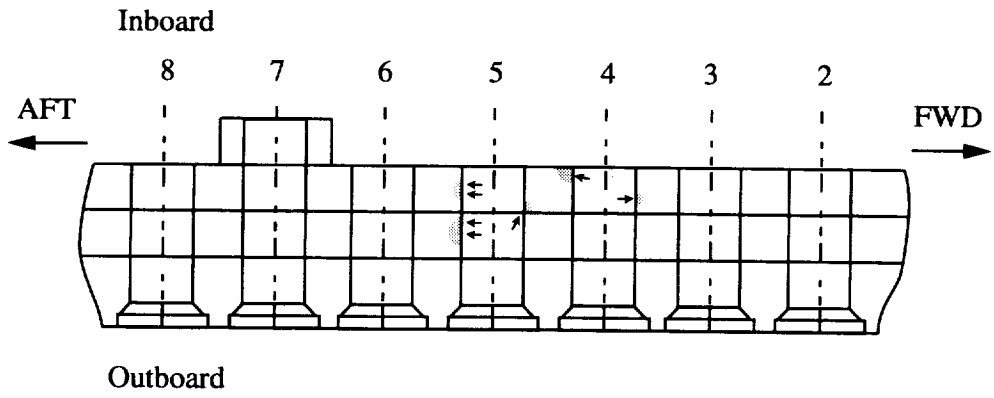

Hole #	Location	Length mm (in)	Type	Initiation site
4 (AFT)	L.tear strap	0.425 (0.017)	Corner	Inboard corner
4 (FWD)	L.tear strap	0.220 (0.009)	Multiple surface	Outboard side of center
5 (1AFT)	U.tear strap	0.210 (0.008)	Multiple surface	Multiple sites in center
5 (2AFT)	L.tear strap	0.100 (0.004)	Multiple surface	Multiple sites in center
5 (FWD)	L.tear strap	0.260 (0.010)	Multiple corner	Outboard corner

Figure 6.6 The through thickness schematic shows the location and initiation site (small arrows) of fatigue cracks found in rivet row J from the bay 1 tear strap/lap splice joint region. The table summarizes crack location, crack length, crack type, and initiation site for each fatigue crack shown.

BAY 1 ROW I

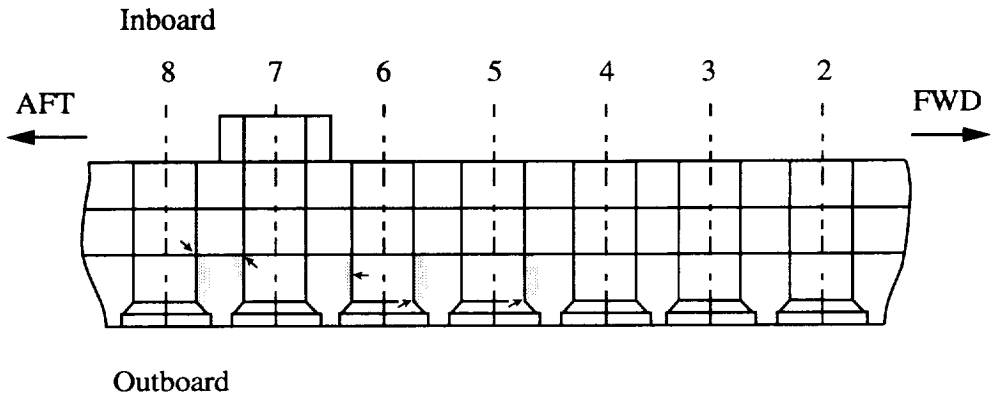

Hole #	Location	Length mm (in)	Type	Initiation site
5 (FWD)	Outer skin	0.420 (0.017)	Countersink	Outboard side of shank
6 (FWD)	Outer skin	1.160 (0.046)	Countersink	Outboard side of shank
6 (AFT)	Outer skin	0.200 (0.008)	Countersink	Center of shank
7 (AFT)	Outer skin	0.150 (0.006)	Countersink	Inboard side of shank
8 (FWD)	Outer skin	1.030 (0.041)	Countersink	Inboard side of shank

Figure 6.7 The through thickness row schematic shows the location and initiation site (small arrows) of fatigue cracks found in rivet row I from the bay 1 tear strap lap/splice joint region. The table summarizes crack location, crack length, crack type, and initiation site for each fatigue crack shown.

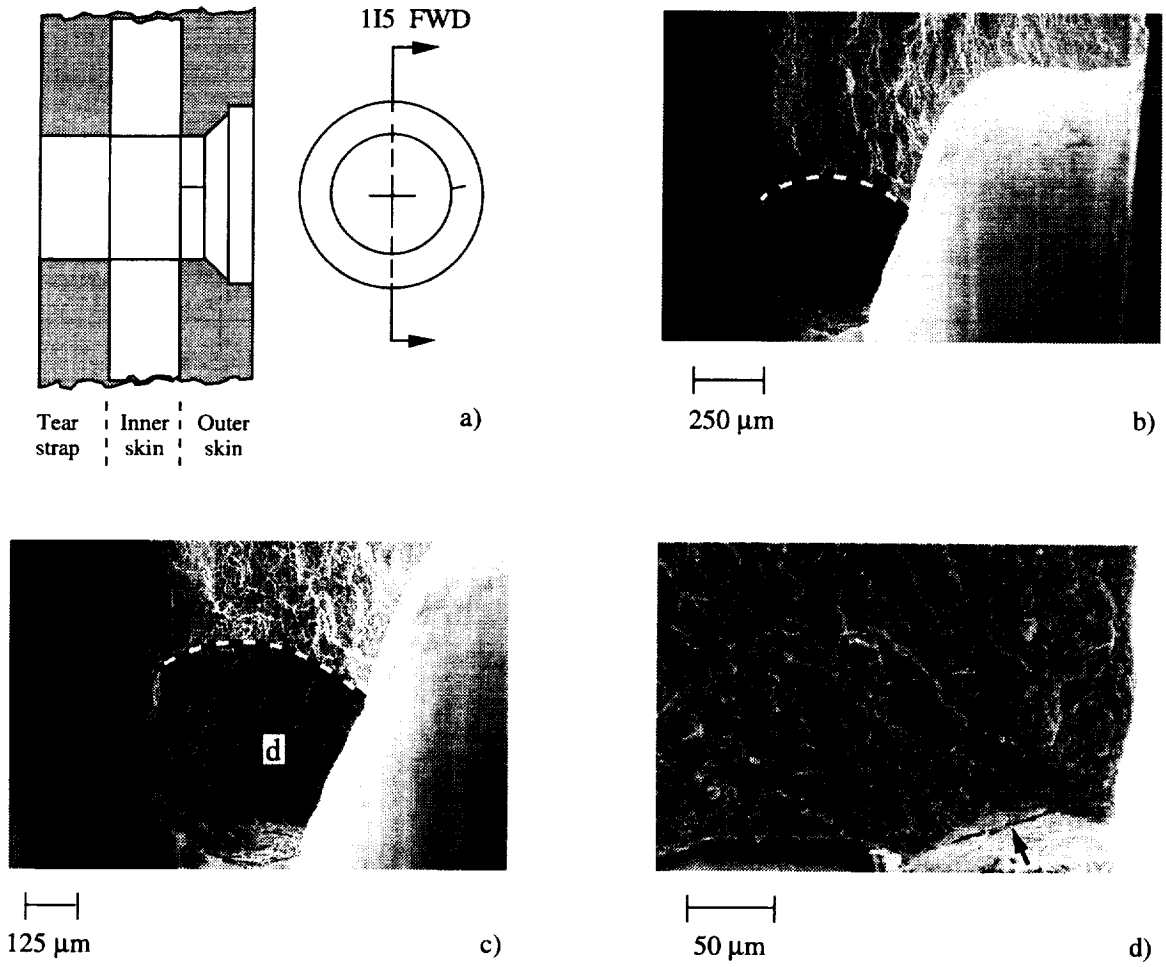

Figure 6.8 a) The schematic shows the rivet hole 1I5 configuration and the location of the outer skin fatigue crack oriented in the forward direction slightly above the 3 o'clock position. b) The SEM micrograph shows the fatigue crack location within the rivet hole. The dashed line marks the fatigue crack front. c) The SEM micrograph shows the fatigue crack region at higher magnification. d) The SEM micrograph shows region "d" in Figure 6.8.c at higher magnification. The likely crack initiation region is marked by an arrow. The mud cracking feature (upper right of arrow) is evidence of corrosion. The rivet was removed after pressure testing and the open rivet hole was exposed to the environment. It is likely corrosion occurred at that time.

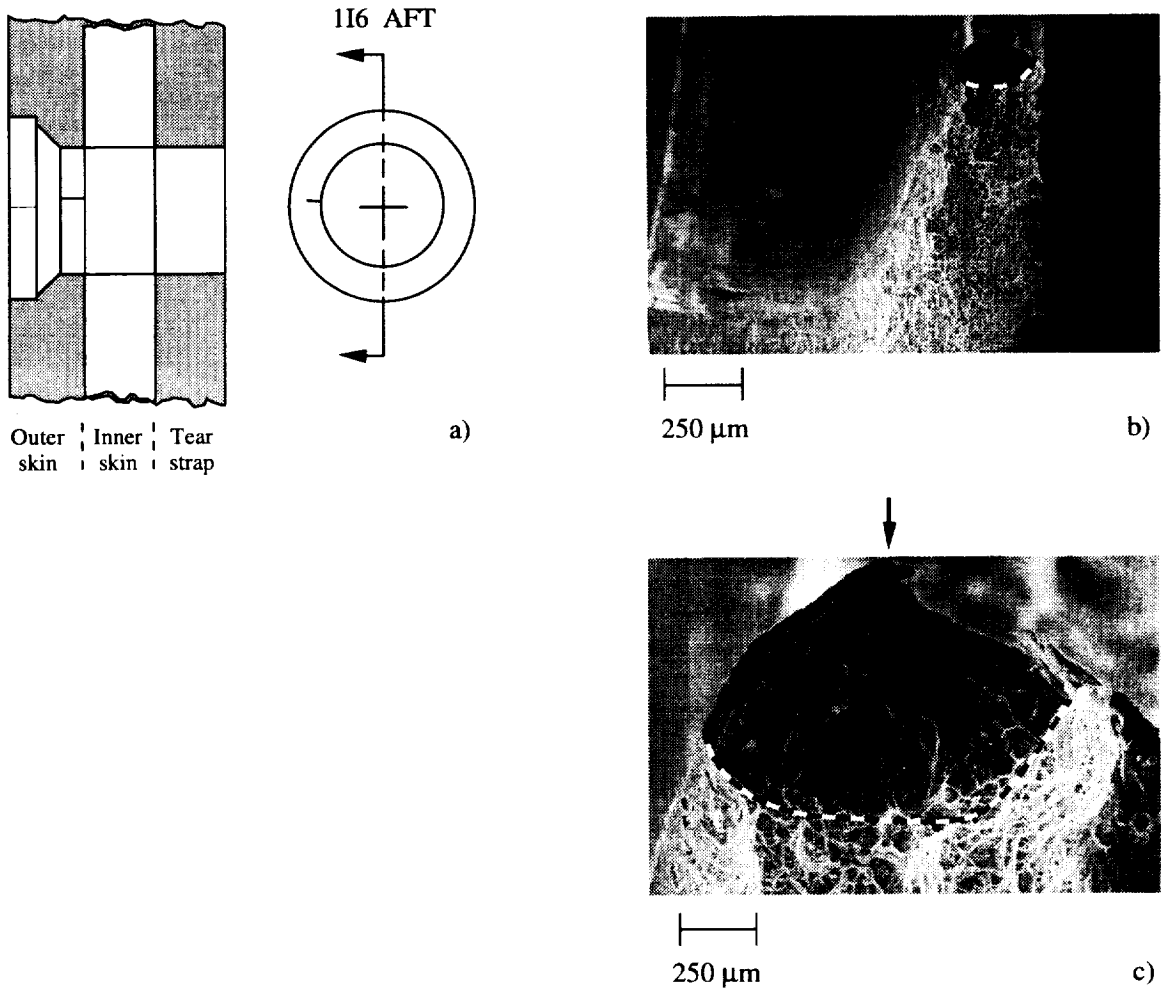

Figure 6.9 a) The schematic shows the rivet hole 1I6 configuration and the location of the outer skin fatigue crack oriented in the aft direction slightly above the 9 o'clock position. b) The SEM micrograph shows the fatigue crack location within the rivet hole. The dashed line marks the fatigue crack front. c) The SEM micrograph shows the fatigue crack region at higher magnification. The arrow marks the likely site of crack initiation. The dashed line marks the fatigue crack front.

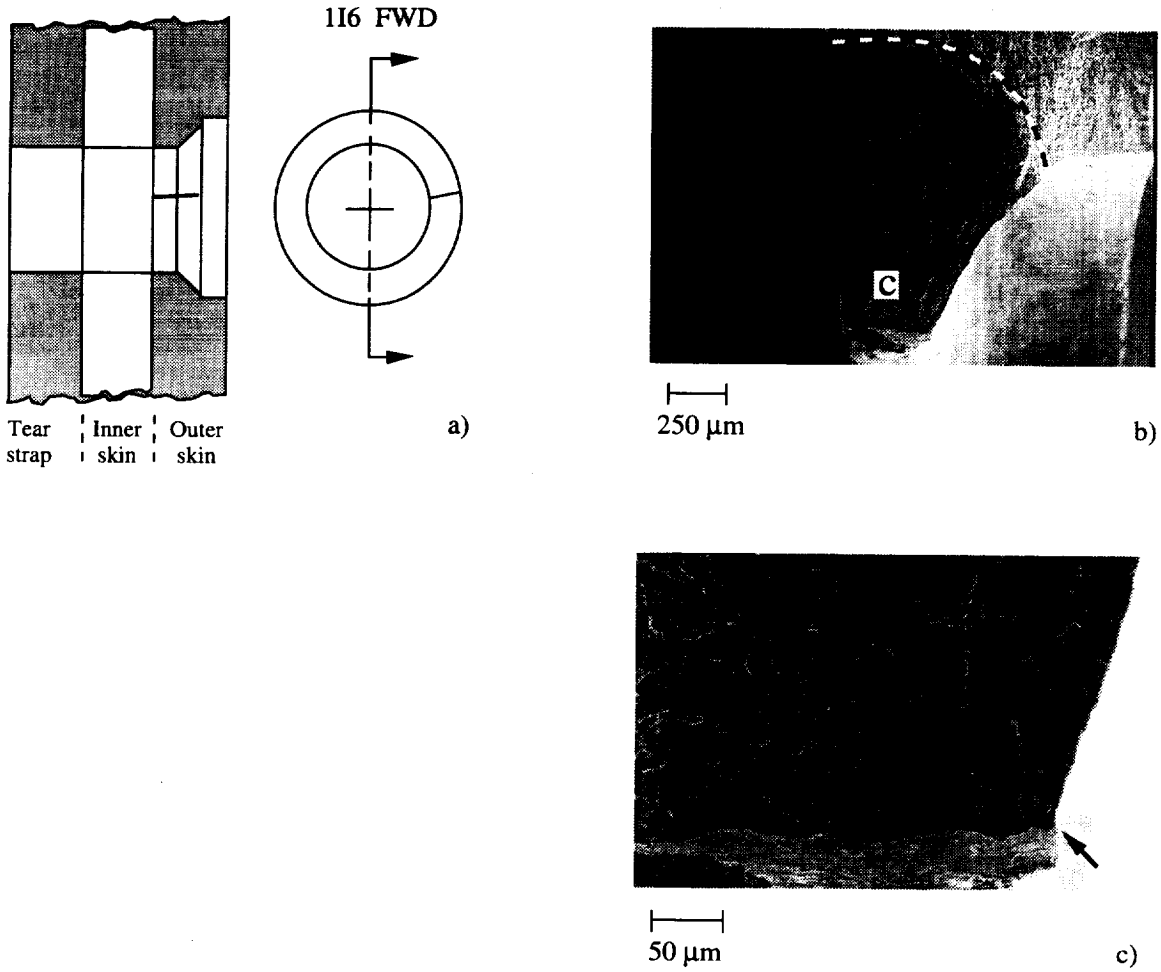

Figure 6.10 a) The schematic shows the rivet hole 1I6 configuration and the location of the outer skin fatigue crack oriented in the forward direction slightly above the 3 o'clock position. b) The SEM micrograph shows the fatigue crack location within the rivet hole. The dashed line marks the fatigue crack front. c) The SEM micrograph shows region "c" in Figure 6.10.b at higher magnification. The arrow marks the likely site of crack initiation.

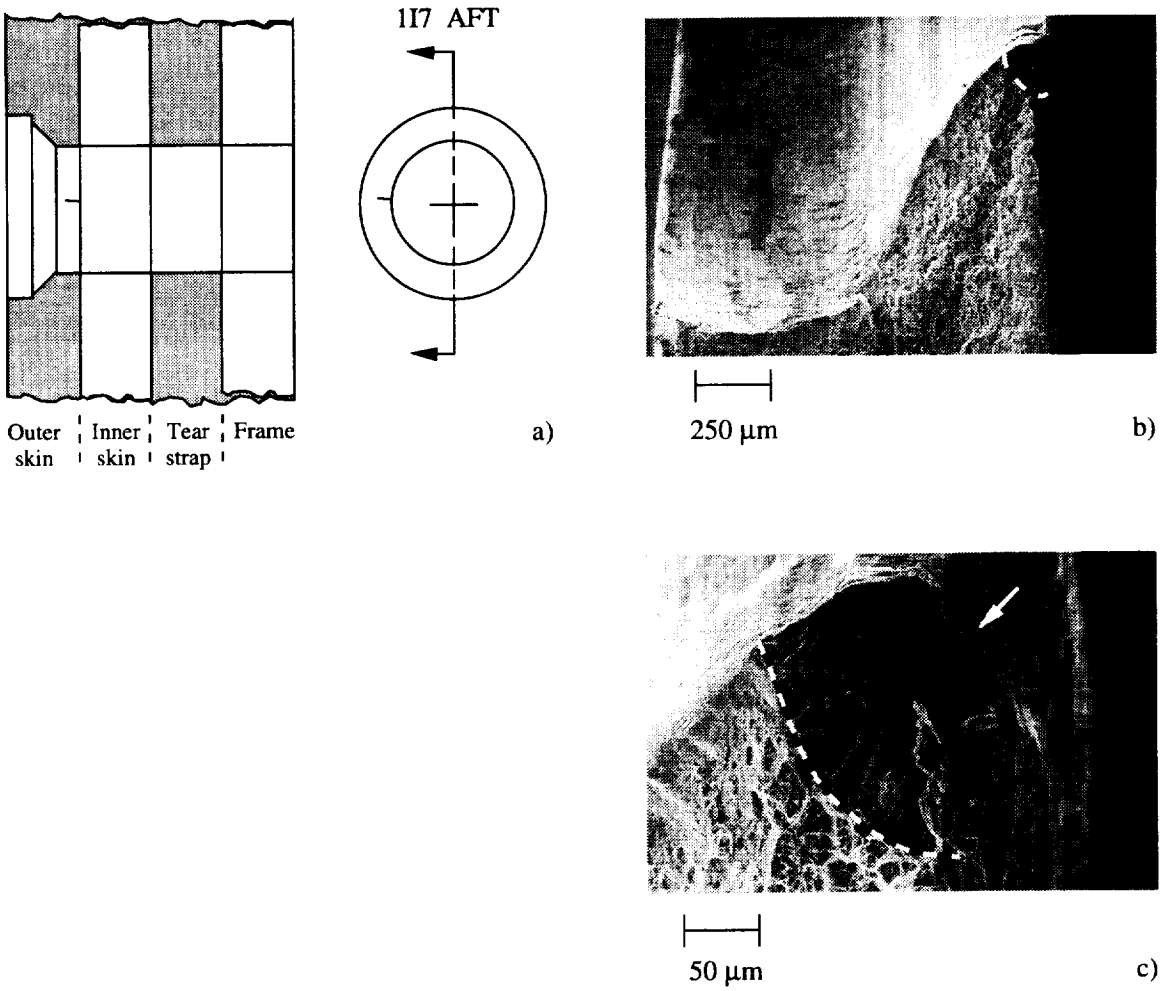

Figure 6.11 a) The schematic shows the rivet hole 1I7 configuration and the location of the outer skin fatigue crack oriented in the aft direction slightly above the 9 o'clock position. b) The SEM micrograph shows the fatigue crack location within the rivet hole. The dashed line marks the fatigue crack front. c) The SEM micrograph shows the fatigue crack region at higher magnification. The arrow marks the likely site of crack initiation.

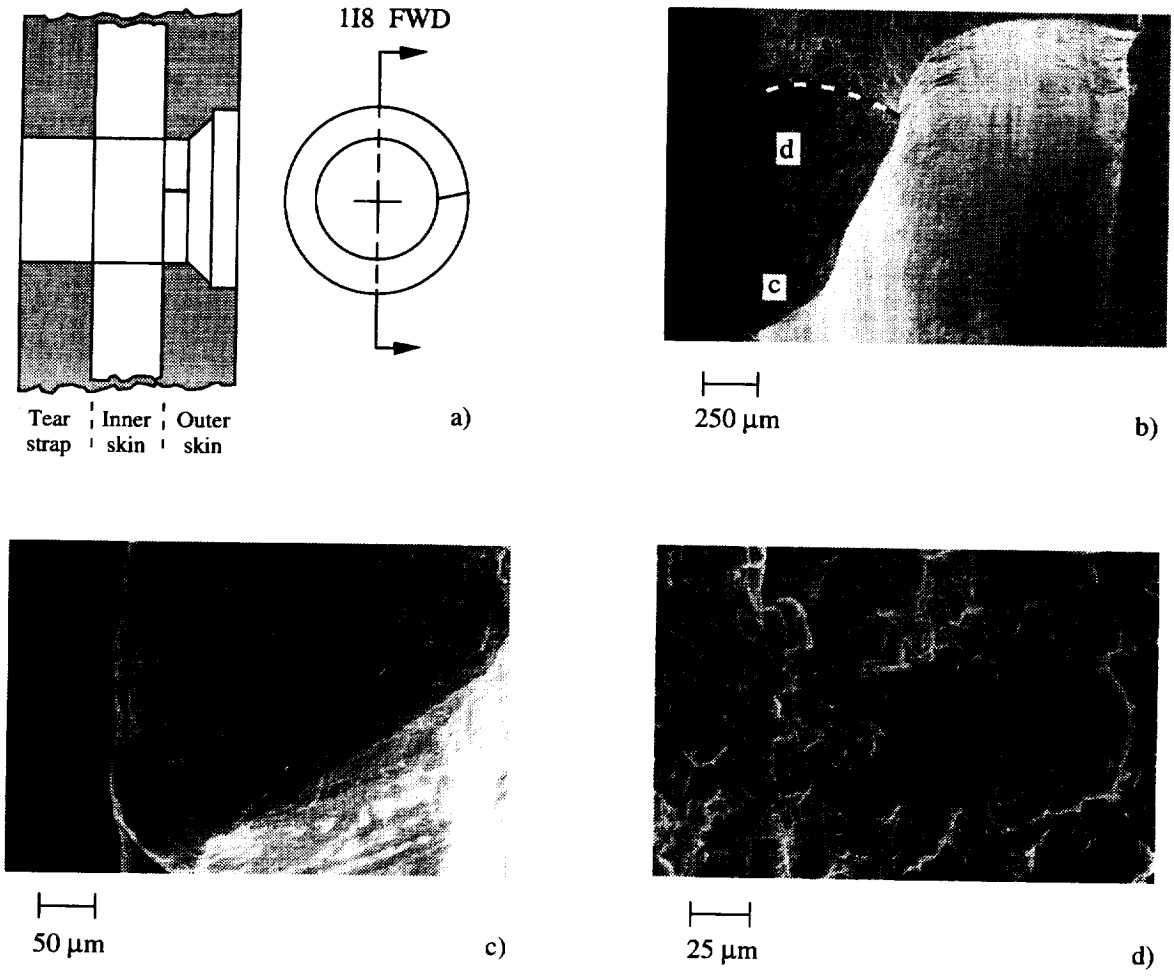

Figure 6.12 a) The schematic shows the rivet hole 1I8 configuration and the location of the outer skin fatigue crack oriented in the forward direction slightly above the 3 o'clock position. b) The SEM micrograph shows the fatigue crack location within the rivet hole. The dashed line marks the fatigue crack front. c) The SEM micrograph shows the crack initiation region "c" in Figure 6.12.b. Oxides covering the fracture surface mask the crack morphology around the site of crack initiation. d) The SEM micrograph shows the transgranular fatigue crack morphology in region "d" in Figure 6.12.b.

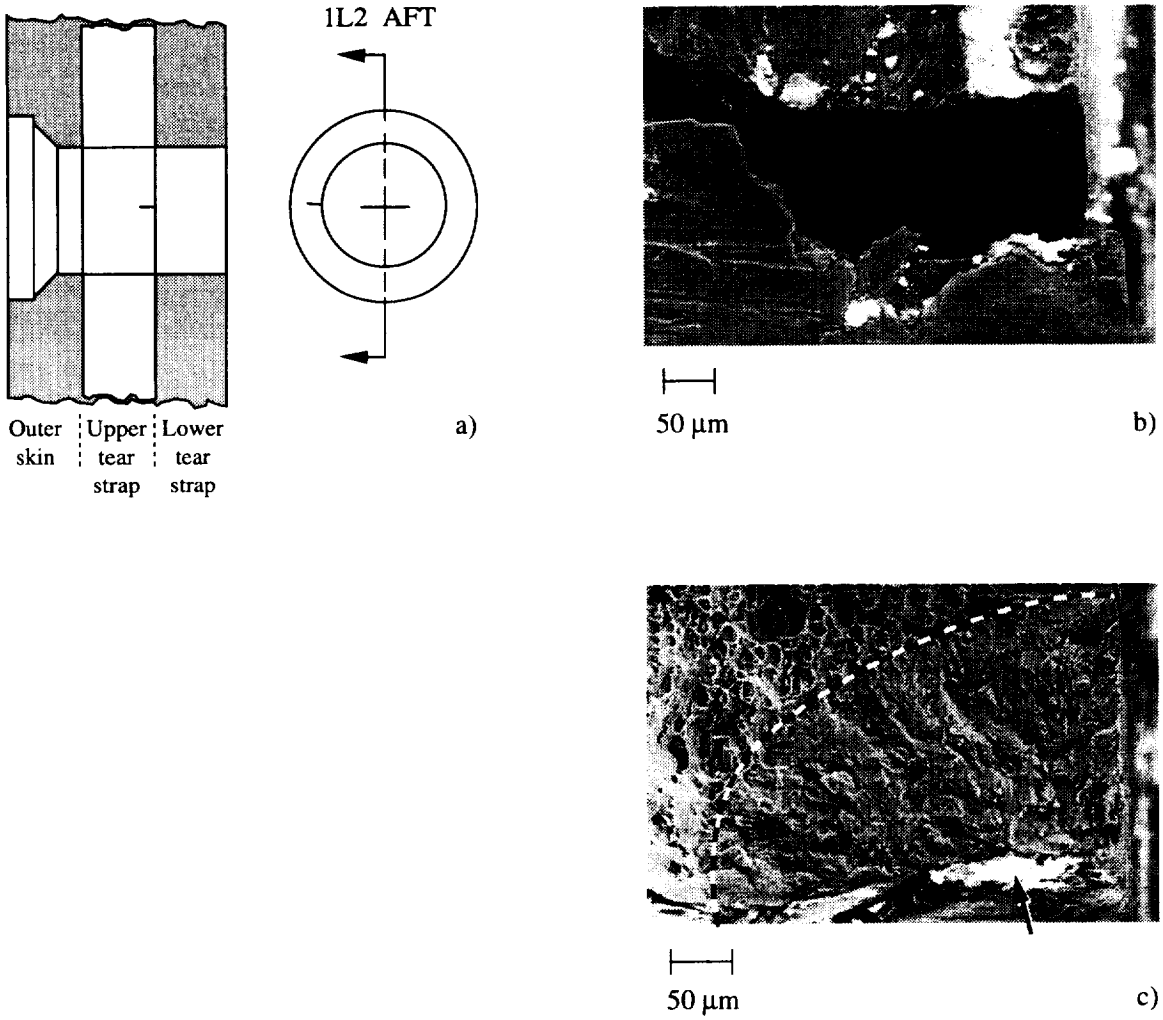

Figure 6.13 a) The schematic shows the rivet hole 1L2 configuration and the location of the upper tear strap fatigue crack oriented in the aft direction slightly above the 9 o'clock position. b) The SEM micrograph shows the corner fatigue crack that has been partially opened during the destructive examination. The surface normal to the fatigue crack is the hole inside surface. This surface exhibits a roughened morphology and oxide debris is observed adjacent to the crack lip. The white color of this debris is associated with electronic charging during the SEM examination and is typically caused by nonconducting surface oxides. c) The SEM micrograph shows the fatigue crack region after final fracture of the specimen. The dashed line marks the fatigue crack front. An arrow marks the likely region of crack initiation which exhibits a rough surface containing oxide debris (white region).

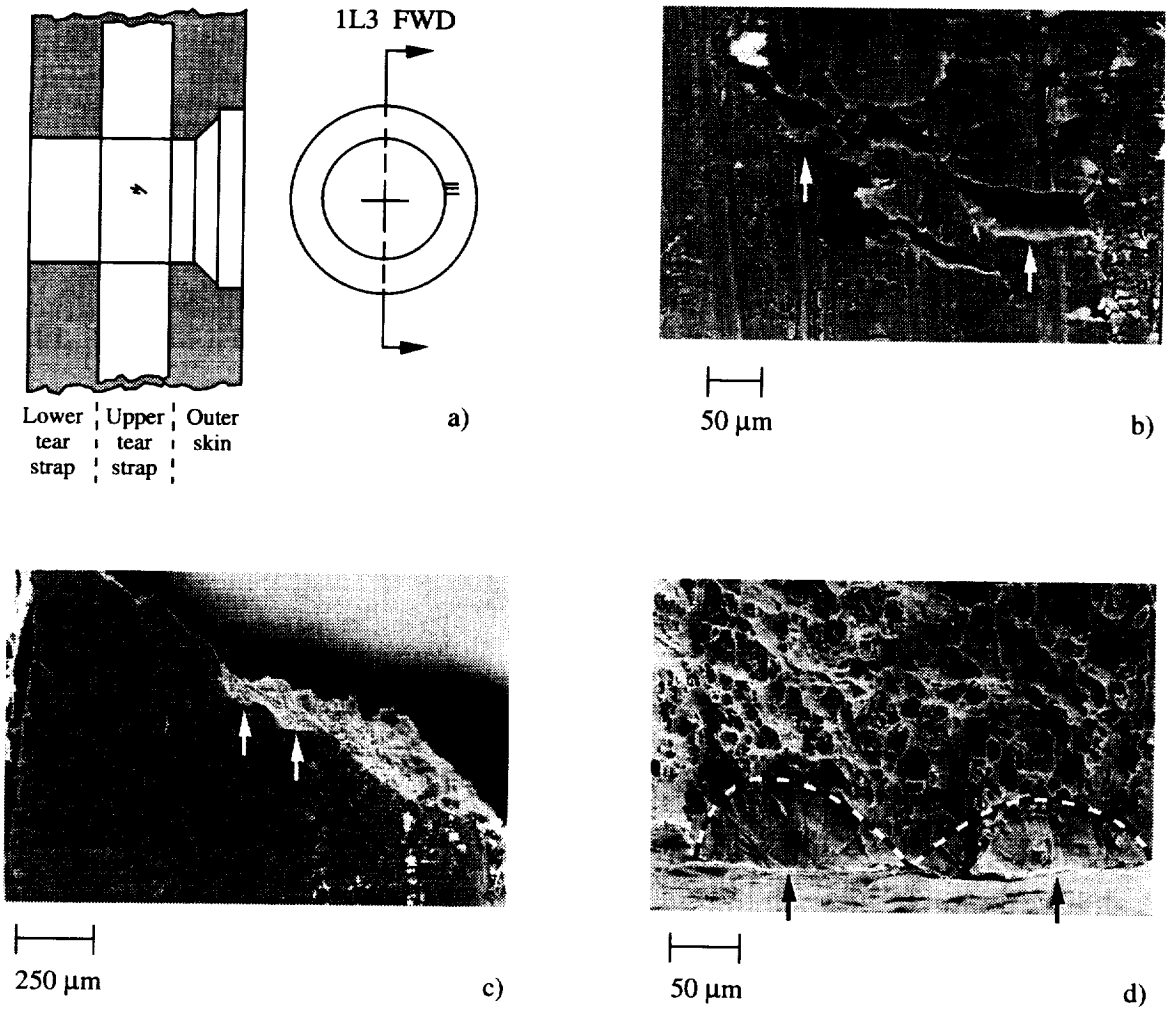

Figure 6.14 a) The schematic shows the rivet hole 1L3 configuration and the location of the upper tear strap fatigue crack oriented in the forward direction at about the 3 o'clock position. b) The SEM micrograph shows the surface fatigue cracks that have been partially opened during the destructive examination. Note the vertical marking on the inside surface of the hole. These markings suggest possible disturbed surface metal in the region of crack initiation marked by the arrows. c) The SEM micrograph shows the fatigue crack location within the rivet hole after the specimen was fractured. Arrows mark approximate regions of fatigue crack initiation. d) The SEM micrograph shows the fatigue fracture surface. The dashed line marks the fatigue crack front. Arrows mark approximate regions of fatigue crack initiation.

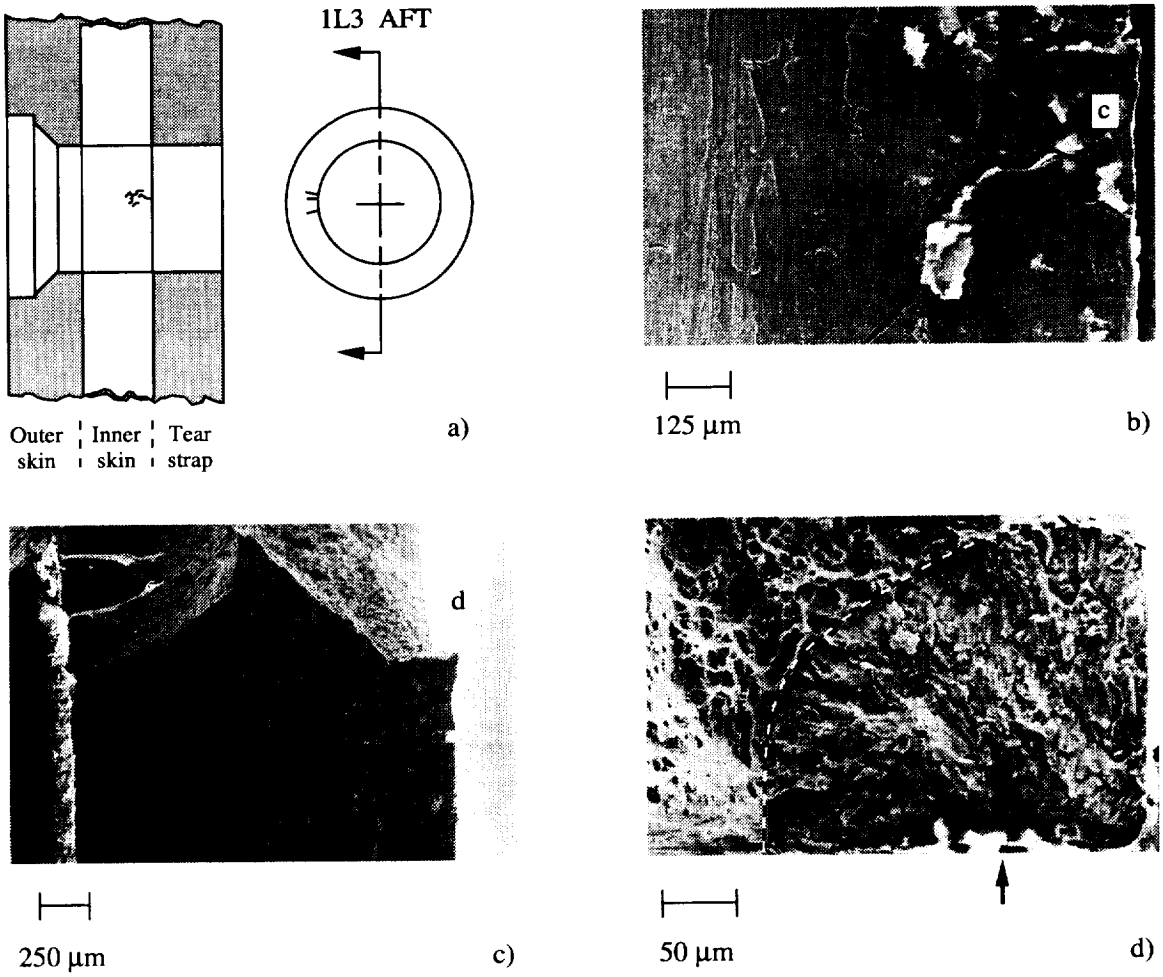

Figure 6.15 a) The schematic shows the rivet hole 1L3 configuration and the location of the upper tear strap fatigue crack oriented in the aft direction and about the 9 o'clock position. b) The SEM micrograph shows the multiple surface and corner fatigue cracks that have been partially opened during the destructive examination. c) The SEM micrograph shows the lower half (region "c" in Figure 6.15.b) fatigue crack region after the specimen was fractured. d) The SEM micrograph shows the fatigue fracture surface of the corner crack at region "d" in Figure 6.15.c. The dashed line marks the fatigue crack front. An arrow marks the likely region of crack initiation which exhibits a rough surface containing oxide debris (white region).

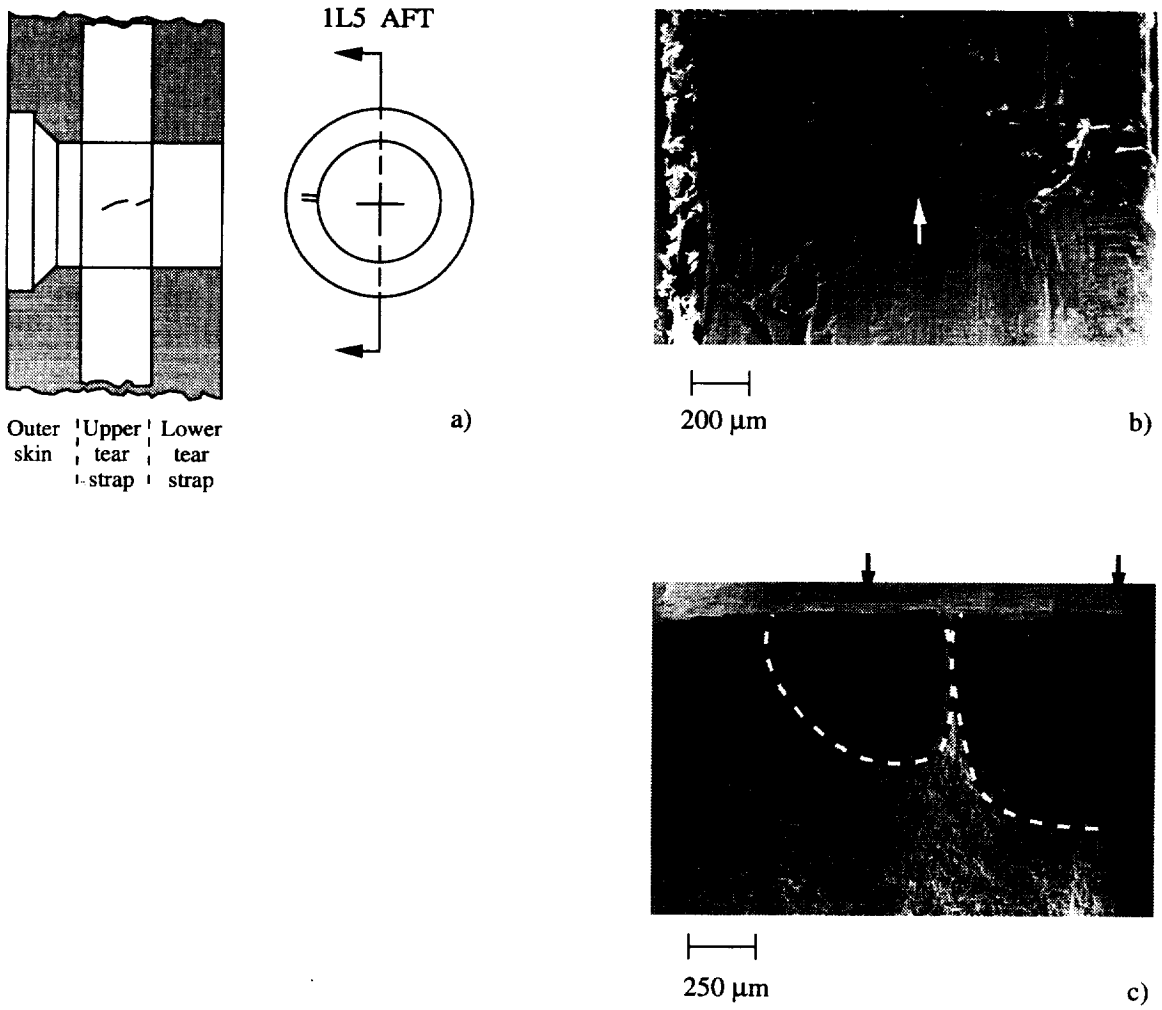

Figure 6.16 a) The schematic shows the rivet hole 1L5 configuration and the location of the upper tear strap fatigue cracks oriented in the aft direction and about the 9 o'clock position. b) The SEM micrograph shows the multiple surface and corner fatigue cracks that have been partially opened during the destructive examination. Arrows mark approximate sites of crack initiation. c) The SEM micrograph shows the fatigue fracture surface of the corner and surface crack. The dashed line marks the fatigue crack front. Note that crack-to-crack interaction has altered the shape of each crack front (marked by dashed lines). Arrows mark the approximate location of crack initiation.

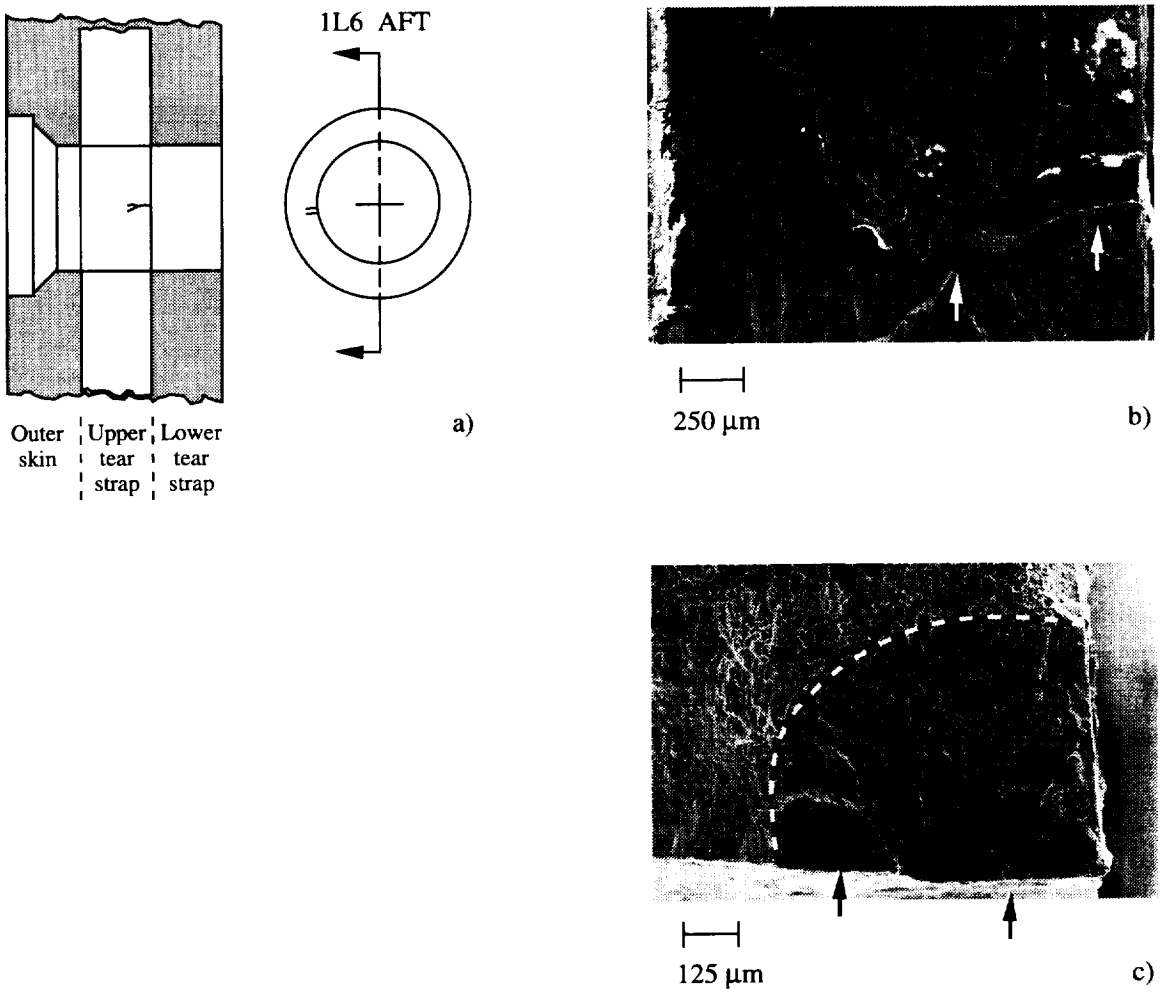

Figure 6.17 a) The schematic shows the rivet hole 1L6 configuration and the location of the upper tear strap fatigue crack oriented in the aft direction and about the 9 o'clock position. b) The SEM micrograph shows the surface and corner fatigue cracks that have been partially opened during the destructive examination. Arrows mark approximate location of crack initiation. c) The SEM micrograph shows the fatigue fracture surface of the corner and surface crack. The dashed line marks the fatigue crack front. Arrows mark the approximate location of crack initiation.

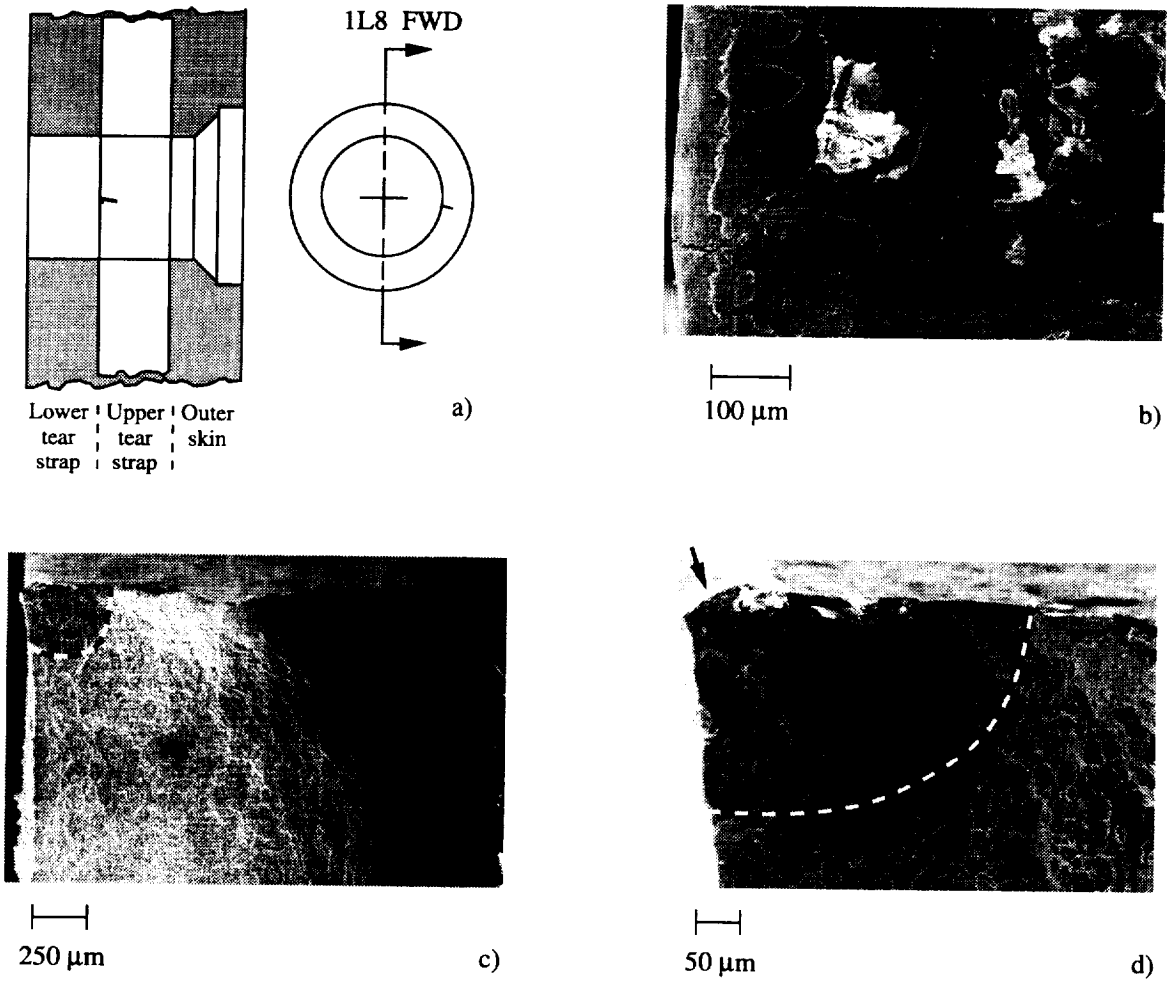

Figure 6.18 a) The schematic shows the rivet hole 1L8 configuration and the location of the upper tear strap fatigue crack oriented in the forward direction and about the 3 o'clock position. b) The SEM micrograph shows the tight corner fatigue crack prior to the destructive examination straining operation. c) The SEM micrograph shows the fatigue fracture surface of the corner crack. The dashed line marks the fatigue crack front. d) The SEM micrograph shows the fatigue fracture surface of the corner crack at higher magnification. White oxide debris near the corner marks the likely region of crack initiation (arrow).

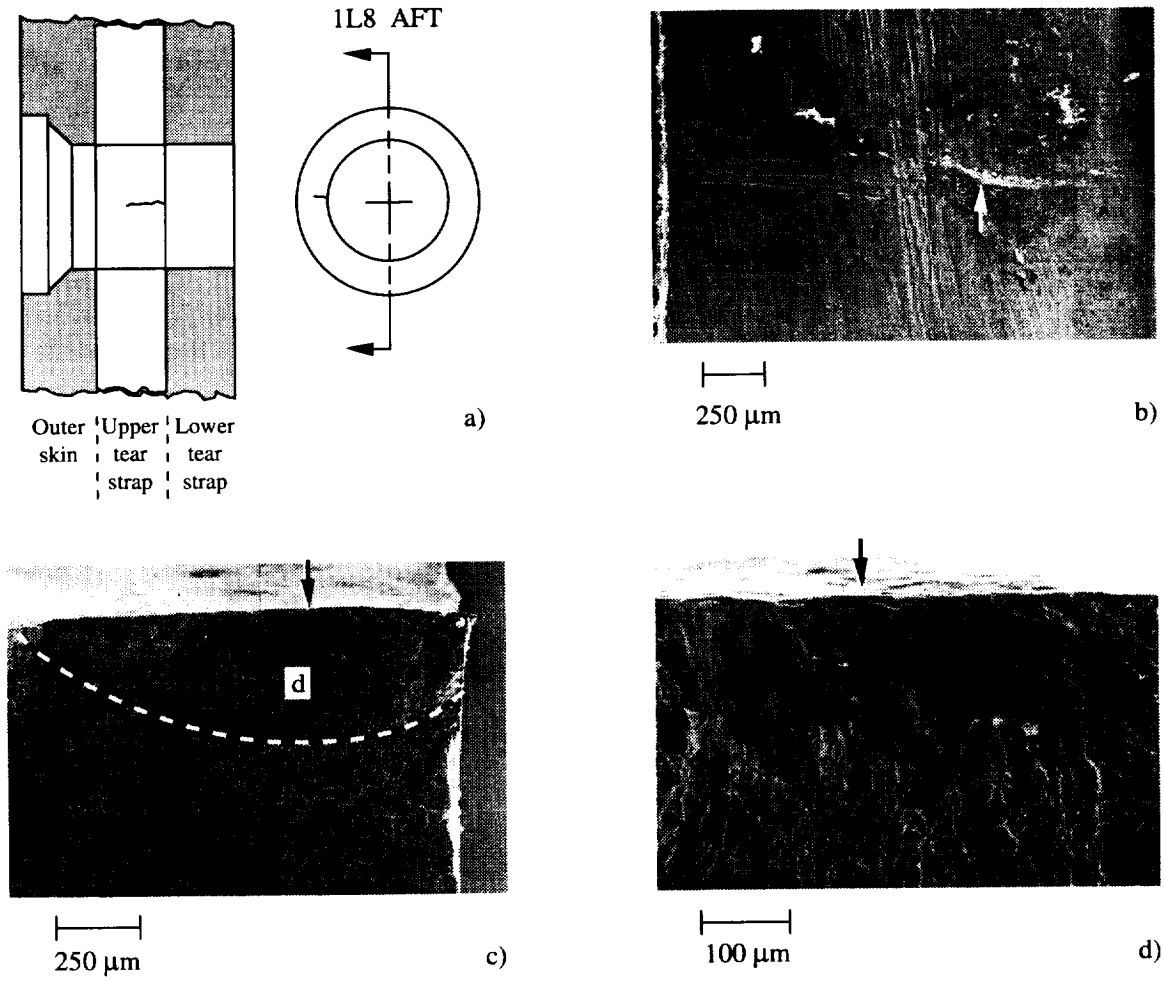

Figure 6.19 a) The schematic shows the rivet hole 1L8 configuration and the location of the upper tear strap fatigue crack oriented in the aft direction and about the 9 o'clock position. b) The SEM micrograph shows the tight corner fatigue crack (barely visible) prior to the destructive examination straining operation. The arrow marks the approximate crack initiation region. Note that a horizontal mark (disturbed metal) is located at the region of crack initiation. Other vertical markings are also visible. c) The SEM micrograph shows the fatigue fracture surface of the surface crack that has intersected the corner of the rivet hole. The arrow marks the approximate crack initiation region. The dashed line marks the fatigue crack front. d) The SEM micrograph shows the fatigue fracture surface of the crack initiation area, region "d" in Figure 6.19.c. Oxide debris is noted at the site of crack initiation.

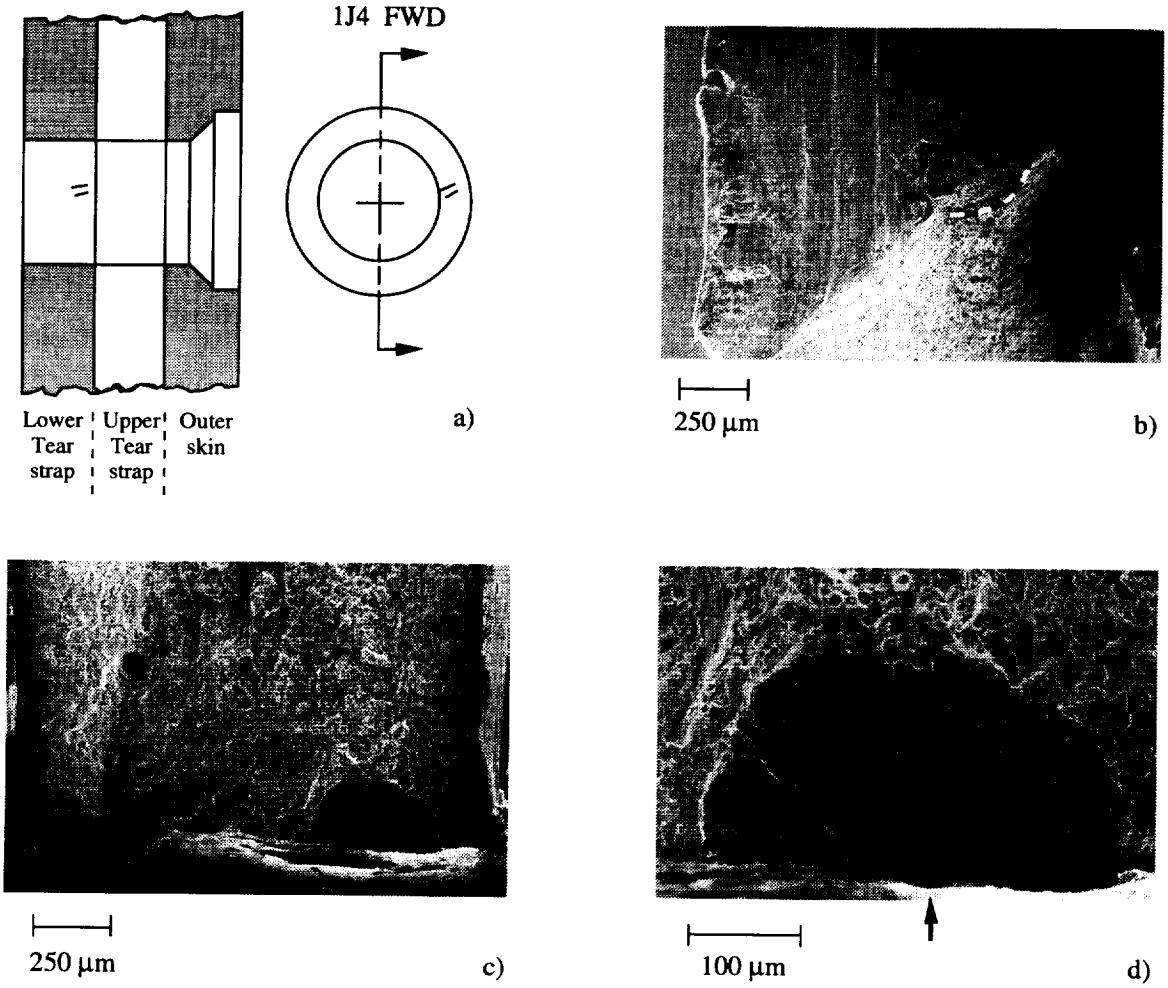

Figure 6.20 a) The schematic shows the rivet hole 1J4 configuration and the location of the lower tear strap fatigue cracks oriented in the forward direction and about the 3 o'clock position. b) The SEM micrograph shows the inside surface of the rivet hole and the fracture surface. The dashed line marks the position of the single surface fatigue crack on the fracture surface. Located above the fatigue fracture surface and on the rivet hole inside diameter are three incipient surface fatigue cracks. c) The SEM micrograph shows the semicircular fatigue fracture surface of the rivet hole surface crack. d) The SEM micrograph shows the semicircular fatigue fracture surface of the rivet hole surface crack at higher magnification. An arrow marks the likely site of fatigue crack initiation, and the dashed line marks the fatigue crack front.

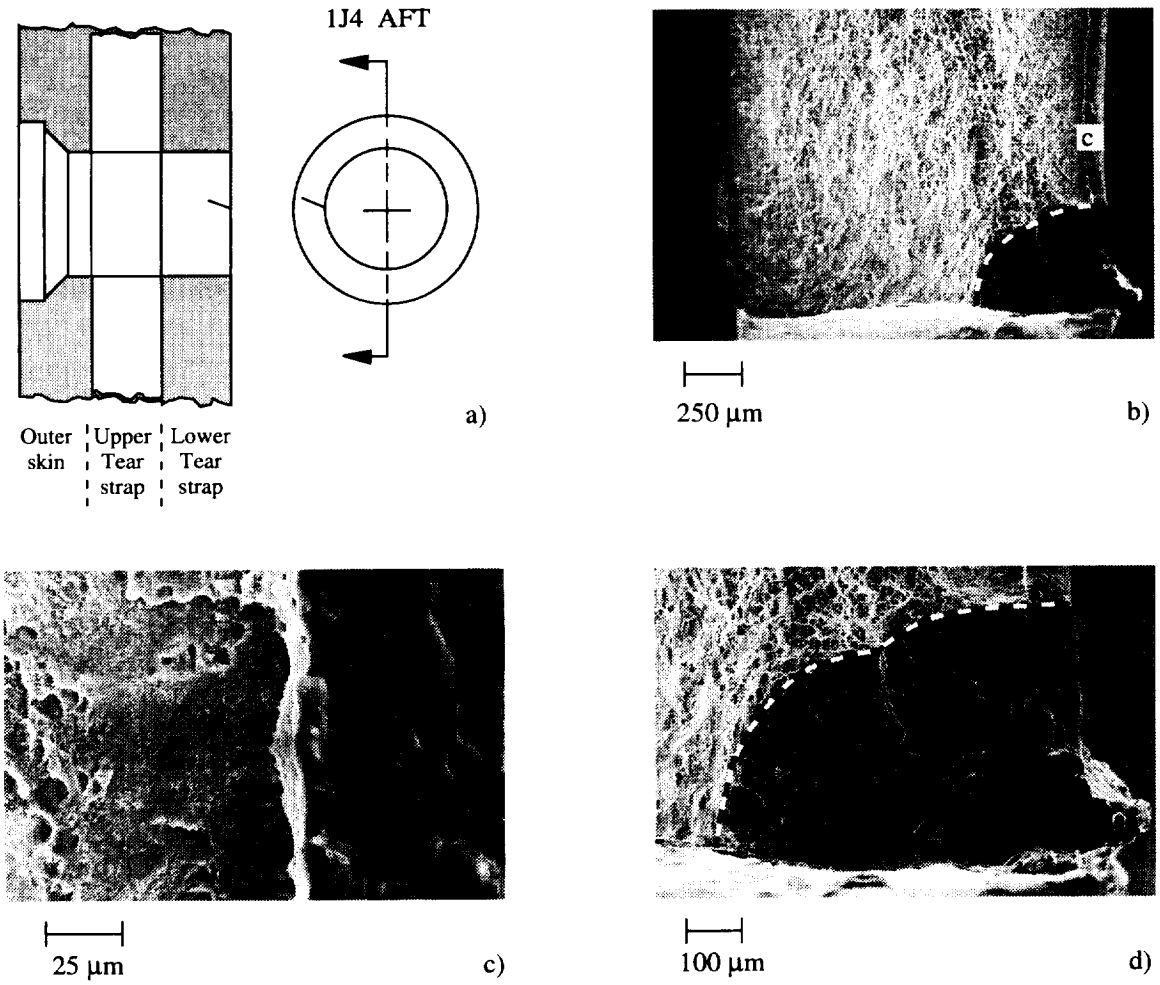

Figure 6.21 a) The schematic shows the rivet hole 1J4 configuration and the location of the lower tear strap fatigue crack oriented in the aft direction and about the 9 o'clock position. b) The SEM micrograph shows fatigue fracture surface of the rivet hole corner crack. Note the corner burr near the likely point of crack initiation (arrow). c) The SEM micrograph shows the clad/alloy interface at region "c" shown in Figure 6.21.c. d) The SEM micrograph shows the fatigue fracture surface of the rivet hole corner crack at high magnification. A dashed line marks the fatigue crack front.

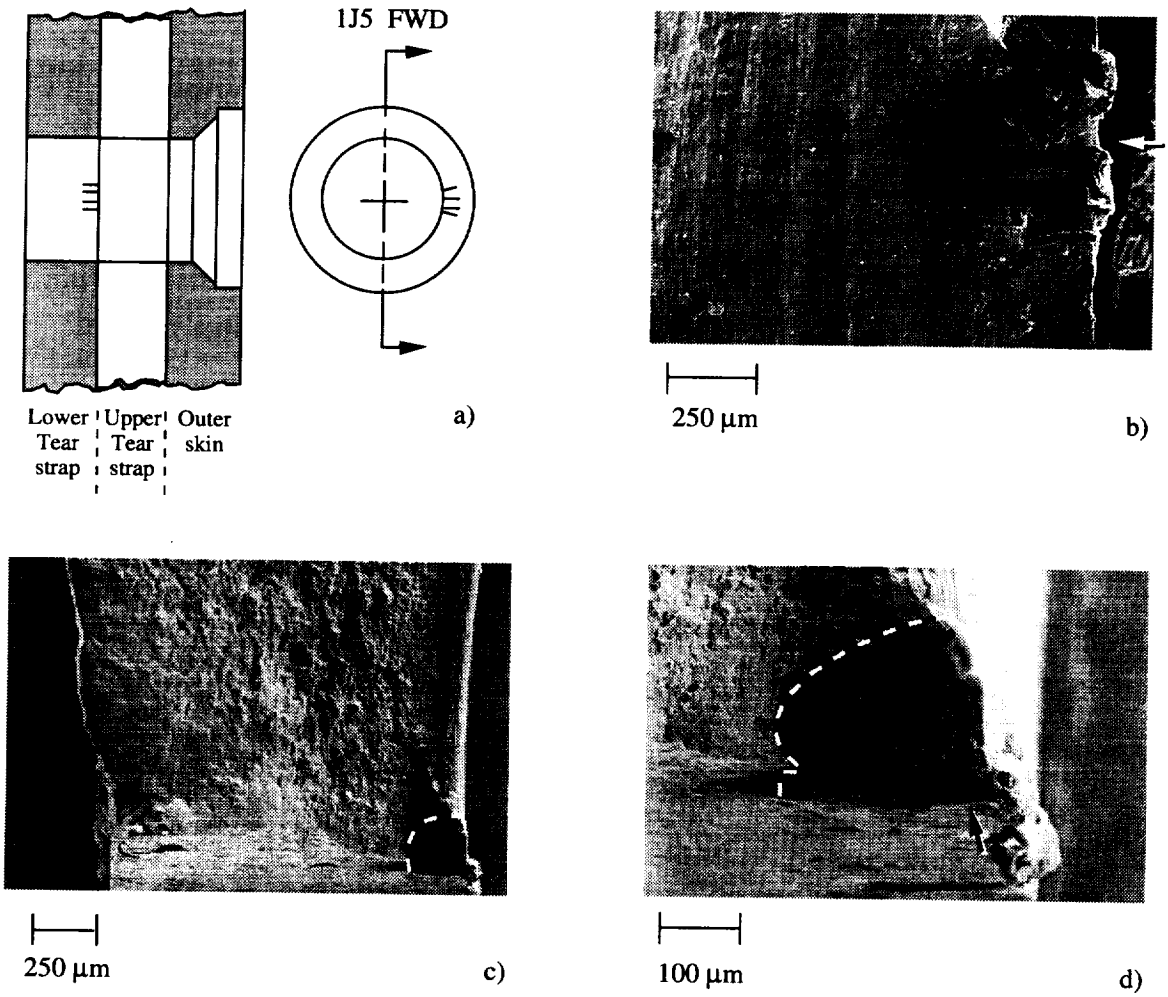

Figure 6.22 a) The schematic shows the rivet hole 1J5 configuration and the location of the multiple lower tear strap corner fatigue cracks oriented in the forward direction and about the 3 o'clock position. b) The SEM micrograph of the rivet hole surface shows the region that contains multiple corner cracks. Note the corner burrs near the likely point of crack initiation. The arrow marks the position of the fracture shown in Figures 6.22.c and 6.22.d. c) The SEM micrograph shows the fracture surface of the corner crack marked by the arrow in Figure 6.22.b. The dashed line marks the fatigue crack front. d) The SEM micrograph shows the fracture surface of the corner crack in Figure 6.22.c at higher magnification. The dashed line marks the fatigue crack front and the arrow marks the likely site of fatigue crack initiation.

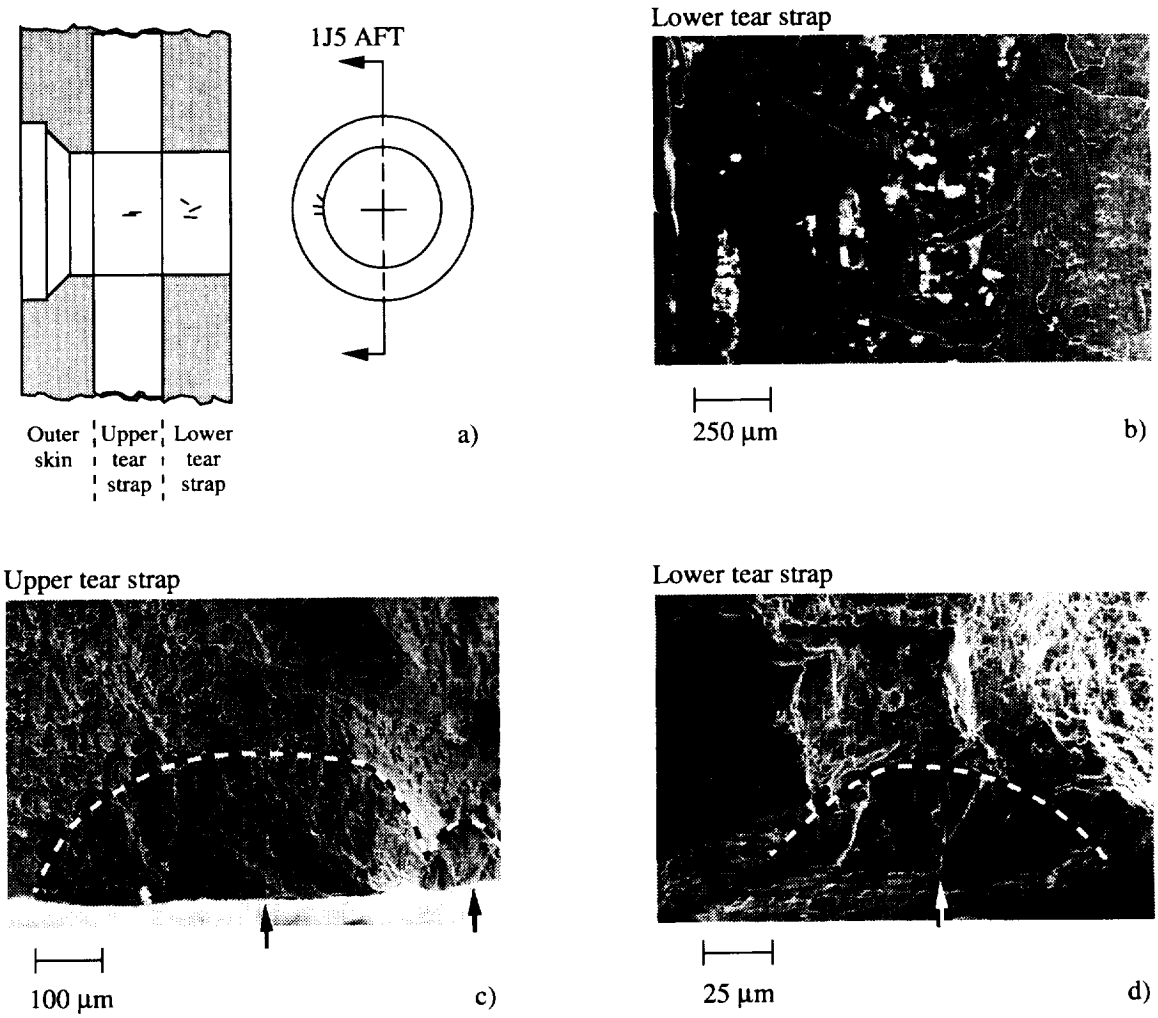

Figure 6.23 a) The schematic shows the rivet hole 1J5 configuration and the location of upper and lower tear strap fatigue cracks oriented in the aft direction and about the 9 o'clock position. b) The SEM micrograph shows the inside surface of the lower tear strap rivet hole and multiple fatigue surface cracks partially opened as a result of the destructive examination straining operation. c) The SEM micrograph shows the fatigue fracture surface of the upper tear strap rivet hole surface cracks. The dashed line marks the fatigue crack front and arrows mark the likely sites of fatigue crack initiation. The irregular shape of the crack front is a due to multiple crack coalescence. d) The SEM micrograph shows the fatigue fracture surface of the lower tear strap rivet hole surface crack (upper most crack in Figure 6.23.b). An arrow marks the site of crack initiation.

7. Destructive Examination of Bay #2

A total of sixty-seven rivet hole locations in bay 2 (identified by the filled hole symbols in Figure 7.1) were destructively examined. All fifteen upper rivet row locations exhibited fatigue cracking (a total of 30 fatigue cracks) prior to crack link-up. A single crack, 47.88 cm (18.85 in.) long, spanning the entire length of the bay 2 lap splice formed when fatigue crack link-up occurred at each upper rivet hole. Twenty-one fatigue cracks were found in the remaining rivet rows contained in bay 2: six cracks in row I, four cracks in row H, and eleven cracks in row G. Figures 7.2 and 7.3 show the location of all fatigue cracks found in the first layer (outer skin) and the second layer (inner skin), respectively. No fatigue cracks were found in the horizontal stiffener or tear strap. Rivet rows J and I contained outer skin cracks and rows H and G contained inner skin cracks. The through-thickness rivet hole schematics shown in Figures 7.4, 7.5 and 7.6 summarize crack location, crack length, crack type, and initiation site for rivet rows I, H, and G, respectively. Because all fatigue cracks are linked in row J and fracture surface detail was destroyed by surface abrasion, a through-thickness schematic detailing fatigue crack information is not shown for the upper row. The following is a detailed description of the fatigue damage in the bay 2 tear strap region. Figures 7.8 through 7.22 are detailed photographs showing the top portion of the long upper row crack (row J) shown in Figure 7.7 and corresponding crack growth data obtained from visual surface measurements performed during pressure testing. Figures 7.23 through 7.43 detail the location and fracture surface morphology of all fatigue cracks found in the remainder of bay 2 (rivet rows G, H, and I).

7.1 Fatigue Cracks Contained in Row J:

Figures 7.7 through 7.22 describe the fatigue crack morphology in row J.

7.2 Fatigue Cracks Contained in Row I:

Figures 7.23 through 7.28 describe the fatigue crack morphology in row I.

7.3 Fatigue Cracks Contained in Row H:

Figures 7.29 through 7.32 describe the fatigue crack morphology in row H.

7.4 Fatigue Cracks Contained in Row G:

Figures 7.33 through 7.43 describe the fatigue crack morphology in row G.

7.5 Bay #2 Summary:

Table 7.1 summarizes the destructive examination results for bay 2 rivet rows G, H, I, and J. The upper row J and bottom row G were found to contain most of the fatigue cracks. Bay 2 cracks range in length from 0.058 mm (0.002 in.) to the long crack which extended 478.8 mm (18.85 in.) along rivet row J. The upper two rows (J and I) contained outer skin cracks. Inner skin cracking was observed in the two lower rivet rows H and G. The following observations were made as a result of fractographic examinations of bay 2.

7.5.1 Crack initiation site(s):

Row J: Most fatigue cracks initiated along the outer/inner skin faying surface in the region under the rivet head. The faying surface exhibited black oxide and disturbed metal suggesting fretting contact at the point of crack initiation.

Row I: Most fatigue cracks initiated along the outer/inner skin faying surface in the region under the rivet head. The faying surface exhibited black oxide and disturbed metal suggesting fretting contact at the point of crack initiation.

Row H: Fatigue cracks initiated in the inner skin rivet hole at the outboard corner facing the outer skin. Burrs and disturbed metal were observed at the point of crack initiation.

Row G: Fatigue crack initiation was observed in three distinct inner skin regions, (1) rivet hole surface, (2) rivet hole corner, and inner/outer skin faying surface.

7.5.2 Crack front shape as a function of crack length:

Row J: Fatigue crack fronts were not discernible.

Row I: Fatigue crack fronts progressed in the outboard direction from faying surface to the outer skin outboard surface.

Row H: Because most cracks were small, limited data was obtained on crack front shape versus crack length.

Row G: Inner skin fatigue crack fronts progressed in the inboard direction from the outer/inner skin faying surface. Fatigue cracks that initiated within the rivet hole exhibited somewhat symmetrical crack front shapes.

7.5.3 Fatigue crack/stable tearing transition crack length:

Row J: Greater than 70% of the crack surface between each rivet hole contain evidence of ductile tearing suggesting either rapid fatigue crack growth or stable tearing.

Row I, H, and G: Fatigue fracture surface is transgranular.

7.5.4 Slant fracture morphology:

Row J: Greater than 70% of the crack surface between each rivet hole contain slant fracture morphology.

Row I, H, and G: No slant fracture morphology was observed.

7.5.5 Evidence of corrosion:

Row J, I, H, and G: No corrosion was observed.

Table 7-1 Bay #2 Fatigue Crack Summary

Rivet Row	No. of Cracks (Holes)	Location	Crack Length mm (in)	Comment
J	30(15)	Outer Skin	a=478.8(18.85)	Fretting
I	2(2)	Outer Skin	0.058(0.002)≤a	High K_T
	4(4)	Outer Skin	≤2.33(0.082)	Fretting
H	4(3)	Inner Skin	0.110(0.004)≤a ≤2.43(0.096)	High K_T
G	12(7)	Inner Skin	0.100(0.004)≤a	High K_T
	1(1)	Inner Skin	≤4.17(0.164)	Fretting

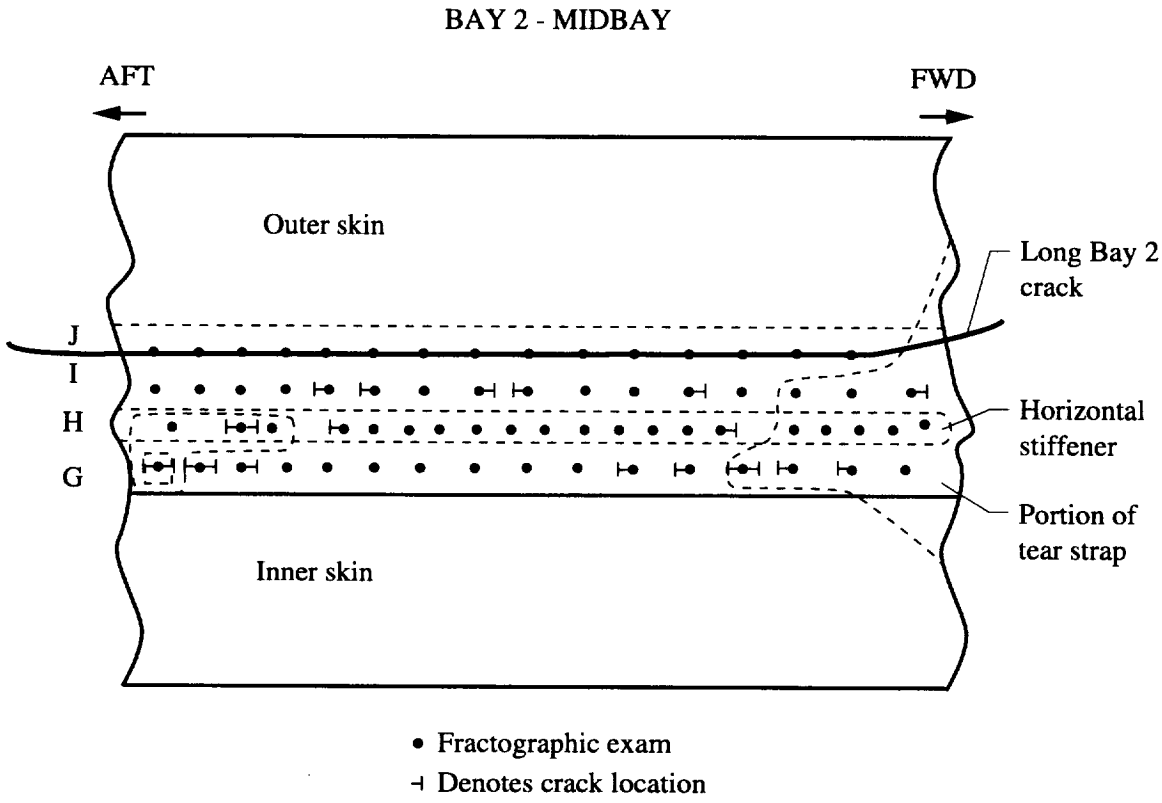

Figure 7.1 The schematic shows the location of all fatigue cracks found in the bay 2 lap splice joint by destructive examination. The long bay 2 crack is visible in row J. All bay 2 rivet holes were destructively examined.

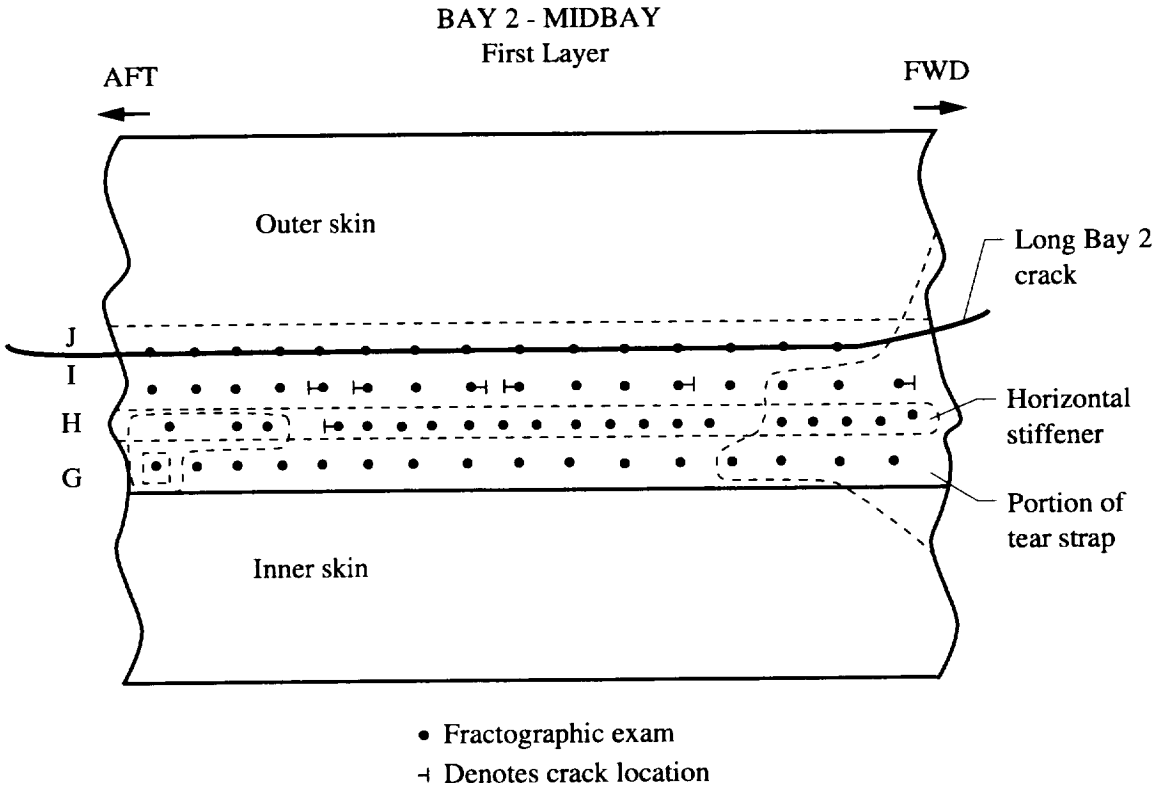

Figure 7.2 The schematic shows the location of fatigue cracks found in the first layer (outer skin) of the bay 2 lap splice joint by destructive examination. The long bay 2 crack is visible in row J.

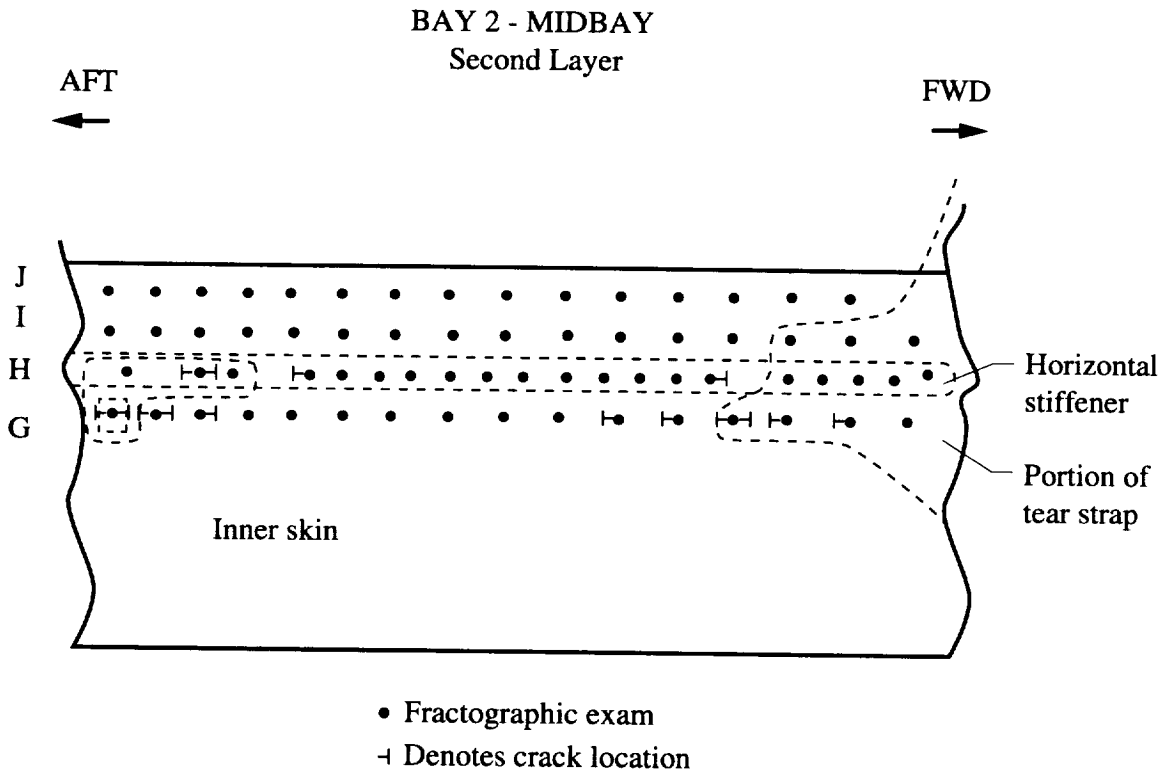

Figure 7.3 The schematic shows the location of fatigue cracks found in the second layer (inner skin) of the bay 2 lap splice joint by destructive examination.

BAY 2 ROW I

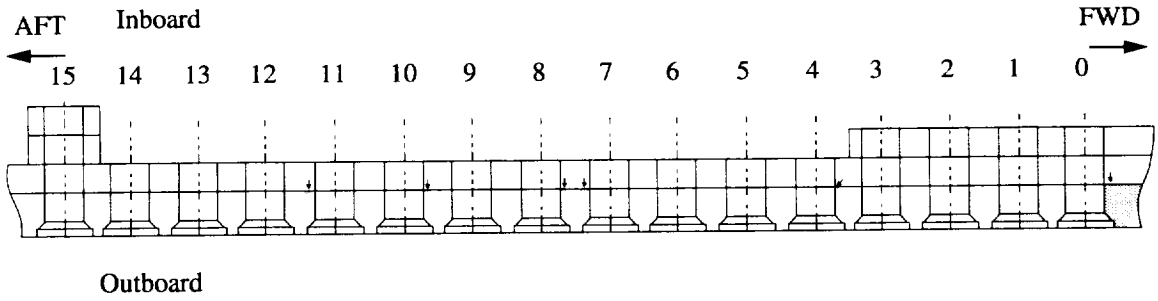

Hole #	Location	Length mm(in)	Type	Initiation-site
0 (FWD)	Outer skin	2.33 (.092)	Through	Inner/outer skin interface
4 (FWD)	Outer skin	0.102 (.004)	Fretting	Inboard corner of shank
7 (Aft)	Outer skin	0.112 (.004)	Fretting	IS/OS
8 (FWD)	Outer skin	0.073 (.003)	Fretting	IS/OS
10 (FWD)	Outer skin	0.140 (.006)	Fretting	IS/OS
11 (Aft)	Outer skin	0.058 (.002)	Fretting	IS/OS

Figure 7.4 The through thickness schematic shows the location and initiation site (small arrows) of fatigue cracks found in rivet row I from bay 2. The table summarizes crack location, crack length, crack type, and initiation site for each fatigue crack shown.

BAY 2 ROW H

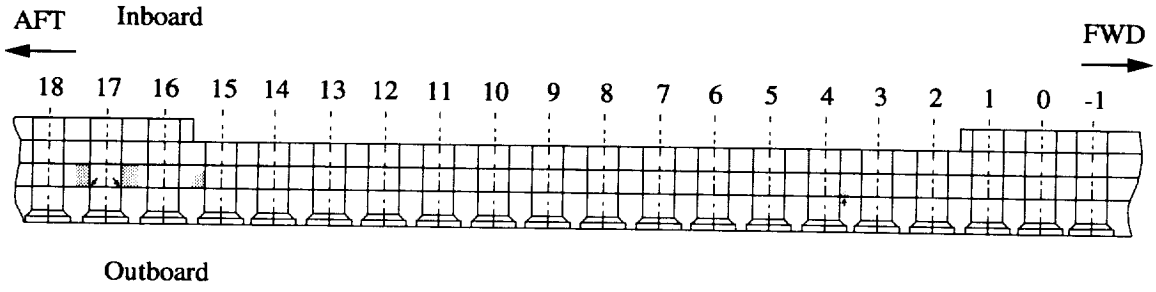

Hole #	Location	Length mm(in)	Type	Initiation site
4 (FWD)	Inner skin	0.110 (.004)	Surface	IS / OS Interface
15 (Aft)	Inner skin	ND	Corner	Not determined
17 (FWD)	Inner skin	>2.43 (.096)	Through	Outboard corner
17 (Aft)	Inner skin	>1.63 (.064)	Through	Outboard corner

Figure 7.5 The through thickness schematic shows the location and initiation site (small arrows) of fatigue cracks found in rivet row H from bay 2. The table summarizes crack location, crack length, crack type, and initiation site for each fatigue crack shown.

BAY 2 ROW G

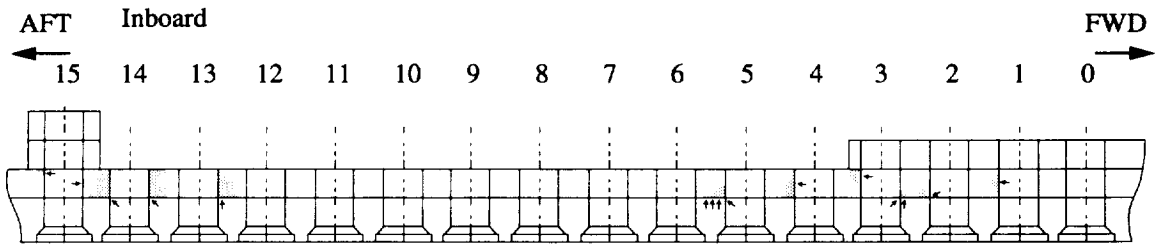

Hole #	Location	Length mm(in.)	Type	Initiation site
1 (Aft)	Inner skin	0.250 (.010)	Surface	Center
2 (Aft)	Inner skin	0.100 (.004)	Corner	Outboard corner (OC)
3 (1FWD)	Inner skin	0.170 (.007)	Corner	OC
3 (2FWD)	Inner skin	0.335 (.013)	Corner	OC
3 (Aft)	Inner skin	0.360 (.014)	Corner	Surface (Inboard side)
4 (Aft)	Inner skin	0.615 (.024)	Through	Center
5 (Aft)	Inner skin	0.680 (.027)	Corner & fretting	Mutiple (OC & fretting)
13 (FWD)	Inner skin	~2.750 (.108)	Through	OC
14 (Aft)	Inner skin	~2.720 (.107)	Through	OC
14 (FWD)	Inner skin	>4.170 (.164)	Through	OC
15 (FWD)	Inner skin	0.163 (.006)	Surface	Center
15 (1-Aft)	Inner skin	0.115 (.004)	Corner	IC
15 (2-Aft)	Inner skin	0.128 (.005)	Corner	IC

Figure 7.6 The through thickness schematic shows the location and initiation site (small arrows) of fatigue cracks found in rivet row G from bay 2. The table summarizes crack location, crack length, crack type, and initiation site for each fatigue crack shown.

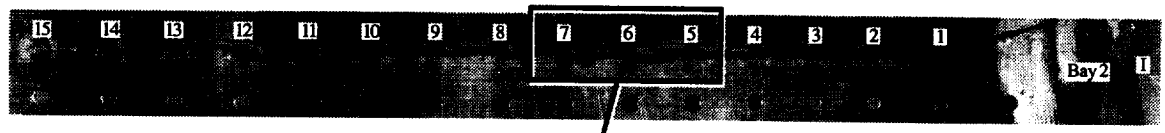

a)

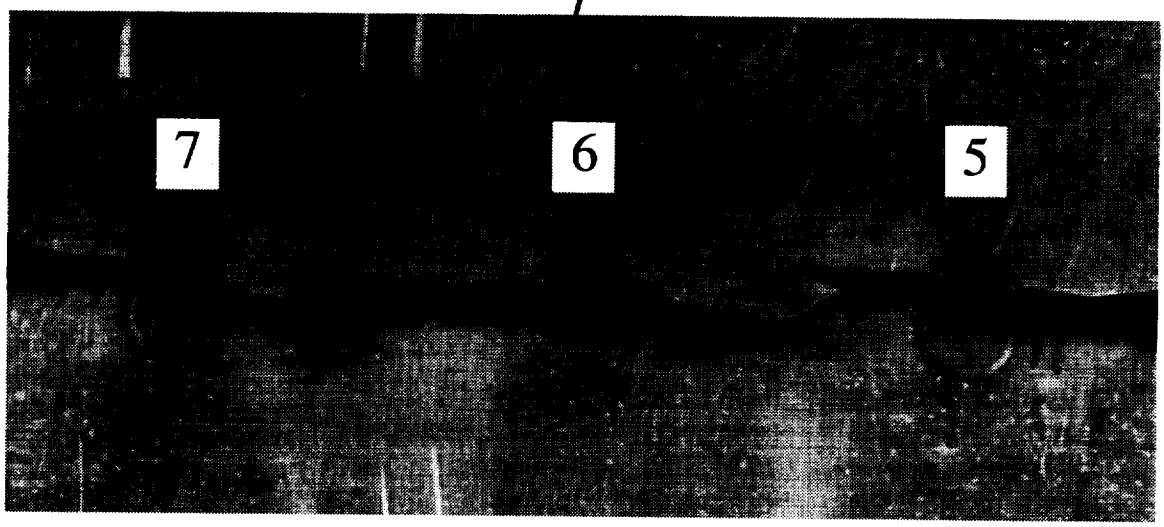

b)

Figure 7.7 a) The photograph shows the 18.85 inch (47.88 cm) long outer skin crack that extends through the entire upper rivet row. b) The photograph shows an enlargement of the region containing rivet holes 2J5, 2J6, and 2J7. The cracked outer skin extends outward (pillowed) and is no longer captured by the rivet heads. The upper portion of the rivet heads shown in Figure 7.7.b are fractured and no longer capture the pillowed outer skin. The cracking between the rivet holes shows a curved crack link-up configuration. The oblong shaped portion of outer skin formed by the linked cracks between holes 5 and 6 is clearly visible.

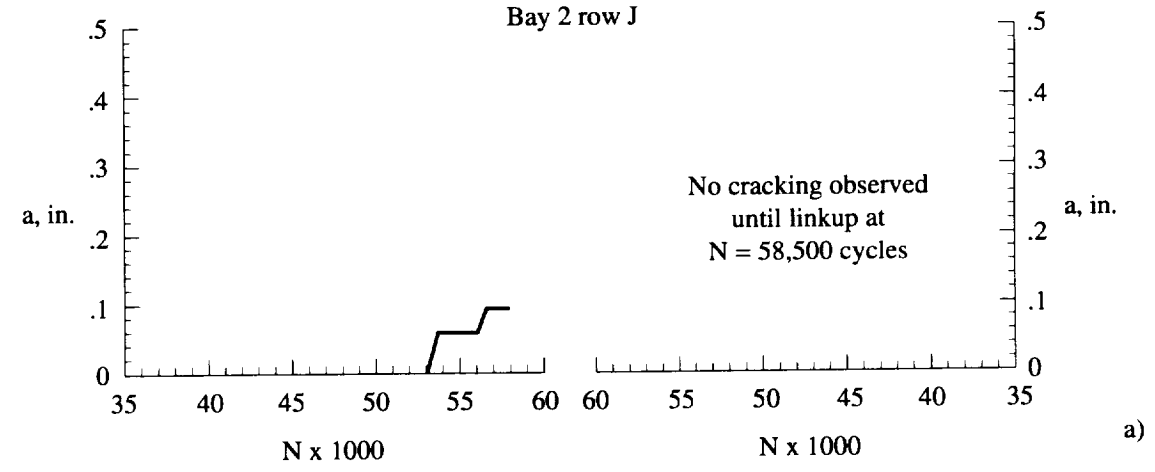

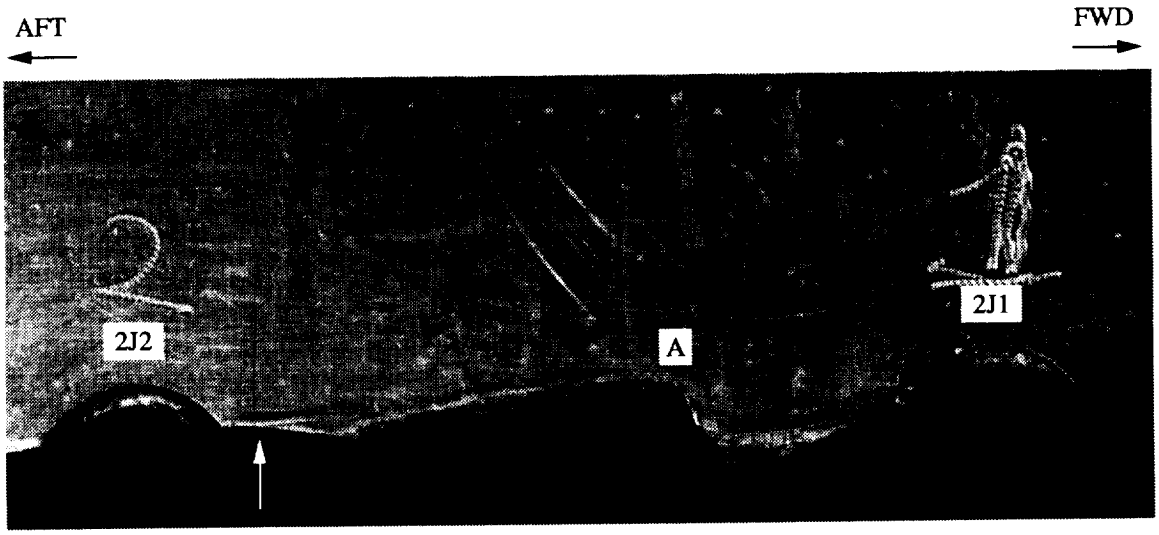

Figure 7.8 a) The figure is a plot of outer skin crack length (a) measured from the rivet outside diameter versus pressurization cycles (N). *In situ* visual crack length measurements were taken during pressure testing. Fatigue crack growth plots are shown for crack segments 2J1 aft and 2J2 forward. No visual cracks were observed from rivet hole 2J1 until after crack link-up (N=60,000 cycles). b) The photograph shows the upper portion of the outer skin crack surface between rivet holes 2J1 and 2J2. An arrow marks the approximate final position of the fatigue crack noted (visually) prior to crack link-up. Region A is the likely position where both cracks linked. Most of the crack surface shown in Figure 7.8.b exhibits a roughened appearance. This slant fracture region is characteristic of ductile tearing produced by relatively high crack tip stress intensity. The slant fracture region contain scratches normal to the direction of crack propagation indicative of fracture surface contact resulting from mode III displacement.

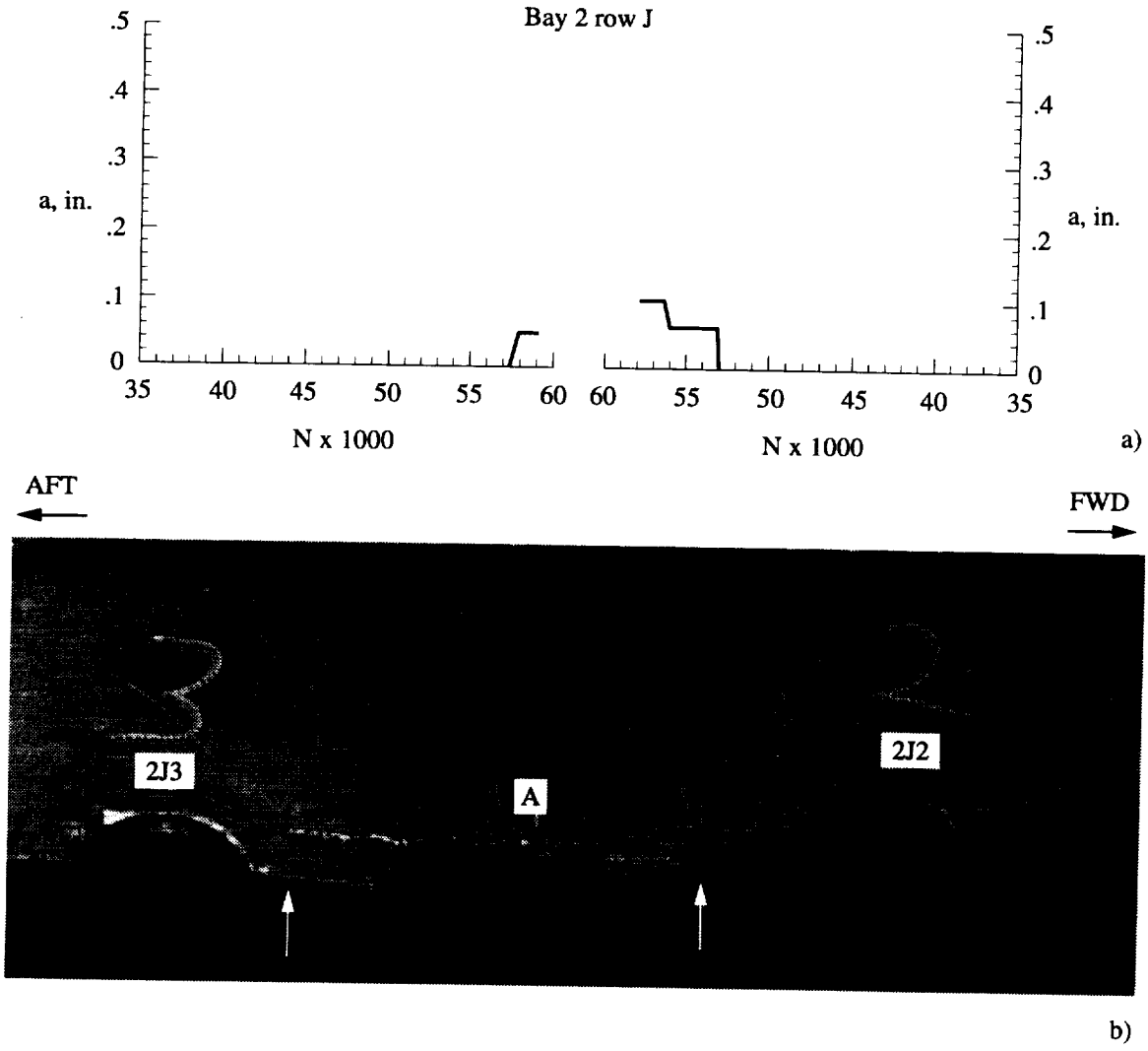

Figure 7.9 a) The figure is a plot of outer skin crack length (a) measured from the rivet outside diameter versus pressurization cycles (N). *In situ* visual crack length measurements were taken during pressure testing. Fatigue crack growth plots are shown for crack segments 2J2 aft and 2J3 forward. b) The photograph shows the upper portion of the outer skin crack surface between rivet holes 2J2 and 2J3. Arrows mark the approximate final position of the fatigue cracks noted (visually) prior to crack link-up. Region A is the likely position where both cracks linked. Most of the crack surface shown in Figure 7.9.b exhibits a roughened appearance. This slant fracture region is characteristic of ductile tearing produced by relatively high crack tip stress intensity. The slant fracture region contains scratches normal to the direction of crack propagation indicative of fracture surface contact resulting from mode III displacement.

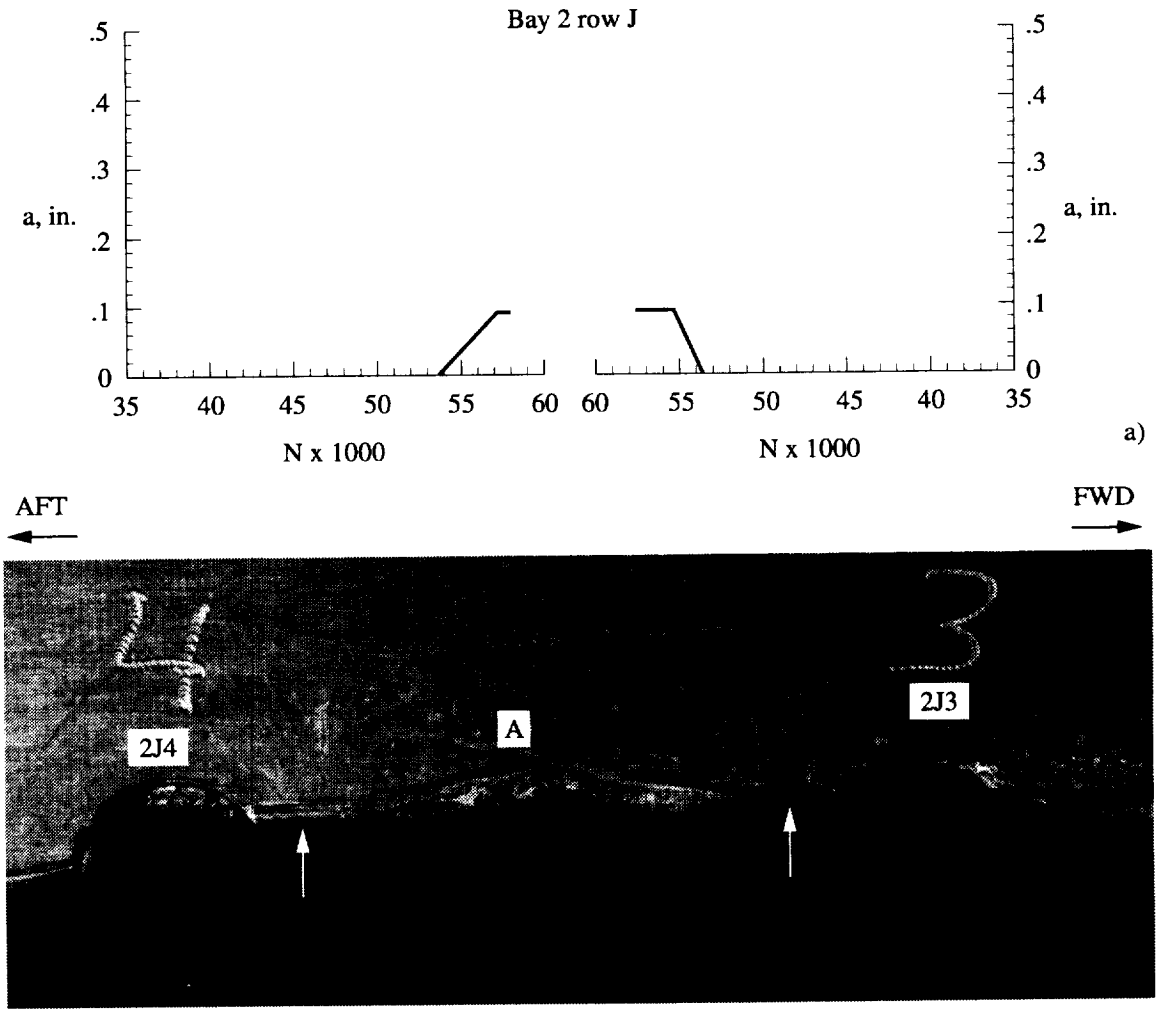

Figure 7.10 a) The figure is a plot of outer skin crack length (a) measured from the rivet outside diameter versus pressurization cycles (N). *In situ* visual crack length measurements were taken during pressure testing. Fatigue crack growth plots are shown for crack segments 2J3 aft and 2J4 forward. b) The photograph shows the upper portion of the outer skin crack surface between rivet holes 2J3 and 2J4. Arrows mark the approximate final position of the fatigue cracks noted (visually) prior to crack link-up. Region A is the likely position where both cracks linked. Most of the crack surface shown in Figure 7.10.b exhibits a roughened appearance. This slant fracture region is characteristic of ductile tearing produced by relatively high crack tip stress intensity. The slant fracture region contains scratches normal to the direction of crack propagation indicative of fracture surface contact resulting from mode III displacement.

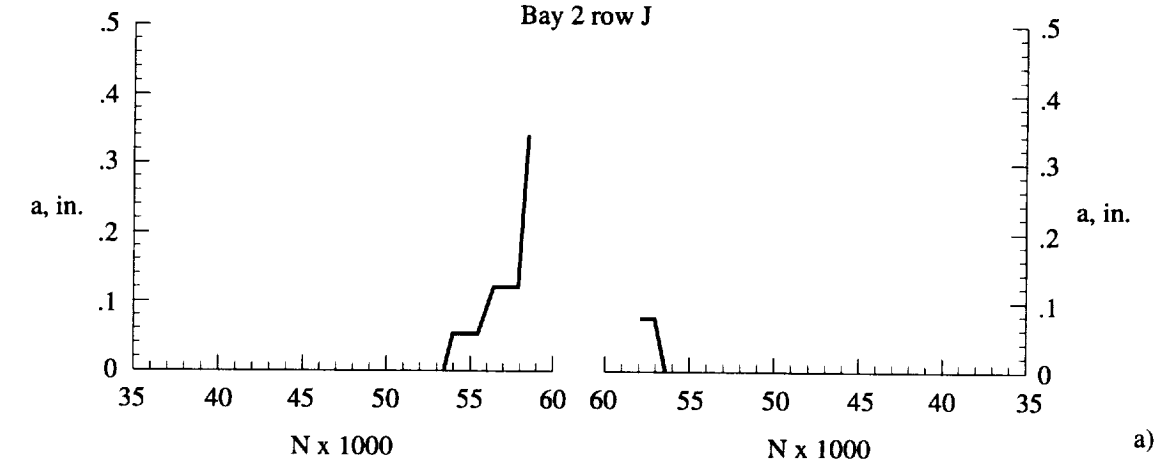

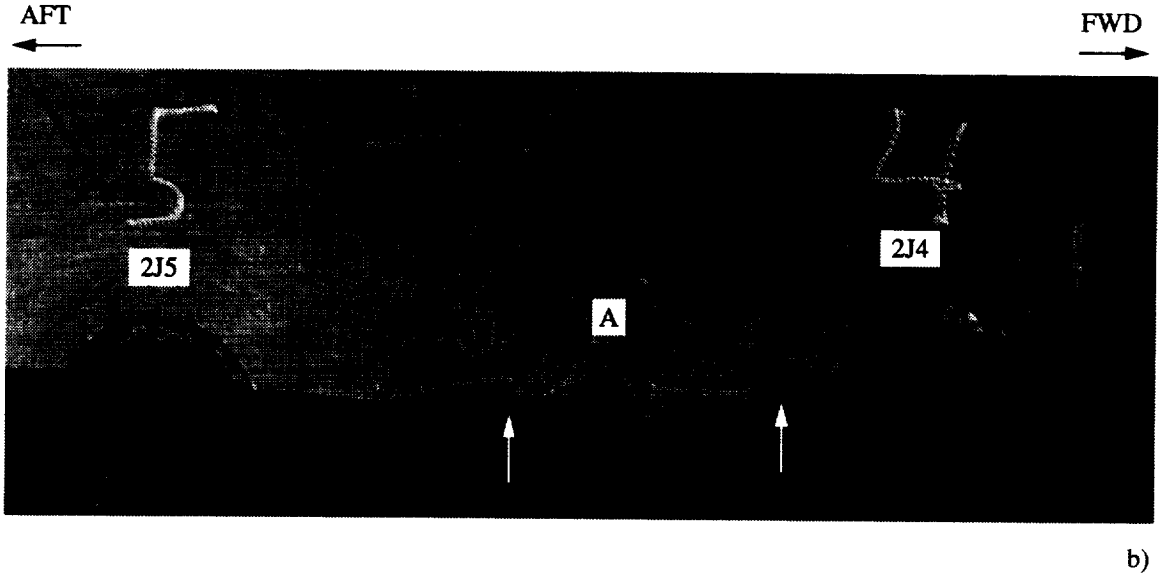

Figure 7.11 a) The figure is a plot of outer skin crack length (a) measured from the rivet outside diameter versus pressurization cycles (N). *In situ* visual crack length measurements were taken during pressure testing. Fatigue crack growth plots are shown for crack segments 2J4 aft and 2J5 forward. The plot for hole 5 shows that very rapid crack growth occurred just prior to crack link-up. b) The photograph shows the upper portion of the outer skin crack surface between rivet holes 2J4 and 2J5. Arrows mark the approximate final position of the fatigue cracks noted (visually) prior to crack link-up. Region A is the likely position where both cracks linked. Most of the crack surface shown in Figure 7.11.b exhibits a roughened appearance. This slant fracture region is characteristic of ductile tearing produced by relatively high crack tip stress intensity. The slant fracture region contains scratches normal to the direction of crack propagation indicative of fracture surface contact resulting from mode III displacement.

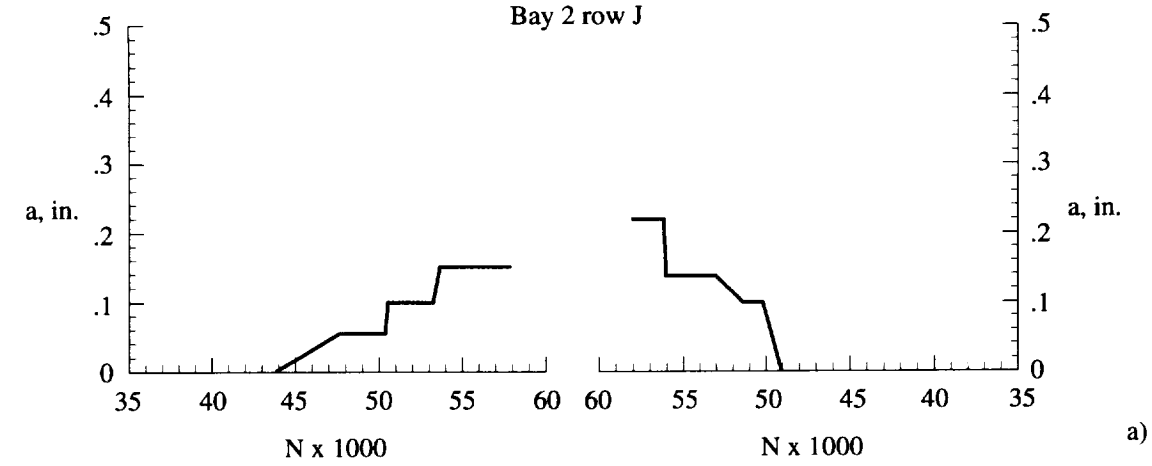

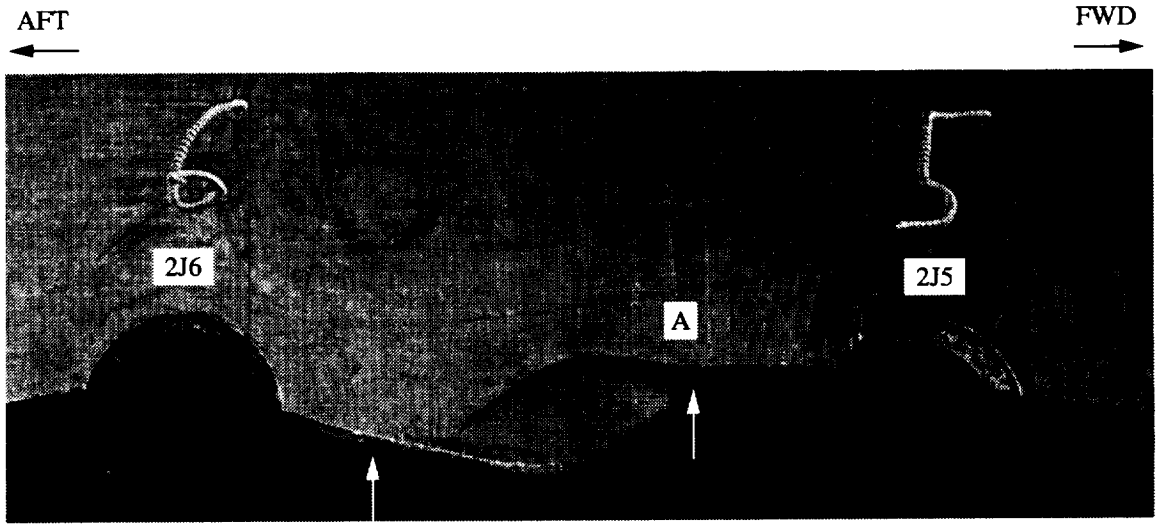

Figure 7.12 a) The figure is a plot of outer skin crack length (a) measured from the rivet outside diameter versus pressurization cycles (N). *In situ* visual crack length measurements were taken during pressure testing. Fatigue crack growth plots are shown for crack segments 2J5 aft and 2J6 forward. b) The photograph shows the upper portion of the outer skin crack surface between rivet holes 2J5 and 2J6. This region is also shown in Figure 7.7.b prior to destructive examination. Arrows mark the approximate final position of the fatigue cracks noted (visually) prior to crack link-up. Region A is the likely position where cracks from both holes had linked. Most of the crack surface shown in Figure 7.12.b exhibits a roughened appearance. This slant fracture region is characteristic of ductile tearing produced by relatively high crack tip stress intensity. The slant fracture region contains no scratches normal to the direction of crack propagation observed in other rivet hole regions. This suggests that this region was captured by the rivets and link-up occurred before large mode III displacement resulted from pillowing.

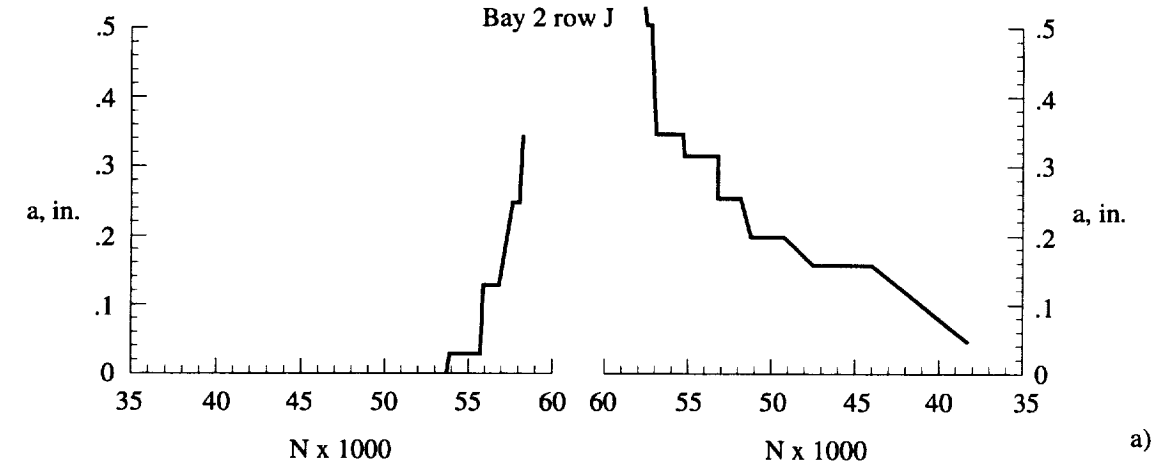

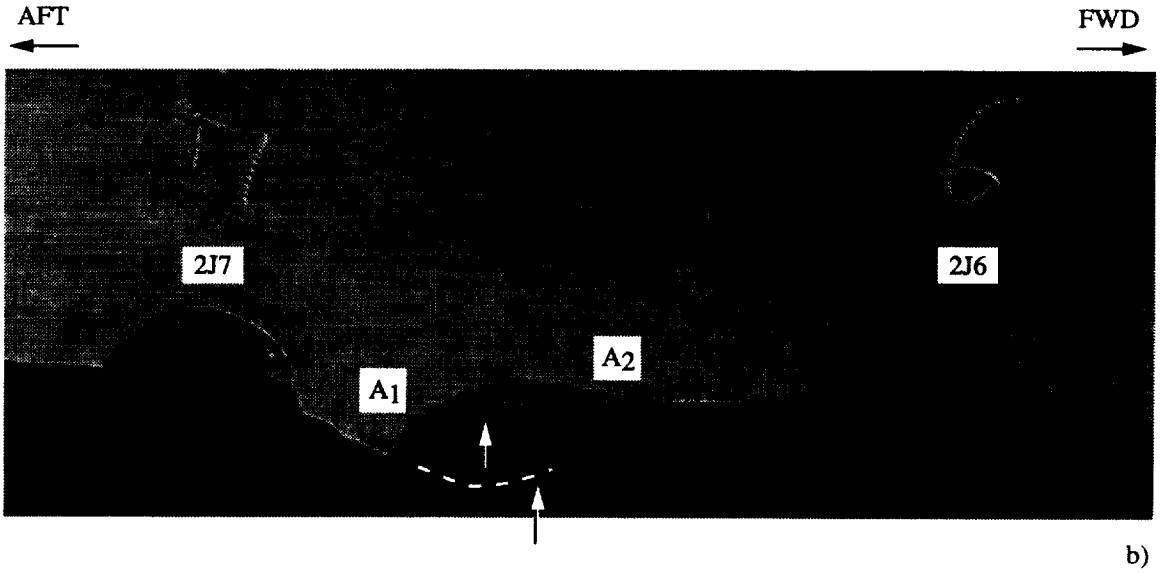

Figure 7.13 a) The figure is a plot of outer skin crack length (a) measured from the rivet outside diameter versus pressurization cycles (N). *In situ* visual crack length measurements were taken during pressure testing. Fatigue crack growth plots are shown for crack segments 2J6 aft and 2J7 forward. The plots for hole 2J6 and 2J7 show that very rapid crack growth occurred just prior to crack link-up. b) The photograph shows the upper portion of the outer skin crack surface between rivet holes 2J6 and 2J7. This region is shown in Figure 7.7.b prior to the destructive examination. Arrows mark the approximate final position of the fatigue cracks noted (visually) prior to crack link-up. Dashed lines represent the approximate path of the crack that propagated from hole 7. Regions A1 or A2 are the likely positions for crack link-up. Most of the crack surface shown in Figure 7.13.b exhibits a roughened appearance. This slant fracture region is characteristic of ductile tearing produced by relatively high crack tip stress intensity. The slant fracture region contains no scratches normal to the direction of crack propagation observed in other rivet hole regions. This suggests that this region was captured by the rivets and link-up occurred before large mode III displacement resulted from pillowing.

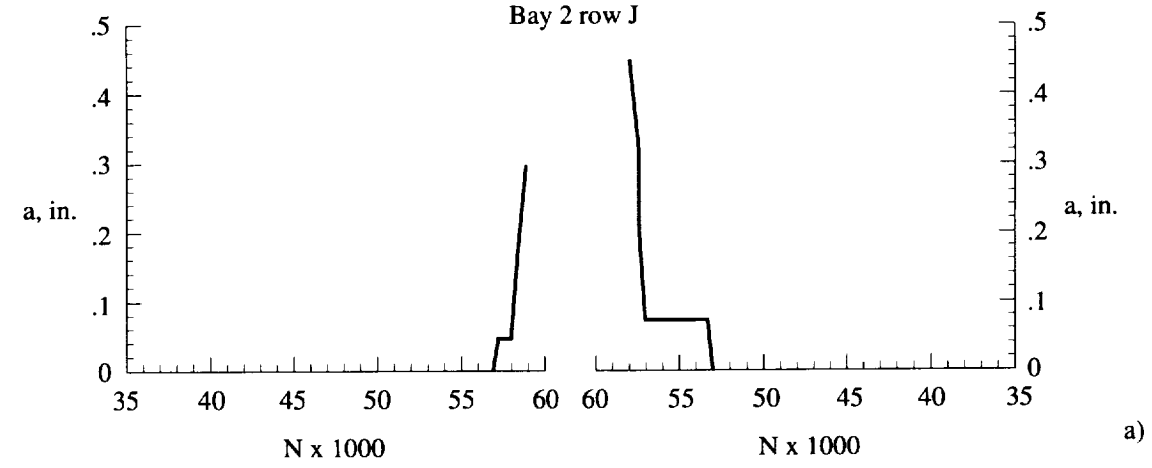

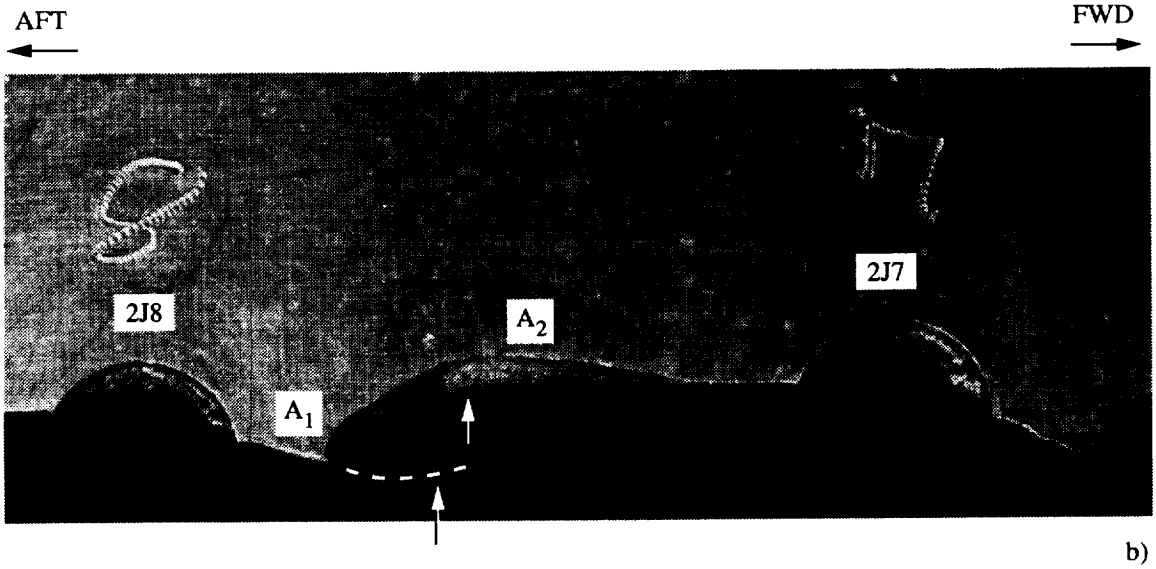

Figure 7.14 a) The figure is a plot of outer skin crack length (a) measured from the rivet outside diameter versus pressurization cycles (N). *In situ* visual crack length measurements were taken during pressure testing. Fatigue crack growth plots are shown for crack segments 2J7 aft and 2J8 forward. The plots for hole 2J7 and 2J8 show that very rapid crack growth occurred just prior to crack link-up. b) The photograph shows the upper portion of the outer skin crack surface between rivet holes 2J7 and 2J8. Arrows mark the approximate final position of the fatigue cracks noted (visually) prior to crack link-up. A dashed line represents the approximate path of the crack that propagated from hole 2J8. Regions A1 or A2 are the likely positions for crack link-up. Most of the crack surface shown in Figure 7.14.b exhibits a roughened appearance. This slant fracture region is characteristic of ductile tearing produced by relatively high crack tip stress intensity. The slant fracture region contains no scratches normal to the direction of crack propagation observed in other rivet hole regions. This suggests that this region was captured by the rivets and link-up occurred before large mode III displacement resulted from pillowing.

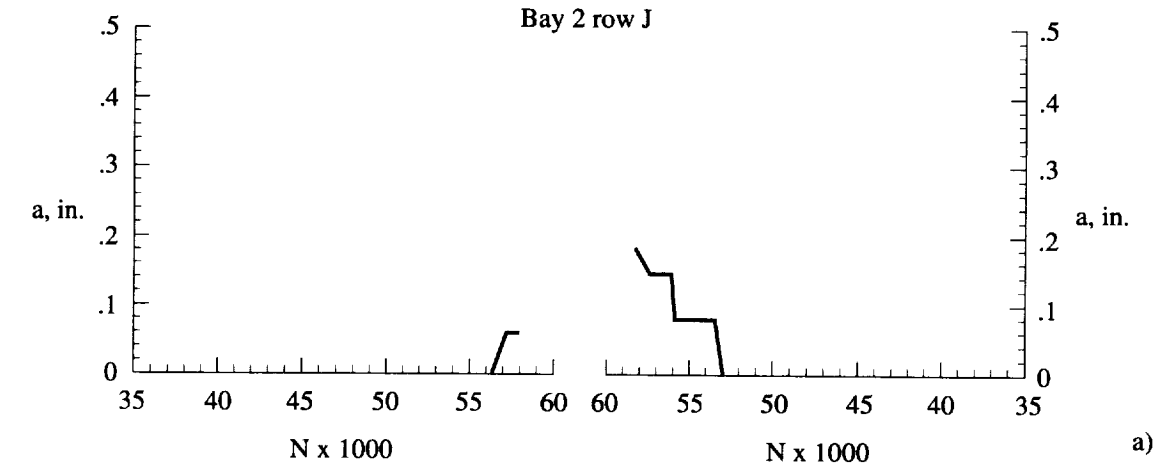

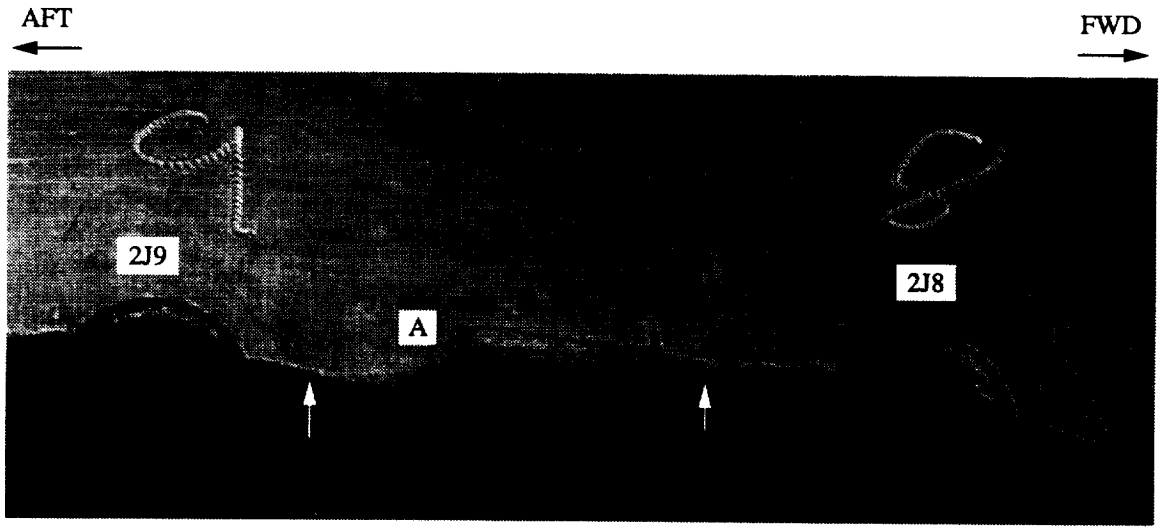

b)

Figure 7.15 a) The figure is a plot of outer skin crack length (a) measured from the rivet outside diameter versus pressurization cycles (N). *In situ* visual crack length measurements were taken during pressure testing. Fatigue crack growth plots are shown for crack segments 2J8 aft and 2J9 forward. b) The photograph shows the upper portion of the outer skin crack surface between rivet holes 2J8 and 2J9. Arrows mark the approximate final position of the fatigue cracks (noted visually) prior to crack link-up. Region A is the location where both cracks had linked. Most of the crack surface shown in Figure 7.15.b exhibits a roughened appearance. This slant fracture region is characteristic of ductile tearing produced by relatively high crack tip stress intensity. The slant fracture region contains scratches normal to the direction of crack propagation indicative of fracture surface contact resulting from mode III displacement.

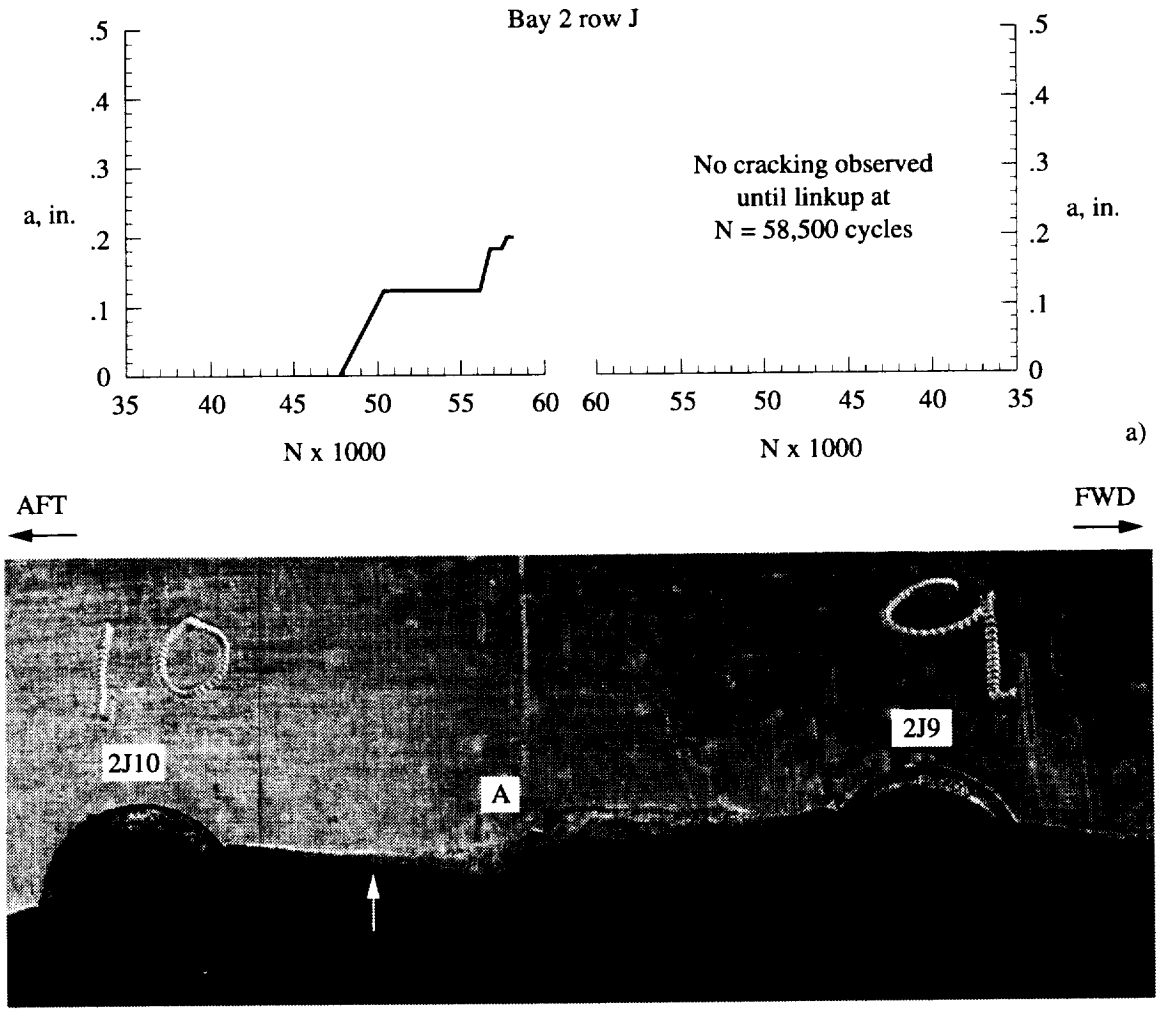

Figure 7.16 a) The figure is a plot of outer skin crack length (a) measured from the rivet outside diameter versus pressurization cycles (N). *In situ* visual crack length measurements were taken during pressure testing. Fatigue crack growth plots are shown for crack segments 2J9 aft and 2J10 forward. No visible cracks were observed from rivet hole 2J9 until after crack link-up. b) The photograph shows the upper portion of the outer skin crack surface between rivet holes 2J9 and 2J10. The arrow marks the approximate final position of the fatigue crack (noted visually) prior to crack link-up. Region A is the location where both cracks had linked. Most of the crack surface shown in Figure 7.16.b exhibits a roughened appearance. This slant fracture region is characteristic of ductile tearing produced by relatively high crack tip stress intensity. The slant fracture region contains scratches normal to the direction of crack propagation indicative of fracture surface contact resulting from mode III displacement.

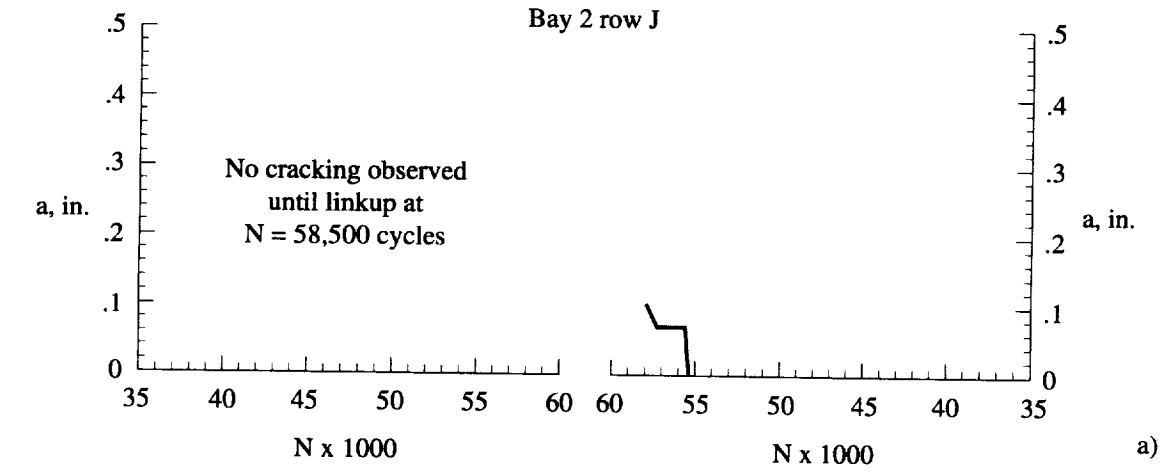

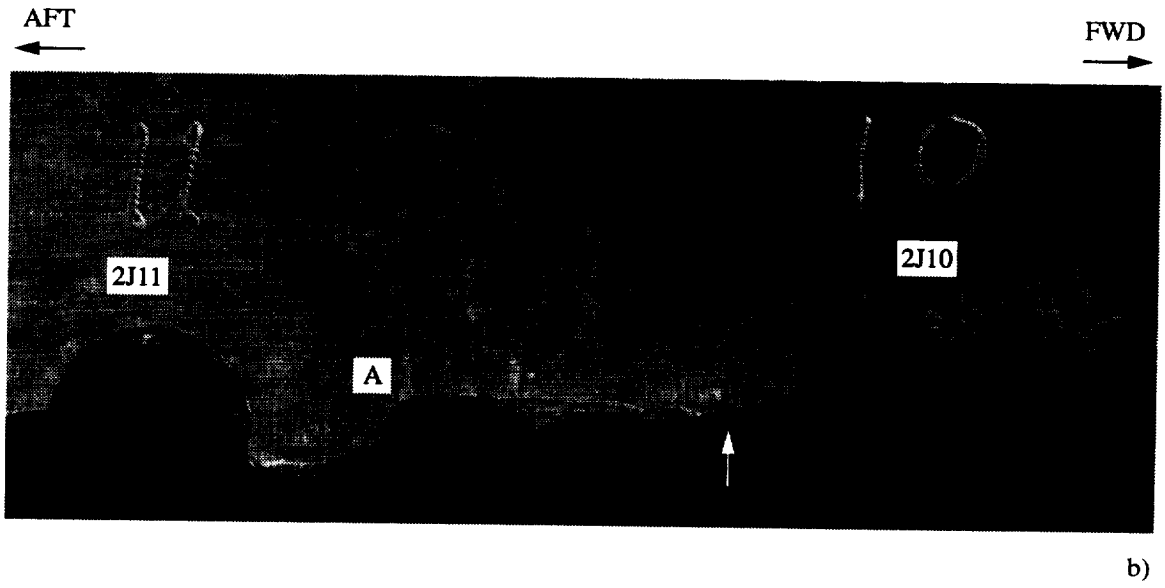

Figure 7.17 a) The figure is a plot of outer skin crack length (a) measured from the rivet outside diameter versus pressurization cycles (N). *In situ* visual crack length measurements were taken during pressure testing. Fatigue crack growth plots are shown for crack segments 2J10 aft and 2J11 forward. No visible cracks were observed from rivet hole 2J11 until after crack link-up. b) The photograph shows the upper portion of the outer skin crack surface between rivet holes 2J10 and 2J11. An arrow marks the approximate final position of the fatigue crack (noted visually) prior to crack link-up. Region A is the location where both cracks had linked. Most of the crack surface shown in Figure 7.17.b exhibits a roughened appearance. This slant fracture region is characteristic of ductile tearing produced by relatively high crack tip stress intensity. The slant fracture region contains scratches normal to the direction of crack propagation indicative of fracture surface contact resulting from mode III displacement.

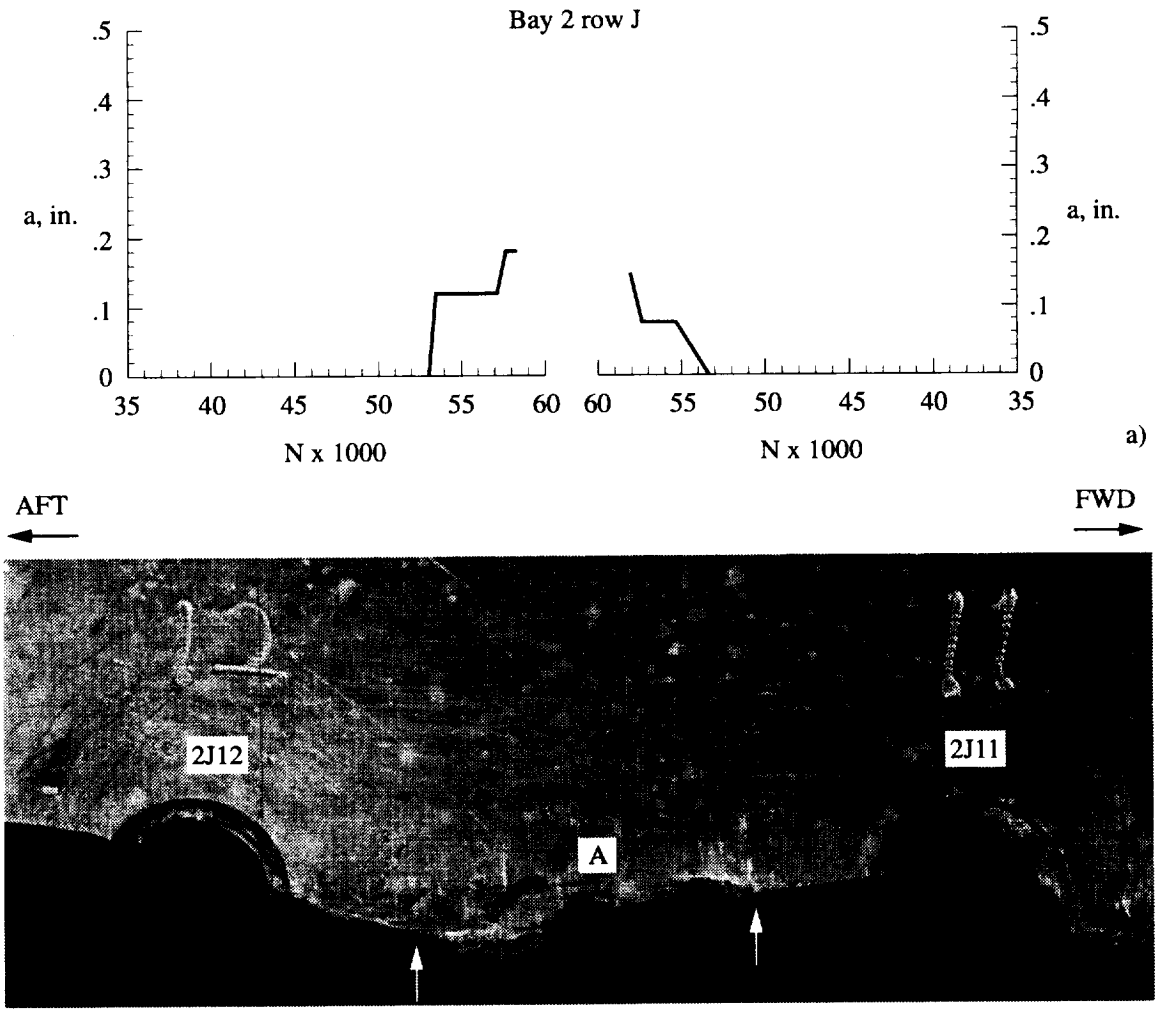

Figure 7.18 a) The figure is a plot of outer skin crack length (a) measured from the rivet outside diameter versus pressurization cycles (N). *In situ* visual crack length measurements were taken during pressure testing. Fatigue crack growth plots are shown for crack segments 2J11 aft and 2J12 forward. b) The photograph shows the upper portion of the outer skin crack surface between rivet holes 2J11 and 2J12. Arrows mark the approximate final position of the fatigue cracks (noted visually) prior to crack link-up. Region A is the location where both cracks had linked. Most of the crack surface shown in Figure 7.18.b exhibits a roughened appearance. This slant fracture region is characteristic of ductile tearing produced by relatively high crack tip stress intensity. The slant fracture region contains scratches normal to the direction of crack propagation indicative of fracture surface contact resulting from mode III displacement.

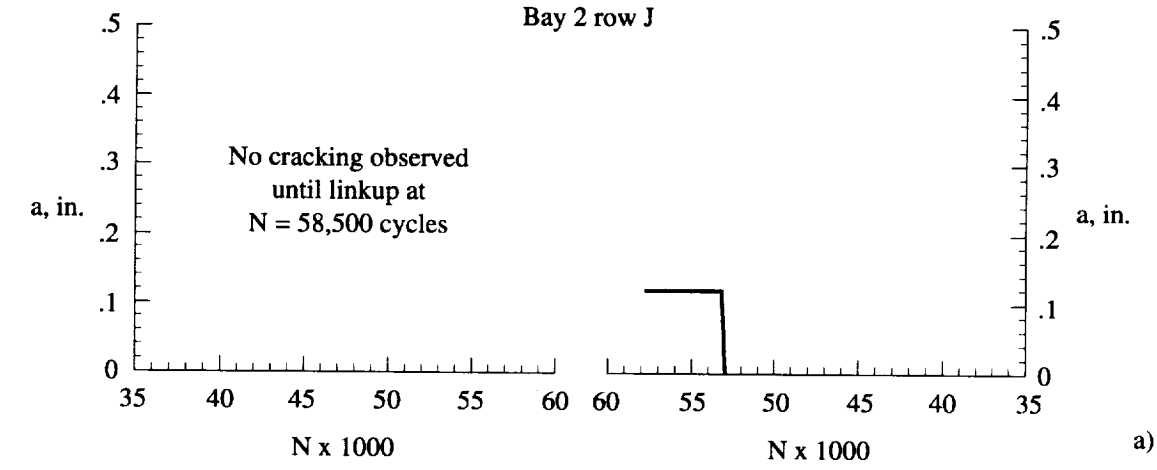

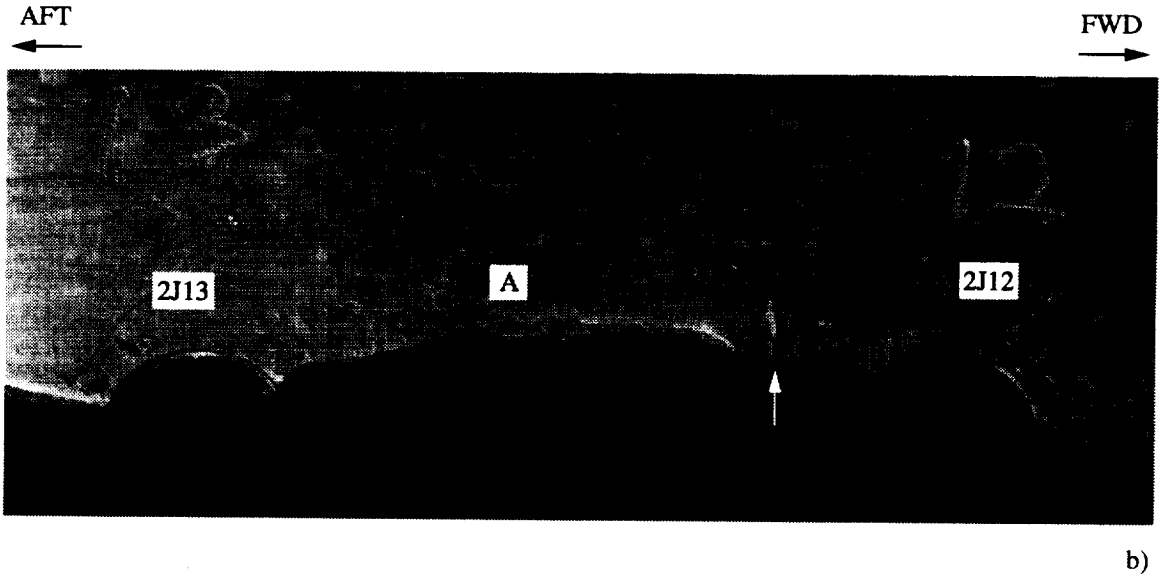

Figure 7.19 a) The figure is a plot of outer skin crack length (a) measured from the rivet outside diameter versus pressurization cycles (N). *In situ* visual crack length measurements were taken during pressure testing. Fatigue crack growth plots are shown for crack segments 2J12 aft and 2J13 forward. No visible cracks were observed from rivet hole 2J13 until after crack link-up. b) The photograph shows the upper portion of the outer skin crack surface between rivet holes 2J12 and 2J13. The arrow marks the approximate final position of the fatigue crack (noted visually) prior to crack link-up. Region A is the likely location for crack link-up. Most of the crack surface shown in Figure 7.19.b exhibits a roughened appearance. This slant fracture region is characteristic of ductile tearing produced by relatively high crack tip stress intensity. The slant fracture region contains scratches normal to the direction of crack propagation indicative of fracture surface contact resulting from mode III displacement.

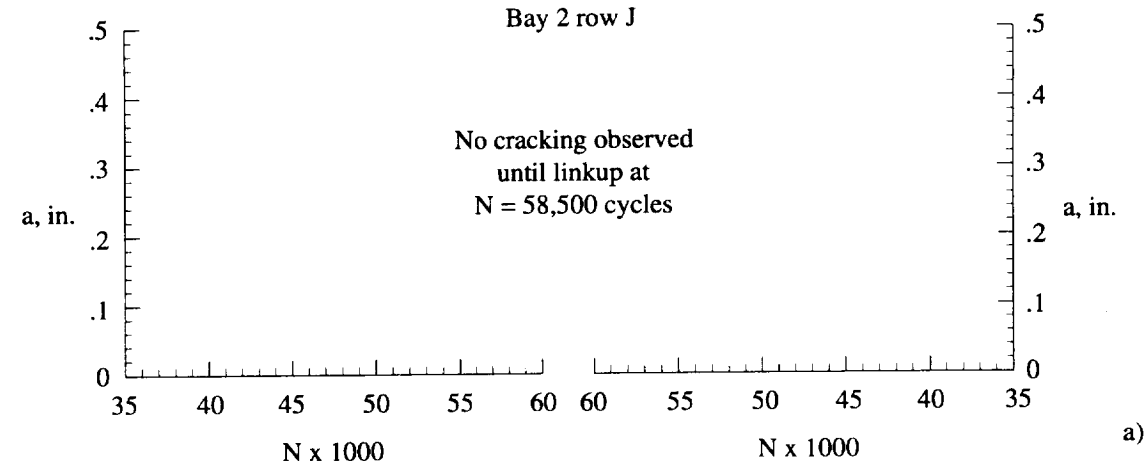

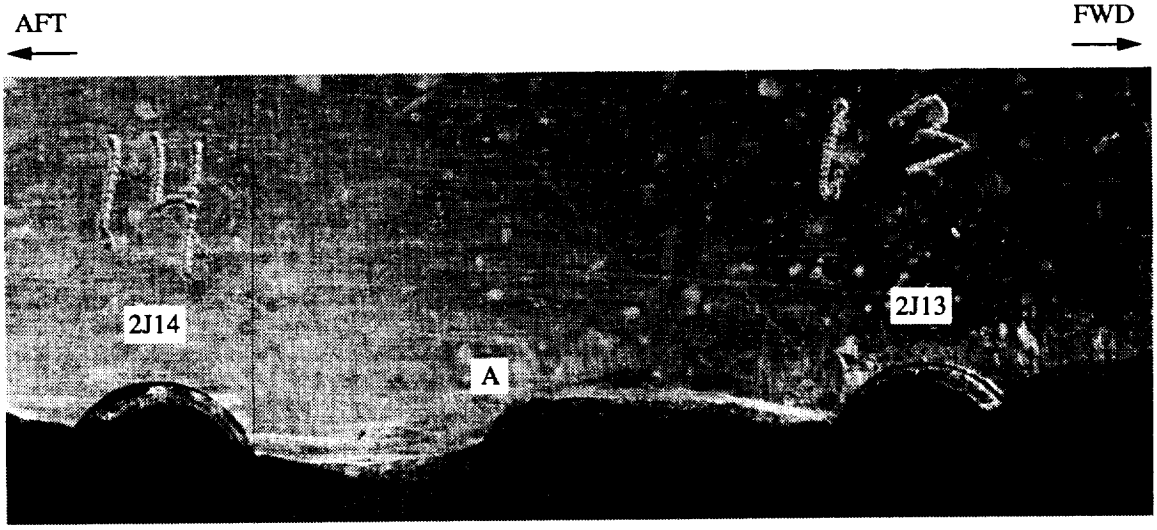

Figure 7.20 a) No visible cracks were observed between rivet holes 2J13 and 2J14 until after crack link-up. b) The photograph shows the upper portion of the crack surface between rivet holes 2J13 and 2J14. Region A is the likely location for crack link-up. Most of the crack surface shown in Figure 7.20.b exhibits a roughened appearance. This slant fracture region is characteristic of ductile tearing produced by relatively high crack tip stress intensity. The slant fracture region contains scratches normal to the direction of crack propagation indicative of fracture surface contact resulting from mode III displacement.

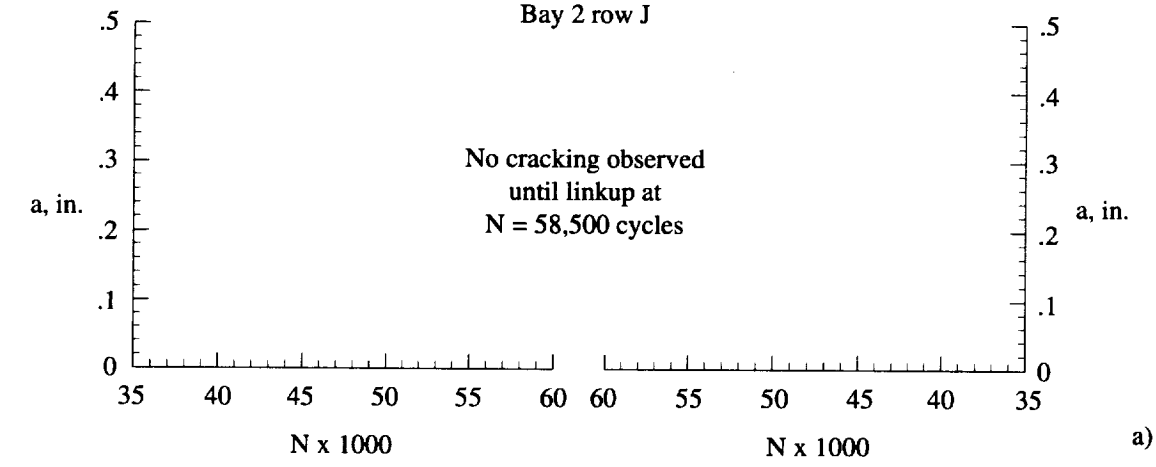

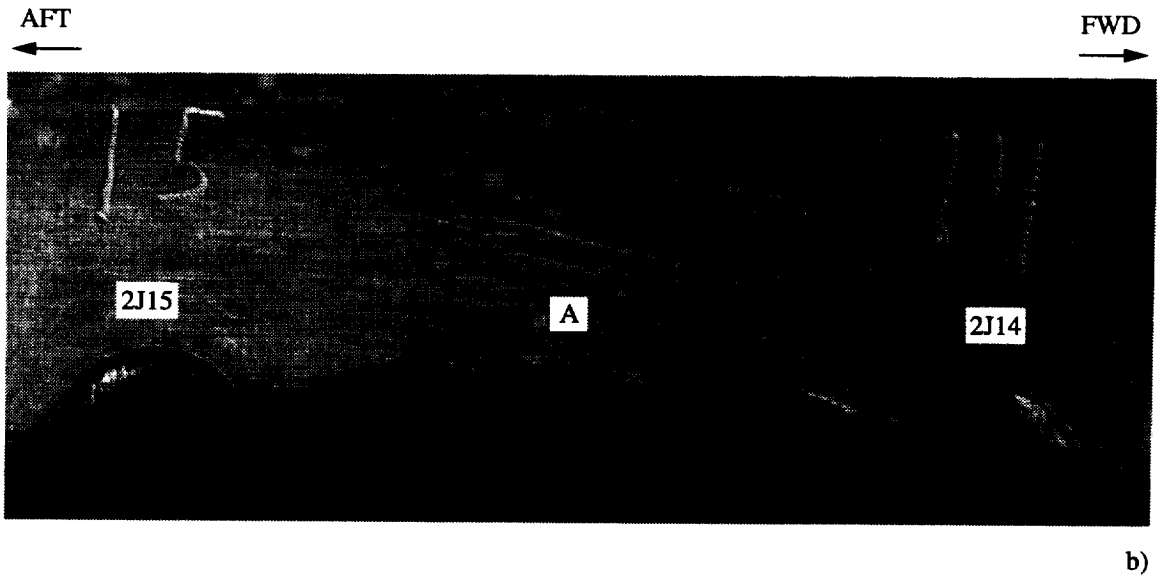

Figure 7.21 a) No visible cracks were observed between rivet holes 2J14 and 2J15 until after crack link-up. b) The photograph shows the upper portion of the crack surface between rivet holes 2J14 and 2J15. The region of crack link-up is less defined between holes 2J14 and 2J15, thus no crack link-up region is defined in Figure 7.21.b. Most of the crack surface shown in Figure 7.21.b exhibits a roughened appearance. This slant fracture region is characteristic of ductile tearing produced by relatively high crack tip stress intensity. The slant fracture region contains scratches normal to the direction of crack propagation indicative of fracture surface contact resulting from mode III displacement.

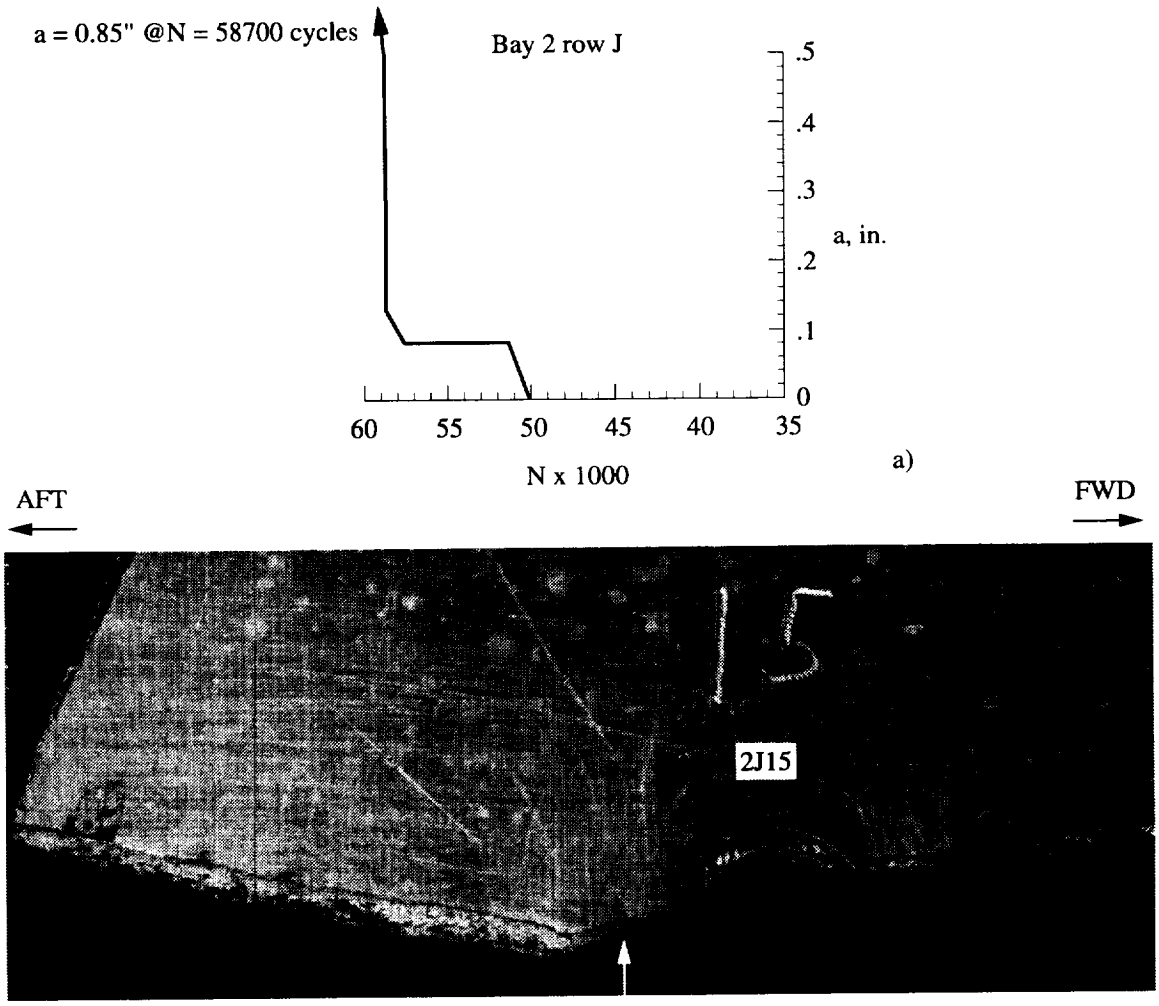

Figure 7.22 a) The figure is a plot of outer skin crack length (a) measured from the rivet outside diameter versus pressurization cycles (N). *In situ* visual crack length measurements were taken during pressure testing. The plot shown for crack segments 2J4 aft reveals that crack growth was very rapid prior to terminating in the tear strap region. b) The photograph shows the upper portion of the outer skin crack surface from hole 2J15. The arrow marks the approximate final position of the fatigue crack (noted visually) prior to crack link-up. Most of the crack surface shown in Figure 7.22.b exhibits a roughened appearance. This slant fracture region is characteristic of ductile tearing produced by relatively high crack tip stress intensity. The slant fracture region contains scratches normal to the direction of crack propagation indicative of fracture surface contact resulting from mode III displacement.

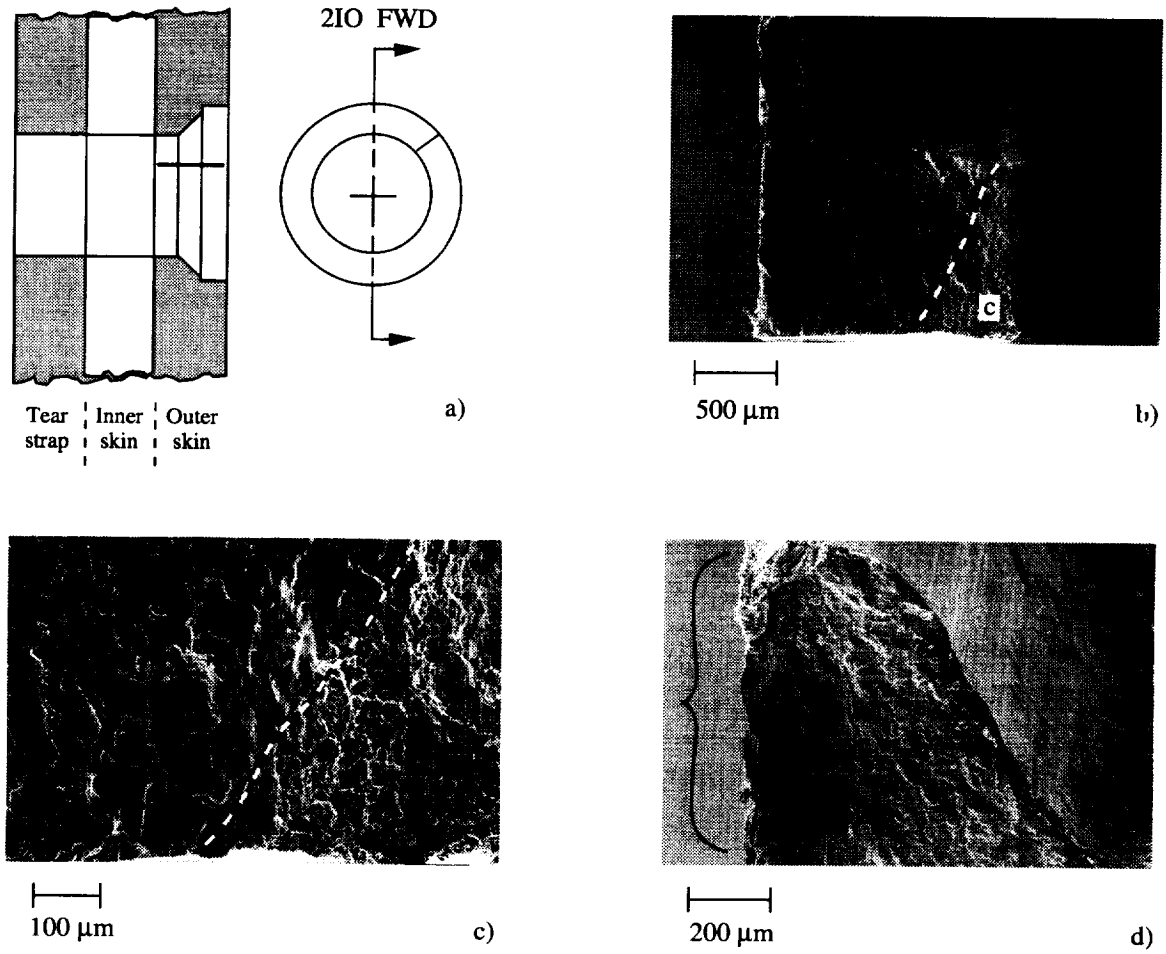

Figure 7.23 a) The schematic shows the rivet hole 2I0 configuration and the location of the outer skin fatigue crack oriented in the forward direction and about the 2 o'clock position. b) The SEM micrograph shows a portion of the fatigue crack and the rivet hole (top of the micrograph). The dashed line marks a portion of the fatigue crack front. The missing portion of the fracture surface was inadvertently cut during the destructive examination. c) The SEM micrograph shows the crack front region (region "c" in Figure 7.23.b), comparing the smooth transgranular fatigue crack morphology to the rough dimpled ductile tearing of the overload fracture surface (the dashed boundary line marks the fatigue crack front and overload regions) produced during destructive examination of the rivet hole. d) The SEM micrograph shows the fatigue fracture surface at the rivet hole shank region. The bracket marks the likely region of crack initiation along the faying surface.

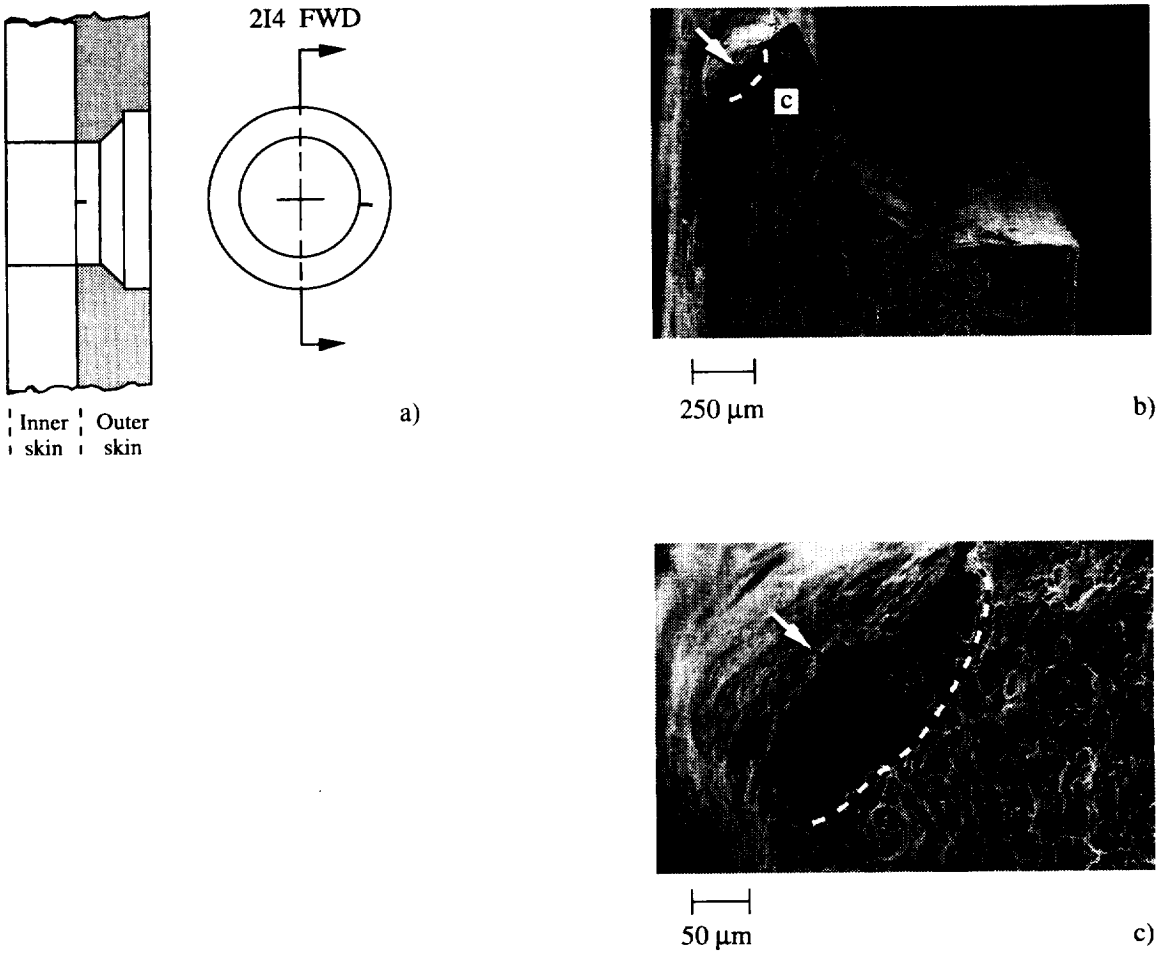

Figure 7.24 a) The schematic shows the rivet hole 2I4 configuration and the location of the outer skin fatigue crack oriented in the forward direction and about the 3 o'clock position. b) The SEM micrograph shows a small fatigue crack at the rivet hole corner marked by an arrow. c) The SEM micrograph shows the fatigue crack in Figure 7.24.b at higher magnification.

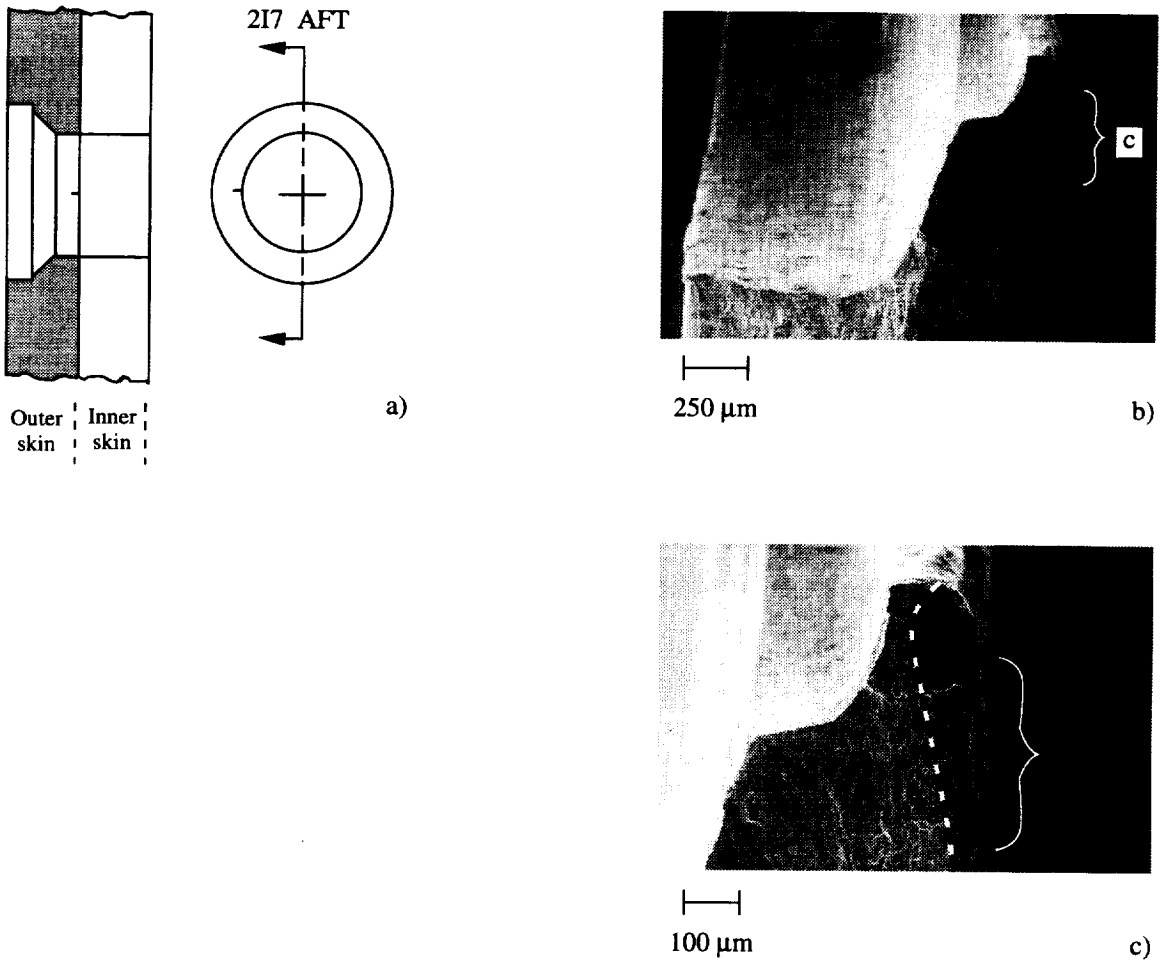

Figure 7.25 a) The schematic shows the rivet hole 2I7 configuration and the location of the outer skin fatigue crack oriented in the aft direction and about the 9 o'clock position. b) The SEM micrograph shows the fatigue crack along the faying surface. The bracket marks the region of crack initiation along the faying surface. Note the rivet hole shank region exhibits an anomalous configuration. c) The SEM micrograph shows the fatigue crack (region "c" in Figure 7.25.b) at high magnification. The dashed line marks the fatigue crack front. The bracket marks the region of crack initiation along the rough faying surface.

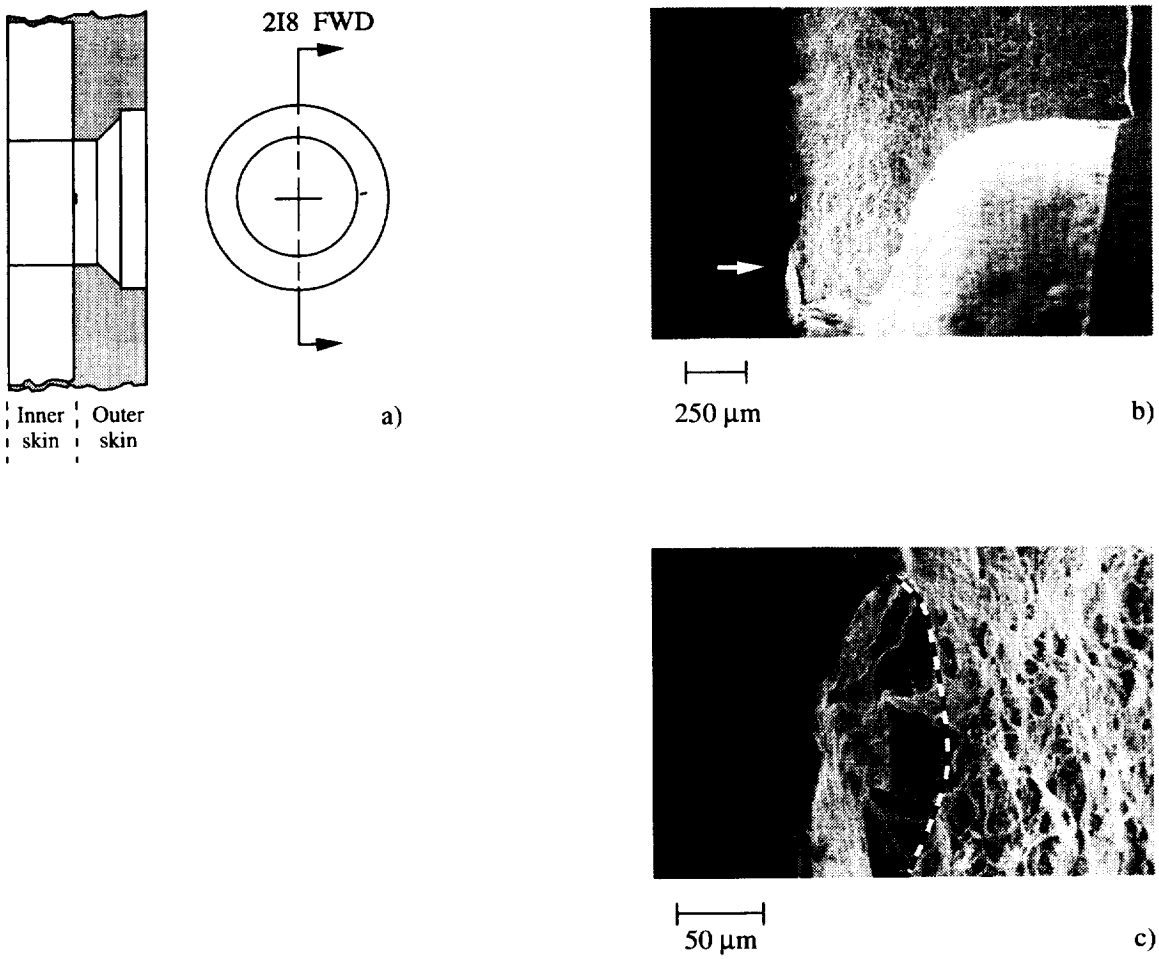

Figure 7.26 a) The schematic shows the rivet hole 2I8 configuration and the location of the outer skin fatigue crack oriented in the forward direction and about the 3 o'clock position. b) The SEM micrograph shows a small fatigue crack (marked by the arrow) located at the faying surface c) The SEM micrograph shows the small fatigue crack contained in the clad layer at high magnification. The dashed line marks the fatigue crack front. The crack initiated in a roughened surface region at the faying surface.

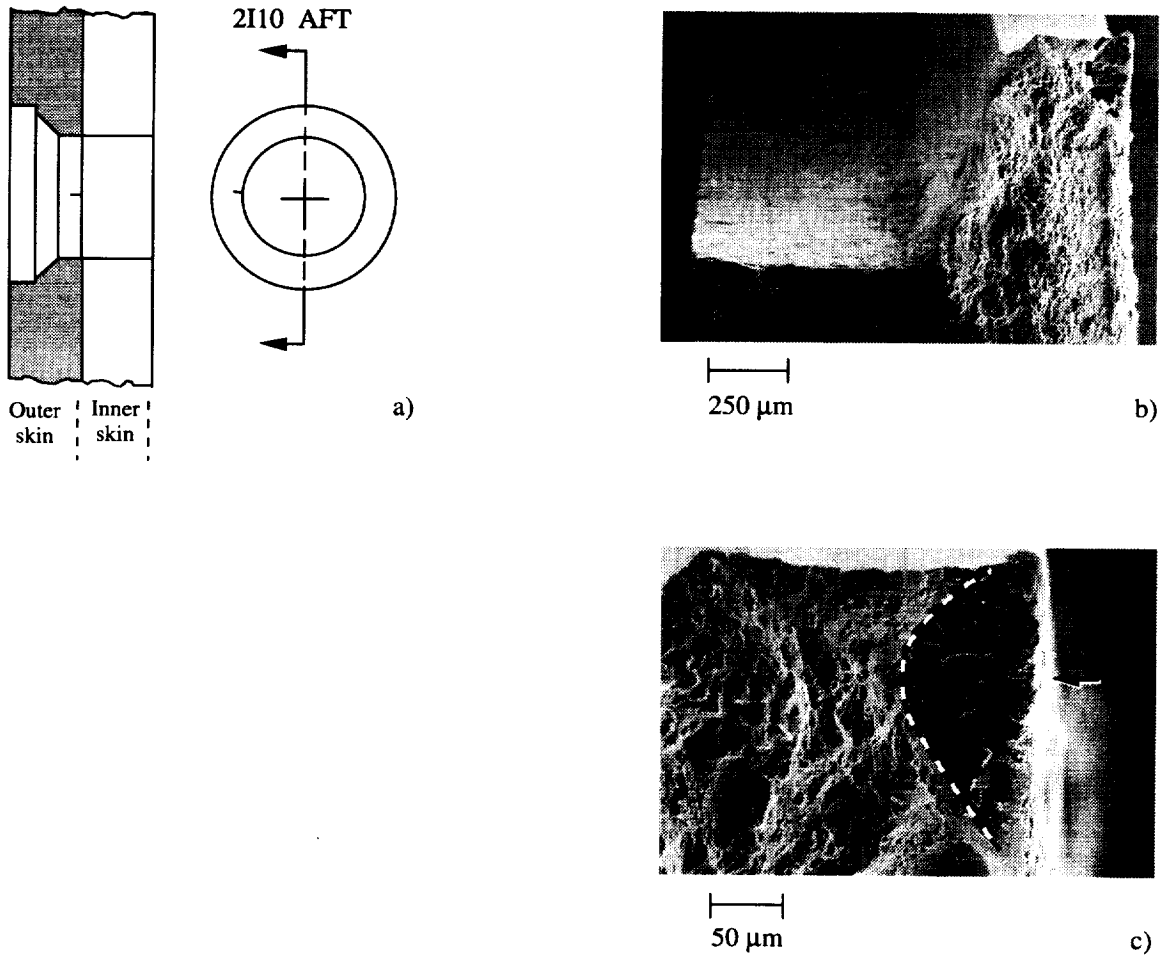

Figure 7.27 a) The schematic shows the rivet hole 2I10 configuration and the location of the outer skin fatigue crack oriented in the aft direction and about the 9 o'clock position. b) The SEM micrograph shows a small fatigue crack located at the rivet hole shank region along the faying surface. The dashed line marks the fatigue crack front. c) The SEM micrograph shows the small fatigue crack at high magnification. The dashed line marks the fatigue crack front. The crack initiated in a roughened region along the faying surface.

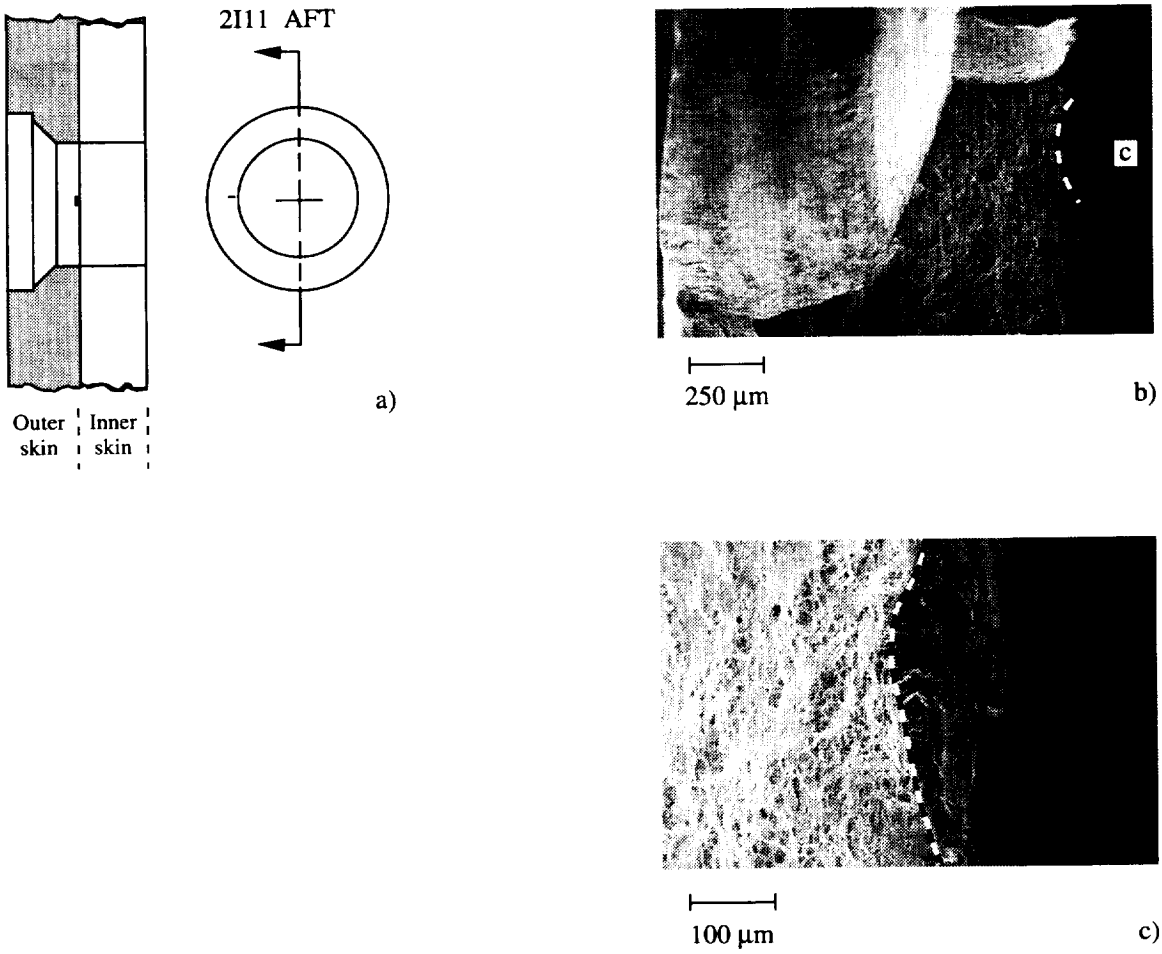

Figure 7.28 a) The schematic shows the rivet hole 2I11 configuration and the location of the outer skin fatigue crack oriented in the aft direction and about the 9 o'clock position. b) The SEM micrograph shows a small elongated fatigue crack located at the faying surface. The dashed line marks the fatigue crack front. c) The SEM micrograph shows the small fatigue crack contained in the clad layer at high magnification, region "c" in Figure 7.28.b. The dashed line marks the fatigue crack front. The crack initiated in a roughened region along the faying surface.

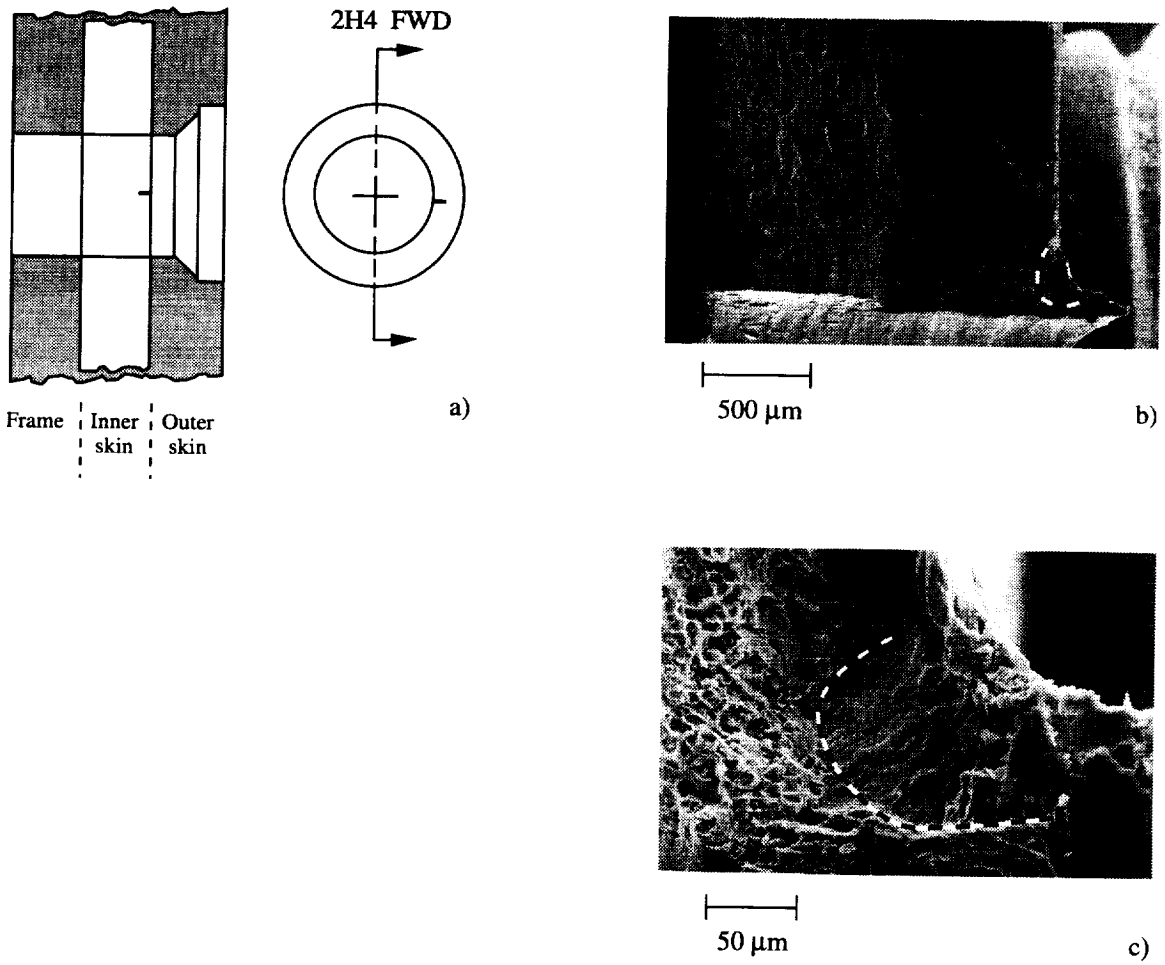

Figure 7.29 a) The schematic shows the rivet hole 2H4 configuration and the location of the inner skin fatigue crack oriented in the forward direction and about the 3 o'clock position. b) The SEM micrograph shows a small fatigue crack located near a rivet hole corner burr. The dashed line marks the fatigue crack front. c) The SEM micrograph shows the small fatigue crack at high magnification.

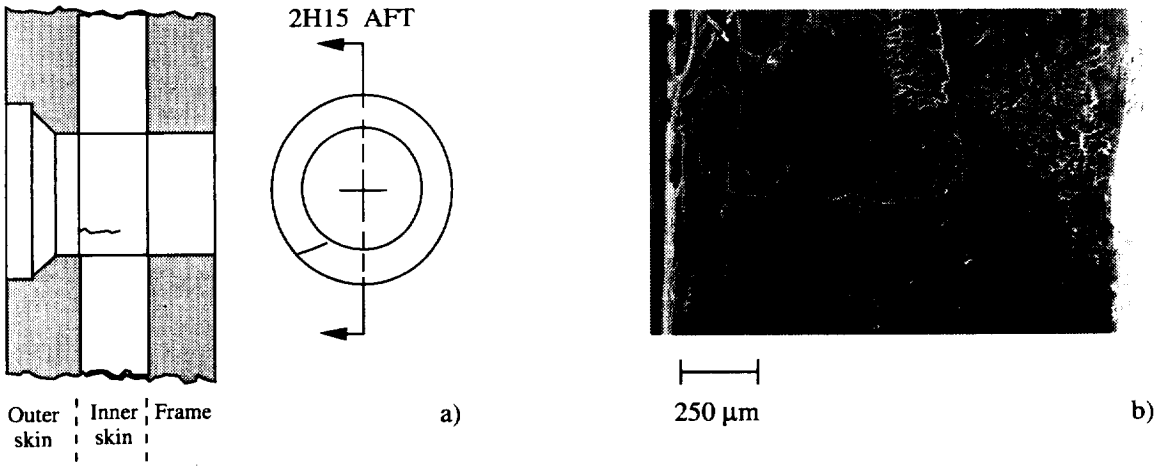

Figure 7.30 a) The schematic shows the rivet hole 2H15 configuration and the location of the inner skin fatigue crack oriented in the aft direction and below the 8 o'clock position. b) The SEM micrograph shows the inside surface of the rivet hole and a fatigue crack extending from the outboard corner. The crack was partially opened during the destructive examination. SEM examination into the partially opened corner crack verified that the crack was a transgranular fatigue crack.

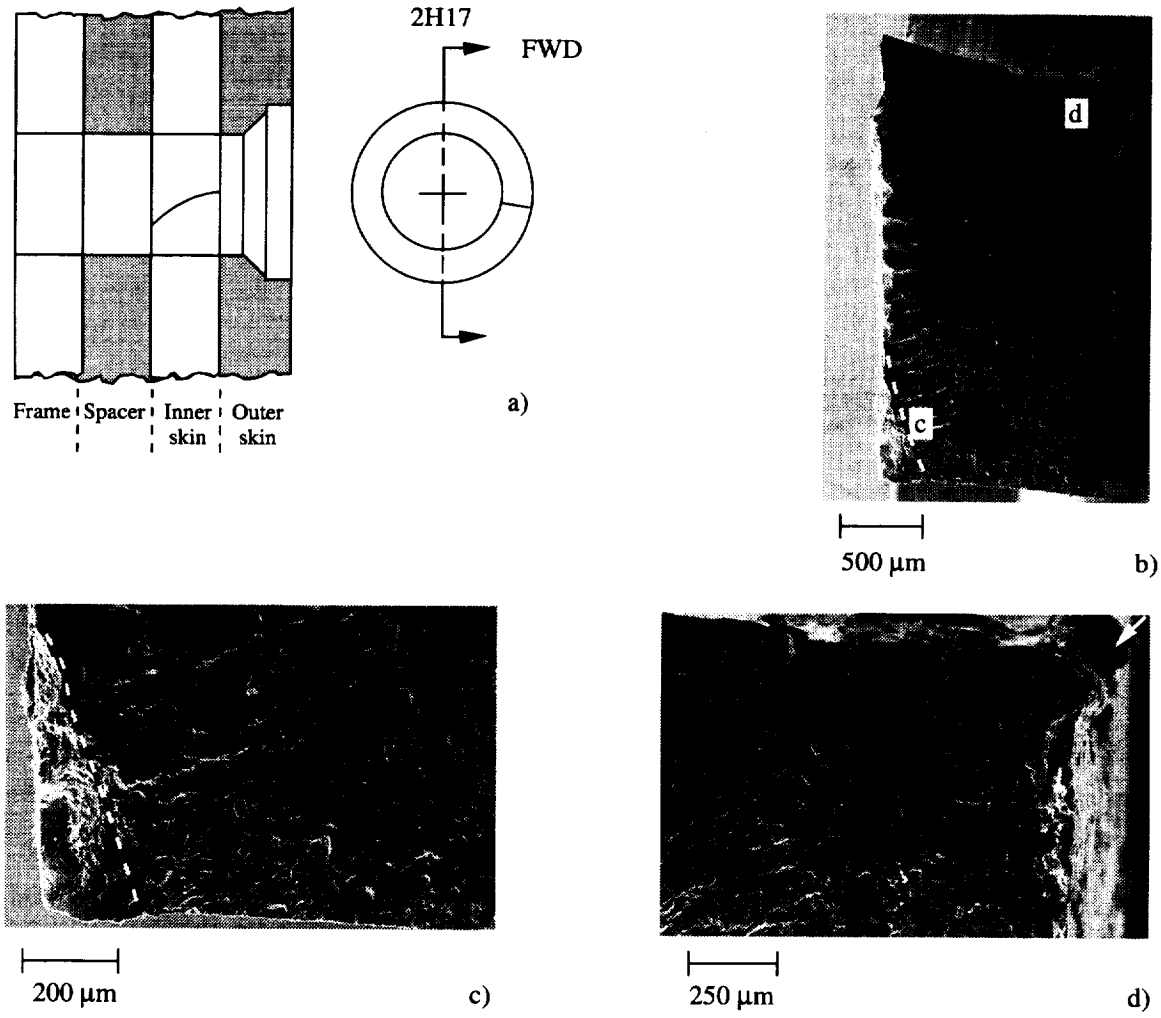

Figure 7.31 a) The schematic shows the rivet hole 2H17 configuration and the location of the inner skin fatigue crack oriented in the forward direction and about the 3 o'clock position. b) The SEM micrograph shows the fatigue crack fracture surface (the direction of crack propagation is from top to bottom of the figure) at the inner skin rivet hole which is located at the top of the micrograph. The fatigue crack was cut during the removal of the specimen from the panel and a portion of the fatigue crack surface is not shown in the figure. c) The SEM micrograph shows the fatigue crack surface at region "c" in Figure 7.31.b. The dashed line marks the remainder of the fatigue crack front. The crack front configuration suggests that the crack extends farther along the outboard surface of the inner skin compared to the inboard surface. d) The SEM micrograph shows the crack initiation region near the outboard corner of the rivet hole (region "d" in Figure 7.31.b). The region of crack initiation (arrow) along the outboard faying surface exhibits disturbed metal.

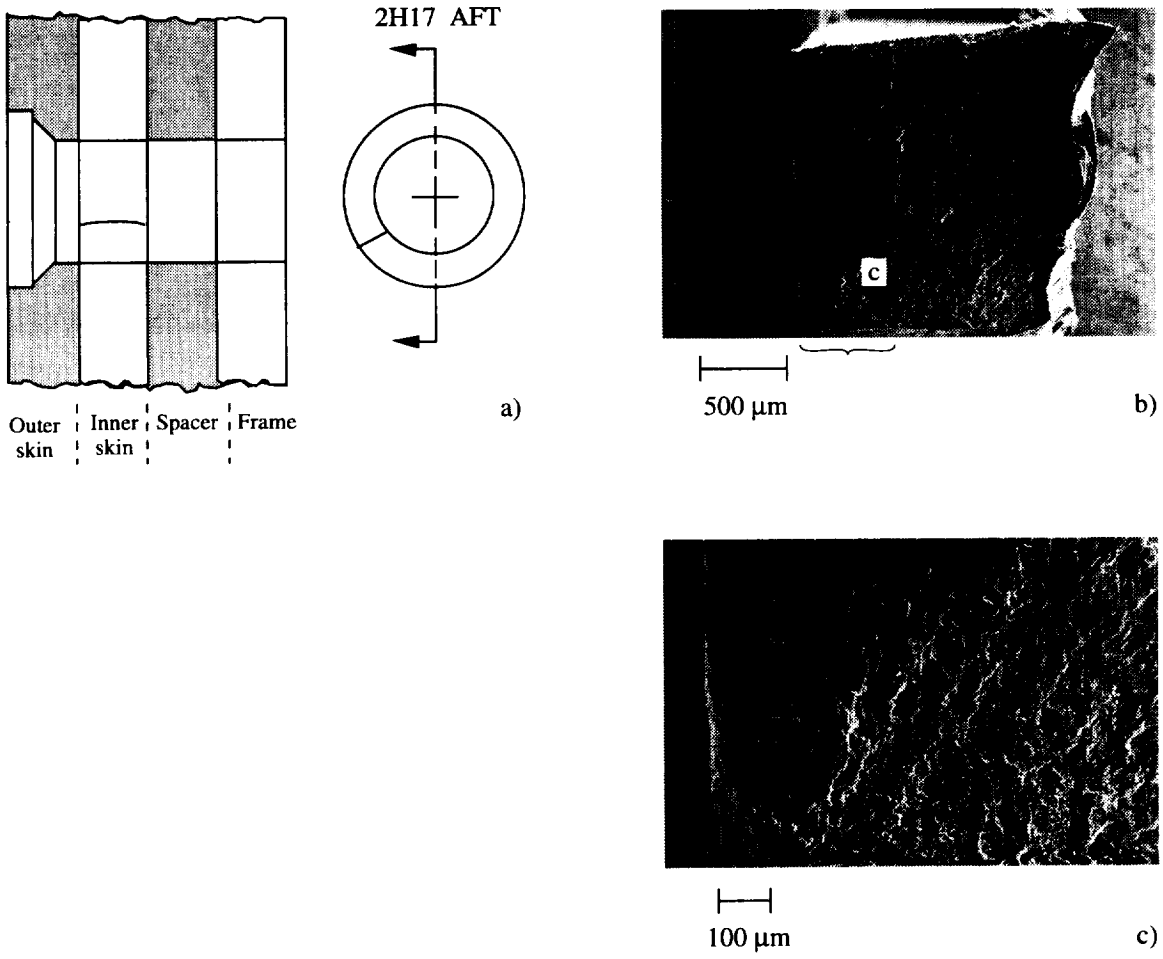

Figure 7.32 a) The schematic shows the rivet hole 2H17 configuration and the location of the inner skin fatigue crack oriented in the aft direction and below the 9 o'clock position. b) The SEM micrograph shows the inner skin fatigue crack fracture surface (the direction of crack propagation is from the bottom to the top of the figure). The rivet hole is located at the bottom of the micrograph. The fatigue crack was cut during the removal of the specimen from the panel and a portion of the fatigue crack surface is not shown in the figure. c) The SEM micrograph shows the fatigue crack surface at the outboard corner (approximate crack initiation site) of the rivet hole, region "c" in Figure 7.31.b.

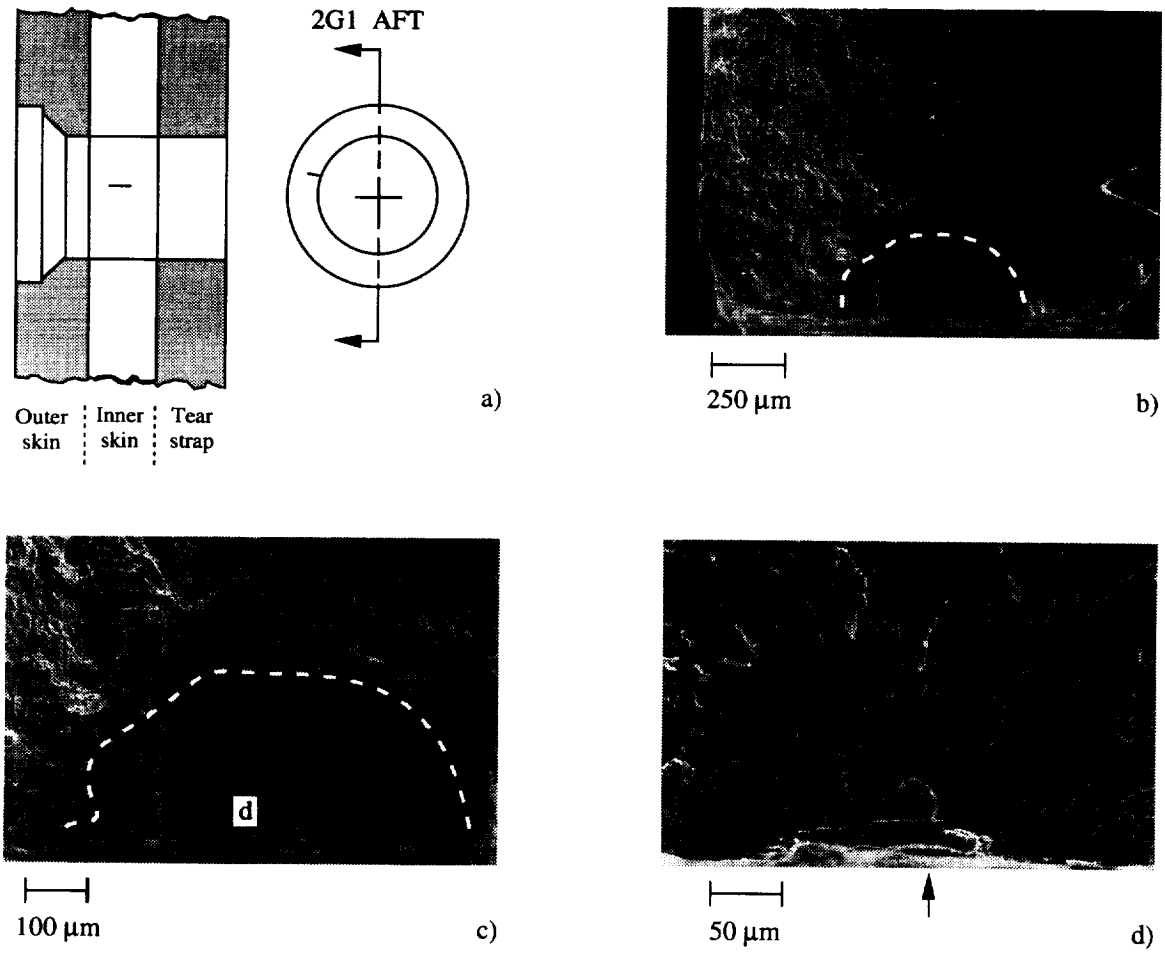

Figure 7.33 a) The schematic shows the rivet hole 2G1 configuration and the location of the inner skin fatigue crack oriented in the aft direction and above the 9 o'clock position. b) The SEM micrograph shows the fatigue crack at the mid-thickness location of the inner skin rivet hole (bottom of the micrograph). The dashed line marks the fatigue crack front. c) The SEM micrograph shows the semicircular shaped surface fatigue crack at higher magnification. The dashed line marks the fatigue crack front. d) The SEM micrograph shows the crack initiation region (region "d" in Figure 7.33.c). The region of crack initiation marked by an arrow along the inside surface of the rivet hole exhibits disturbed metal.

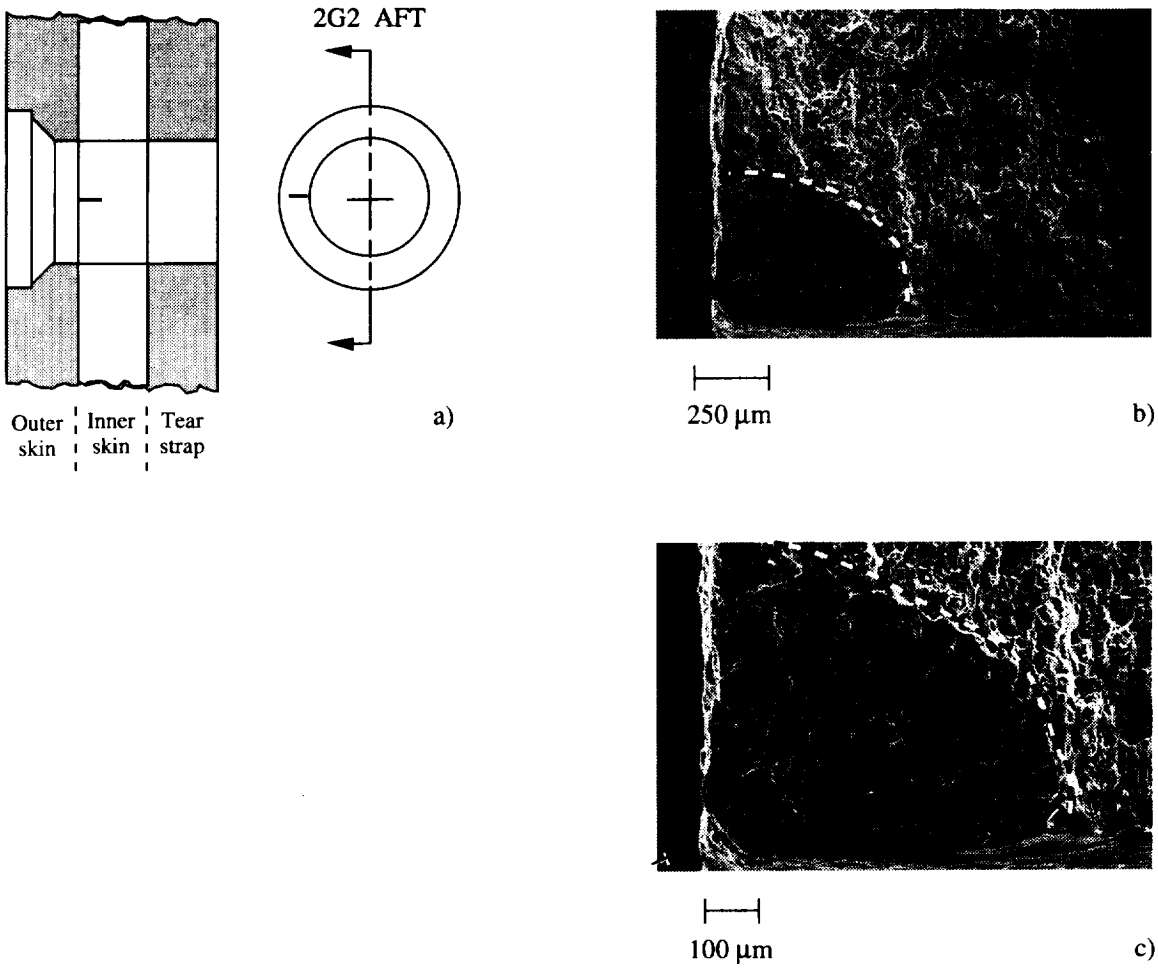

Figure 7.34 a) The schematic shows the rivet hole 2G2 configuration and the location of the inner skin fatigue crack oriented in the aft direction and at the 9 o'clock position. b) The SEM micrograph shows the fatigue crack fracture surface located at the outboard corner of the rivet hole (bottom-left of the micrograph). The dashed line marks the fatigue crack front. c) The SEM micrograph shows the corner fatigue crack at higher magnification. The arrow marks the region of crack initiation and the dashed line marks the fatigue crack front.

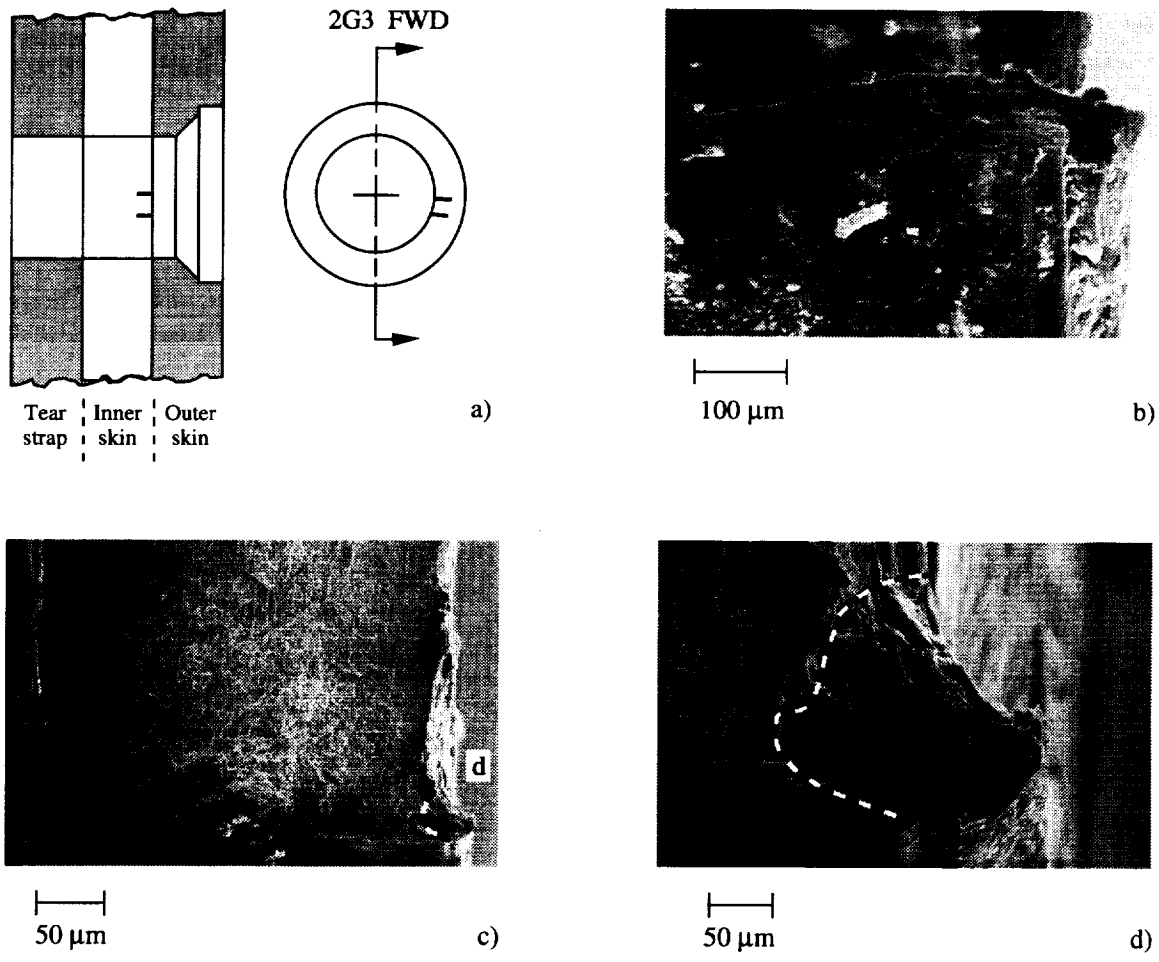

Figure 7.35 a) The schematic shows the rivet hole 2G3 configuration and the location of two inner skin fatigue cracks oriented in the forward direction and slightly below the 3 o'clock position. b) The SEM micrograph shows the surface of the rivet hole and a partially opened fatigue crack at the outboard corner after the initial destructive examination straining operation. A burr and disturbed metal are observed at the corner. c) The SEM micrograph shows the corner fatigue crack surface at the outboard corner of the rivet hole. The dashed line marks the fatigue crack front. d) The SEM micrograph shows the corner fatigue crack at high magnification (region "d" in Figure 7.35.c). The region of crack initiation is located near disturbed metal produced by a corner burr.

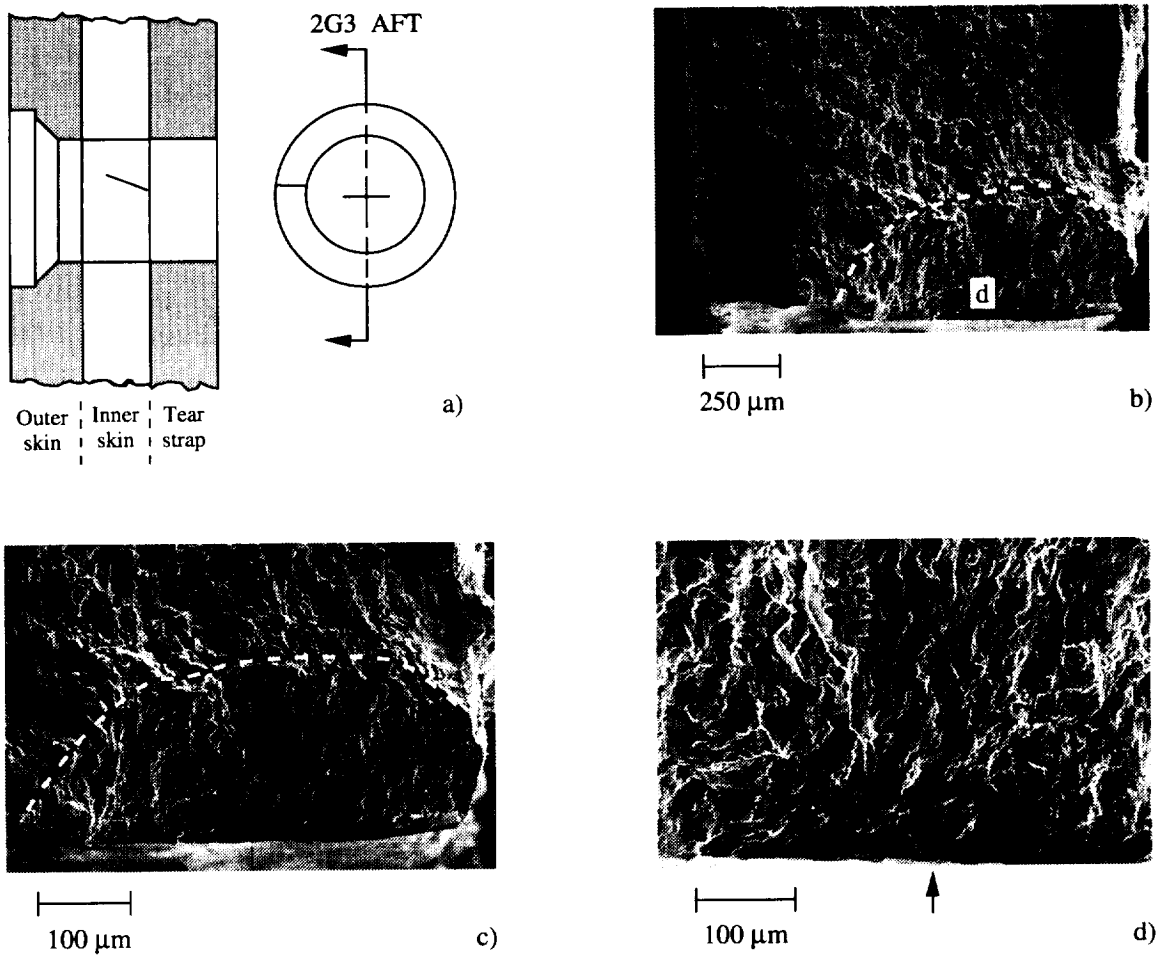

Figure 7.36 a) The schematic shows the rivet hole 2G3 configuration and the location of the inner skin fatigue crack oriented in the aft direction and about the 9 o'clock position. b) The SEM micrograph shows the fatigue crack located along the rivet hole (bottom of the micrograph). The dashed line marks the fatigue crack front. c) The SEM micrograph shows the fatigue crack surface at higher magnification. The dashed line marks the fatigue crack front. d) The SEM micrograph shows the fatigue crack along the rivet hole inside surface (region "d" in Figure 7.36.b). The arrow marks the likely site of crack initiation.

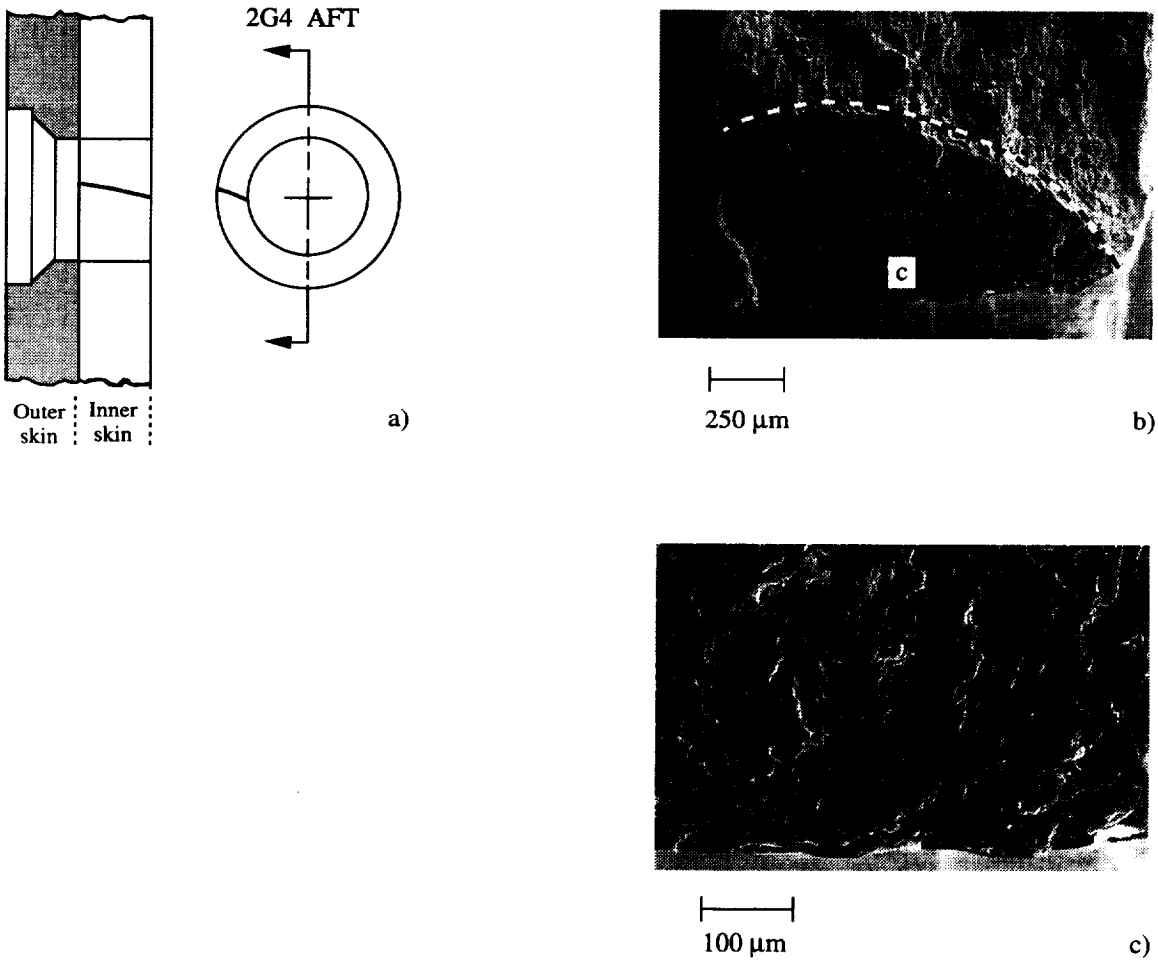

Figure 7.37 a) The schematic shows the rivet hole 2G4 configuration and the location of the inner skin fatigue crack oriented in the aft direction and about the 9 o'clock position. b) The SEM micrograph shows the fatigue crack fracture surface located along the rivet hole (bottom of micrograph). The fatigue crack extends nearly through the thickness of the inner skin. The dashed line marks the fatigue crack front. c) The SEM micrograph shows the rough surface of the rivet hole and the likely site of crack initiation (region "c" in Figure 7.36.b).

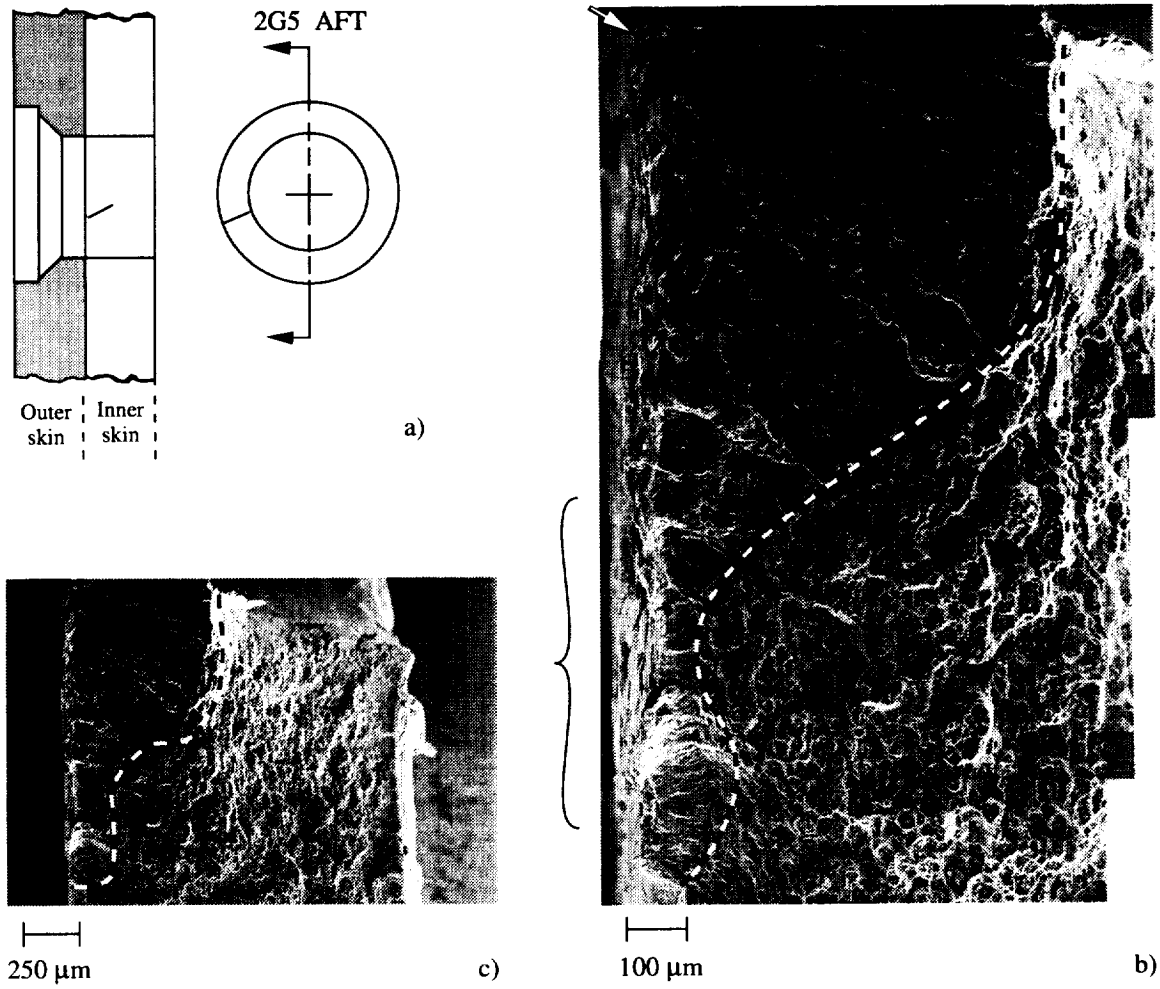

Figure 7.38 a) The schematic shows the rivet hole 2G5 configuration and the location of the inner skin fatigue crack oriented in the aft direction and slightly below the 9 o'clock position. b) The SEM micrograph shows the fatigue crack fracture surface that extends along the faying surface (left of micrograph). The rivet hole is located at the top of the micrograph. The dashed line marks the fatigue crack front. The crack front geometry suggests that a number of surface fatigue cracks initiated along the faying surface and have coalesced to form a nonsemicircular shaped fatigue crack front. Possible crack initiation sites are marked by an arrow at the corner and a bracket along the faying surface. c) The SEM micrograph shows the relationship of the fatigue crack surface with the rivet hole (top) and inboard skin surface. The dashed line marks the fatigue crack front.

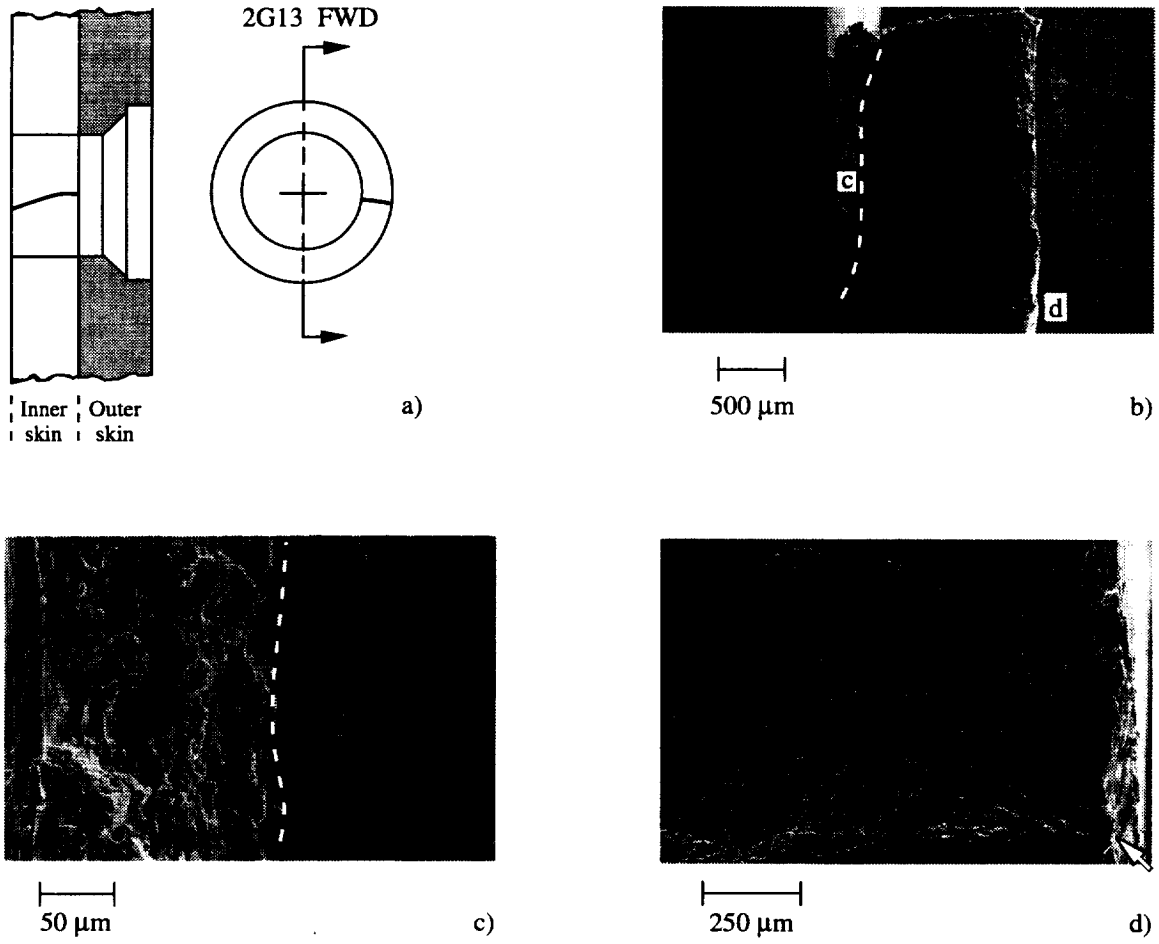

Figure 7.39 a) The schematic shows the rivet hole 2G13 configuration and the location of the inner skin fatigue crack oriented in the forward direction and about the 3 o'clock position. b) The SEM micrograph shows the fatigue crack fracture surface (the direction of crack propagation is from bottom to top of the figure) in the inner skin. The rivet hole is located at the bottom of the micrograph. The fatigue crack was cut during the removal of the specimen from the panel and a portion of the fatigue crack surface is not shown in the figure. The dashed line shows a portion of the fatigue crack front that extends nearly parallel to the inboard surface of the inner skin. c) The SEM micrograph shows the fatigue crack front region (dashed line) at region "c" in Figure 7.39.b. The fatigue fracture surface (right) exhibits a transgranular morphology while the overload fracture (left) exhibits a ductile appearance. d) The SEM micrograph region shows the outboard corner of the rivet hole (region "d" in Figure 7.39.b) at higher magnification. The arrow marks the likely site of crack initiation. The faying surface is located along the right side of the micrograph and the rivet hole is located at the bottom.

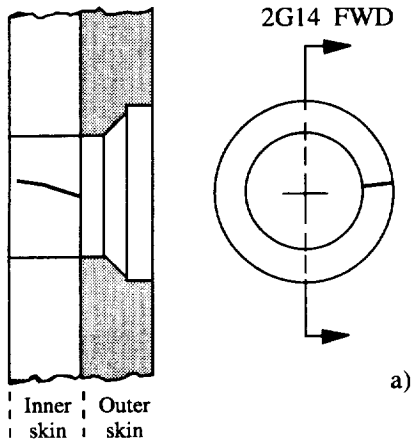

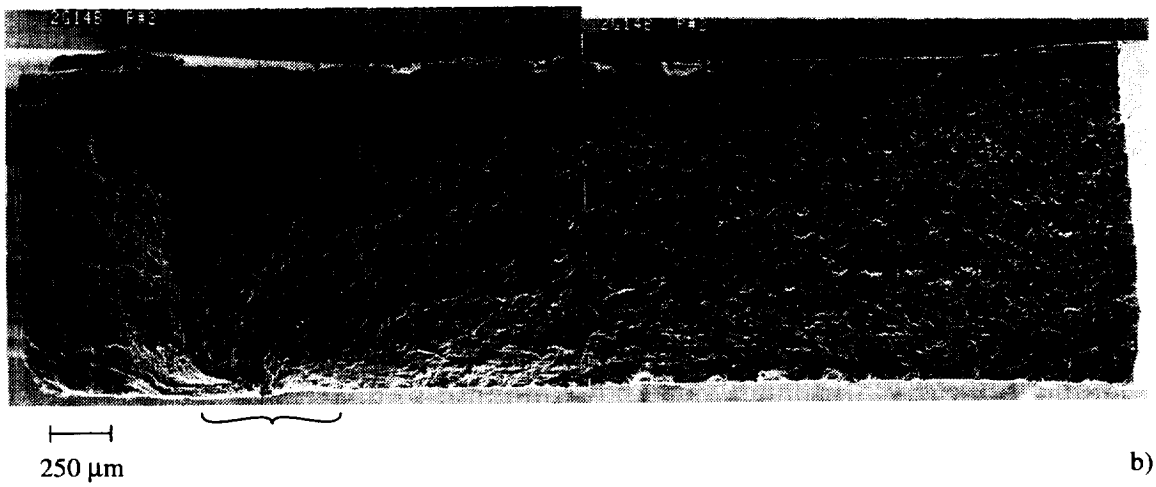

Figure 7.40 a) The schematic shows the rivet hole 2G14 configuration and the location of the inner skin fatigue crack oriented in the forward direction and about the 3 o'clock position. b) The SEM micrograph shows the fatigue crack that grew (the general direction of crack propagation is left to right) from the inner skin rivet hole which is located at the left of the micrograph. The fatigue crack was cut during the removal of the specimen from the panel and a portion of the fatigue crack surface is not shown in the figure. The fatigue crack initiated at the outboard corner of the rivet (bracket) hole at the faying surface (bottom left region of the micrograph).

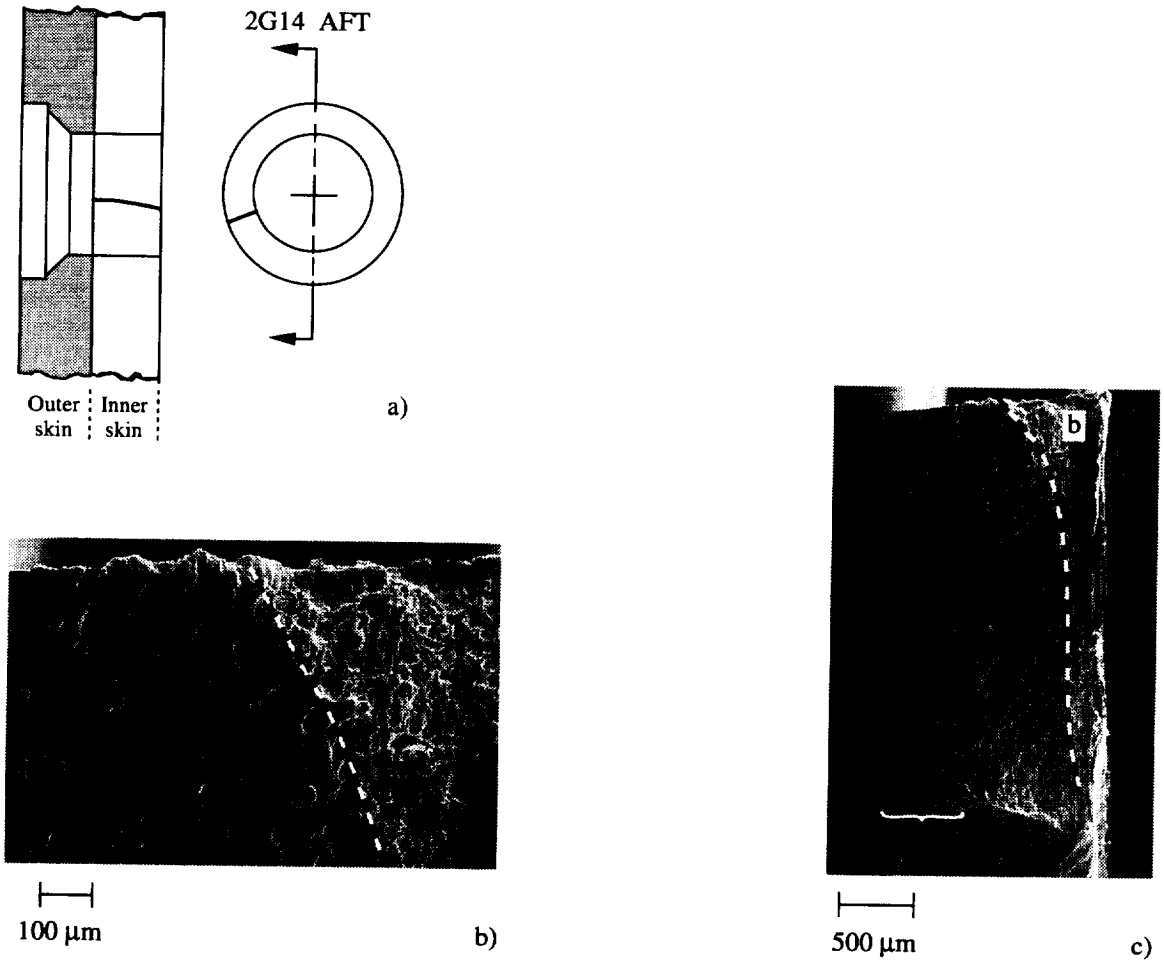

Figure 7.41 a) The schematic shows the rivet hole 2G14 configuration and the location of the inner skin fatigue crack oriented in the aft direction and below the 9 o'clock position. b) The SEM micrograph shows a portion of the fatigue crack front region (dashed line) at region "b" in Figure 7.41.c. The fatigue surface (left of the dashed line) exhibits a transgranular morphology and the overload fracture (right of the dashed line) exhibits a ductile appearance. A small portion of the fatigue crack surface is not shown in the figure. The fatigue crack was inadvertently cut during the removal of the specimen from the panel. c) The SEM micrograph shows the fatigue crack that grew (the direction of crack propagation is from bottom to top of the figure) from the inner skin rivet hole located at the bottom of the micrograph. The dashed line shows the fatigue crack front that extends nearly parallel to the inboard surface of the inner skin. A small portion of the fatigue crack surface is not shown in the figure. A bracket marks the fatigue crack initiation region.

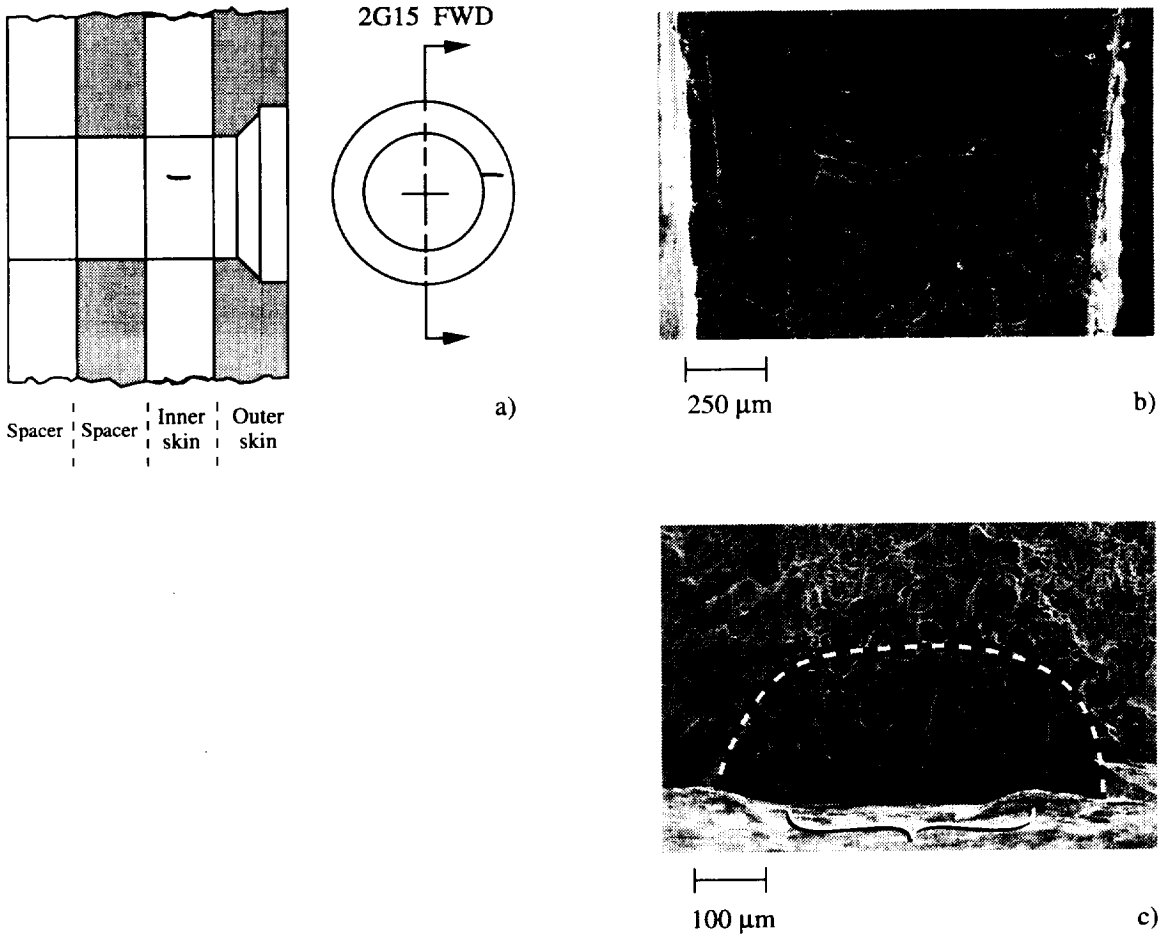

Figure 7.42 a) The schematic shows the rivet hole 2G15 configuration and the location of the inner skin fatigue crack oriented in the forward direction and above the 3 o'clock position. b) The SEM micrograph shows the partially opened surface crack on the inside diameter of the inner skin rivet hole. The fatigue crack was partially opened by the straining operation prior to breaking the specimen c) The SEM micrograph shows the surface fatigue crack extending from the rivet hole after the specimen was fractured. The dashed line marks the fatigue crack front. The crack initiated at multiple sites along the irregular surface of the rivet hole followed by cracks coalescing to form the single non semicircular fatigue crack. The bracket marks the region of crack initiation.

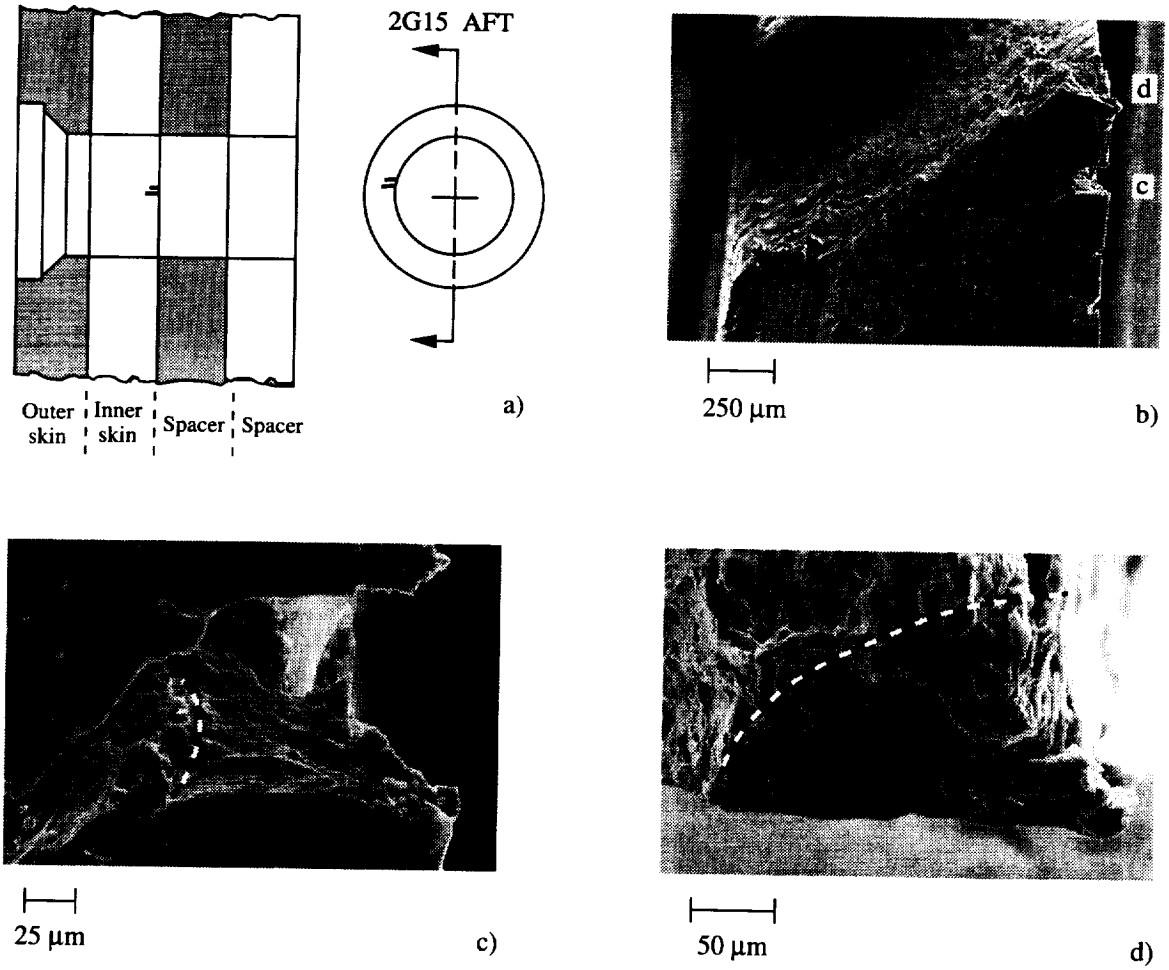

Figure 7.43 a) The schematic shows the rivet hole 2G15 configuration and the location of the inner skin fatigue crack oriented in the aft direction and about the 9 o'clock position. b) The SEM micrograph shows the rivet hole surface that has been partially fractured during the straining operation. Two fatigue cracks are noted at "c" and "d" along the outboard corner. c) The SEM micrograph shows the partially opened corner fatigue crack at region "c" in Figure 7.43.b. The dashed line marks the fatigue crack front. d) The SEM micrograph shows the corner fatigue crack at region "d" in Figure 7.43.b). The dashed line marks the fatigue crack front. The crack initiated at the burr on the corner.

8. Destructive Examination of Bay 2/3 Tear Strap

Figure 8.1 shows the bay 2/3 tear strap (T.S.) region, identifies most structural components, and locates the position of the long outer skin crack that extended into the T.S. region from bay 2. Identified in Figure 8.1 are the twenty-three rivet hole locations that were destructively examined (identified by the filled hole symbols in Figure 8.1), and the nineteen rivet hole locations that contain fatigue cracks. Figures 8.2, 8.3, 8.4 and 8.5 show the locations of thirty-one fatigue cracks observed in the outer skin, the upper tear strap and inner skin regions, the lower tear strap, and the frame, respectively. The through-thickness crack schematics shown in Figures 8.6 through 8.11 summarize location, length, type, and initiation site for all cracks found in rivet rows G through L, respectively.

8.1 Fatigue Cracks Contained in Bay 2/3 Tear Strap:

Figures 8.12 through 8.36 describe the fatigue crack morphology in the bay 2/3 tear strap region.

8.2 Bay 2/3 Tear Strap Summary:

Table 8.1 summarizes the destructive examination results for the bay 2/3 tear strap region. Fatigue cracks were observed in all layers, i.e., outer skin, inner skin, tear strap and a single fatigue crack was found in the frame. The bay 2/3 tear strap region contained cracks that range in length from 0.05 mm (0.002 in.) to 2.60 mm (0.102 in.). Tear strap fatigue cracking was isolated to a region that contained rivet holes 1 through 10 shown in Figure 8.1. Inner and outer skin fatigue cracks were observed in a region containing rivet holes 11 through 23 below the intrusion of the large bay 2 crack shown in Figure 8.1. The following observations were made as a result of fractographic examinations of bay 2.

8.2.1 Crack initiation site(s): Most fatigue cracks initiated at high K_T regions. These high K_T regions included rivet hole corners, areas of disturbed metal, and small surface imperfections. Damage due to fretting did not appear to play a significant role in crack initiation.

8.2.2 Crack front shape as a function of crack length: No crack front shape versus crack length correlation was made.

8.2.3 Fatigue crack/stable tearing transition crack length: No evidence of ductile tearing suggesting either rapid fatigue crack growth or stable tearing was observed in the bay 2/3 tear strap region.

8.2.4 Slant fracture morphology: No slant fracture was observed.

8.2.5 Evidence of corrosion: No corrosion was observed.

Table 8-1 Bay 2/3 Tear Strap Fatigue Crack Summary

Rivet No.	No. of Cracks (Holes)	Location	Crack Length mm (in)	Comment
1,2,3	5(3)	Upper T.S.	0.052(0.002)≤a	High K_T
		Lower T.S.	≤1.540(0.061)	
	1(1)	Frame		
4,5,6,7	5(3)	Upper T.S.	0.050(0.002)≤a	High K_T
		Lower T.S.	≤0.815(0.032)	
8,9,10	5(3)	Upper T.S.	0.143(0.006)≤a	High K_T
		Lower T.S.	≤1.818(0.072)	
11,12,13,14	5(3)	Outer Skin	0.052(0.002)≤a	High K_T
		Inner Skin	≤1.270(0.050)	Fretting
	1(1)			
15,16,17,18,19	4(3)	Inner Skin	0.110(0.004)≤a	High K_T
			≤0.776(0.031)	
20,21,22,23	5(3)	Inner Skin	0.168(0.007)≤a	High K_T
			≤2.600(0.102)	

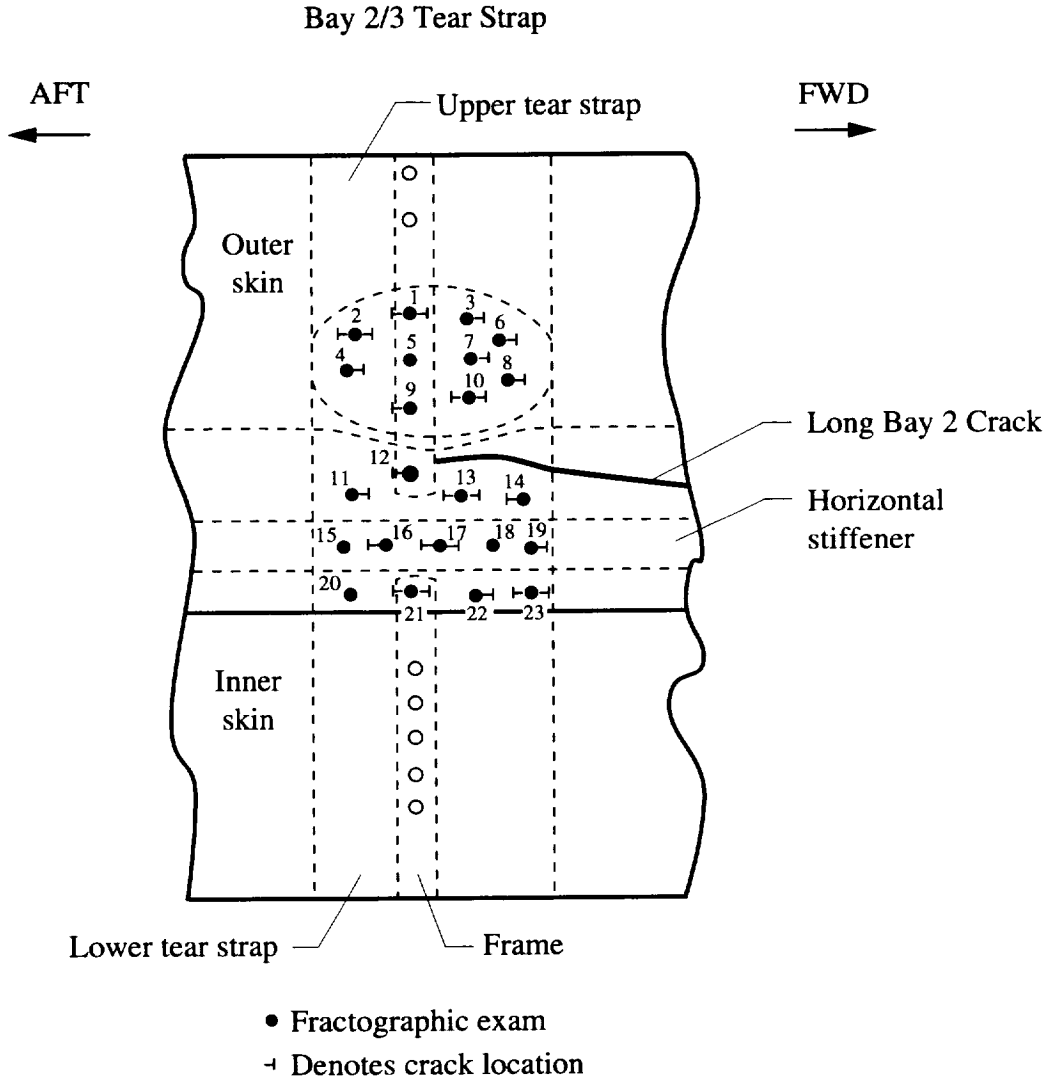

Figure 8.1 The schematic shows the location of all fatigue cracks found in the bay 2/3 tear strap by destructive examination. The solid dark line depicts one end of the long bay 2 crack extending into the tear strap.

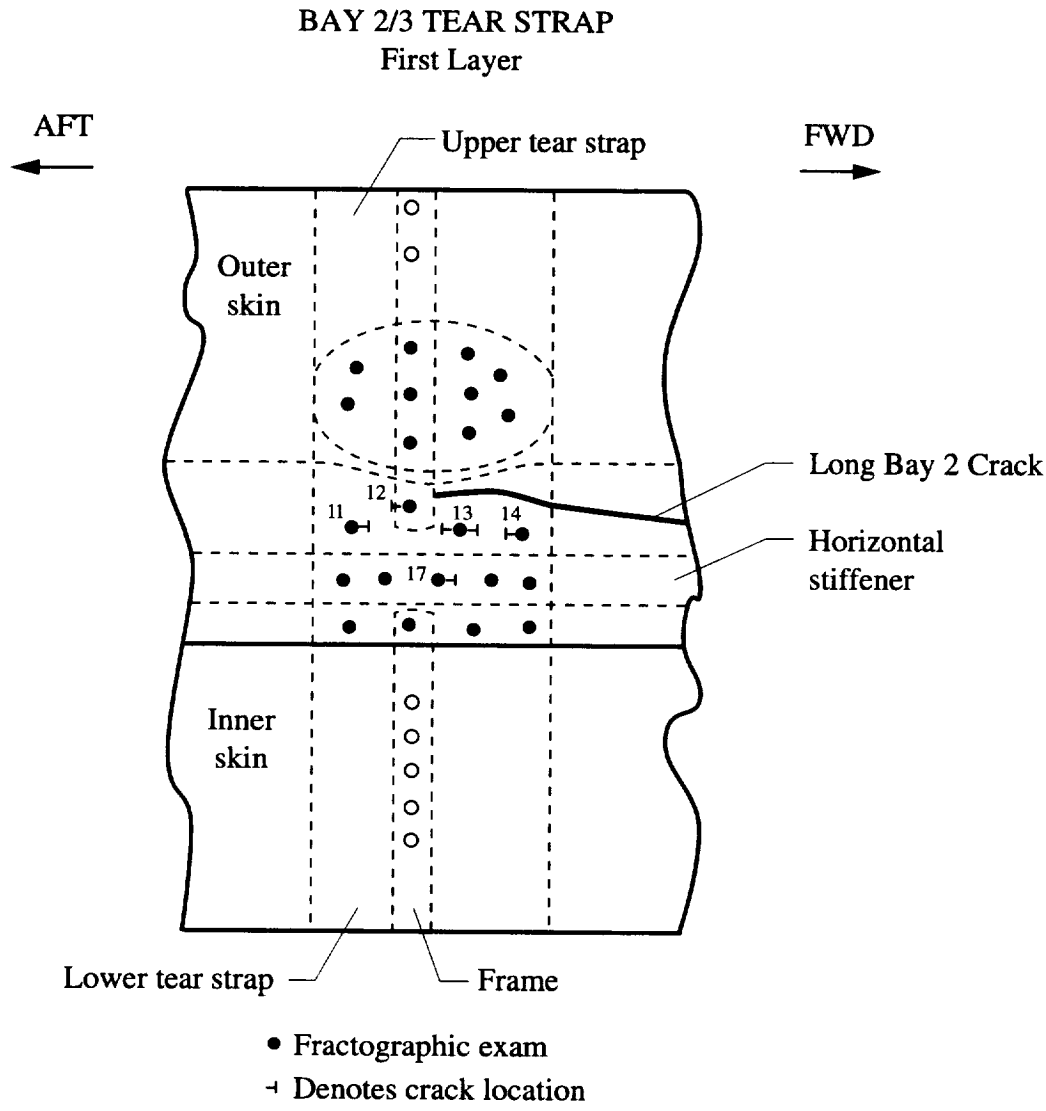

Figure 8.2 The schematic shows the location of fatigue cracks found in the first layer (outer skin) of the bay 2/3 tear strap by destructive examination. The solid dark line depicts one end of the long bay 2 crack extending into the tear strap.

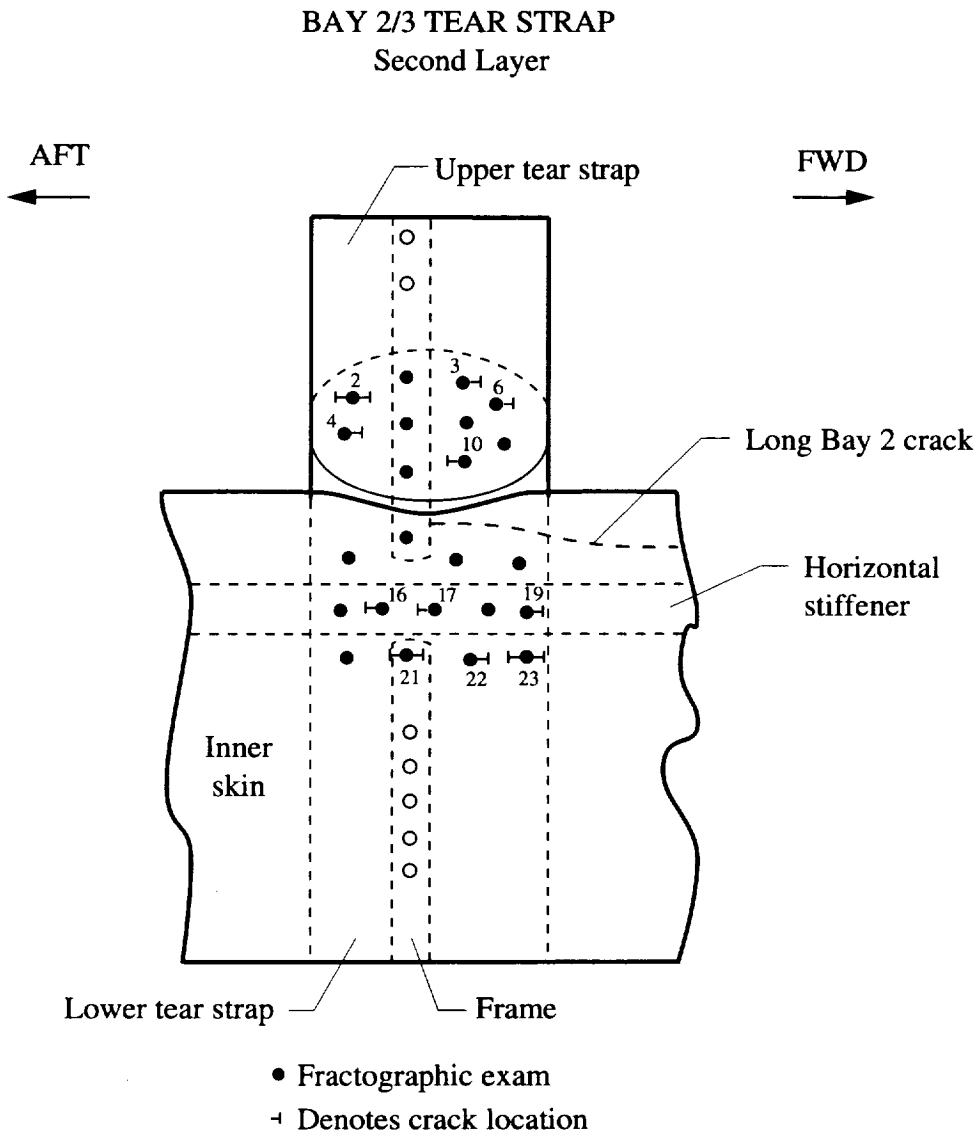

Figure 8.3 The schematic shows the location of fatigue cracks found in the second layer (upper tear strap and inner skin) of the bay 2/3 tear strap by destructive examination. The dashed dark line depicts one end of the long bay 2 crack extending into the tear strap.

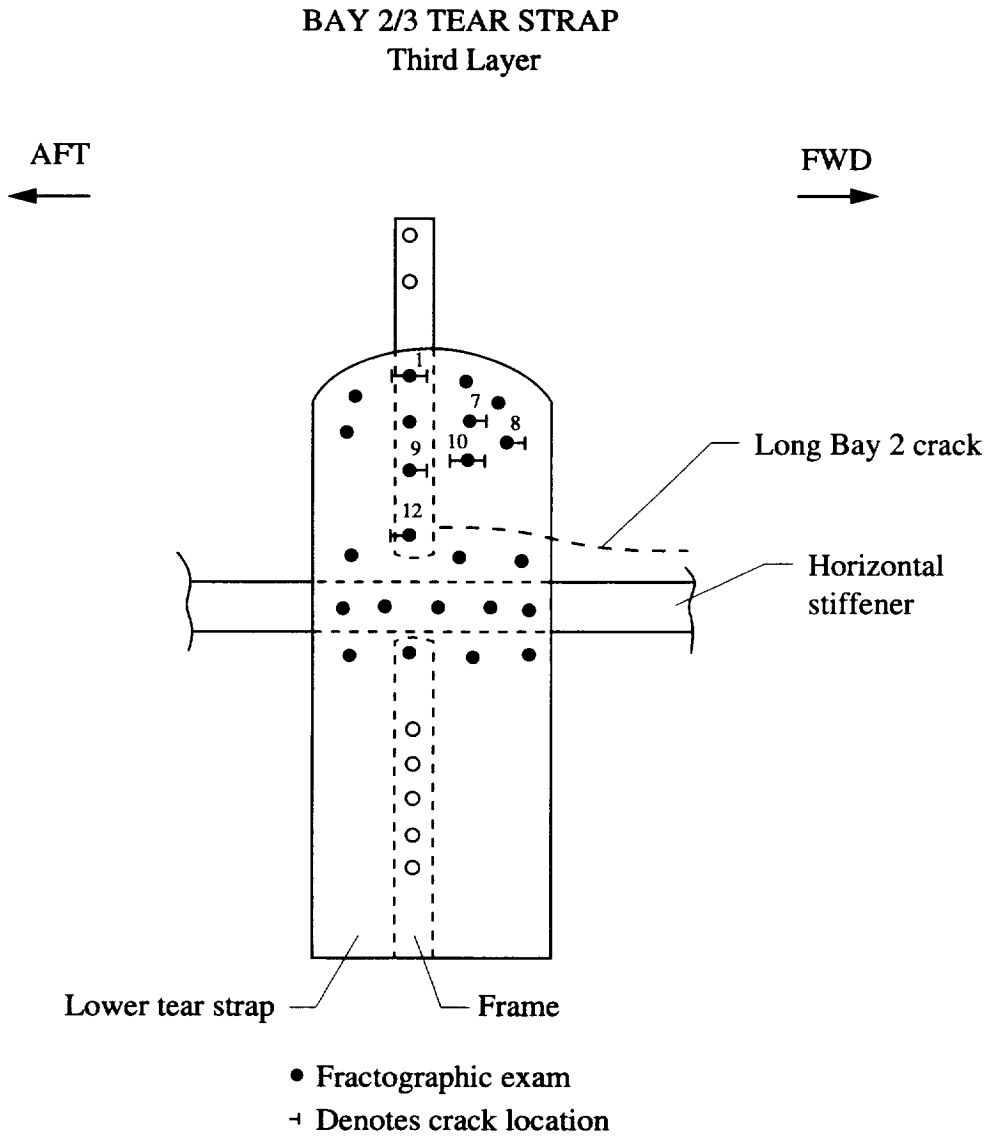

Figure 8.4 The schematic shows the location of fatigue cracks found in the third layer (lower tear strap) of the bay 2/3 tear strap by destructive examination. The dashed dark line depicts one end of the long bay 2 crack extending into the tear strap.

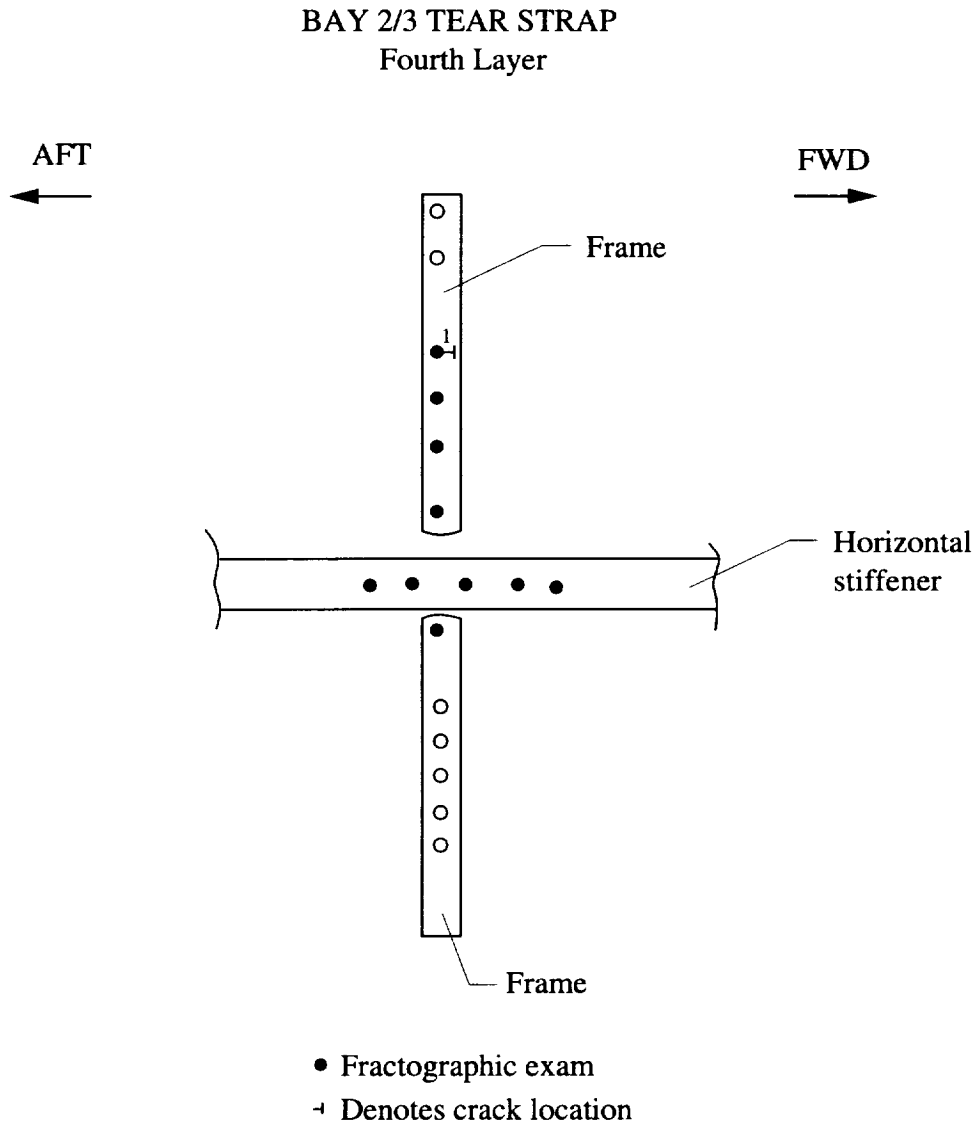

Figure 8.5 The schematic shows the location of the single fatigue crack found in the fourth layer (frame and horizontal stiffener) of the bay 2/3 tear strap.

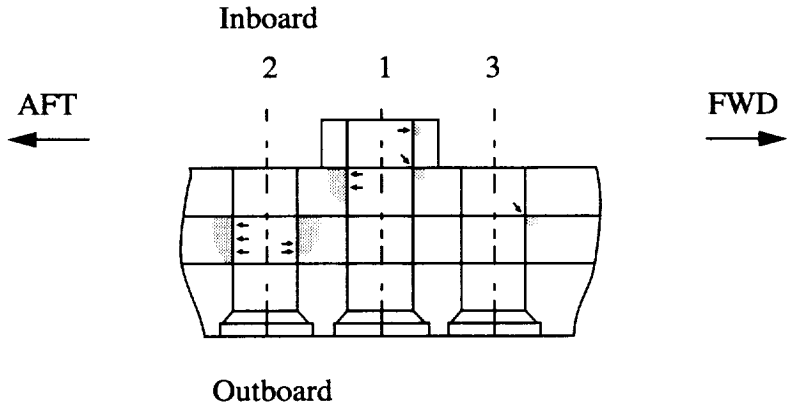

Hole #	Location	Length mm (in)	Type	Initiation site
2 (Aft)	Upper tear strap	1.540 (0.061)	Through	Multiple surface
2 (Fwd)	Upper tear strap	1.470 (0.058)	Corner	Multiple surface
1 (Aft)	Lower tear strap	0.350 (0.014)	Corner	Multiple surface
1 (1Fwd)	Lower tear strap	0.209 (0.008)	Corner	Inboard Corner
1 (2Fwd)	Frame	0.052 (0.002)	Surface	Surface
3 (Fwd)	Upper tear strap	0.124 (0.005)	Corner	Inboard Corner

Figure 8.6 The through thickness schematic shows the location and initiation site of fatigue cracks found in holes number 1, 2 and 3 in the bay 2/3 tear strap. The table summarizes crack location, crack length, crack type, and initiation site for each fatigue crack shown.

Bay 2/3 Tear Strap

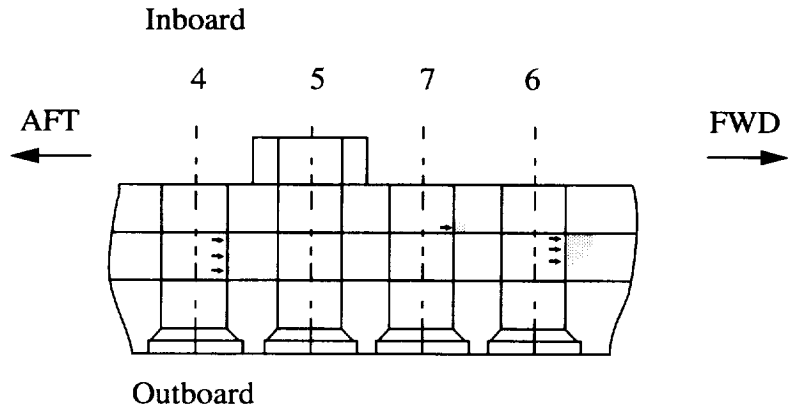

Hole #	Location	Length mm (in)	Type	Initiation site
4 (Fwd)	Upper tear strap	0.214 (0.008)	Surface	Multiple surface
6 (Fwd)	Lower tear strap	0.815 (0.032)	Corner	Surface
7 (Fwd)	Lower tear strap	0.419 (0.016)	Corner	Outboard corner

Figure 8.7 The through hickness schematic shows the location and initiation site of fatigue cracks found in holes number 4, 5, 6, and 7 in the bay 2/3 tear strap. The table summarizes crack location, crack length, crack type, and initiation site for each fatigue crack shown.

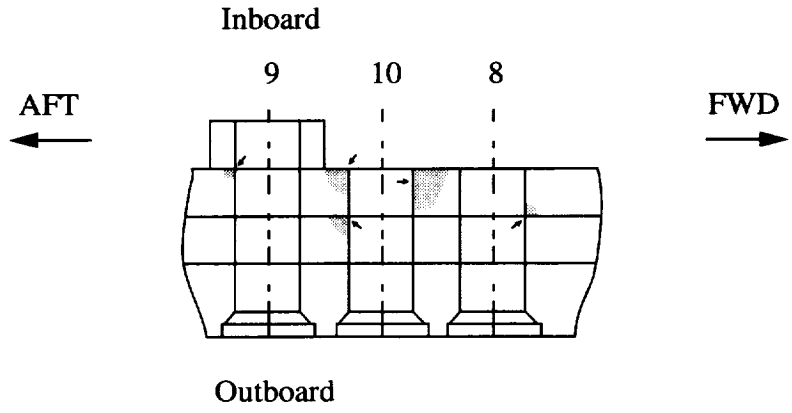

Hole #	Location	Length mm (in)	Type	Initiation site
8 (Fwd)	Lower tear strap	0.926 (0.036)	Corner	Not determined
9 (Aft)	Lower tear strap	0.143 (0.006)	Corner	Inboard Corner (IC)
10 (Aft)	Upper tear strap	0.324 (0.013)	Corner	IC
10 (Aft)	Lower tear strap	1.277 (0.057)	Corner	IC
10 (Fwd)	Lower tear strap	1.818 (0.072)	Corner	Surface

Figure 8.8 The through thickness schematic shows the location and initiation site of fatigue cracks found in holes number 8, 9 and 10 in the bay 2/3 tear strap. The table summarizes crack location, crack length, crack type, and initiation site for each fatigue crack shown.

Bay 2/3 Tear Strap

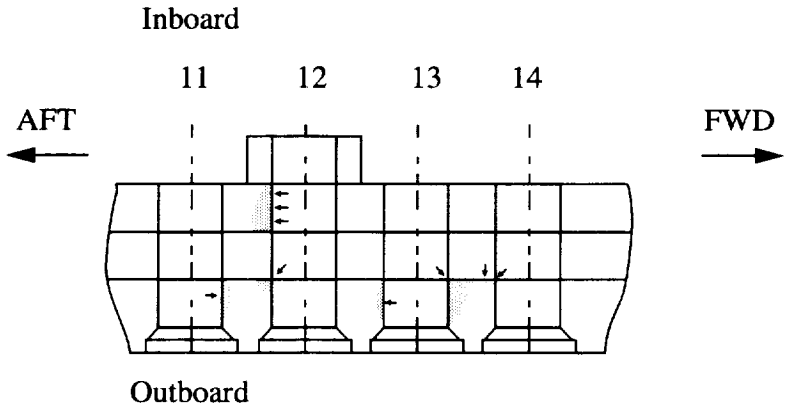

Hole #	Location	Length mm (in)	Type	Initiation site
11 (Fwd)	Outer Skin	<0.052 (<0.002)	Countersink	Center of shank
12 (Aft)	Tear strap	0.109 (0.004)	Countersink	Inboard side of shank
12 (Aft)	Inner Skin	1.190 (0.047)	Through	Multiple Surface
13 (Aft)	Outer Skin	0.214 (0.008)	Countersink	Center of shank
13 (Fwd)	Outer Skin	1.270 (0.050)	Countersink	Inboard side of shank
14 (1 Aft)	Outer Skin	0.166 (0.007)	Fretting	Inner skin / outer skin
14 (2 Aft)	Outer Skin	0.157 (0.006)	Fretting	Inner skin / outer skin

Figure 8.9 The through thickness schematic shows the location and initiation site of fatigue cracks found in holes number 11, 12, 13, and 14 in the bay 2/3 tear strap. The table summarizes crack location, crack length, crack type, and initiation site for each fatigue crack shown.

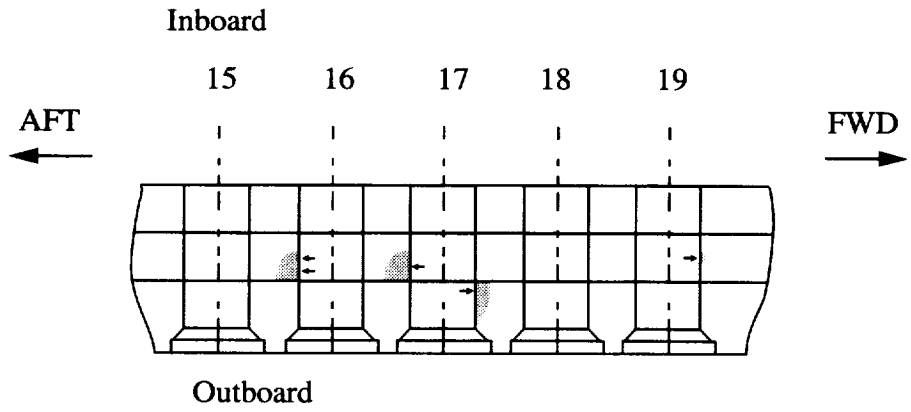

Hole #	Location	Length mm (in)	Type	Initiation site
16 (Aft)	Inner Skin	0.539 (0.021)	Corner	Multiple surface
17 (Aft)	Inner Skin	0.776 (0.031)	Corner	Surface
17 (Fwd)	Outer Skin	0.186 (0.007)	Counter sink	Inboard side of shank
19 (Fwd)	Inner Skin	0.110 (0.004)	Surface	Surface

Figure 8.10 The through thickness schematic shows the location and initiation site of fatigue cracks found in holes number 15, 16, 17, 18, and 19 in the bay 2/3 tear strap. The table summarizes crack location, crack length, crack type, and initiation site for each fatigue crack shown.

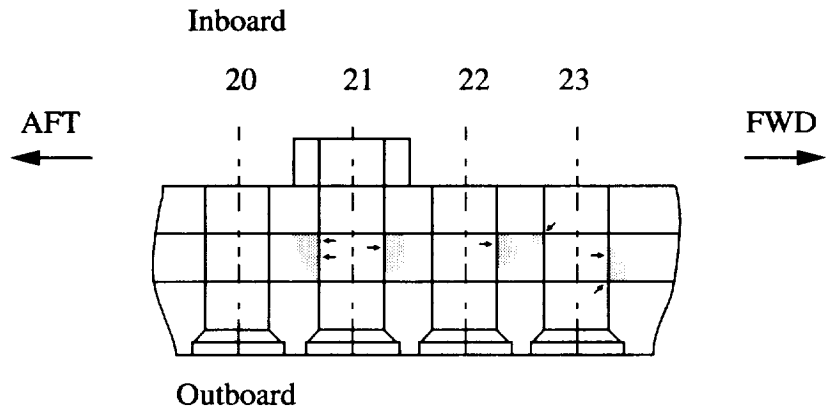

Hole #	Location	Length mm (in)	Type	Initiation site
21 (Aft)	Inner Skin	2.600 (0.102)	Through	Multiple Surface
21 (Fwd)	Inner Skin	0.532 (0.021)	Corner	Surface
22 (Fwd)	Inner Skin	0.597 (0.023)	Surface	Surface
23 (Aft)	Inner Skin	0.168 (0.007)	Corner	Inboard corner
23 (Fwd)	Inner Skin	0.686 (0.027)	Corner	Surface and corner

Figure 8.11 The through thickness schematic shows the location and initiation site of fatigue cracks found in holes number 20, 21, 22, and 23 in the bay 2/3 tear strap. The table summarizes crack location, crack length, crack type, and initiation site for each fatigue crack shown.

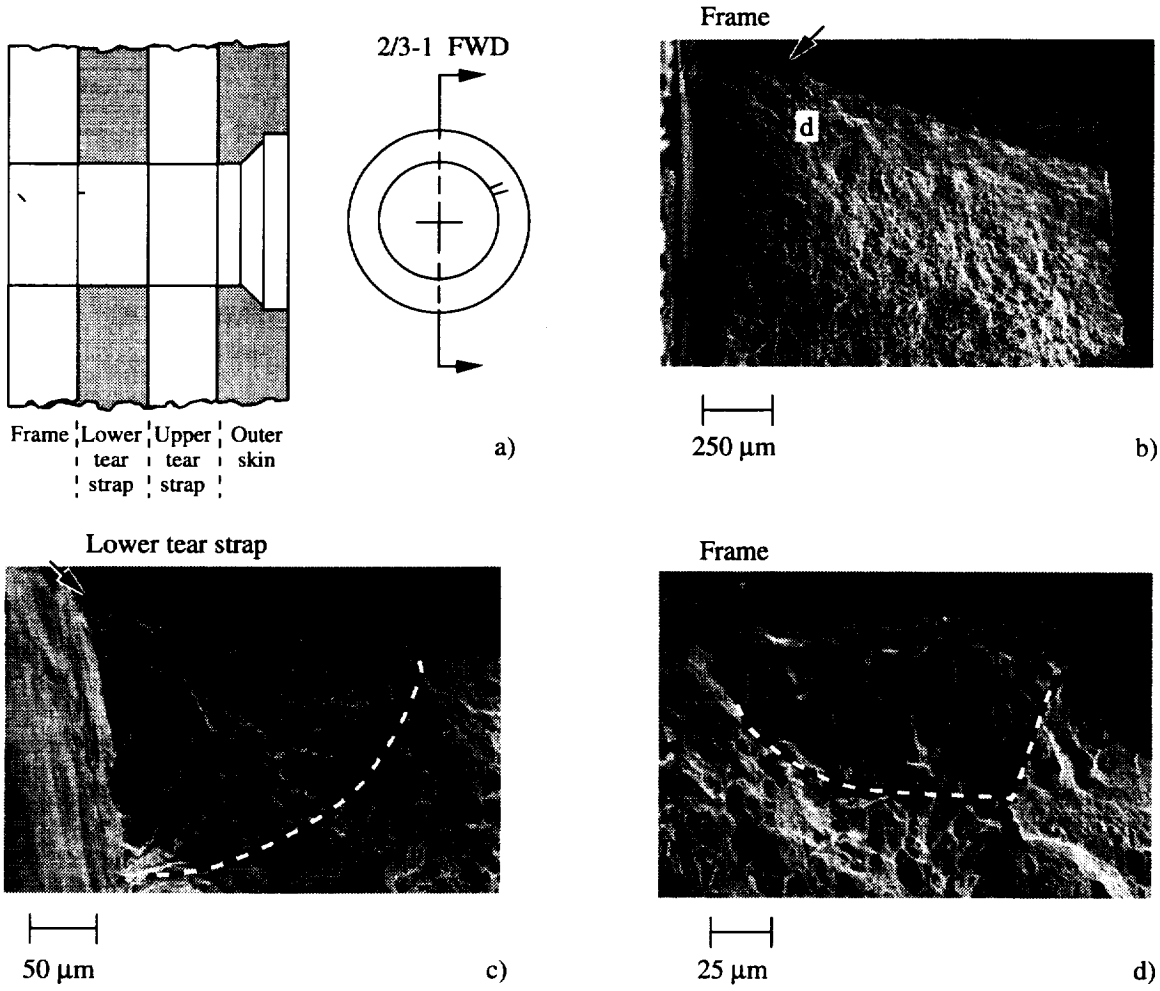

Figure 8.12 a) The schematic shows the rivet hole 2/3-1 configuration and the location of lower T.S. and frame fatigue cracks oriented in the forward direction and about the 2 o'clock position. b) The SEM micrograph shows the location of a small fatigue crack located (arrow) at the inside surface of the rivet hole. The rivet hole is located at the top of the micrograph. c) The SEM micrograph shows the fatigue crack located on the inboard corner of the lower T.S. rivet hole. The rivet hole is located at the top of the micrograph. d) The SEM micrograph shows the fatigue fracture surface of region "d" in Figure 8.12.b at high magnification.

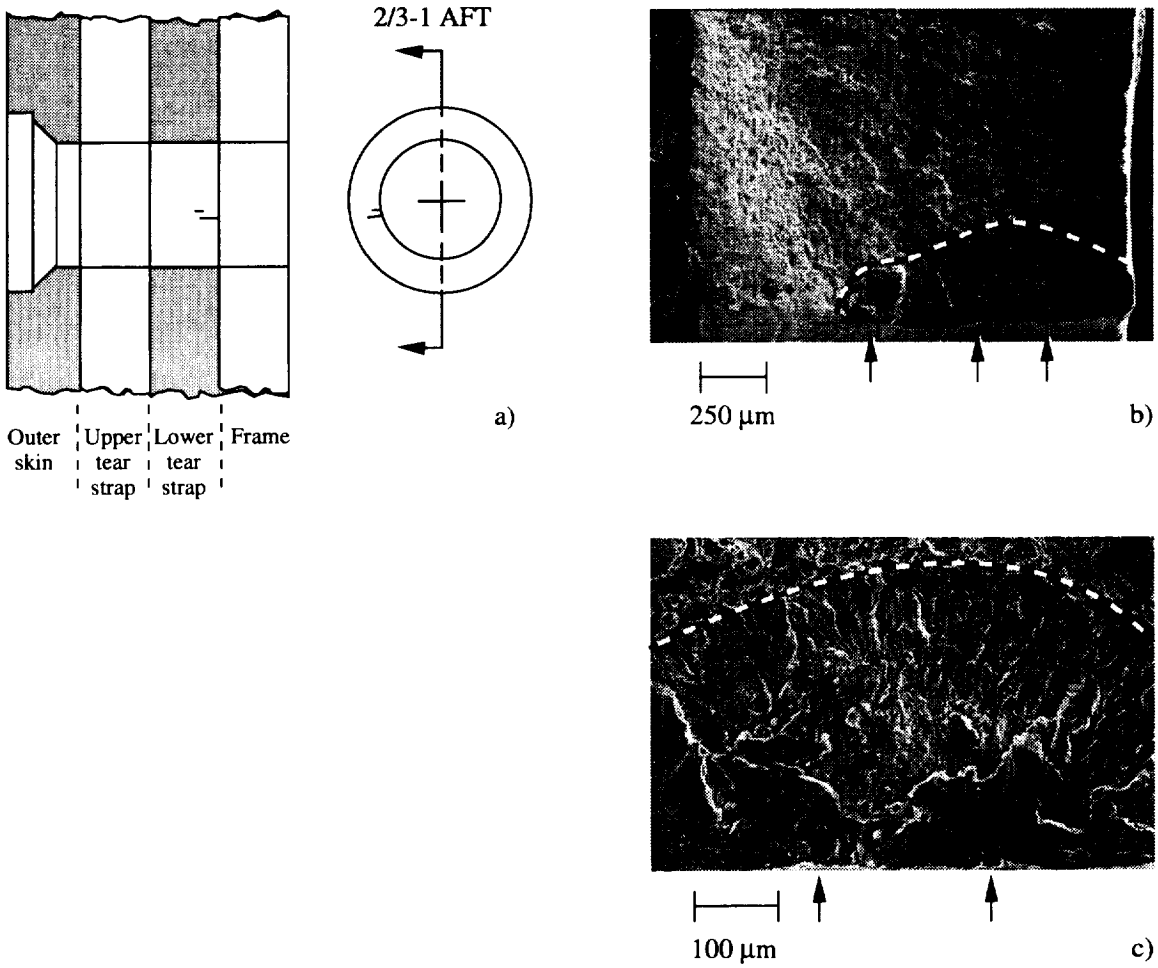

Figure 8.13 a) The schematic shows the rivet hole 2/3-1 configuration and the location of two lower T.S. fatigue cracks oriented in the aft direction and below the 9 o'clock position. b) The SEM micrograph shows the fatigue crack located at the inside surface of the rivet hole. The dashed line marks the shape of the irregular crack front which suggests the initiation, growth and coalescence of multiple cracks. Arrows mark likely sites of crack initiation. c) The SEM micrograph shows the regions of crack initiation (arrows) at high magnification. The dashed line shows the location of the fatigue crack front.

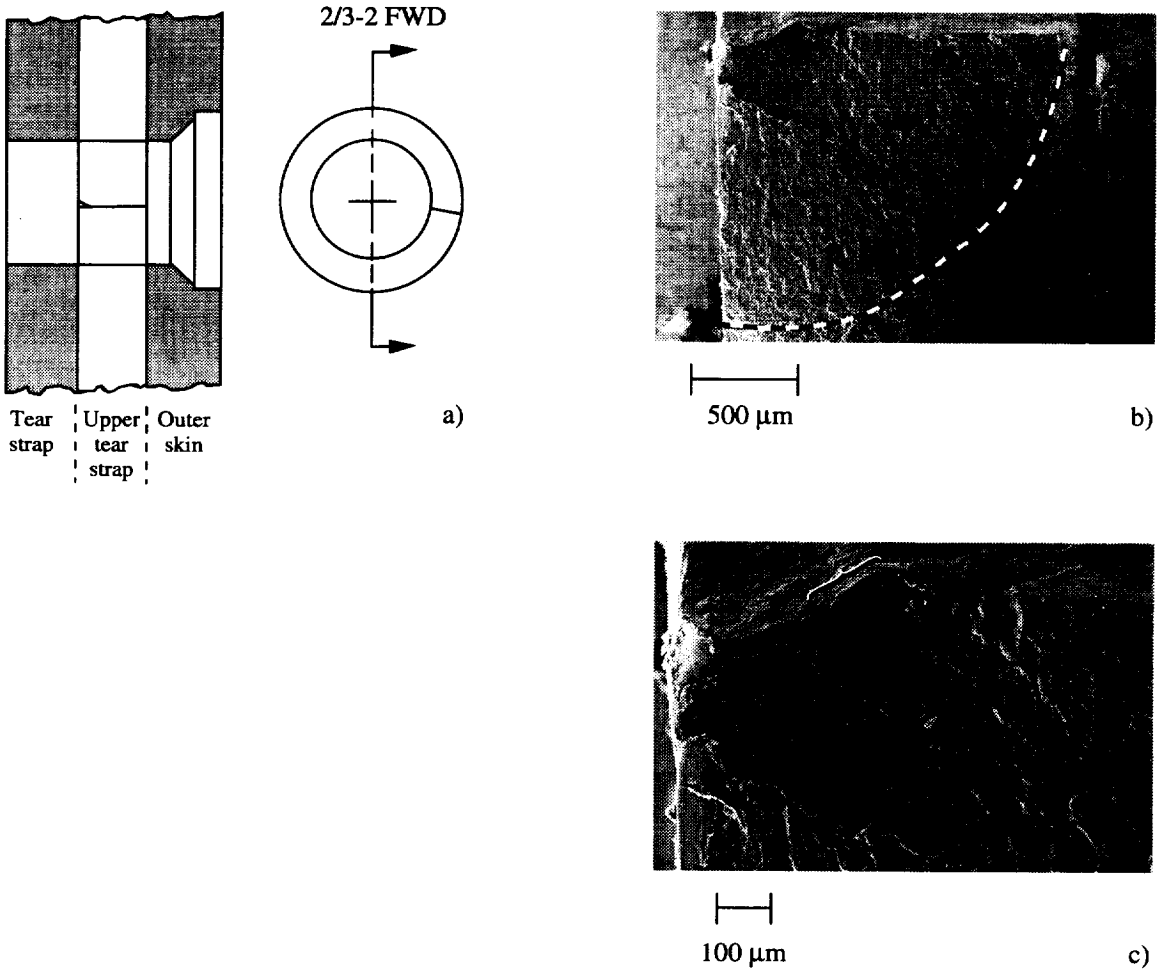

Figure 8.14 a) The schematic shows the rivet hole 2/3-2 configuration and the location of an upper T.S. fatigue crack oriented in the forward direction and about the 3 o'clock position. b) The SEM micrograph shows the location of the corner fatigue crack at the inside surface of the rivet hole contained in the lower T.S. The dashed line marks the shape of the crack front. c) The SEM micrograph shows the region of crack initiation located on the inside corner of the lower T.S. rivet hole. The bracket marks the approximate location of crack initiation.

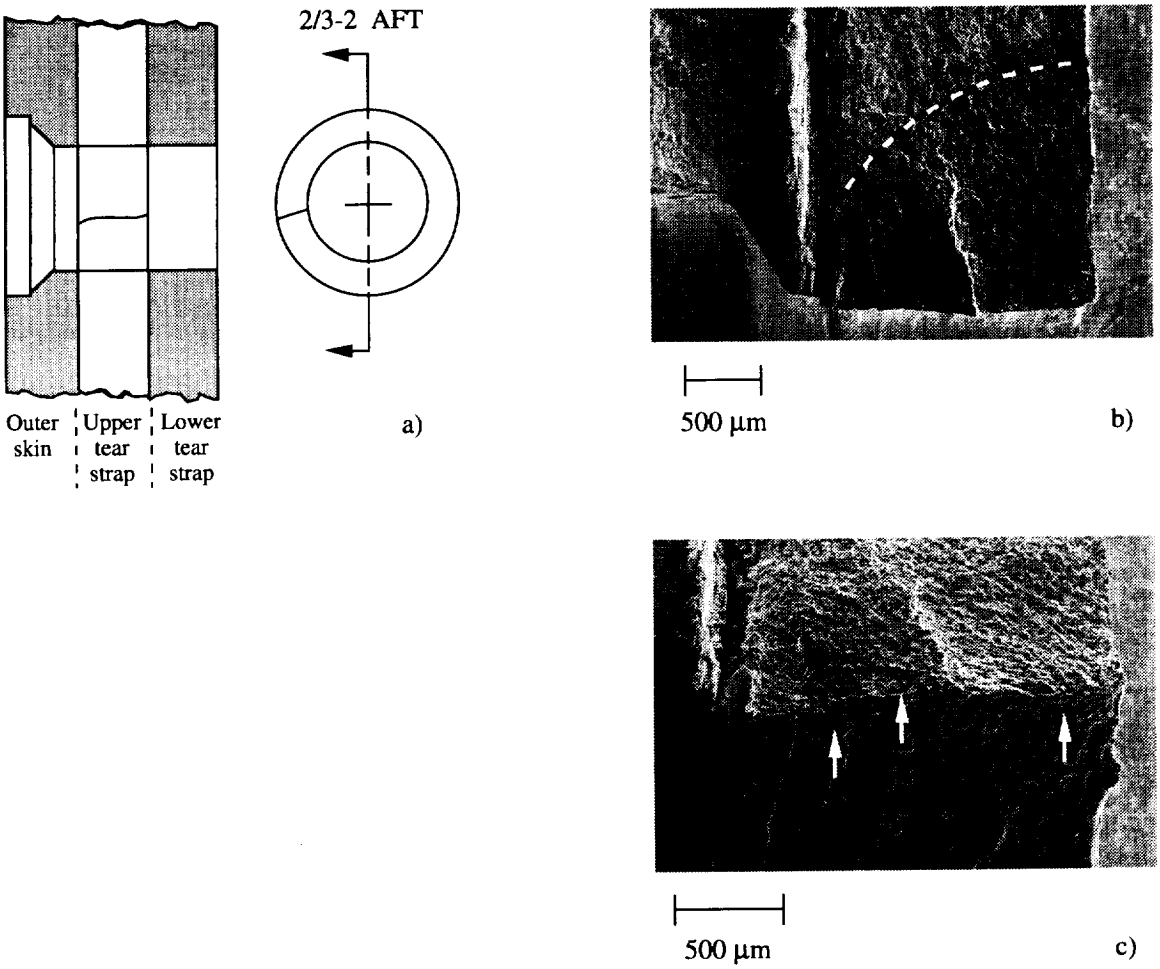

Figure 8.15 a) The schematic shows the rivet hole 2/3-2 configuration and the location of a upper T.S. fatigue crack oriented in the aft direction and about the 9 o'clock position. b) The SEM micrograph shows the location of the through-thickness fatigue crack contained in the upper T.S. The micrograph shows the lower T.S. and outer skin rivet hole countersink region to the left. The dashed line marks the shape of the crack front. c) The SEM micrograph shows the region of crack initiation located on the inside surface of the rivet hole contained in the upper T.S. Arrows mark possible crack initiation sites.

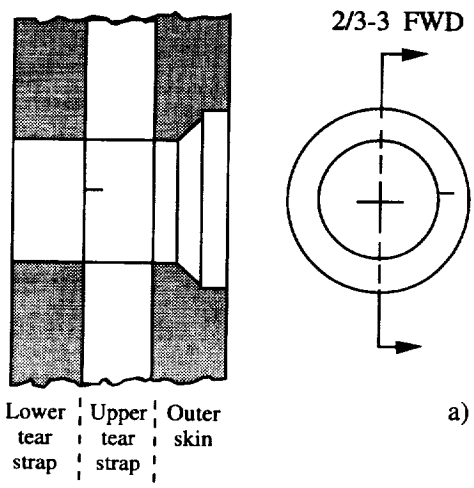

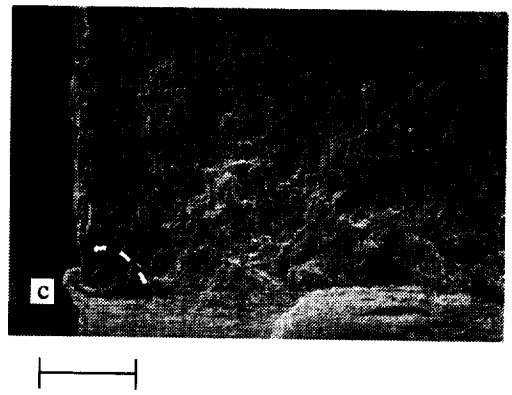

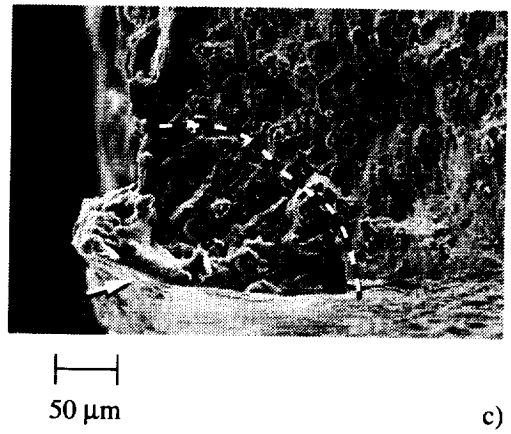

Figure 8.16 a) The schematic shows the rivet hole 2/3-3 configuration and the location of a upper T.S. fatigue crack oriented in the forward direction and above the 3 o'clock position. b) The SEM micrograph shows the location of a fatigue crack at the inboard corner of the upper T.S. rivet hole. The dashed line marks the shape of the crack front. c) The SEM micrograph shows region "c" in Figure 8.16.b. The crack initiated at a burr located on the corner of the rivet hole (arrow).

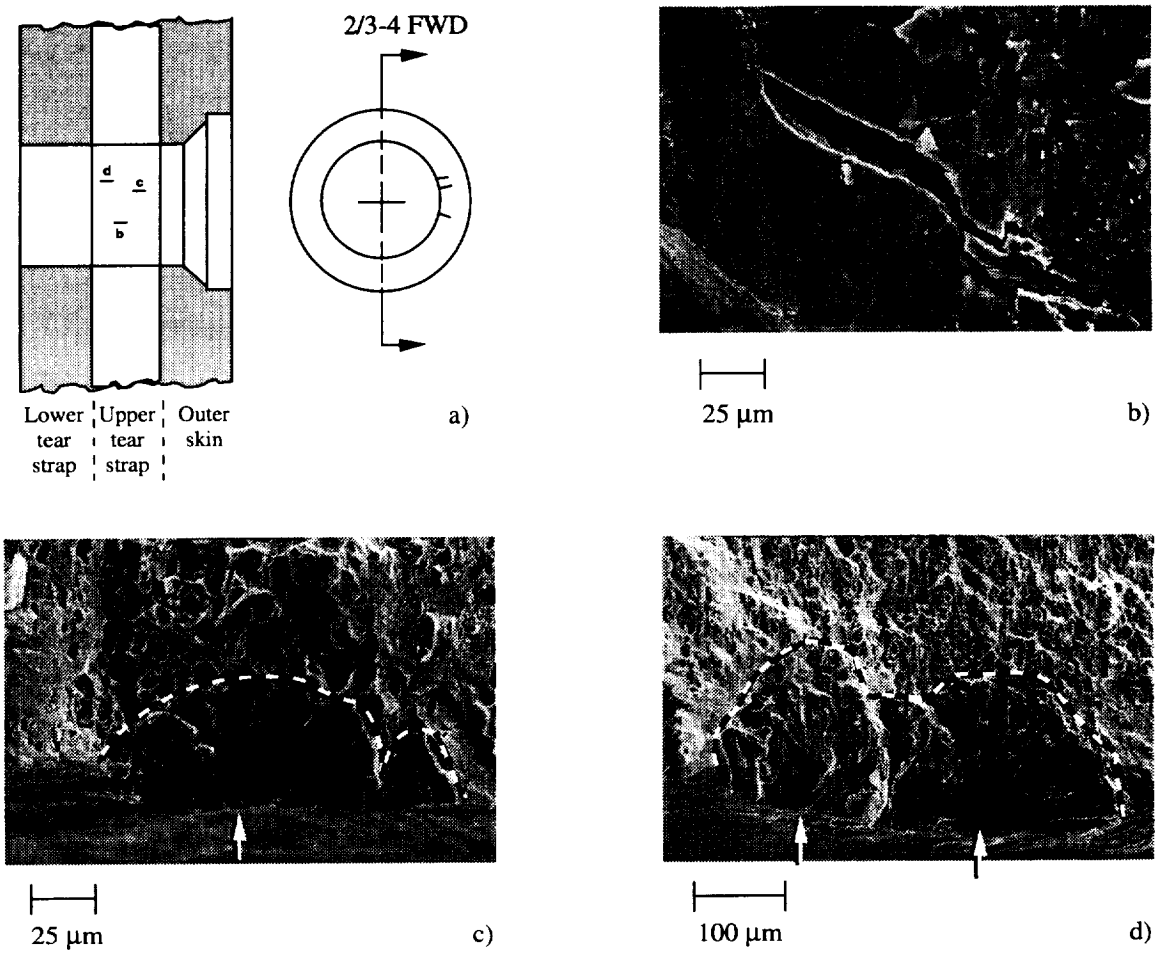

Figure 8.17 a) The schematic shows the rivet hole 2/3-4 configuration and the location of three upper T.S. fatigue cracks oriented in the forward direction and at the 2 to 4 o'clock positions. b) The SEM micrograph shows a surface fatigue crack at the inside surface of the rivet hole contained in the upper T.S. shown at location "b" in Figure 8.17.a. The crack was partially opened during the destructive examination. c) The SEM micrograph shows the rivet hole surface crack at region "c" in Figure 8.17.a. The dashed line marks the irregular crack front of two surface cracks that have coalesced. d) The SEM micrograph shows the rivet hole surface crack at region "d" in Figure 8.17.a. The dashed line marks the irregular crack from two or possibly three surface cracks that have coalesced.

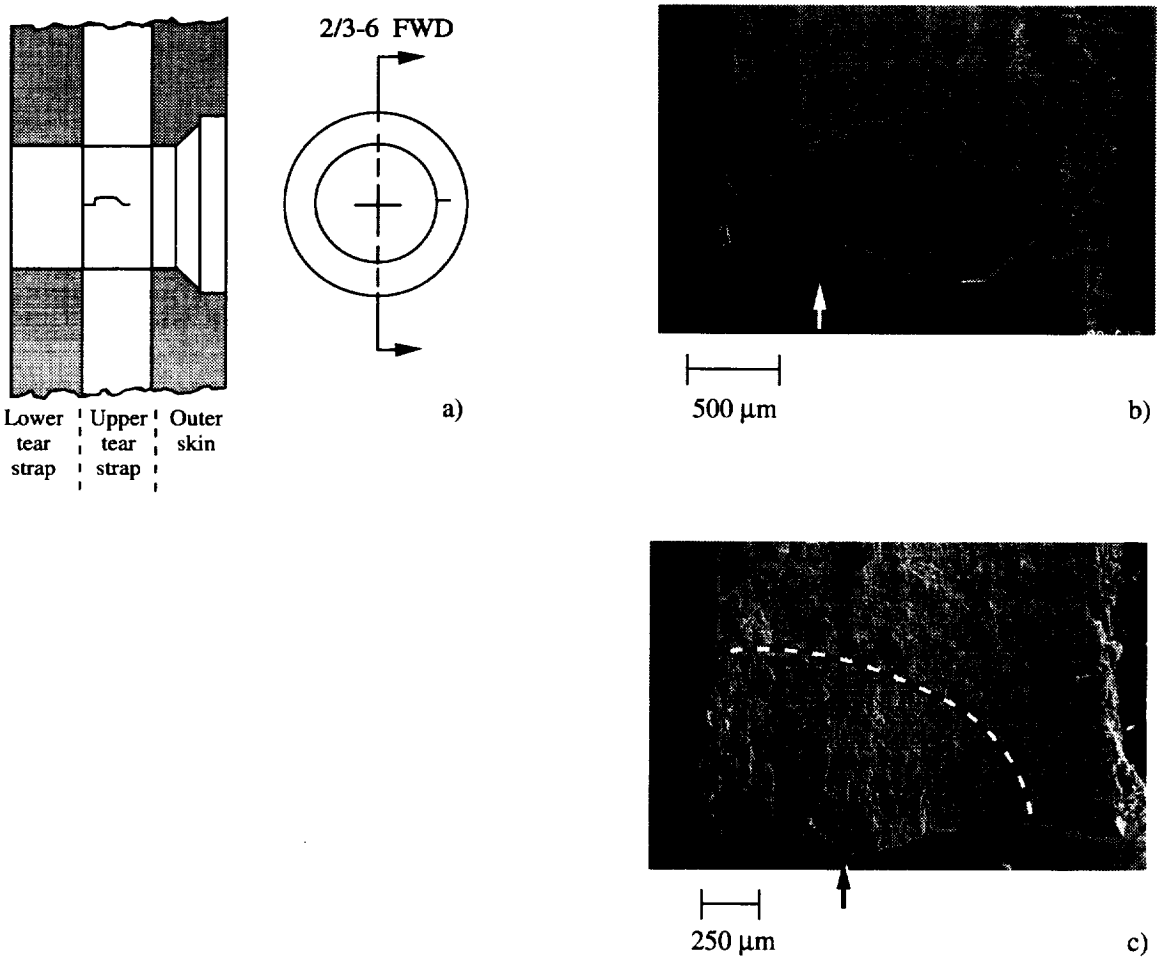

Figure 8.18 a) The schematic shows the rivet hole 2/3-6 configuration and the location of the upper T.S. fatigue crack oriented in the forward direction and at the 3 o'clock position. b) The SEM micrograph shows the fatigue crack along the rivet hole surface. The left edge of the specimen is the faying surface in contact with the lower T.S. The arrow marks the location of crack initiation. c) The SEM micrograph shows the fatigue crack fracture surface in the upper T.S. The dashed line marks the fatigue crack front. The arrow marks the likely site of crack initiation.

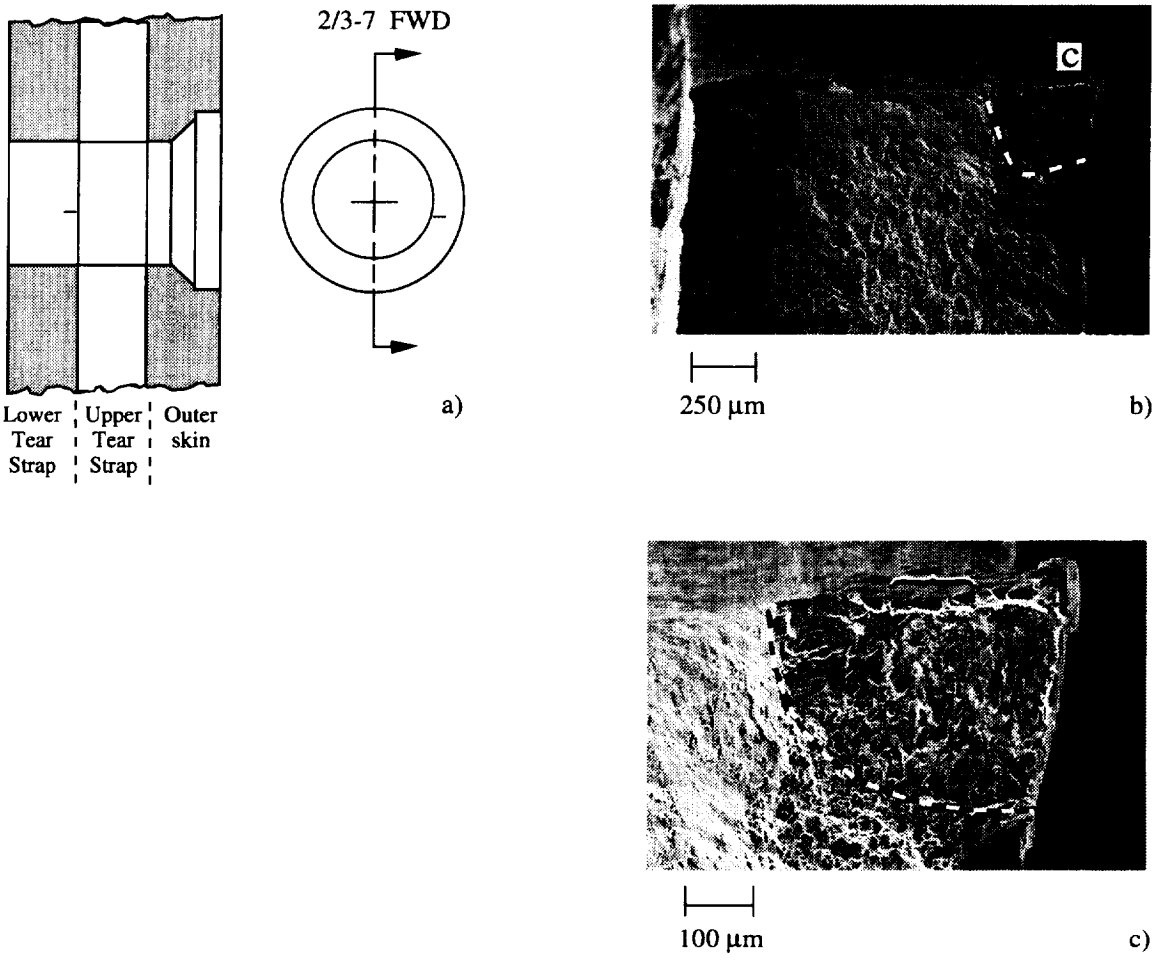

Figure 8.19 a) The schematic shows the rivet hole 2/3-7 configuration and the location of the lower T.S. fatigue crack oriented in the forward direction and below the 3 o'clock position. b) The SEM micrograph shows a corner fatigue crack at the outboard corner of the rivet hole contained in the lower T.S. The fatigue crack front is marked by a dashed line. c) The SEM micrograph shows the corner, region "c" in Figure 8.19.b, at high magnification. The dashed line marks the fatigue crack front and the bracket marks the likely region of crack initiation.

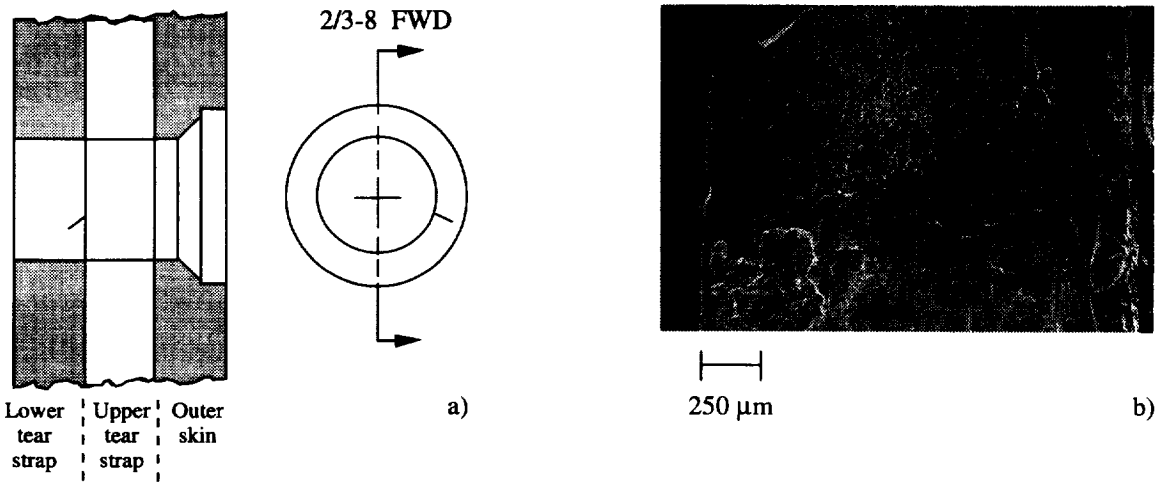

Figure 8.20 a) The schematic shows the rivet hole 2/3-8 configuration and the location of the lower T.S. fatigue crack oriented in the forward direction and at the 4 o'clock position. b) The SEM micrograph shows the corner fatigue crack at the outboard corner of the rivet hole surface contained in the lower T.S. The crack was partially opened as a result of the straining operation during the destructive examination but opened no further when the specimen was strained to failure.

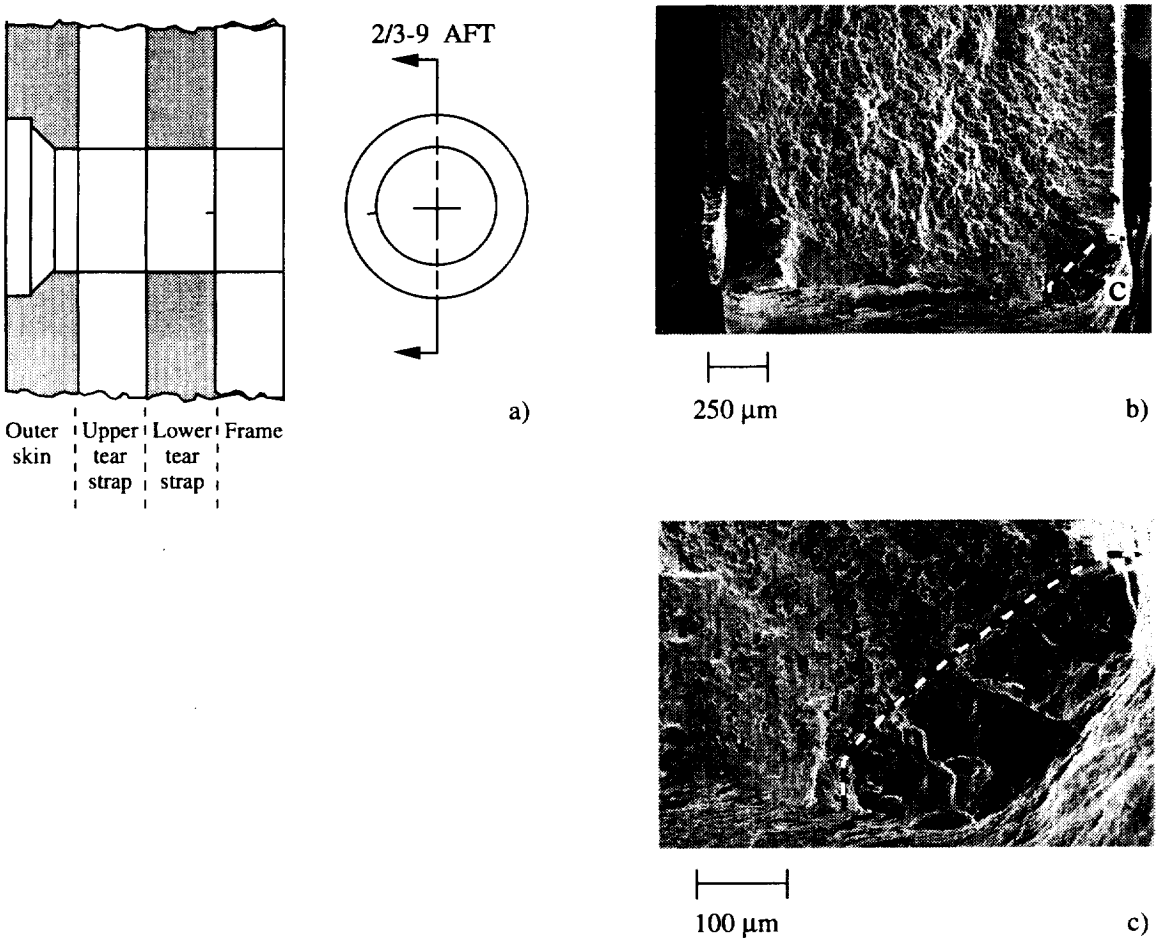

Figure 8.21 a) The schematic shows the rivet hole 2/3-9 configuration and the location of the lower T.S. fatigue crack oriented in the aft direction and at the 9 o'clock position. b) The SEM micrograph shows the corner fatigue crack at the inboard corner of the rivet hole contained between the lower T.S. and frame. The dashed line marks the fatigue crack front. c) The SEM micrograph shows the corner crack at region "c" in Figure 8.21.b at high magnification. The dashed line marks the fatigue crack front.

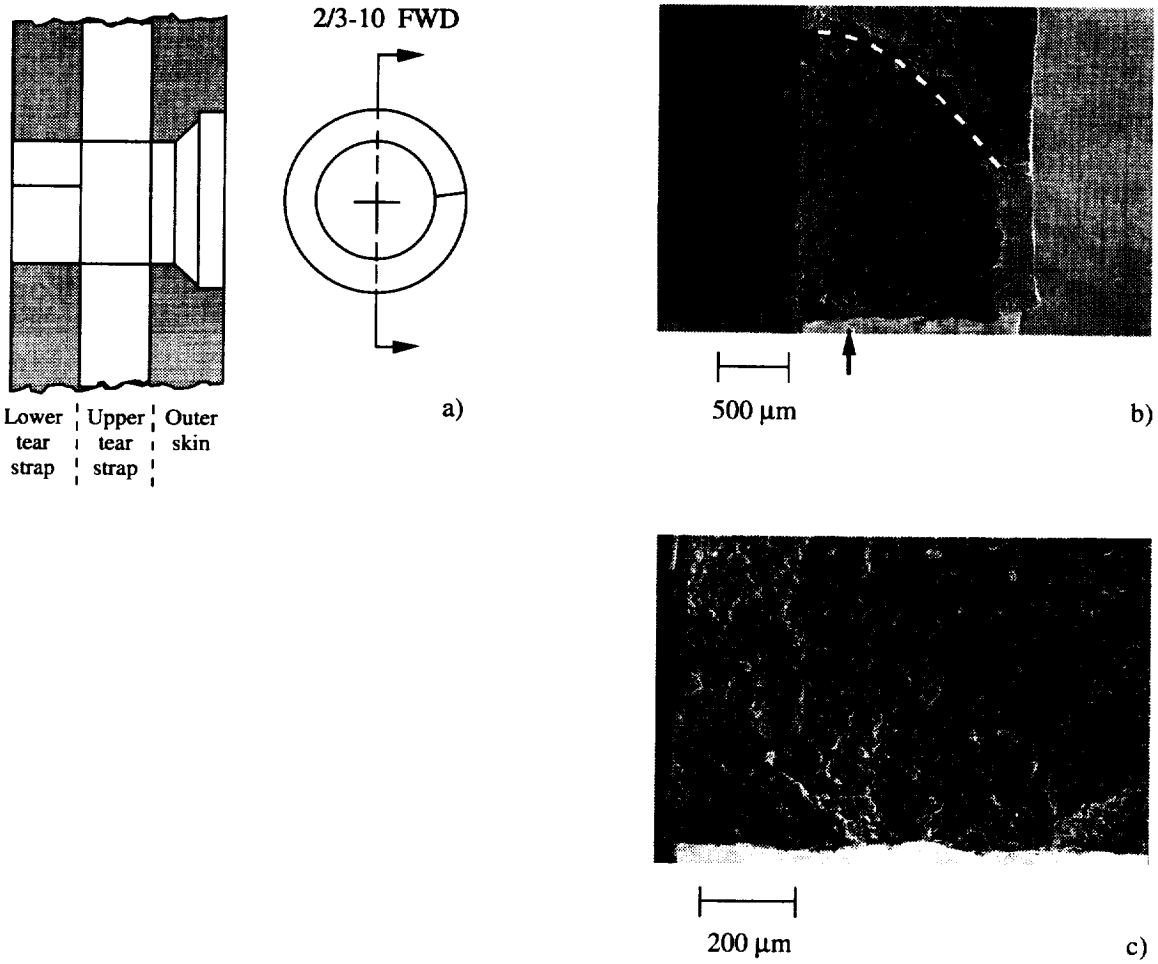

Figure 8.22 a) The schematic shows the rivet hole 2/3-10 configuration and the location of the lower T.S. fatigue crack oriented in the forward direction and about the 3 o'clock position. b) The SEM micrograph shows the fatigue crack contained in the lower T.S. The arrow marks the approximate location of crack initiation at the rivet hole. The dashed line marks the location of the fatigue crack front. c) The SEM micrograph shows the fatigue crack initiation region marked by the arrow in Figure 8.22.b.

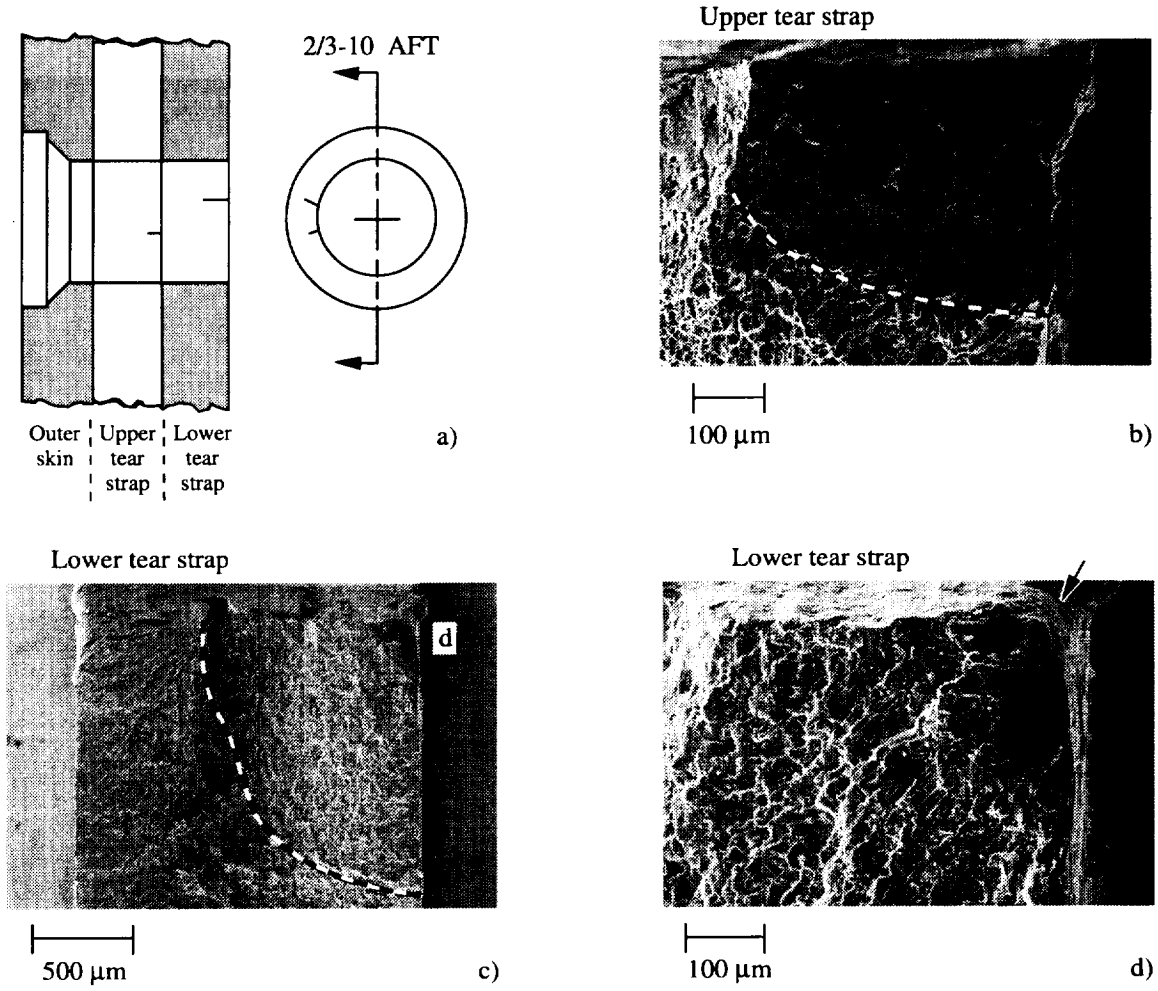

Figure 8.23 a) The schematic shows the rivet hole 2/3-10 configuration and the location of one upper T.S. fatigue crack and one lower T.S. fatigue crack oriented in the aft direction and at about the 9 o'clock position. b) The SEM micrograph shows the corner fatigue crack at the inboard corner of the rivet hole contained in the upper T.S. The dashed line marks the fatigue crack front. c) The SEM micrograph shows the corner fatigue crack at the inboard corner of the rivet hole contained in the lower T.S. The dashed line marks the fatigue crack front. d) The arrow in the SEM micrograph marks the likely crack initiation region "d" in Figure 8.23.c.

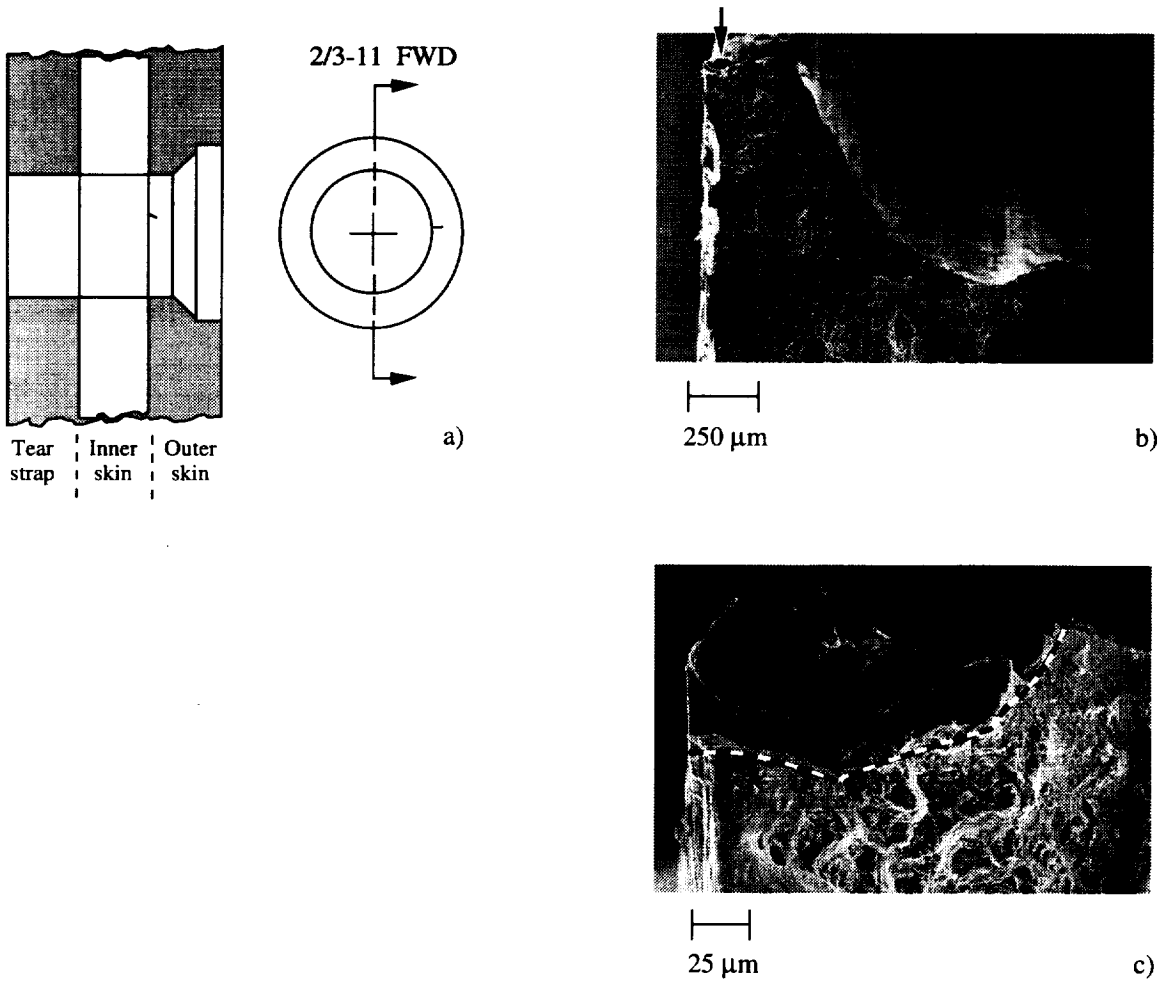

Figure 8.24 a) The schematic shows the rivet hole 2/3-11 configuration and the location of the outer skin fatigue crack oriented in the forward direction and above 3 o'clock position. b) The SEM micrograph shows the countersink region of the rivet hole. The arrow marks the location of the small fatigue crack at the rivet hole shank region. c) The SEM micrograph shows the small fatigue crack at the region marked by the arrow in Figure 8.24.b at high magnification.

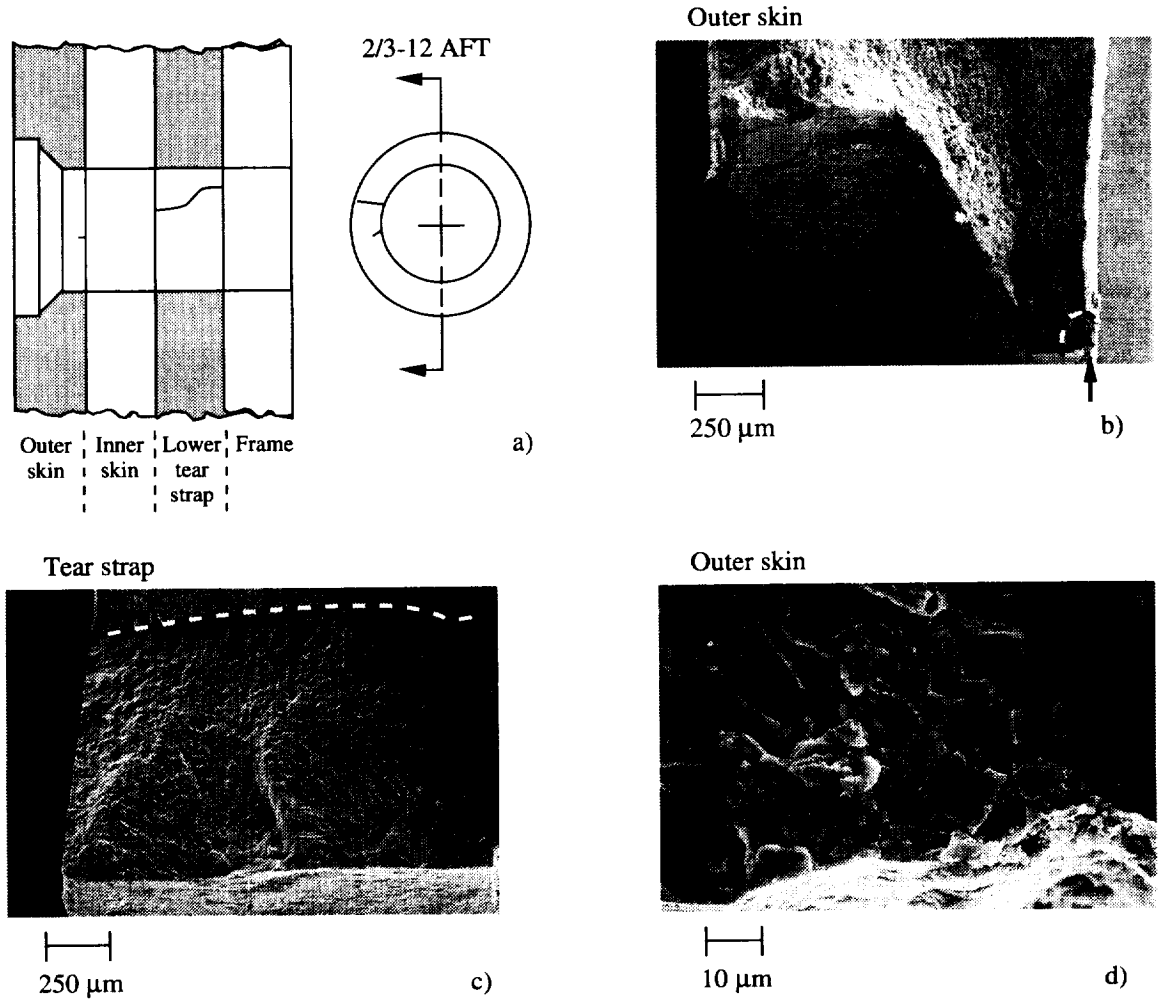

Figure 8.25 a) The schematic shows the rivet hole 2/3-12 configuration and the location of one outer skin fatigue crack and one lower T.S. fatigue crack oriented in the aft direction and at about the 9 and 10 o'clock positions, respectively. b) The SEM micrograph shows the fatigue crack fracture surface (arrow) located at the shank region of the rivet hole contained in the outer skin. The dashed line marks the fatigue crack front. c) The SEM micrograph shows the through-thickness fatigue crack that has propagated from the rivet hole (bottom on Figure 8.35.c) in the lower T.S. The dashed line marks the fatigue crack front. d) The SEM micrograph shows the crack initiation region marked by arrow in Figure 8.25.b.

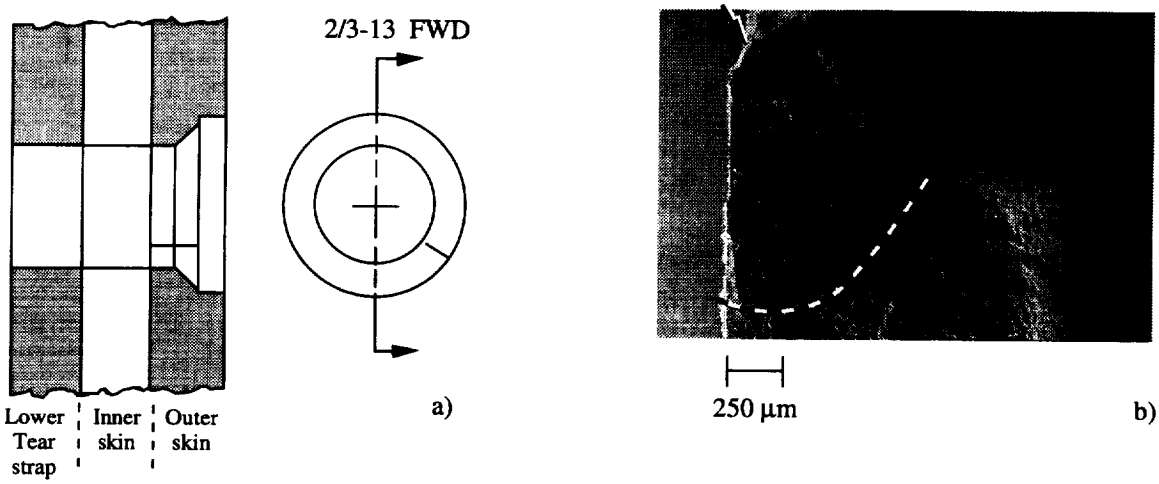

Figure 8.26 a) The schematic shows the rivet hole 2/3-13 configuration and the location of the outer skin fatigue crack oriented in the forward direction and at about the 4 o'clock position. b) The SEM micrograph shows the fatigue crack fracture surface located at the rivet hole contained in the outer skin. The dashed line marks the fatigue crack front and the arrow marks the likely site of crack initiation.

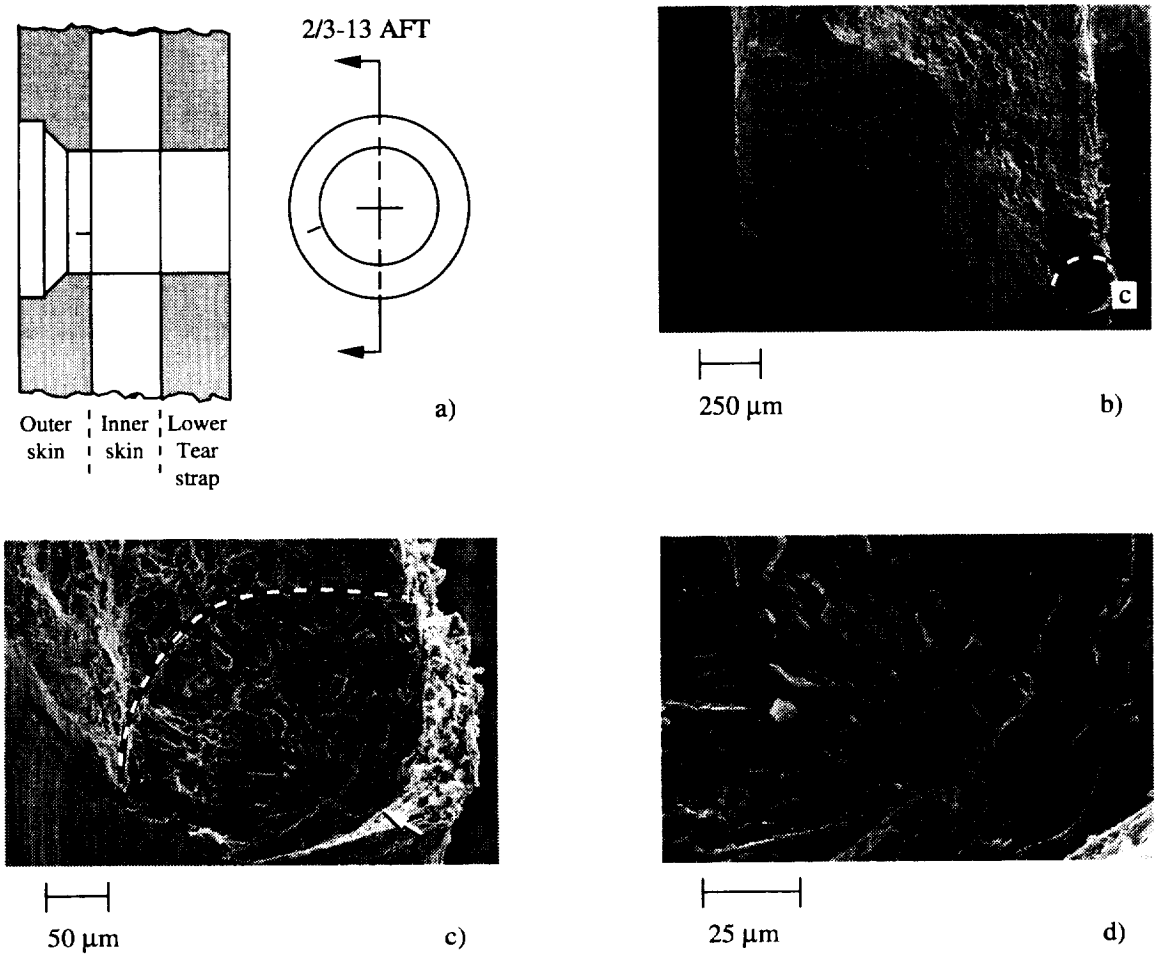

Figure 8.27 a) The schematic shows the rivet hole 2/3-13 configuration and the location of the outer skin fatigue crack oriented in the aft direction and at about the 8 o'clock position. b) The SEM micrograph shows the fatigue crack fracture surface located at the shank region of the rivet hole contained in the outer skin. The dashed line marks the fatigue crack front. c) The SEM micrograph shows region "c" in Figure 8.27.b at higher magnification. The arrow marks the crack initiation site and the dashed line marks the fatigue crack front. d) The SEM micrograph shows the crack initiation region marked by the arrow in Figure 8.27.c.

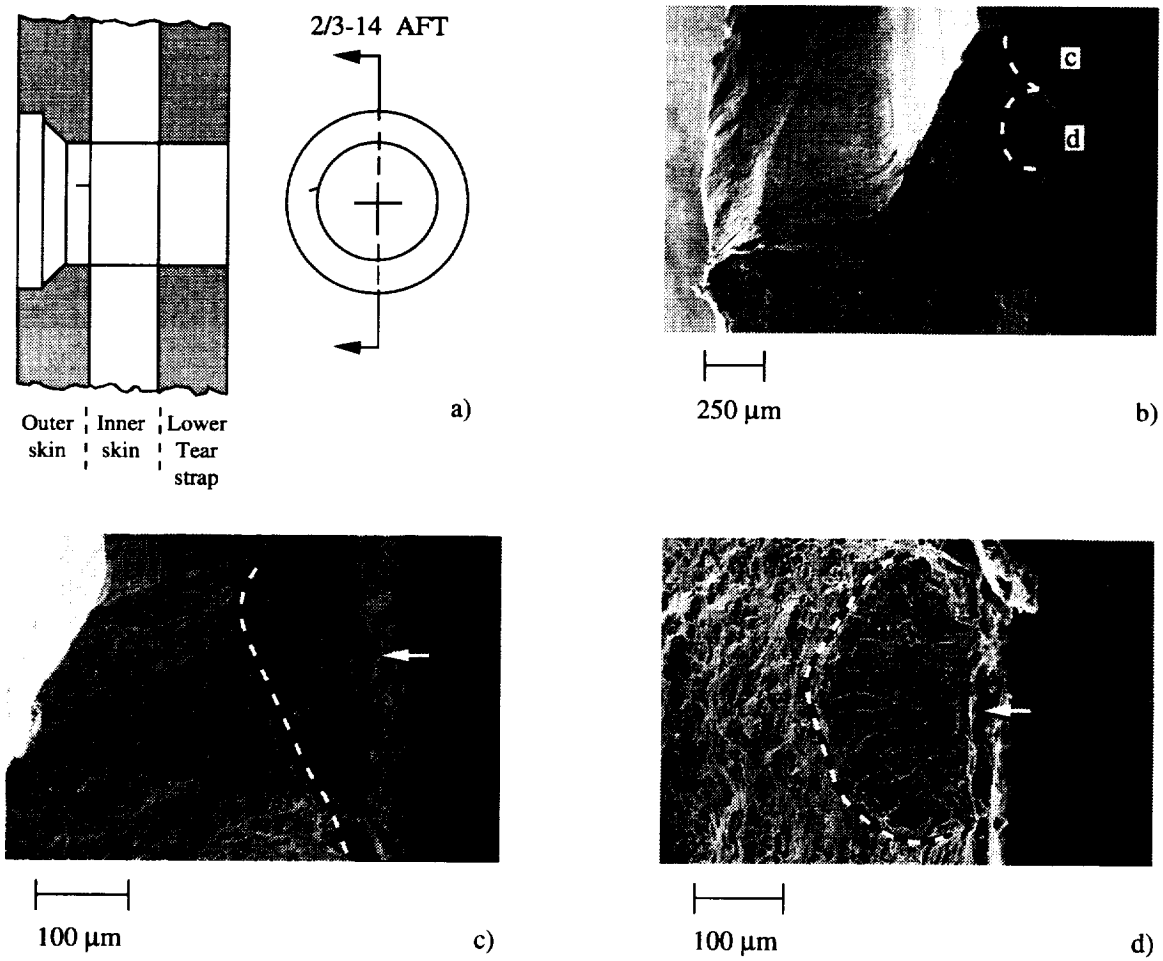

Figure 8.28 a) The schematic shows the rivet hole 2/3-14 configuration and the location of the outer skin fatigue crack oriented in the aft direction and above the 9 o'clock position. b) The SEM micrograph shows two fatigue cracks located along the faying surface. c) The SEM micrograph shows the faying surface fatigue crack at region "c" in Figure 8.28.b. The arrow marks the crack initiation site along the rough faying surface and the dashed line marks the fatigue crack front. d) The SEM micrograph shows the faying surface fatigue crack at region "d" in Figure 8.28.b. The arrow marks the crack initiation site along the rough faying surface and the dashed line marks the fatigue crack front.

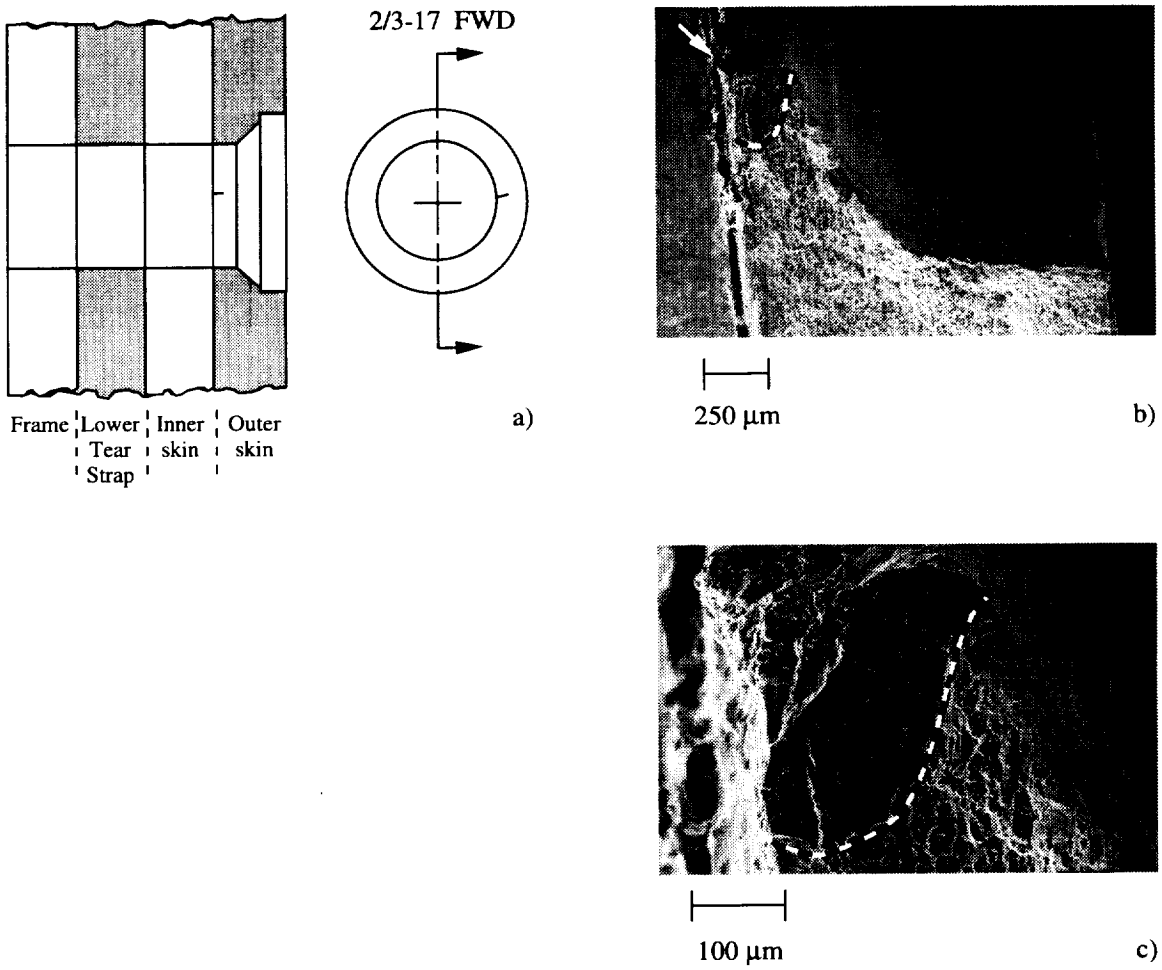

Figure 8.29 a) The schematic shows the rivet hole 2/3-17 configuration and the location of the outer skin fatigue crack oriented in the forward direction and above the 3 o'clock position. b) The SEM micrograph shows the fatigue crack fracture (arrow) surface located at the inboard corner of the rivet hole contained in the outer skin. The dashed line marks the fatigue crack front. c) The SEM micrograph shows the region marked by the arrow in Figure 8.29.b. The dashed line marks the fatigue crack front.

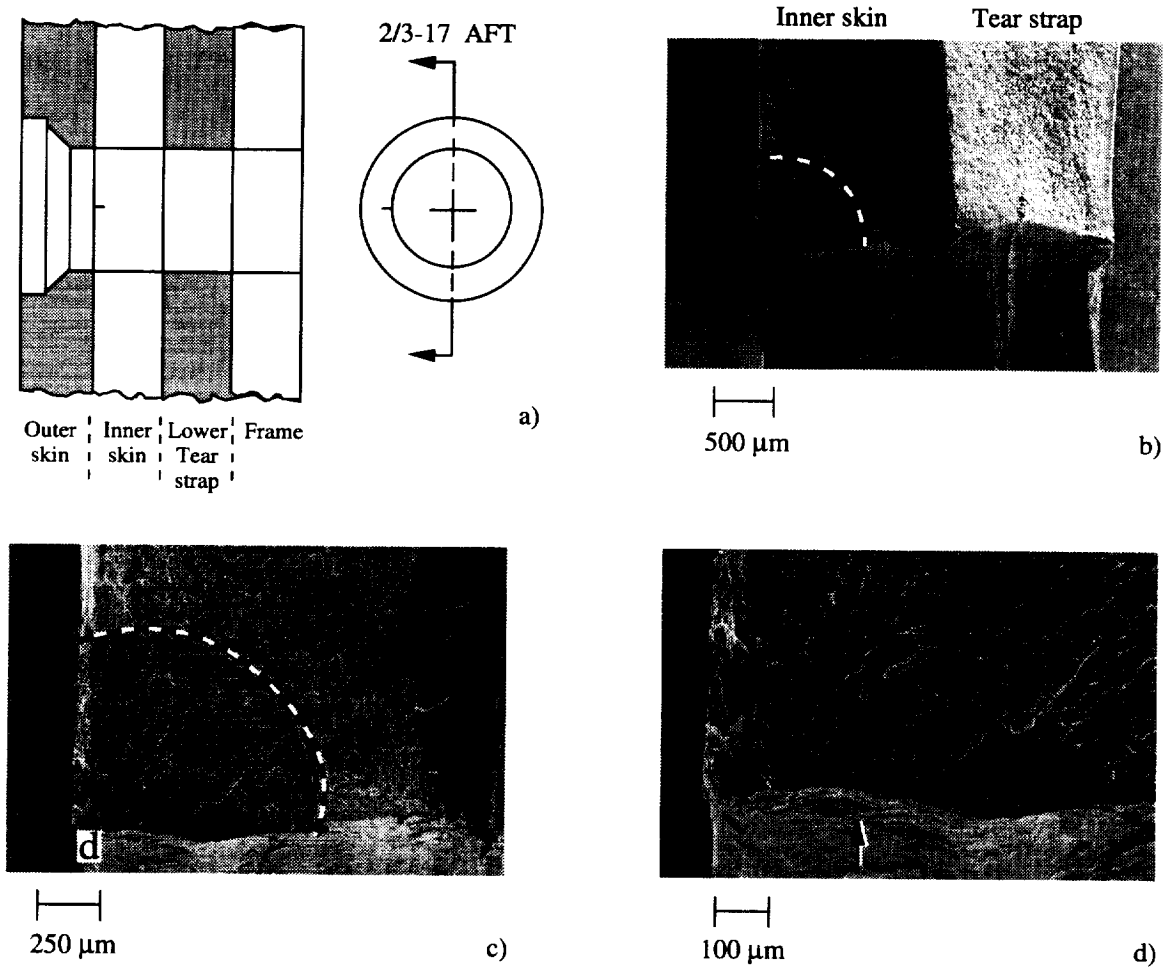

Figure 8.30 a) The schematic shows the rivet hole 2/3-17 configuration and the location of the inner skin corner fatigue crack oriented in the aft direction and at about the 9 o'clock position. b) The SEM micrograph shows the corner fatigue crack fracture surface located at the outboard corner of the inner skin rivet hole. The dashed line marks the fatigue crack front. The tear strap is located to the right of the inner skin. c) The SEM micrograph shows the inner skin corner crack at higher magnification. The dashed line marks the fatigue crack front. The bonded joint between the inner skin and tear strap is located on the far right of the micrograph. d) The SEM micrograph shows the crack initiation region "d" in Figure 8.30.c. An arrow marks the likely site of crack initiation.

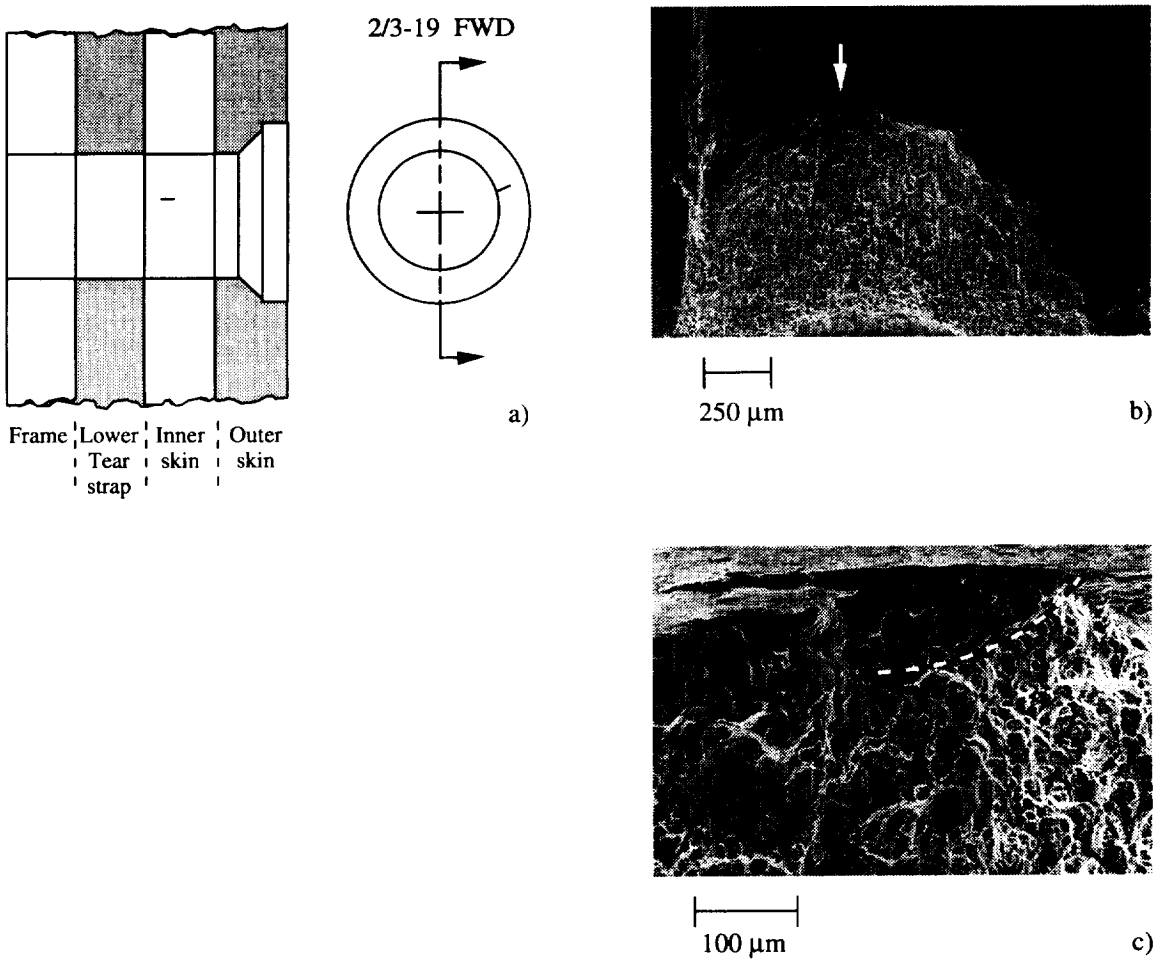

Figure 8.31 a) The schematic shows the rivet hole 2/3-19 configuration and the location of the inner skin fatigue crack oriented in the forward direction and at about the 2 o'clock position. b) The SEM micrograph shows the fatigue crack (arrow) located at the surface of the inner skin rivet hole (top of the micrograph). c) The SEM micrograph shows the surface fatigue crack at higher magnification. The inner skin rivet hole surface is located along the top of the micrograph. The dashed line marks the crack front of the partially hidden fatigue crack.

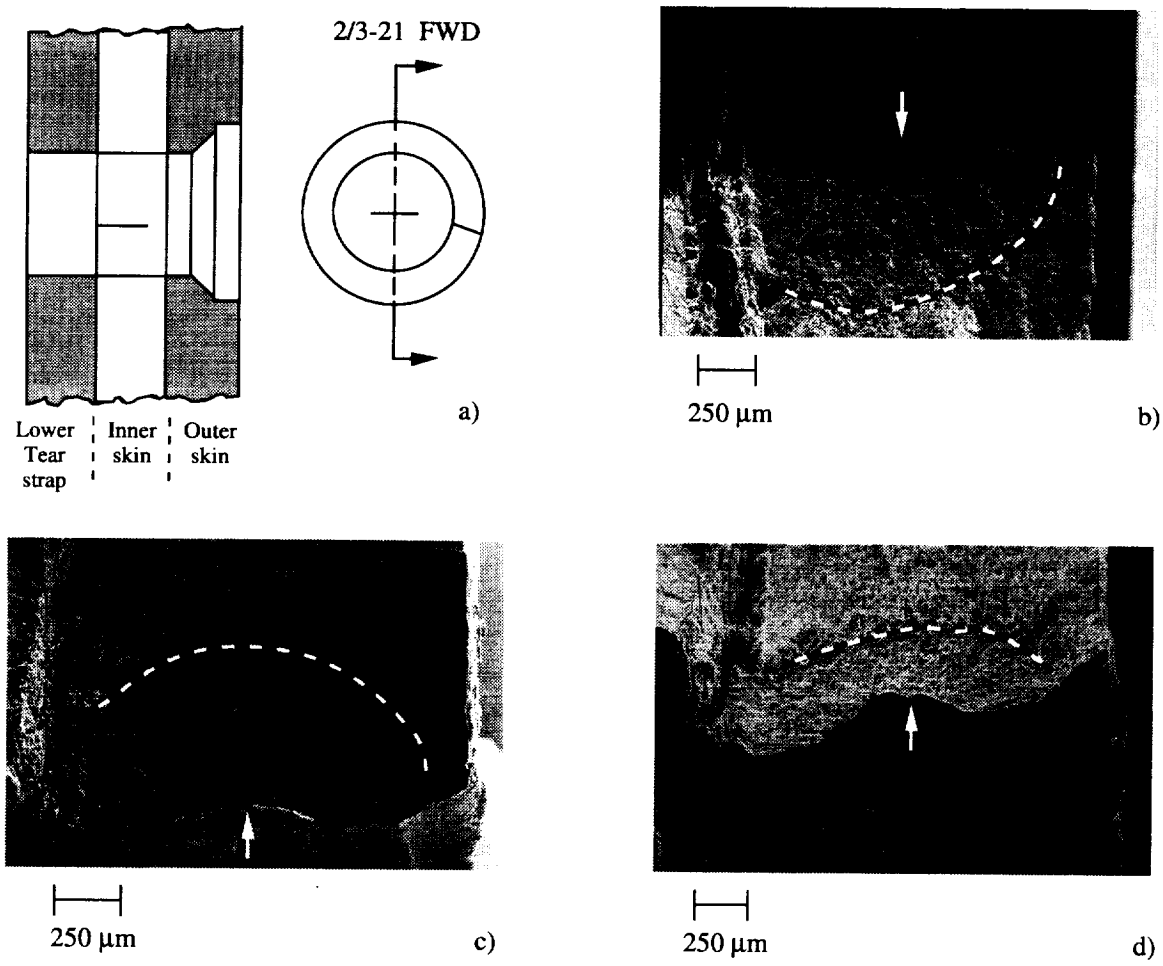

Figure 8.32 a) The schematic shows the rivet hole 2/3-21 configuration and the location of the inner skin fatigue crack oriented in the forward direction and below the 3 o'clock position. b) The SEM micrograph shows the fatigue crack fracture surface located along the rivet hole contained in the inner skin. The arrow marks the region of crack initiation, coincident with a rivet hole indentation. The dashed line marks the fatigue crack front. The region on the left side of the micrograph is the bond between the inner skin and tear strap. c) The SEM micrograph shows the inner skin rivet hole fatigue crack oriented at a 45° angle to the SEM beam. The arrow marks the crack initiation site and the dashed line marks the fatigue crack front. d) The SEM micrograph shows the inner skin fatigue crack at a third orientation. Here, the irregular rivet hole surface is highlighted with respect to the fatigue crack (crack front marked by the dashed line) fracture surface and the crack initiation site (arrow).

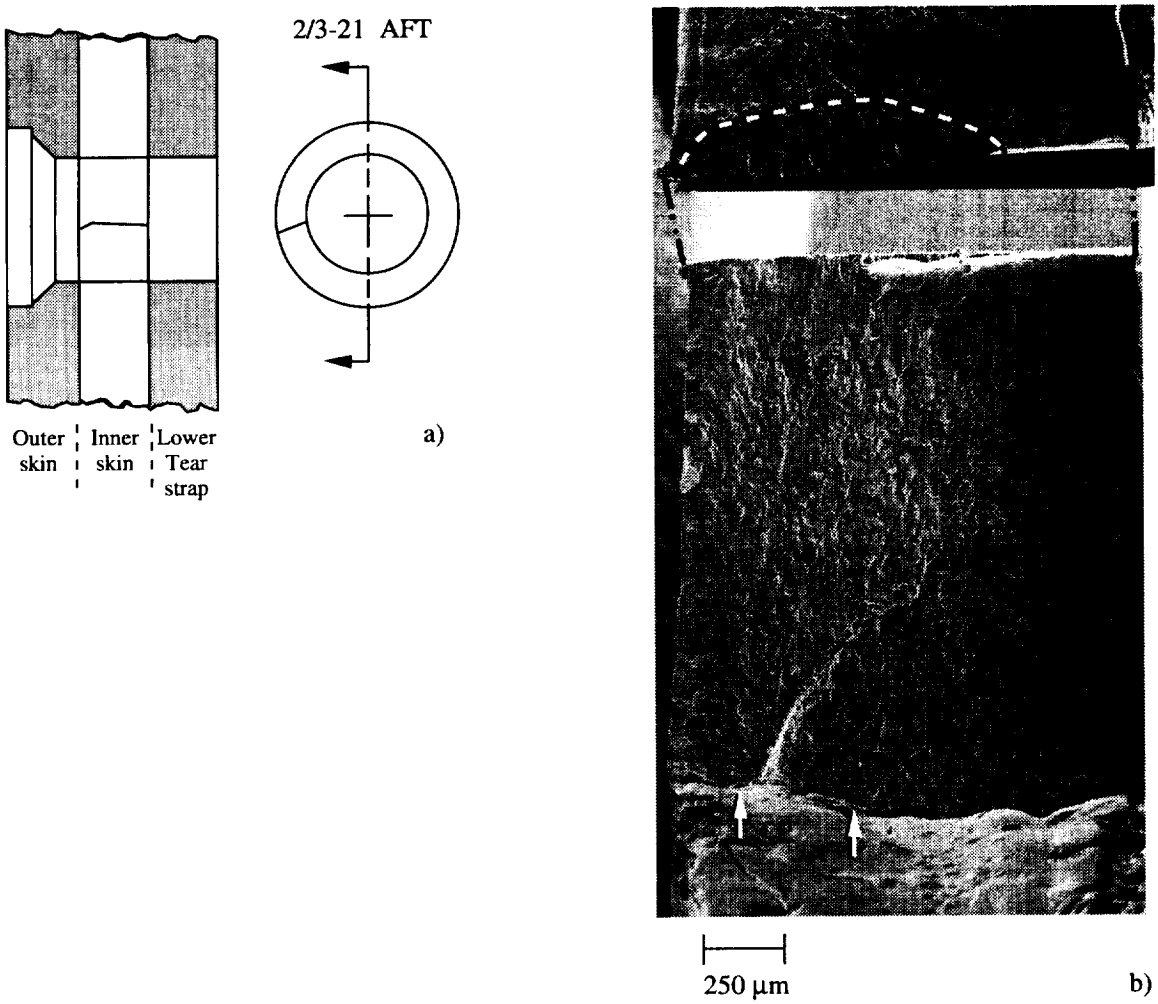

Figure 8.33 a) The schematic shows the rivet hole 2/3-21 configuration and the location of the inner skin fatigue crack oriented in the aft direction and below the 9 o'clock position. b) The SEM micrograph shows the inner skin through thickness fatigue crack fracture surface. The crack initiated at multiple sites (arrows) at the rivet hole (bottom of the micrograph). Here, the fracture surface was inadvertently cut during the destructive examination. A second specimen containing the remainder of the fatigue fracture surface is located at the top of the micrograph. The dashed line marks part of the fatigue crack front.

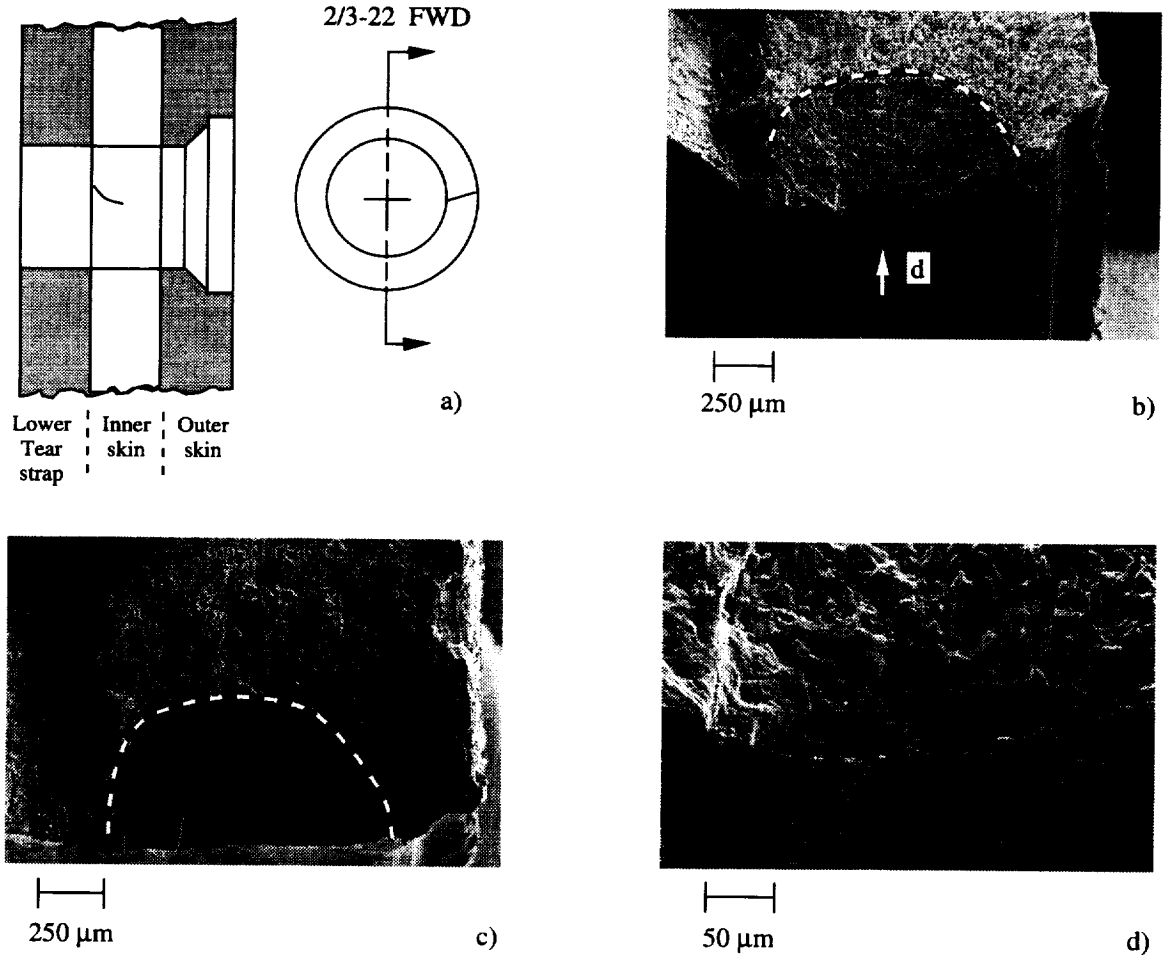

Figure 8.34 a) The schematic shows the rivet hole 2/3-22 configuration and the location of the inner skin fatigue crack oriented in the forward direction and at about the 3 o'clock position. b) The SEM micrograph shows the fatigue crack fracture surface located at the inner skin rivet hole. The specimen is oriented 45° to the SEM beam. The arrow marks the area of crack initiation on the surface of the rivet hole and the dashed line marks the fatigue crack front. The area to the left is the bonded region between the inner skin and tear strap. c) The SEM micrograph shows another view of the inner skin fatigue crack with a nearly semicircular crack marked by the dashed line. d) The SEM micrograph shows the crack initiation region "d" in Figure 8.34.b.

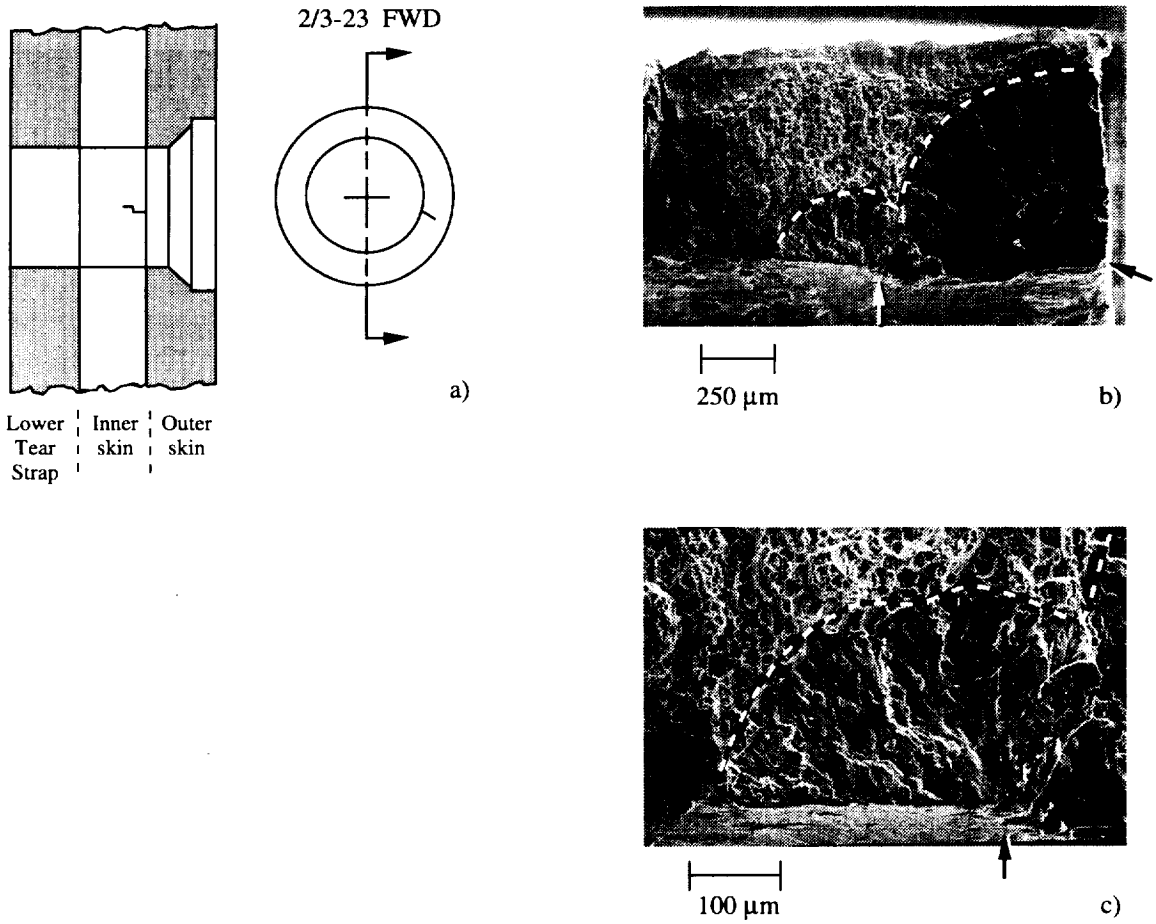

Figure 8.35 a) The schematic shows the rivet hole 2/3-23 configuration and the location of the inner skin fatigue crack oriented in the forward direction and below the 3 o'clock position. b) The SEM micrograph shows a fatigue crack fracture surface located at the outboard corner of the rivet hole contained in the inner skin. The dashed line marks the fatigue crack front showing that a corner crack and surface crack located in the rivet hole had coalesced. Arrows mark the likely sites of crack initiation. c) The SEM micrograph shows the portion of the fatigue crack located at mid thickness at high magnification. The arrow marks the crack initiation site and the dashed line marks the fatigue crack front.

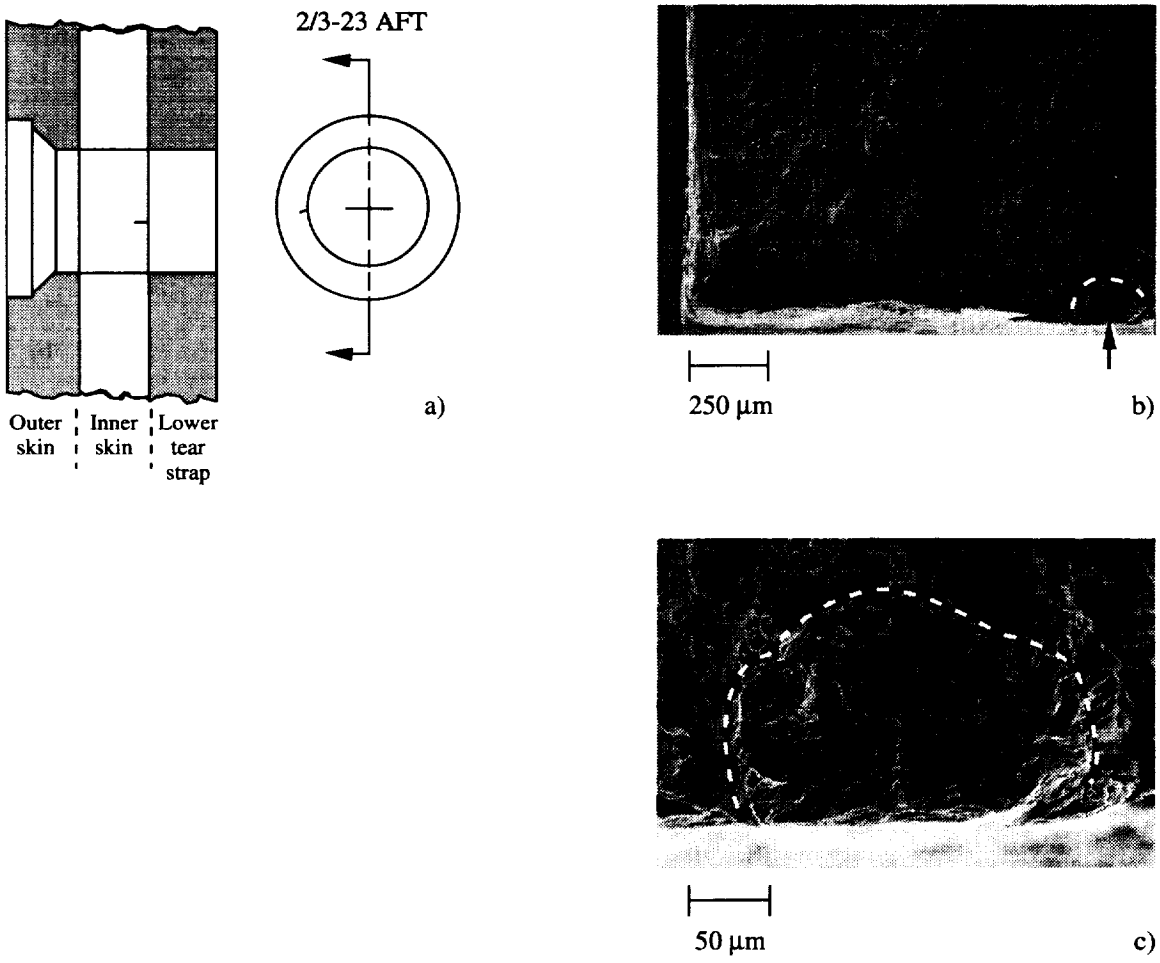

Figure 8.36 a) The schematic shows the rivet hole 2/3-23 configuration and the location of the inner skin fatigue crack oriented in the aft direction and below the 9 o'clock position. b) The SEM micrograph shows the fatigue crack fracture surface located at the inboard corner of the inner skin. The arrow marks the crack initiation site and the dashed line marks the fatigue crack front. c) The SEM micrograph shows the corner fatigue crack at higher magnification. The dashed line marks the fatigue crack front.

9. Destructive Examination of Bay 3

All rivet holes shown in Figure 9.1, a total of sixty-six rivet hole locations, were destructively examined. Fourteen of the fifteen upper rivet row locations exhibited fatigue cracking (a total of 24 fatigue cracks). The remaining rivet rows contained fourteen fatigue cracks in 9 rivet hole locations: six cracks in row I, six cracks in row H, and two cracks in the bottom row G. Figures 9.2 and 9.3 show the location of all fatigue cracks found in the first layer (outer skin) and the second layer (inner skin), respectively. Rivet rows J and I contained outer skin cracks and rows H and G contained both inner and outer skin cracks. The through-thickness schematics shown in Figures 9.4, 9.5, 9.6, 9.7, and 9.8 summarize crack location, crack length crack type and initiation site for rivet rows J, I, H, and G, respectively. The following is a detailed description of the fatigue damage in bay 3.

9.1 Fatigue Cracks Contained in Row J:

Figures 9.9 through 9.32 describe the fatigue crack morphology in row J.

9.2 Fatigue Cracks Contained in Row I:

Figures 9.3 through 9.38 describe the fatigue crack morphology in row I.

9.3 Fatigue Cracks Contained in Row H:

Figures 9.39 through 9.43 describe the fatigue crack morphology in row H.

9.4 Fatigue Cracks Contained in Row G:

Figures 9.44 and 9.45 describe the fatigue crack morphology in row G.

9.5 Bay 3 Summary:

Table 9.1 summarizes the destructive examination results for bay 3 rivet rows G, H, I, and J. Row J was found to contain most of the fatigue cracks, twenty-four. Bay 3 cracks, range in length from 0.055 mm (0.002 in.) to 4.890 mm (0.192 in.). The upper rivet rows J and I contained outer skin cracks. Rows H and G contained both outer and inner skin cracking. The following observations were made as a result of fractographic examinations of bay 3.

9.5.1 Crack initiation site(s):

Row J: Most fatigue cracks initiated along the outer/inner skin faying surface in the region under the rivet head. The faying surfaces exhibited black oxide and disturbed metal suggesting fretting contact at the point of crack initiation.

Row I: Most outer skin fatigue cracks initiated at the rivet hole shank region. Cracks initiated at deformed areas and regions having disturbed surfaces.

Row H: Fatigue cracks initiated in the inner skin rivet hole at the outboard corner facing the outer skin. Burrs and disturbed metal were observed at the point of crack initiation.

Row G: Fatigue crack initiation was observed in three distinct inner skin regions, (1) rivet hole surface, (2) rivet hole corner, and (3) inner/outer skin faying surface.

9.5.2 Crack front shape as a function of crack length:

Row J: A distinct pattern in crack front shape was observed. Cracks initiated and grew from the faying surface and continued to grow as subsurface fatigue cracks. The subsurface cracks formed a thin ligament along the outboard surface of the outer skin. The fatigue cracks continued to propagate along the faying surface to a distance equivalent to 2 - 3 skin thicknesses without becoming through-thickness fatigue cracks.

Row I, H and G: Fatigue cracks were small and no data on crack shape versus crack length was obtained.

9.5.3 Fatigue crack/stable tearing transition crack length:

Row J, I, H, and G: All cracks exhibited a transgranular morphology. Little stable tearing was observed.

9.5.4 Slant fracture morphology:

Row J, I, H, and G: No slant fracture morphology was observed.

9.5.5 Evidence of corrosion:

Row J, I, H, and G: No corrosion was observed.

Table 9-1 Bay 3 Fatigue Crack Summary

Rivet Row	No. of Cracks (Holes)	Location	Crack Length mm (in)	Comment
J	12(11)	Outer Skin	0.307(0.012)≤a	High K_T
	12(9)	Outer Skin	≤4.890(0.192)	Fretting
I	5(4)	Outer Skin	0.084(0.003)≤a	High K_T
	1(1)	Outer Skin	≤0.336(0.013)	High K_T
H	2(2)	Outer Skin	a=0.055(0.002)	High K_T
			a=0.125(0.005)	High K_T
	4(4)	Inner Skin	0.170(0.008)≤a ≤0.246(0.010)	High K_T
G	1(1)	Outer Skin	a=0.091(0.004)	Fretting
	1(1)	Inner Skin	a=0.120(0.005)	High K_T

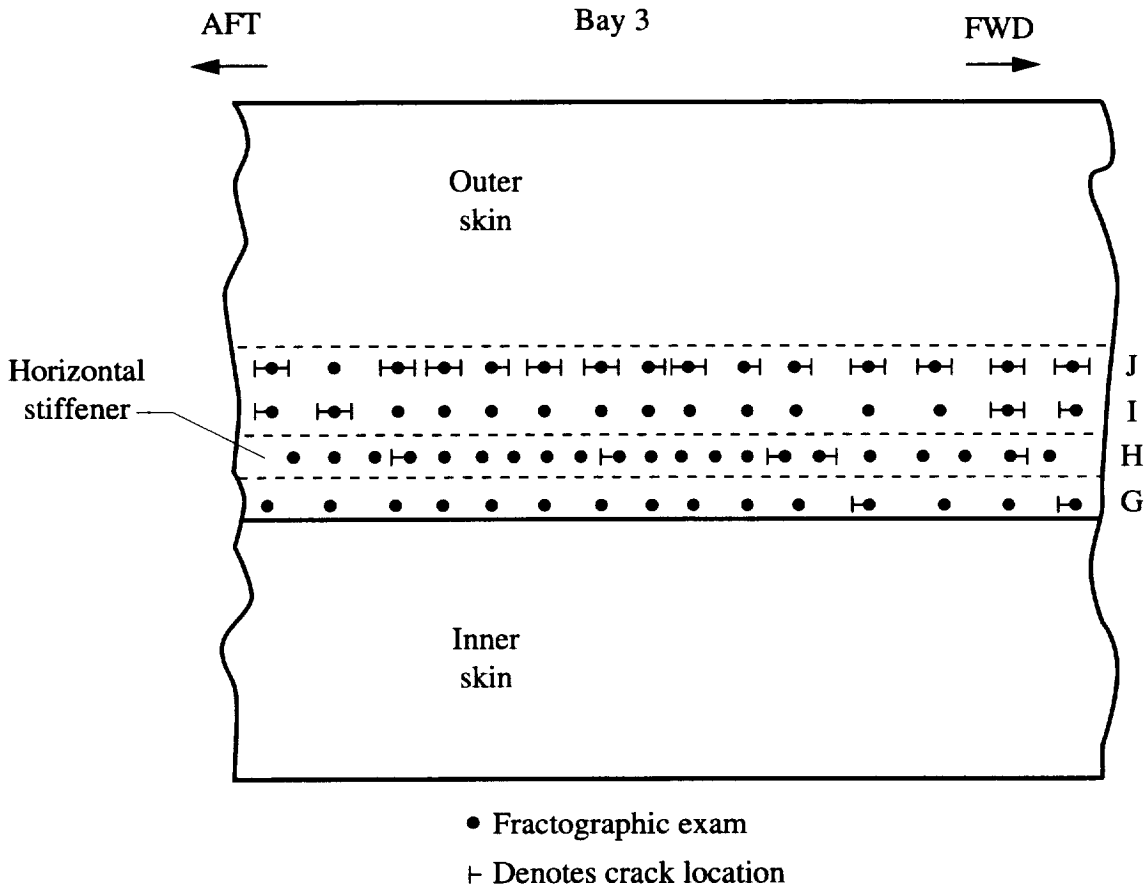

Figure 9.1 The schematic shows the location of all fatigue cracks found in the bay 3 lap splice joint by destructive examination. All bay 3 rivet holes were destructively examined.

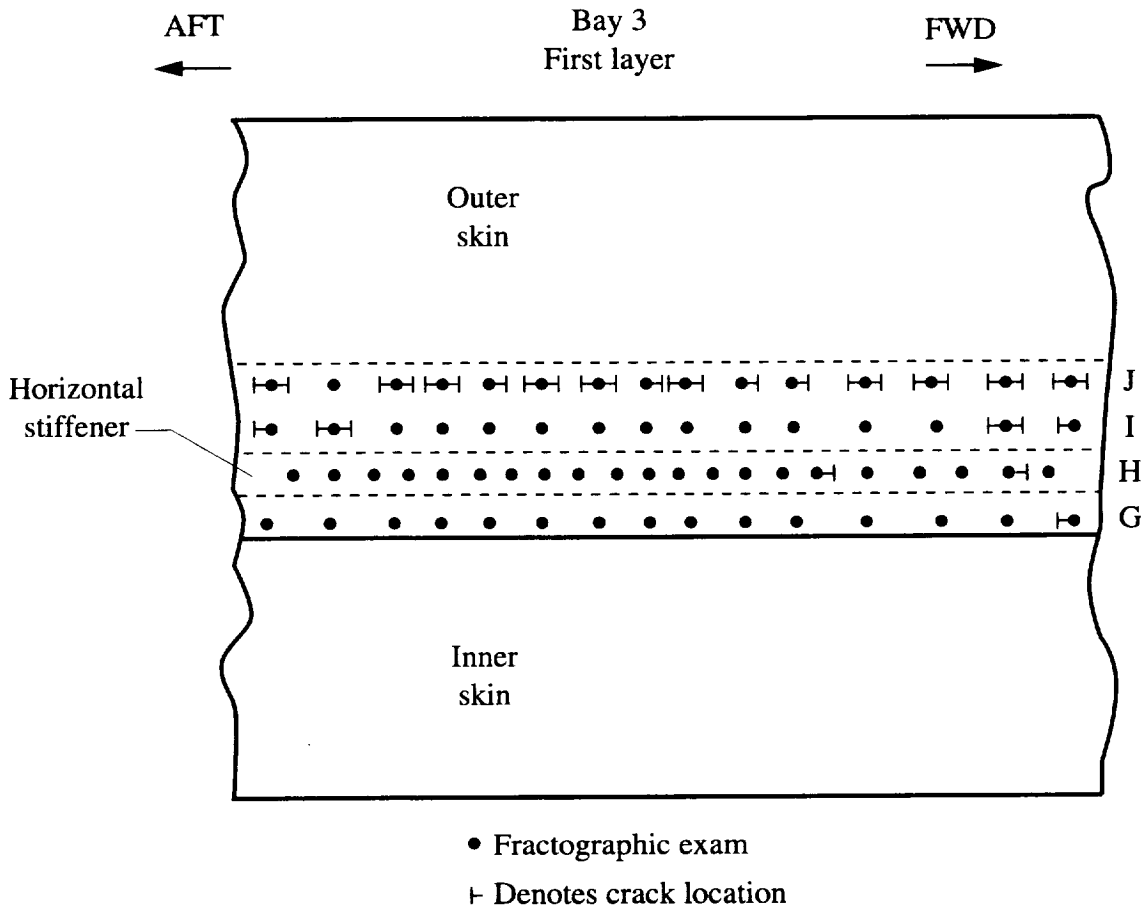

Figure 9.2 The schematic shows the location of fatigue cracks found in the first layer (outer skin) of the bay 3 lap splice joint by destructive examination.

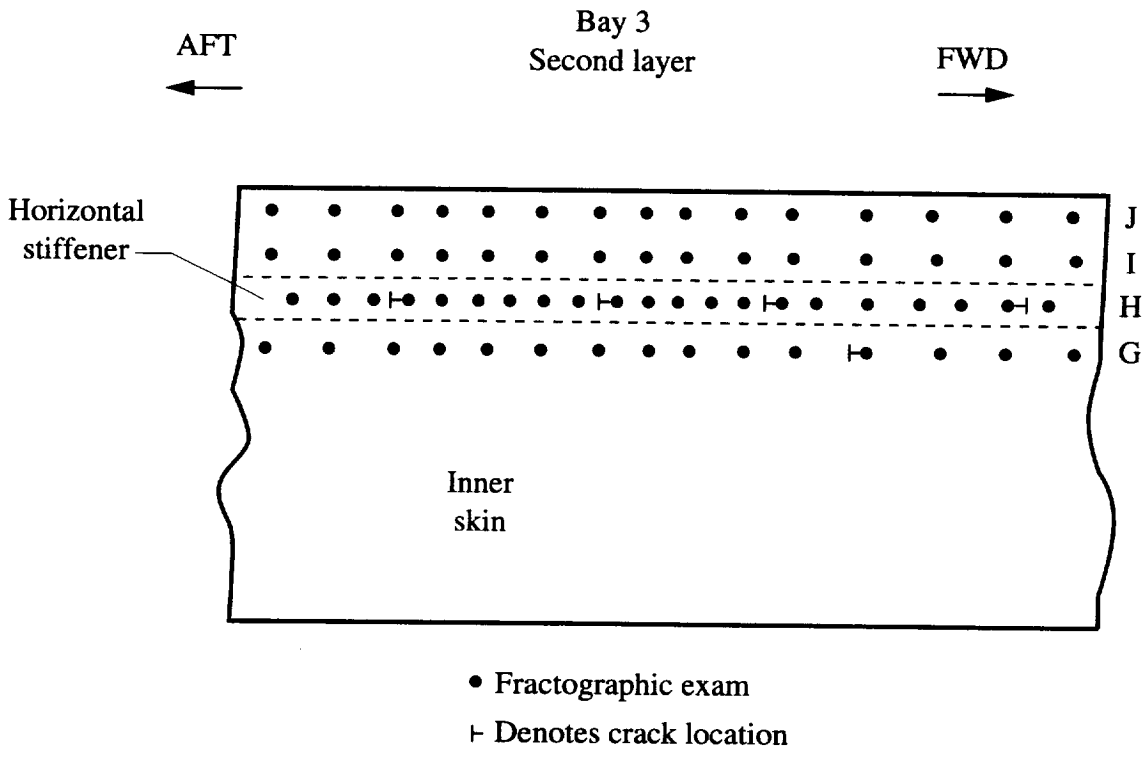

Figure 9.3 The schematic shows the location of fatigue cracks found in the second layer (inner skin) of the bay 3 lap splice joint by destructive examination.

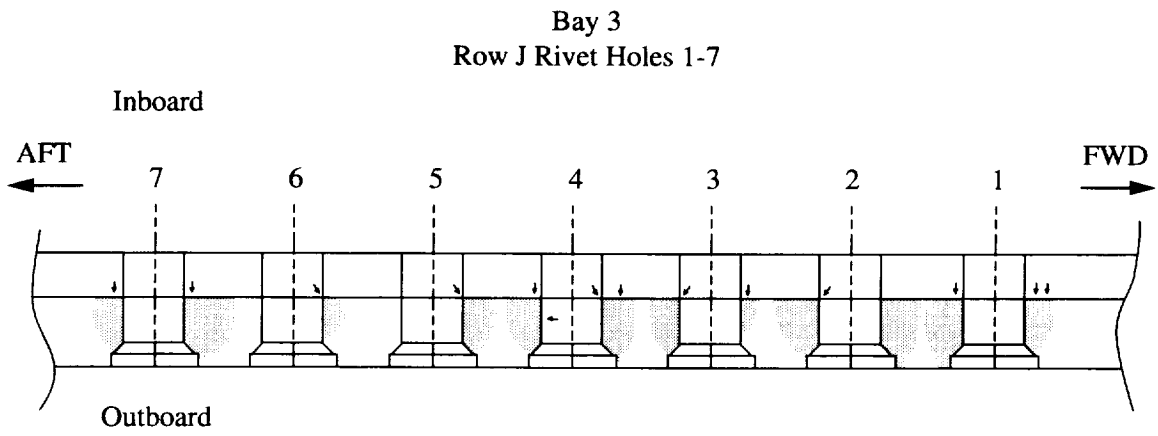

Hole #	Location	Length mm (in)	Type	Initiation site
1 (Aft)	Outer Skin	4.733 (0.186)	Through	Inner skin / outer skin
1 (Fwd)	Outer Skin	2.550 (0.100)	Through	Inner skin / outer skin
2 (Aft)	Outer Skin	2.300 (0.091)	Countersink	Inboard corner of shank
2 (Fwd)	Outer Skin	4.222 (0.166)	Through	Not determined
3 (Aft)	Outer Skin	1.625 (0.064)	Countersink	Inboard side of shank
3 (Fwd)	Outer Skin	1.071 (0.042)	Fretting	Inner skin / outer skin
4 (Aft)	Outer Skin	1.833 (0.072)	Countersink	Multiple sites
4 (Fwd)	Outer Skin	2.439 (0.096)	Countersink	Multiple sites
5 (Fwd)	Outer Skin	1.737 (0.068)	Countersink	Inner skin / outer skin
6 (Fwd)	Outer Skin	0.662 (0.026)	Countersink	Inboard side of shank
7 (Aft)	Outer Skin	1.419 (0.056)	Countersink	Inner skin / outer skin
7 (Fwd)	Outer Skin	2.500 (0.098)	Fretting	Inner skin / outer skin

Figure 9.4 The through thickness schematic shows the location and initiation site of fatigue cracks found in rivet row J (holes 1-7) of bay 3. The table summarizes crack location, crack length, crack type, and initiation site for each fatigue crack shown.

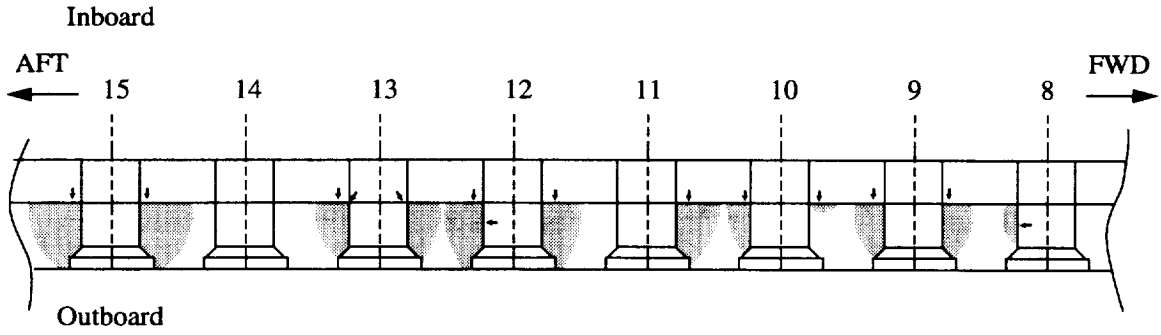

Hole #	Location	Length mm (in)	Type	Initiation site
8 (Aft)	Outer Skin	0.742 (0.029)	Countersink	Center of shank
9 (Aft)	Outer Skin	1.737 (0.068)	Countersink	Inner skin / outer skin
9 (Fwd)	Outer Skin	1.130 (0.044)	Countersink	Inner skin / outer skin
10 (Aft)	Outer Skin	0.905 (0.036)	Countersink	Inner skin / outer skin
10 (Fwd)	Outer Skin	0.307 (0.012)	Fretting	Inner skin / outer skin
11 (Fwd)	Outer Skin	4.160 (0.164)	Countersink	Inner skin / outer skin
12 (Aft)	Outer Skin	3.220 (0.127)	Through	Multiple sites
12 (Fwd)	Outer Skin	4.890 (0.192)	Through	Inner skin / outer skin
13 (Aft)	Outer Skin	2.030 (0.080)	Countersink	Multiple sites
13 (Fwd)	Outer Skin	2.500 (0.098)	Countersink	Inner skin / outer skin
15 (Aft)	Outer Skin	3.040 (0.120)	Through	Inner skin / outer skin
15 (Fwd)	Outer Skin	2.980 (0.115)	Through	Inner skin / outer skin

Figure 9.5 The through thickness schematic shows the location and initiation site of fatigue cracks found in rivet row J (holes 8-15) of bay 3. The table summarizes crack location, crack length, crack type, and initiation site for each fatigue crack shown.

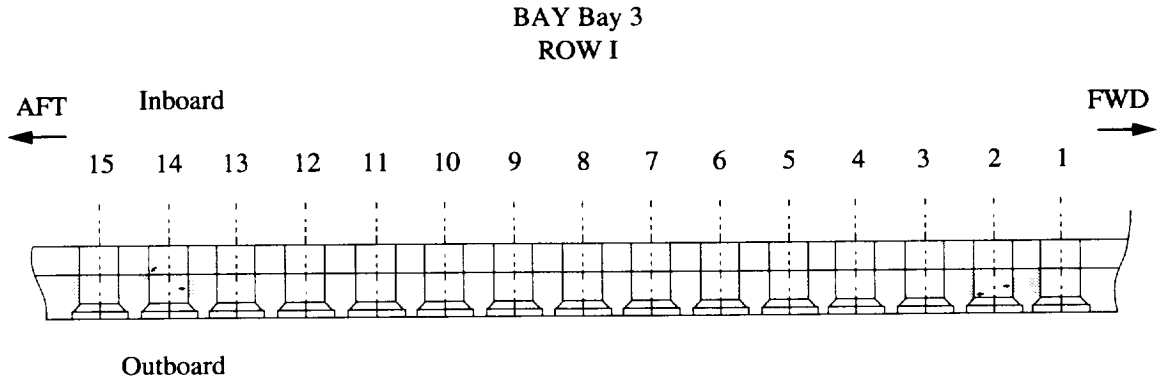

Hole #	Location	Length mm (in)	Type	Initiation site
1 (Aft)	Outer Skin	Not determined	Countersink	Not determined
2 (Aft)	Outer Skin	0.336 (0.013)	Countersink	Outboard side of shank
2 (Fwd)	Outer Skin	0.088 (0.003)	Countersink	Center of shank
14 (Aft)	Outer Skin	0.084 (0.003)	Countersink	Inboard side of shank
14 (Fwd)	Outer Skin	0.174 (0.007)	Countersink	Center of shank
15 (Aft)	Outer Skin	0.148 (0.006)	Countersink	Center of shank

Figure 9.6 The through thickness schematic shows the location and initiation site of fatigue cracks found in rivet row I of bay 3. The table summarizes crack location, crack length, crack type, and initiation site for each fatigue crack shown.

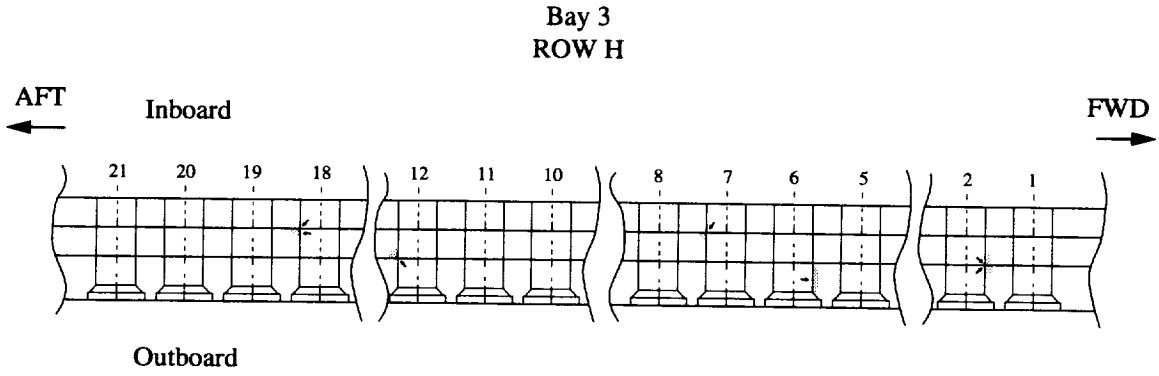

Hole #	Location	Length mm(in)	Type	Initiation site
2(1 Fwd)	Inner skin	0.246 (0.010)	Corner	Outboard corner
2(2 Fwd)	Outer skin	0.055 (0.002)	Countersink	Inboard corner of shank
6(Fwd)	Outer skin	0.125 (0.005)	Countersink	Center of shank
7(Aft)	Inner skin	0.183 (0.007)	Corner	Inboard corner
12(Aft)	Inner skin	0.170 (0.007)	Corner	Outboard corner
18(Aft)	Inner skin	0.184 (0.007)	Corner/surface	Corner and surface

Figure 9.7 The through thickness schematic shows the location and initiation site of fatigue cracks found in rivet row H of bay 3. The table summarizes crack location, crack length, crack type, and initiation site for each fatigue crack shown.

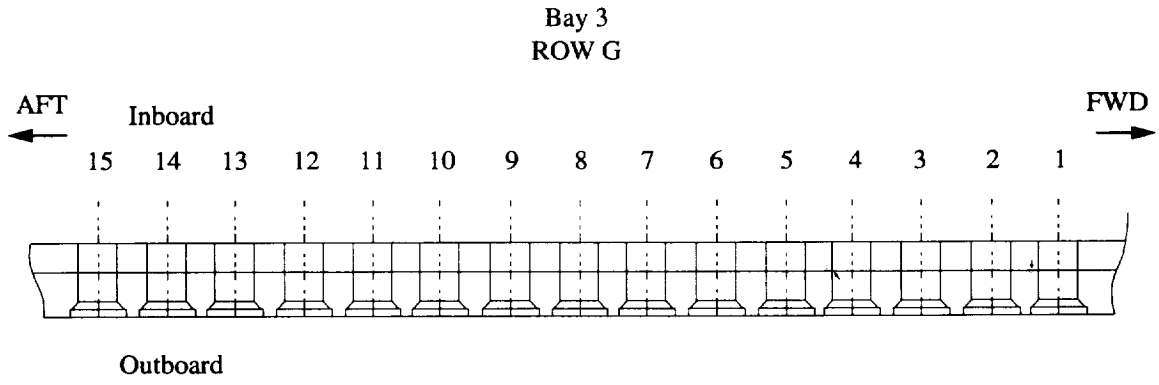

Hole #	Location	Length mm(in)	Type	Initiation site
1(Aft)	Countersink	0.091 (0.004)	Fretting	Inner skin/outer skin
4(Aft)	Inner skin	0.120 (0.005)	Corner	Outboard corner

Figure 9.8 The through thickness schematic shows the location and initiation site of fatigue cracks found in rivet row G of bay 3. The table summarizes crack location, crack length, crack type, and initiation site for each fatigue crack shown.

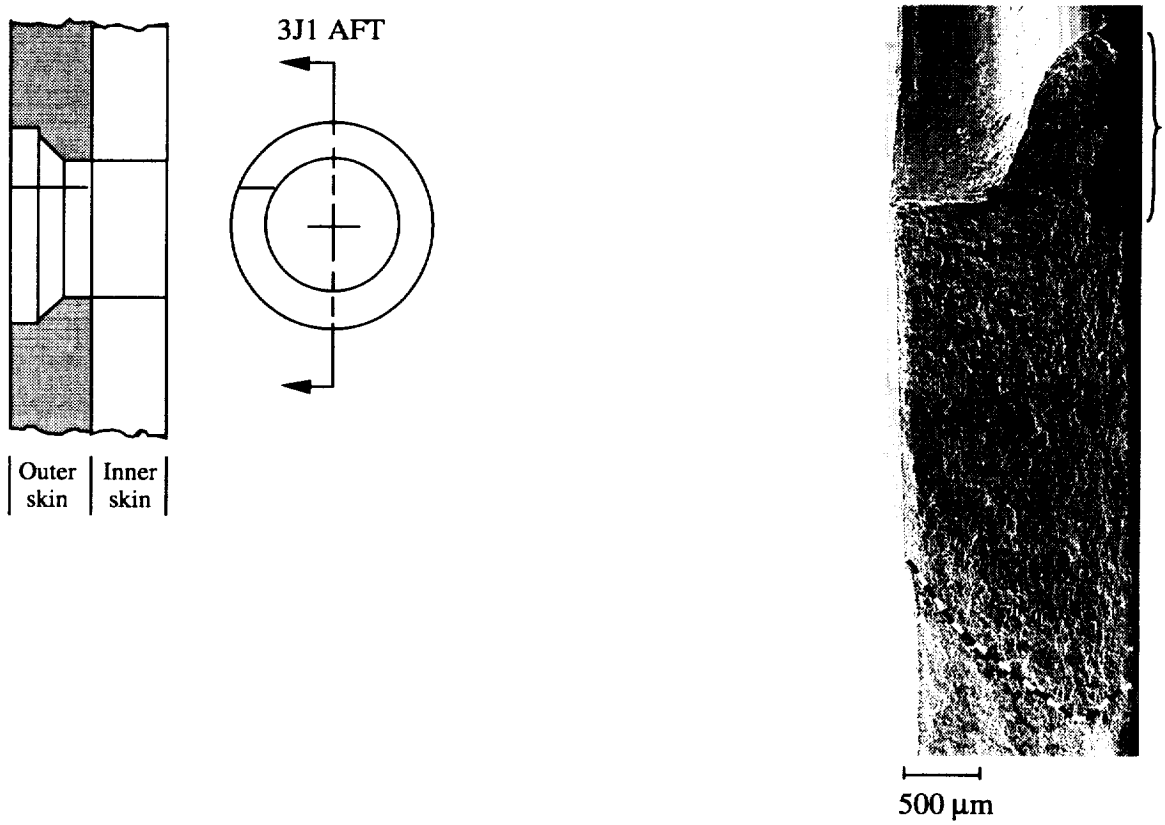

Figure 9.9 a) The schematic shows the rivet hole 3J1 configuration and the location of the outer skin fatigue crack oriented in the aft direction and about the 10 o'clock position. b) The SEM micrograph shows the through-thickness fatigue crack and the rivet hole (top). The bracket shows the likely crack initiation region along the faying surface and the dashed line marks the fatigue crack front. Considerable oxide was noted in the region of crack initiation.

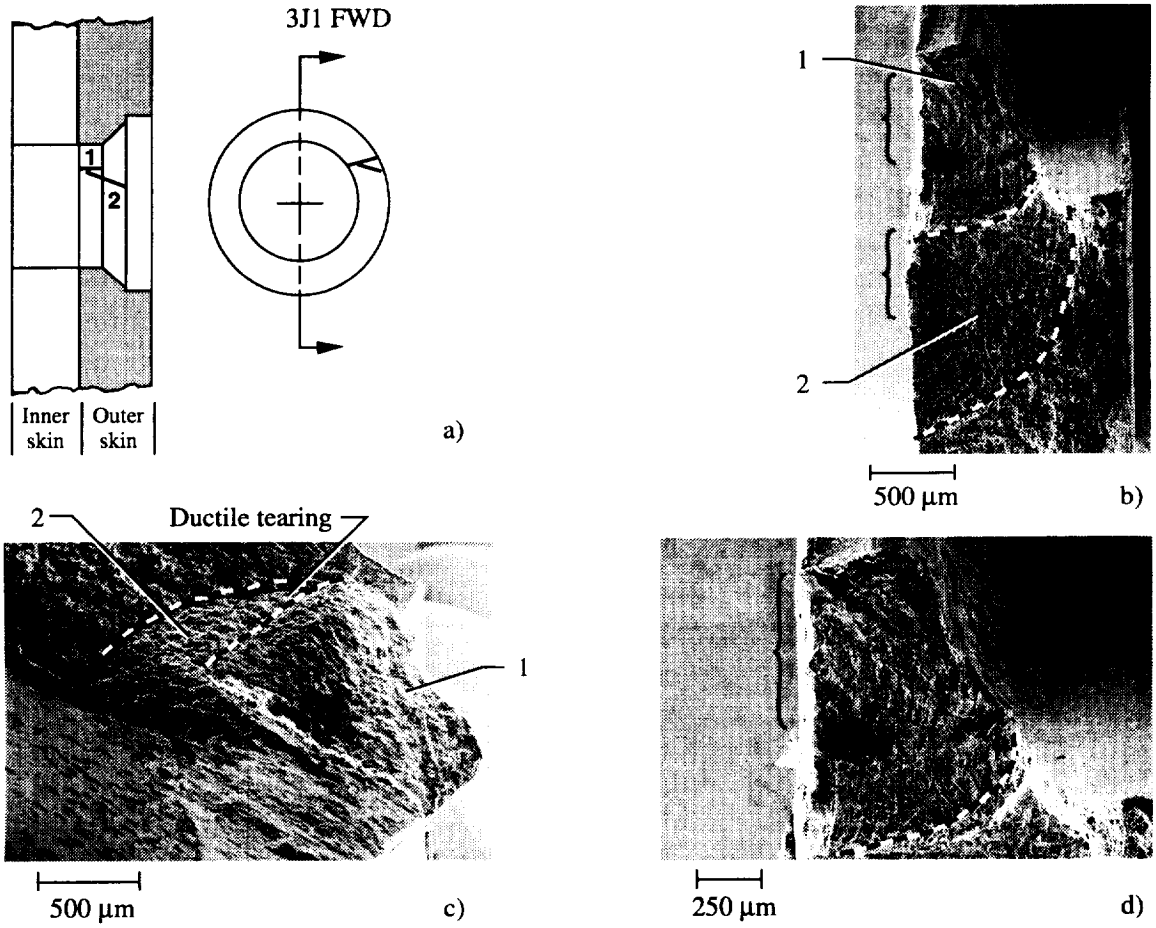

Figure 9.10 a) The schematic shows the rivet hole 3J1 configuration and the location of two outer skin fatigue cracks oriented in the forward direction and about the 2 o'clock position. b) The SEM micrograph shows the fracture surface of two (1 & 2) fatigue cracks and the rivet hole (top). The dashed lines mark both fatigue crack fronts. Brackets identify the crack initiation regions of both cracks along the faying surface. c) The SEM micrograph shows the fatigue fracture surface at an oblique angle. The dashed line marks a region of ductile tearing, suggesting that a portion of the crack fronts had not joined until this region was destructively examined. d) The SEM micrograph shows the fracture surface of crack #1 and the region of crack initiation (bracket) at higher magnification.

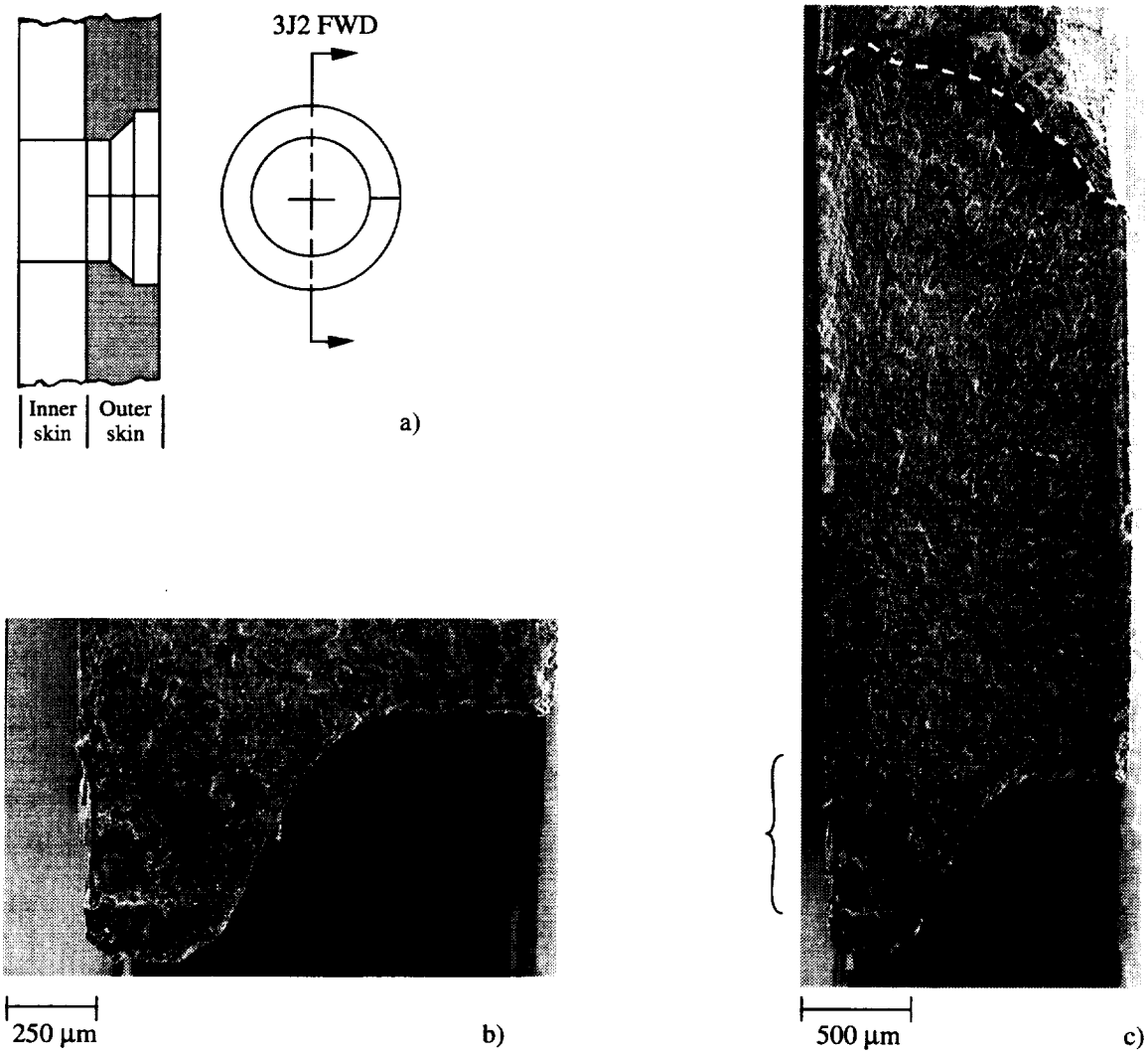

Figure 9.11 a) The schematic shows the rivet hole 3J2 configuration and the location of the outer skin fatigue crack oriented in the forward direction and about the 3 o'clock position. b) The SEM micrograph shows the fatigue fracture surface at the rivet hole (bottom of micrograph). c) The SEM micrograph shows the shank region of the through-thickness fatigue crack and the rivet hole (bottom of the micrograph). The dashed line marks the fatigue crack front and the bracket shows the likely region of initiation.

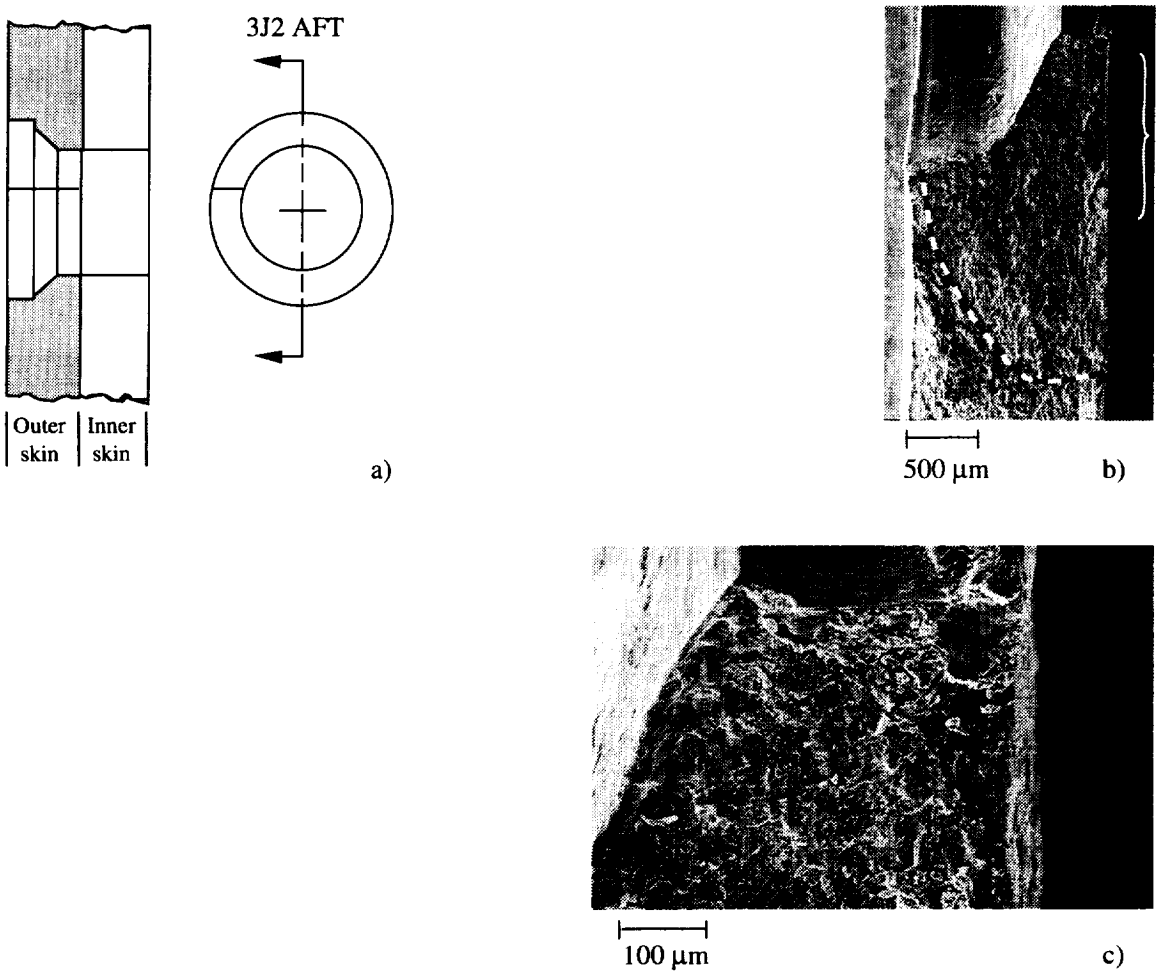

Figure 9.12 a) The schematic shows the rivet hole 3J2 configuration and the location of the outer skin fatigue crack oriented in the aft direction and about the 10 o'clock position. b) The SEM micrograph shows the through-thickness fatigue crack and the rivet hole (top). The bracket shows the likely crack initiation region along the faying surface and the dashed line marks the fatigue crack front. c) The SEM micrograph shows the rivet hole shank region at higher magnification.

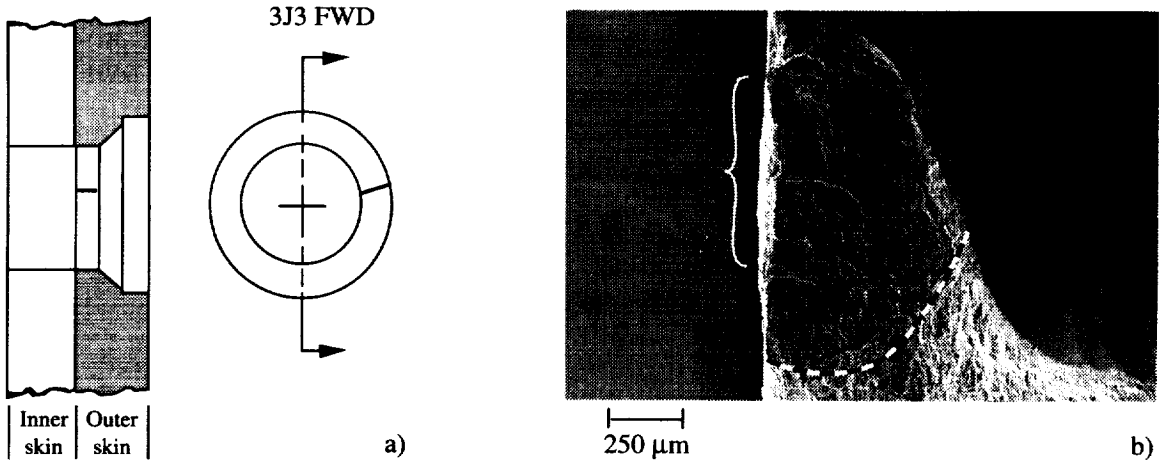

Figure 9.13 a) The schematic shows the rivet hole 3J3 configuration and the location of the outer skin fatigue crack oriented in the forward direction above the 3 o'clock position. b) The SEM micrograph shows the fatigue crack located at the rivet hole. The bracket shows the likely crack initiation region along the faying surface and the dashed line marks the fatigue crack front.

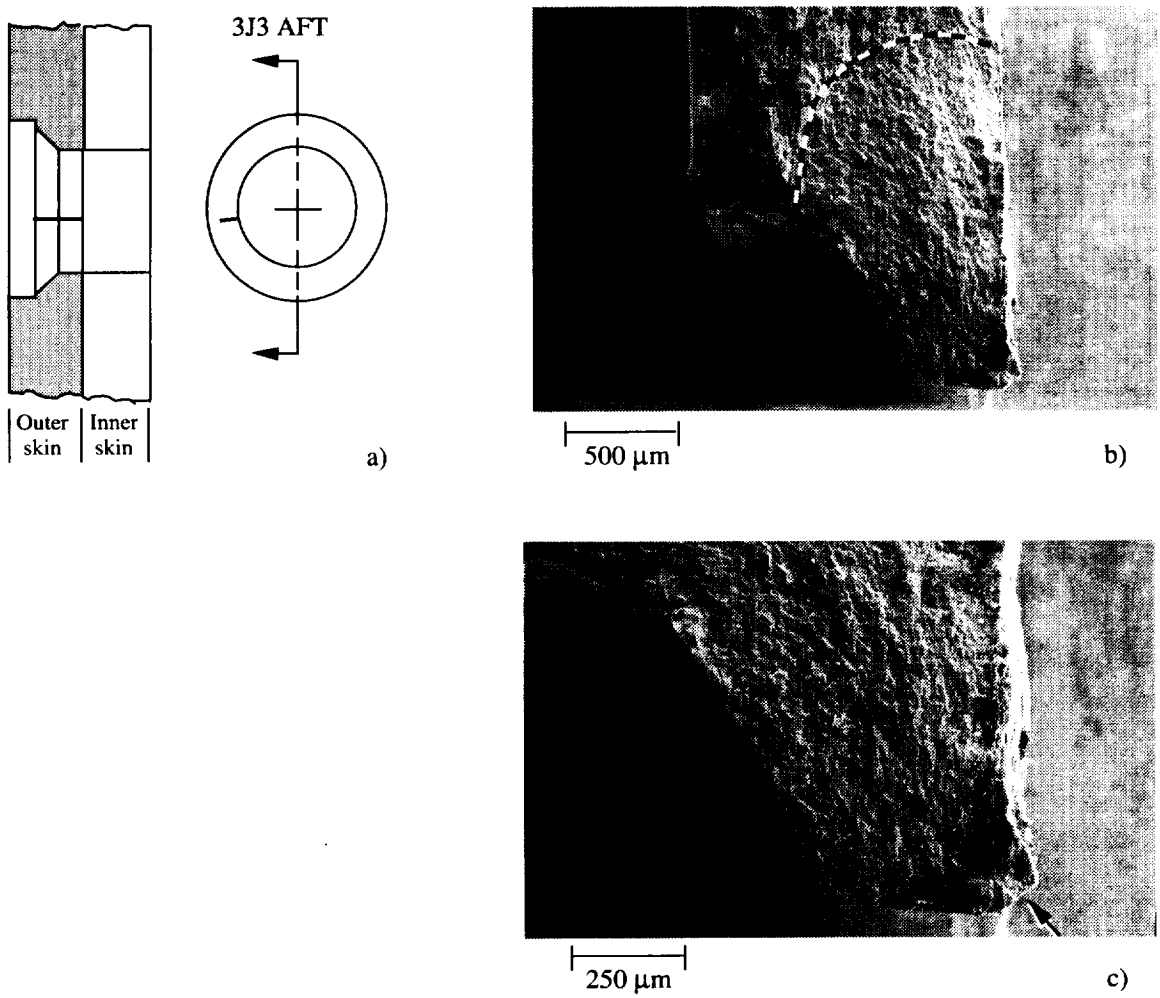

Figure 9.14 a) The schematic shows the rivet hole 3J3 configuration and the location of the outer skin fatigue crack oriented in the aft direction below the 9 o'clock position. b) The SEM micrograph shows the fatigue crack located at the rivet hole. The dashed line marks the fatigue crack front. c) The SEM micrograph shows the fatigue crack fracture surface at the rivet hole shank region. The arrow marks the likely region of crack initiation at the inboard corner of the rivet hole.

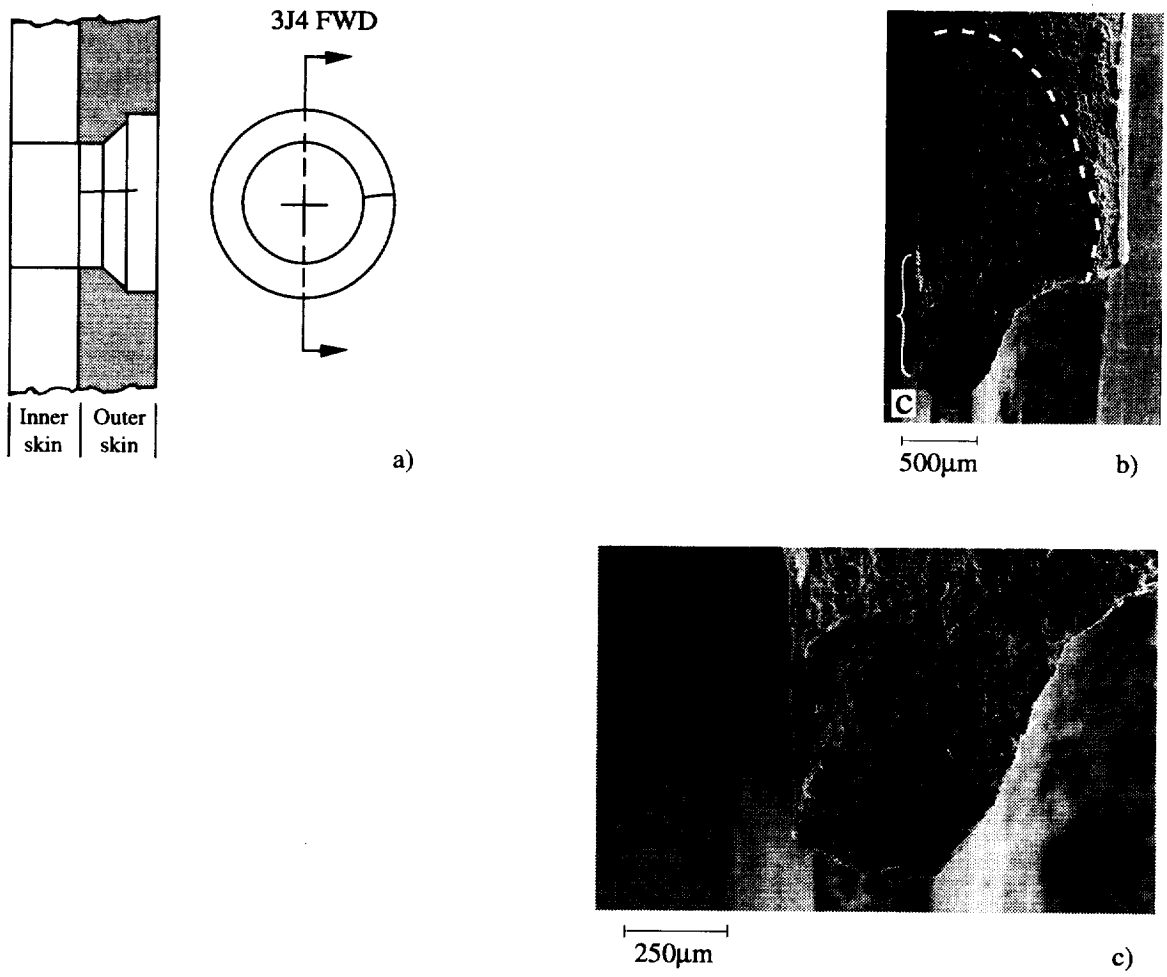

Figure 9.15 a) The schematic shows the rivet hole 3J4 configuration and the location of the outer skin fatigue crack oriented in the forward direction above the 3 o'clock position. b) The SEM micrograph shows the fatigue crack at the rivet hole (bottom). The bracket shows the likely crack initiation region along the faying surface and the dashed line marks the fatigue crack front. c) The SEM micrograph shows the fatigue crack fracture surface at the rivet hole shank region.

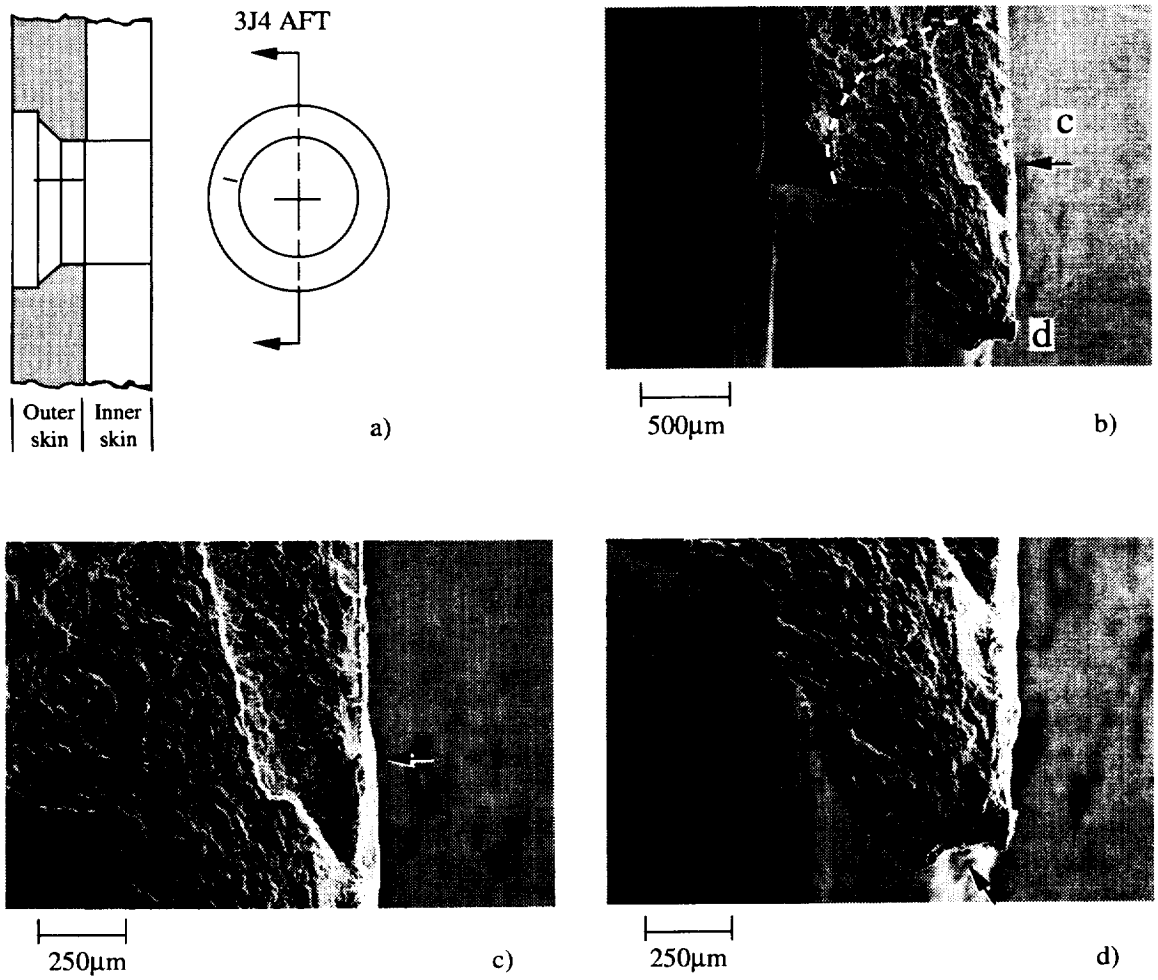

Figure 9.16 a) The schematic shows the rivet hole 3J4 configuration and the location of the outer skin fatigue crack oriented in the aft direction and about the 10 o'clock position. b) The SEM micrograph shows the fatigue crack at the rivet hole (bottom). The micrograph reveals that cracking occurred along two fracture planes ("c" and "d"). An arrow marks the likely crack initiation region for crack "c" along the faying surface. The dashed line marks the fatigue crack front. c) The SEM micrograph shows the fatigue crack surface at region "c". The arrow marks the likely crack initiation site along the faying surface. d) The SEM micrograph shows the fatigue crack surface at the rivet hole shank region "d" in Figure 9.16.b. The arrow marks the likely region of crack initiation.

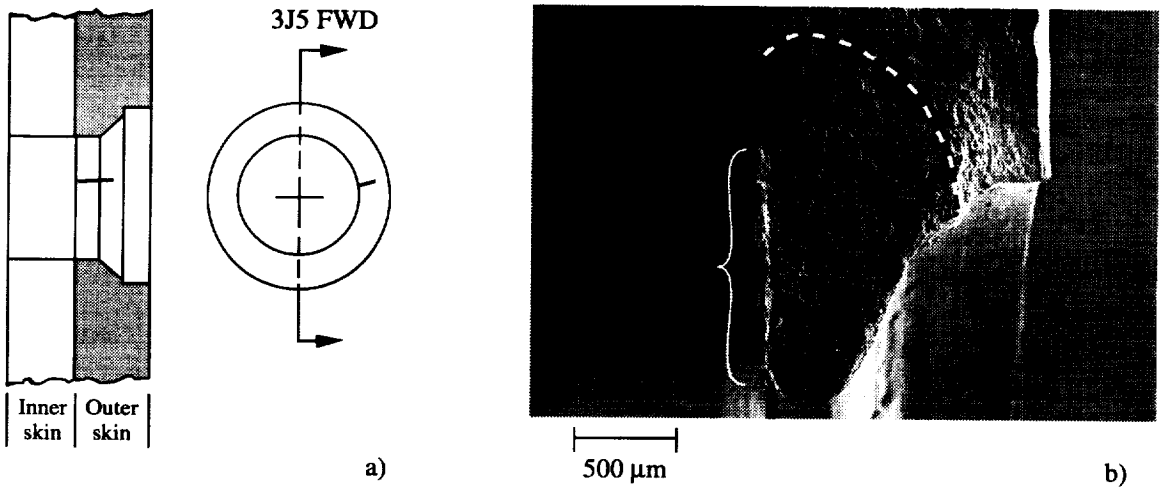

Figure 9.17 a) The schematic shows the rivet hole 3J5 configuration and the location of the outer skin fatigue crack oriented in the forward direction above the 3 o'clock position. b) The SEM micrograph shows the fatigue crack at the rivet hole (bottom). The bracket shows the likely crack initiation region along the faying surface and the dashed line marks the fatigue crack front.

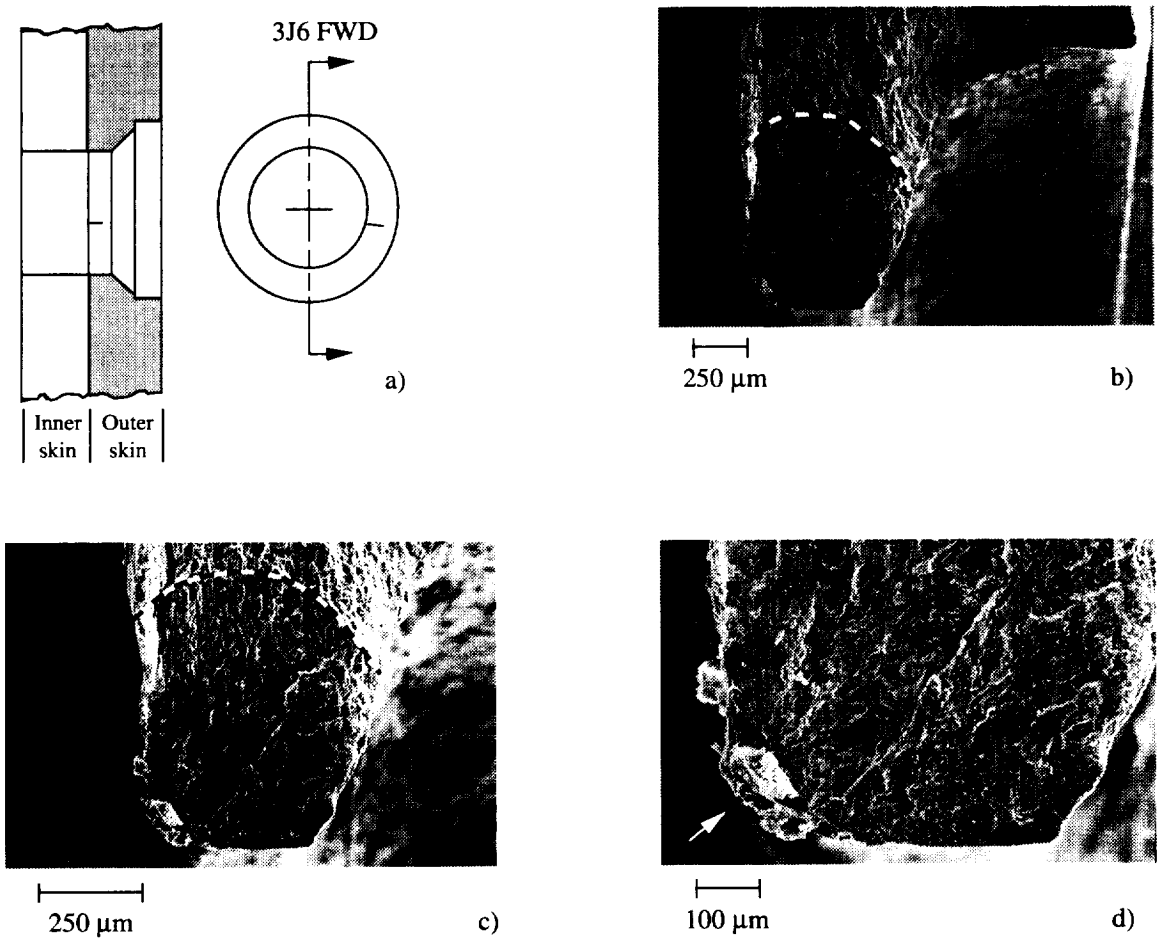

Figure 9.18 a) The schematic shows the rivet hole 3J6 configuration and the location of the outer skin fatigue crack oriented in the forward direction below the 3 o'clock position. b) The SEM micrograph shows the fatigue crack at the rivet hole. The dashed line marks the fatigue crack front. c) The SEM micrograph shows the fatigue crack fracture surface at the rivet hole shank region. The dashed line marks the fatigue crack front. d) The SEM micrograph shows the crack initiation site at the inboard corner of the rivet hole (arrow) at high magnification.

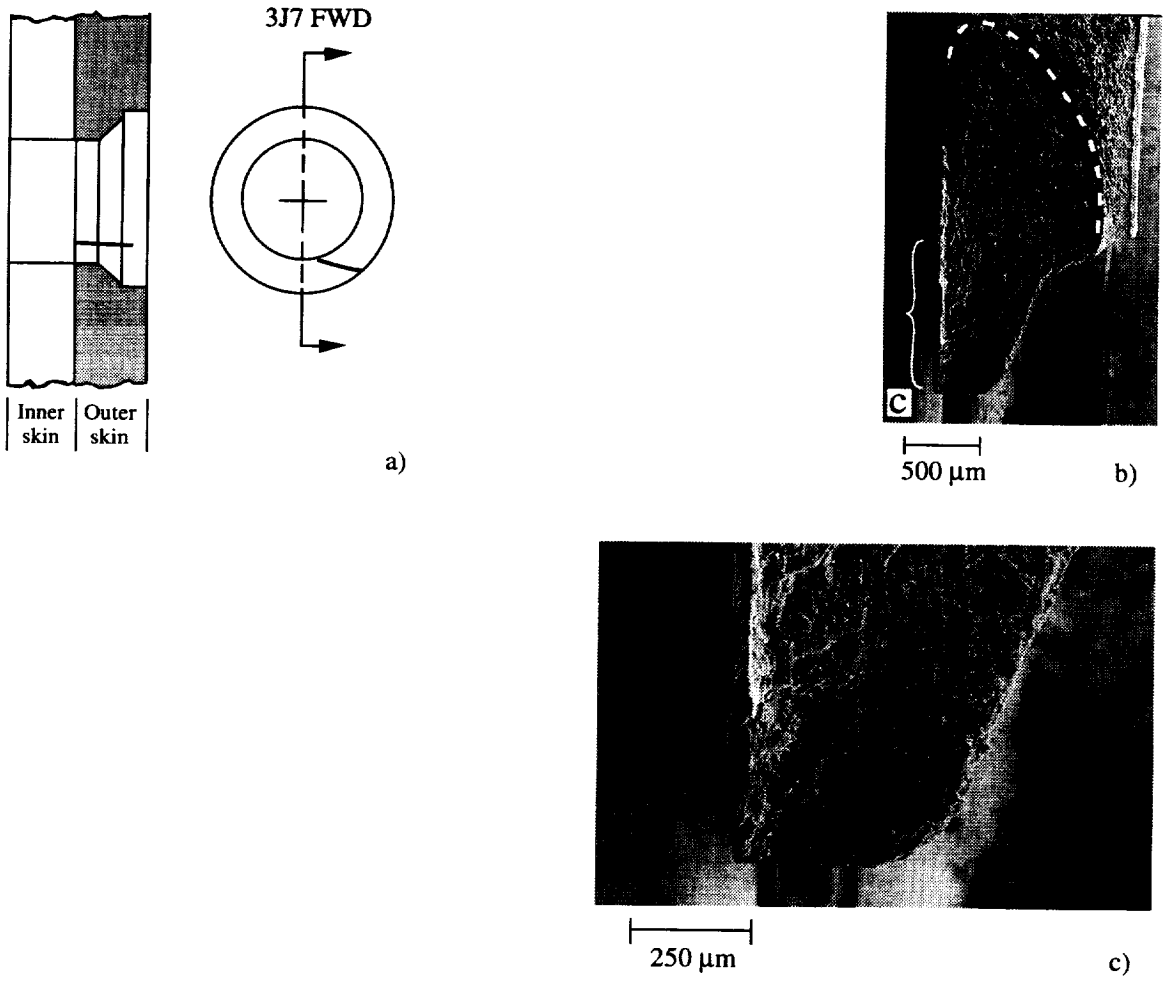

Figure 9.19 a) The schematic shows the rivet hole 3J7 configuration and the location of the outer skin fatigue crack oriented in the forward direction and about the 5 o'clock position. b) The SEM micrograph shows the fatigue crack at the rivet hole (bottom). The bracket shows the likely crack initiation region along the faying surface and the dashed line marks the fatigue crack front. c) The SEM micrograph shows the fatigue crack fracture surface at the rivet hole shank region.

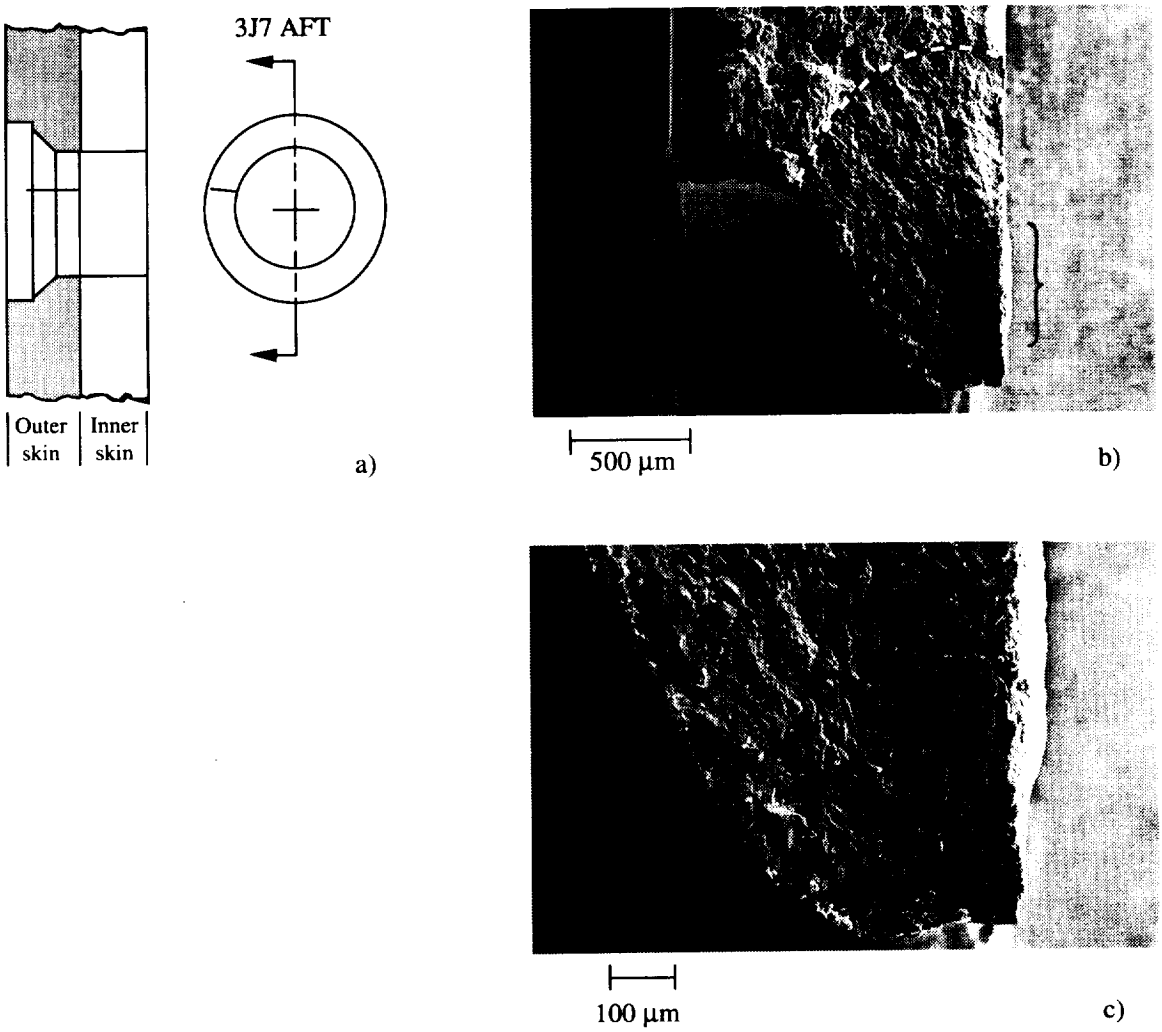

Figure 9.20 a) The schematic shows the rivet hole 3J7 configuration and the location of the outer skin fatigue crack oriented in the aft direction above the 9 o'clock position. b) The SEM micrograph shows the fatigue crack at the rivet hole (bottom). The bracket shows the likely crack initiation region along the faying surface and the dashed line marks the fatigue crack front. c) The SEM micrograph shows the fatigue crack fracture surface at the rivet hole shank region.

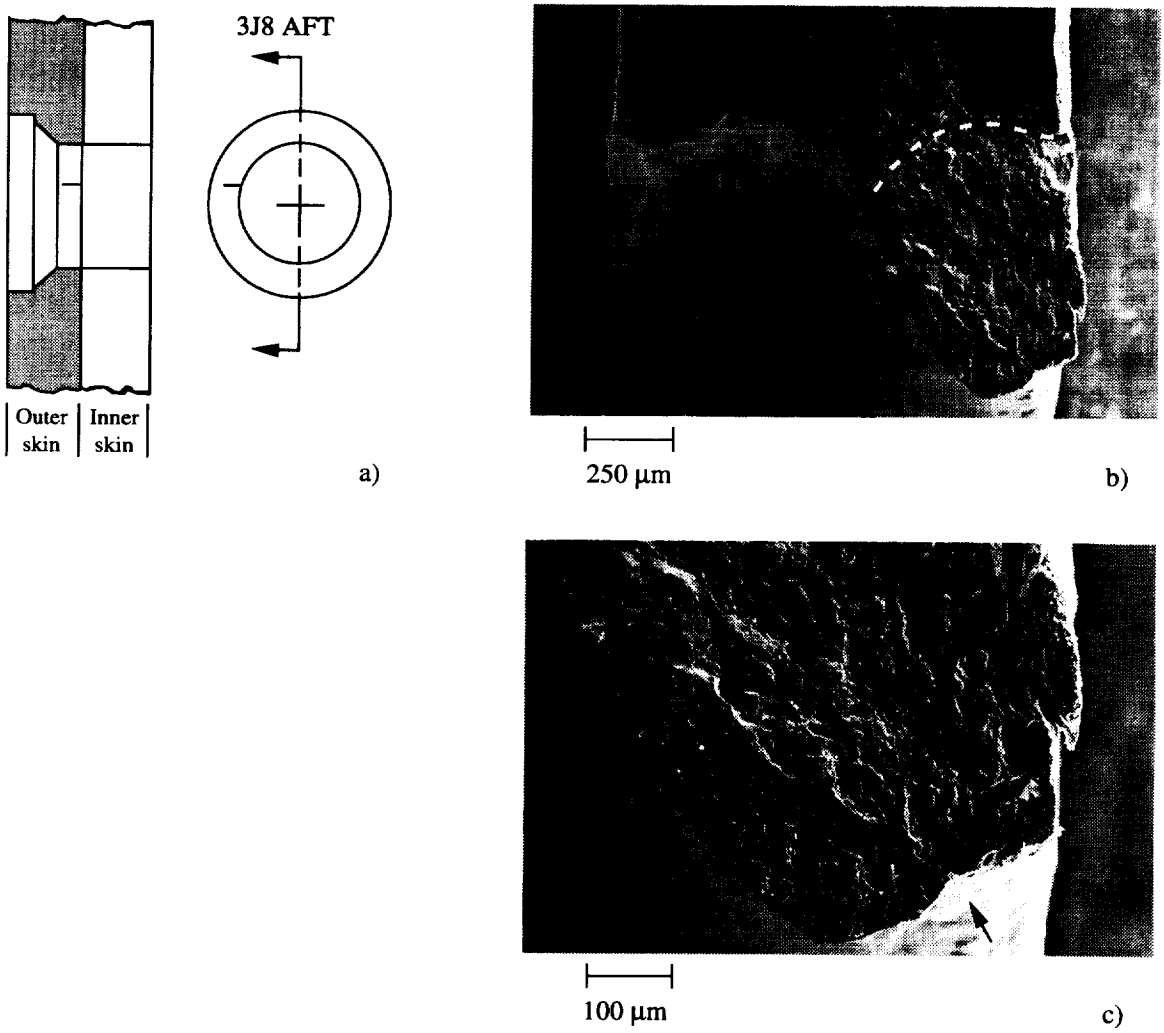

Figure 9.21 a) The schematic shows the rivet hole 3J8 configuration and the location of the outer skin fatigue crack oriented in the aft direction and about the 10 o'clock position. b) The SEM micrograph shows the fatigue crack at the rivet hole (bottom). The dashed line marks the fatigue crack front. c) The SEM micrograph shows the fatigue crack fracture surface at the rivet hole shank region. The arrow marks the likely region of crack initiation.

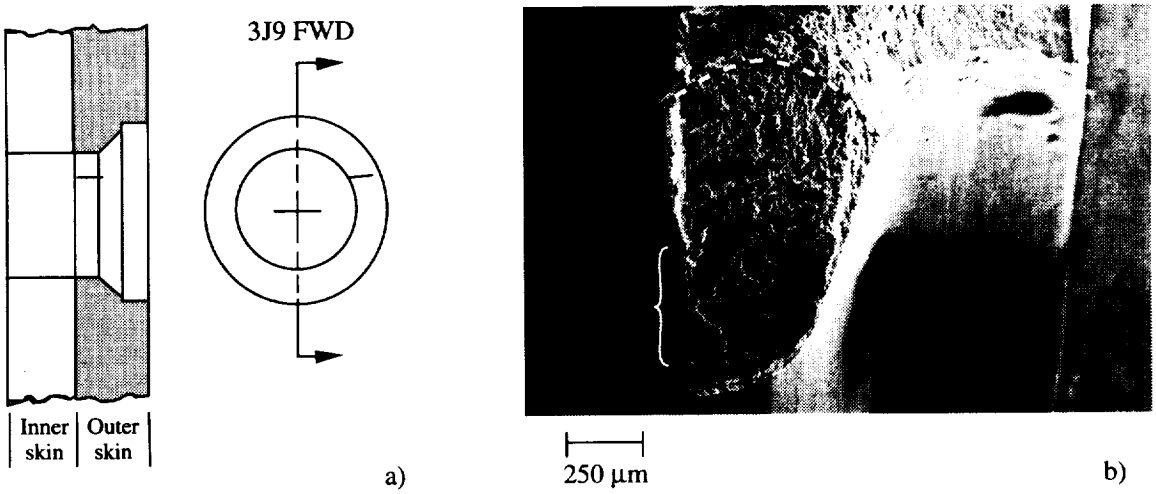

Figure 9.22 a) The schematic shows the rivet hole 3J9 configuration and the location of the outer skin fatigue crack oriented in the forward direction and about the 2 o'clock position. b) The SEM micrograph shows the fatigue crack at the rivet hole (bottom). The bracket shows the likely crack initiation region along the faying surface and the dashed line marks the fatigue crack front.

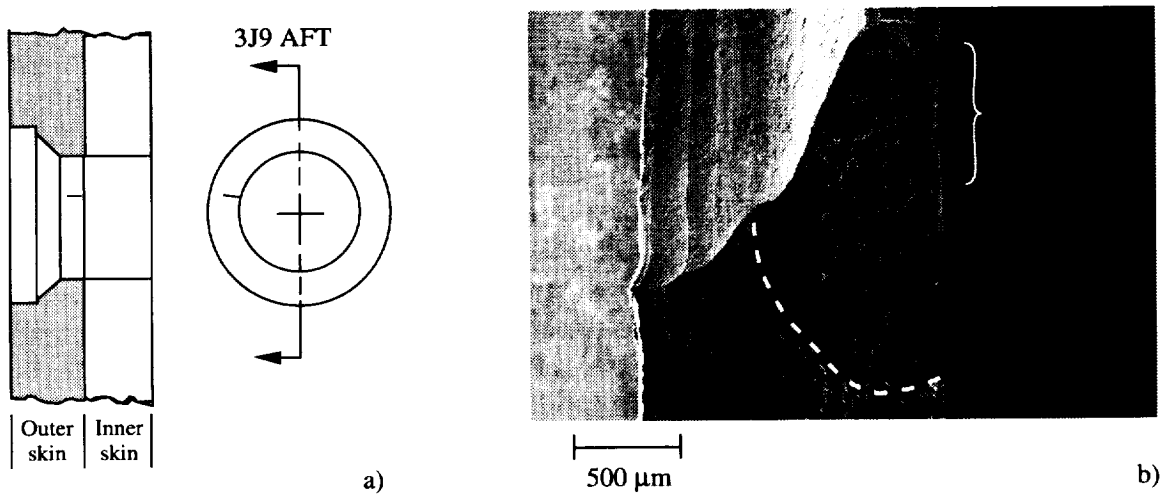

Figure 9.23 a) The schematic shows the rivet hole 3J9 configuration and the location of the outer skin fatigue crack oriented in the aft direction above the 9 o'clock position. b) The SEM micrograph shows the fatigue crack at the rivet hole (top). The bracket shows the likely crack initiation region along the faying surface and the dashed line marks the fatigue crack front.

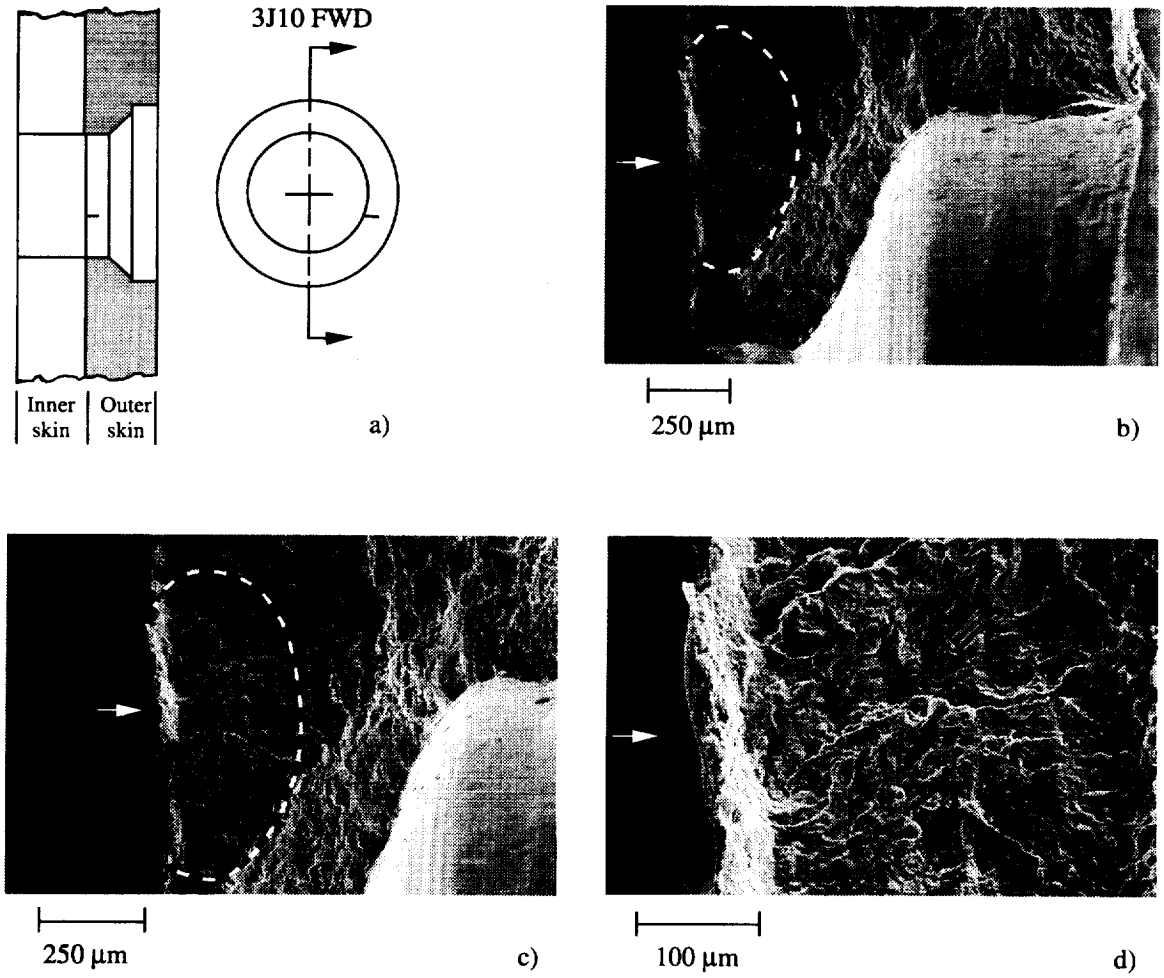

Figure 9.24 a) The schematic shows the rivet hole 3J10 configuration and the location of the outer skin fatigue crack oriented in the forward direction and about the 4 o'clock position. b) The SEM micrograph shows the faying surface fatigue crack at the rivet hole (bottom). The arrow identifies the likely crack initiation region along the faying surface and the dashed line marks the fatigue crack front. c) The SEM micrograph shows the faying surface fatigue crack fracture surface and the region of crack initiation (arrow). d) The SEM micrograph shows the rough faying surface at the site of crack initiation (arrow).

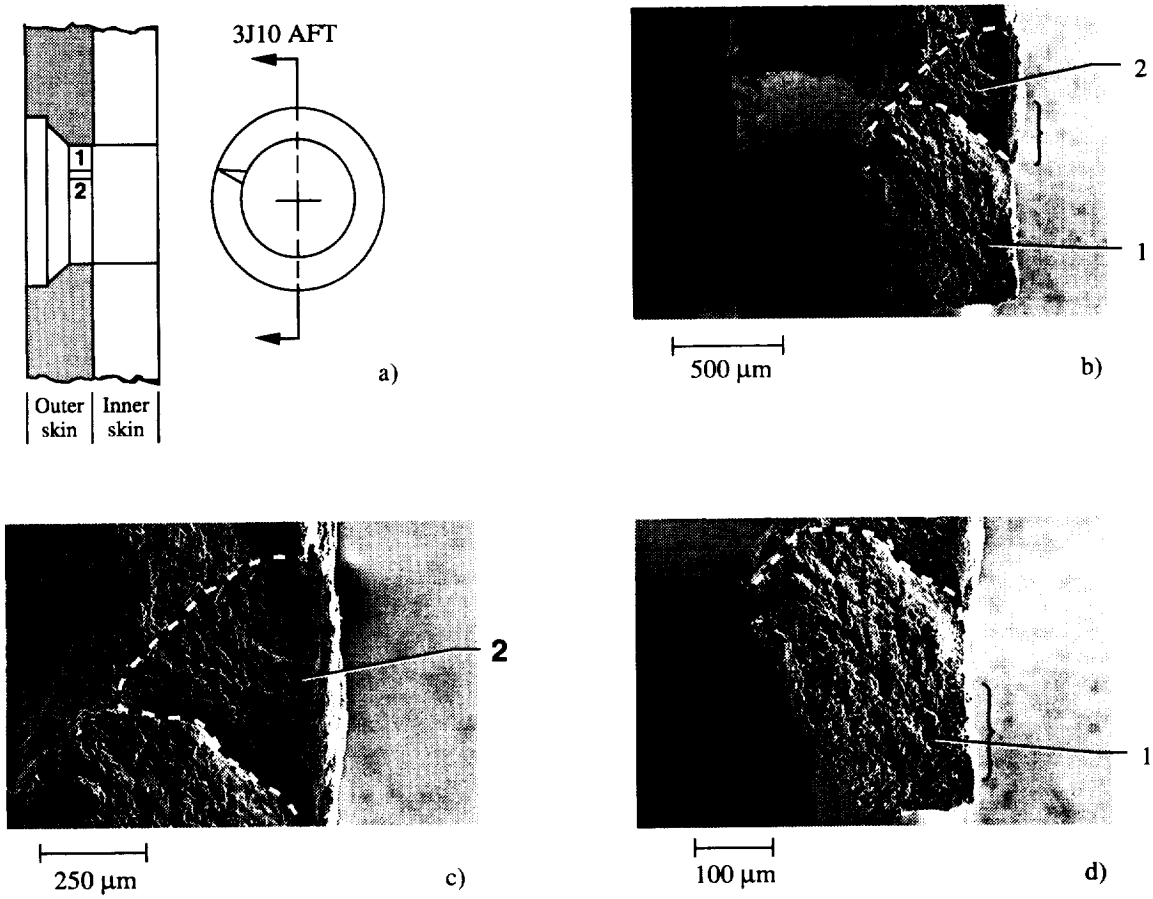

Figure 9.25 a) The schematic shows the rivet hole 3J10 configuration and the location of two outer skin fatigue cracks (1 and 2) oriented in the aft direction and about the 10 o'clock position. b) The SEM micrograph shows the fatigue crack at the rivet hole (bottom). The micrograph reveals that cracking occurred along two fracture planes (1 and 2). A bracket marks the likely crack initiation region for crack "2" along the faying surface and the region where the two cracks coalesced. The dashed line marks the fatigue crack front. c) The SEM micrograph shows the fatigue crack surface at the region of crack "2" shown in Figure 9.25.b. The dashed lines mark the fatigue crack front and the region where the two crack planes linked. d) The SEM micrograph shows the fatigue crack surface at the rivet hole shank and crack "1" in Figure 9.25.b. The bracket marks the likely region of crack initiation for crack "1".

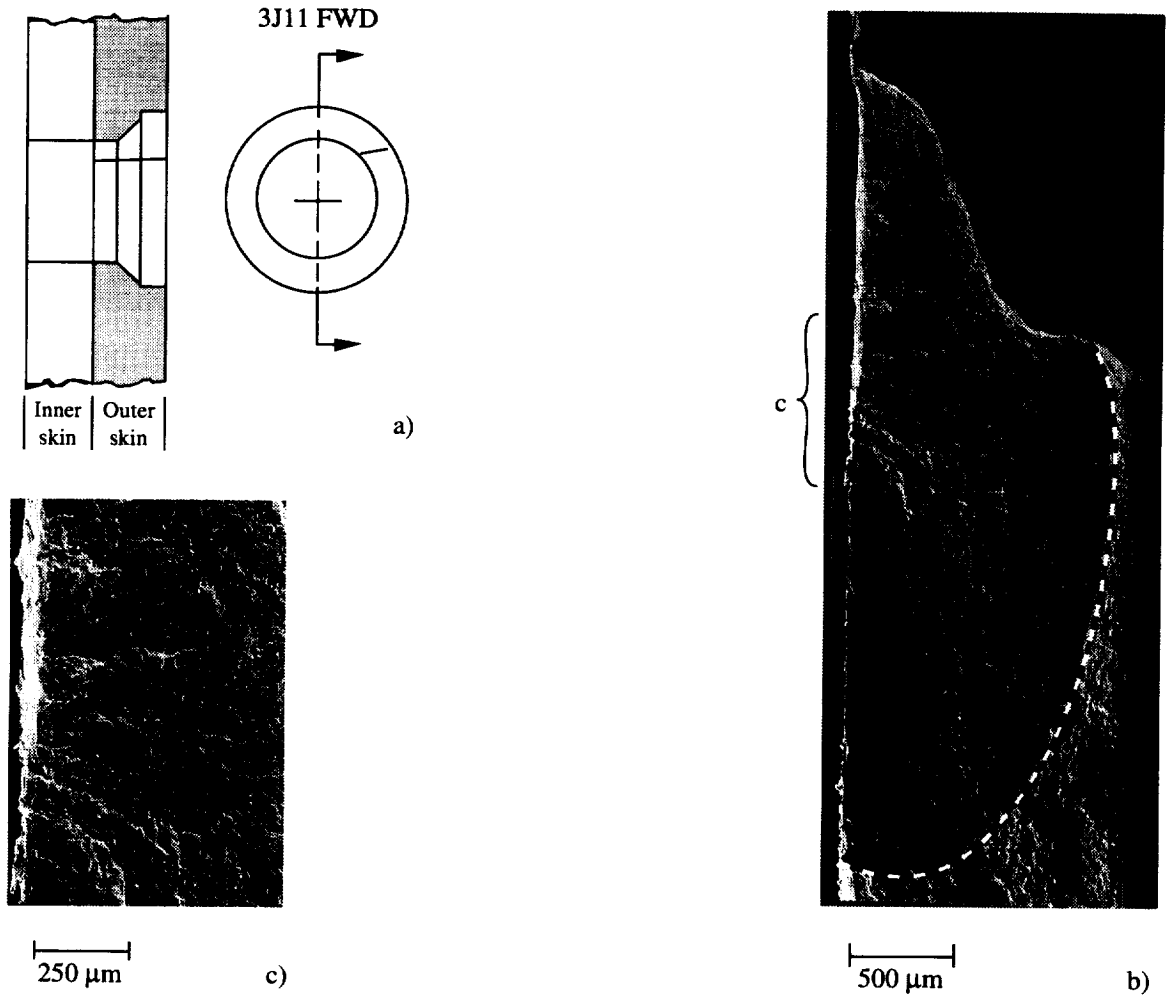

Figure 9.26 a) The schematic shows the rivet hole 3J11 configuration and the location of the outer skin fatigue crack oriented in the forward direction and about the 2 o'clock position. b) The SEM micrograph shows the fatigue crack at the rivet hole (top). The bracket locates the region of crack initiation along the faying surface and the dashed line marks the fatigue crack front. c) The SEM micrograph shows the crack initiation region "c" in Figure 9.26.b.

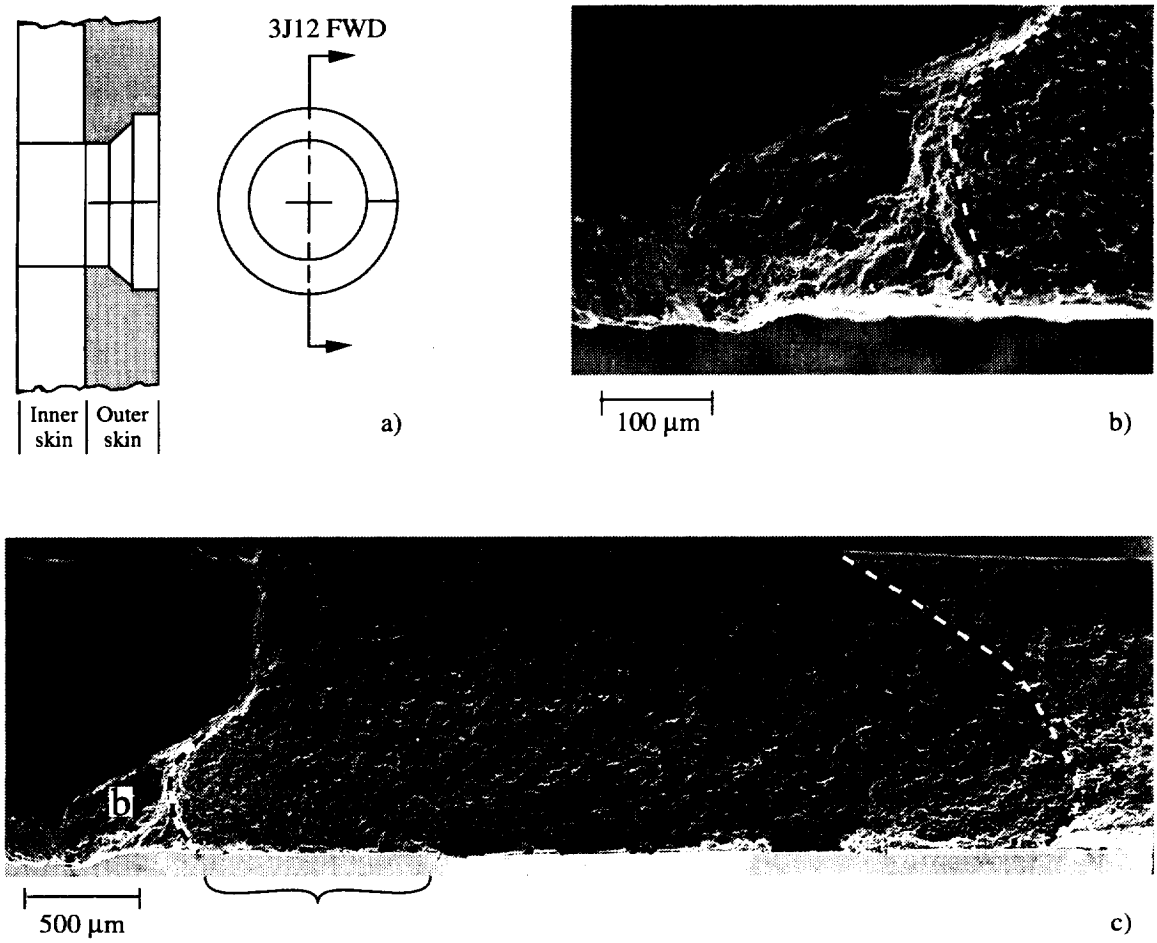

Figure 9.27 a) The schematic shows the rivet hole 3J12 configuration and the location of the outer skin fatigue crack oriented in the forward direction and about the 3 o'clock position. b) The SEM micrograph shows the fatigue crack surface at the rivet hole shank region "b" in Figure 9.27.c. The dashed line marks the fatigue crack front; to the right of the dashed line is the transgranular fatigue crack fracture surface and to the left is a region (ligament) that exhibits a ductile tearing morphology. c) The SEM micrograph shows the fatigue crack fracture surface extending from the rivet hole (left). The bracket marks the likely region of crack initiation along the faying surface and the dashed lines mark the fatigue crack fronts. Presumably, the crack initiated at a site located a considerable distance from the rivet hole, forming a ligament that failed by ductile tearing.

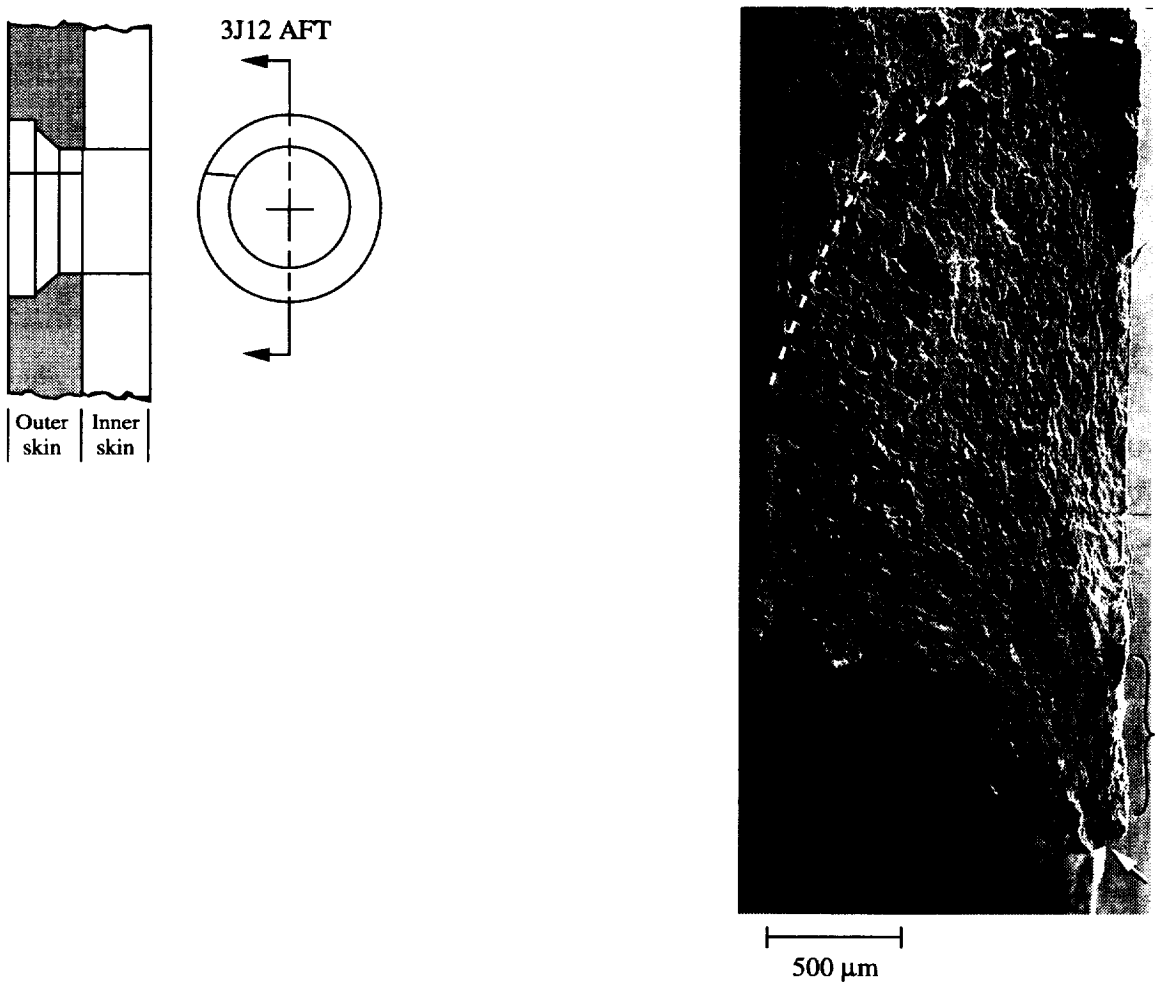

Figure 9.28 a) The schematic shows the rivet hole 3J12 configuration and the location of the outer skin fatigue crack oriented in the aft direction and about the 10 o'clock position. b) The SEM micrograph shows the fatigue crack fracture surface extending from the rivet hole (bottom). The arrow and bracket mark the likely regions of crack initiation at the inboard corner and faying surface of the rivet hole and the dashed line marks the fatigue crack front.

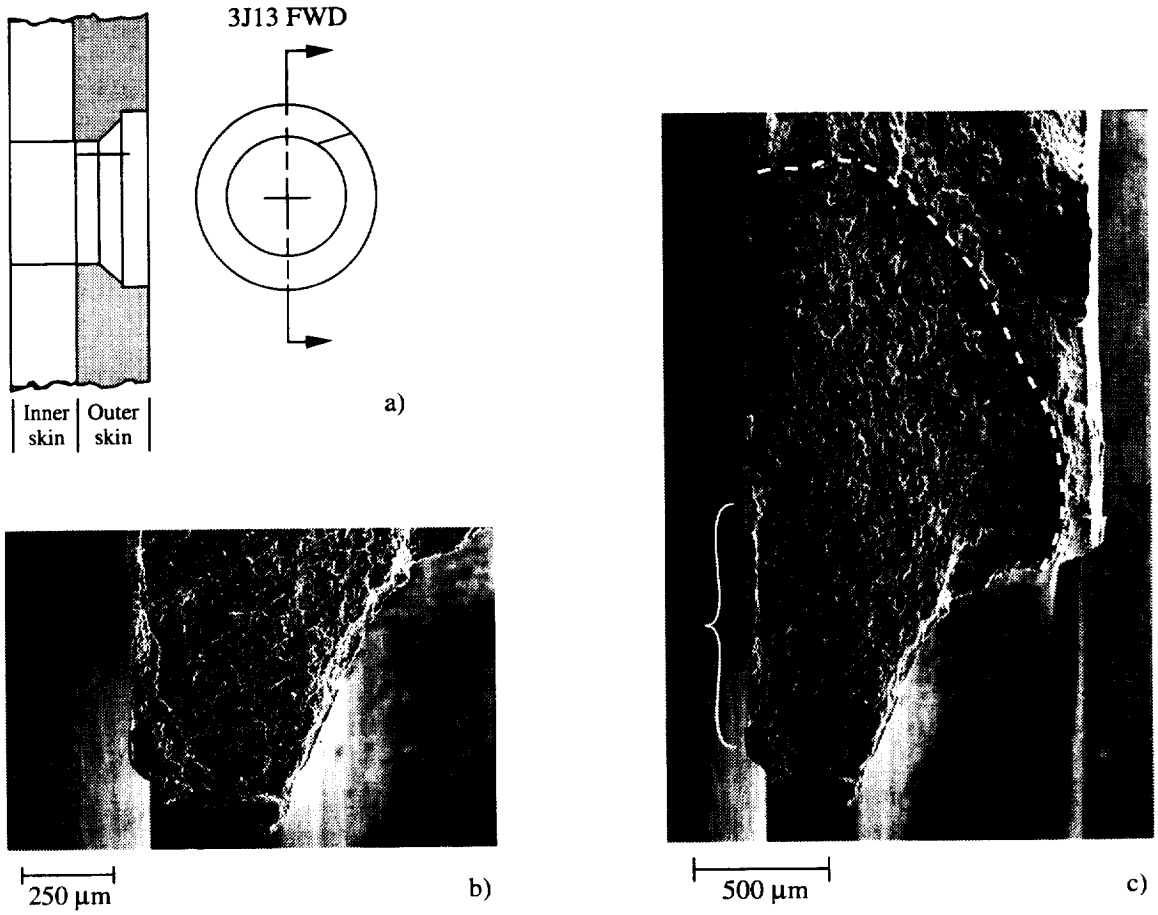

Figure 9.29 a) The schematic shows the rivet hole 3J13 configuration and the location of the outer skin fatigue crack oriented in the forward direction and about the 1 o'clock position. b) The SEM micrograph shows the fatigue crack surface at the rivet hole shank region c) The SEM micrograph shows the fatigue crack fracture surface extending from the rivet hole (bottom). The bracket marks the likely region of crack initiation along the faying surface and the dashed line marks the fatigue crack front.

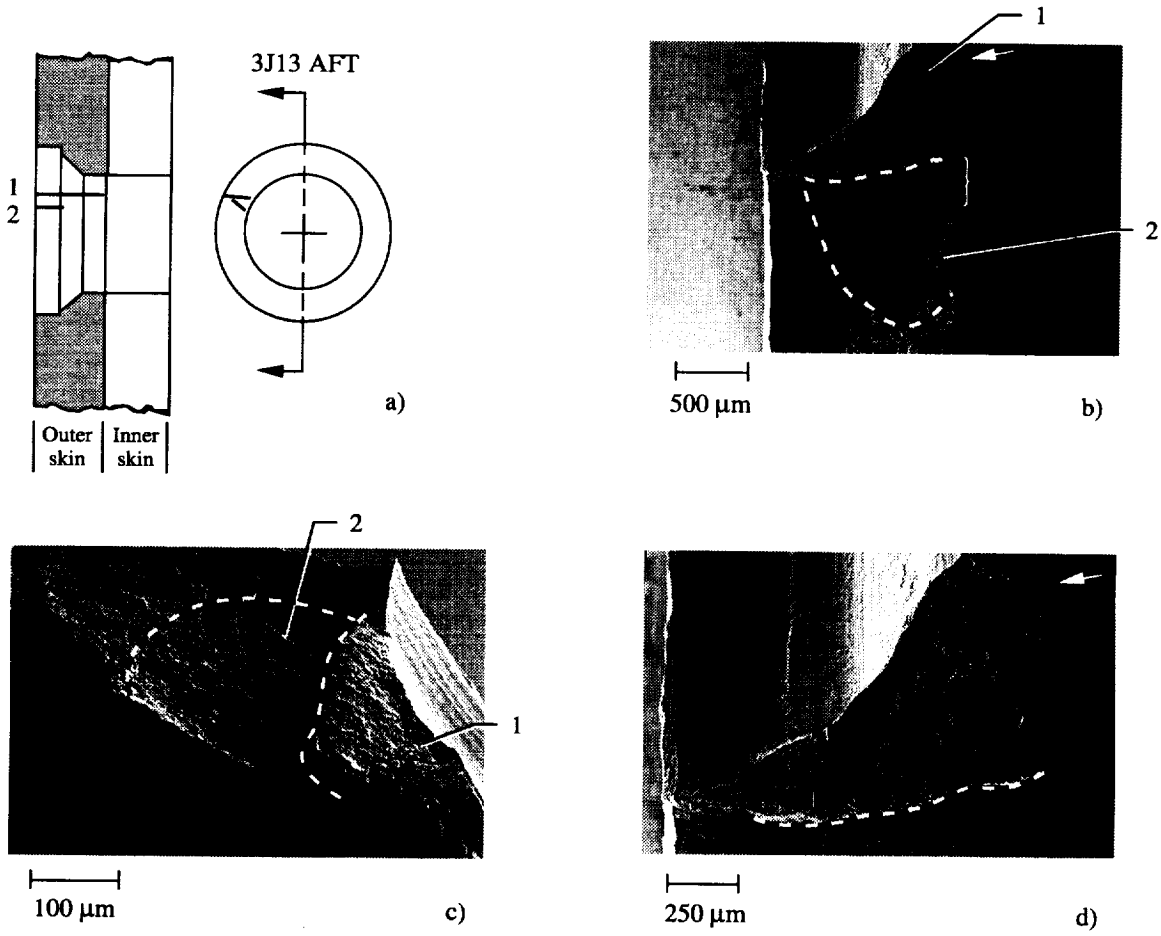

Figure 9.30 a) The schematic shows the rivet hole 3J13 configuration and the location of two outer skin fatigue cracks (1 and 2) oriented in the aft direction and about the 10 o'clock position. b) The SEM micrograph shows the fatigue crack at the rivet hole (top). The micrograph reveals that cracking occurred along two fracture planes (1 and 2). The brackets and arrow mark the likely crack initiation region for cracks "2" and "1", respectively, along the faying surface. The nearly horizontal dashed line near the middle of the fracture surface marks the region where both cracks coalesced. The dashed line extending to the bottom of the micrograph marks the final fatigue crack front. c) The SEM micrograph shows the fatigue crack surfaces of cracks "1" and "2" at an oblique angle. The dashed line on the left marks the final fatigue crack front. The near vertical dashed line marks the region where the cracks coalesced. d) The SEM micrograph shows the fatigue crack surface at the rivet hole shank and crack "1" in Figure 9.25.b. The arrow marks the site of crack initiation.

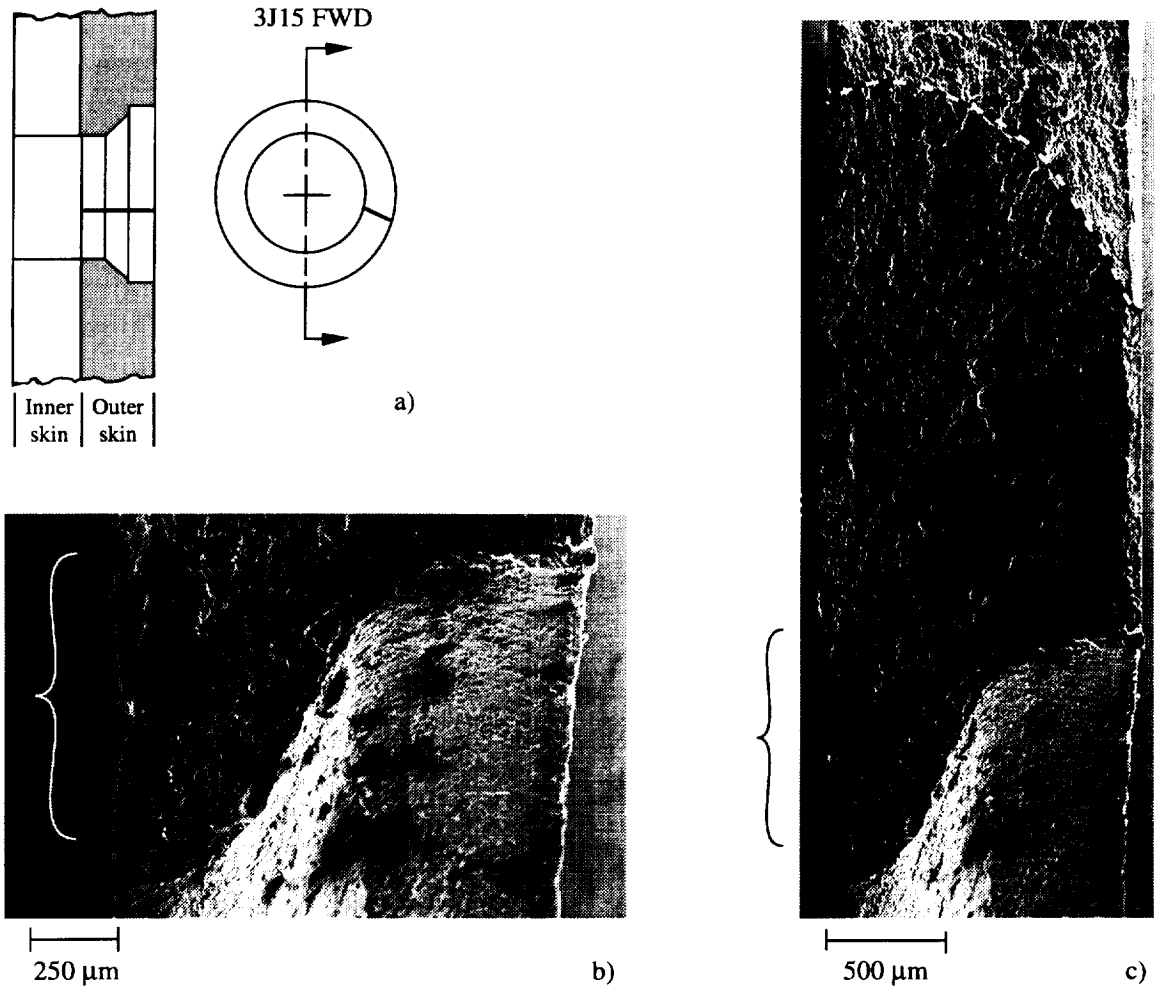

Figure 9.31 a) The schematic shows the rivet hole 3J15 configuration and the location of the outer skin fatigue crack oriented in the forward direction below the 9 o'clock position. b) The SEM micrograph shows the fatigue crack at the rivet hole. The bracket marks the likely region of crack initiation along the faying surface. c) The SEM micrograph shows the fatigue crack at the rivet hole (bottom). The bracket locates the region of crack initiation along the faying surface and the dashed line marks the fatigue crack front.

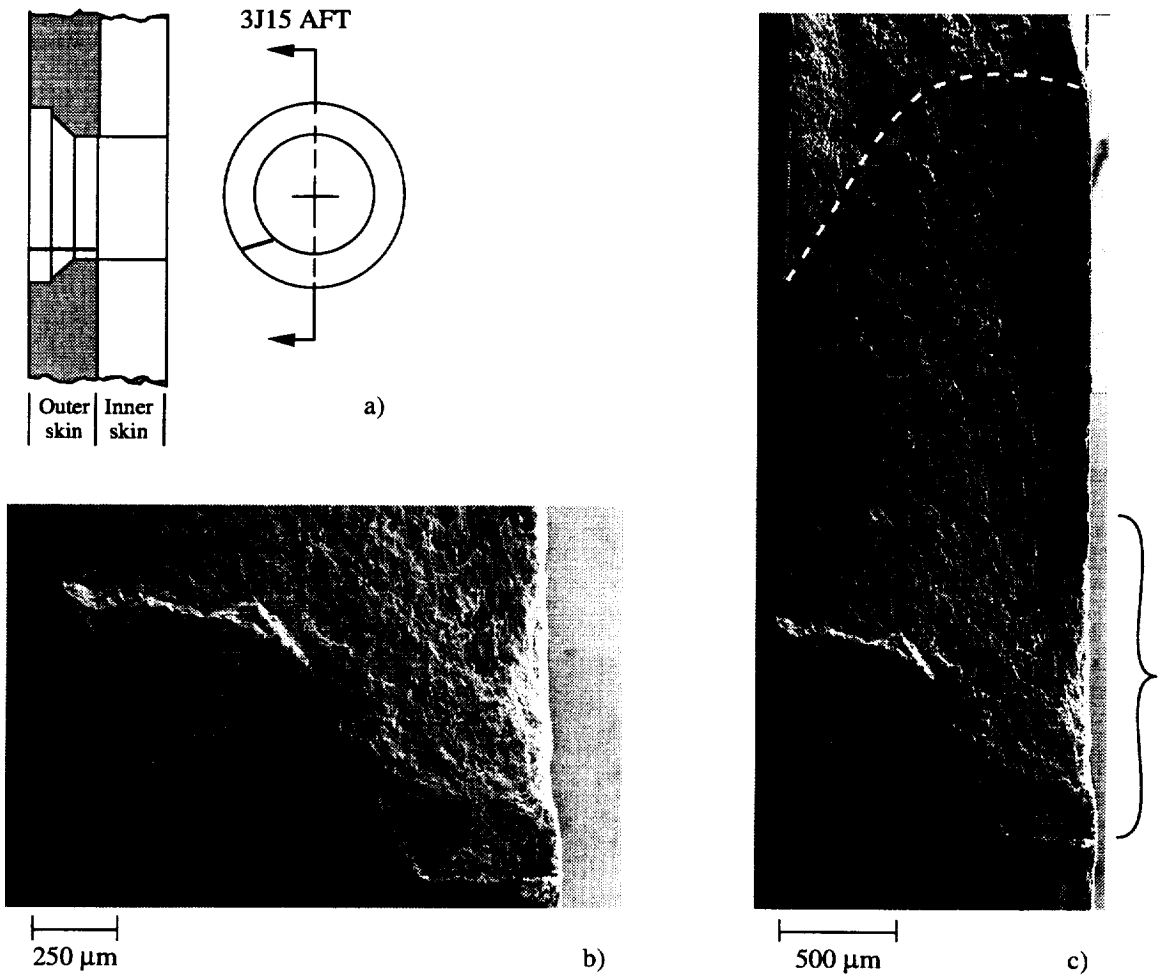

Figure 9.32 a) The schematic shows the rivet hole 3J15 configuration and the location of the outer skin fatigue crack oriented in the aft direction and about the 8 o'clock position. b) The SEM micrograph shows the fatigue crack region, marked by the bracket in Figure 9.32.c, at high magnification. c) The SEM micrograph shows the fatigue crack at the rivet hole (bottom). The bracket locates the region of crack initiation along the faying surface and the dashed line marks the fatigue crack front.

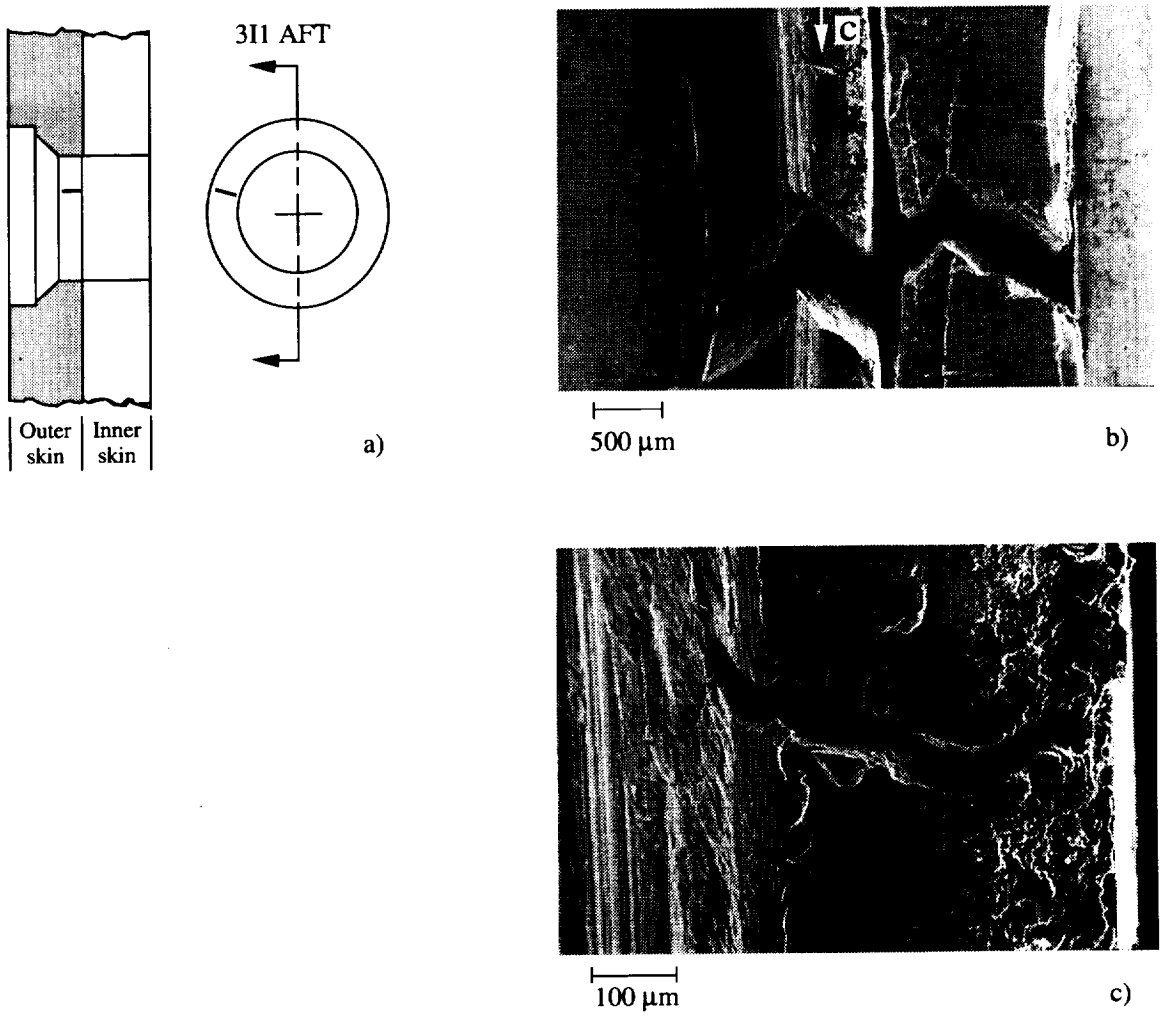

Figure 9.33 a) The schematic shows the rivet hole 3I1 configuration and the location of the outer skin fatigue crack oriented in the aft direction and about the 10 o'clock position. b) The SEM micrograph shows the partially strained to failure specimen oriented as shown in Figure 9.33.a.; shown is the outer skin on the left and the inner skin to the right. The partially opened outer skin fatigue crack is identified by the arrow. c) The SEM micrograph shows region "c" in Figure 9.33.b at high magnification. The fatigue crack was partially opened during the destructive examination. SEM examination into the opened crack confirmed transgranular fatigue crack growth.

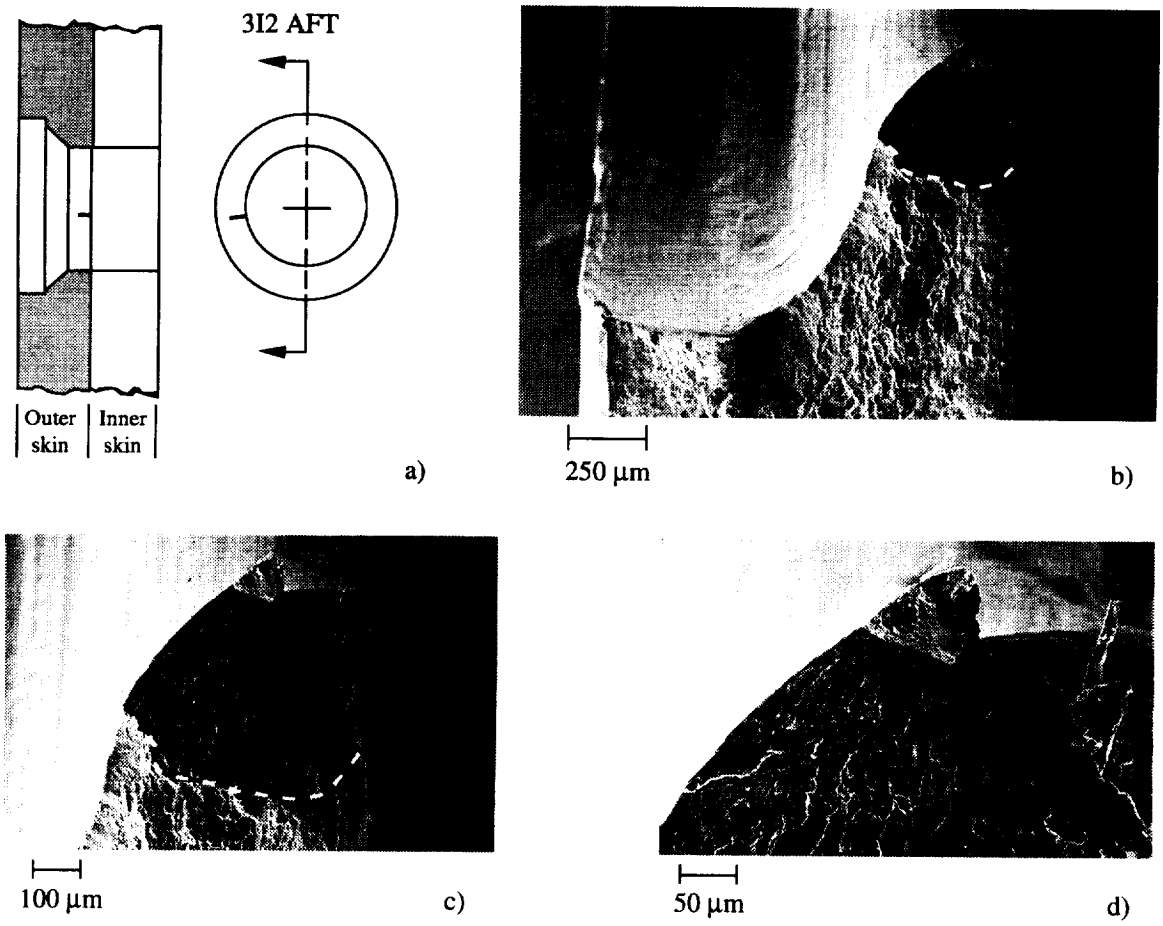

Figure 9.34 a) The schematic shows the rivet hole 3I2 configuration and the location of the outer skin fatigue crack oriented in the aft direction below the 9 o'clock position. b) The SEM micrograph shows the fatigue crack and the rivet hole. The dashed line marks the fatigue crack front. c) The SEM micrograph shows the fatigue crack region. The dashed line marks the fatigue crack front. d) The SEM micrograph shows the region of crack initiation at the deformed rivet hole shank.

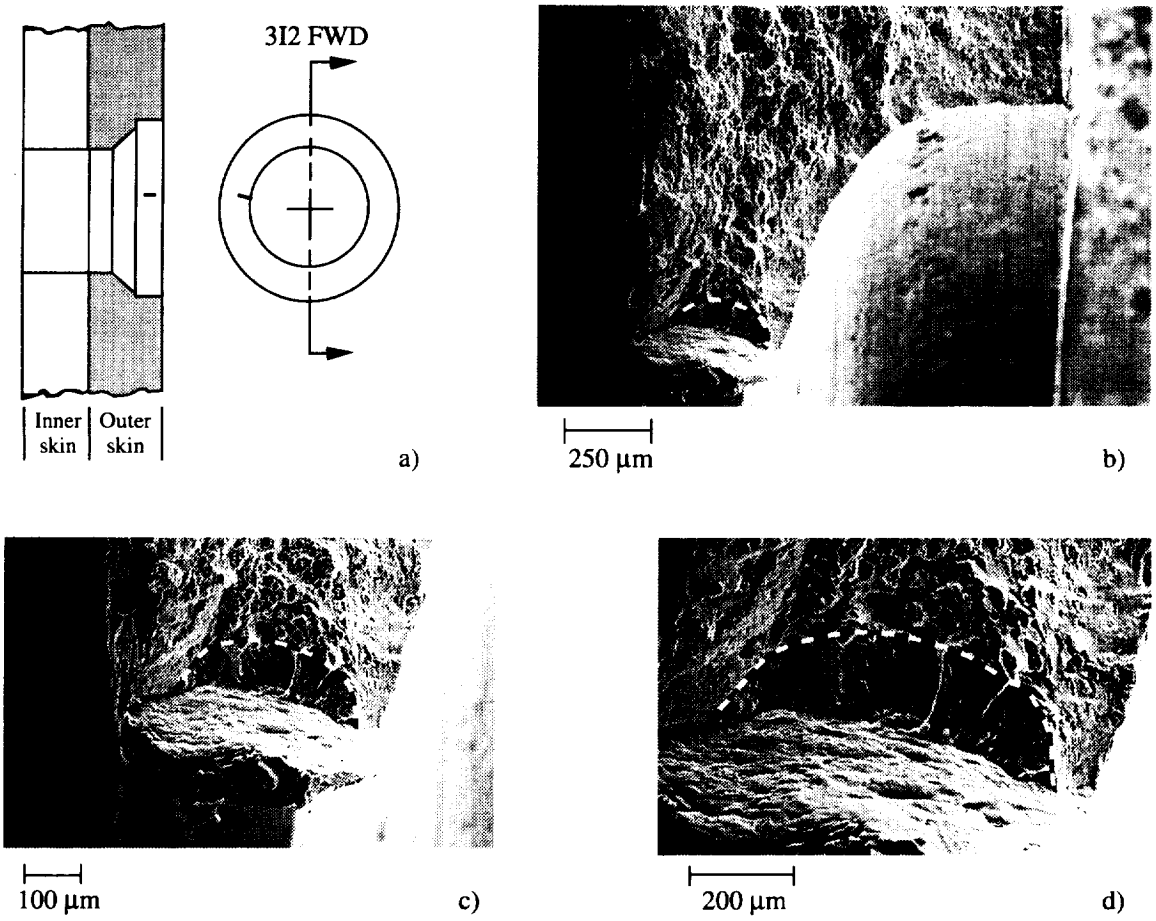

Figure 9.35 a) The schematic shows the rivet hole 3I2 configuration and the location of the outer skin fatigue crack oriented in the forward direction above the 9 o'clock position. b) The SEM micrograph shows the fatigue crack and the rivet hole. The dashed line marks the fatigue crack front. c) The SEM micrograph shows the rivet hole shank region. The dashed line marks the fatigue crack front. d) The SEM micrograph shows the region of crack initiation at the rough surface of the rivet hole shank.

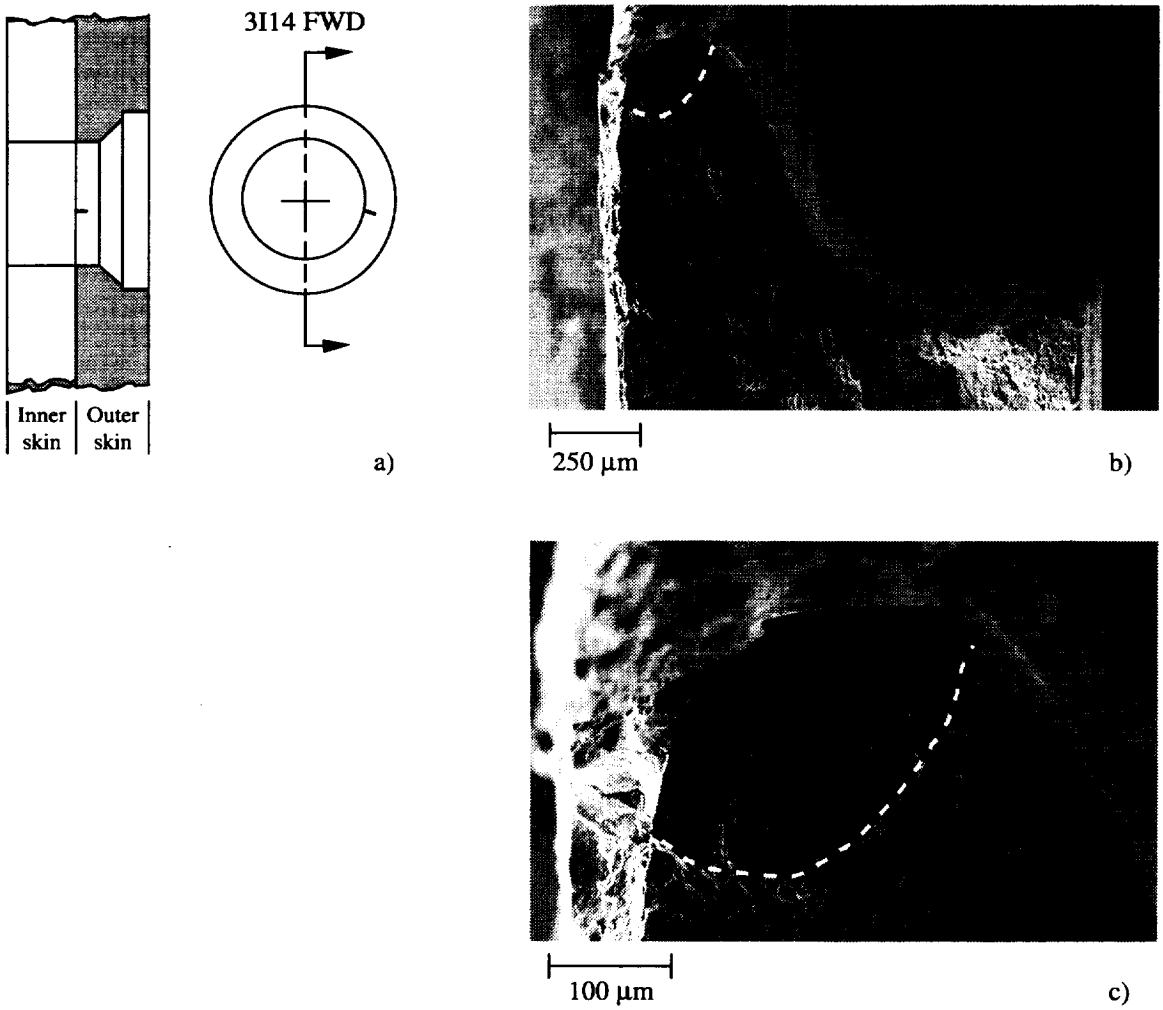

Figure 9.36 a) The schematic shows the rivet hole 3I14 configuration and the location of the outer skin fatigue crack oriented in the forward direction below the 3 o'clock position. b) The SEM micrograph the fatigue crack and the rivet hole. The dashed line marks the fatigue crack front. c) The SEM micrograph shows the region of crack initiation at the rivet hole shank.

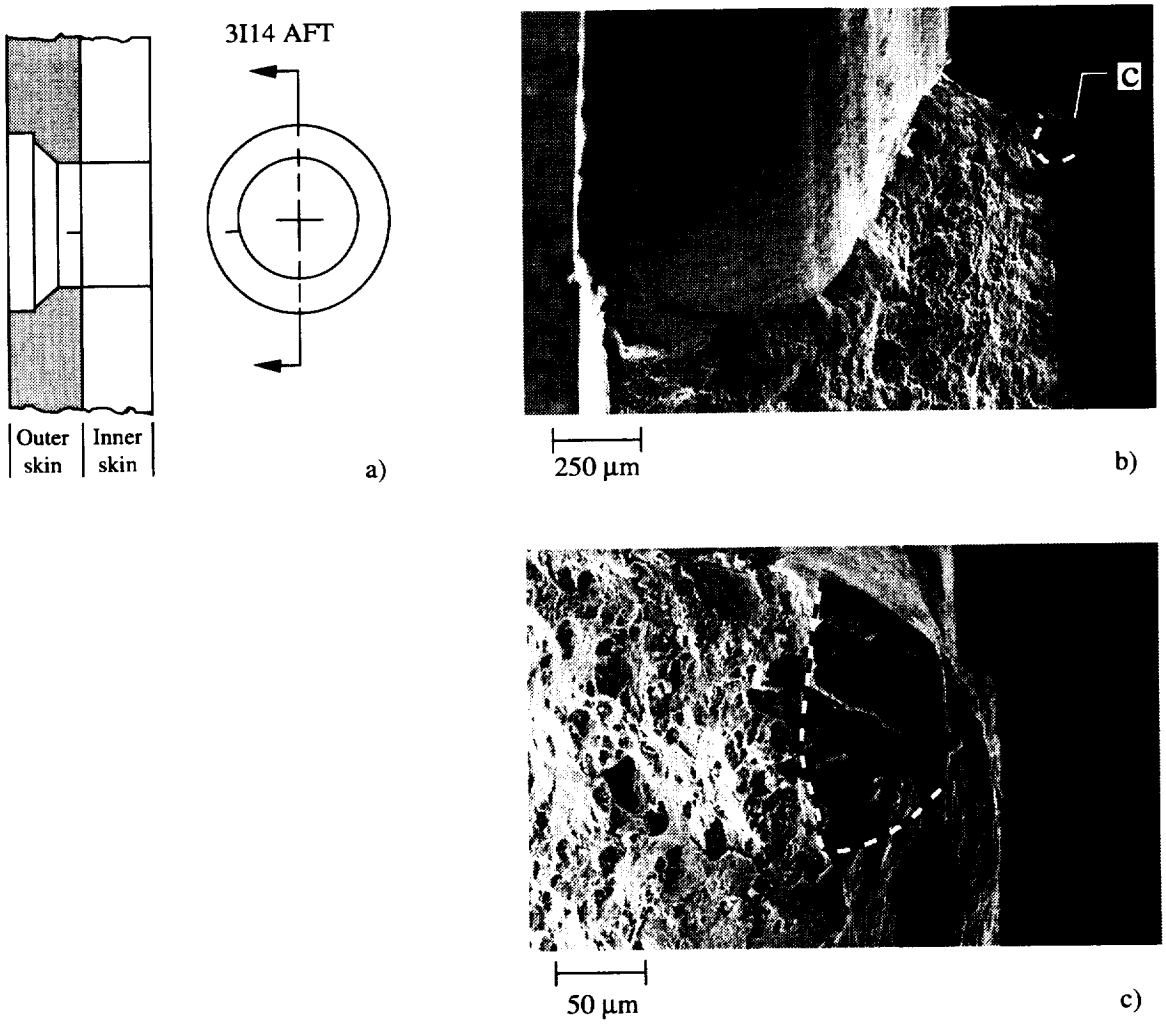

Figure 9.37 a) The schematic shows the rivet hole 3I14 configuration and the location of the outer skin fatigue crack oriented in the aft direction below the 9 o'clock position. b) The SEM micrograph shows the fatigue crack at the inboard corner of the rivet hole. The dashed line marks the fatigue crack front. c) The SEM micrograph shows the region of crack initiation at the rivet hole shank region "c" in Figure 9.37.b. The dashed line marks the fatigue crack front.

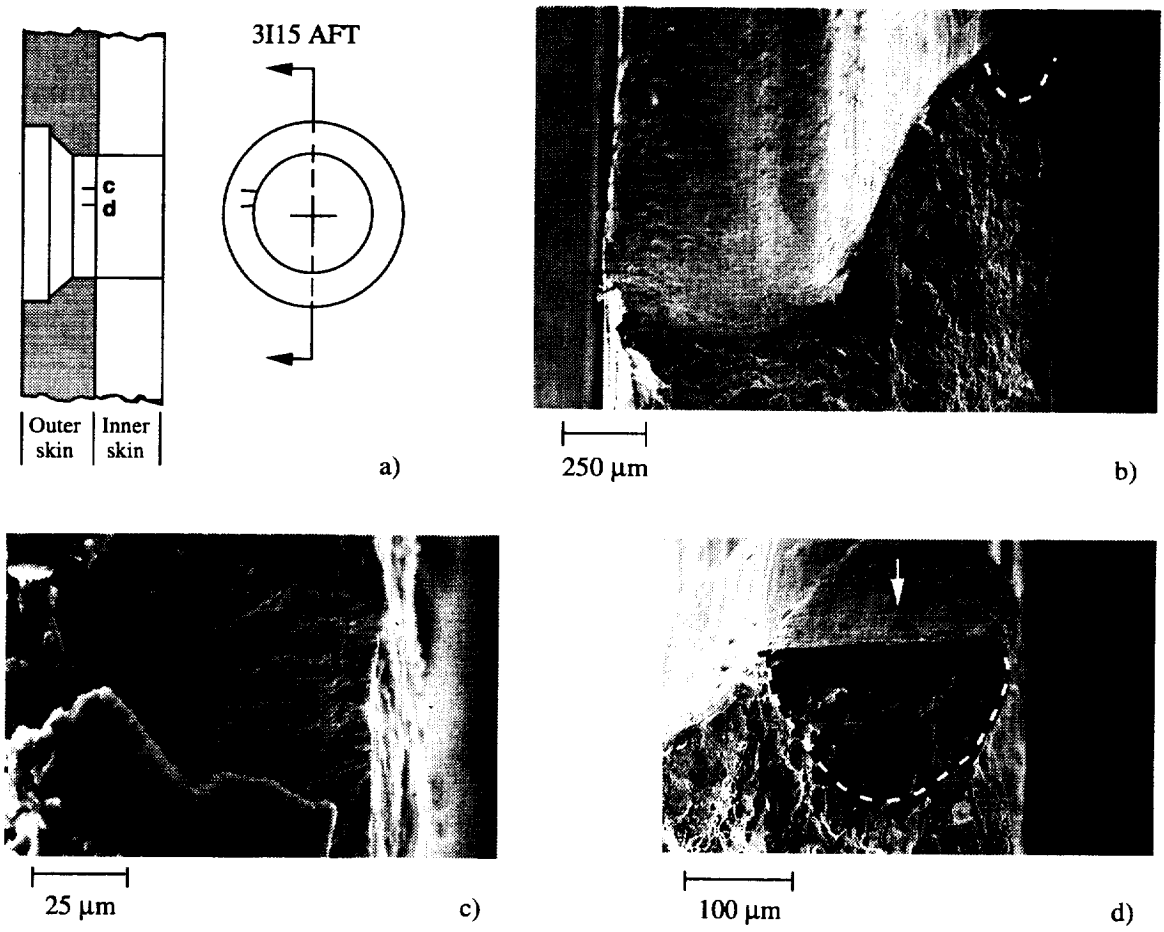

Figure 9.38 a) The schematic shows the rivet hole 3I15 configuration and the location of two outer skin fatigue cracks ("c" and "d") oriented in the aft direction and about the 9 and 10 o'clock positions. b) The SEM micrograph shows fatigue crack "d" at the rivet hole. The dashed line marks the fatigue crack front. c) The SEM micrograph shows the partially opened fatigue crack "c" in Figure 9.38.a located at the inboard corner of the rivet hole. d) The SEM micrograph shows the fatigue crack "d" located at the rivet hole shank.

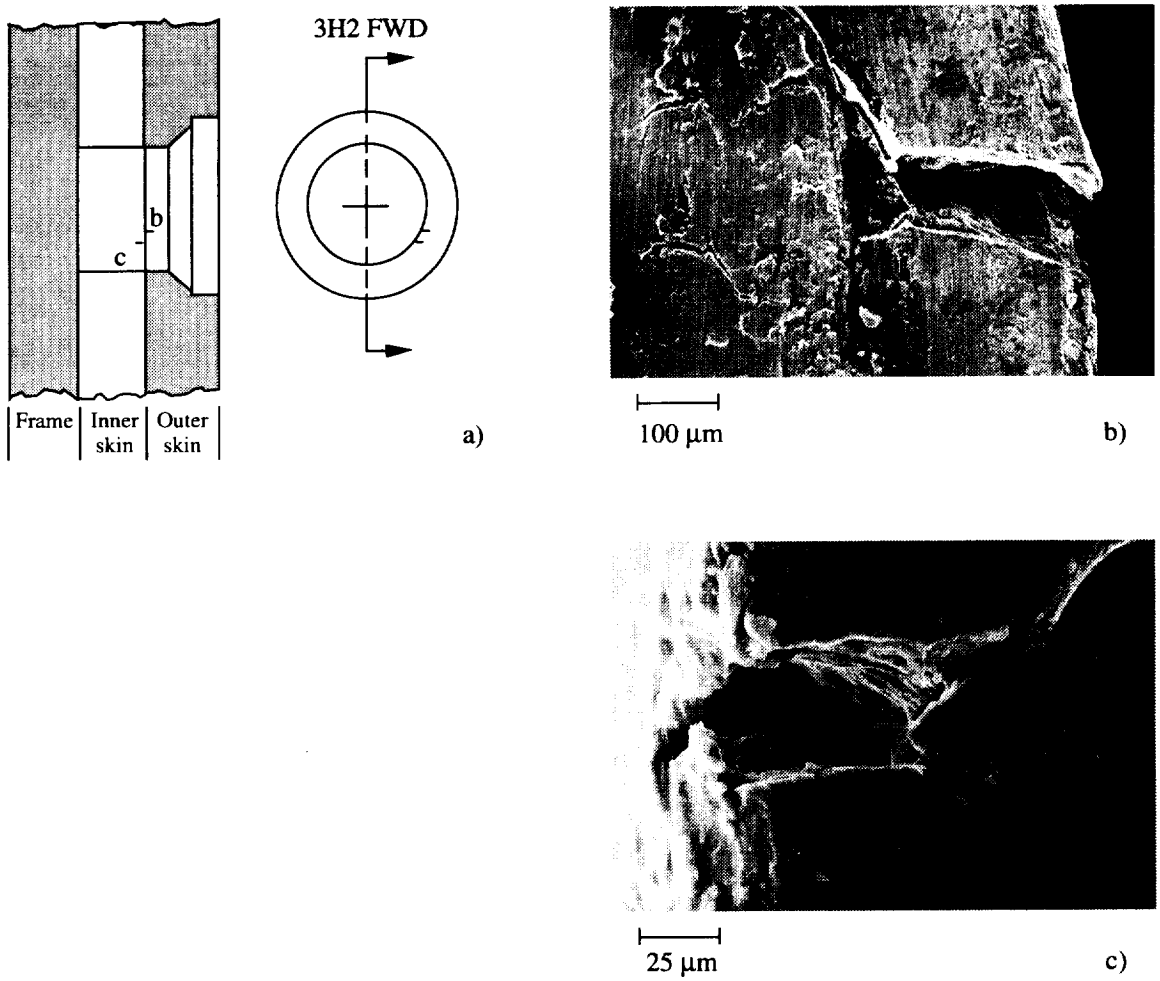

Figure 9.39 a) The schematic shows the rivet hole 3H2 configuration and the location of two fatigue cracks, ("b" and "c") oriented in the forward direction and about the 4 o'clock position. Crack "b" is located at the outboard corner of the inner skin and crack "c" is located at the inboard corner of the outer skin rivet hole. b) The SEM micrograph shows the partially opened inner skin fatigue crack "b" shown in Figure 9.40.a. c) The SEM micrograph shows the partially opened outer skin fatigue crack "c" shown in Figure 9.40.a.

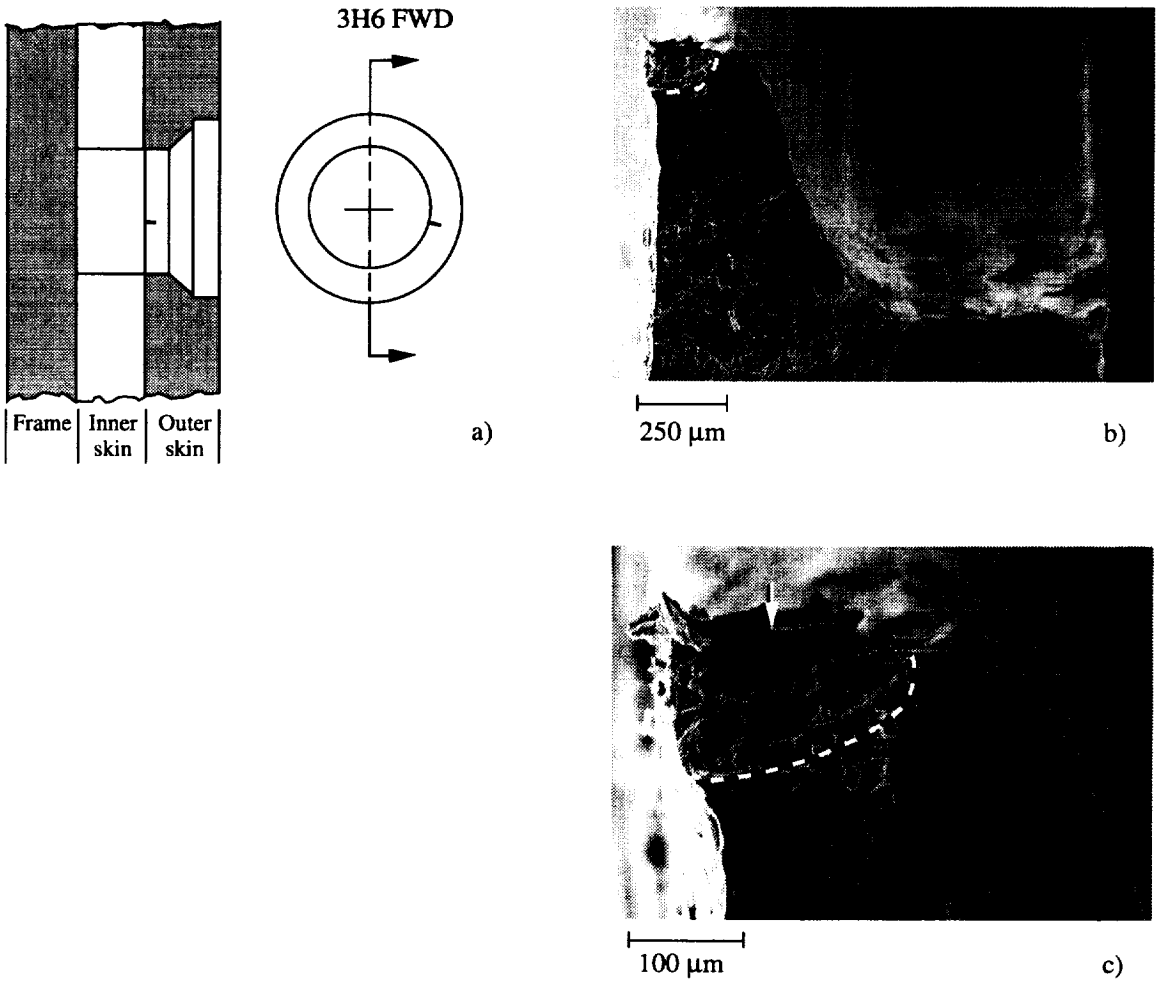

Figure 9.40 a) The schematic shows the rivet hole 3H6 configuration and the location of the outer skin fatigue crack oriented in the forward direction below the 3 o'clock position. b) The SEM micrograph shows the fatigue crack at the rivet hole shank region. The dashed line marks the fatigue crack front. c) The SEM micrograph shows the region of crack initiation (arrow) at the rivet hole shank. The dashed line marks the fatigue crack front.

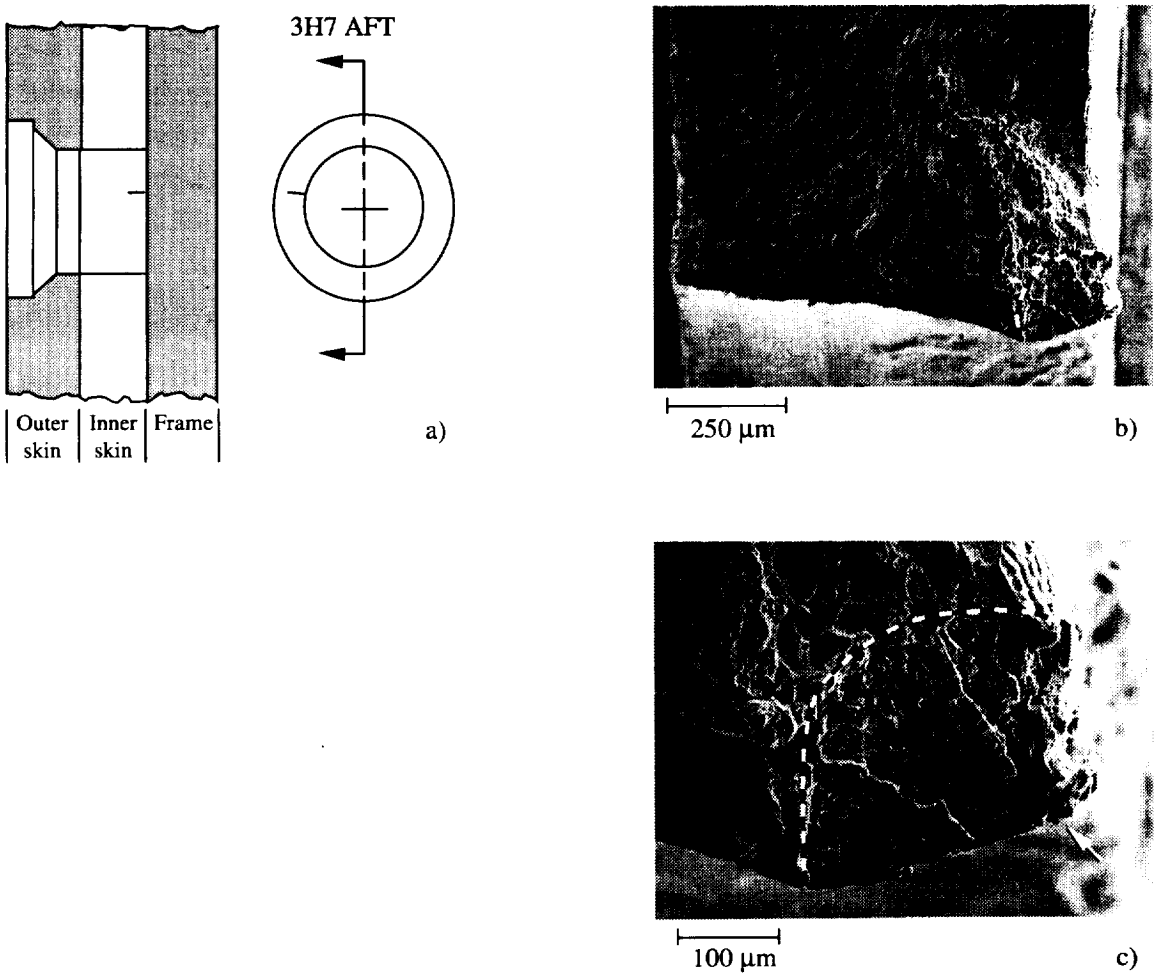

Figure 9.41 a) The schematic shows the rivet hole 3H7 configuration and the location of the inner skin fatigue crack oriented in the aft direction above the 9 o'clock position. b) The SEM micrograph shows the fatigue crack at the inboard corner of the rivet hole. The dashed line marks the fatigue crack front. c) The SEM micrograph shows the region of crack initiation (arrow) at the inboard corner of the rivet hole. The dashed line marks the fatigue crack front.

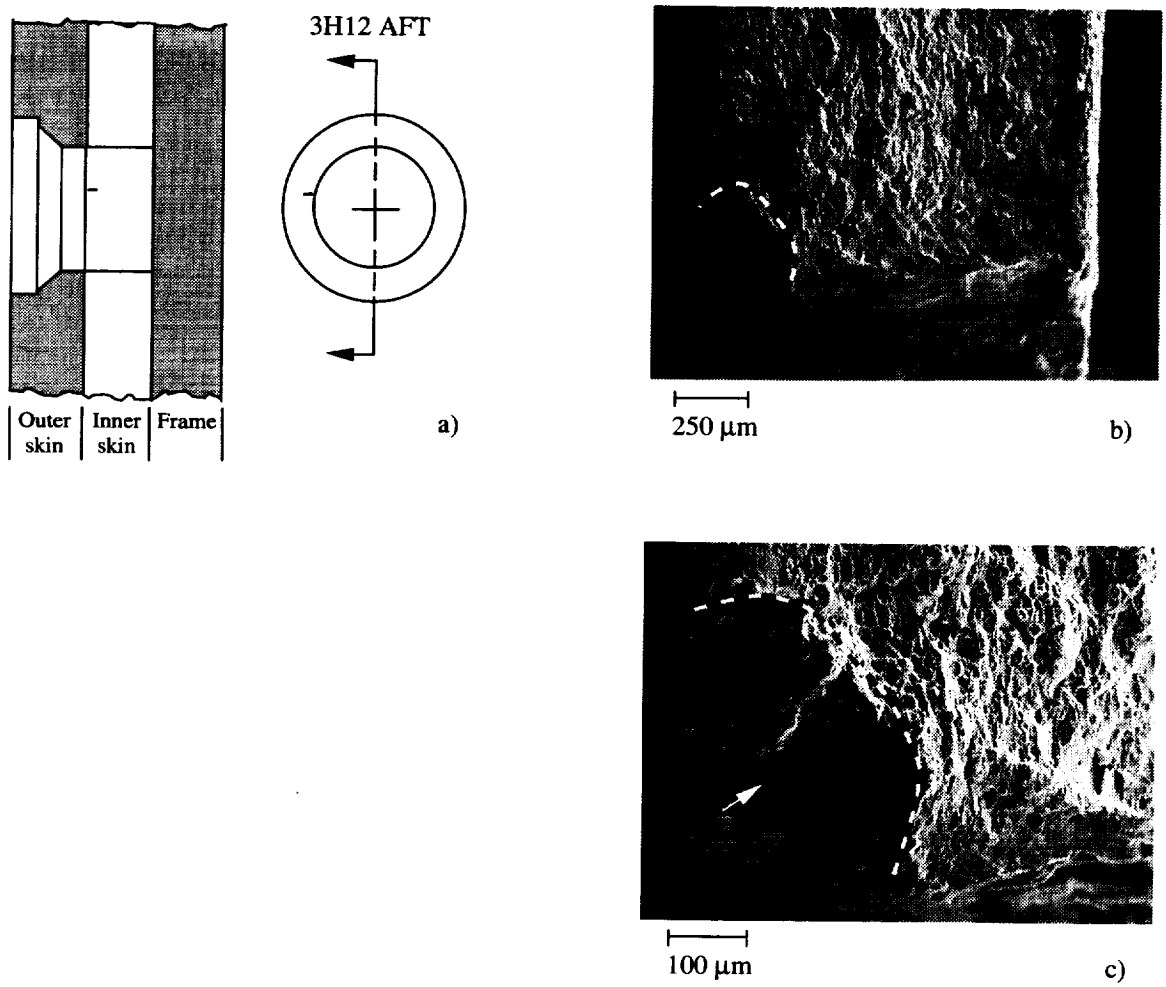

Figure 9.42 a) The schematic shows the rivet hole 3H12 configuration and the location of the inner skin fatigue crack oriented in the aft direction above the 9 o'clock position. b) The SEM micrograph shows the fatigue crack at the outboard corner of the rivet hole. The dashed line marks the fatigue crack front. c) The SEM micrograph shows the region of crack initiation (arrow) at the outboard corner of the rivet hole. The dashed line marks the fatigue crack front.

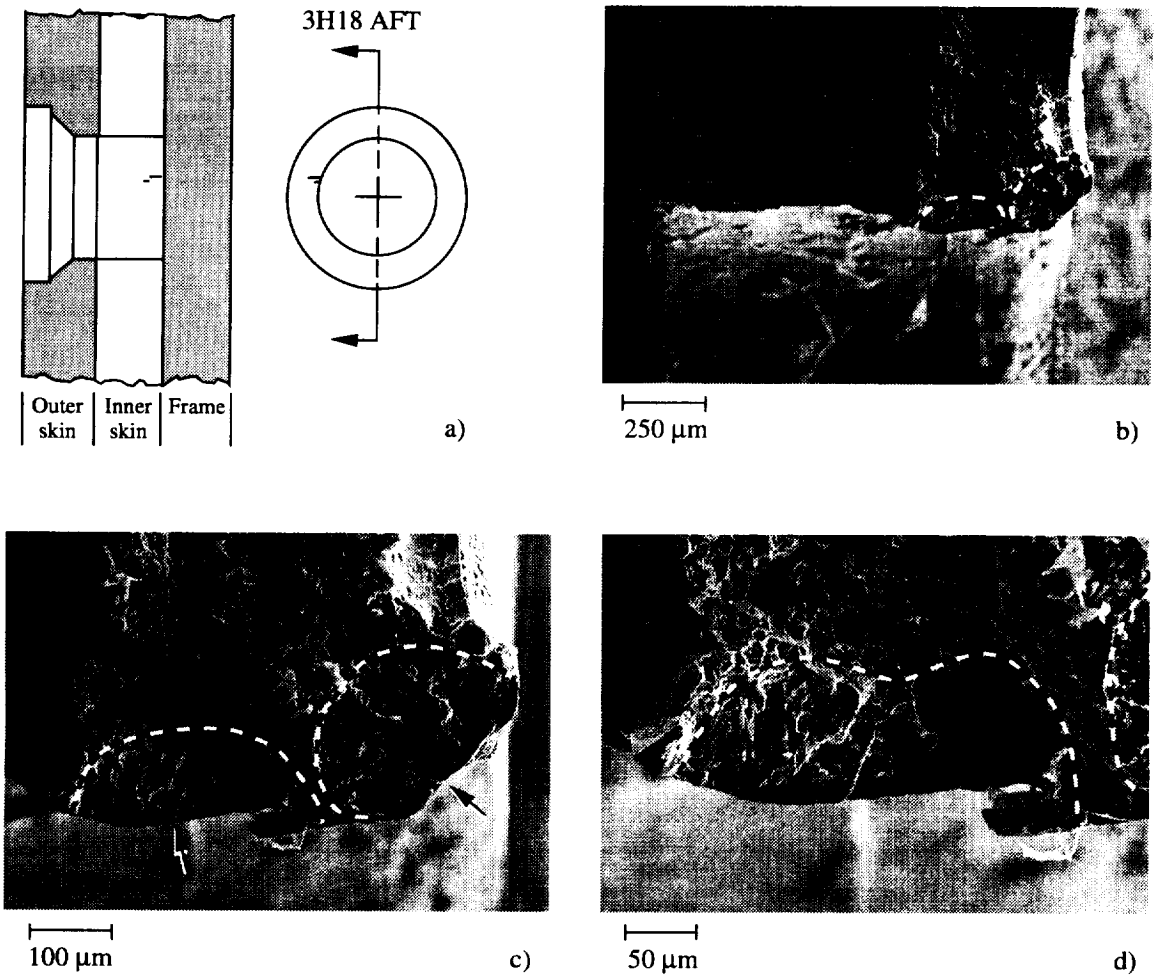

Figure 9.43 a) The schematic shows the rivet hole 3H18 configuration and the location of two inner skin fatigue cracks oriented in the aft direction above the 9 o'clock position. b) The SEM micrograph shows the fatigue cracks at the inboard corner of the rivet hole and at the rivet hole surface. The dashed lines mark the fatigue crack front. c) The SEM micrograph shows the region of crack initiation (arrows) of the inboard corner and surface fatigue cracks. The dashed lines mark the fatigue crack fronts. d) The SEM micrograph shows the rivet hole surface crack at high magnification.

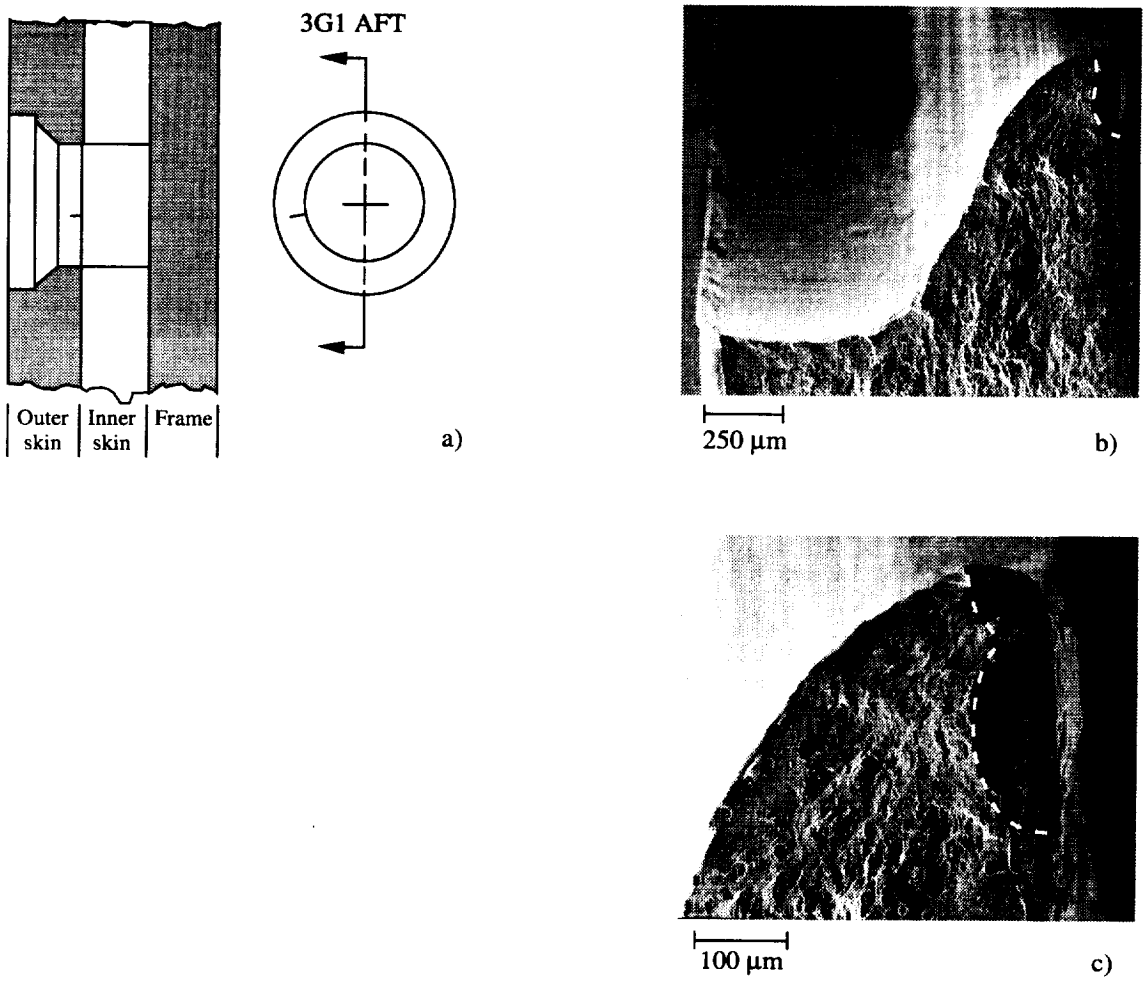

Figure 9.44 a) The schematic shows the rivet hole 3G1 configuration and the location of the outer skin fatigue crack oriented in the aft direction below the 9 o'clock position. b) The SEM micrograph shows the fatigue crack at the rivet hole faying surface. The dashed line marks the fatigue crack front. c) The SEM micrograph shows the fatigue crack region at high magnification. The dashed line marks the fatigue crack front.

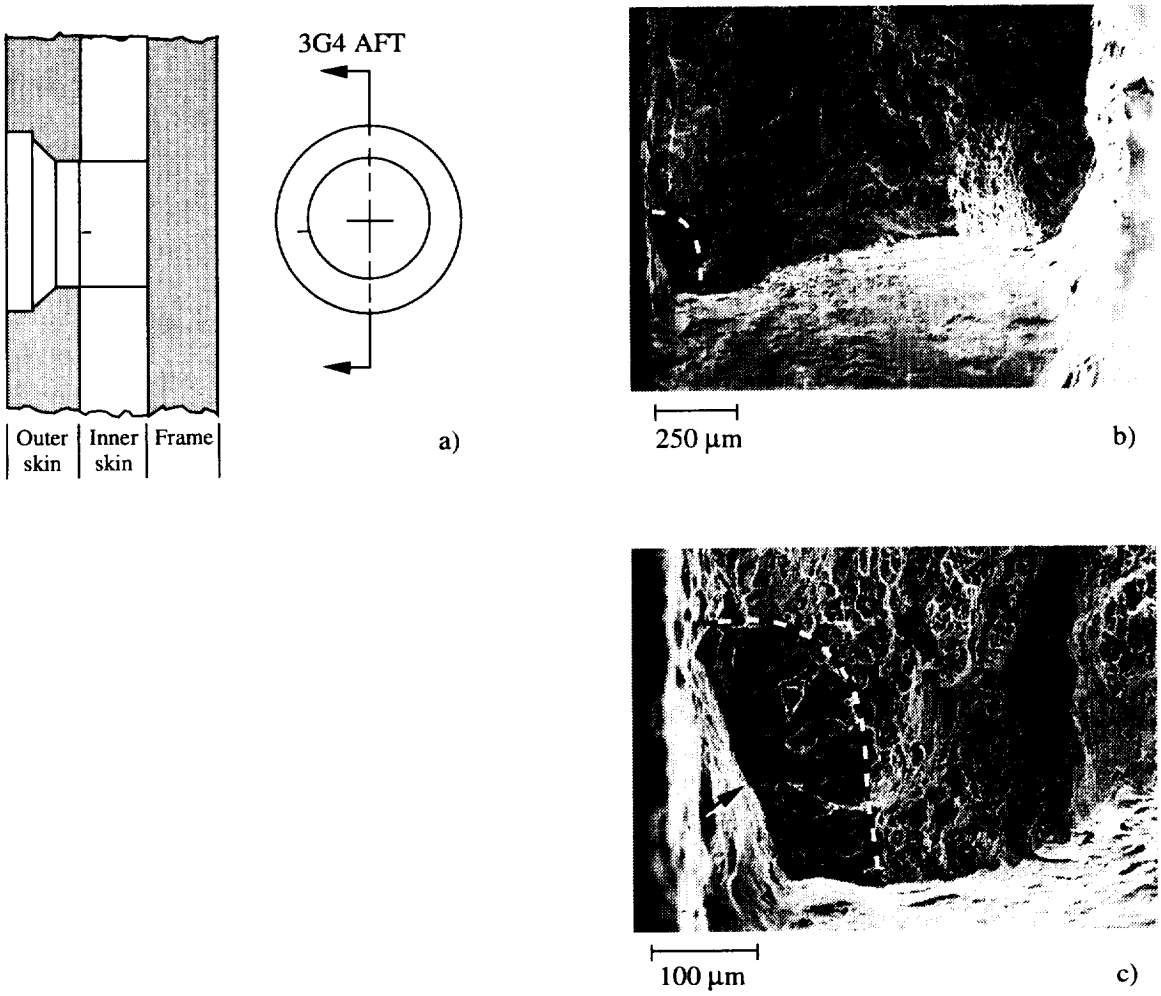

Figure 9.45 a) The schematic shows the rivet hole 3G4 configuration and the location of the inner skin fatigue crack oriented in the aft direction below the 9 o'clock position. b) The SEM micrograph shows the fatigue crack at the outboard corner of the rivet hole. The dashed line marks the fatigue crack front. c) The SEM micrograph shows the region of crack initiation (arrow) at the outboard corner of the rivet hole. The dashed line marks the fatigue crack front.

10. Destructive Examination of Bay 3/4 Tear Strap

Figure 10.1 shows the bay 3/4 tear strap (T.S.) region and most structural components. Identified in Figure 10.1 are thirty-four rivet hole locations that were destructively examined. Sixteen rivet hole locations were found to contain fatigue cracks. A total of seven fatigue cracks were observed at six outer skin rivet hole locations shown in Figure 10.2. Thirteen fatigue cracks were observed at eight upper tear strap rivet hole locations shown in Figure 10.3. Three fatigue cracks were found at two lower tear strap rivet hole locations shown in Figure 10.4. The fatigue cracks observed in the bay 3/4 T.S. region exhibited crack lengths ranging from 0.069 mm (0.003 in) to 2.388 mm (0.094 in). The through-thickness crack schematics shown in Figures 10.5 through 10.9 summarize crack location, crack length, crack type, and initiation sites for rivets numbered 1 through 34. The following is a detailed description of the fatigue damage in bay 3/4 tear strap region.

10.1 Fatigue Cracks Contained in Bay 3/4 Tear Strap:

Figures 10.10 through 10.29 describe the fatigue crack morphology in the bay 3/4 tear strap region.

10.2 Bay 2/3 Tear Strap Summary:

Table 10.1 summarizes the destructive examination results for the bay 3/4 tear strap region. The outer skin fatigue cracks range in length from 0.052 mm (0.002 in.) to 2.529 mm (0.021 in.) and the tear strap cracks ranged between 0.069 mm (0.003 in.) to 5.224 mm (0.206 in) in length. Tear strap fatigue cracking was contained in rivet rows I, J, K, and L. Outer skin fatigue cracks were observed in rows G and I. The following observations were made as a result of fractographic examinations of bay 2.

10.2.1 Crack initiation site(s): All fatigue cracks initiated at high K_T regions. These regions included rivet hole corners, areas of disturbed metal, and small surface imperfections.

10.2.2 Crack front shape as a function of crack length: No crack front shape versus crack length correlation was made.

10.2.3 Fatigue crack/stable tearing transition crack length: No evidence of ductile tearing suggesting either rapid fatigue crack growth or stable tearing was observed in the bay 2/3 tear strap region.

10.2.4 Slant fracture morphology: No slant fracture was observed.

10.2.5 Evidence of corrosion: No corrosion was observed.

Table 10-1 Bay 3/4 Tear Strap Fatigue Crack Summary

Rivet Hole Number	No. of Cracks (Holes)	Location	Crack Length mm (in)	Comment
1–6	10(5)	Upper T.S.	0.143(0.006)≤a ≤2.388(0.094)	High K_T
7–11	1(1)	Upper T.S.	a=0.069(0.003)	High K_T
12–16	2(2)	Upper T.S.	a_1=0.076(0.003)	High K_T
			a_2=0.284(0.011)	High K_T
	3(2)	Lower T.S.	0.177(0.007)≤a ≤0.377(0.015)	High K_T
17–22	6(6)	Outer Skin	0.052(0.002)≤a ≤1.270(0.050)	High K_T
		Lower T.S.	a_1=0.213(0.008)	High K_T
			a_2=5.224(0. 206)	High K_T
23–29	No Fatigue Cracks Found	------	------	------
30–34	3(5)	Outer Skin	0.123(0.005)≤a ≤2.529(0.021)	High K_T

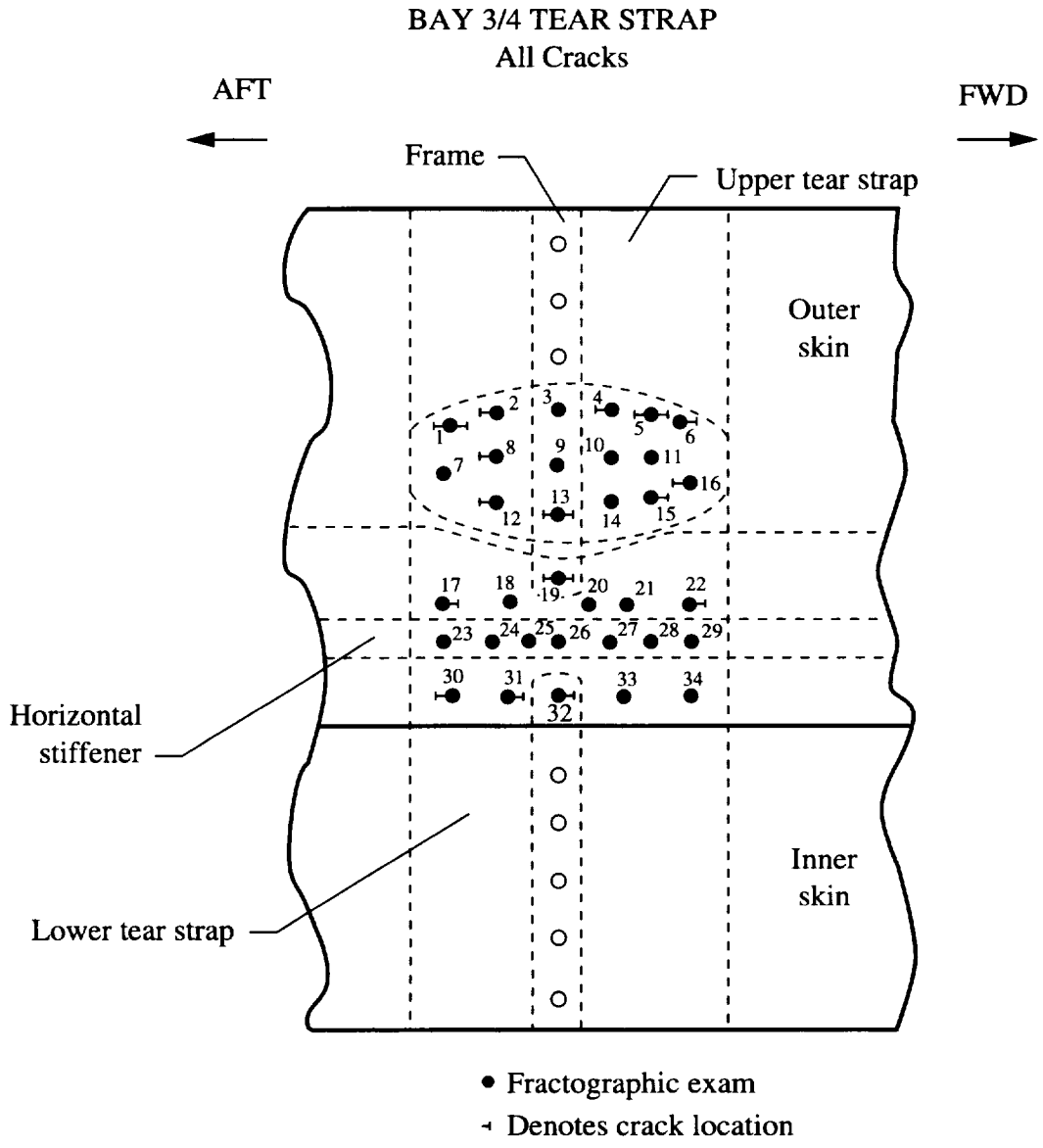

Figure 10.1 The schematic shows the location of all fatigue cracks found in the bay 3/4 tear strap by destructive examination. All filled and numbered rivet holes were destructively examined.

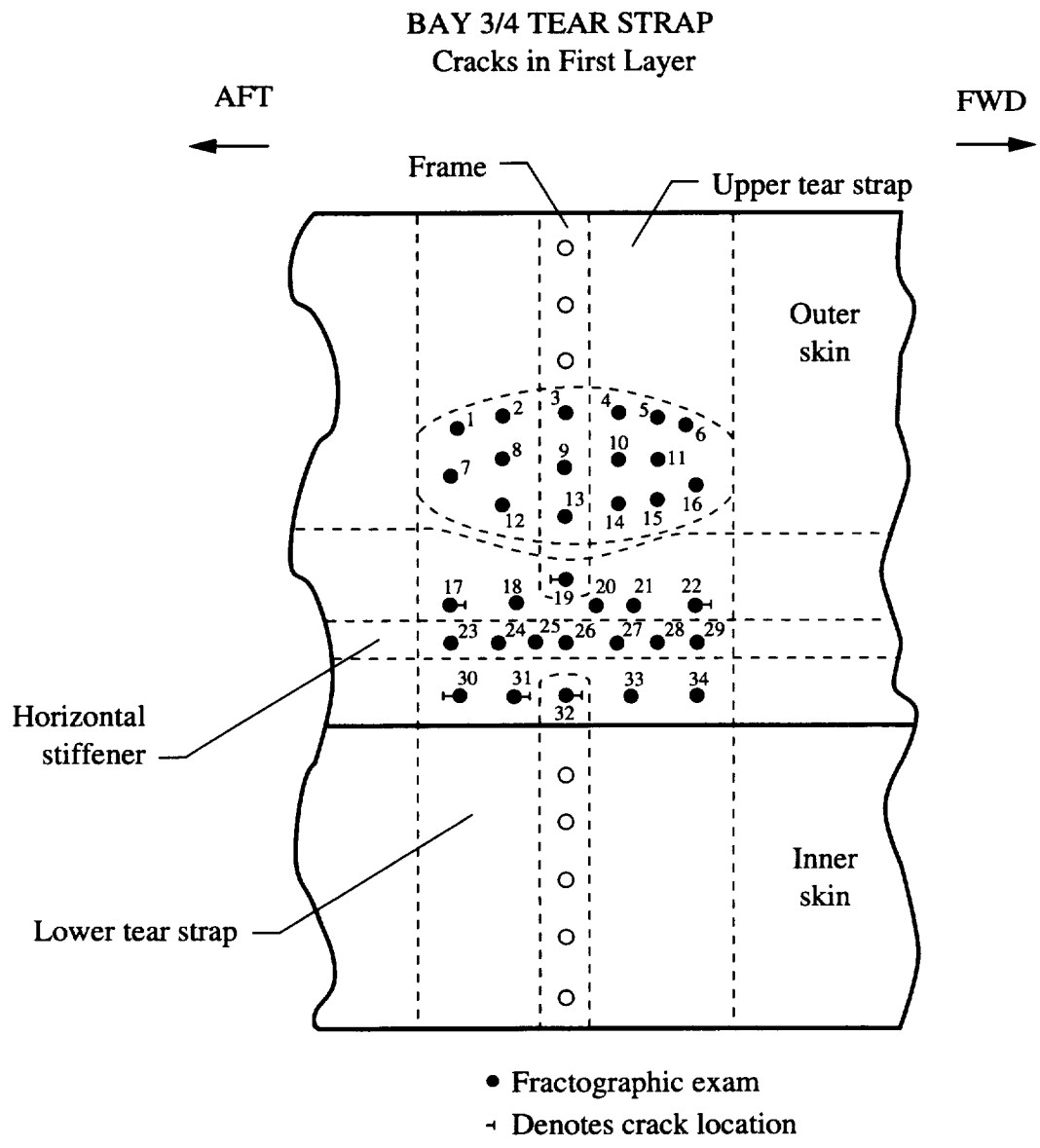

Figure 10.2 The schematic shows the location of fatigue cracks found in the first layer (outer skin) of the bay 3/4 tear strap by destructive examination.

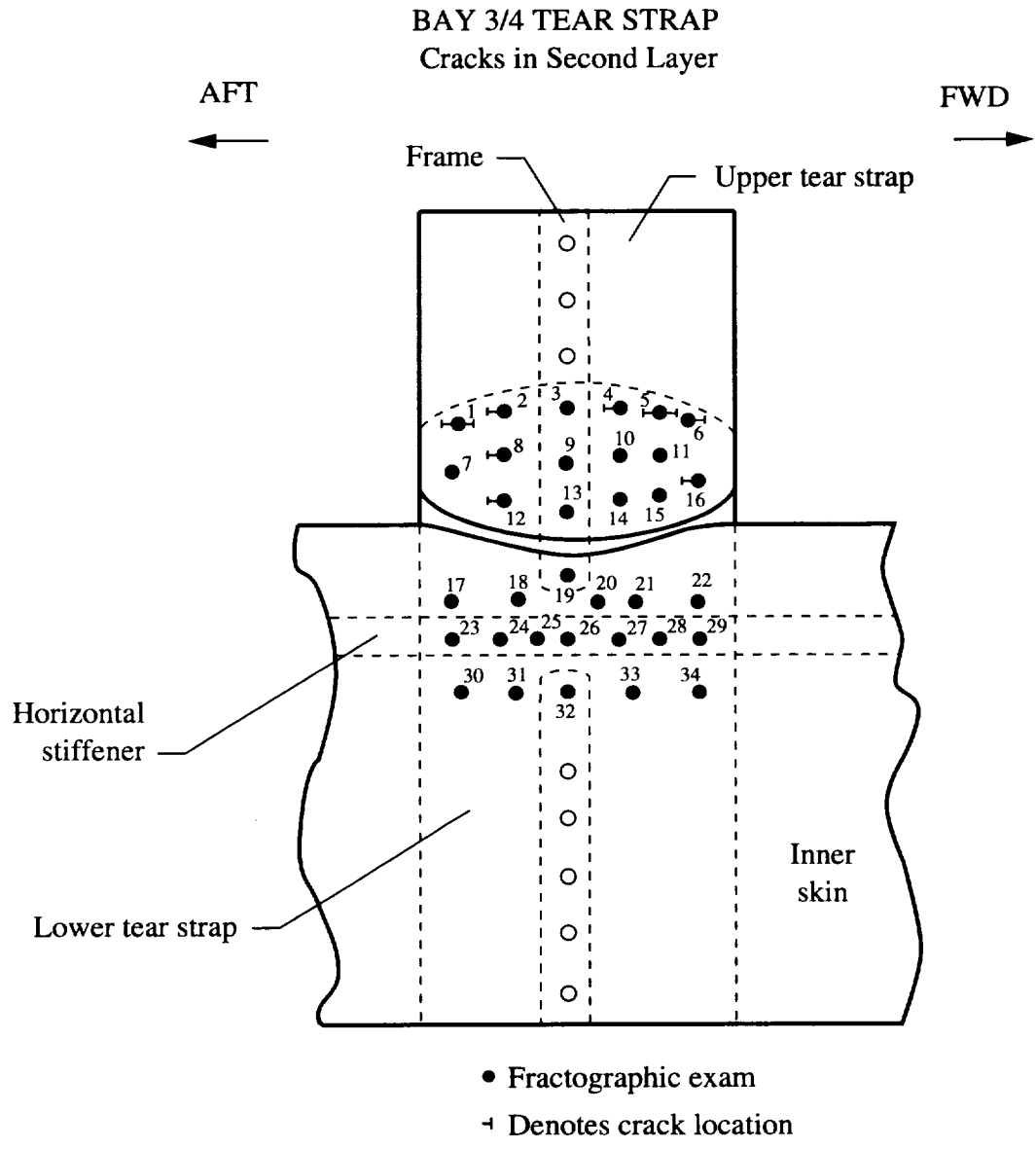

Figure 10.3 The schematic shows the location of fatigue cracks found in the second layer (inner skin and upper tear strap) of the bay 3/4 tear strap by destructive examination.

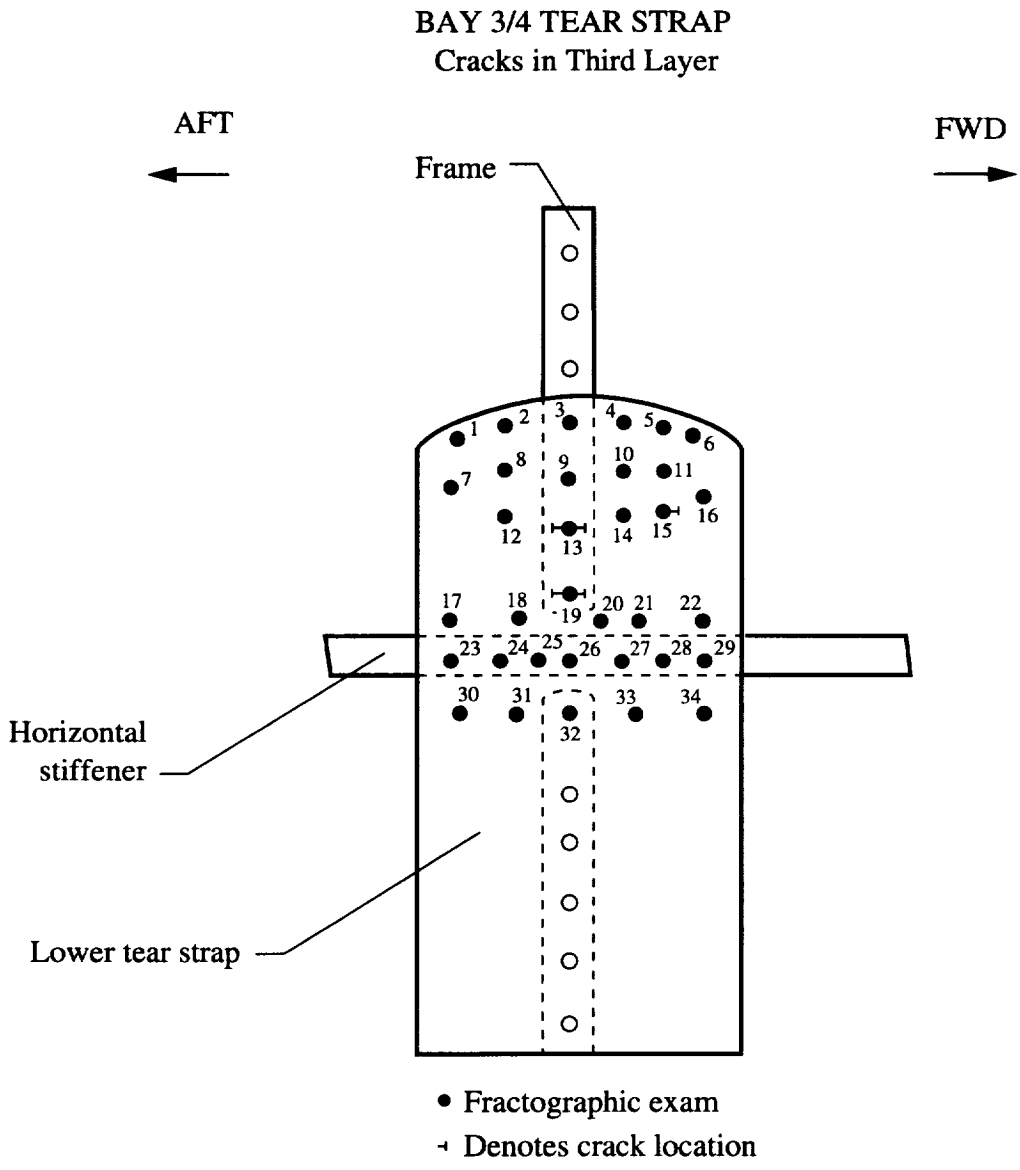

Figure 10.4 The schematic shows the location of one fatigue crack found in the third layer (lower tear strap) of the bay 3/4 tear strap by destructive examination.

Bay 3/4 Tear Strap Row L
Holes 1-6

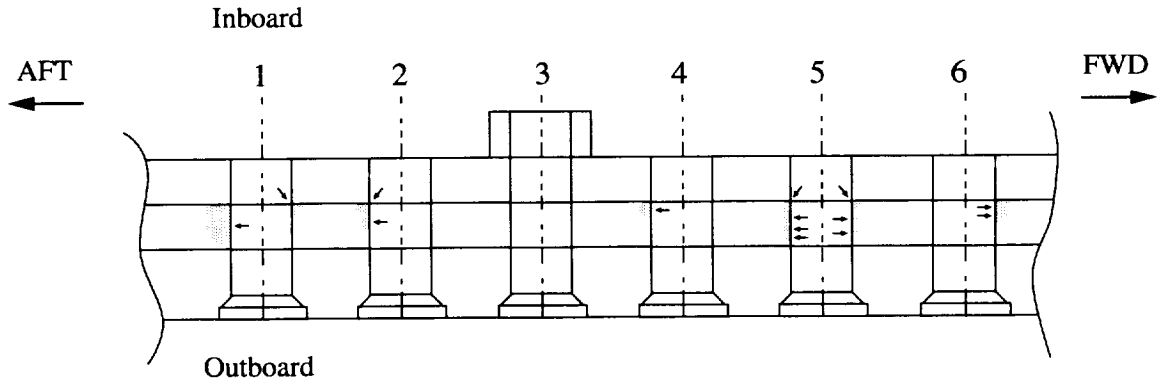

Hole #	Location	Length mm(in)	Type	Initiation site
1 (Aft)	Upper tear strap	2.388 (0.094)	Through	Surface
1 (Fwd)	Upper tear strap	0.143 (0.006)	Corner	Inboard corner
2 (Aft)	Upper tear strap	0.176 (0.007)	Corner	Multiple inboard corner
2 (Aft)	Upper tear strap	0.336 (0.013)	Surface	Surface
4 (Aft)	Upper tear strap	0.353 (0.014)	Corner	Surface
5 (Aft)	Upper tear strap	0.180 (0.007)	Surface	Multiple surface
5 (Aft)	Upper tear strap	0.171 (0.007)	Corner	Inboard corner
5 (Fwd)	Upper tear strap	0.619 (0.024)	Corner	Inboard corner
5 (Fwd)	Upper tear strap	0.143 (0.006)	Surface	Multiple surface
6 (Fwd)	Upper tear strap	0.603 (0.024)	Corner	Multiple surface

Figure 10.5 The through the thickness row schematic shows the location and initiation site of fatigue cracks found in holes number 1, 2, 3, 4, 5, and 6 (row L) in the bay 3/4 tear strap. The table summarizes crack location, crack length, crack type, and initiation site for each fatigue crack shown.

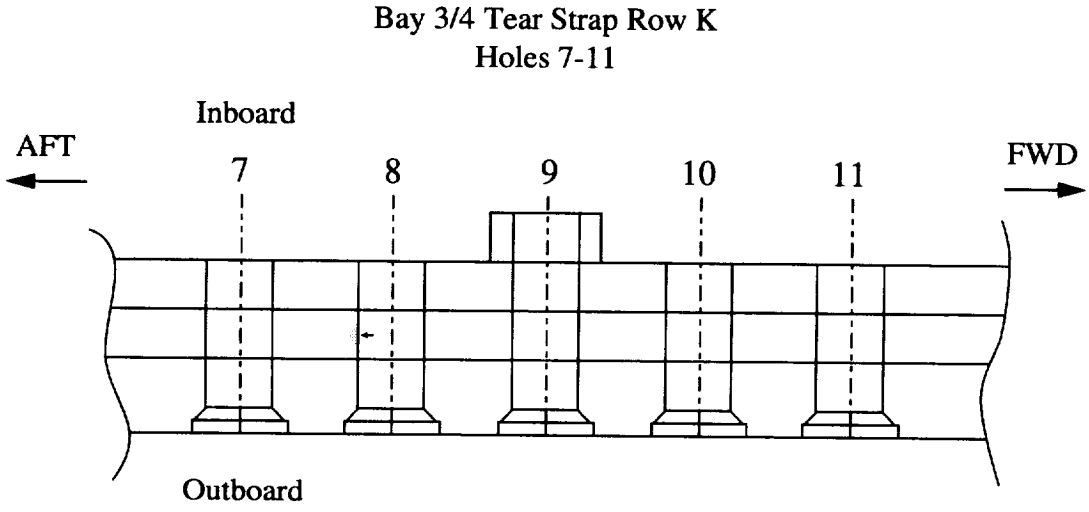

Hole #	Location	Length mm(in)	Type	Initiation site
8 (Aft)	Upper tear strap	0.069 (0.003)	Surface	Surface

Figure 10.6 The through the thickness row schematic shows the location and initiation site of fatigue cracks found in holes number 7, 8, 9, 10, and 11 (row K) in the bay 3/4 tear strap. The table summarizes crack location, crack length, crack type, and initiation site for each fatigue crack shown.

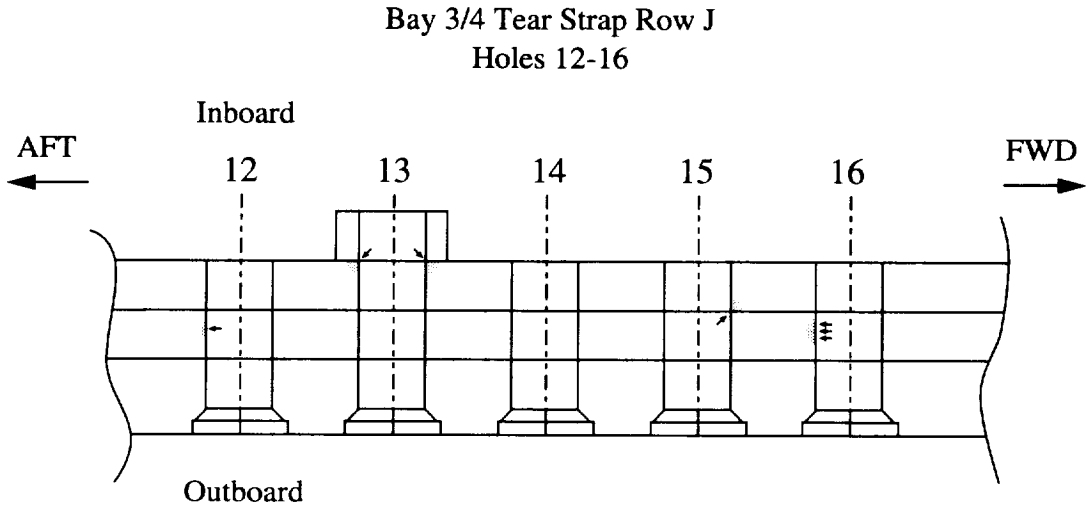

Hole #	Location	Length mm(in)	Type	Initiation site
12 (Aft)	Upper tear strap	0.284 (0.011)	Surface	Surface
13 (Aft)	Lower tear strap	0.377 (0.015)	Corner	Outboard corner
13 (Fwd)	Lower tear strap	0.177 (0.007)	Corner	Multiple corner
15 (Fwd)	Lower tear strap	0.196 (0.008)	Corner	Outboard corner
16 (Aft)	Upper tear strap	0.076 (0.003)	Surface	Multiple surface

Figure 10.7 The through the thickness row schematic shows the location and initiation site of fatigue cracks found in holes number 12, 13, 14, 15, and 16 (row J) in the bay 3/4 tear strap. The table summarizes crack location, crack length, crack type, and initiation site for each fatigue crack shown.

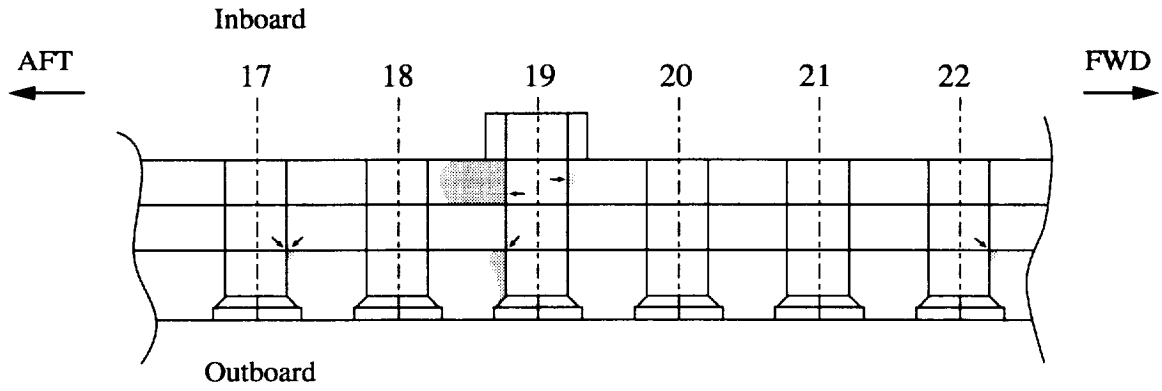

Hole #	Location	Length mm(in)	Type	Initiation site
17 (1 Fwd)	Outer skin	0.216 (0.008)	Countersink	Inboard side of shank
17 (2 Fwd)	Outer skin	0.470 (0.019)	Countersink	Inboard side of shank
19 (1 Aft)	Lower tear strap	5.224 (0.206)	Through	Surface
19 (2 Aft)	Outer skin	0.325 (0.013)	Countersink	Inboard side of shank
19 (Fwd)	Lower tear strap	0.213 (0.008)	Surface	Surface
22 (Fwd)	Outer skin	0.154 (0.006)	Countersink	Inboard side of shank

Figure 10.8 The through the thickness row schematic shows the location and initiation site of fatigue cracks in holes number 17, 18, 19, 20, 21, and 22 (row I) in the bay 3/4 tear strap. The table summarizes crack location, crack length, crack type, and initiation site for each fatigue crack shown.

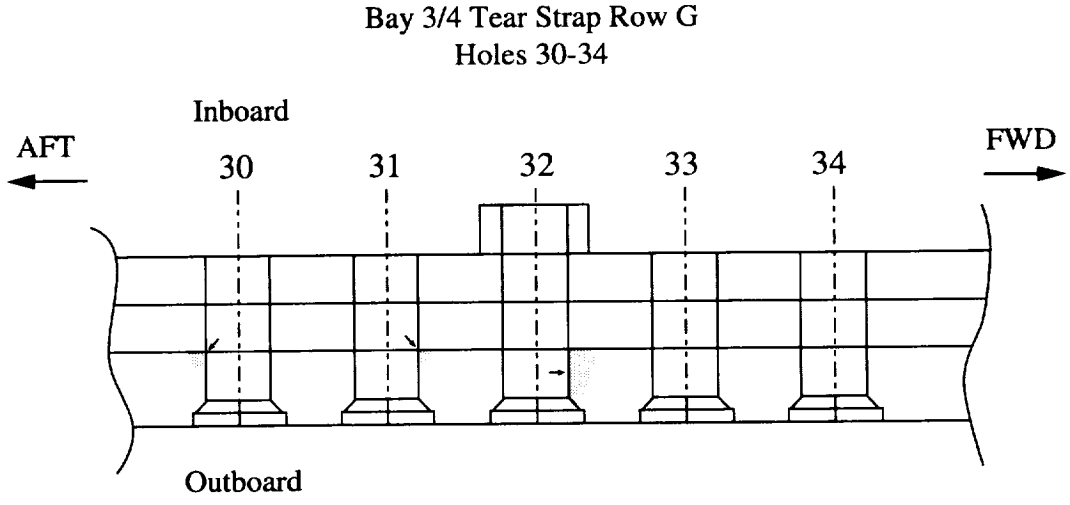

Hole #	Location	Length mm(in)	Type	Initiation site
30 (Aft)	Outer skin	0.208 (0.008)	Countersink	Inboard side of shank
31 (Fwd)	Outer skin	0.123 (0.005)	Countersink	Inboard side of shank
32 (Fwd)	Outer skin	0.529 (0.021)	Countersink	Outboard of shank

Figure 10.9 The through the thickness row schematic shows the location and initiation site of fatigue cracks in holes number 30, 31, 32, 33, and 34 (row G) in the bay 3/4 tear strap. The table summarizes crack location, crack length, crack type, and initiation site for each fatigue crack shown.

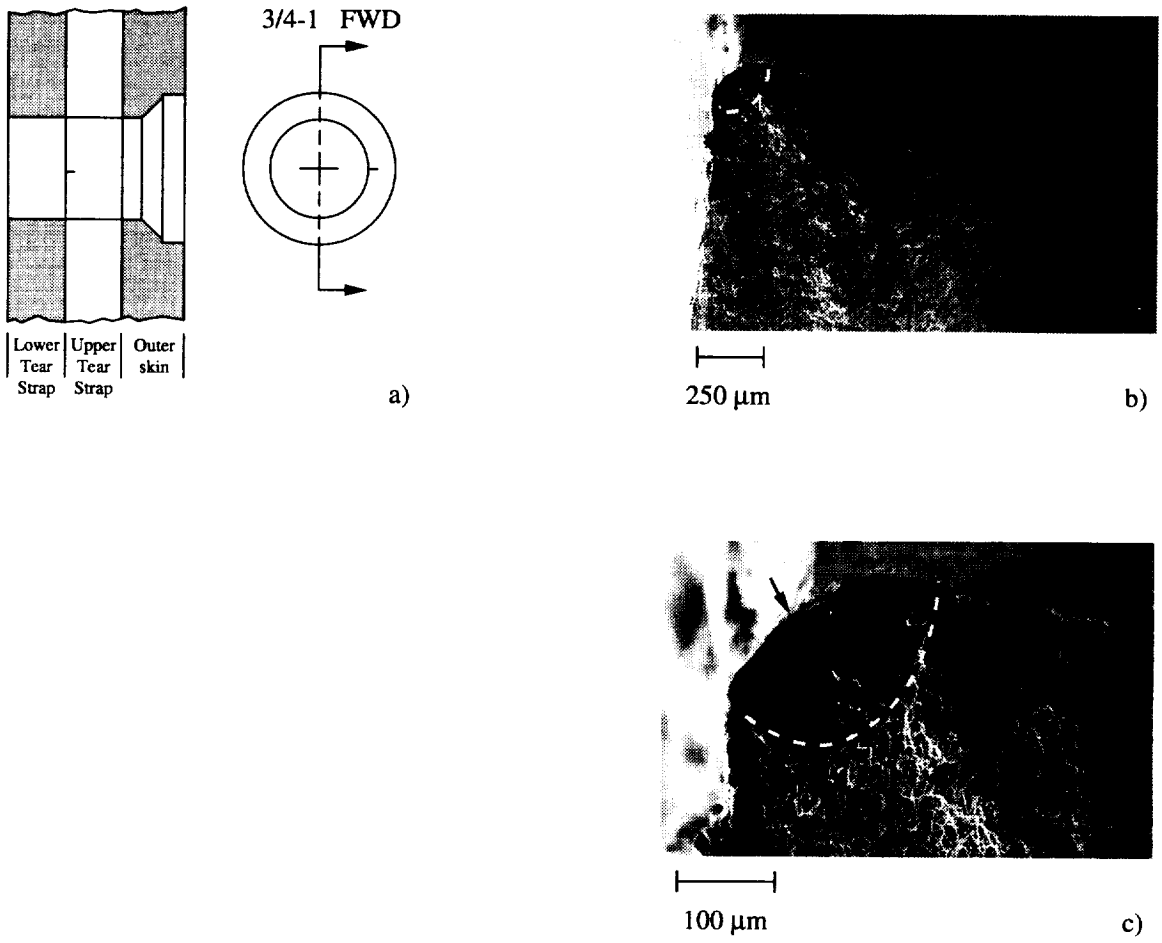

Figure 10.10 a) The schematic shows the rivet hole 3/4-1 configuration and the location of an upper T.S. fatigue crack oriented in the forward direction and about the 3 o'clock position. b) The SEM micrograph shows the location of a small fatigue crack at the inside corner of the upper T.S. rivet hole. The dashed line marks the fatigue crack front. c) The SEM micrograph shows the corner crack at high magnification. The arrow marks the likely crack initiation site and the dashed line marks the fatigue crack front.

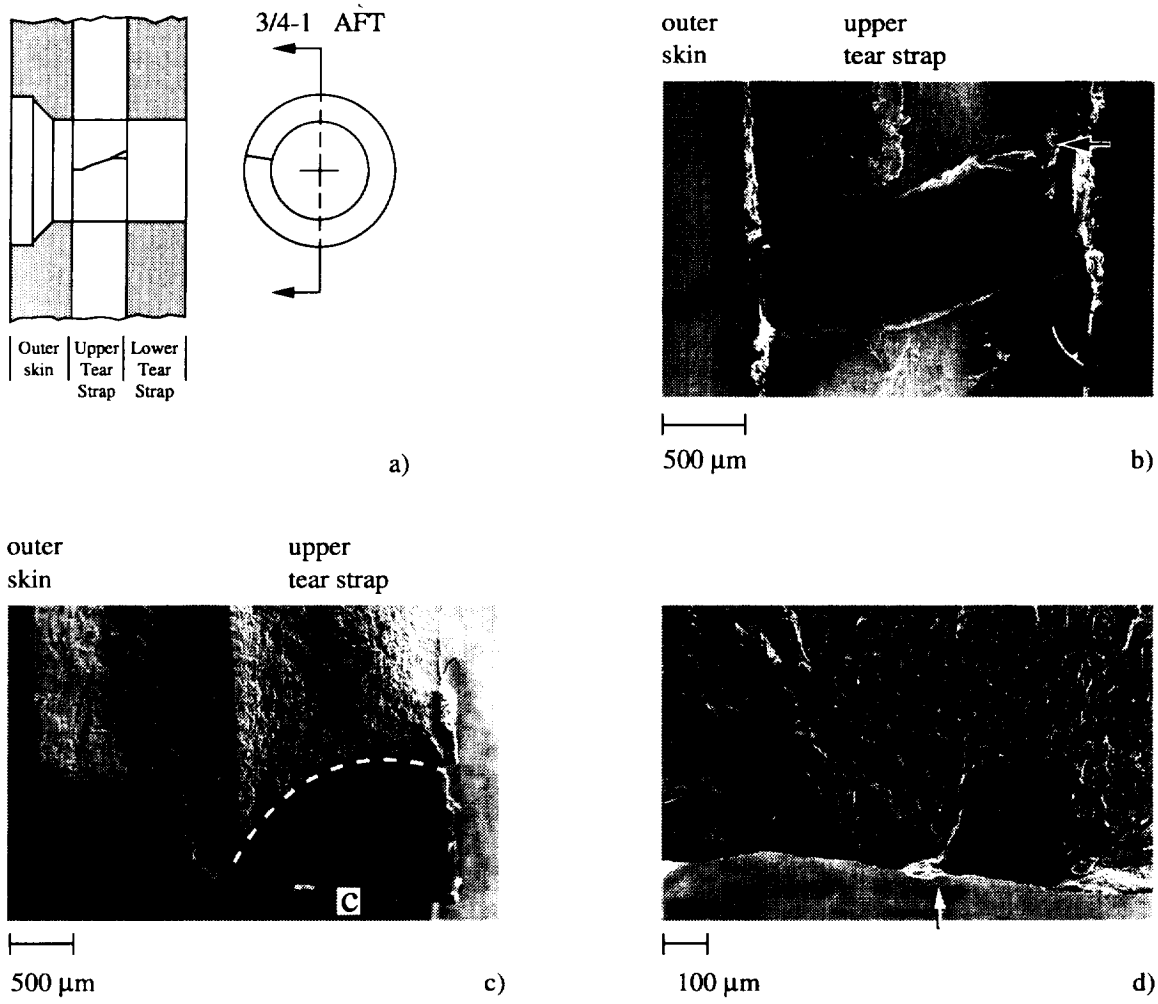

Figure 10.11 a) The schematic shows the rivet hole 3/4-1 configuration and the location of an upper T.S. fatigue crack oriented in the aft direction above the 9 o'clock position. b) The SEM micrograph shows the partially opened upper T.S. crack at the rivet hole surface. To the left is the fractured outer skin. A small partially opened fatigue crack is visible above the main fracture surface (arrow). c) The SEM micrograph shows the location of the fatigue crack contained in the upper T.S. The dashed line marks the fatigue crack front. Here the rivet hole is located at the bottom of the micrograph and the outer skin is located to the left of the fatigue crack region. d) The SEM micrograph shows the region of crack initiation at high magnification, region "c" in Figure 10.10.d. The arrow marks the likely crack initiation site.

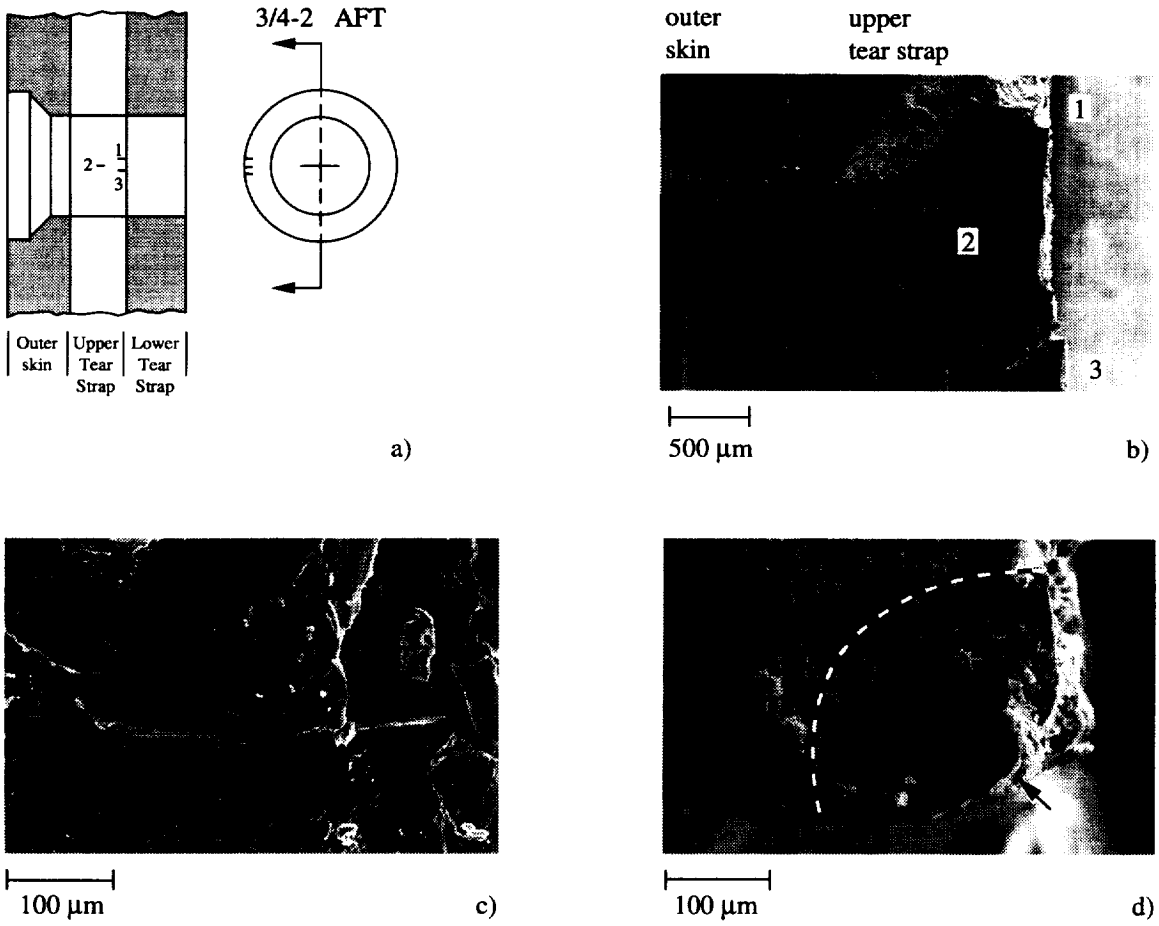

Figure 10.12 a) The schematic shows the rivet hole 3/4-2 configuration and the location of three upper T.S. fatigue cracks oriented in the aft direction and about the 9 o'clock position. b) The SEM micrograph shows the location of two partially opened upper T.S. cracks, crack #2 on the rivet hole surface and crack #3 at the inboard corner. Crack #1 is located at the inboard corner on the main fracture surface. c) The SEM micrograph shows the partially opened fatigue crack #2 in Figure 10.12.b on the disturbed metal surface of the upper skin rivet hole. d) The SEM micrograph shows corner crack #1 in Figure 10.12.b. The arrow marks the site of crack initiation and the dashed line marks the fatigue crack front.

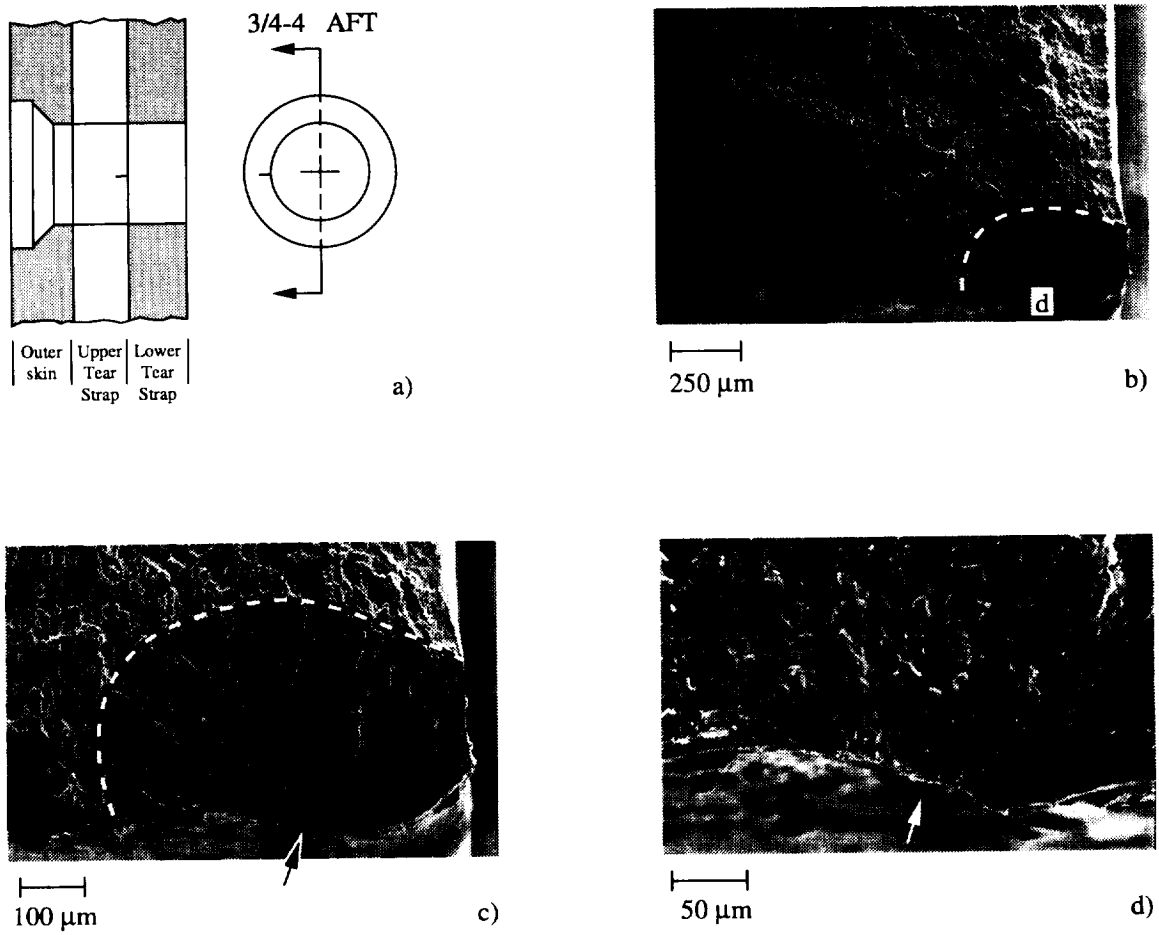

Figure 10.13 a) The schematic shows the rivet hole 3/4-4 configuration and the location of an upper T.S. fatigue crack oriented in the aft direction and about the 9 o'clock position. b) The SEM micrograph shows the upper T.S. fatigue crack located at the inboard corner of the rivet hole. The dashed line marks the fatigue crack front. c) The SEM micrograph shows the upper T.S. corner crack. The arrow marks the likely site of crack initiation and the dashed line marks the fatigue crack front. d) The SEM micrograph shows the region of crack initiation at high magnification, region "d" in Figure 10.13.b. The arrow marks the likely crack initiation site.

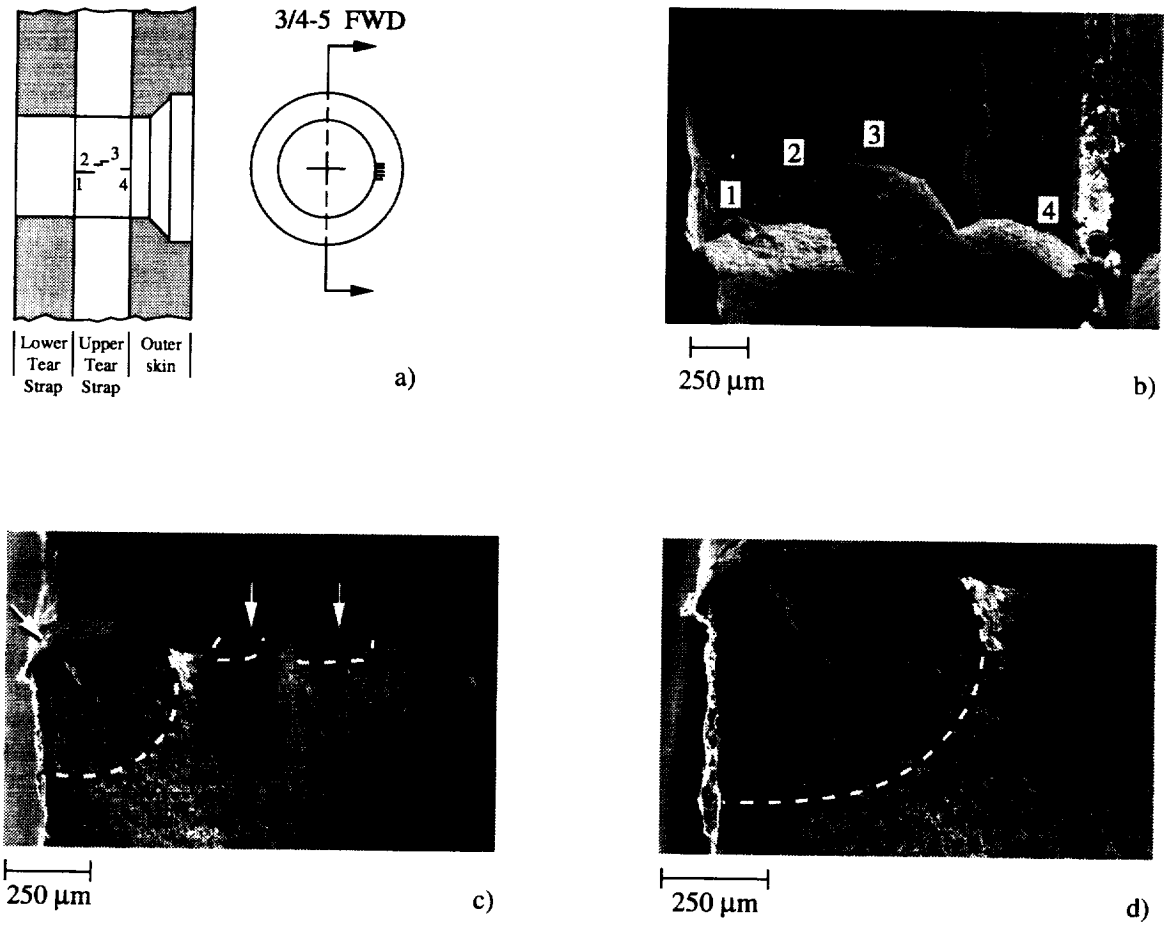

Figure 10.14 a) The schematic shows the rivet hole 3/4-5 configuration and the location of four upper T.S. fatigue cracks oriented in the forward direction and about the 3 o'clock position. b) The SEM micrograph shows the inside surface of the upper T.S. rivet hole. The main fracture surface is located at the bottom of the micrograph. c) The SEM micrograph shows three upper T.S. fatigue cracks located on the main fracture surface (arrows). Starting at the left, a fatigue crack initiated at the inboard rivet hole corner (crack #1), the middle arrow marks a surface crack (crack #3) partially hidden by a partially fractured ligament seen in Figure 10.14.b. The third arrow, located slightly to the right of center, marks the location of the third rivet hole surface crack (crack #4). Dashed lines mark the crack fronts. d) The SEM micrograph shows the inboard corner crack at higher magnification. The dashed line marks the fatigue crack front.

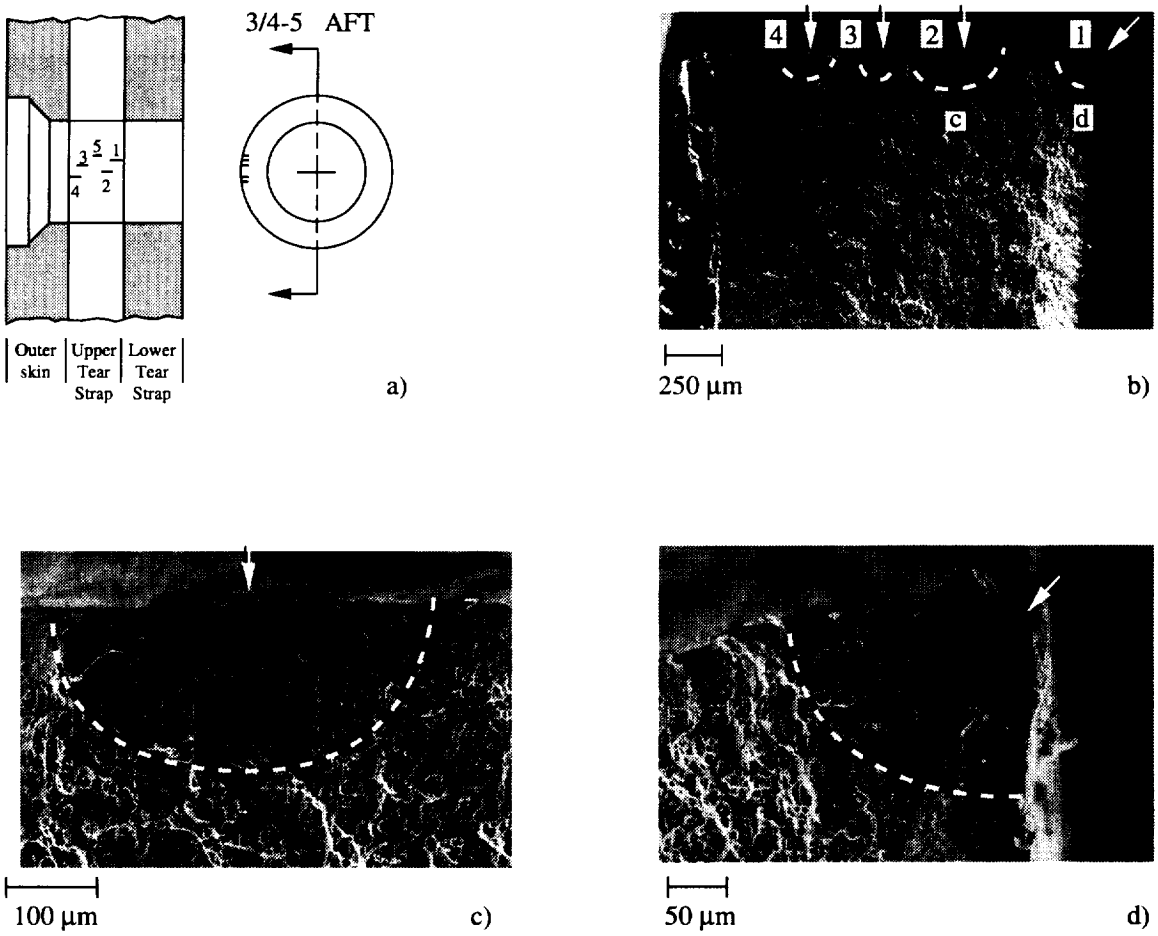

Figure 10.15 a) The schematic shows the rivet hole 3/4-5 configuration and the location of five upper T.S. fatigue cracks oriented in the aft direction and about the 9 o'clock position. b) The SEM micrograph shows the location of four fatigue cracks at the upper tear strap rivet hole (top). Cracks #2, #3, and #4 are rivet hole surface cracks and crack #1 is located on the inboard corner. The dashed line marks the fatigue crack fronts. The arrows mark the likely sites of crack initiation. c) The SEM micrograph shows the fatigue fracture surface of fatigue crack #2 at region "c" in Figure 10.15.b. The arrow marks the area of crack initiation and the dashed line marks the fatigue crack front. d) The SEM micrograph shows the inboard corner crack, region "d" in Figure 10.15.b, at higher magnification. The arrow marks the crack initiation site and the dashed line marks the fatigue crack front.

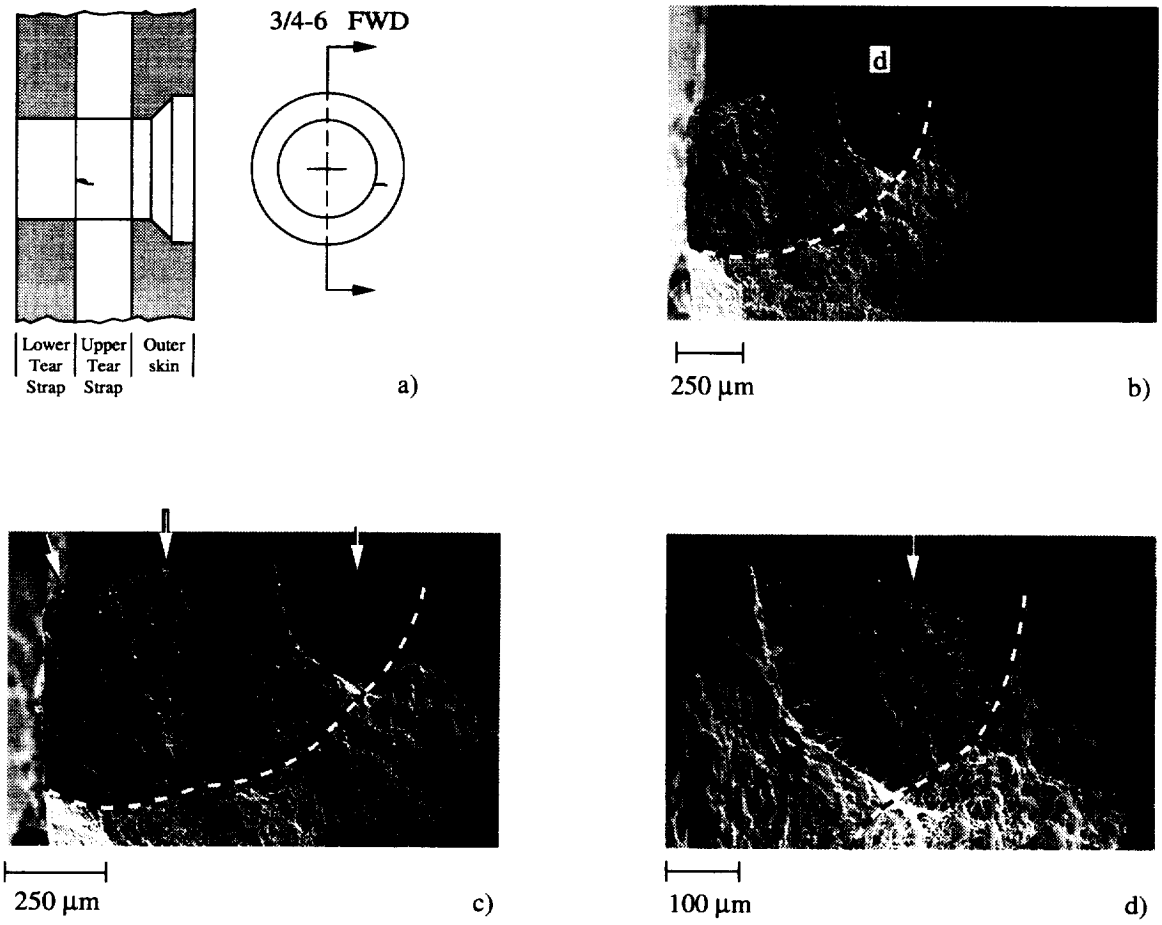

Figure 10.16 a) The schematic shows the rivet hole 3/4-6 configuration and the location of an upper T.S. fatigue crack oriented in the forward direction and about the 4 o'clock position. b) The SEM micrograph shows the fatigue crack located on the inboard corner of the upper T.S. rivet hole. The dashed line marks the fatigue crack front. c) The SEM micrograph shows three possible sites (arrows) where fatigue cracks initiated and subsequently coalesced into a corner crack marked by the dashed line. Two fracture surface ridges mark the location where the small fatigue cracks joined to form a single corner crack. d) The SEM micrograph shows region "d" in Figure 10.16.b at high magnification. The arrow marks the approximate site of crack initiation and the dashed line marks a portion of the fatigue crack front. A ridge created by cracks that coalesced runs from the upper left to the lower middle of the micrograph.

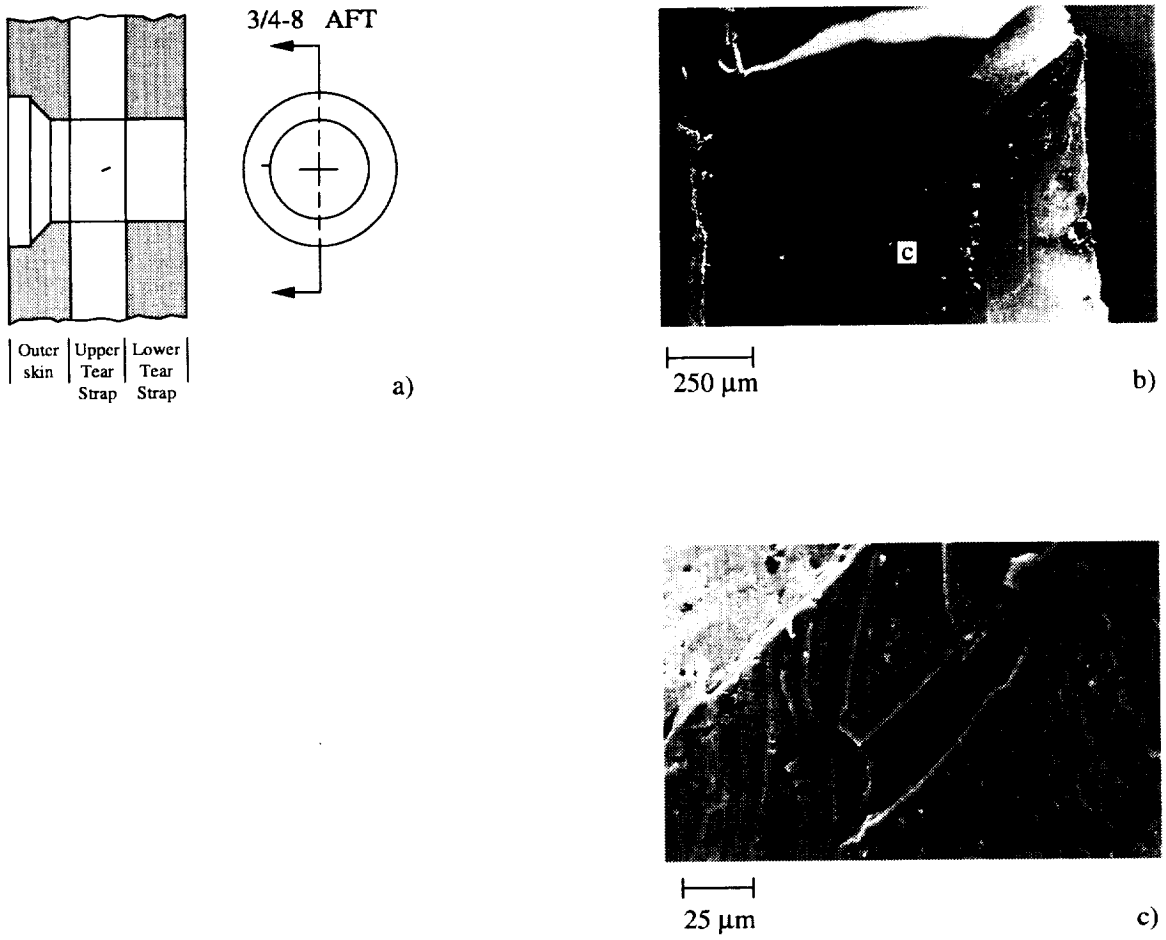

Figure 10.17 a) The schematic shows the rivet hole 3/4-8 configuration and the location of an upper T.S. fatigue crack oriented in the aft direction and about the 9 o'clock position. b) The SEM micrograph shows the inside surface of the upper T.S. rivet hole and the location of a small fatigue crack barely visible at the region marked "c". The main fracture surface produced during the destructive examination is located just above region "c". c) The SEM micrograph shows the partially opened surface fatigue crack located at region "c" in Figure 10.17.b. The crack mouth was opened during the destructive examination. SEM examination into the crack mouth confirmed transgranular fatigue crack growth.

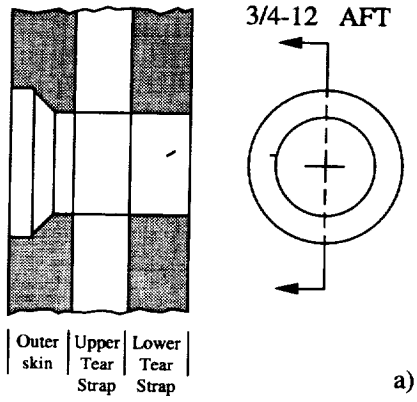

a)

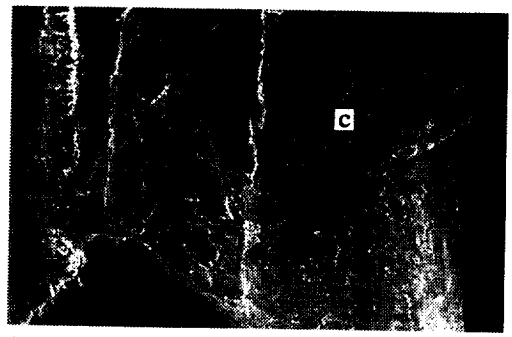

b)

c)

Figure 10.18 a) The schematic shows the rivet hole 3/4-12 configuration and the location of an upper T.S. fatigue crack oriented in the aft direction and about the 9 o'clock position. b) The SEM micrograph shows the inside surface of the upper T.S. rivet hole and the location of a fatigue crack at region "c". The main fracture surface produced during the destructive examination is partially visible at the bottom of the micrograph. c) The SEM micrograph shows the partially opened surface fatigue crack located at region "c" in Figure 10.18.b. The crack mouth was opened during the destructive examination. SEM examination into the crack mouth confirmed transgranular fatigue crack growth.

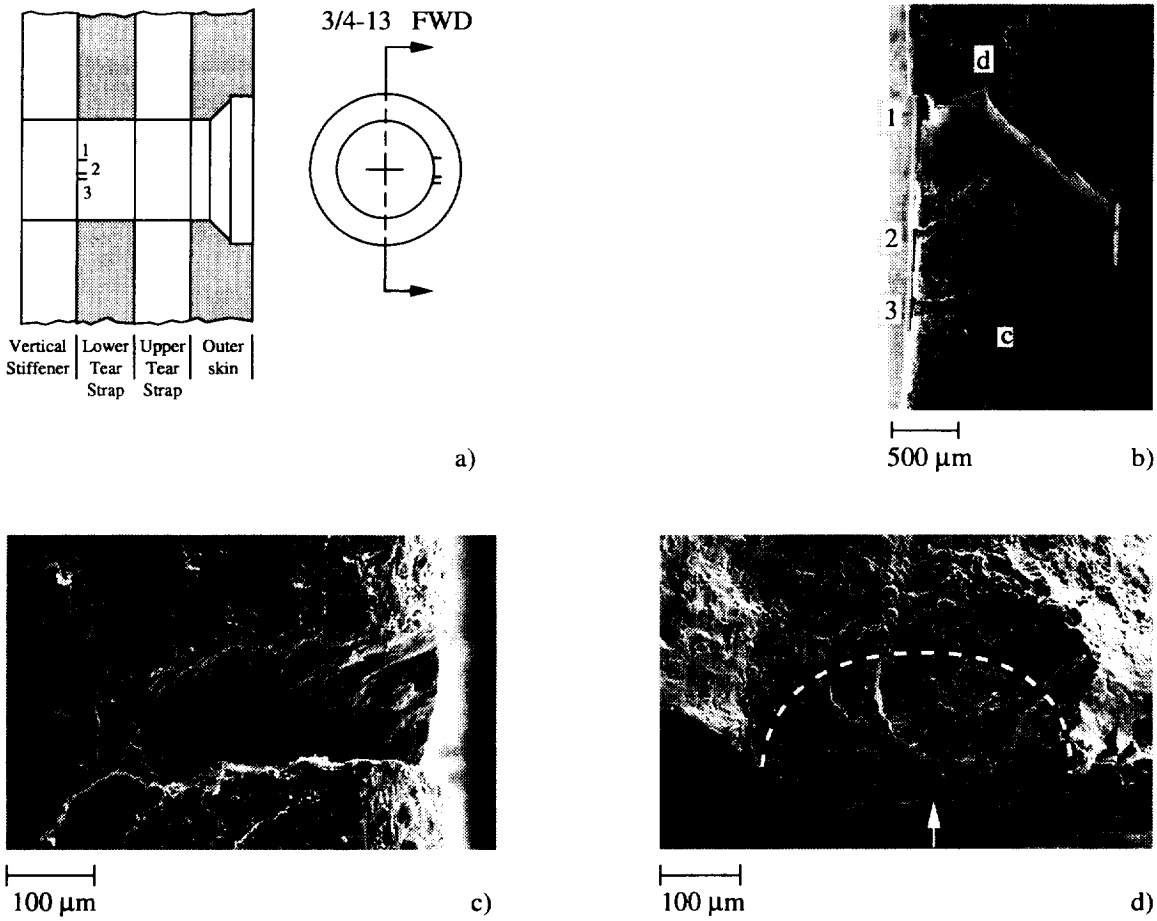

Figure 10.19 a) The schematic shows the rivet hole 3/4-8 configuration and the location of three lower T.S. fatigue cracks oriented in the forward direction and about the 3 o'clock position. b) The SEM micrograph shows the inside surface of the lower T.S. rivet hole and the location of the three small cracks along the inboard corner of the rivet hole. Crack #1 is located on the main fracture surface and cracks #2 and #3 are partially opened. c) The SEM micrograph shows the partially opened rivet hole corner fatigue crack #3 located at region "c" in Figure 10.19.b. The crack mouth was opened during the destructive examination. d) The SEM micrograph shows the surface fatigue crack #1 located near the inboard corner at region "d" in Figure 10.19.b.

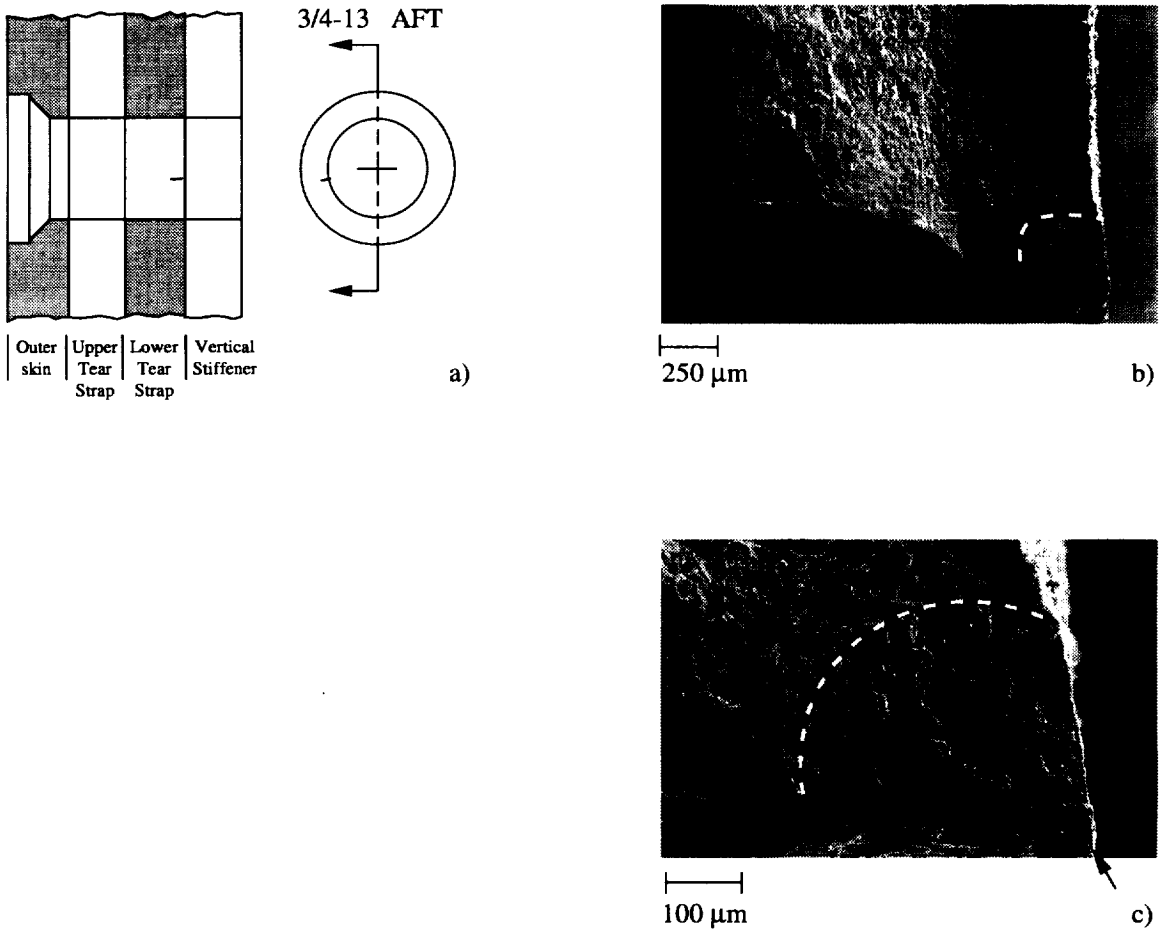

Figure 10.20 a) The schematic shows the rivet hole 3/4-13 configuration and the location of a lower T.S. fatigue crack oriented in the aft direction and below the 9 o'clock position. b) The SEM micrograph shows the fatigue fracture surface of the corner crack located on the inboard corner of the rivet hole. The dashed line marks the fatigue crack front. c) The SEM micrograph shows the fatigue fracture surface of the corner crack. The arrow marks the likely site of crack initiation and the dashed line marks the fatigue crack front.

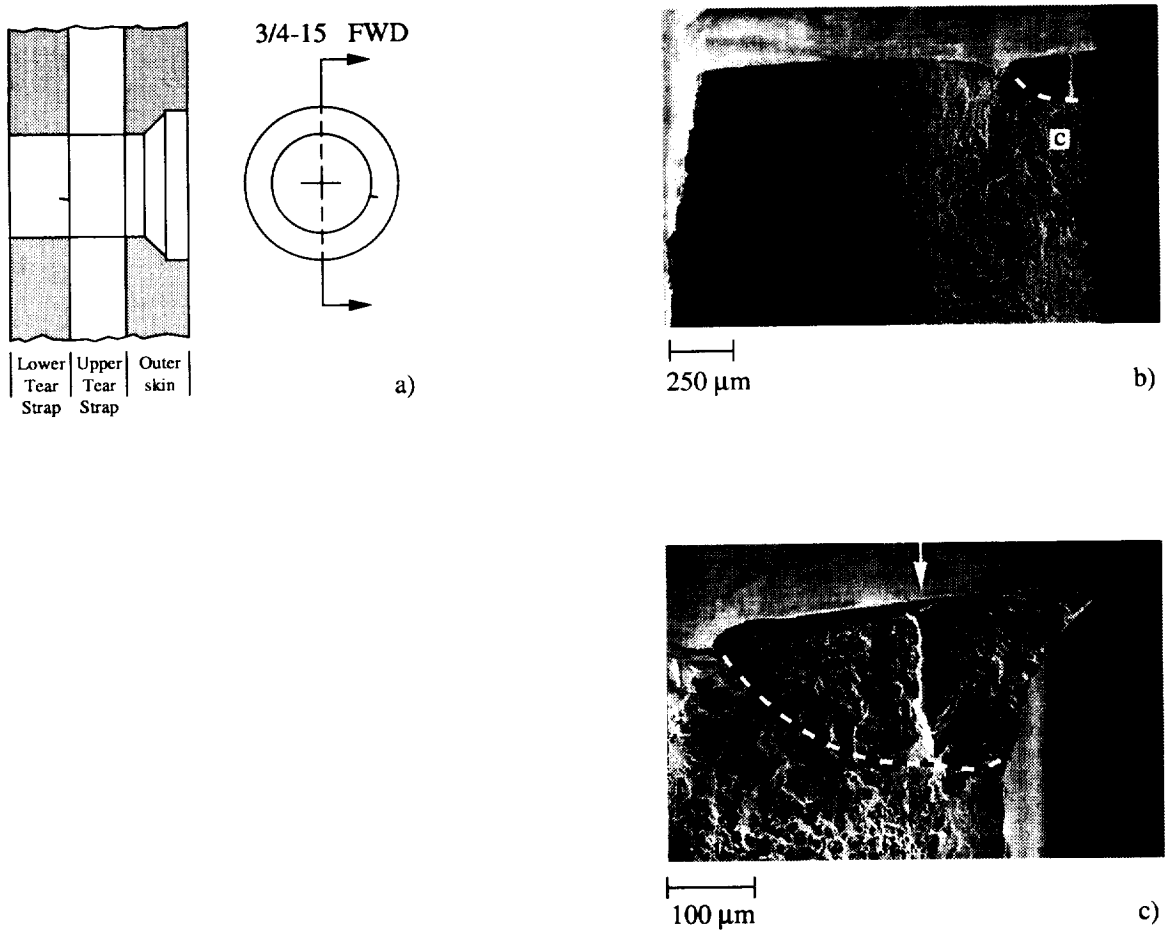

Figure 10.21 a) The schematic shows the rivet hole 3/4-15 configuration and the location of a lower T.S. fatigue crack oriented in the forward direction and about the 3 o'clock position. b) The SEM micrograph shows the fatigue fracture surface of the corner crack located on the outboard corner of the rivet hole. The dashed line marks the fatigue crack front. c) The SEM micrograph shows the fatigue fracture surface of the corner crack (region "c" in Figure 10.21.b). The arrow marks the likely site of crack initiation and the dashed line marks the fatigue crack front.

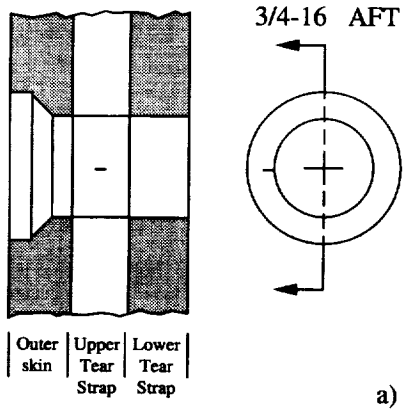

a)

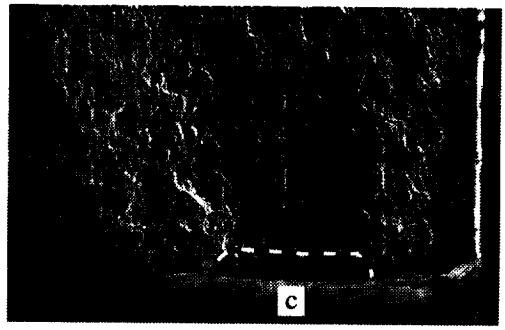

b)

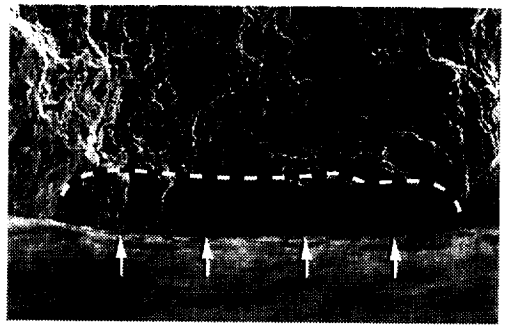

c)

Figure 10.22 a) The schematic shows the rivet hole 3/4-16 configuration and the location of an upper T.S. fatigue crack oriented in the aft direction and about the 9 o'clock position. b) The SEM micrograph shows the fatigue fracture surface of the crack located on the surface of the rivet hole. The dashed line marks the fatigue crack front. c) The SEM micrograph shows the fatigue fracture surface of the rivet hole surface crack, region "c" in Figure 10.22.b. The four arrows mark the likely sites of crack initiation and the dashed line marks the fatigue crack front.

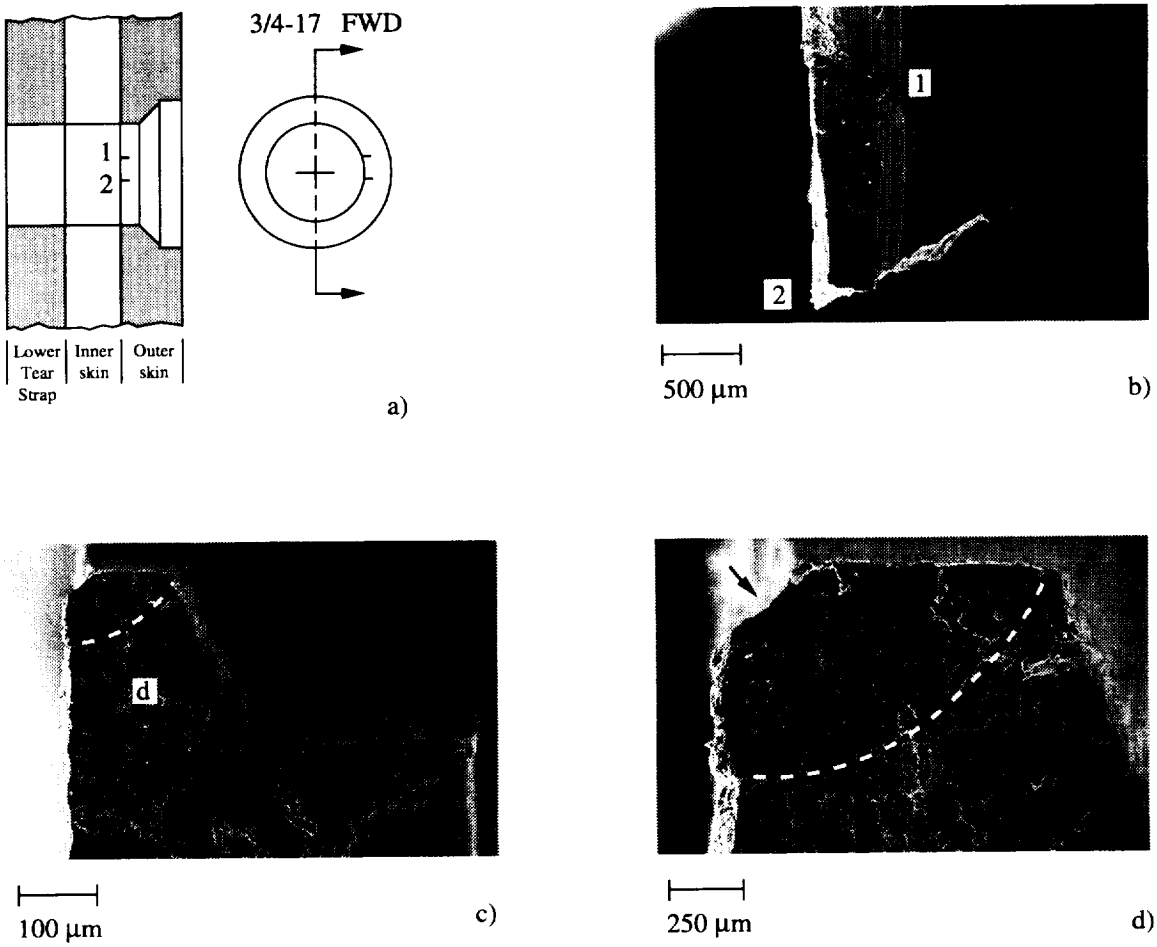

Figure 10.23 a) The schematic shows the rivet hole 3/4-17 configuration and the location of two outer skin fatigue cracks oriented in the forward direction and about the 3 o'clock position. b) The SEM micrograph shows the inside surface of the outer skin rivet hole. Fatigue crack #1 is partially opened along the shank region of the rivet hole and crack #2 is located on the main fracture surface. c) The SEM micrograph shows fatigue crack #2 located in the shank region of the rivet hole. The dashed line marks the fatigue crack front. d) The SEM micrograph shows the fatigue crack #2 located at region "d" in Figure 10.19.c at high magnification. The arrow marks the likely site of crack initiation at the inboard corner of the rivet hole and the dashed line marks the fatigue crack front.

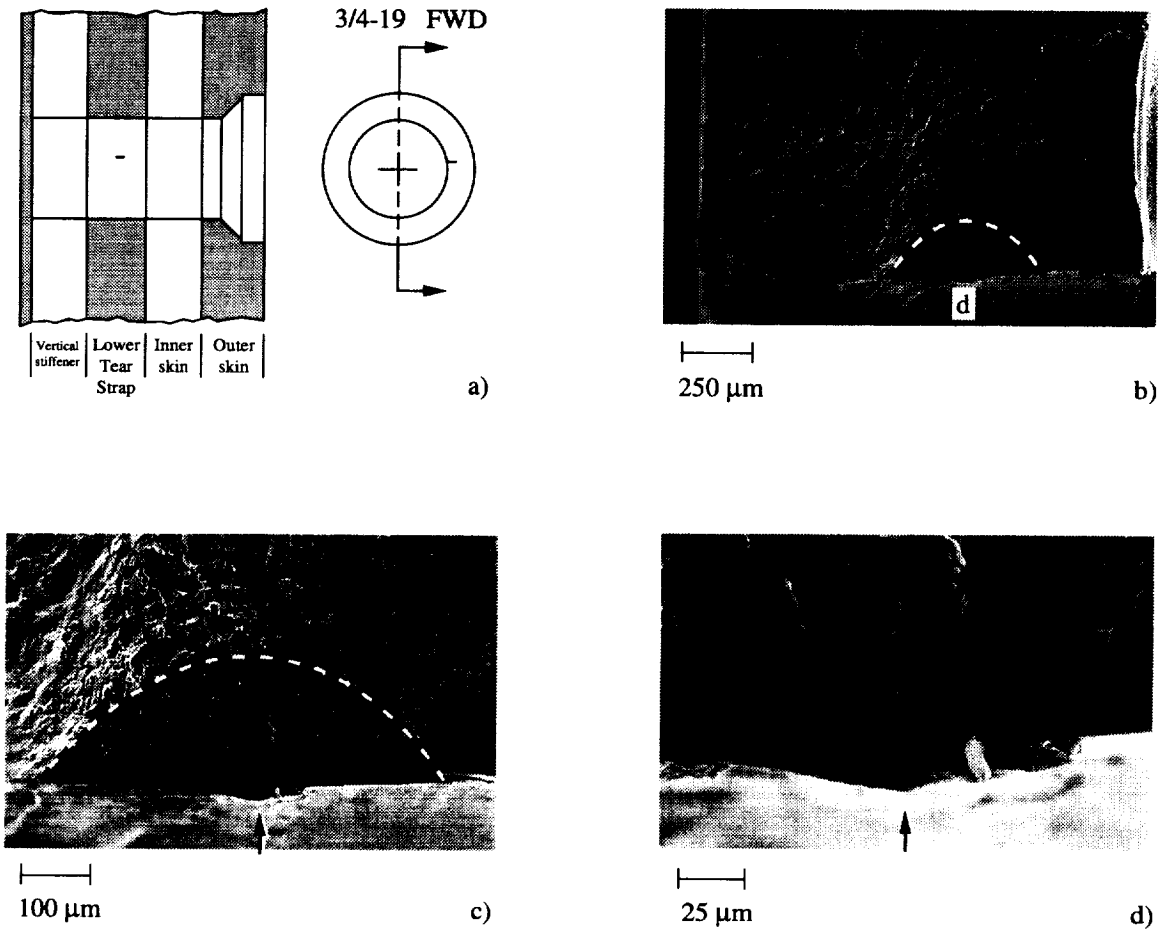

Figure 10.24 a) The schematic shows the rivet hole 3/4-19 configuration and the location of the lower T.S. fatigue crack oriented in the forward direction and above the 3 o'clock position. b) The SEM micrograph shows the fracture surface of the fatigue crack located on the inside surface of the lower T.S. rivet hole. The dashed line marks the fatigue crack front. c) The SEM micrograph shows the surface fatigue crack located at region "d" in Figure 10.34.b. The arrow marks the site of crack initiation and the dashed line marks the fatigue crack front. d) The SEM micrograph shows the crack initiation site (arrow) at high magnification.

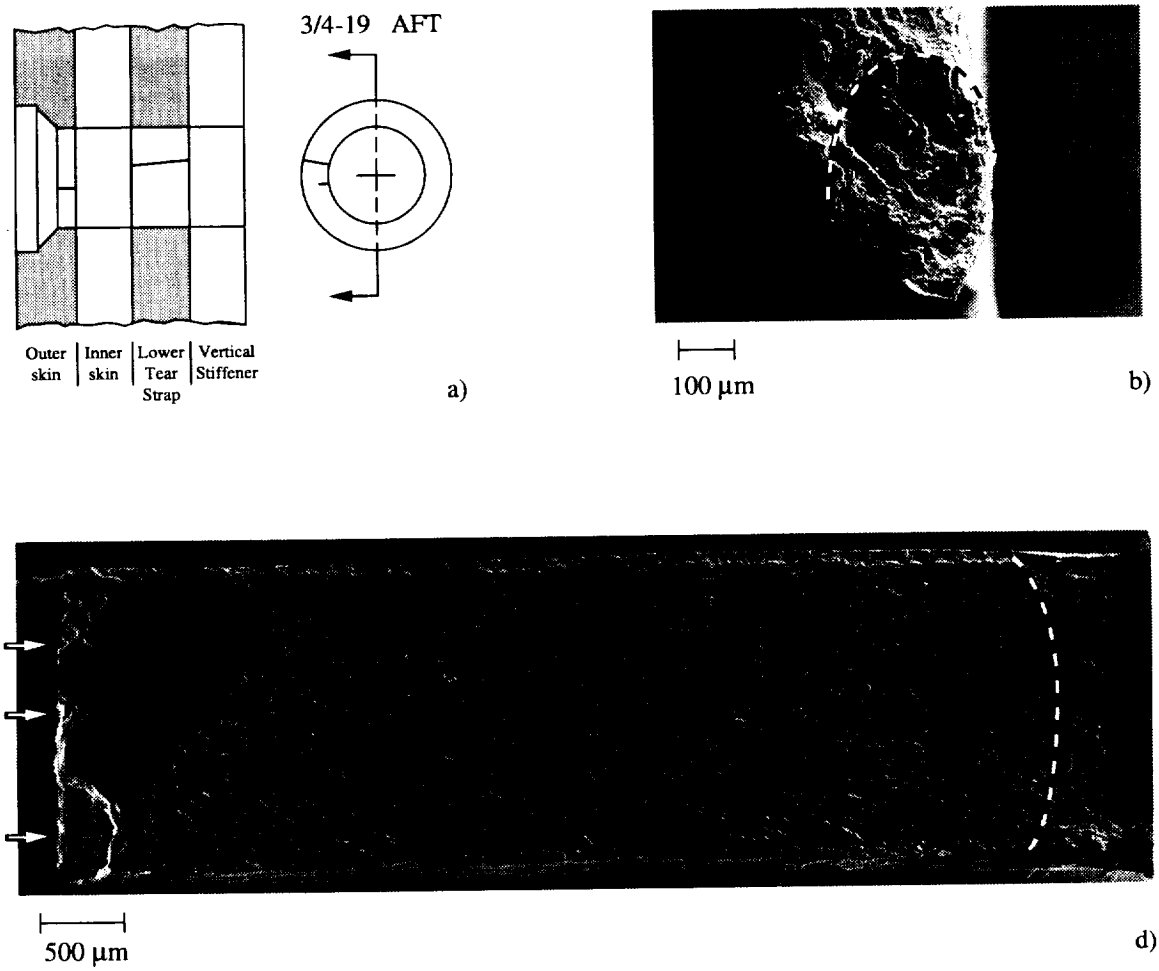

Figure 10.25 a) The schematic shows the rivet hole 3/4-19 configuration and the location of an outer skin fatigue crack and a lower T.S. fatigue crack oriented in the aft direction and about the 3 o'clock position b) The SEM micrograph shows the fracture surface of the fatigue crack located at the shank region of the outer skin rivet hole. The dashed line marks the fatigue crack front. c) The SEM micrograph shows the fracture surface of the lower T.S. fatigue crack. Arrows mark the likely crack initiation sites at the rivet hole surface and the dashed line marks the fatigue crack front.

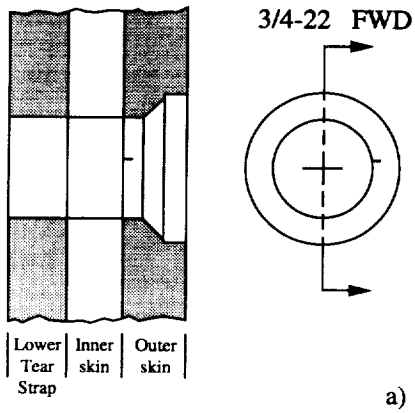

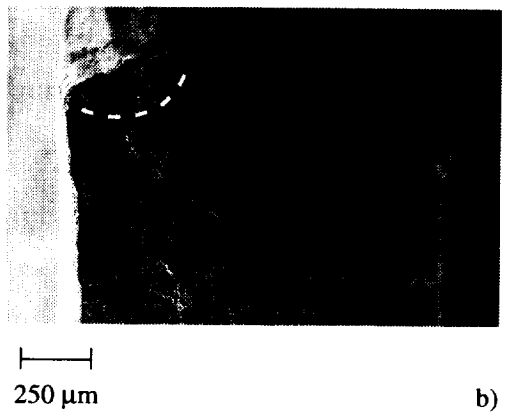

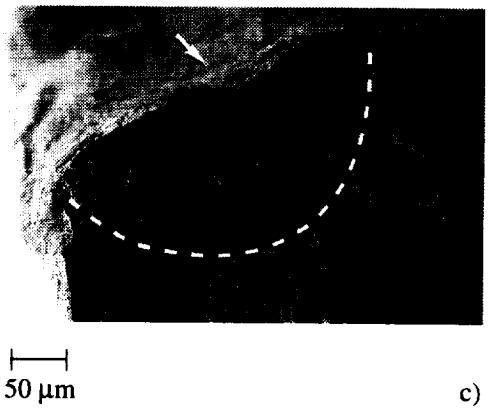

Figure 10.26 a) The schematic shows the rivet hole 3/4-22 configuration and the location of the outer skin fatigue crack oriented in the forward direction and about the 3 o'clock position. b) The SEM micrograph shows the fracture surface of the fatigue crack located at the shank region of the outer skin rivet hole. The dashed line marks the fatigue crack front. c) The SEM micrograph shows the fatigue crack at higher magnification. The arrow marks the likely site of crack initiation and the dashed line marks the fatigue crack front.

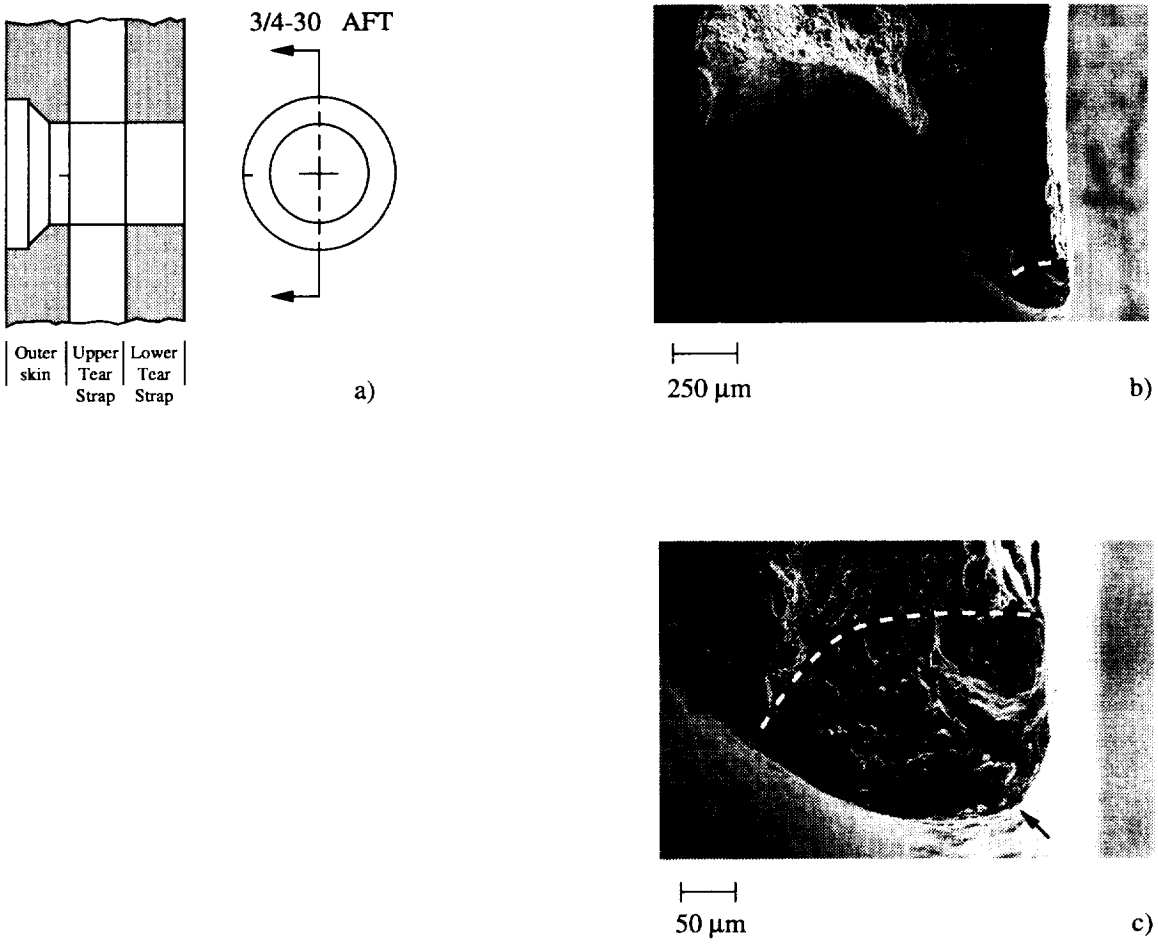

Figure 10.27 a) The schematic shows the rivet hole 3/4-30 configuration and the location of the outer skin fatigue crack oriented in the aft direction and about the 9 o'clock position. b) The SEM micrograph shows the fracture surface of the fatigue crack located at the shank region of the outer skin rivet hole. The dashed line marks the fatigue crack front. c) The SEM micrograph shows the fatigue crack at higher magnification. The arrow marks the likely site of crack initiation and the dashed line marks the fatigue crack front.

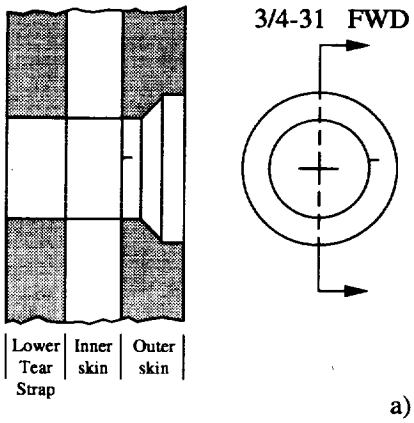

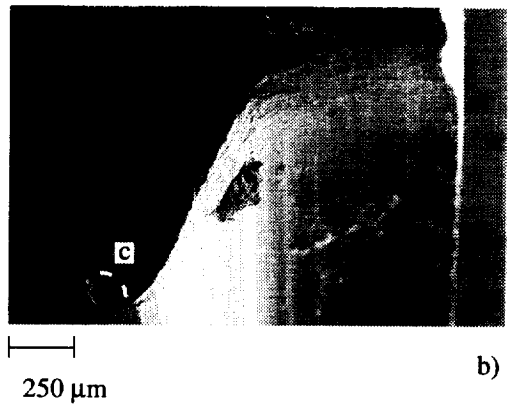

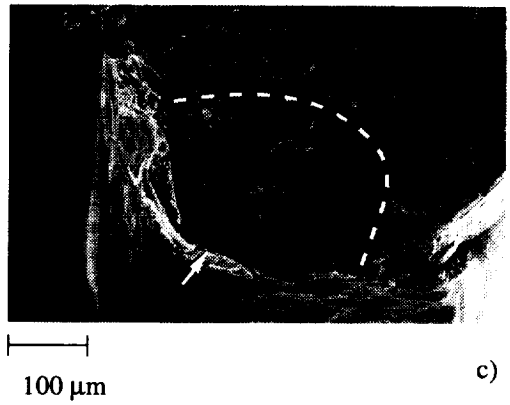

Figure 10.28 a) The schematic shows the rivet hole 3/4-31 configuration and the location of the outer skin fatigue crack oriented in the forward direction and about the 3 o'clock position. b) The SEM micrograph shows the fracture surface of the fatigue crack located at the shank region of the outer skin rivet hole. The dashed line marks the fatigue crack front. c) The SEM micrograph shows the fatigue crack at region "c" in Figure 10.28.b at higher magnification. The arrow marks the likely site of crack initiation and the dashed line marks the fatigue crack front.

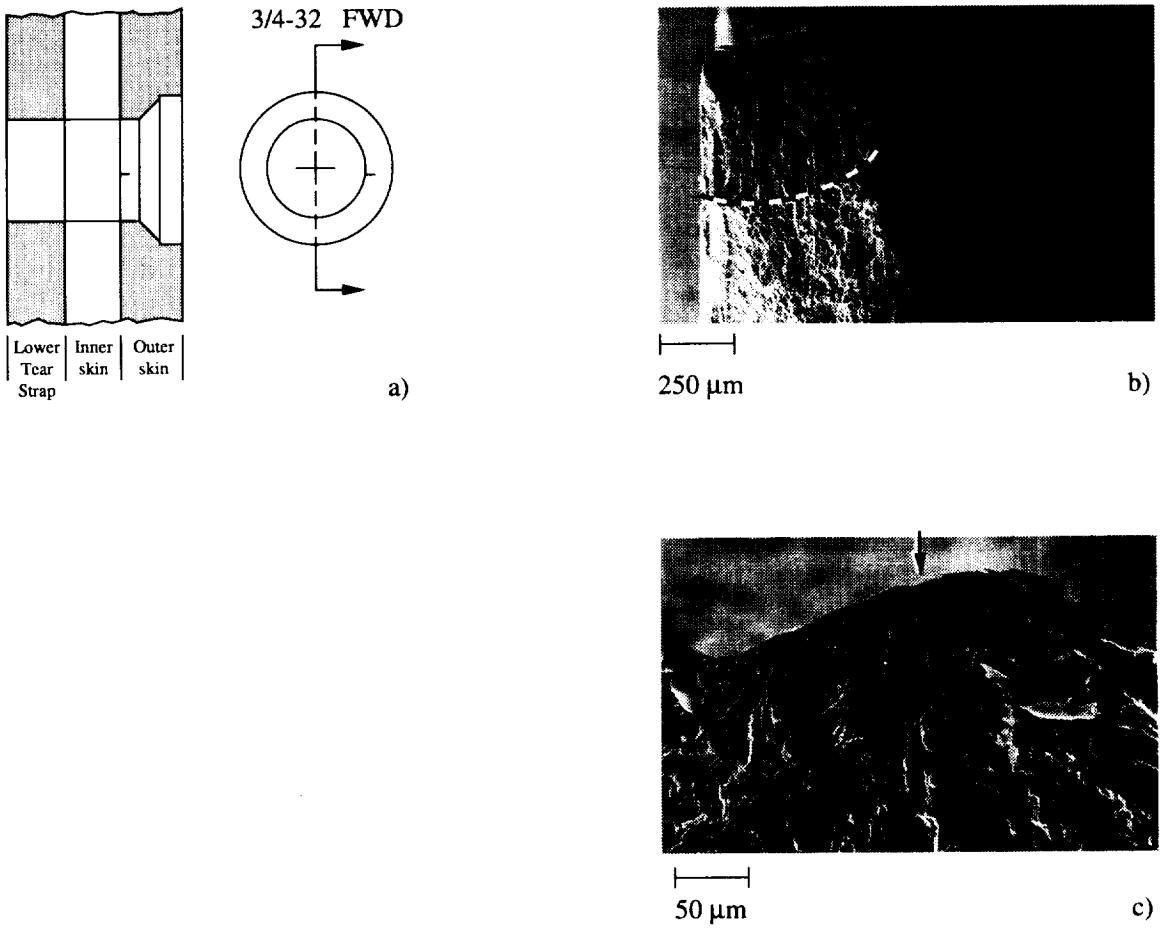

Figure 10.29 a) The schematic shows the rivet hole 3/4-32 configuration and the location of the outer skin fatigue crack oriented in the forward direction and about the 3 o'clock position. b) The SEM micrograph shows the fracture surface of the fatigue crack located at the shank region of the outer skin rivet hole. The dashed line marks the fatigue crack front. c) The SEM micrograph shows the fatigue crack at higher magnification. The arrow marks the likely site of crack initiation.

11. Destructive Examination of Bay 4

For rivet holes shown in Figure 11.1, a total of sixty-five rivet hole locations in bay 4, were destructively examined. All fifteen rivet holes in the upper row J contained fatigue cracks; a total of 29 fatigue cracks were found. Crack link-up was observed between two rivet holes located near the center of row J. The remaining rivet rows contained twelve fatigue cracks: six cracks in row I, two in row H, and four in the bottom row G. Figures 11.2 and 11.3 show the location of all fatigue cracks found in the first layer (outer skin) and the second layer (inner skin), respectively. Rivet rows J and I contained outer skin cracks, row H contained both inner and outer skin cracks, and row G contained only inner skin cracks. The through-thickness crack schematics shown in Figures 11.4, 11.5, 11.6, 11.7, and 11.8 summarize crack location, crack length, crack type and initiation site for rivet rows J, I, H, and G, respectively. The following is a detailed description of the fatigue damage in bay 4 tear strap region.

11.1 Fatigue Cracks Contained in Row J:

Figures 11.9 through 11.37 describe the fatigue crack morphology in row J.

11.2 Fatigue Cracks Contained in Row I:

Figures 11.38 through 11.43 describe the fatigue crack morphology in row I.

11.3 Fatigue Cracks Contained in Row H:

Figures 11.44 through 11.45 describe the fatigue crack morphology in row H.

11.4 Fatigue Cracks Contained in Row G:

Figures 11.46 through 11.48 describe the fatigue crack morphology in row G.

11.5 Bay #4 Summary:

Table 10.1 summarizes the destructive examination results for bay 4 rivet rows G, H, I, and J. Row J was found to contain twenty-nine fatigue cracks. Bay 4 cracks, range in length from 0.039 mm (0.002 in.) to 12.964 mm (0.510) in. Rivet rows J and I contained outer skin cracks and rows H and G contained both outer and inner skin cracking. The following observations were made as a result of fractographic examinations of bay 4.

11.5.1 Crack initiation site(s):

Row J: Fatigue cracks initiated along the outer/inner skin faying surface and the inboard corner of the rivet hole. The faying surface exhibited black oxide and disturbed metal suggesting fretting contact at the point of crack initiation.

Row I: Most outer skin fatigue cracks initiated at the inboard corner rivet hole shank region and along the faying surface. Cracks initiated at deformed regions and regions having disturbed surfaces.

Row H and G: Fatigue cracks initiated at outboard corners of inner skin rivet holes. Areas of disturbed metal were observed at the point of crack initiation. A few outer skin fatigue cracks were noted at the rivet hole faying surface, similar to those found in row J.

11.5.2 Crack front shape as a function of crack length:

Row J: A distinct pattern in crack front shape was observed. Cracks initiated at the faying surface and grew subsurface to the outboard surface. The subsurface fatigue cracks formed a thin ligament along the outboard surface of the outer skin. The fatigue cracks propagated along the faying surface a distance of 2 to 3 skin thicknesses before becoming through-thickness cracks.

Rows I, H, and G: In general, fatigue cracks were small and no data on crack shape was obtained.

11.5.3 Fatigue crack/stable tearing transition crack length:

Rows J, I, H, and G: All cracks exhibited a transgranular morphology characteristic of fatigue cracks.

11.5.4 Slant fracture morphology:

Row J, I, H, and G: No slant fracture morphology was observed.

11.5.5 Evidence of corrosion:

Row J, I, H, and G: No corrosion was observed.

Table 11-1 Bay #4 Fatigue Crack Summary

Rivet Row	No. of Cracks (Holes)	Location	Crack Length mm (in)	Comment
J	25(14)	Outer Skin	0.769(0.030)≤a	Fretting
	4(3)		≤12.954(0.510)	High K_T
I	4(3)	Outer Skin	0.039(0.002)≤a	High K_T
	2(1)		≤0.284(0.011)	Fretting
H	1(1)	Outer Skin	a=0.102(0.004)	High K_T
	1(1)	Inner Skin	a=0.237(0.009)	High K_T
G	2(2)	Inner Skin	0.121(0.005)≤a	Fretting
	2(2)		≤0.313(0.012)	High K_T

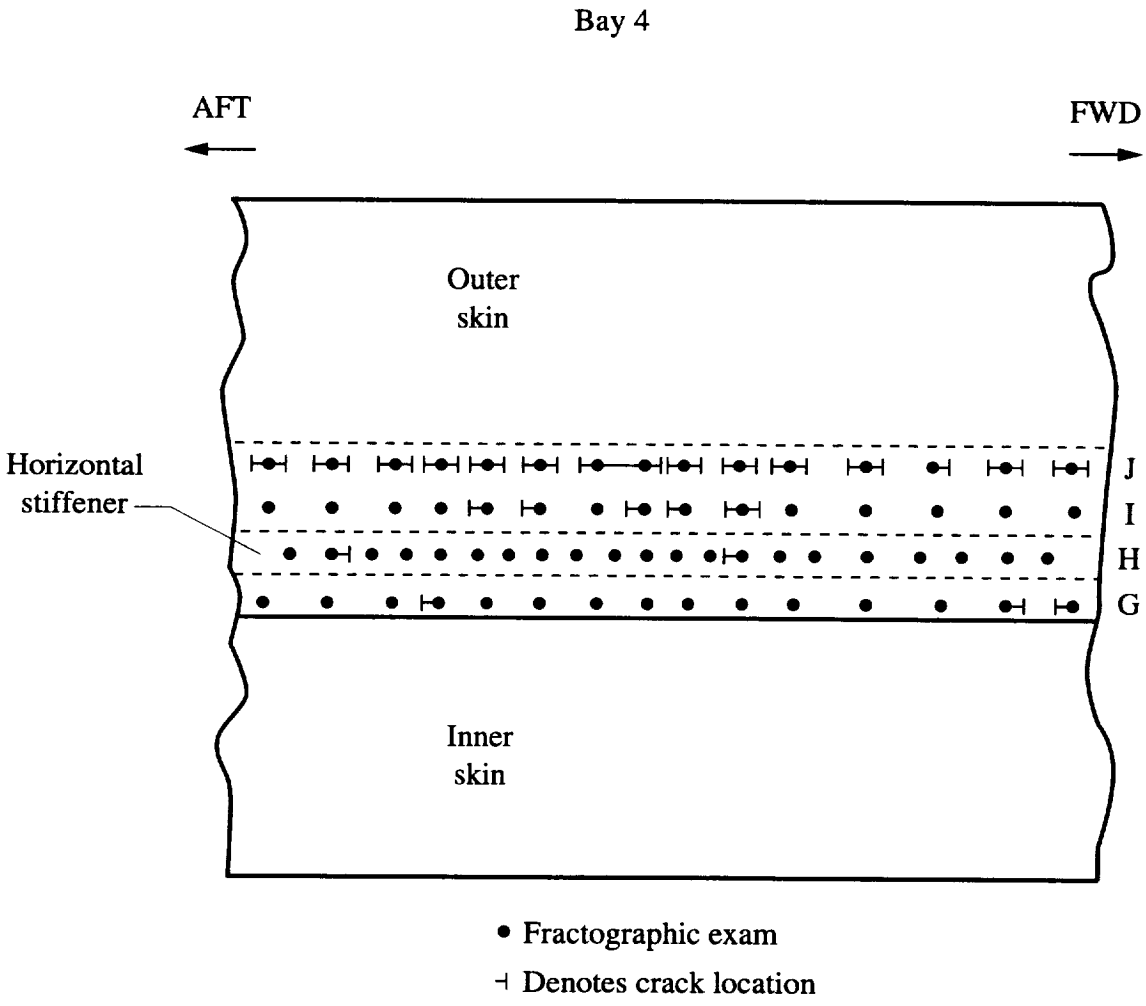

Figure 11.1 The schematic shows the location of all fatigue cracks found in the bay 4 lap splice joint by destructive examination. All bay 4 rivet holes were examined.

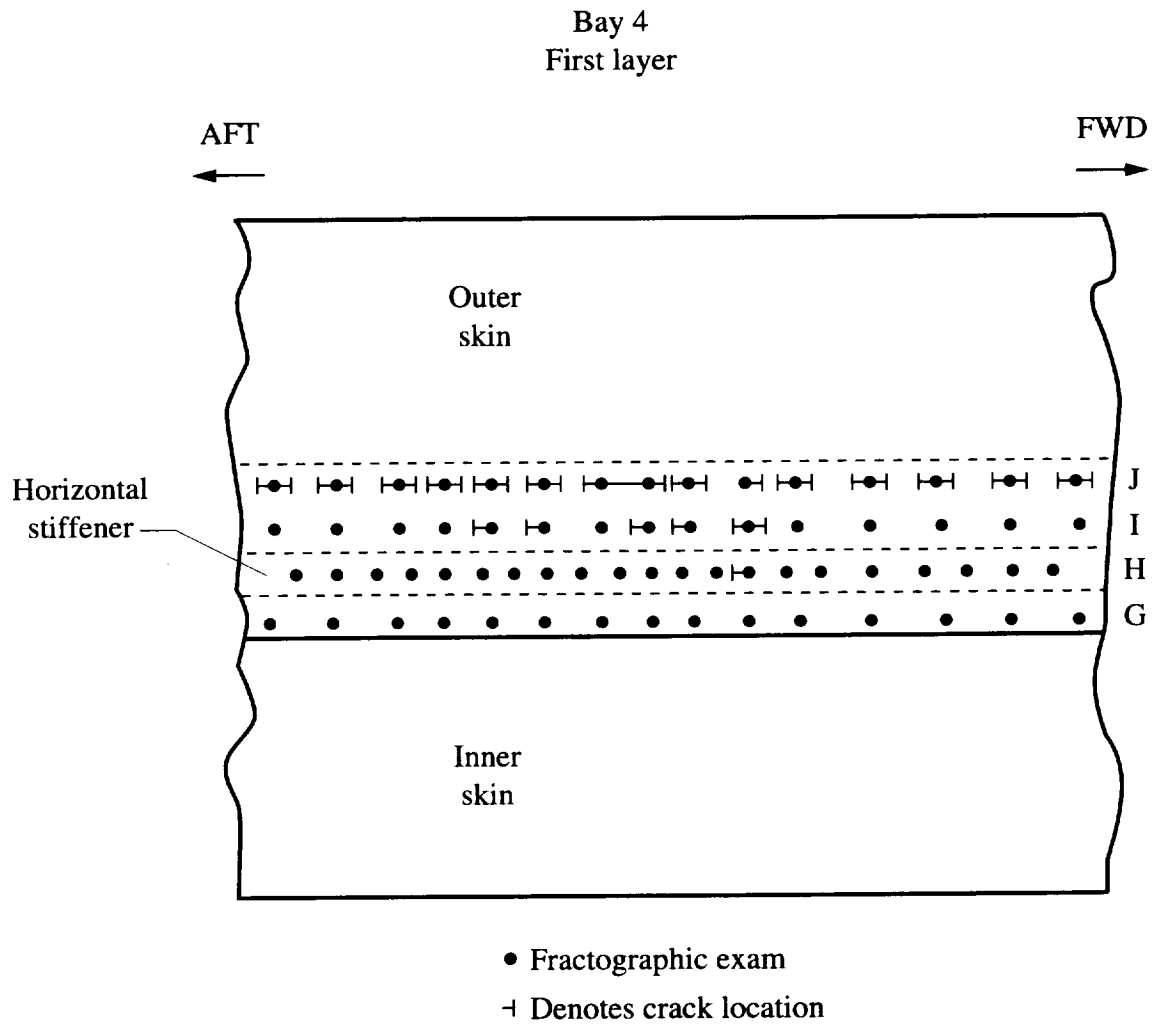

Figure 11.2 The schematic shows the location of fatigue cracks found in the first layer (outer skin) of the bay 4 lap splice joint by destructive examination.

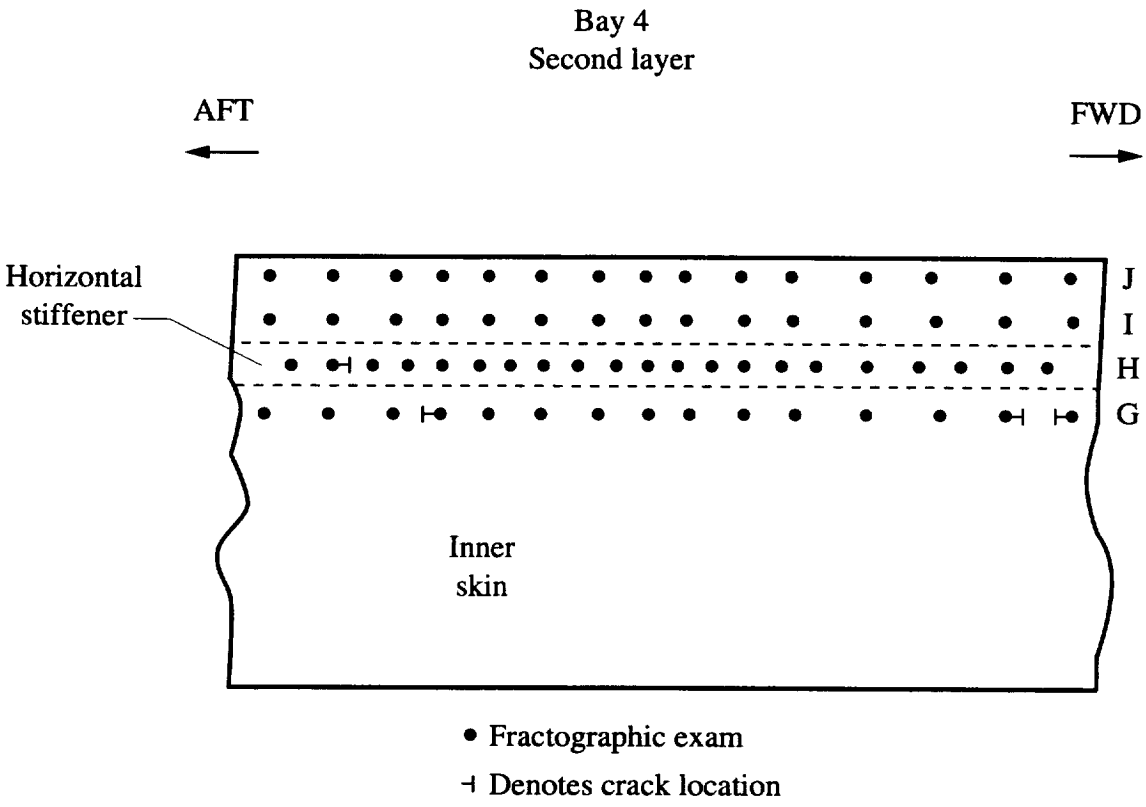

Figure 11.3 The schematic shows the location of fatigue cracks found in the second layer (inner skin) of the bay 4 lap splice joint by destructive examination.

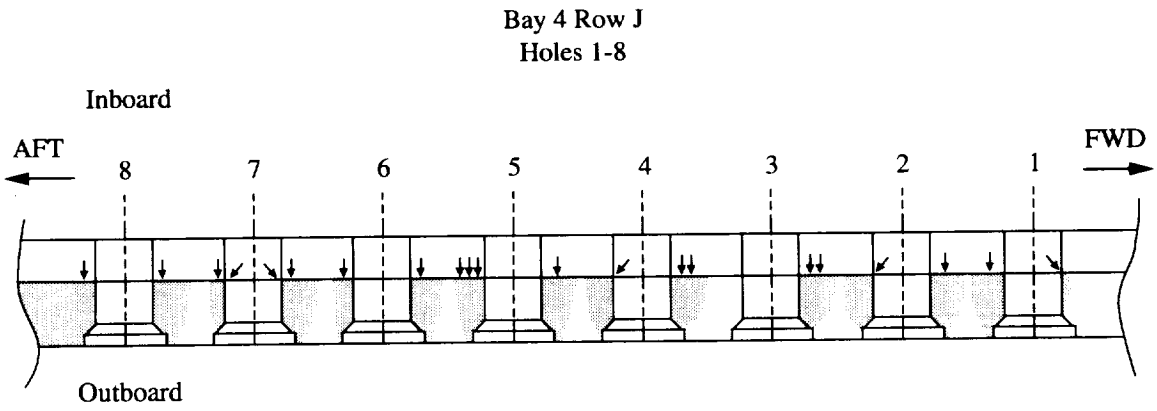

Hole #	Location	Length mm(in)	Type	Initiation site
1 (Aft)	Outer skin	2.893 (0.114)	Fretting	Inner skin/Outer skin
1 (Fwd)	Outer skin	0.769 (0.030)	Fretting	IS/OS
2 (Aft)	Outer skin	0.905 (0.036)	Fretting	IS/OS
2 (Fwd)	Outer skin	2.814 (0.111)	Fretting	IS/OS
3 (Fwd)	Outer skin	2.427 (0.096)	Fretting	IS/OS multiple
4 (Aft)	Outer skin	2.497 (0.098)	Fretting	IS/OS
4 (Fwd)	Outer skin	2.700 (0.106)	Fretting	IS/OS
5 (Aft)	Outer skin	5.334 (0.210)	Fretting	IS/OS multiple
5 (Fwd)	Outer skin	5.279 (0.207)	Fretting	IS/OS
6 (Aft)	Outer skin	2.714 (0.107)	Fretting	IS/OS
6 (Fwd)	Outer skin	3.848 (0.152)	Fretting	IS/OS
7 (Aft)	Outer skin	1.113 (0.044)	Fretting	IS/OS, inboard corner
7 (Fwd)	Outer skin	3.310 (0.130)	Fretting	IS/OS, inboard corner
8 (Aft)	Outer skin	Linkup with 4J9 (Fwd)	Fretting	IS/OS
8 (Fwd)	Outer skin	12.954 (0.510)	Fretting	IS/OS

Figure11.4 The through thickness schematic shows the location and initiation site of fatigue cracks found in rivet row J (holes 1-8) from bay 4. The table summarizes crack location, crack length, crack type, and initiation site for each fatigue crack shown.

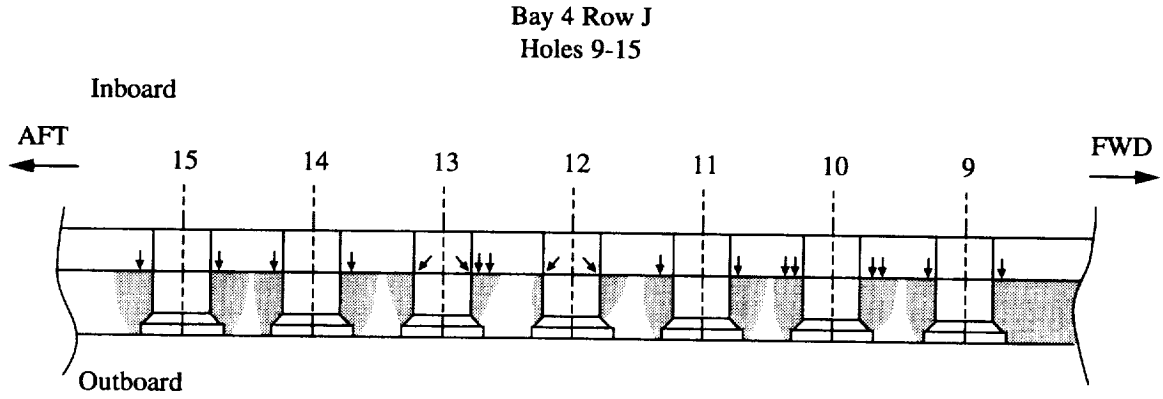

Hole #	Location	Length mm(in)	Type	Initiation site
9 (Aft)	Outer skin	8.265 (0.325)	Fretting	Inner skin/Outer skin
9 (Fwd)	Outer skin	Linkup with 4J8(Aft)	Fretting	IS/OS
10 (Aft)	Outer skin	4.194 (0.165)	Fretting	IS/OS multiple
10 (Fwd)	Outer skin	3.042 (0.120)	Fretting	IS/OS multiple
11 (Aft)	Outer skin	5.397 (0.212)	Fretting	IS/OS
11 (Fwd)	Outer skin	5.675 (0.223)	Fretting	IS/OS
12 (Aft)	Outer skin	1.874 (0.074)	Countersink	Inboard corner of shank
12 (Fwd)	Outer skin	2.460 (0.097)	Countersink	Inboard corner of shank
13 (Aft)	Outer skin	1.835 (0.072)	Countersink	Inboard corner of shank
13 (Fwd)	Outer skin	1.102 (0.043)	Fretting	IC,IS/OS multiple
14 (Aft)	Outer skin	2.995 (0.118)	Fretting	IS/OS multiple
14 (Fwd)	Outer skin	2.810 (0.111)	Fretting	IS/OS
15 (Aft)	Outer skin	8.559 (0.337)	Fretting	IS/OS
15 (Fwd)	Outer skin	6.959 (0.274)	Fretting	IS/OS

Figure 11.5 The through thickness schematic shows the location and initiation site of fatigue cracks found in rivet row J (holes 9-15) from bay 4. The table summarizes crack location, crack length, crack type, and initiation site for each fatigue crack shown.

Bay 4 Row I

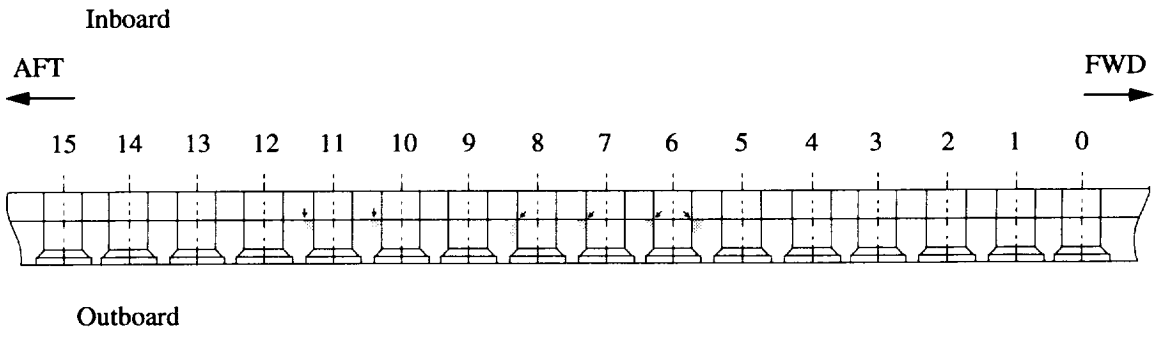

Hole #	Location	Length mm(in)	Type	Initiation site
6(Aft)	Outer skin	0.116 (0.005)	Countersink	Inboard corner of shank
6(Fwd)	Outer skin	0.285 (0.011)	Countersink	Inboard corner of shank
7(Aft)	Outer skin	0.105 (0.004)	Countersink	Inboard corner of shank
8(Aft)	Outer skin	0.199 (0.008)	Countersink	Inboard corner of shank
10(Aft)	Outer skin	0.089 (0.003)	Fretting	IS/OS
11(Aft)	Outer skin	0.039 (0.002)	Fretting	IS/OS

Figure 11.6 The through thickness schematic shows the location and initiation site of fatigue cracks found in rivet row I from bay 4. The table summarizes crack location, crack length, crack type, and initiation site for each fatigue crack shown.

Bay 4 Row H

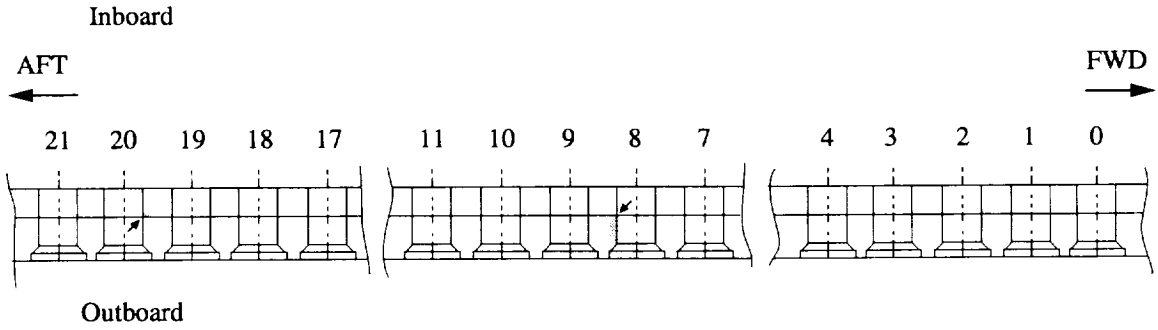

Hole #	Location	Length mm(in)	Type	Initiation site
8(Aft)	Outer skin	0.102 (0.004)	Countersink	Inboard corner of shank
20(Fwd)	Inner skin	0.237 (0.009)	Corner	Outboard corner

Figure 11.7 The through thickness schematic shows the location and initiation site of fatigue cracks found in rivet row H from bay 4. The table summarizes crack location, crack length, crack type, and initiation site for each fatigue crack shown.

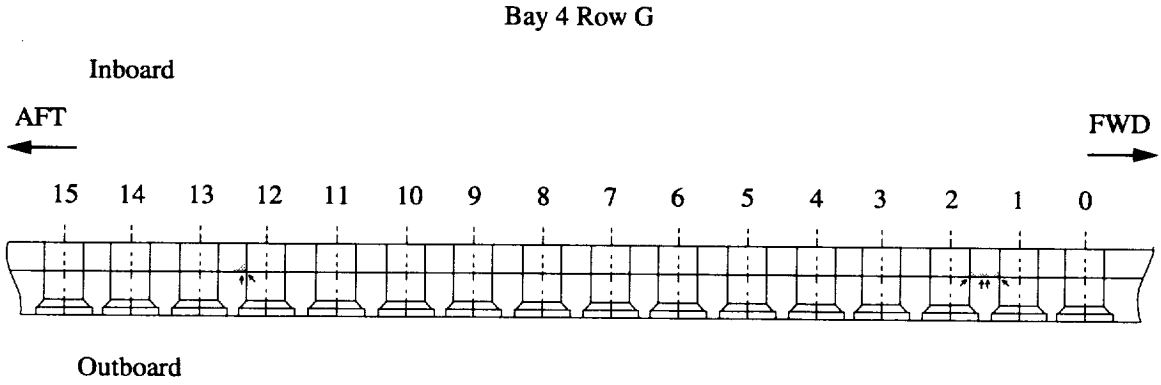

Hole #	Location	Length mm(in)	Type	Initiation site
1(Aft)	Inner skin	0.121 (0.005)	Corner	Outboard corner
2(Fwd)	Inner skin	0.131 (0.005)	Fretting and Corner	IS/OS,Outboard corner
2(Fwd)	Inner skin	0.180 (0.007)	Fretting	Innerskin/outerskin
12(Aft)	Inner skin	0.313 (0.012)	Fretting and Corner	IS/OS,Outboard corner

Figure 11.8 The through thickness schematic shows the location and initiation site of fatigue cracks found in rivet row G from bay 4. The table summarizes crack location, crack length, crack type, and initiation site for each fatigue crack shown.

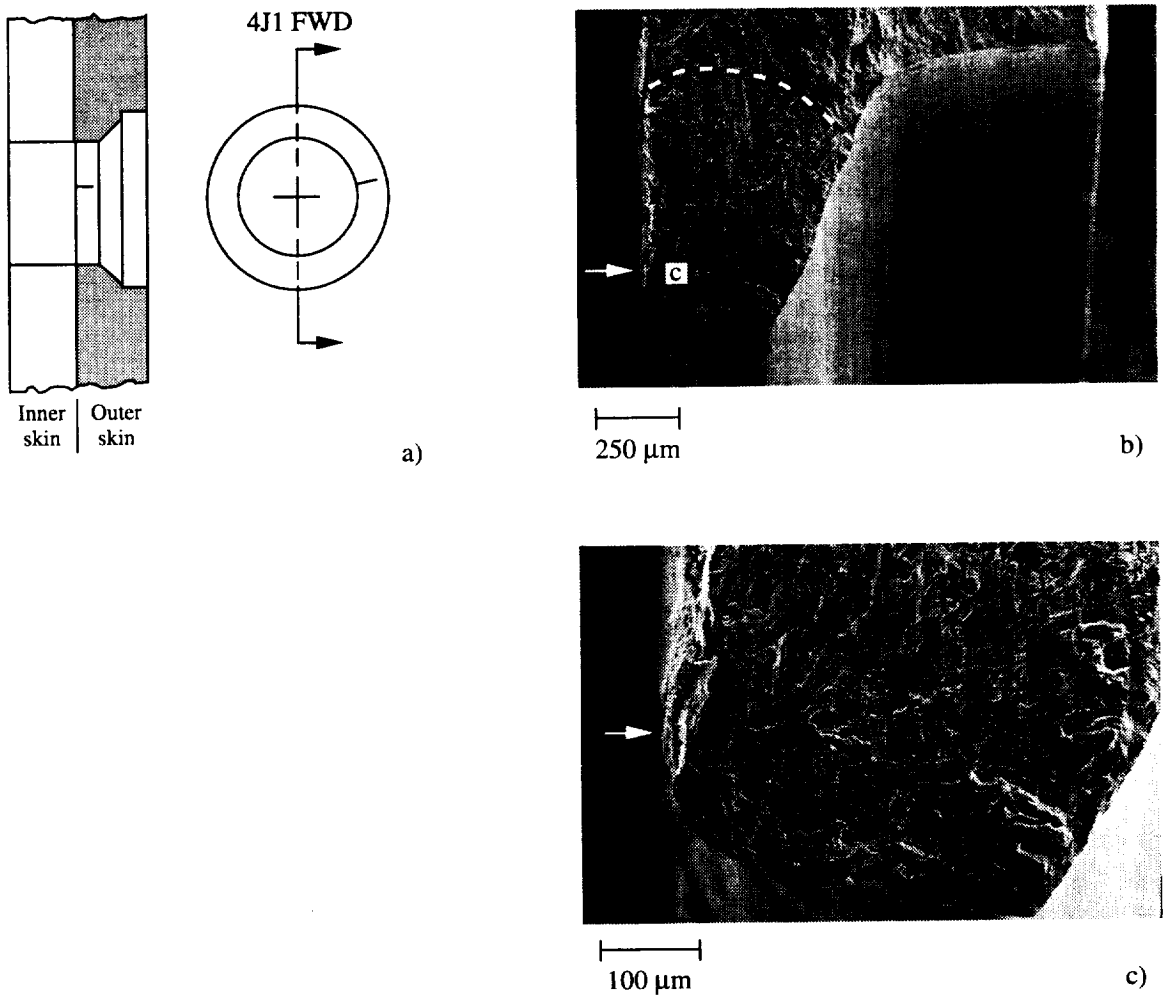

Figure 11.9 a) The schematic shows the rivet hole 4J1 configuration and the location of the outer skin fatigue crack oriented in the forward direction and above the 3 o'clock position. b) The SEM micrograph shows the fatigue crack fracture surface located at the rivet hole shank region. The arrow marks the likely crack initiation region along the faying surface and the dashed line marks the fatigue crack front. c) The SEM micrograph shows the fatigue crack fracture surface at region "c" in Figure 11.9.b. The arrow marks the likely crack initiation region along the faying surface.

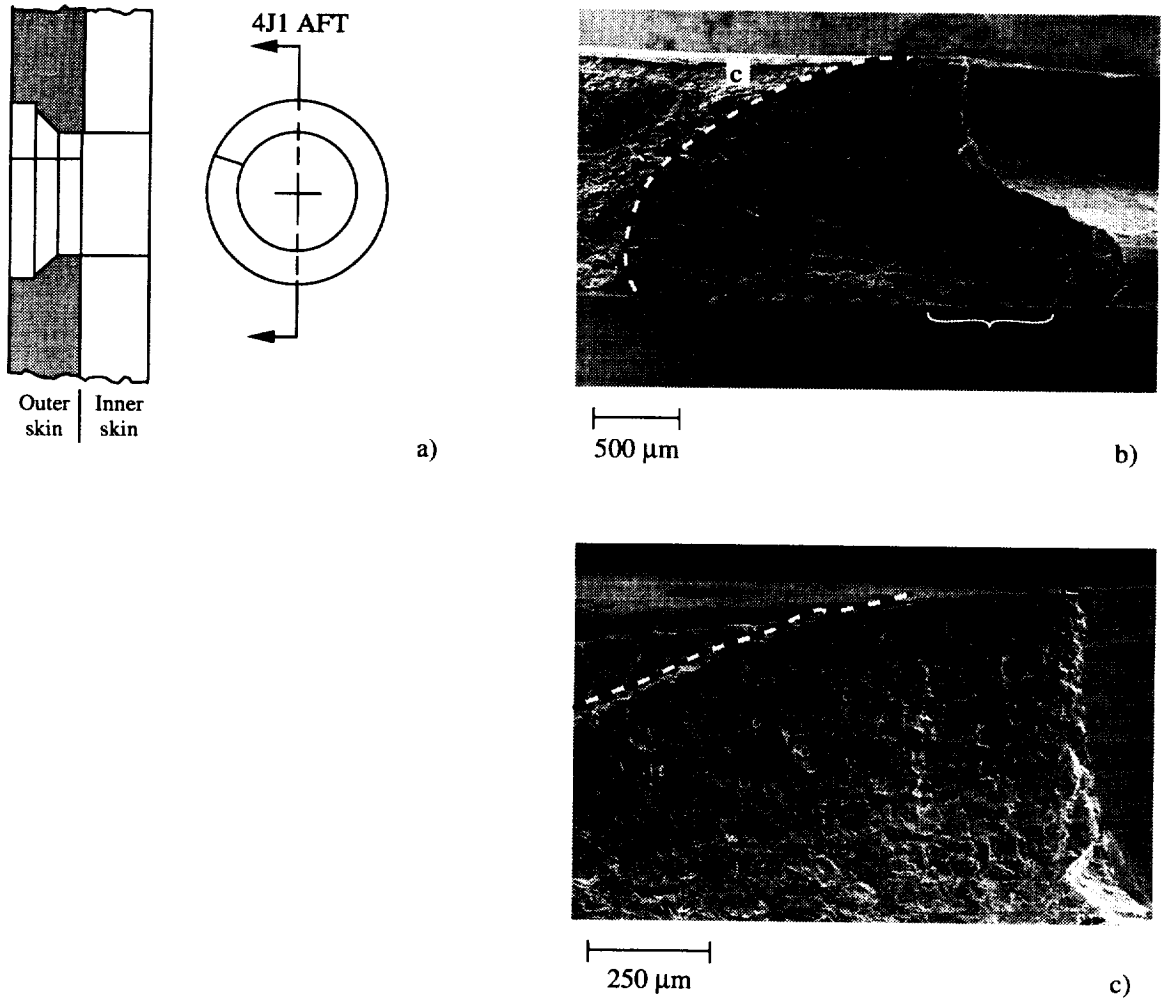

Figure 11.10 a) The schematic shows the rivet hole 4J1 configuration and the location of the outer skin fatigue crack oriented in the aft direction and about the 10 o'clock position. b) The SEM micrograph shows the fatigue crack fracture surface located at the outer skin rivet hole (right). The dashed line marks the fatigue crack front. The bracket marks the region of crack initiation. c) The SEM micrograph shows the fatigue crack front, region "c" in Figure 11.10.b. The dashed line marks the fatigue crack front as it intersects the outboard surface of the outer skin.

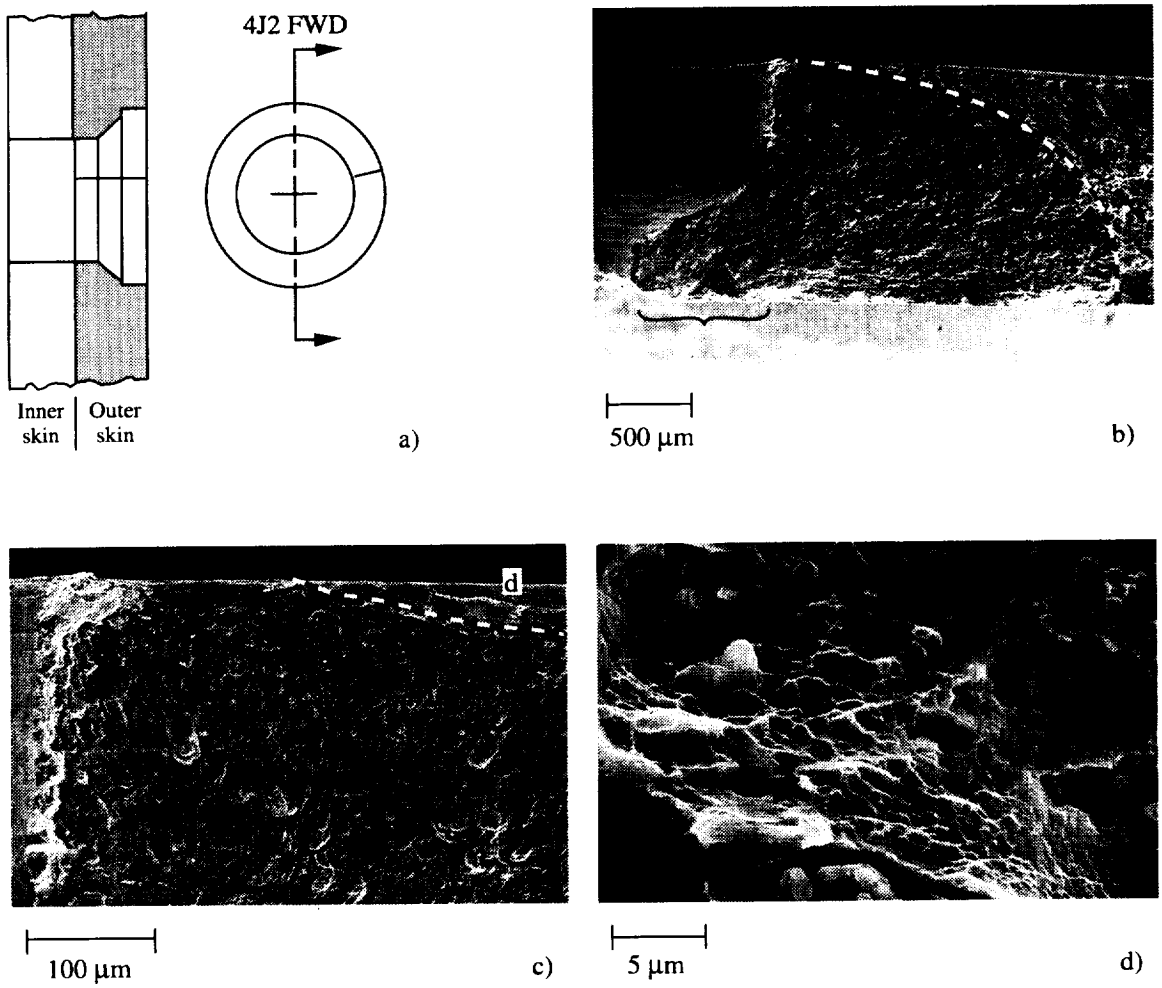

Figure 11.11 a) The schematic shows the rivet hole 4J2 configuration and the location of the outer skin fatigue crack oriented in the forward direction and above the 3 o'clock position. b) The SEM micrograph shows the fatigue crack fracture surface located at the outer skin rivet hole (left). The bracket marks the likely region of crack initiation and the dashed line marks the fatigue crack front. c) The SEM micrograph shows the fatigue crack front region (dashed line) as it intersects the outboard surface of the outer skin. The rivet hole is located to the left. d) The SEM micrograph shows the ductile morphology of the over load fracture surface at region "d" in Figure 11.11c at high magnification.

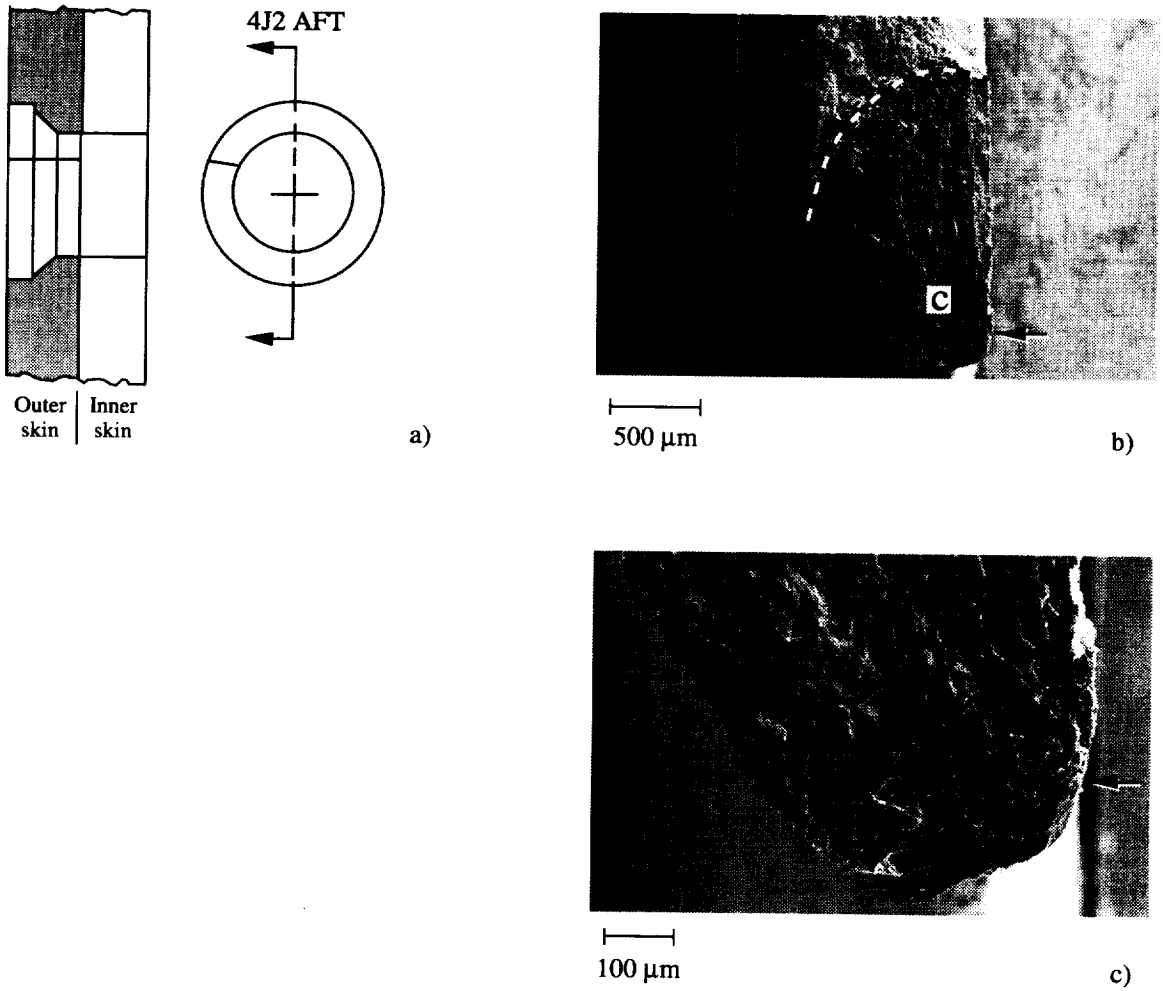

Figure 11.12 a) The schematic shows the rivet hole 4J2 configuration and the location of the outer skin fatigue crack oriented in the aft direction and about the 10 o'clock position. b) The SEM micrograph shows the fatigue crack fracture surface located at the outer skin rivet hole (bottom). The arrow marks the likely crack initiation site and the dashed line marks the fatigue crack front. c) The SEM micrograph shows the fatigue crack front region "c" in Figure 11.12.b. The arrow marks the region of crack initiation.

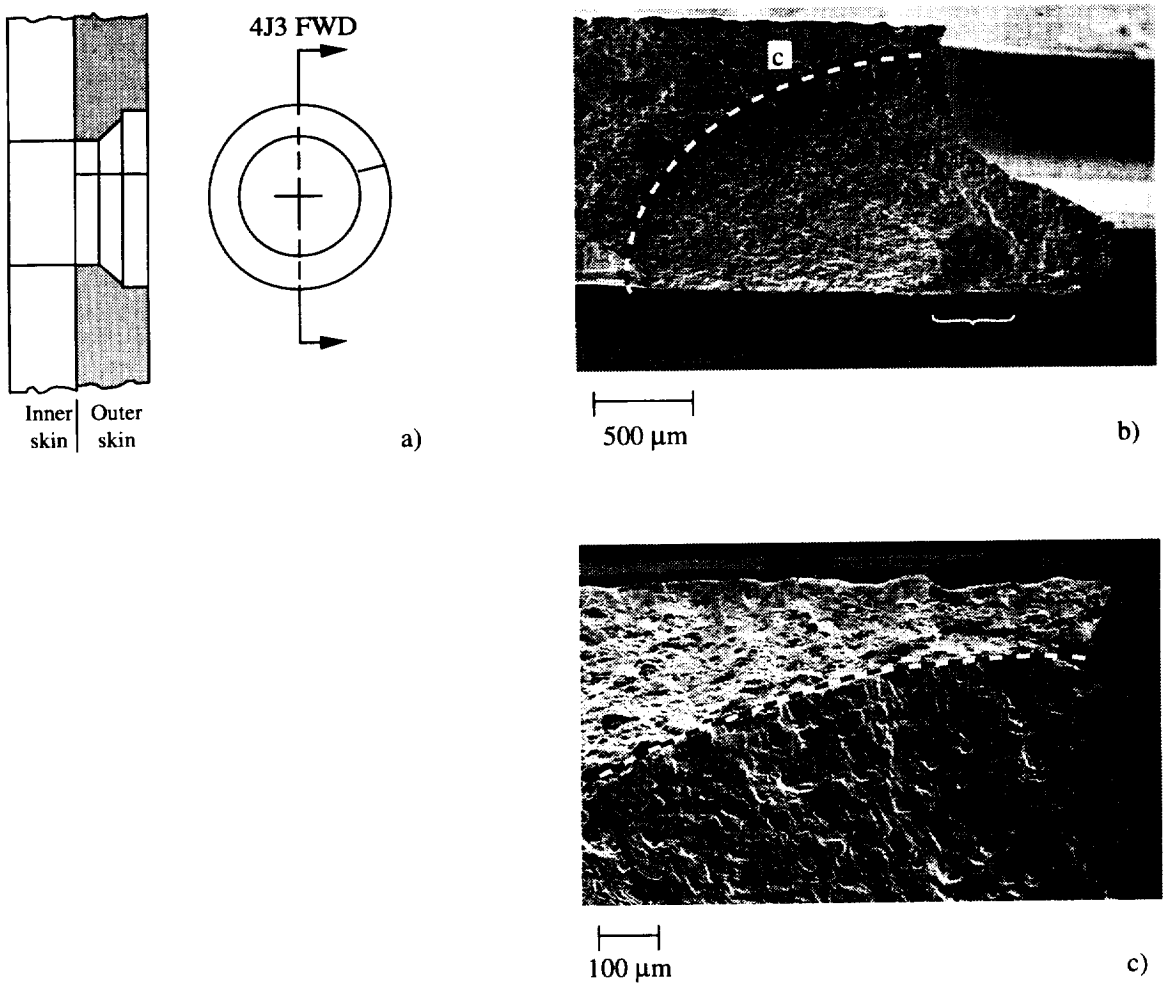

Figure 11.13 a) The schematic shows the rivet hole 4J3 configuration and the location of the outer skin fatigue crack oriented in the forward direction and about the 2 o'clock position. b) The SEM micrograph shows the fatigue crack fracture surface located at the outer skin rivet hole (right). The dashed line marks the fatigue crack front and the bracket marks the region of crack initiation. c) The SEM micrograph shows the fatigue crack front and the ligament, region "c", in Figure 11.13.b. The dashed line marks the fatigue crack front where it intersects the rivet hole (right). The outboard surface of the outer skin is located at the top of the micrograph.

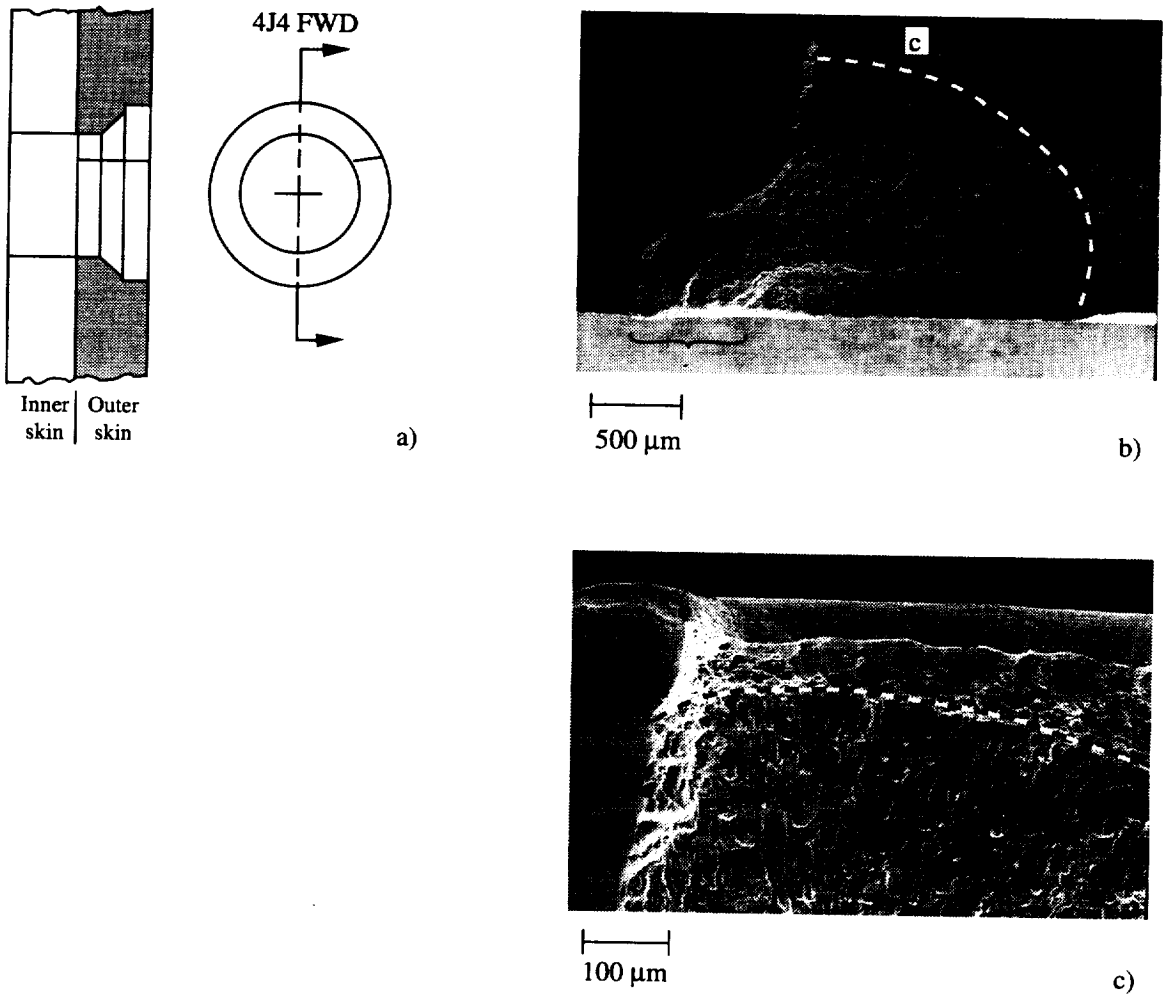

Figure 11.14 a) The schematic shows the rivet hole 4J4 configuration and the location of the outer skin fatigue crack oriented in the forward direction and about the 2 o'clock position. b) The SEM micrograph shows the fatigue crack fracture surface located at the outer skin rivet hole (left). The bracket shows the region of crack initiation and the dashed line marks the fatigue crack front. c) The SEM micrograph shows the fatigue crack front region "c" in Figure 11.14.b. The dashed line marks the fatigue crack front where it intersects the rivet hole (left). The outboard surface of the outer skin is located at the top of the micrograph.

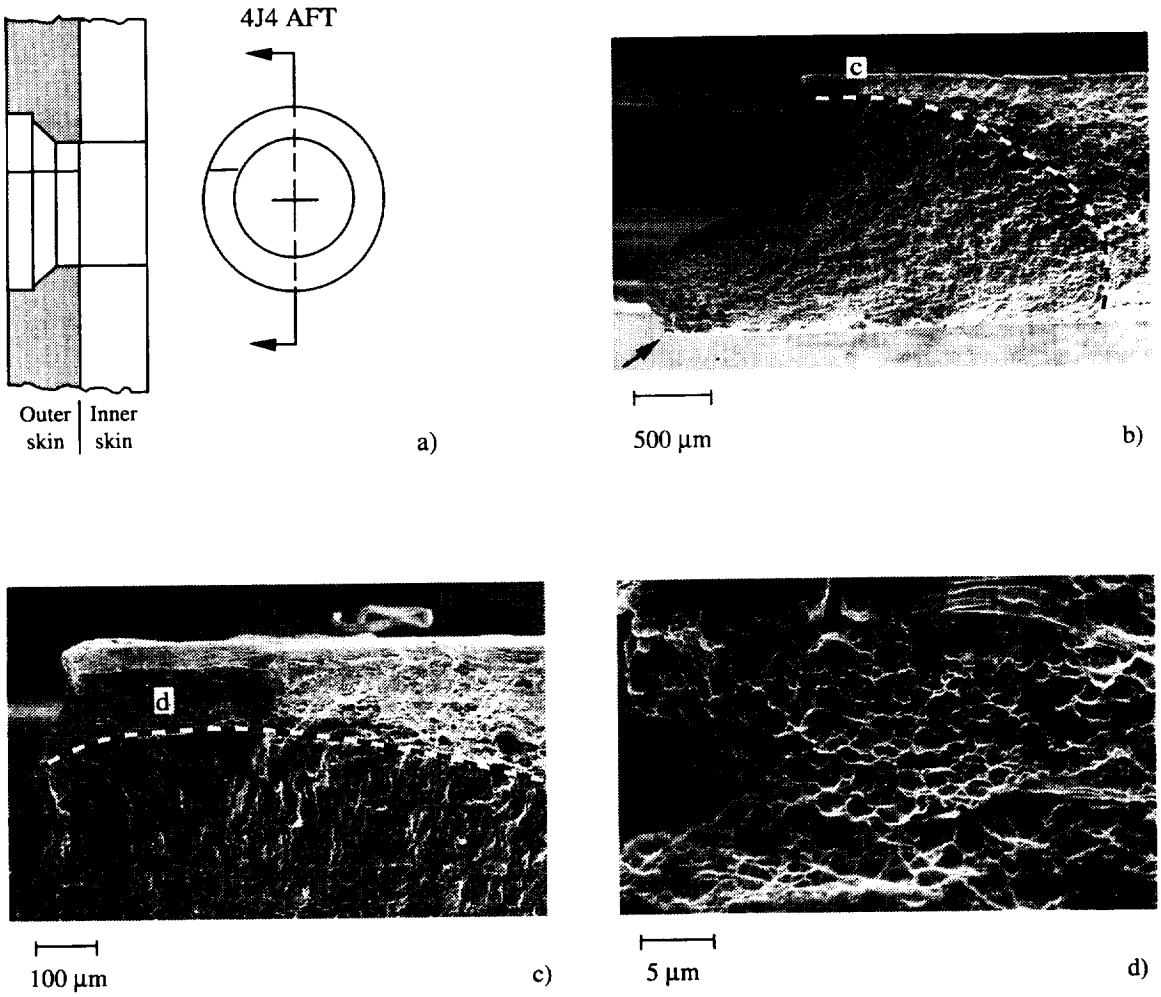

Figure 11.15 a) The schematic shows the rivet hole 4J4 configuration and the location of the outer skin fatigue crack oriented in the aft direction and about the 10 o'clock position. b) The SEM micrograph shows the fatigue crack fracture surface located at the outer skin rivet hole (left). The arrow marks the likely region of crack initiation and the dashed line marks the fatigue crack front. c) The SEM micrograph shows the fatigue crack front and the ligament, region "c" in Figure 11.15.b. The dashed line marks the fatigue crack front where it intersects the rivet hole (left). The outboard surface of the outer skin is located at the top of the micrograph. d) The SEM micrograph shows the ductile morphology of the overload fracture surface at region "d" in Figure 11.15.b at high magnification.

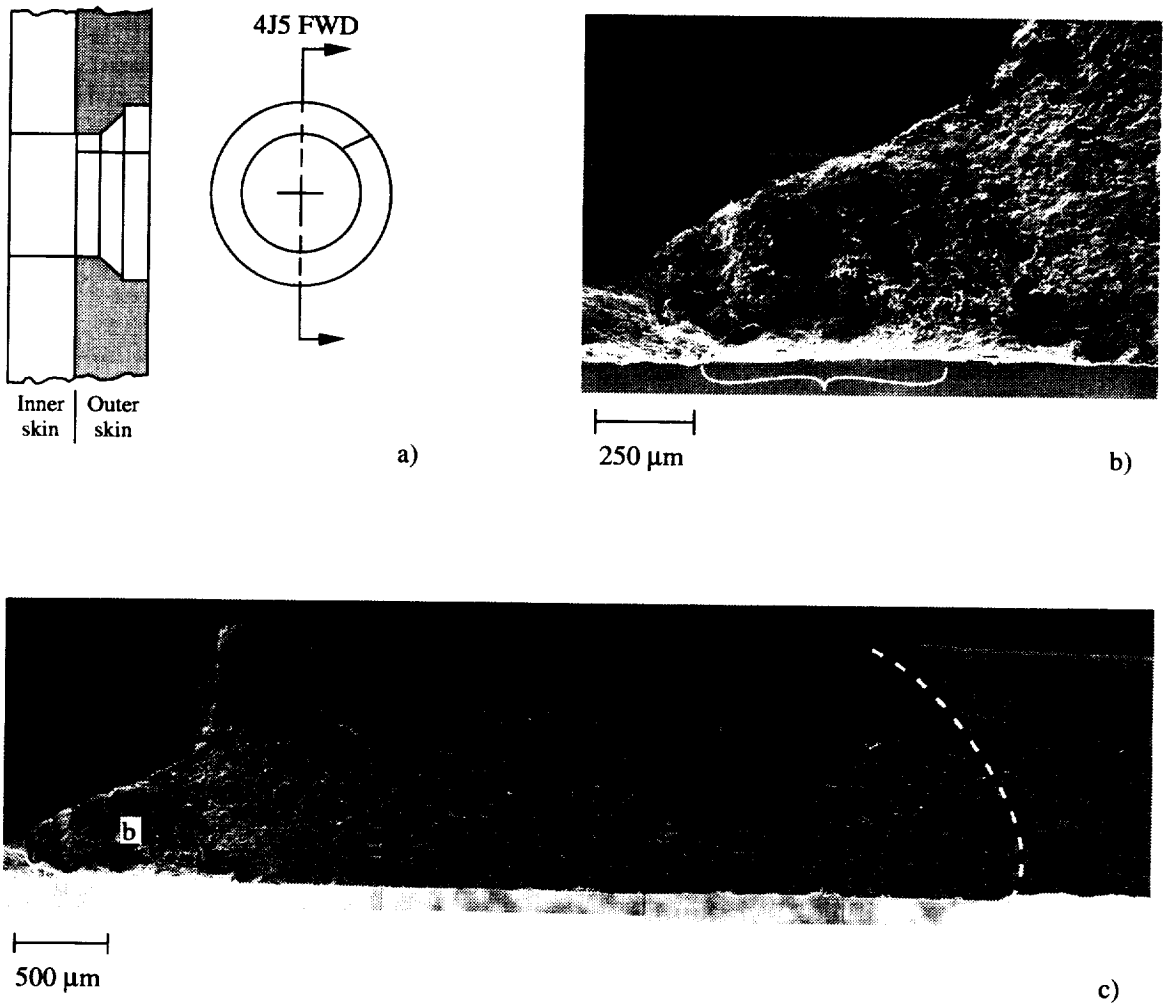

Figure 11.16 a) The schematic shows the rivet hole 4J5 configuration and the location of the outer skin fatigue crack oriented in the forward direction and about the 2 o'clock position. b) The SEM micrograph shows the fatigue crack fracture surface located at the shank, region "b" in Figure 11.16.c. The bracket marks the likely region of crack initiation. c) The SEM micrograph shows the fatigue crack fracture surface located at the outer skin rivet hole (left). The dashed line marks the fatigue crack front.

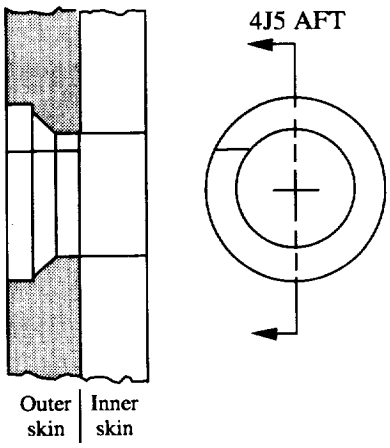

a)

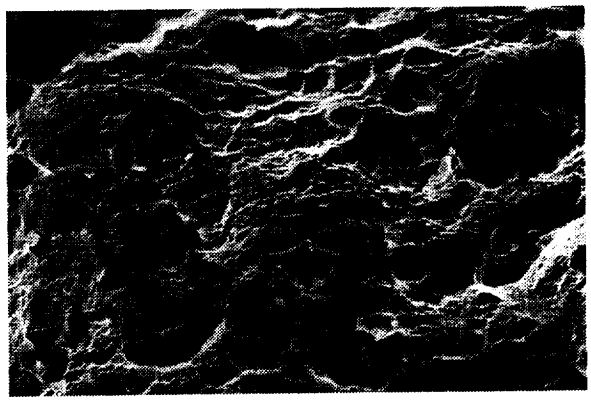

b)

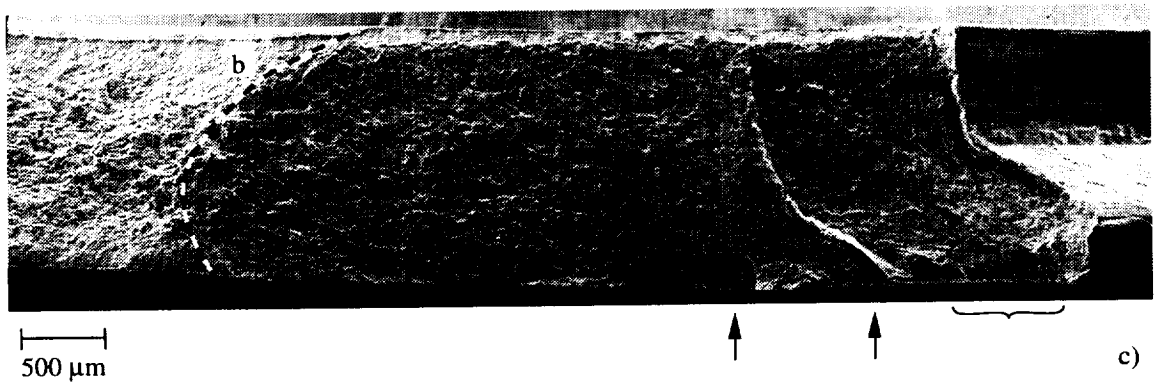

c)

Figure 11.17 a) The schematic shows the rivet hole 4J5 configuration and the location of the outer skin fatigue crack oriented in the aft direction and about the 10 o'clock position. b) The SEM micrograph shows the ductile tearing morphology of the overload fracture surface at region "b" in Figure 11.17.c at high magnification. c) The SEM micrograph shows the fatigue crack fracture surface located at the outer skin rivet hole (right). The bracket and arrows mark the likely regions of crack initiation and the dashed line marks the fatigue crack front. Here, multiple fatigue fracture surface planes suggest that multiple fatigue cracks initiated along the faying surface and eventually coalesced into a single crack.

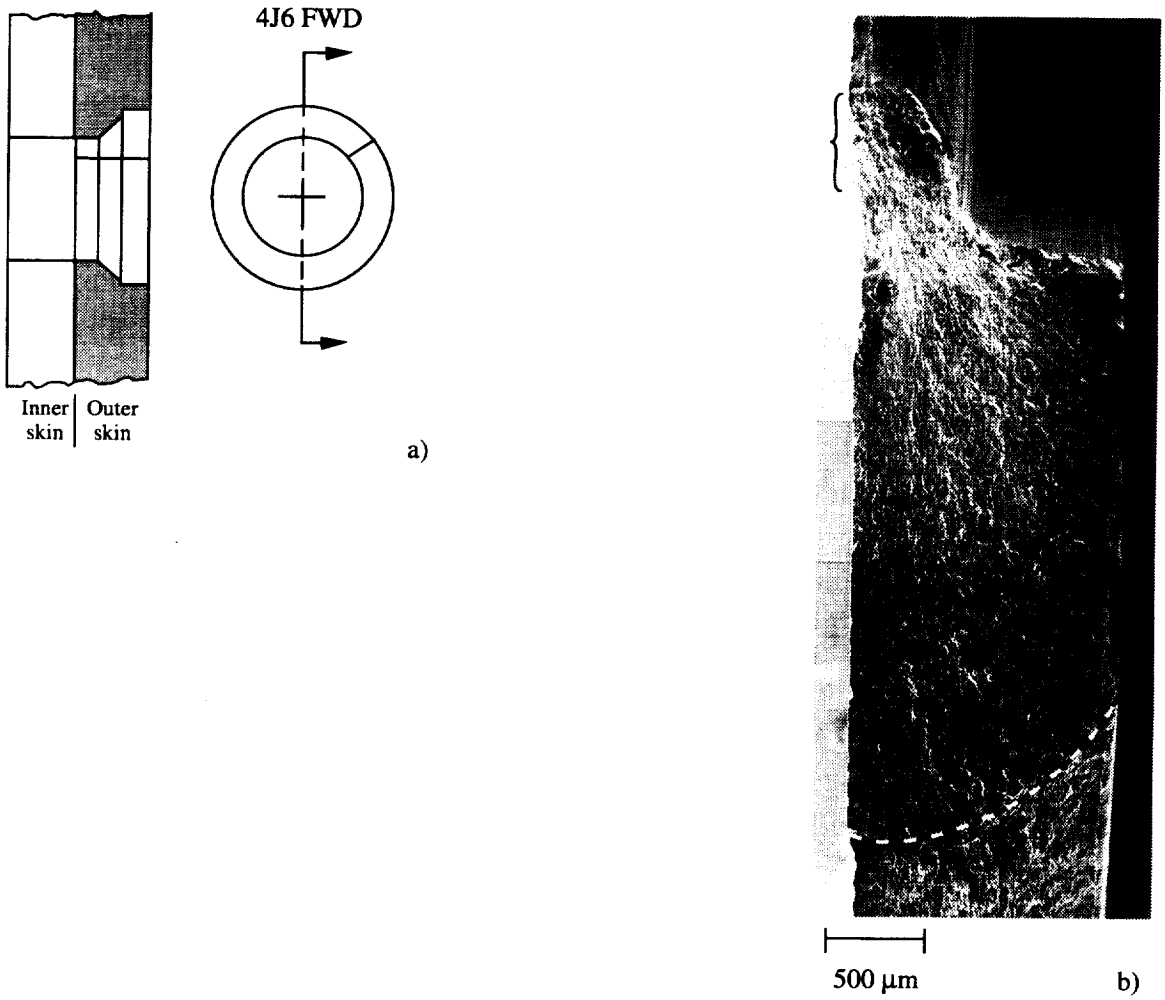

Figure 11.18 a) The schematic shows the rivet hole 4J6 configuration and the location of the outer skin fatigue crack oriented in the forward direction and about the 2 o'clock position. b) The SEM micrograph shows the fatigue crack fracture surface located at the outer skin rivet hole (top). The bracket marks the likely region of crack initiation and dashed line marks the fatigue crack front.

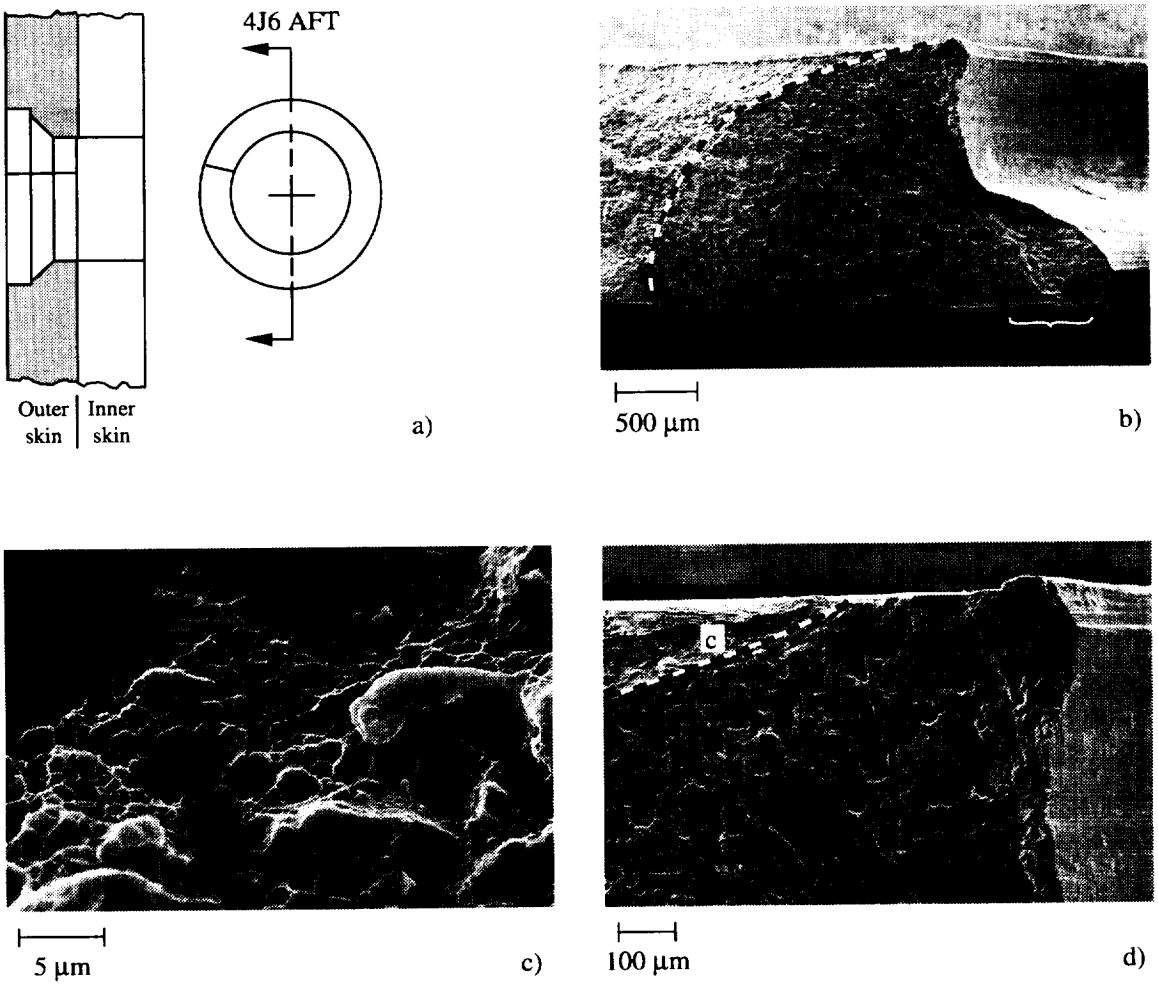

Figure 11.19 a) The schematic shows the rivet hole 4J6 configuration and the location of the outer skin fatigue crack oriented in the aft direction and about the 10 o'clock position. b) The SEM micrograph shows the fatigue crack fracture surface located at the outer skin rivet hole (right). The dashed line marks the fatigue crack front and the bracket marks the region of crack initiation. c) The SEM micrograph shows the ductile tearing morphology of the overload fracture surface at region "c" in Figure 11.11.d at high magnification. c) The SEM micrograph shows the fatigue crack front region (dashed line) as it intersects the outboard surface of the outer skin. The rivet hole is located to the right.

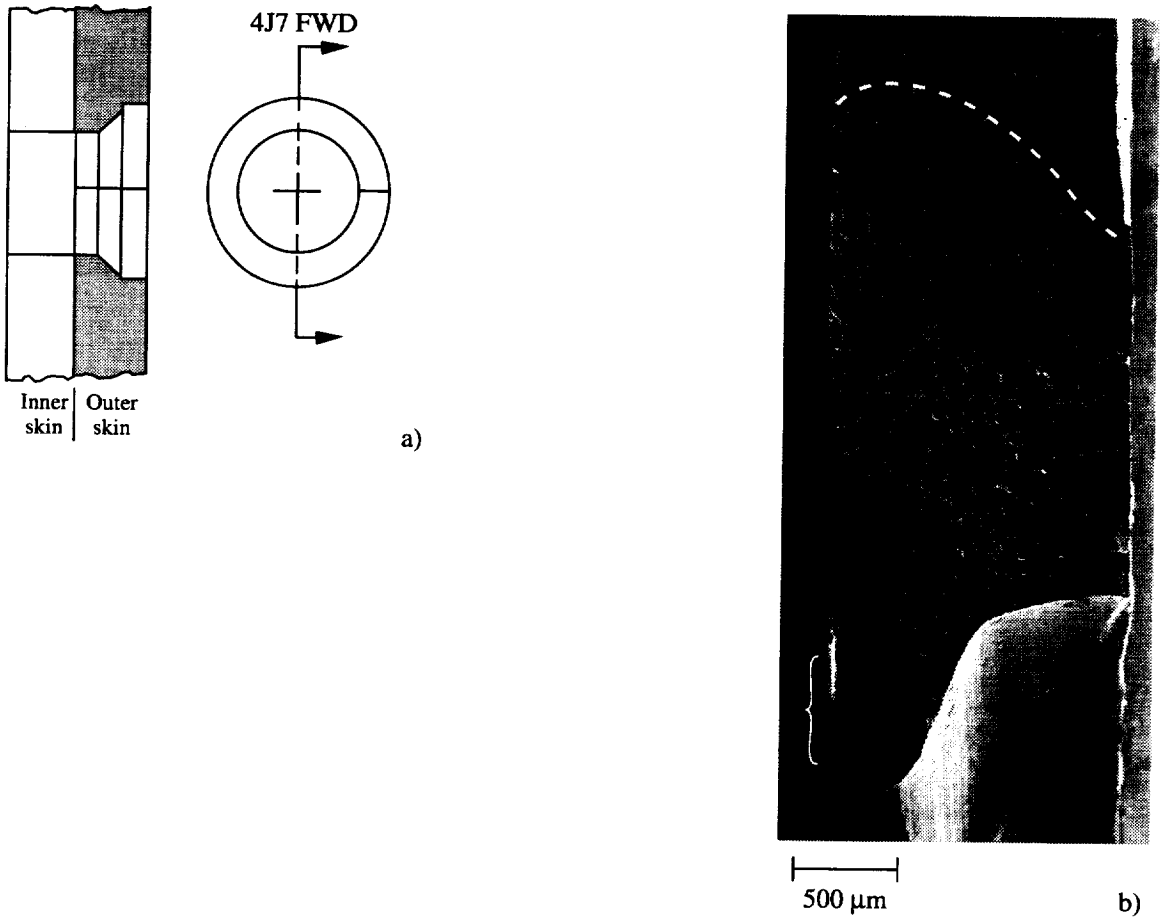

Figure 11.20 a) The schematic shows the rivet hole 4J7 configuration and the location of the outer skin fatigue crack oriented in the forward direction and about the 3 o'clock position. b) The SEM micrograph shows the fatigue crack fracture surface located at the outer skin rivet hole (bottom). The bracket marks the likely region of crack initiation and the dashed line marks the fatigue crack front.

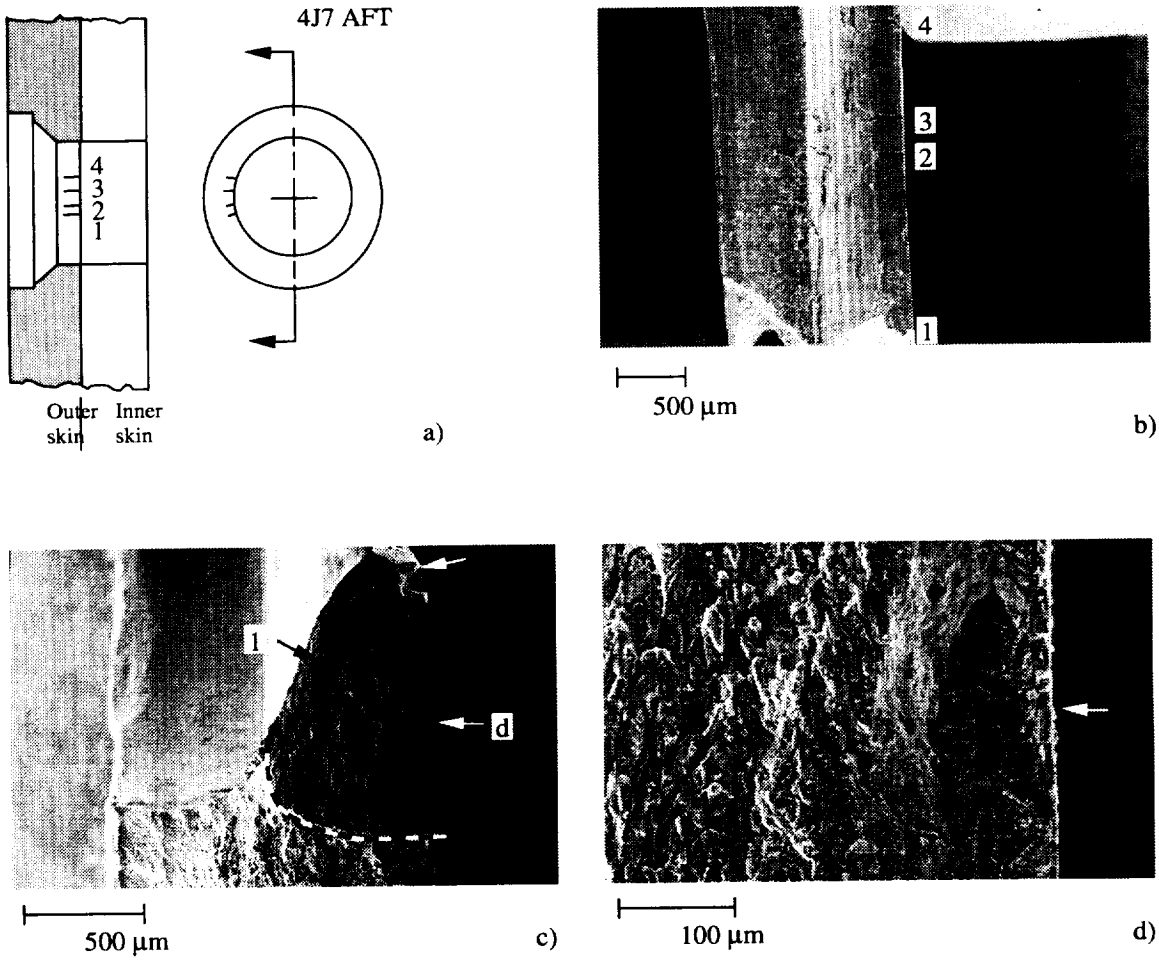

Figure 11.21 a) The schematic shows the rivet hole 4J7 configuration and the location of four outer skin fatigue cracks oriented in the aft direction and about the 9 o'clock position. b) The SEM micrograph shows the inner surface of the outer skin rivet hole and location of four fatigue cracks along the inboard region of the rivet hole. The main fracture surface is partially shown at the bottom of the micrograph. c) The SEM micrograph shows the main fatigue crack fracture surface (crack #1) at the rivet hole. The arrows mark the likely regions of crack initiation and the dashed line marks the fatigue crack front. d) The SEM micrograph shows the fatigue crack initiation site at region "d" in Figure 11.21.c at high magnification.

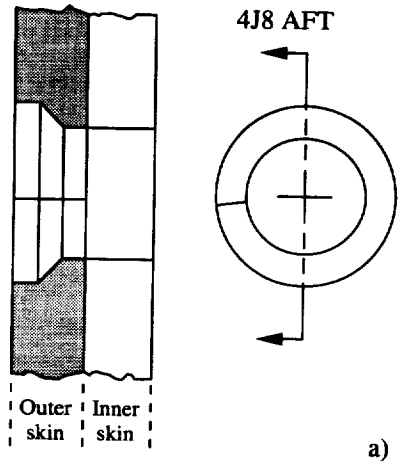

a)

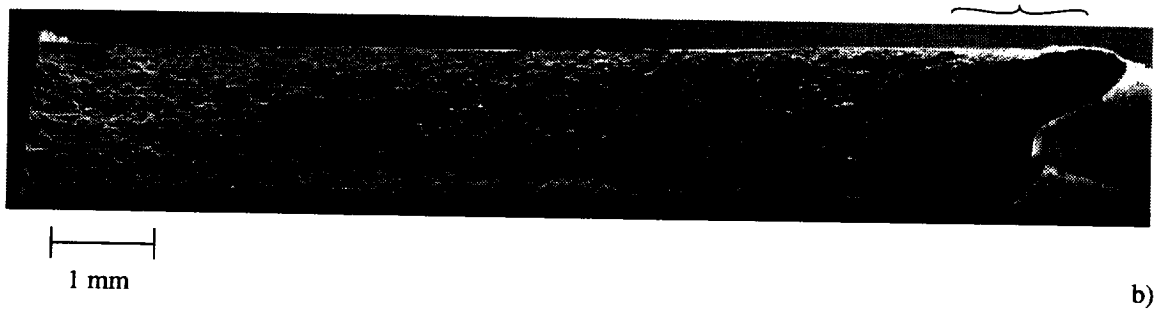

b)

Figure 11.22 a) The schematic shows the rivet hole 4J8 configuration and the location of the outer skin fatigue crack oriented in the aft direction and about the 9 o'clock position. b) The SEM micrograph shows the fatigue crack fracture surface located at the outer skin rivet hole (right). The bracket marks the likely region of crack initiation. The crack front is not visible. This crack linked-up with rivet hole 4J9.

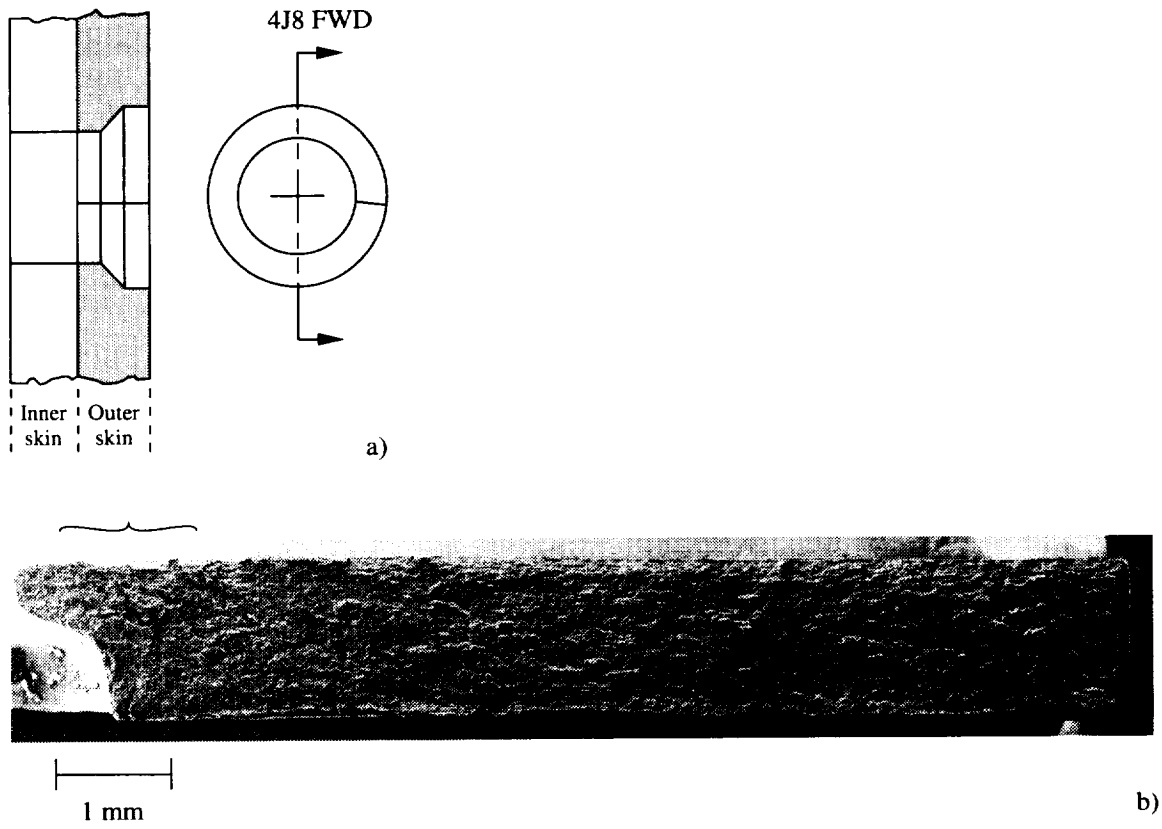

Figure 11.23 a) The schematic shows the rivet hole 4J8 configuration and the location of the outer skin fatigue crack oriented in the forward direction and about the 3 o'clock position. b) The SEM micrograph shows the fatigue crack fracture surface located at the outer skin rivet hole (left). The bracket marks the likely region of crack initiation. The crack front is not visible.

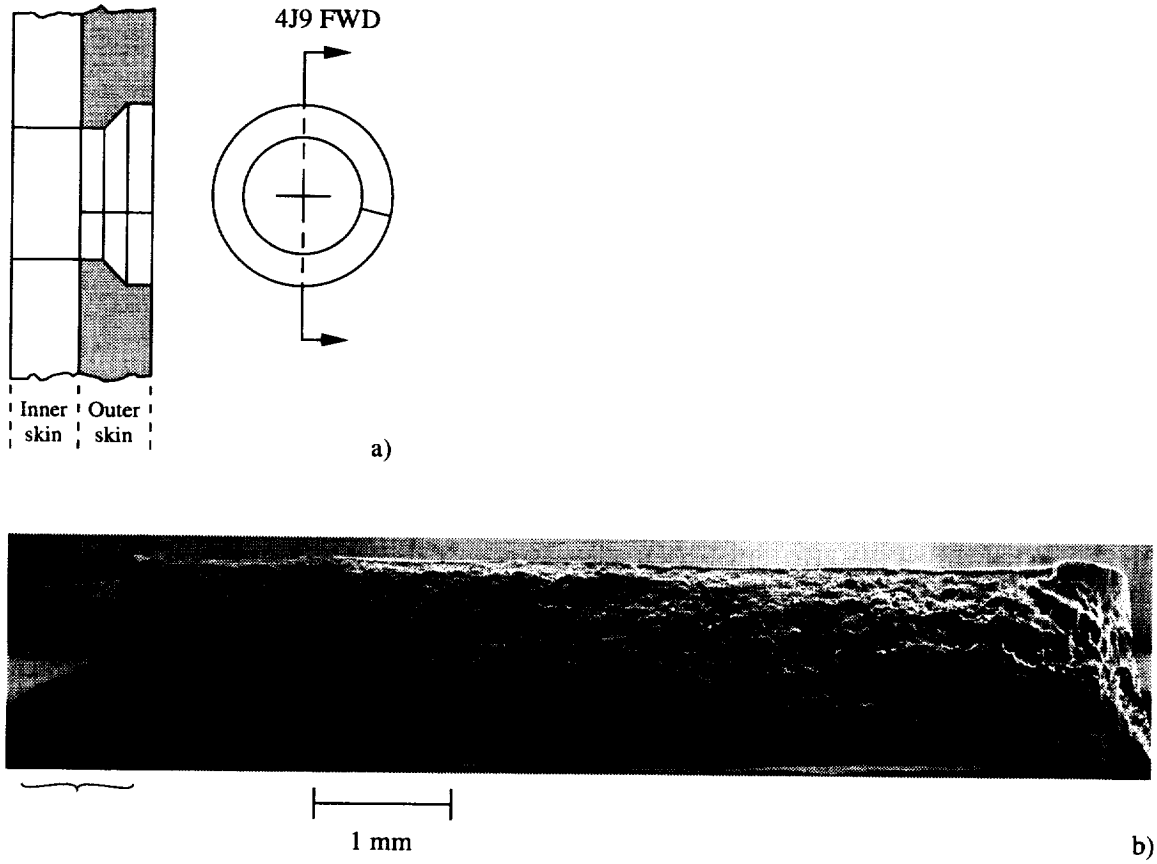

Figure 11.24 a) The schematic shows the rivet hole 4J9 configuration and the location of the outer skin fatigue crack oriented in the forward direction and just below the 3 o'clock position. b) The SEM micrograph shows the fatigue crack fracture surface located at the outer skin rivet hole (left). The bracket marks the likely region of crack initiation. The crack front is not visible.

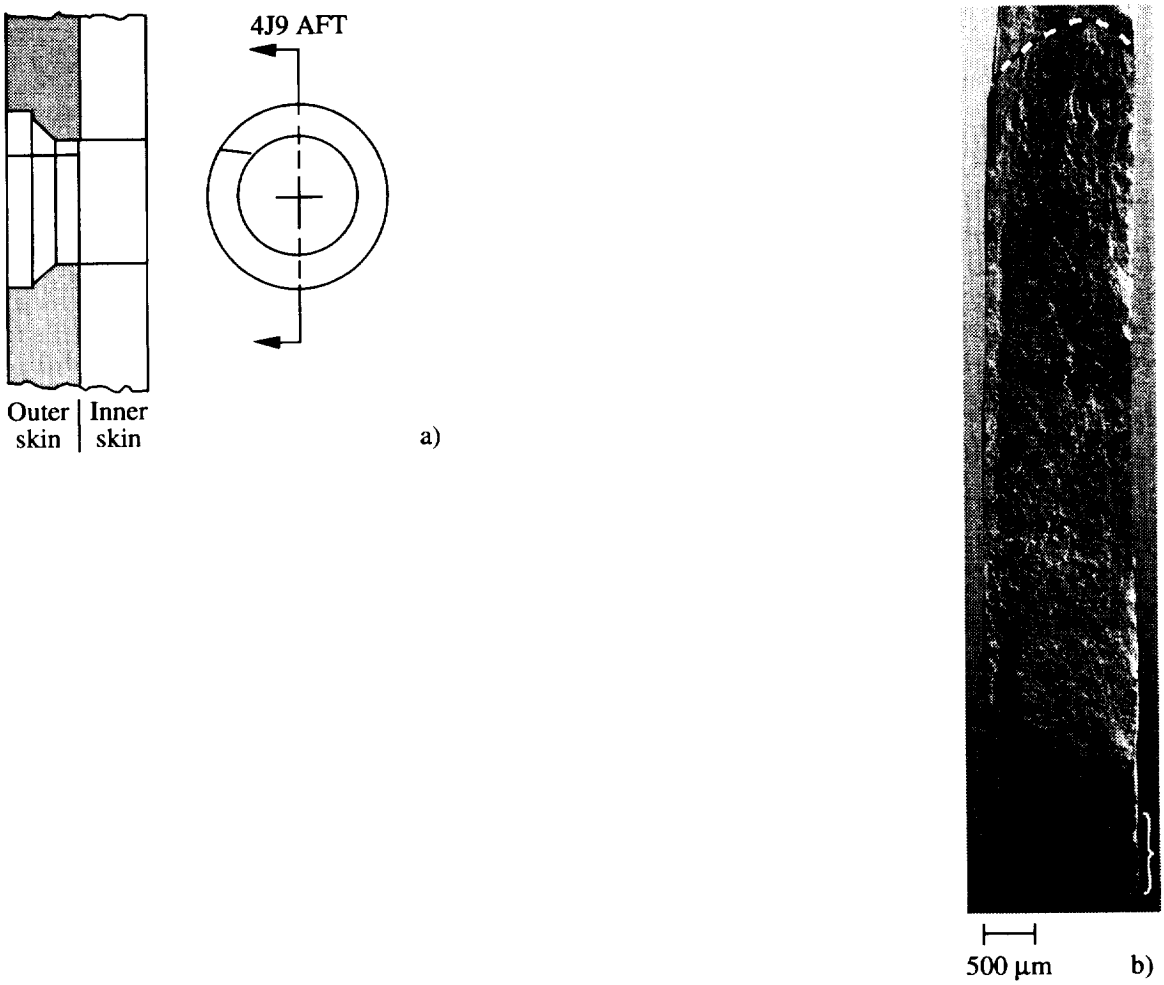

Figure 11.25 a) The schematic shows the rivet hole 4J9 configuration and the location of the outer skin fatigue crack oriented in the aft direction and about the 10 o'clock position. b) The SEM micrograph shows the fatigue crack fracture surface located at the outer skin rivet hole (bottom). The bracket marks the likely region of crack initiation and the dashed line marks the fatigue crack front.

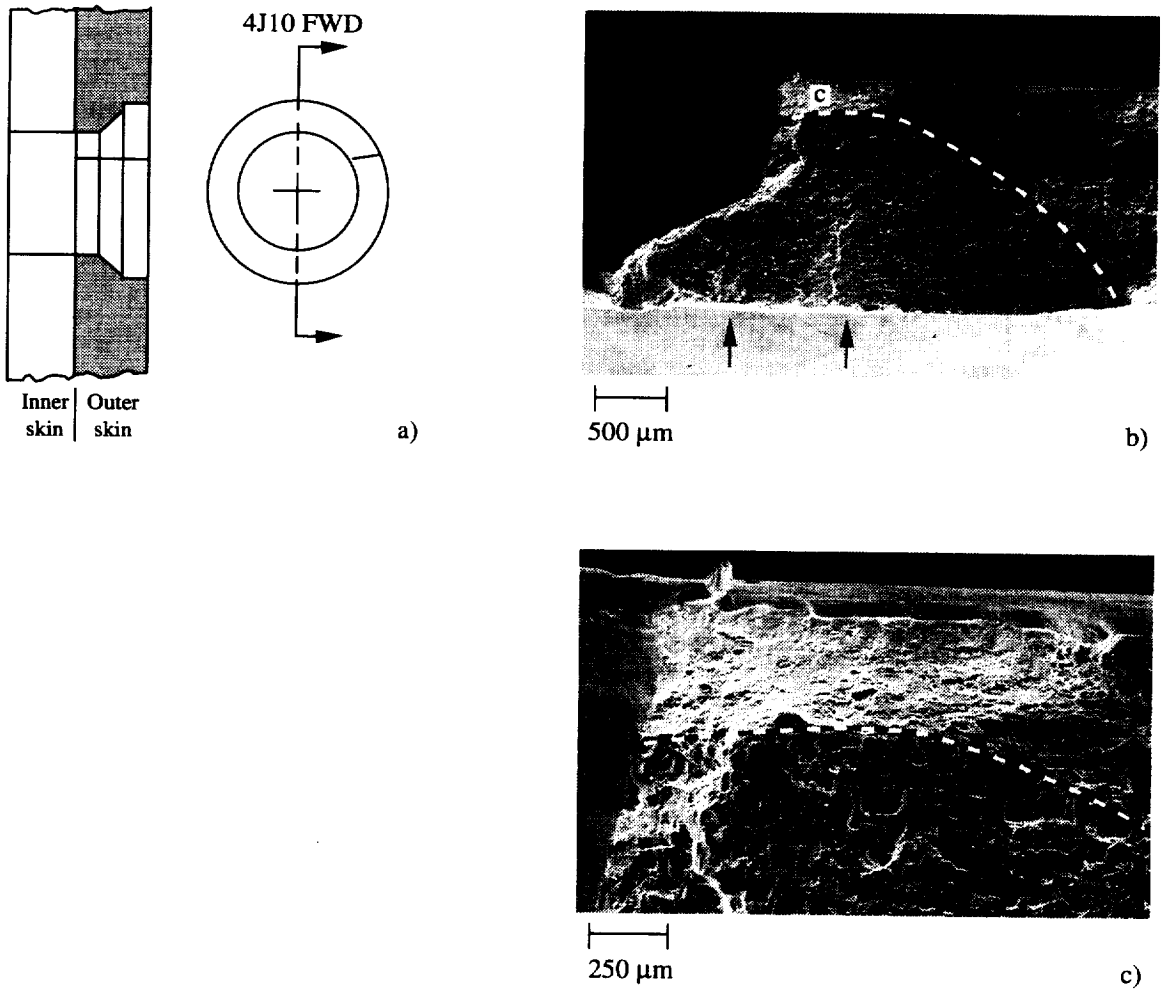

Figure 11.26 a) The schematic shows the rivet hole 4J10 configuration and the location of the outer skin fatigue crack oriented in the forward direction and about the 2 o'clock position. b) The SEM micrograph shows the fatigue crack fracture surface located at the outer skin rivet hole (left). The arrows mark the likely regions of crack initiation and the dashed line marks the fatigue crack front. c) The SEM micrograph shows the fatigue crack front ligament at region "c" in Figure 11.23.b. The dashed line marks the fatigue crack front where it intersects the rivet hole (left). The outboard surface of the outer skin is located at the top of the micrograph.

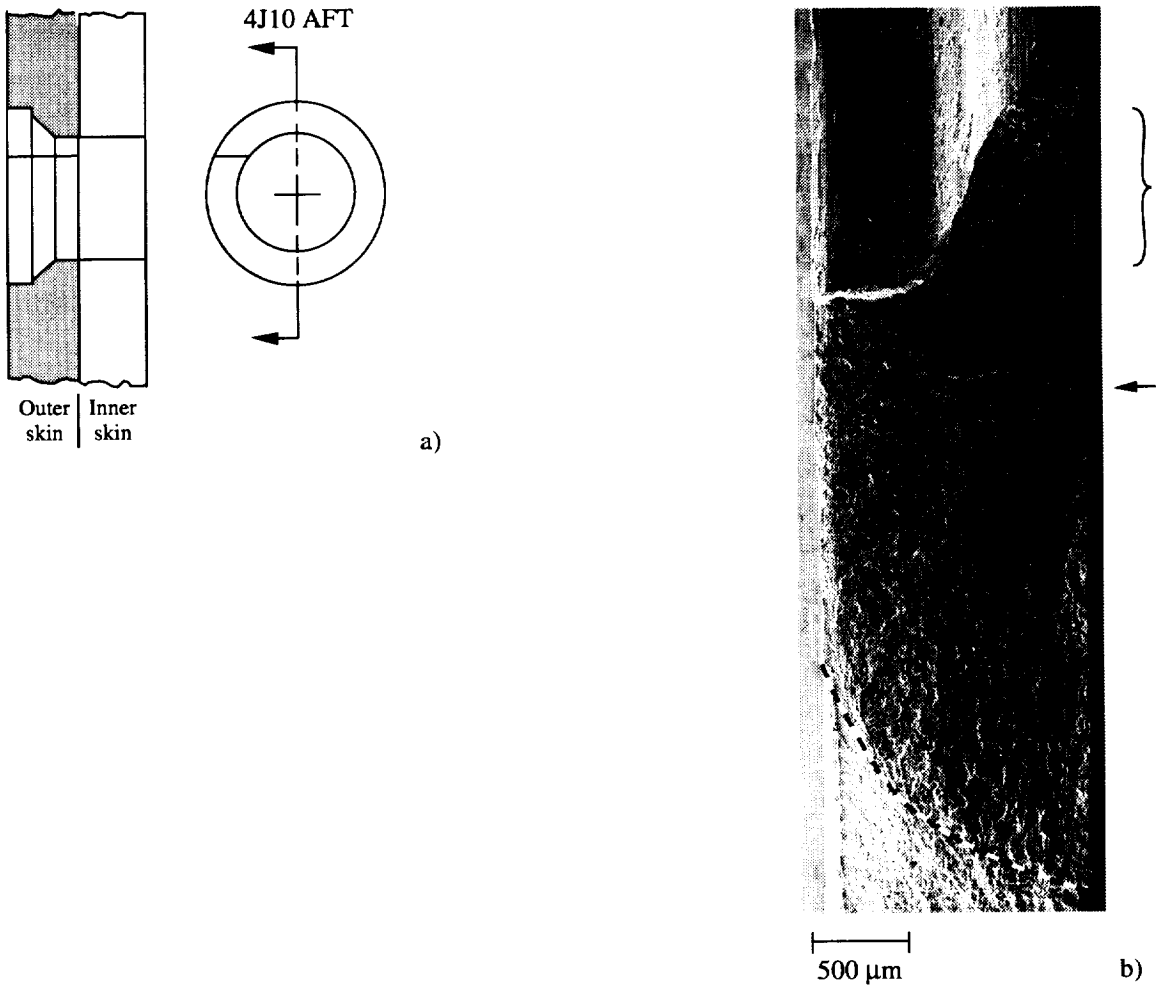

Figure 11.27 a) The schematic shows the rivet hole 4J10 configuration and the location of the outer skin fatigue crack oriented in the aft direction and about the 10 o'clock position. b) The SEM micrograph shows the fatigue crack fracture surface located at the outer skin rivet hole (top). Crack initiation occurred at multiple sites (bracket and arrow) along the faying surface. The dashed line marks the fatigue crack front.

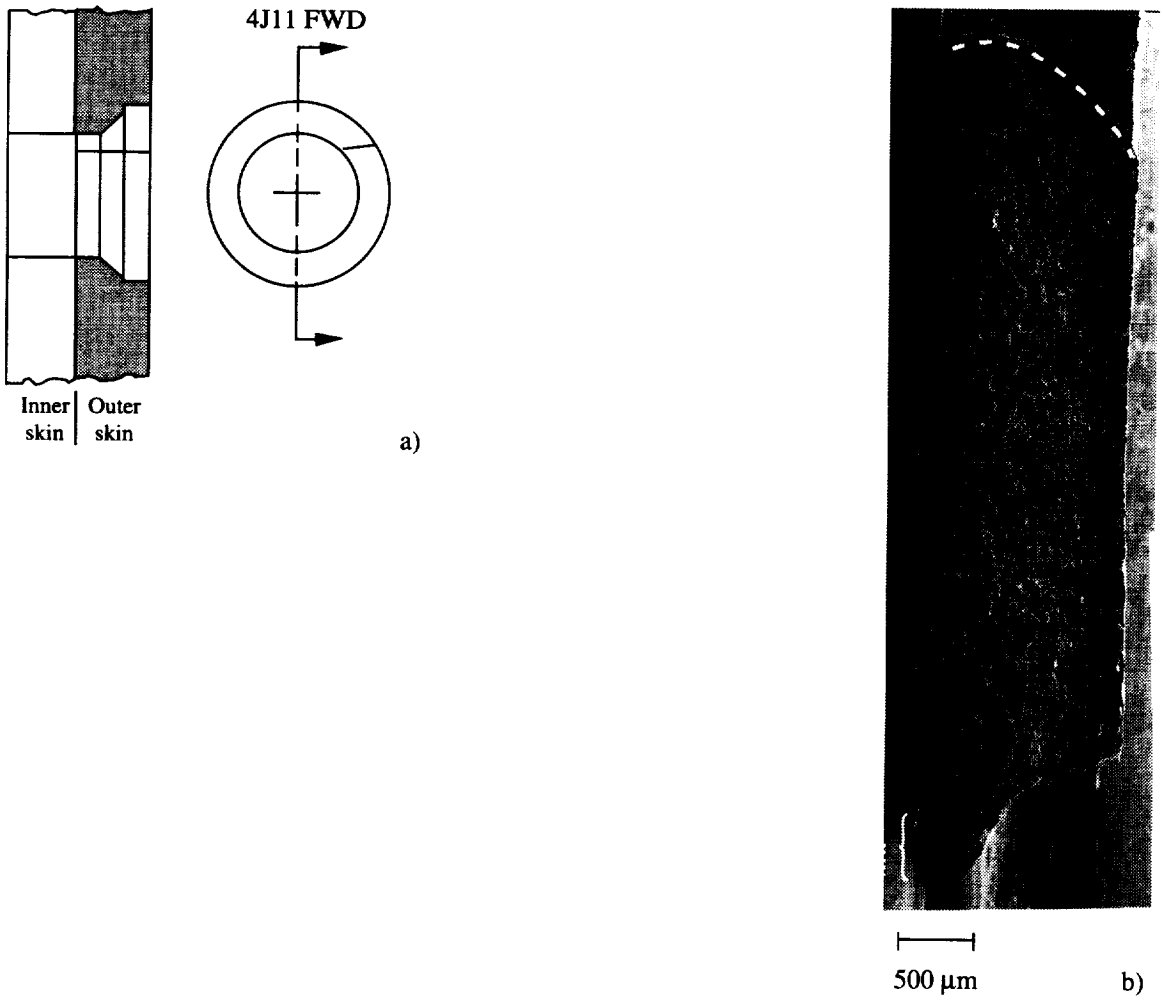

Figure 11.28 a) The schematic shows the rivet hole 4J11 configuration and the location of the outer skin fatigue crack oriented in the forward direction and about the 2 o'clock position. b) The SEM micrograph shows the fatigue crack fracture surface located at the outer skin rivet hole (bottom). The bracket shows the likely region of crack initiation and the dashed line marks the fatigue crack front.

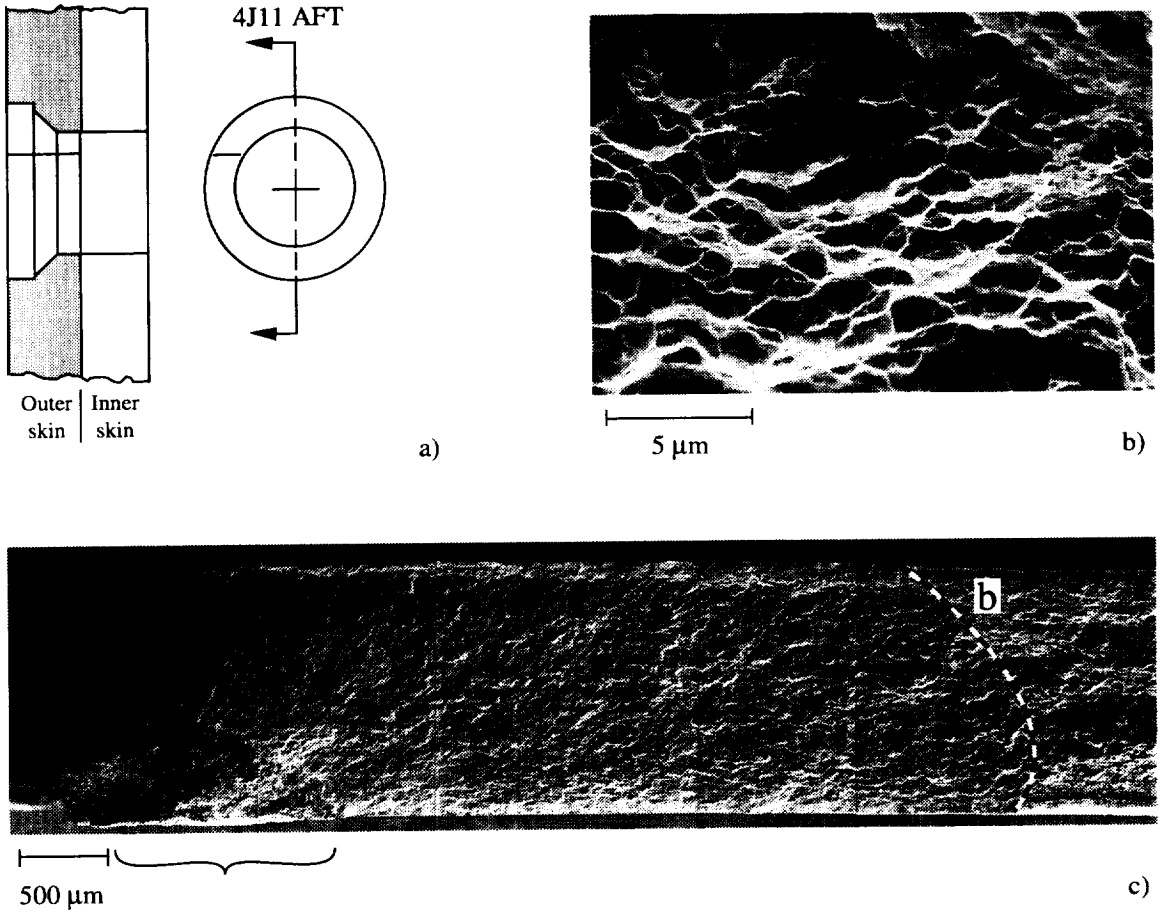

Figure 11.29 a) The schematic shows the rivet hole 4J11 configuration and the location of the outer skin fatigue crack oriented in the aft direction and about the 10 o'clock position. b) The SEM micrograph shows the ductile tearing morphology of the overload fracture surface at region "b" in Figure 11.26.c. c) The SEM micrograph shows the fatigue crack fracture surface located at the outer skin rivet hole (left). The bracket shows the region of crack initiation along the faying surface and the dashed line marks the fatigue crack front.

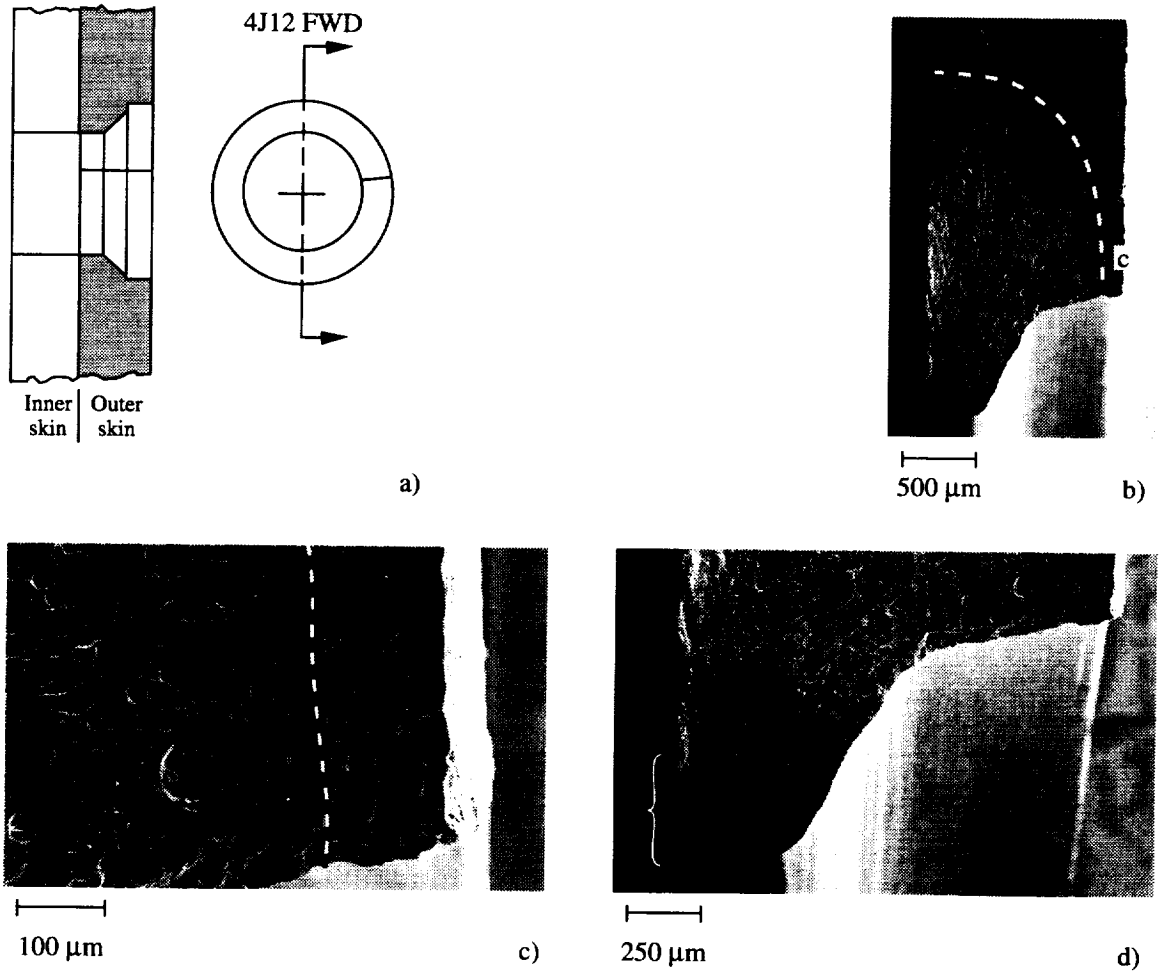

Figure 11.30 a) The schematic shows the rivet hole 4J12 configuration and the location of the outer skin fatigue crack oriented in the forward direction and above the 3 o'clock position. b) The SEM micrograph shows the fatigue crack fracture surface located at the outer skin rivet hole (bottom). The dashed line marks the fatigue crack front. c) The SEM micrograph shows the fatigue crack front at region "c" in Figure 11.27.b. The dashed line marks the fatigue crack front where it intersects the rivet hole (bottom). The outboard surface of the outer skin is located at the right of the micrograph. d) The SEM micrograph shows the fatigue crack initiation region located at the faying surface (bracket).

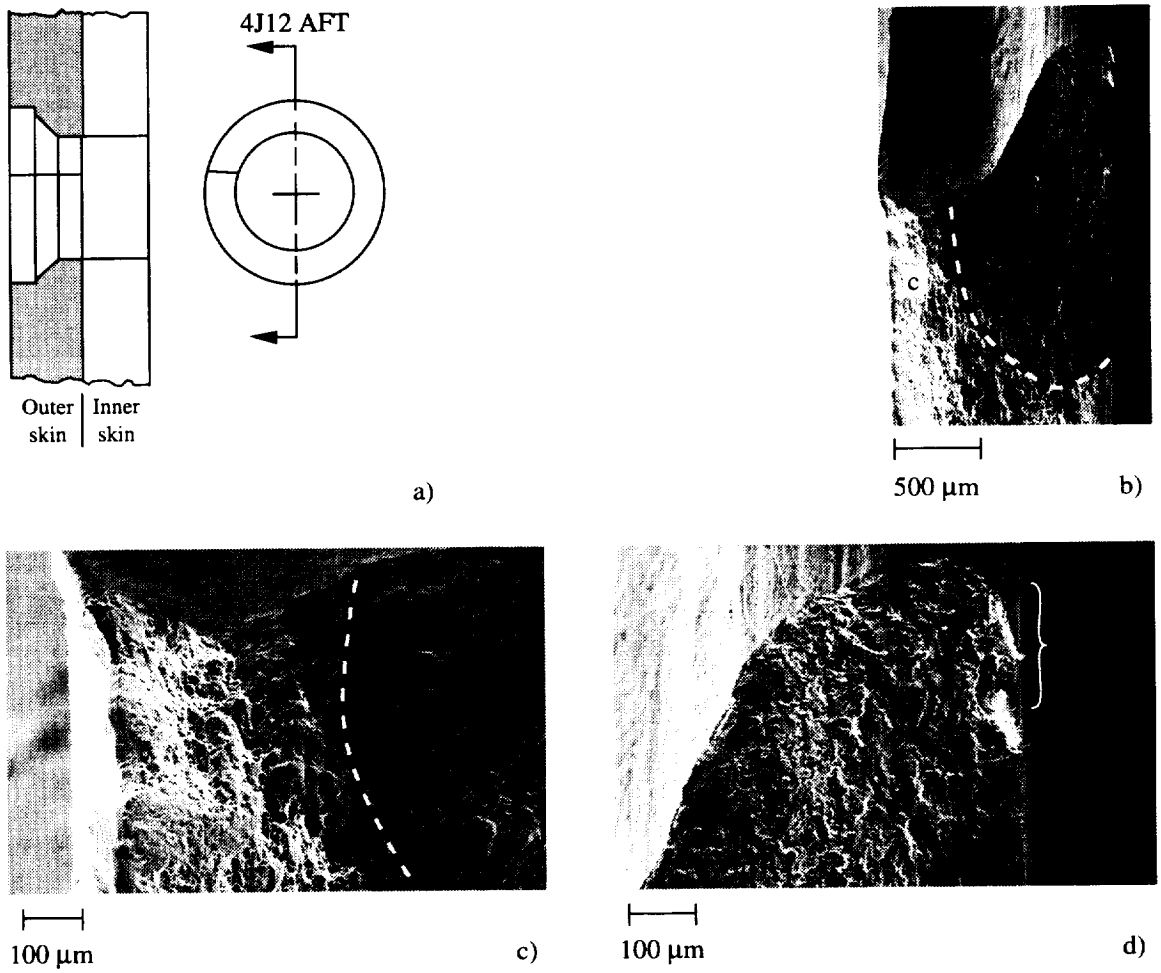

Figure 11.31 a) The schematic shows the rivet hole 4J12 configuration and the location of the outer skin fatigue crack oriented in the aft direction and above the 9 o'clock position. b) The SEM micrograph shows the fatigue crack fracture surface located at the outer skin rivet hole (top). The dashed line marks the fatigue crack front. c) The SEM micrograph shows the fatigue crack front at region "c" in Figure 11.28.b. The dashed line marks the fatigue crack front where it intersects the rivet hole (bottom). The outboard side of the outer skin is located at the left of the micrograph. d) The SEM micrograph shows the fatigue crack initiation region located along the faying surface (bracket).

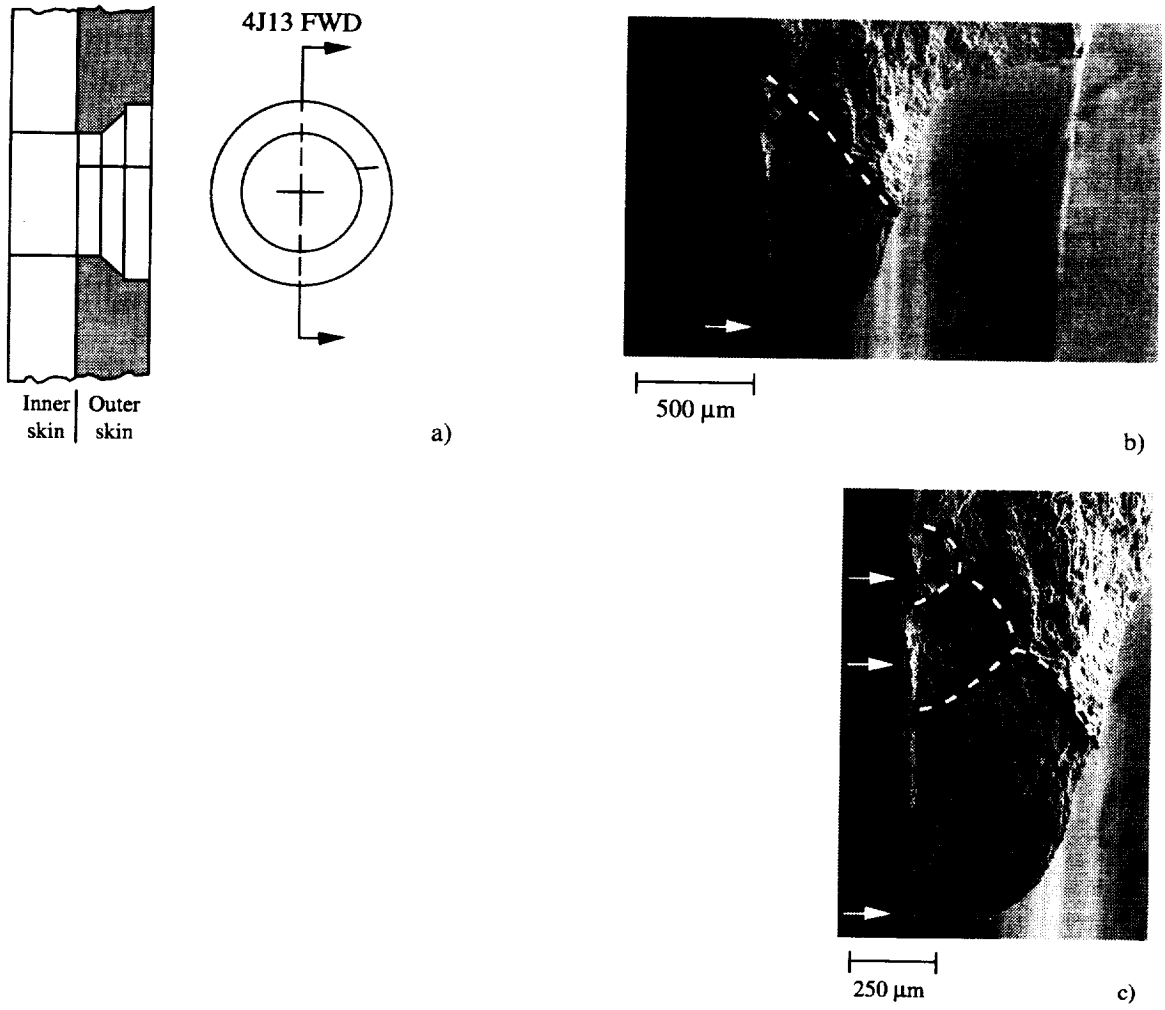

Figure 11.32 a) The schematic shows the rivet hole 4J13 configuration and the location of the outer skin fatigue crack oriented in the forward direction and below the 2 o'clock position. b) The SEM micrograph shows the fatigue crack fracture surface located at the outer skin rivet hole (bottom). The dashed line marks the fatigue crack front. c) The SEM micrograph shows the fatigue crack initiation region located along the faying surface (arrows). The dashed lines mark the crack front.

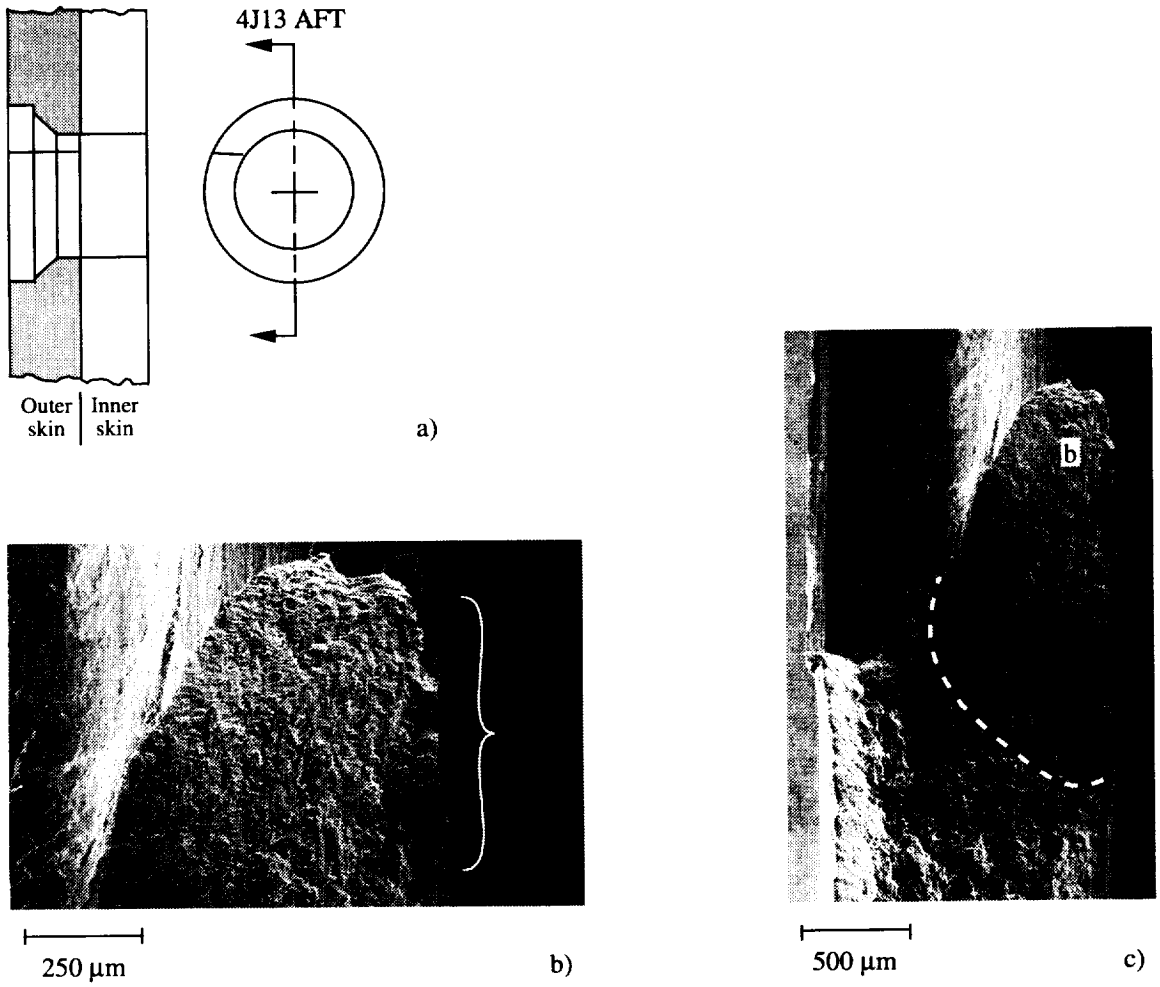

Figure 11.33 a) The schematic shows the rivet hole 4J13 configuration and the location of the outer skin fatigue crack oriented in the aft direction and about the 10 o'clock position. b) The SEM micrograph shows the rivet hole shank region and the likely fatigue crack initiation region located at the inboard corner of the rivet hole (bracket). c) The SEM micrograph shows the fatigue crack fracture surface located at the outer skin rivet hole (top). The dashed line marks the fatigue crack front.

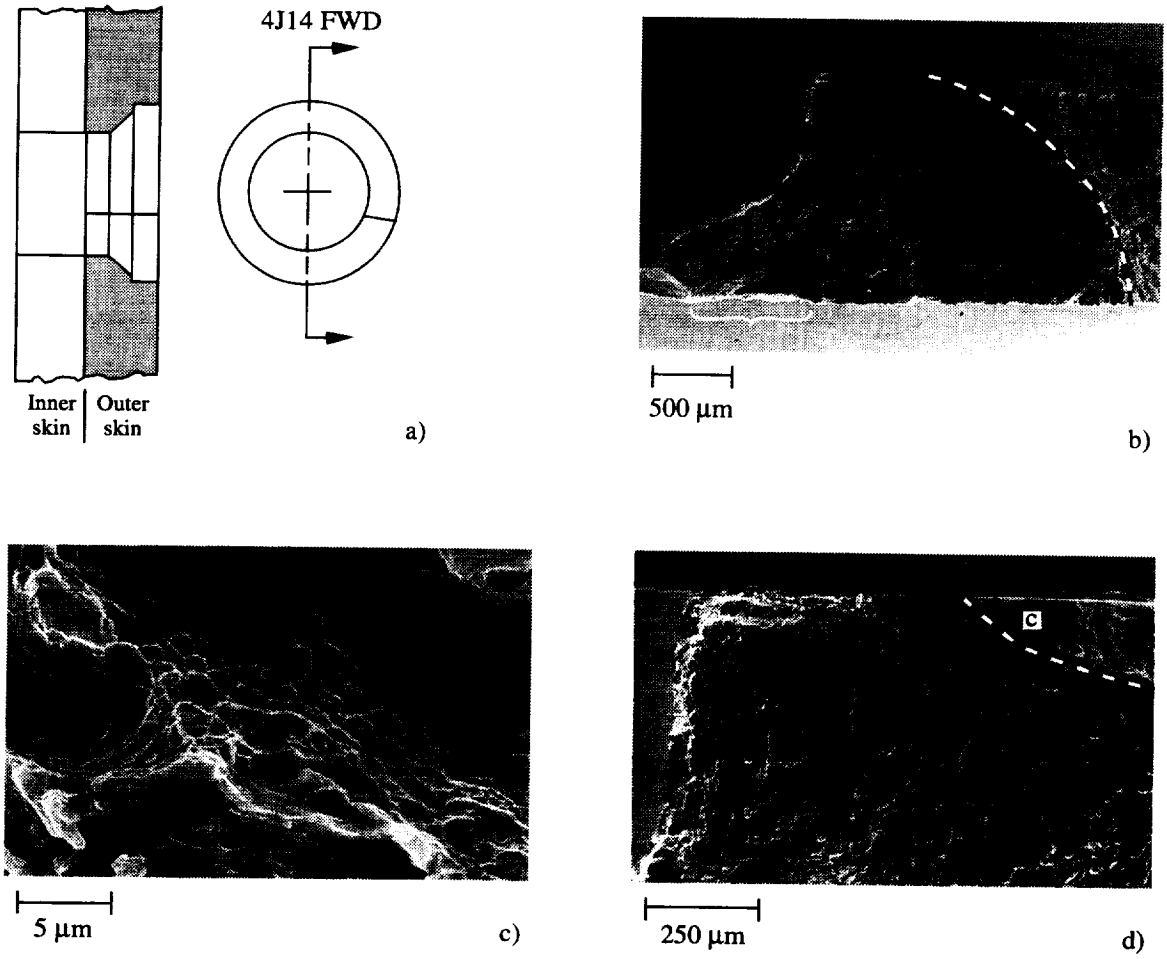

Figure 11.34 a) The schematic shows the rivet hole 4J14 configuration and the location of the outer skin fatigue crack oriented in the forward direction and about the 4 o'clock position. b) The SEM micrograph shows the fatigue crack fracture surface located at the outer skin rivet hole (left). The bracket marks the likely crack initiation site and the dashed line marks the fatigue crack front. c) The SEM micrograph shows the ductile tearing morphology of the overload fracture surface at region "c" in Figure 11.11.d at high magnification. d) The SEM micrograph shows the fatigue crack front region (dashed line) as it intersects the outboard surface of the outer skin. The rivet hole is located to the left.

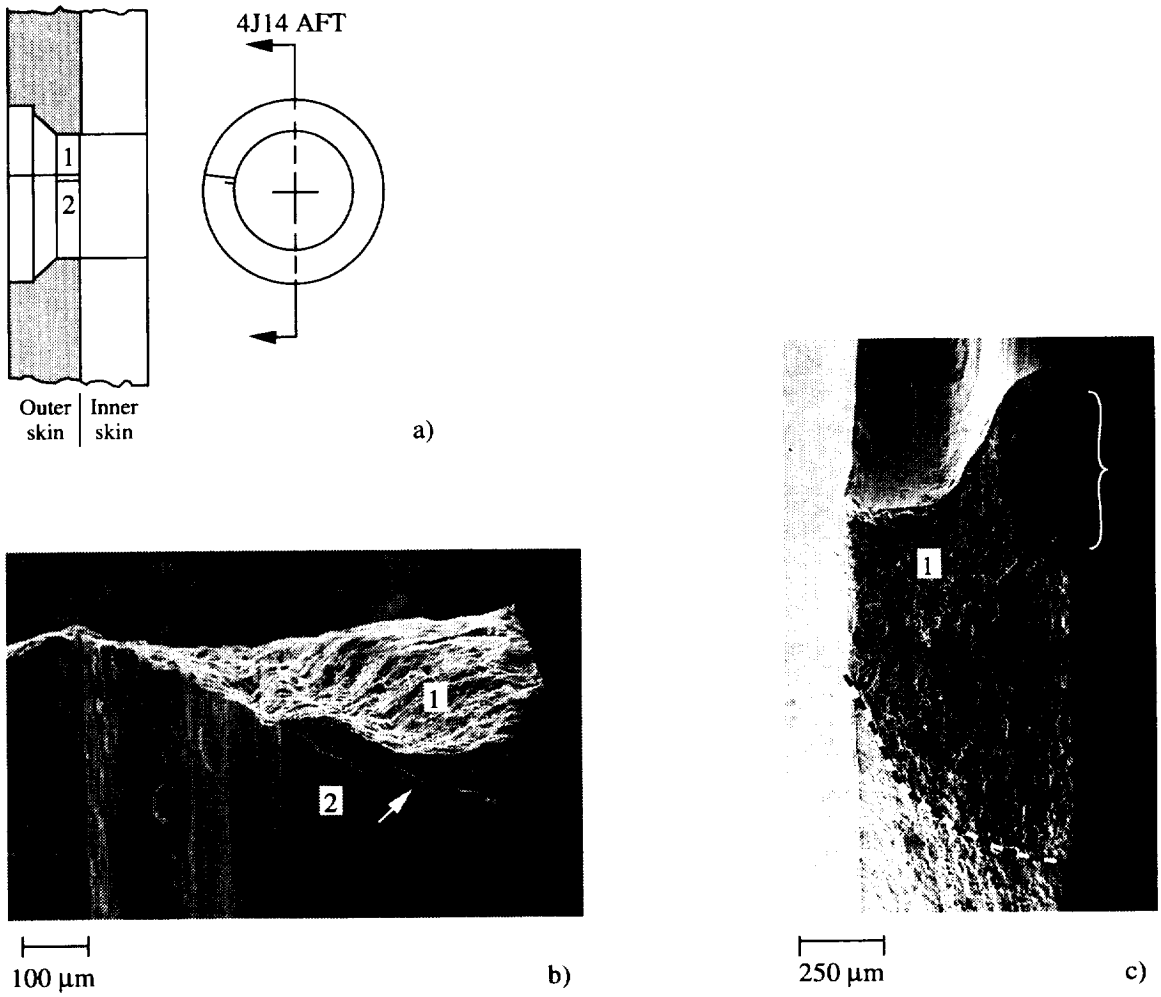

Figure 11.35 a) The schematic shows the rivet hole 4J14 configuration and the location of two outer skin fatigue cracks oriented in the aft direction and above the 9 o'clock position. b) The SEM micrograph shows the rivet hole surface and the fatigue crack fracture surface at an oblique angle. Fatigue crack #2 is located below the main fracture surface that contains fatigue crack #1. c) The SEM micrograph shows the fatigue crack fracture surface located at the outer skin rivet hole (top). The bracket marks the likely region of crack initiation along the faying surface and the dashed line marks the fatigue crack front.

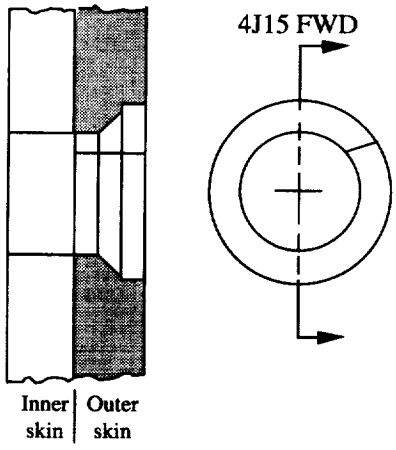

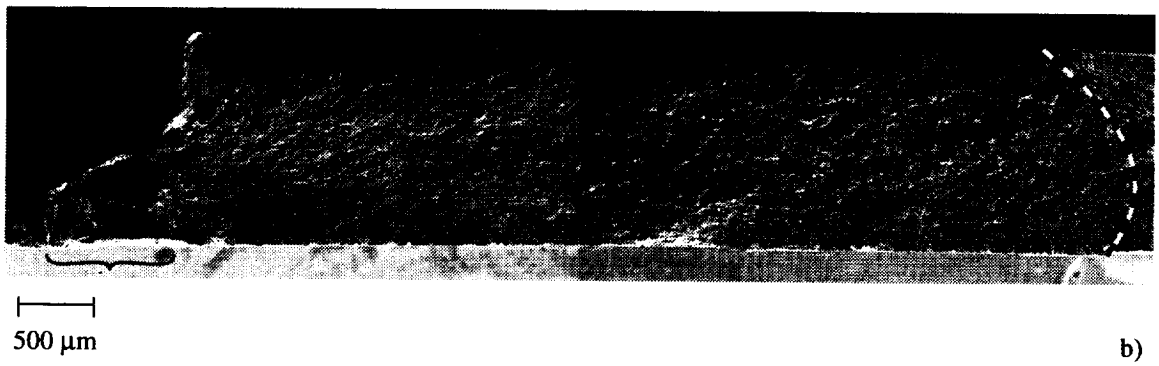

Figure 11.36 a) The schematic shows the rivet hole 4J15 configuration and the location of the outer skin fatigue crack oriented in the forward direction and about the 2 o'clock position. b) The SEM micrograph shows the fatigue crack fracture surface located at the outer skin rivet hole (left). The bracket marks the region of crack initiation along the faying surface and the dashed line marks the fatigue crack front.

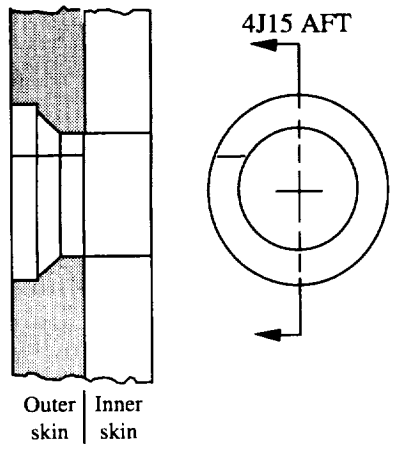

a)

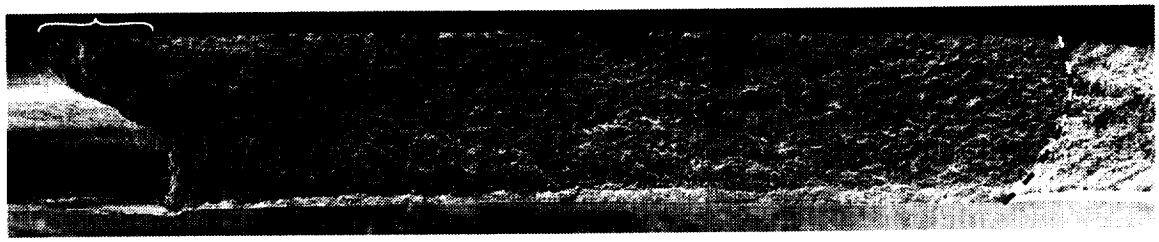

b)

Figure 11.37 a) The schematic shows the rivet hole 4J15 configuration and the location of the outer skin fatigue crack oriented in the aft direction and about the 10 o'clock position. b) The SEM micrograph shows the fatigue crack fracture surface located at the outer skin rivet hole (left). The bracket marks the region of crack initiation along the faying surface and the dashed line marks the fatigue crack front.

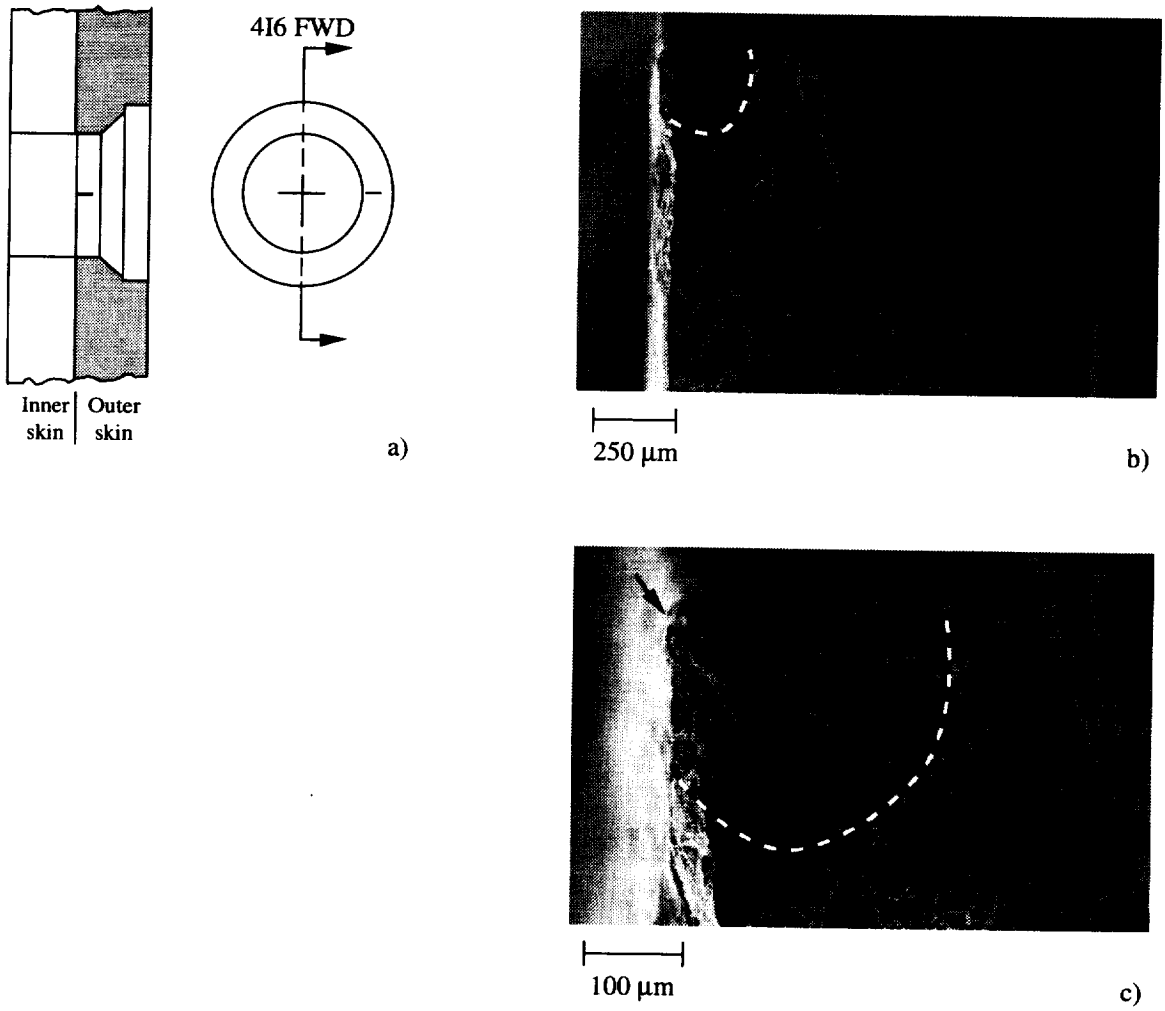

Figure 11.38 a) The schematic shows the rivet hole 4I6 configuration and the location of the outer skin fatigue crack oriented in the forward direction and about the 3 o'clock position. b) The SEM micrograph shows the fatigue crack fracture surface located at the outer skin rivet hole (top). The dashed line marks the fatigue crack front. c) The SEM micrograph shows the fatigue crack fracture surface at the rivet hole shank region. The arrow marks the likely site of crack initiation and the dashed line marks the fatigue crack front.

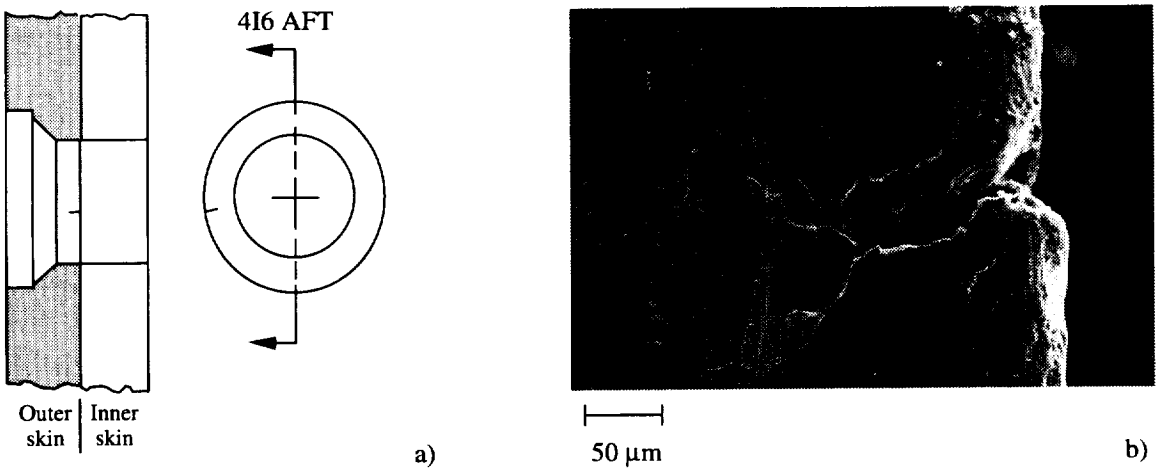

Figure 11.39 a) The schematic shows the rivet hole 4I6 configuration and the location of the outer skin fatigue crack oriented in the aft direction and below the 9 o'clock position. b) The SEM micrograph shows the small partially opened fatigue crack located at the inboard corner of the rivet hole shank region. The crack was partially opened during the destructive examination.

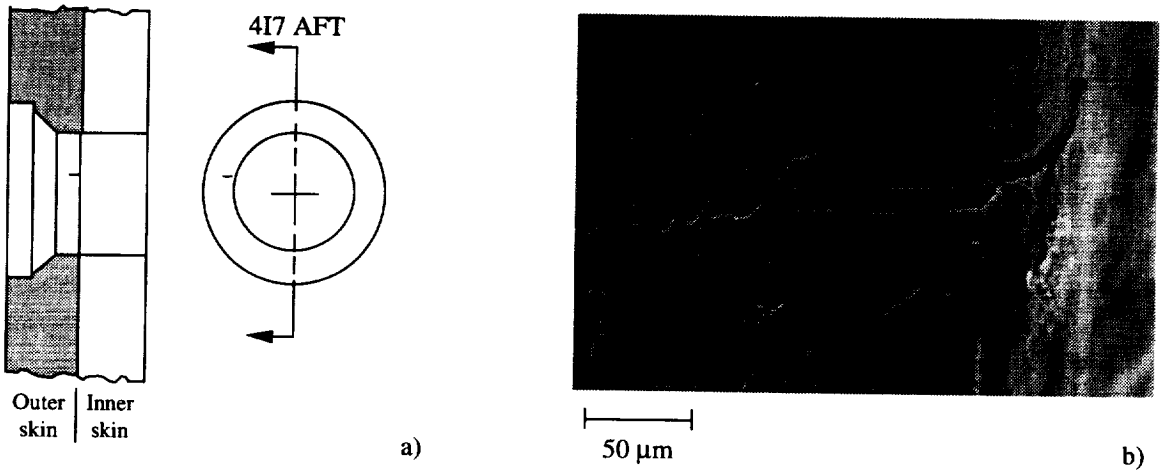

Figure 11.40 a) The schematic shows the rivet hole 4I7 configuration and the location of the outer skin fatigue crack oriented in the aft direction and above the 9 o'clock position. b) The SEM micrograph shows the small partially opened fatigue crack located at the inboard corner of the rivet hole shank region. The crack was partially opened during the destructive examination.

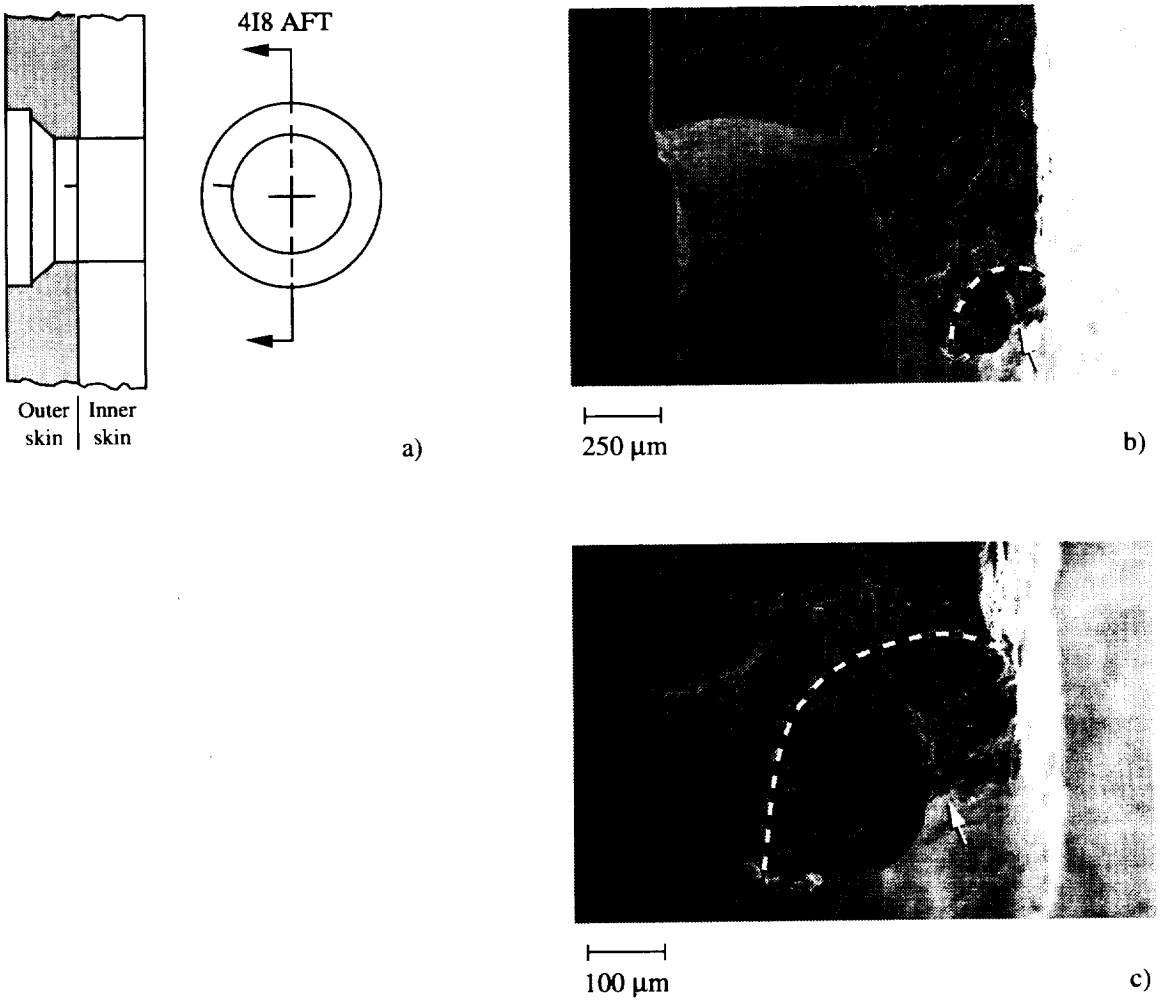

Figure 11.41 a) The schematic shows the rivet hole 4I8 configuration and the location of the outer skin fatigue crack oriented in the aft direction and above the 9 o'clock position. b) The SEM micrograph shows the fatigue crack fracture surface located at the outer skin rivet hole (bottom). The arrow marks the likely crack initiation site and the dashed line marks the fatigue crack front at high magnification. c) The SEM micrograph shows the fatigue crack fracture surface at the rivet hole shank region. The arrow marks the likely site of crack initiation and the dashed line marks the fatigue crack front.

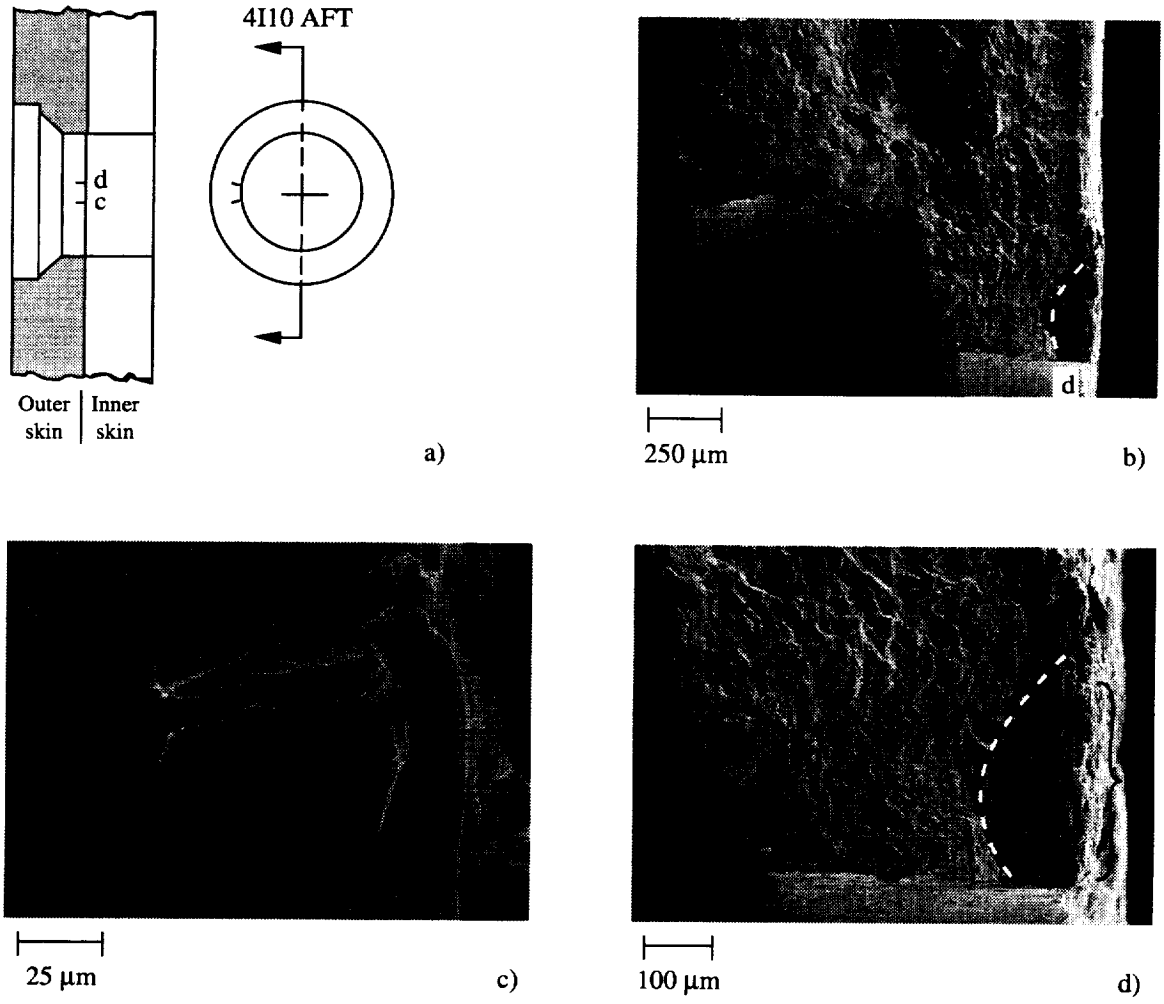

Figure 11.42 a) The schematic shows the rivet hole 4I10 configuration and the location of two outer skin fatigue cracks oriented in the aft direction and about the 9 o'clock position. b) The SEM micrograph shows the fatigue crack fracture surface located at the outer skin rivet hole (bottom). The dashed line marks the fatigue crack front. c) The SEM micrograph shows the inside surface of the rivet hole and a small partially opened fatigue crack (crack "c" in Figure 11.39.a) located at the inboard corner of the rivet hole. d) The SEM micrograph shows the fatigue crack fracture surface (crack "d" in Figure 11.39.a) at the rivet hole shank region at high magnification. The bracket marks the likely region of crack initiation along the faying surface and the dashed line marks the fatigue crack front.

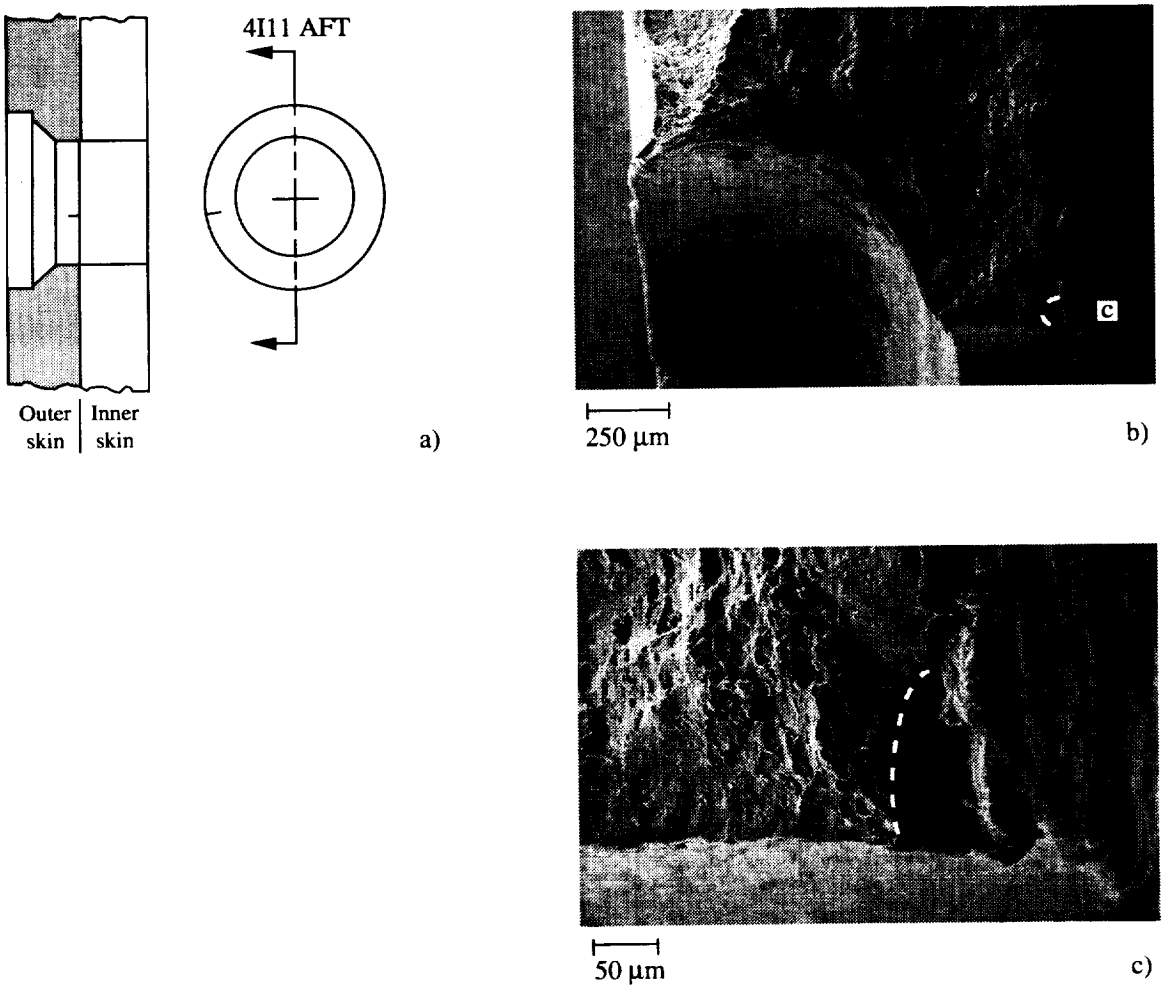

Figure 11.43 a) The schematic shows the rivet hole 4I11 configuration and the location of the outer skin fatigue crack oriented in the aft direction and below the 9 o'clock position. b) The SEM micrograph shows the location of a small fatigue crack (region "c") located at the inboard corner of the outer skin rivet hole. c) The SEM micrograph shows the fatigue crack, region "c" in Figure 11.40.b, located at the rivet hole shank region at high magnification. The dashed line marks the fatigue crack front.

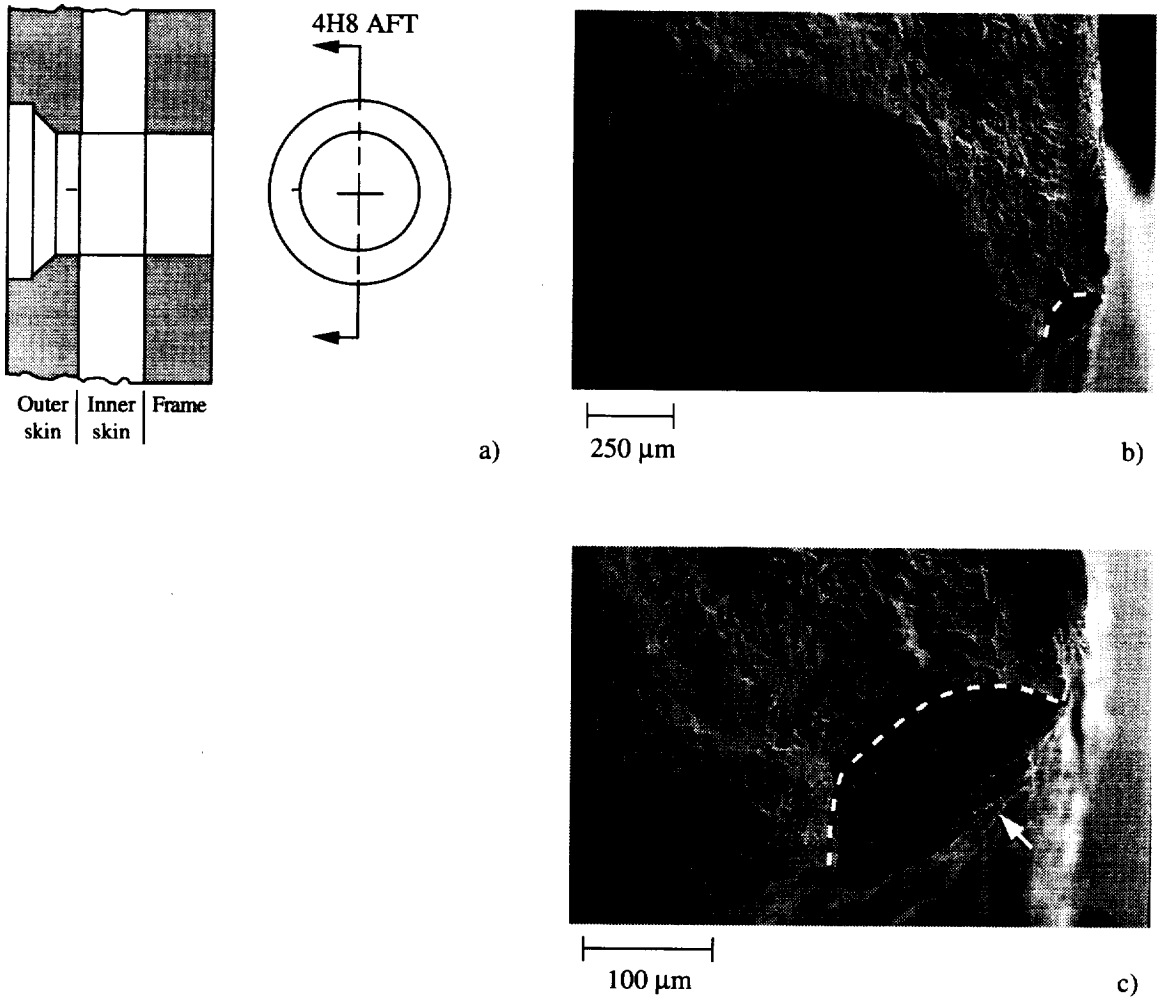

Figure 11.44 a) The schematic shows the rivet hole 4H8 configuration and the location of the outer skin fatigue crack oriented in the aft direction and about the 9 o'clock position. b) The SEM micrograph shows the location of a small fatigue crack located at the inboard corner of the outer skin rivet hole. The dashed line marks the fatigue crack front. c) The SEM micrograph shows the fatigue crack fracture surface at the rivet hole shank region at high magnification. The arrow marks the likely site of crack initiation and the dashed line marks the fatigue crack front.

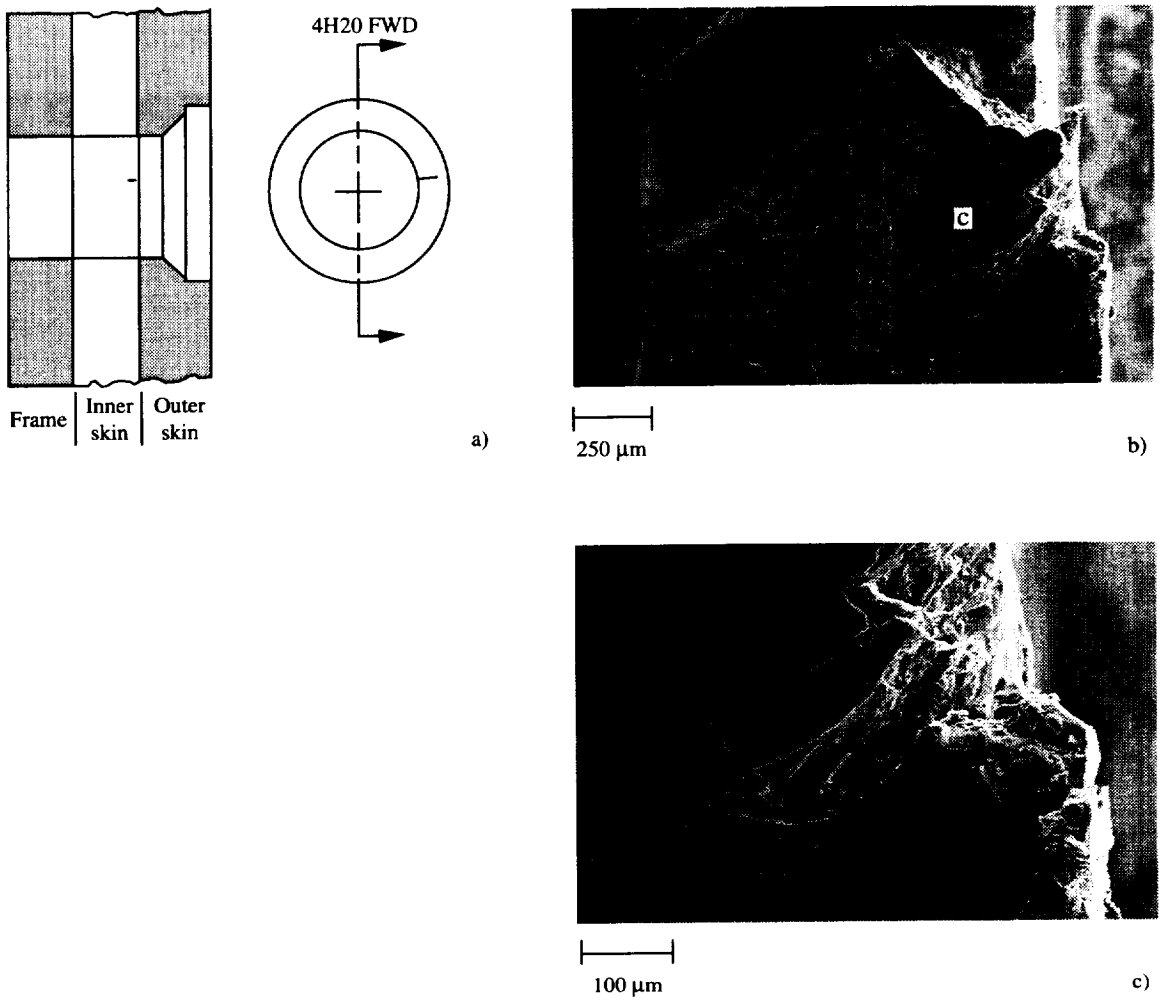

Figure 11.45 a) The schematic shows the rivet hole 4H20 configuration and the location of the inner skin fatigue crack oriented in the forward direction and above the 3 o'clock position. b) The SEM micrograph shows the inside surface of the inner skin rivet hole. A small partially opened fatigue crack is located below the main fracture surface at region "c". The crack was partially opened during the destructive examination. c) The SEM micrograph shows the small partially opened fatigue crack at high magnification at region "c" in Figure 11.42.b. The fatigue crack is located near the outboard corner of the inner skin.

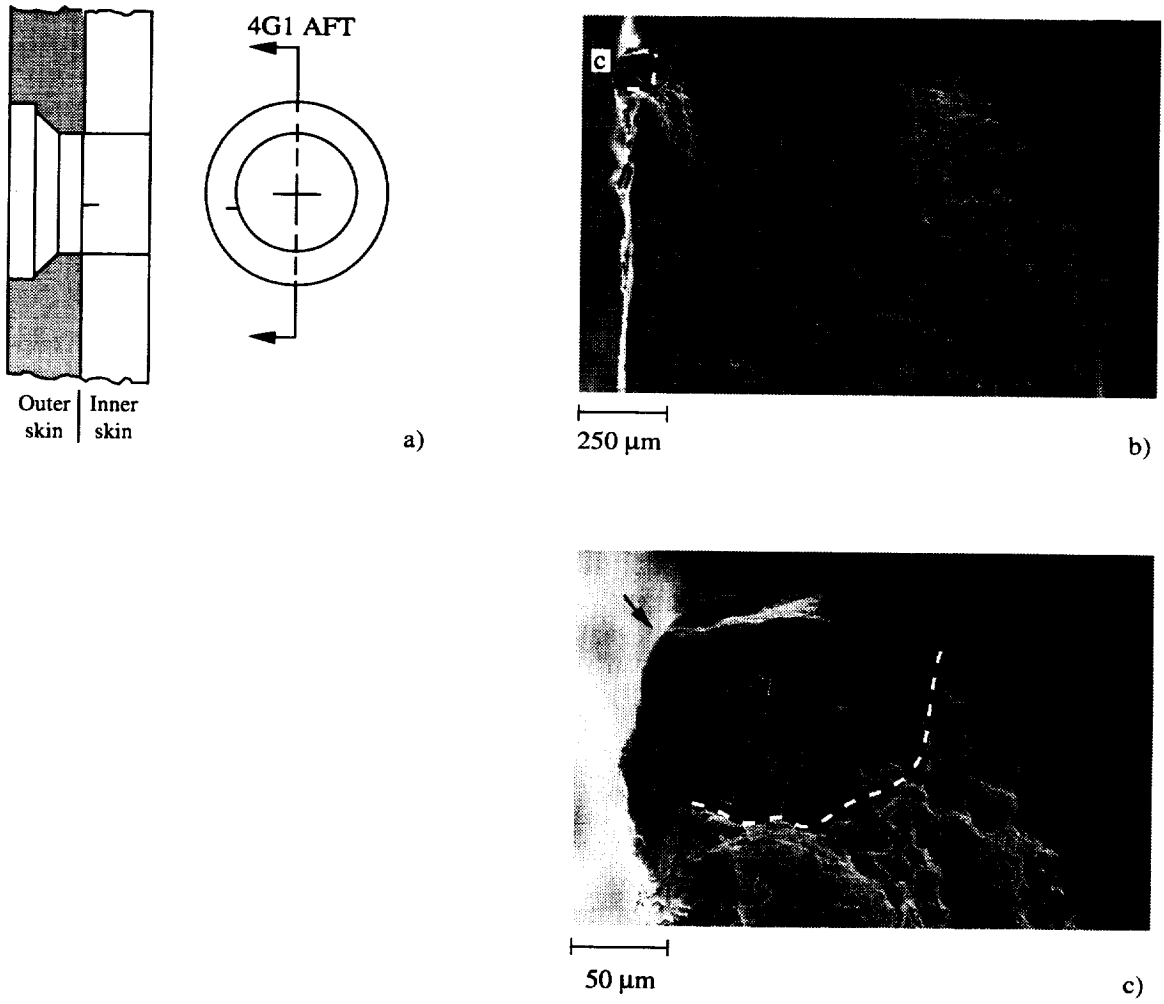

Figure 11.46 a) The schematic shows the rivet hole 4G1 configuration and the location of the inner skin fatigue crack oriented in the aft direction and below the 9 o'clock position. b) The SEM micrograph shows a small fatigue crack (region "c") located at the outboard corner of the inner skin rivet hole. The dashed line marks the fatigue crack front. c) The SEM micrograph shows the small fatigue crack region at high magnification. The arrow marks the likely site of fatigue crack initiation and the dashed line marks the fatigue crack front.

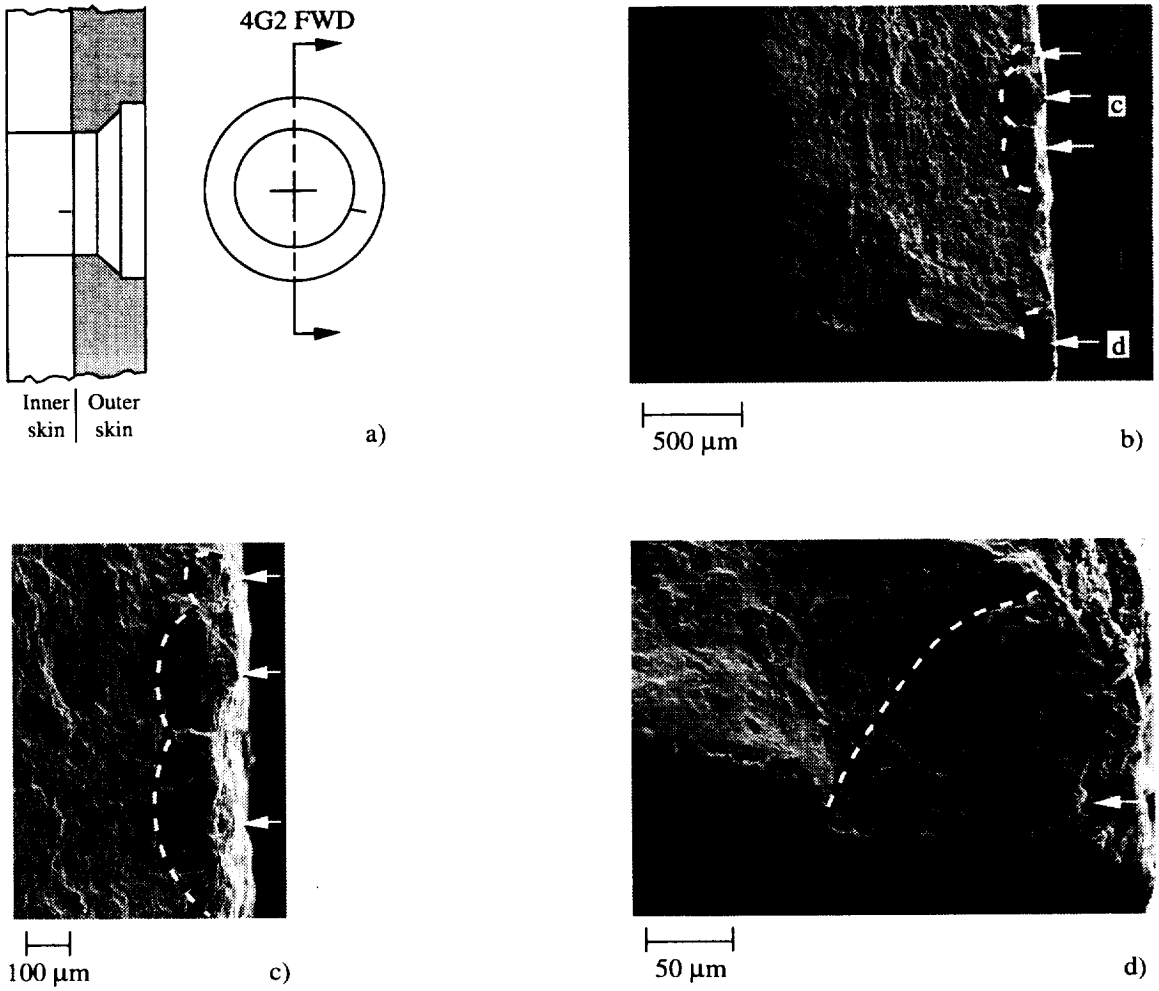

Figure 11.47 a) The schematic shows the rivet hole 4G2 configuration and the location of the outer skin fatigue crack oriented in the forward direction and about the 4 o'clock position. b) The SEM micrograph shows the location of small fatigue cracks located at the outboard corner and faying surface of the inner skin. The arrows mark the likely sites of fatigue crack initiation and the dashed lines mark the fatigue crack fronts. c) The SEM micrograph shows the fatigue crack, region "c" in Figure 11.44.b, along the inner skin faying surface at high magnification. The arrow marks likely sites of crack initiation and the dashed line marks the fatigue crack front. d) The SEM micrograph shows the outboard corner fatigue crack at region "d" in Figure 11.44.b. The arrow marks the crack initiation site and the dashed line marks the crack front.

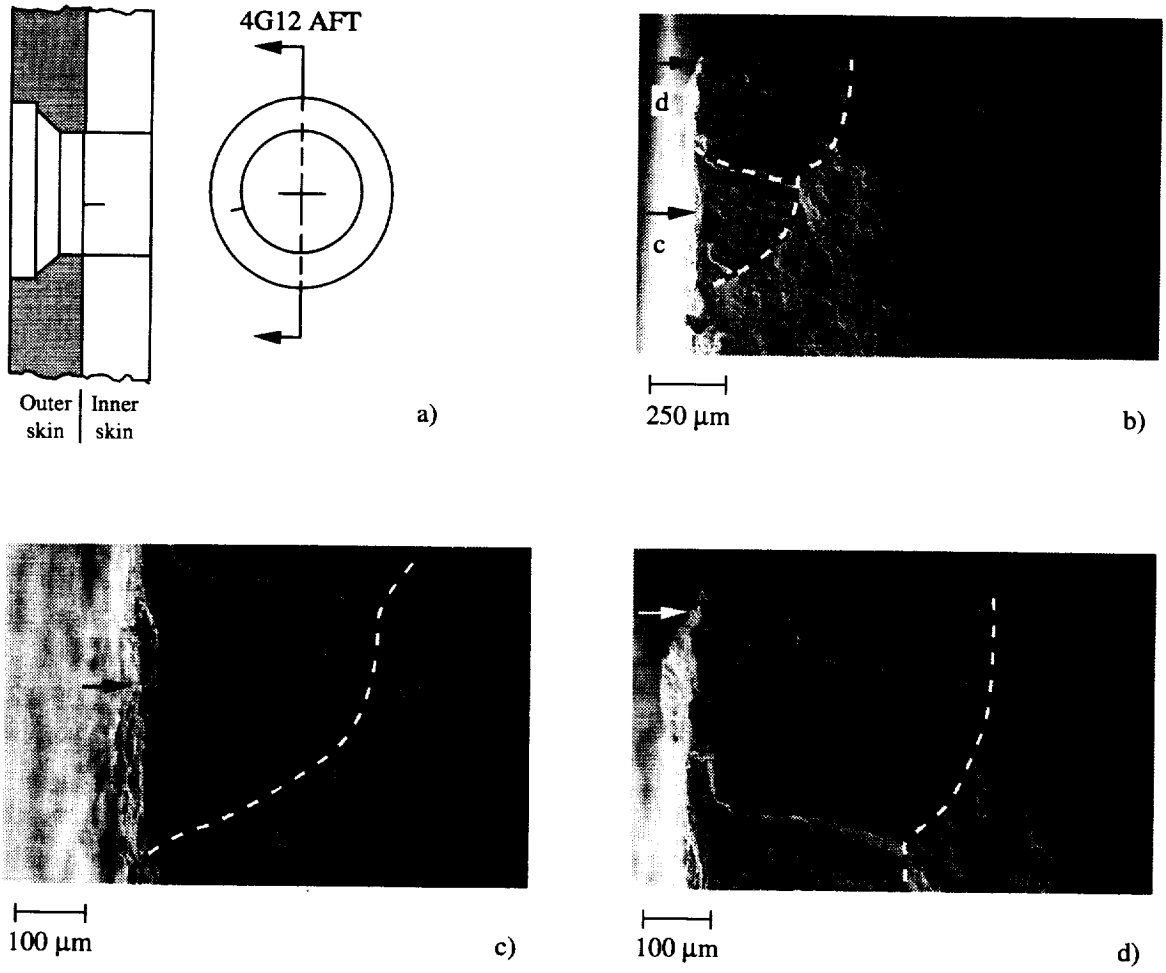

Figure 11.48 a) The schematic shows the rivet hole 4G12 configuration and the location of the inner skin fatigue crack oriented in the aft direction and below the 9 o'clock position. b) The SEM micrograph shows the fatigue crack fracture surface located at the outboard corner of the inner skin rivet hole. The arrows mark likely sites of crack initiation along the faying surface. The irregular shape of the fatigue crack front marked by the dashed lines suggests that two fatigue cracks coalesced at the fracture surface ridge (horizontal dashed line). c) The SEM micrograph shows the fatigue crack, region "c" in Figure 11.45.b, at high magnification. The arrow marks the crack initiation site and the dashed line marks the fatigue crack front. d) The SEM micrograph shows the fatigue crack region "d" in Figure 11.45.b at high magnification. The arrow marks the crack initiation site and the dashed line marks the fatigue crack front.

12. Crack Initiation and Crack Front Shape

The evolution of fatigue cracking from rivet holes contained in the lap splice joint is summarized in this section. Presented is the location of crack initiation and the final crack front shape for all fatigue cracks contained in the lap splice and tear strap regions. Collectively, these data identify the critical regions of crack initiation and the overall fatigue crack morphology of multi-site damage in the fuselage riveted lap splice structure.

12.1 Crack Initiation:

The schematics shown in Figures 12.1 and 12.2 summarize the cracking in lap splice bays 2, 3, and 4. The majority of lap splice outer skin fatigue cracks initiated along the faying surface (Figure 12.1) or at the inboard corner of the rivet hole and propagated as subsurface fatigue cracks for a substantial length before penetrating the outboard surface. Note that bays 3 and 4 exhibited three dominant crack initiation sites (circled numbers) along the faying surface Most fatigue cracks initiated along the faying surface or near the inboard corner of the rivet hole. Fewer fatigue cracks initiated in the rivet hole shank region. Lap splice inner skin fatigue cracks shown in Figure 12.2 are isolated to the bottom two rivet rows in bays 2, 3, and 4. Most inner skin fatigue cracks initiated at the inboard corner of the rivet hole. The inner skin cracks found in bays 3 and 4 are small compared to those observed in bay 2. Presumably, bay 2 inner skin loads were higher compared to inner skin loads in bays 3 and 4, a likely result of crack link-up that occurred along bay 2 outer skin upper rivet row. A summary of crack initiation sites in bay 2/3 and 3/4 tear strap regions are shown in Figures 12.3, 12.4, 12.5 and 12.6. Most of the fatigue cracks observed in the tear strap region initiated within the rivet hole or at the inboard rivet hole corner.

The majority of fatigue cracks found in the outer skin of the lap splice joint initiated along the faying surface under the rivet head. A summary of crack initiation location data for bays 2, 3, and 4 are shown in Figures 12.7, 12.8, and 12.9, respectively. These plots show the frequency of occurrence of outer skin fatigue crack initiation sites as a function of the distance (X) from the rivet hole along the faying surface. The data in Figure 12.7 shows the faying surface crack initiation site distribution for a total twenty-nine fatigue cracks observed in bay 2. Here, the location of 38 crack initiation sites are plotted; the number of initiation sites is larger than the total number of fatigue cracks because many fatigue cracks exhibited multiple initiation sites. It is important to note that a considerable number of cracks initiated a significant distance, ranging from 0.25 mm (0.01 inch) to 2.0 mm (0.08 inch), from the rivet hole. Crack initiation along the faying surface suggest that fretting damage between the inner and outer skin surfaces promote fatigue cracking in the lap splice joint rivet holes. Similar faying surface crack initiation distributions were observed for bays 3 and 4.

12.2 Crack Front Shape:

The summary of crack front shapes from outer skin fatigue cracks is also depicted in Figures 12.1 through 12.6. Indicated adjacent to each crack front is the number of fatigue cracks observed with similar final crack front shape and crack length. For example in Figure 12.1, two bay 2, four bay 3, and four bay 4 cracks exhibited similar crack front shapes at a crack length of 3B, where B is the skin thickness. Note that bay 2 contained 28 fatigue cracks of lengths greater than 3B; these cracks were located in the upper rivet row, where crack link-up occurred, forming the long crack. These results show that all outer skin fatigue cracks grow with similar crack front shapes and crack lengths range from two to three skin thicknesses (2B to 3B) before penetrating the outboard surface of the outer skin. Subsurface cracking noted in the outer skin may result from two effects, (1) out-of-plane bending, and/or (2) residual compressive stress imparted by the radial expansion of the rivet head into the counter bore region. Both effects limit fatigue crack growth in the outboard direction and possibly promote the observed outer skin subsurface fatigue cracking. Different crack front shapes are noted along the inner skin shown in Figure 12.2. The irregular inner skin crack front shape noted in bay 2 is likely due to multiple cracks coalescing along the outboard surface.

The schematic shown in Figure 12.3 reveals the crack front shape for fatigue cracks contained in the lap

splice outer skin for the 2/3 and 3/4 tear strap regions. All fatigue cracks found in the outer skin were small, although, these limited data suggest similar crack front shapes to those contained in bays 2, 3, and 4. Fatigue cracks contained in the lap splice inner skin, Figure 12.4, and tear straps, Figures 12.5 and 12.6, are nearly semicircular or quarter-circular in shape. This symmetry may suggest minimal out-of-plane loading in the tear strap.

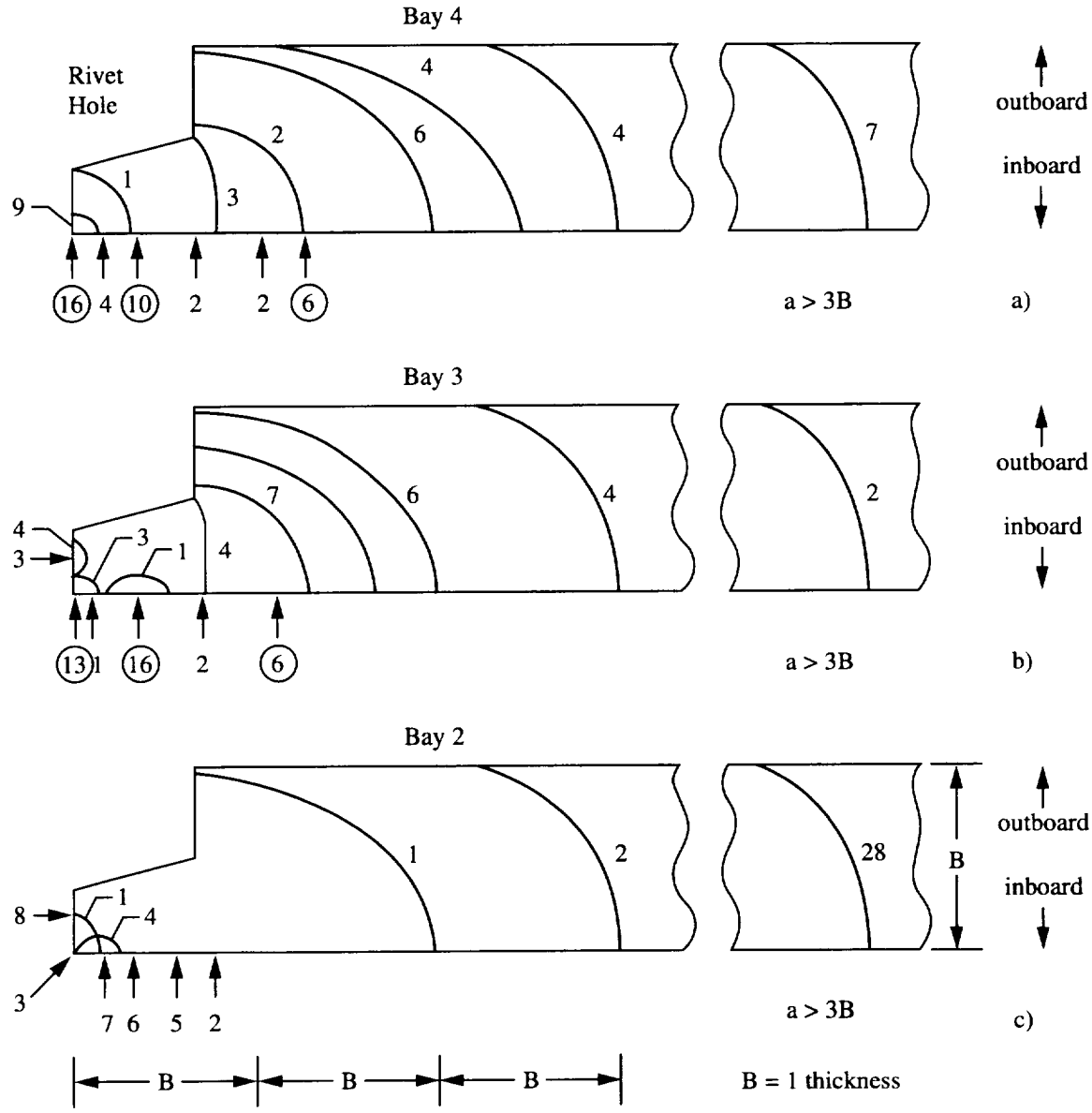

Figure 12.1 A schematic of the lap splice outer skin rivet hole region summarizes the location of fatigue crack initiation sites (arrows) and the final fatigue crack front configuration (curved lines) for a) bay 4, b) bay 3, and c) bay 2. The numbers denote the quantity of fatigue cracks or initiation sites found in the given crack front and initiation regions.

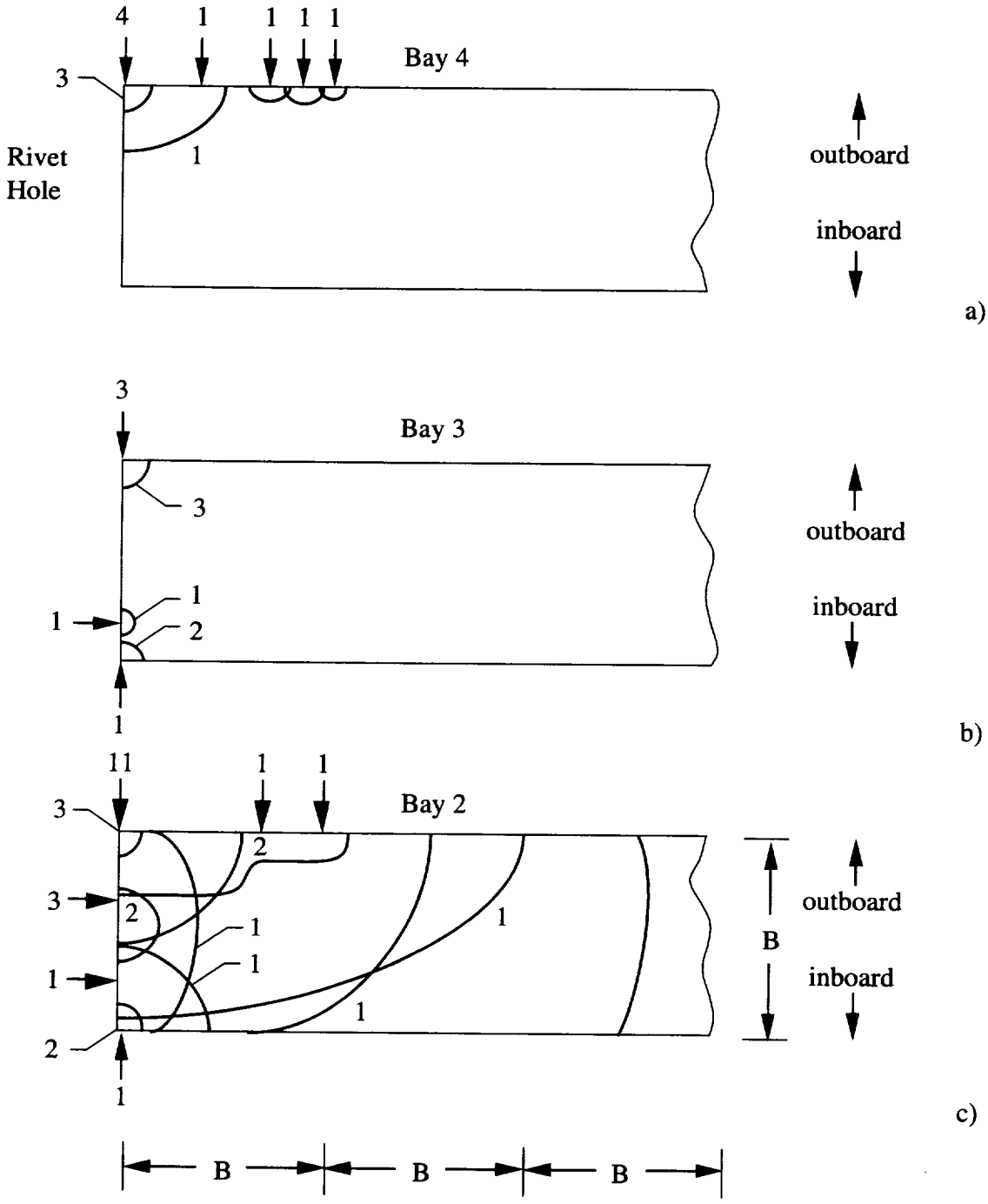

Figure 12.2 A schematic of the lap splice inner skin rivet hole region summarizes the location of fatigue crack initiation (arrows) and the final fatigue crack front configuration (curved lines) for a) bay 4, b) bay 3, and c) bay 2. The numbers denote the quantity of fatigue cracks or initiation sites found in the given crack front and initiation regions.

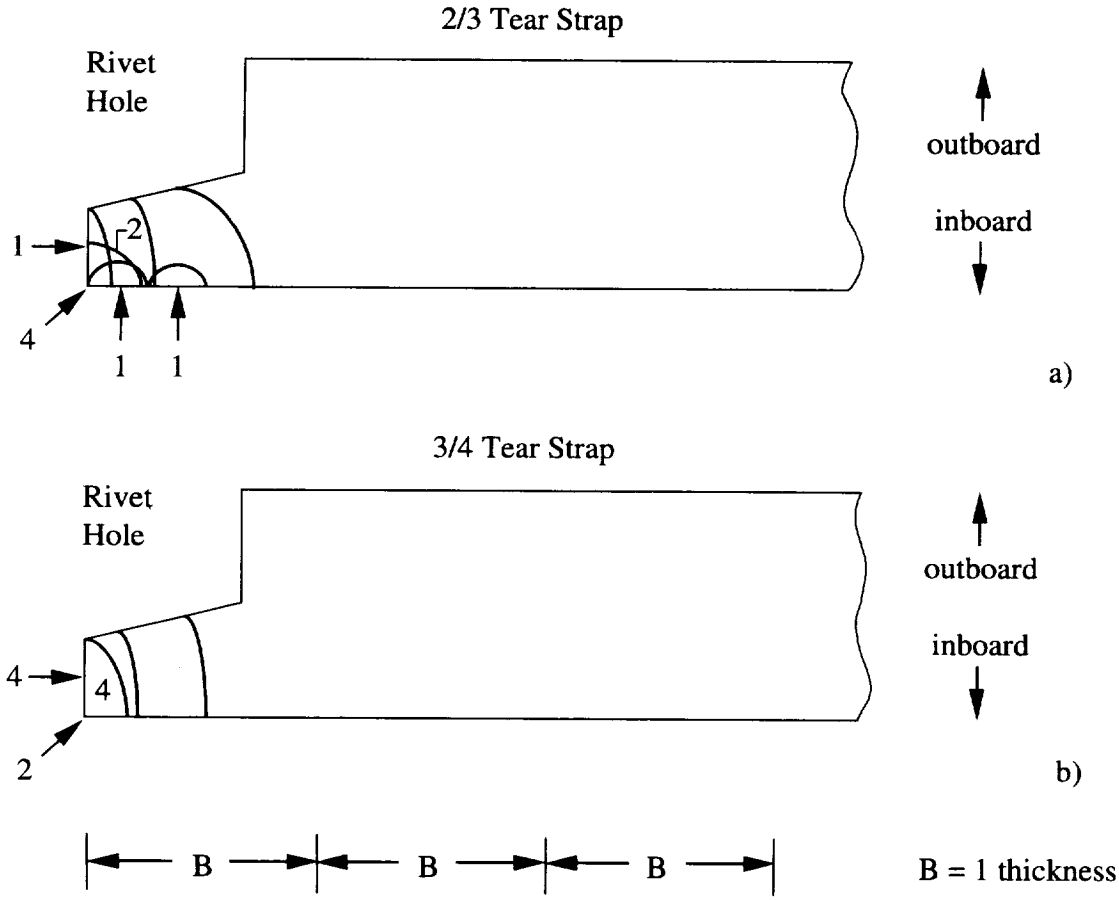

Figure 12.3 A schematic of a) bay 2/3 tear strap and b) bay 3/4 tear strap outer skin rivet hole region and the location of fatigue crack initiation (arrows) and the final fatigue crack front configuration (curved lines). The numbers denote the quantity of fatigue cracks or initiation sites found in the given crack front and initiation regions.

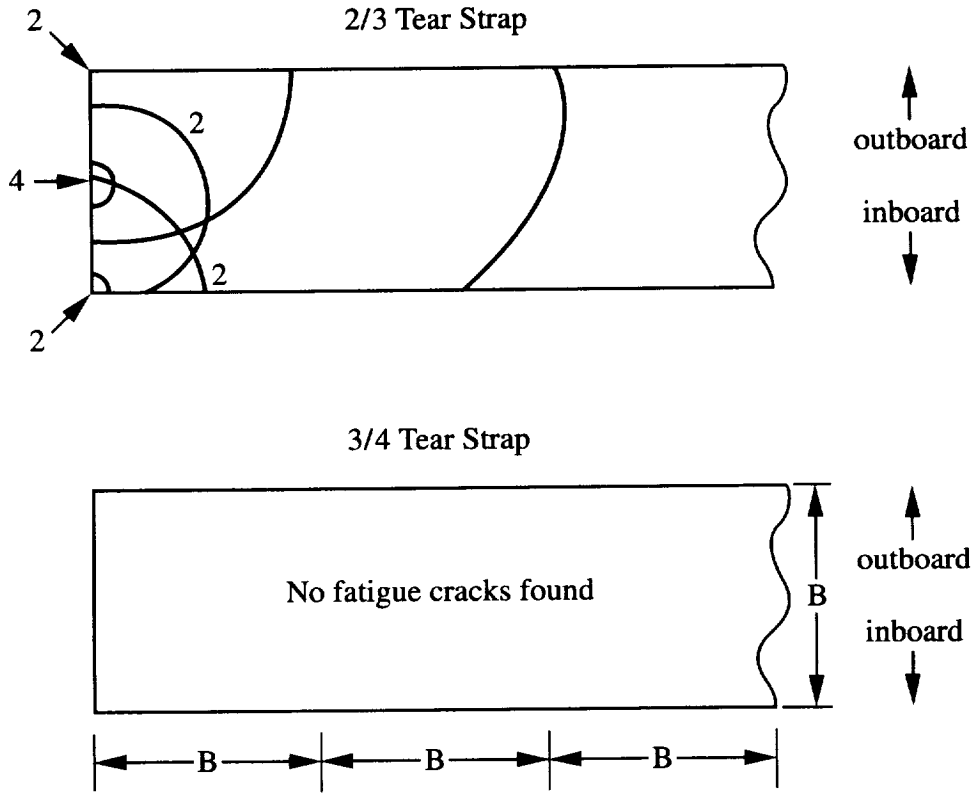

Figure 12.4 A schematic of a) bay 2/3 tear strap and b) bay 3/4 tear strap inner skin rivet hole region and the location of fatigue crack initiation (arrows) and the final fatigue crack front configuration (curved lines). The numbers denote the quantity of fatigue cracks or initiation sites found in the given crack front and initiation regions.

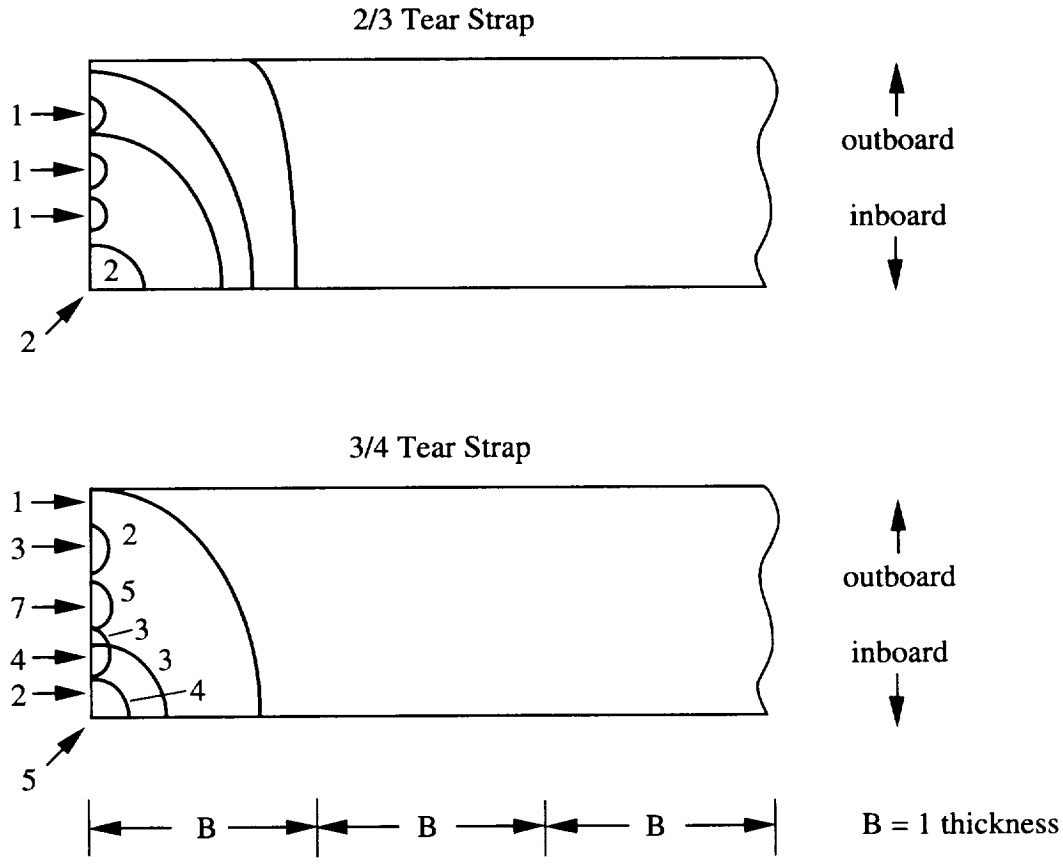

Figure 12.5 A schematic of a) bay 2/3 tear strap and b) bay 3/4 tear strap upper tear strap rivet hole region and the location of fatigue crack initiation (arrows) and the final fatigue crack front configuration (curved lines). The numbers denote the quantity of fatigue cracks or initiation sites found in the given crack front and initiation regions.

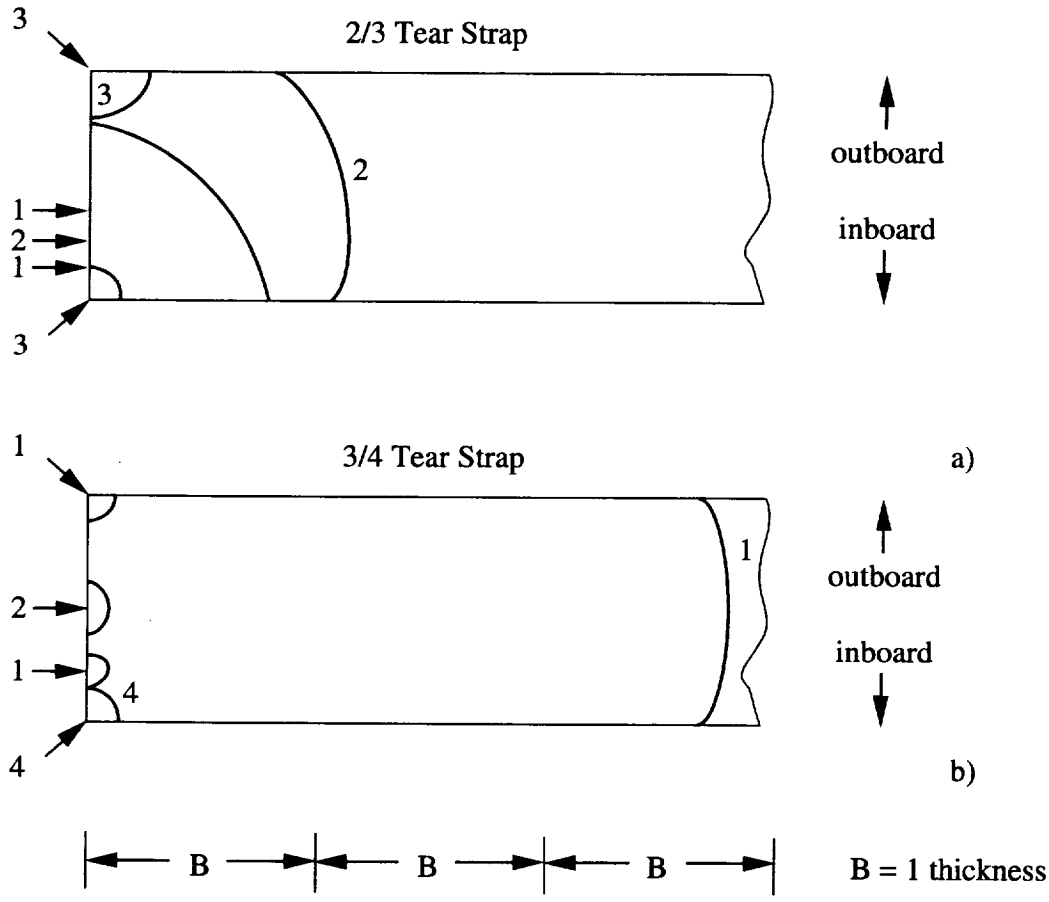

Figure 12.6 A schematic of a) bay 2/3 tear strap and b) bay 3/4 tear strap lower tear strap rivet hole region and the location of fatigue crack initiation (arrows) and the final fatigue crack front configuration (curved lines). The numbers denote the quantity of fatigue cracks or initiation sites found in the given crack front and initiation regions.

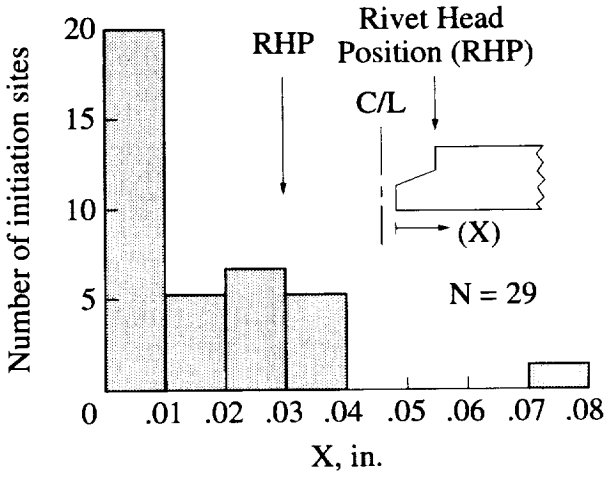

Figure. 12.7 The graph shows the distribution of bay 2 fatigue crack initiation sites located along the X-direction (faying surface) defined in the schematic. For orientation purposes the edge of the rivet hole (RHP) is shown at X=0.03" from the edge of the rivet shank.

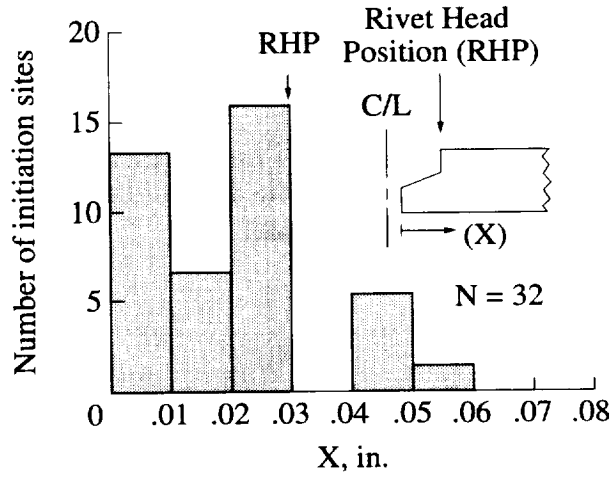

Figure 12.8 The graph shows the distribution of bay 3 fatigue crack initiation sites located along the X-direction (faying surface) defined in the schematic. For orientation purposes the edge of the rivet hole (RHP) is shown at X=0.03" from the edge of the rivet shank.

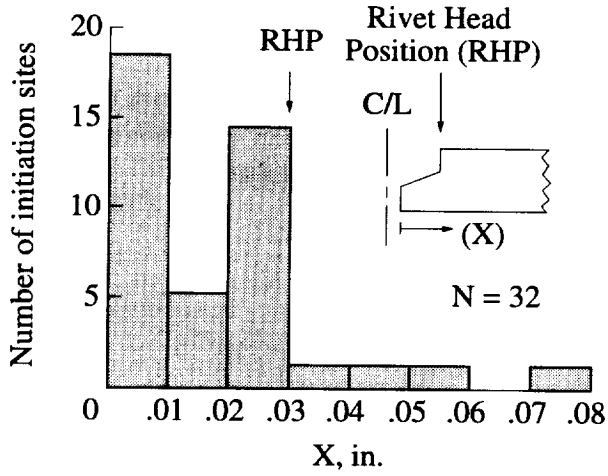

Figure 12.9 The graph shows the distribution of bay 4 fatigue crack initiation sites located along the X-direction (faying surface) defined in the schematic. For orientation purposes the edge of the rivet hole (RHP) is marked at 0.03" from the edge of the rivet shank.

13. Faying Surface Fretting

13.1 Observations:

The observation that faying surface crack initiation occurred in a damaged region characterized by a black aluminum oxide debris zone confirms that upper rivet row outer skin fatigue cracking was initiated by a fretting damage mechanism The results of the destructive examination revealed that the majority of lap splice joint outer skin fatigue cracks initiated along the faying surface. The typical outer skin fatigue crack initiated in the clad layer and within a localized region adjacent to the rivet hole as shown in Figures 7.25, 7.26, and 7.28. Figure 7.26 shows a small (30 μm in depth) fatigue crack located in the damaged (roughened surface) clad layer which is nominally 60 μm to 80 μm thick. The clad layer fatigue cracks shown in Figures 7.25 and 7.28 exhibit an elongated morphology, suggesting multiple crack initiation along the damaged faying surface followed by crack coalescence. Further examination of the fatigue crack initiation sites along the lap splice upper rivet row, revealed a black oxide debris region on the outer skin faying surface and around the rivet hole circumference.

13.2 Characterization of Faying Surface Fretting:

To relate upper rivet row fatigue cracking to fretting damage, it was necessary to document the extent of black oxide debris. Depicted in Figures 13.1, 13.2, and 13.3 is an estimate (area drawn to scale) of fretting debris (black oxide region) observed on the faying surface of bays 2, 3, and 4, respectively. The rivet hole locations containing fretting initiated fatigue cracks are identified and small arrows mark the approximate location of cracking. To obtain an full understanding of the fretting initiated crack morphology, the reader should refer to the fracture surface micrographs (Sections 7, 9, and 11) for those rivet location containing fretting initiated fatigue cracks. An estimate of the extent of fretting was performed by determining the arithmetic average of fretted area per the procedure shown in Figure 13.4. Here, a scaling factor was assigned to estimate the amount of black oxide area in each quadrant. The value of "0" was assigned when no damage or black oxide was observed and "5" represented the highest degree of fretting. A "fretting average" (FA) was estimated for each rivet position and is summarized for each rivet hole position in the Figures 13.1, 13.2, and 13.3. Correlation's of FA and cracking showed that substantial fretting (FA > 3.0) was present in the majority of regions that contained fatigue cracks that initiated along the faying surface. The following observations were made from the fretting debris estimates.

1. The upper rivet row J contained the greatest evidence of fretting damage (highest FA level). The majority of upper rivet row fatigue cracks initiated along the faying surface.
2. Bottom rivet row G contained the second highest FA level and also exhibited a few fatigue cracks that initiated along the faying surface.
3. Middle rows, H and I, contained significantly less evidence of fretting compared to rows J and G. One fatigue crack initiated at the faying surface.

The tear strap regions contained little evidence of fretting along the faying surfaces. Here, all but one fatigue crack initiated at rivet hole corners and along the rivet hole surface; one fatigue crack initiated at the faying surface.

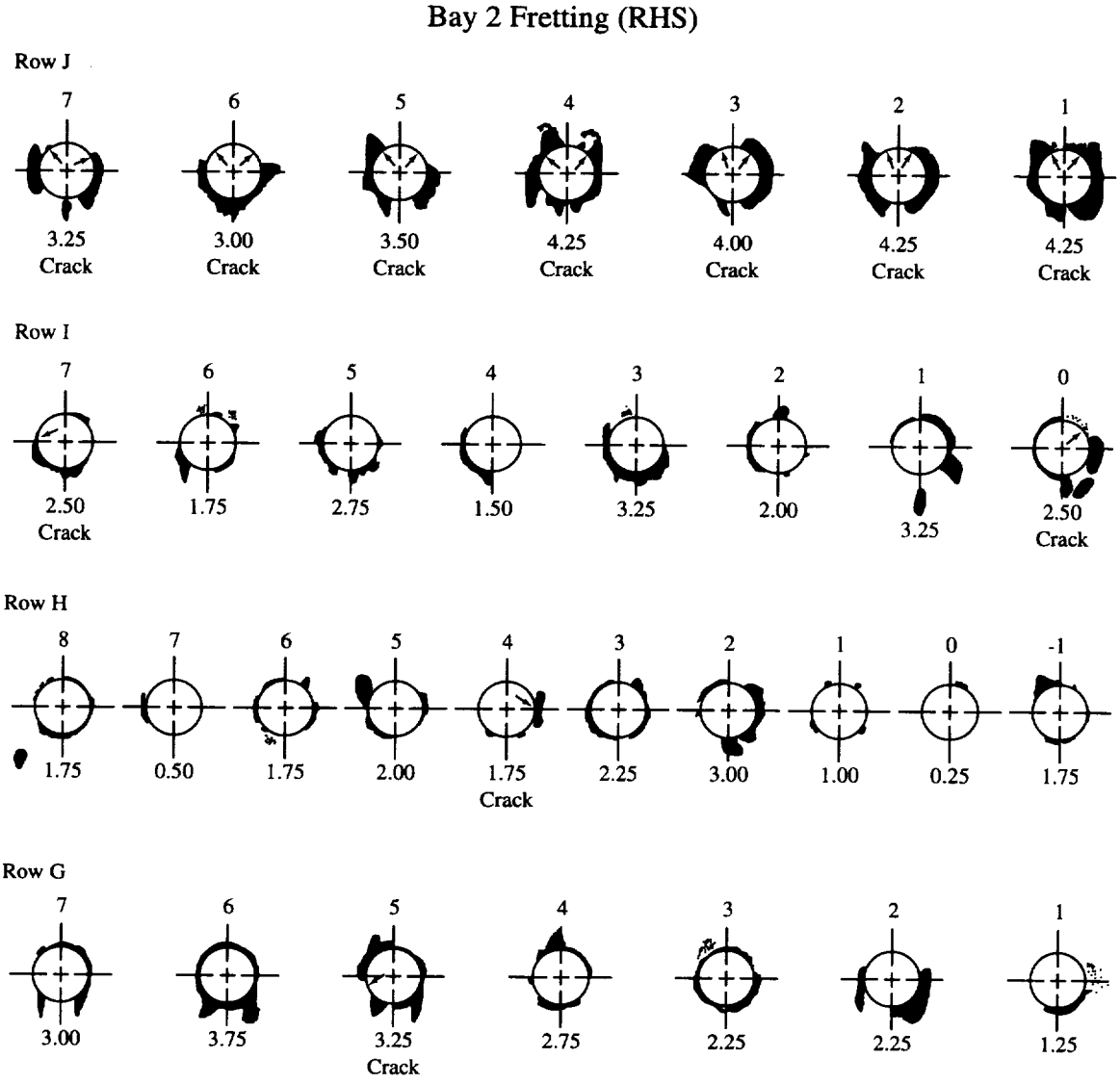

Figure 13.1a A schematic showing a portion of the inboard surface of the bay 2 lap splice outer skin. Illustrated is the location of black oxide fretting debris, the location of fretting initiated fatigue cracks (arrows), and the fretting average (FA) value defined in Figure 13.4.

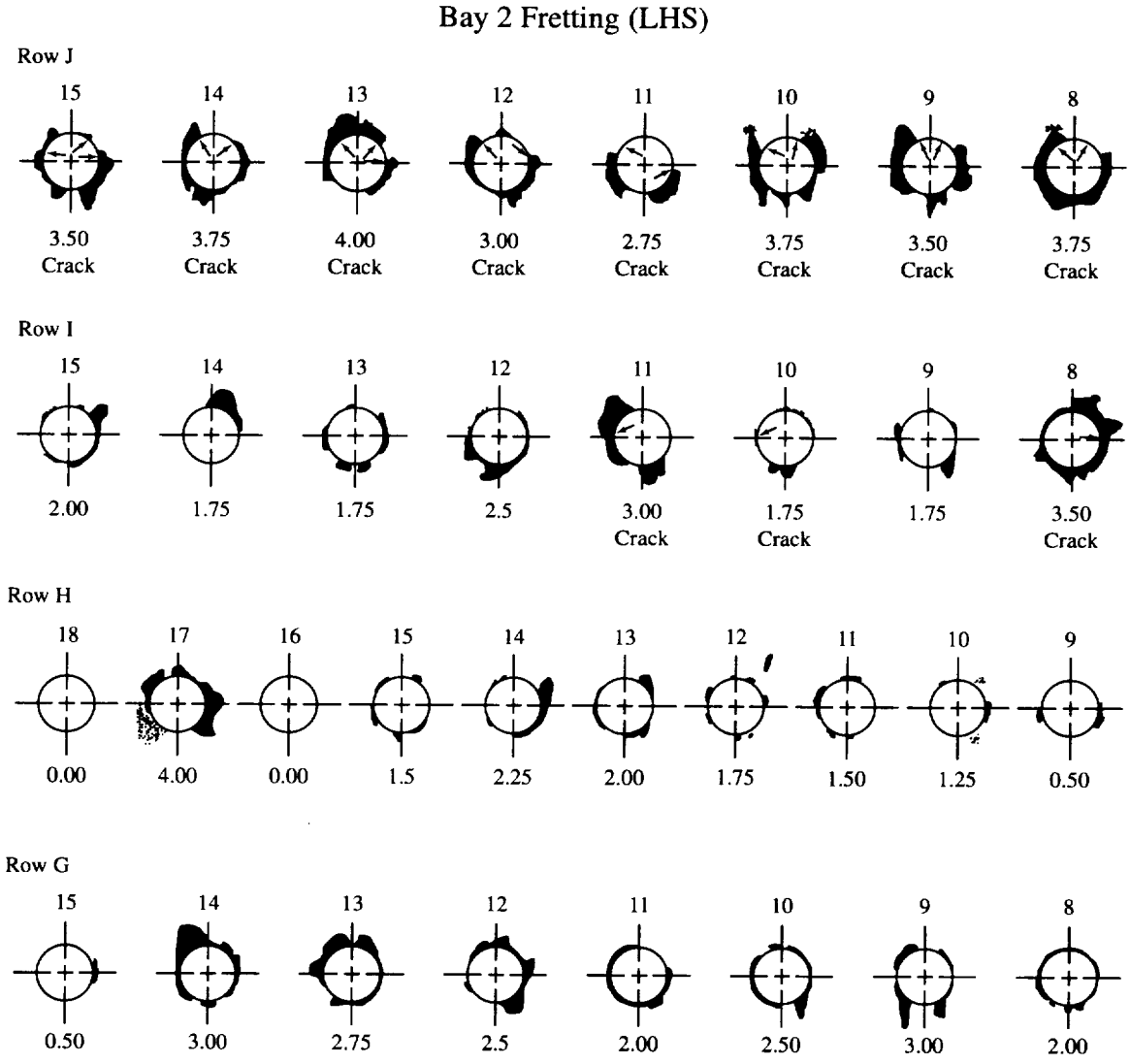

Figure 13.1b A schematic showing a portion of the inboard surface of the bay 2 lap splice outer skin. Illustrated is the location of black oxide fretting debris, the location of fretting initiated fatigue cracks (arrows), and the fretting average (FA) value defined in Figure 13.4.

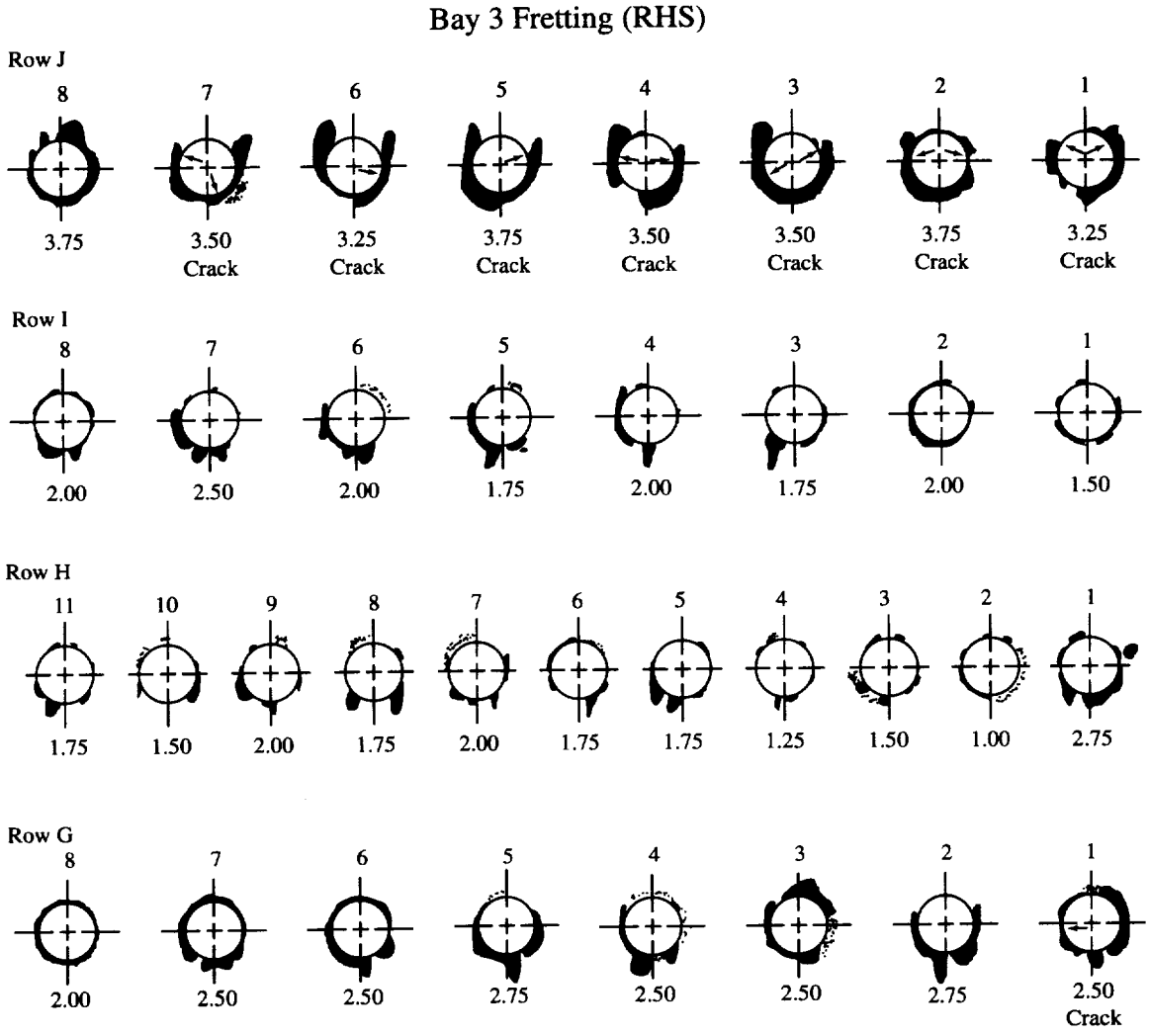

Figure 13.2a A schematic showing a portion of the inboard surface of the bay 3 lap splice outer skin. Illustrated is the location of black oxide fretting debris, the location of fretting initiated fatigue cracks (arrows), and the fretting average (FA) value defined in Figure 13.4.

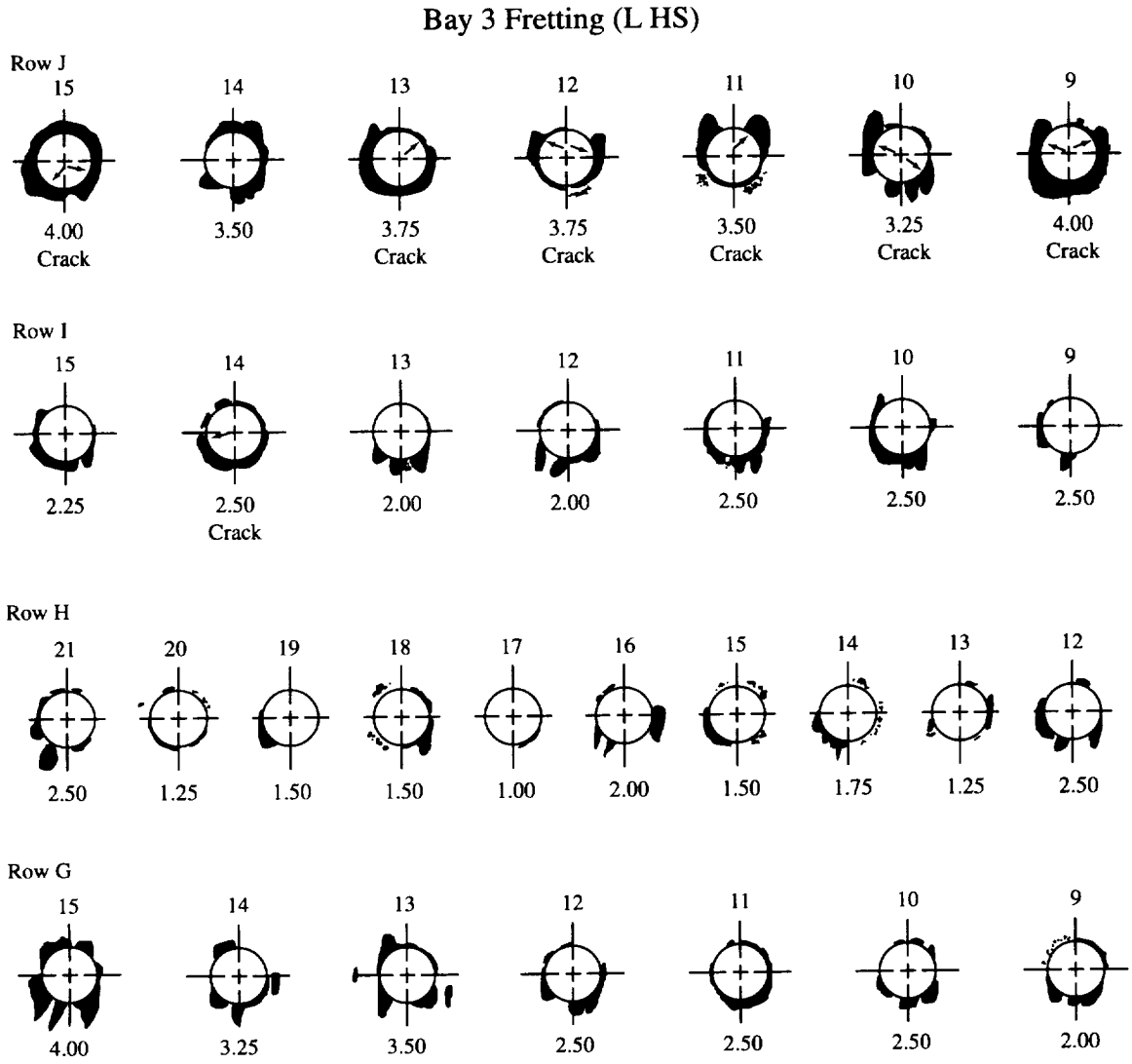

Figure 13.2b A schematic showing a portion of the inboard surface of the bay 3 lap splice outer skin. Illustrated is the location of black oxide fretting debris, the location of fretting initiated fatigue cracks (arrows), and the fretting average (FA) value defined in Figure 13.4.

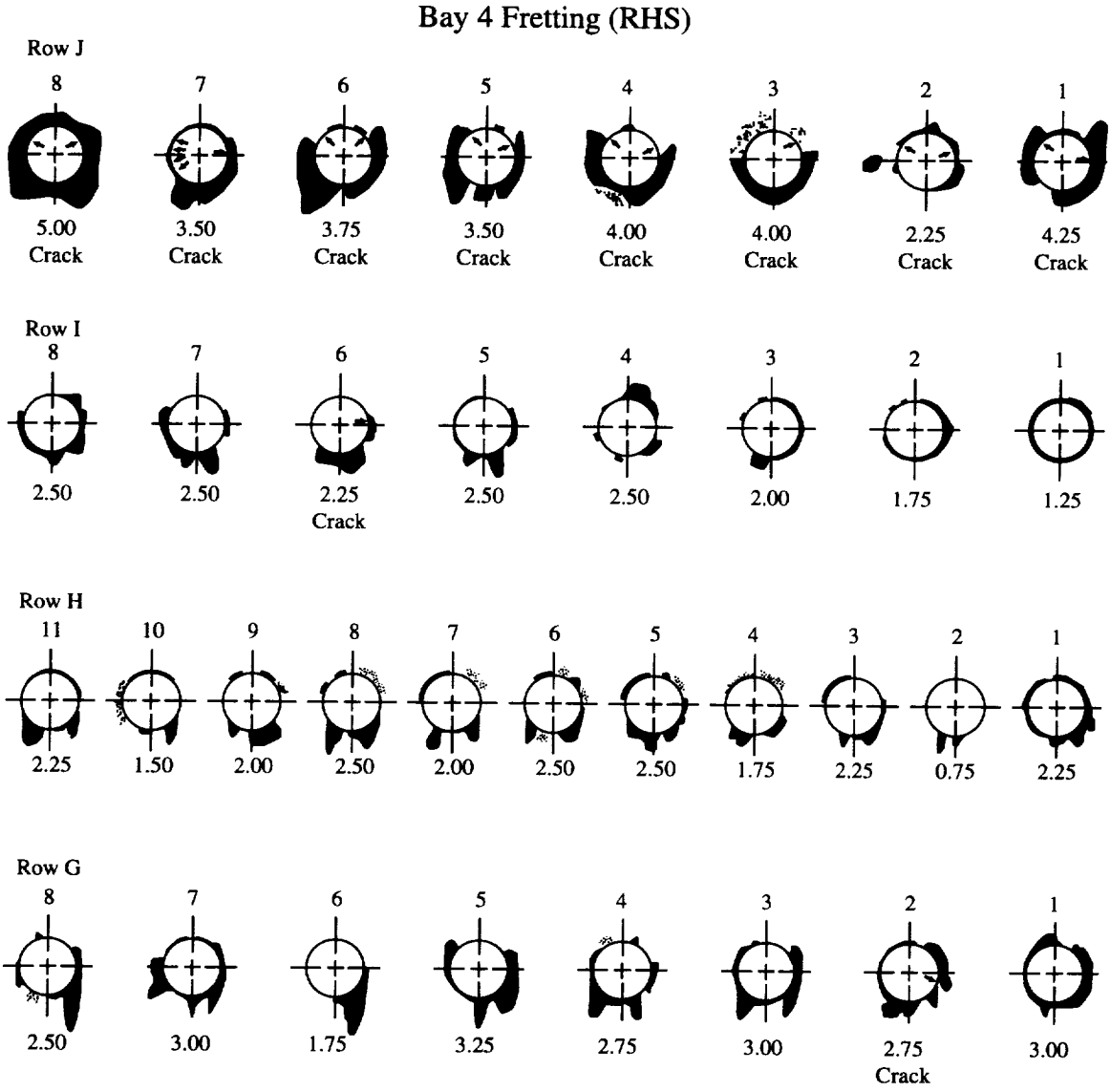

Figure 13.3a A schematic showing a portion of the inboard surface of the bay 4 lap splice outer skin. Illustrated is the location of black oxide fretting debris, the location of fretting initiated fatigue cracks (arrows), and the fretting average (FA) value defined in Figure 13.4.

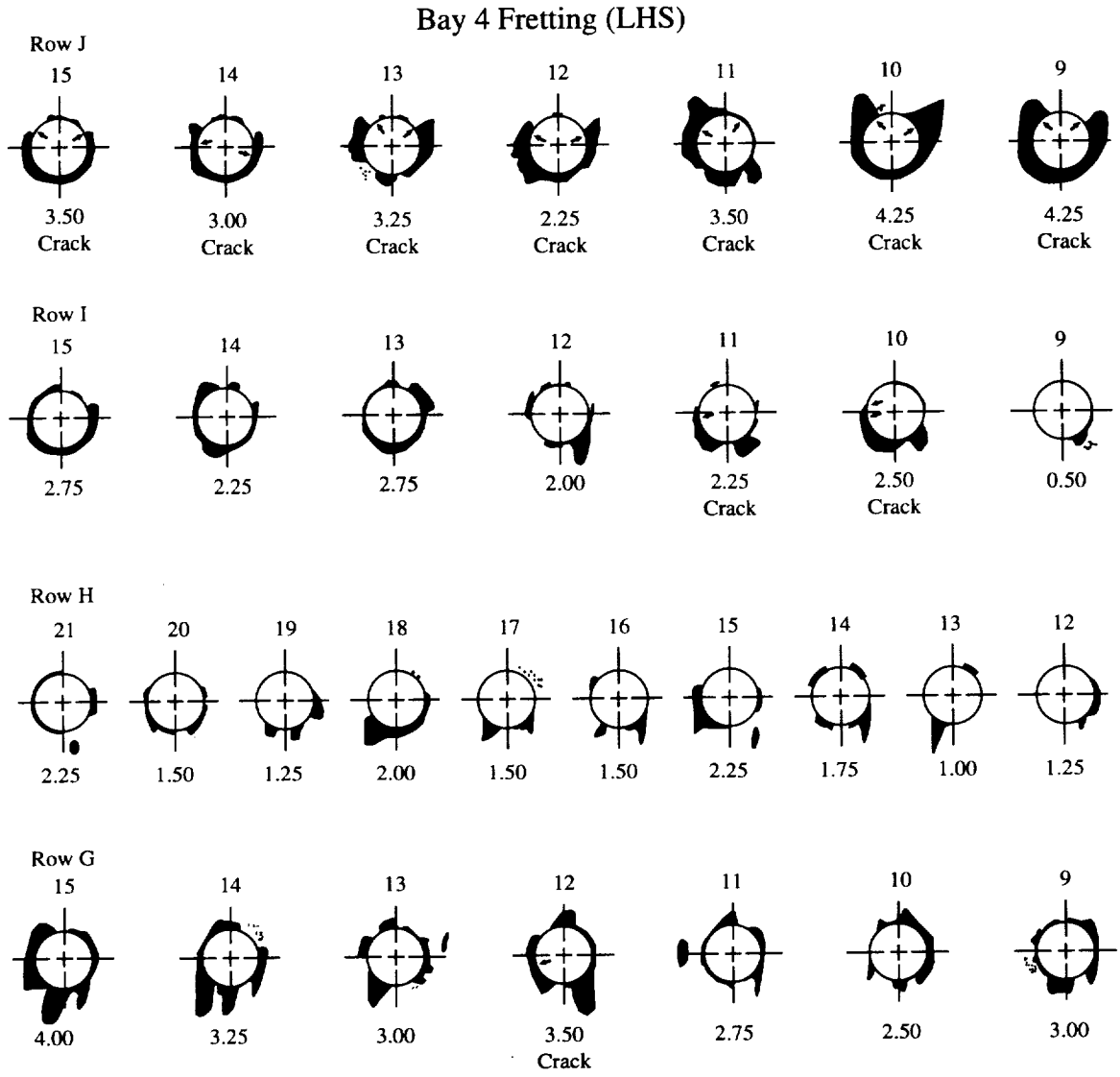

Figure 13.3b A schematic showing a portion of the inboard surface of the bay 3 lap splice outer skin. Illustrated is the location of black oxide fretting debris, the location of fretting initiated fatigue cracks (arrows), and the fretting average (FA) value defined in Figure 13.4.

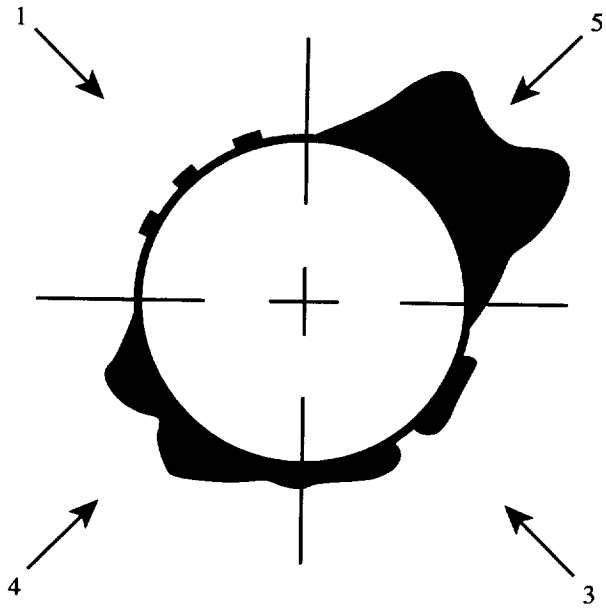

Fretting average = (1 + 5 + 4 + 3)/4 = 3.25

Figure 13.4 A schematic showing the procedure for quantification of fretting by assigning a fretting average to fretting damage (amount of black oxide present between the faying surfaces). Each of four quadrants is assigned a number from 0-5 that describes the total area of black oxide present. The four values are then averaged to obtain the fretting average.

14. Fatigue Crack Growth - Marker Band Analysis

An understanding of small crack growth kinetics is paramount to the prediction of the onset of WFD in airframe structure. To determine the fatigue crack length (a) versus pressure cycle (N) history of small fatigue cracks contained in the lap splice joint, a detailed analysis of fracture surface marker bands was performed on the upper rivet row fatigue cracks contained in bays 3 and 4 outer skin. Characterized herein are the fatigue crack growth characteristics of cracks ranging in size from 0.10 mm (0.004 in.) to 4.29 mm (0.169 in).

14.1 Fatigue Fracture Surface Marker Band Analysis:

The fatigue fracture surface of aluminum alloys, such as 2024T3, exhibit well defined crack arrest marks called fatigue striations. The fact that striations represent successive positions of the crack front enables investigators to theoretically determine the exact position of the crack front as function of load cycle. By introducing subtle changes in the applied load, groups of microscopic striations, termed marker bands, can be introduced to mark the fatigue fracture surface to facilitate locating the crack front by fractography. After every 10,000 (10K) full pressure cycles, a coded block of pressure cycles containing a periodic sequence of alternating full and reduced pressure cycles was used to mark the fracture surface. The combination of full and reduced pressure loads mark the fatigue crack fracture surface by creating microscopic features along the crack front that are easily detected by optical or scanning electron microscopy (SEM)[1]. Figure 14.1 shows SEM micrographs that reveal the distinctive fracture surface marker bands that correspond to the location of the fatigue crack front at 30,000, 40,000, and 50,000 pressure cycles.

Fatigue fracture surfaces from thirty rivet holes contained in bays 3 and 4 upper row rivet row J were examined for the presence marker bands. No marker band data was obtained from bay 2; here, the upper rivet row fracture surfaces were damaged by out-of-plane movement during the formation of the long bay 2 crack. The bay 2 upper rivet row fracture surfaces were also obscured by a thick tenacious oxide layer that could not be removed without further damaging the specimen. Summarized in this section are the marker band analysis results from those fracture surfaces that contained definitive marker bands along the upper rivet row.

14.2 Marker Band Analysis Procedure:

Detailed fractography required the cleaning of each fracture surface to remove black surface oxides that obscured portions of the fatigue crack. The cleaning process required acetone, acetone-based adhesive (butyl acetate was used for this study), and acetate thin film. The acetone-adhesive mixture was applied to the acetate film and fracture surface. The film was pressed firmly onto the fracture surface, dried for about ten minutes, and removed from the fracture surface. The process of removing the dried adhesive from the fatigue fracture surface lifted the black oxides from the specimen. The specimen was cleaned in a ultrasonic bath of acetone, dried, and examined optically at 400X. This cleaning process was repeated four to ten times until the specimen was adequately cleaned before marker band analysis was performed.

Optical microscopy, at magnifications of 400X to 600X, was the primary tool used to search for and locate the marker bands. Scanning electron microscopy was used to investigate regions that required extremely high resolution. Marker band locations were recorded in two dimensional space with an (x,y) coordinate system. An arbitrary reference point on the fracture surface was chosen for each specimen as the coordinate origin and a (0,0) coordinate value was assigned to it. Points along each marker band were located by and x and y dimension relative to the origin; this allowed each marker band to be plotted and the accurate determination of fatigue crack lengths between marker bands.

---

[1] Marker band techniques have been used by many investigators. Refer to McMillan, J. C., and Pelloux, R. M. N., "Fatigue Crack Propagation Under Program and Random Loads", *Fatigue Crack Propagation*, ASTM STP 415, Am. Soc. Testing Mats., 1967, p. 105, for a comprehensive study of marker bands.

14.3 Mapping of Marker Band Locations:

Summarized in Figures 14.2 through 14.35 are data that identify the location of all marker bands found on the fracture surfaces from upper rivet row fatigue cracks contained in bays 3 and 4. A schematic of the outer skin counter bore rivet hole region (aft or forward orientation) is shown with the approximate position of each marker band plotted relative to a reference point labeled (0,0). Depending on the number of marker bands found on the fracture surface, the schematic reveals the crack front shape as the crack grew from the initiation region marked by an arrow or bracket. Each figure also lists the coordinates of each marker band and crack front, the marker band code and cycle count, and comments on marker band region quality.

14.4 Determination of Crack Length From Marker Bands:

Tables 14.1 and 14.2 list the crack length and corresponding pressure cycle for all marker band and final fatigue crack front locations found in bays 3 and 4 upper rivet row, respectively. Crack lengths were determined by plotting the coordinates established for each marker band and crack front, similar to the schematics shown in Figures 14.2 - 14.35, on an expanded scale. As shown in Figure 14.36, crack length was estimated by determining the distance from the site of crack initiation to the approximate center of the crack front (marker band). The crack length data reported in Tables 14.1 and 14.2 were measurements to an accuracy of ± 25 μm. Figure 14.37 is a plot of fatigue crack length versus pressure cycles for thirteen fatigue cracks contained in bay 3 and eighteen fatigue cracks contained in bay 4. Fatigue cracks in bay 3 exhibit a maximum crack length of approximately 4.3 mm at 60,000 pressure cycles. Although most fatigue cracks in bay 4 exhibit a similar range of crack lengths compared to that observed in bay 3, a few upper rivet holes locations contain cracks that are significantly longer. Fatigue cracks at rivet hole locations 4J2, 4J8, 4J9, and 4J15 are approximately 5 mm to nearly 13 mm in length.

14.5 Fatigue Crack Growth Rate:

Tables 14.3 and 14.4 list the average crack length, $(a)_{av}$, and average fatigue crack growth rate, $(\Delta a/\Delta N)_{av}$, determined from each set of fracture surface marker bands found on fatigue cracks in the upper rivet row outer skin of bays 3 and 4, respectively. Figure 14.36 describes the method used to determine the marker band based crack lengths and crack growth rates. Crack lengths were measured from the crack initiation site to the approximate center of the crack front (dashed lines in Figure 14.36) that was established from the marker band coordinates. The average crack length, a_{av}, and average fatigue crack growth rate, $(\Delta a/\Delta N)_{av}$, determinations for each set of marker bands is plotted (solid symbols) in Figure 14.38 for crack lengths ranging from 0.5 to 4.5 mm. A comparison of the linear regression analysis (solid line) for bays 3 and 4 shown in Figures 14.38a and 14.38b suggests that the fatigue crack growth characteristics of short cracks located in both lap splice bays are similar.

A dilemma arises in estimating the growth rate for the initial stage of fatigue cracking ($a < 1$ mm) prior to the first marker band; here, the number of pressure cycles to crack initiation is unknown. To estimate of crack growth rate behavior during the initial stage of fatigue cracking, the number of pressure cycles to crack initiation was assumed and $(\Delta a/\Delta N)_{av}|_1$ was estimated by assuming $N_i = 0$. The dashed line in Figure 14.38 is a linear regression analysis of estimated crack growth rate data (open symbols) for the initial stage of fatigue cracking in bays 3 and 4. A comparison of the fatigue crack growth estimates for crack lengths less than 4.5 mm also suggests that all fatigue cracks in bays 3 and 4 grow in similar manner.

Table 14-1 Bay 3 Crack Length/Pressure Cycle Data

Hole #	a (mm)	N	Hole #	a (mm)	N
3J1	0.20	30000	3J9	0.51	50000
3J1	1.17	40000	3J9	1.27	60000
3J1	2.31	50000	3J11	0.41	40000
3J1	4.22	60000	3J11	2.44	60000
3J2	0.33	50000	3J12	0.89	40000
3J2	2.62	60000	3J12	1.98	50000
3J2	0.41	30000	3J12	3.56	60000
3J2	1.17	40000	3J12	0.33	30000
3J2	2.18	50000	3J12	0.81	40000
3J2	4.34	60000	3J12	1.96	50000
3J4	0.41	30000	3J12	3.81	60000
3J4	0.86	40000	3J13	0.25	30000
3J4	1.30	50000	3J13	1.14	40000
3J4	1.98	60000	3J15	3.30	60000
3J4	0.71	40000	3J15	0.30	30000
3J4	1.37	50000	3J15	0.79	40000
3J4	2.24	60000	3J15	1.80	50000
3J7	0.38	40000	3J15	2.90	60000
3J7	1.14	50000	3J15	0.84	40000
3J7	2.11	60000	3J15	1.93	60000

Table 14-2 Bay 4 Crack Length/Pressure Cycle Data

Hole #	a(mm)	N	Hole #	a(mm)	N	Hole #	a(mm)	N
4J2	0.76	40000	4J6	0.25	30000	4J14	0.53	40000
4J2	1.42	50000	4J6	0.94	40000	4J14	1.42	50000
4J2	2.36	60000	4J6	2.21	50000	4J14	2.82	60000
4J2	0.51	40000	4J6	4.11	60000	4J12	0.64	50000
4J2	1.78	60000	4J6	0.76	30000	4J12	1.78	60000
4J1	0.51	30000	4J6	2.60	60000	4J10	0.64	40000
4J1	1.22	40000	4J5	0.66	30000	4J10	1.96	50000
4J1	2.62	60000	4J5	1.57	40000	4J10	4.04	60000
4J5	0.58	30000	4J5	5.44	60000	4J15	0.46	30000
4J5	1.27	40000	4J7	0.38	40000	4J15	1.42	40000
4J5	2.54	50000	4J7	3.56	60000	4J15	7.14	60000
4J5	5.21	60000	4J9	1.27	30000	4J15	0.30	20000
4J4	0.41	40000	4J9	1.70	40000	4J15	1.57	30000
4J4	1.24	50000	4J9	2.46	60000	4J15	2.97	40000
4J4	2.51	60000	4J8	0.43	20000	4J15	8.56	60000
4J3	0.25	30000	4J8	1.50	30000	4J14	0.28	30000
4J3	2.03	60000	4J8	3.07	40000	4J14	0.84	40000
						4J14	1.47	50000

Table 14-3 Bay 3 Marker Band Based a_{av} and $(\Delta a/\Delta N)_{av}$ Results

Hole #	(a_{av}) (mm)	$(\Delta a/\Delta N)_{av}$ (mm/cycle)	Hole #	(a_{av}) (mm)	$(\Delta a/\Delta N)_{av}$ (mm/cycle)
3J1	0.10	$(6.86 \times 10^{-6})^*$	3J9	0.25	$(1.02 \times 10^{-5})^*$
3J1	0.69	9.65×10^{-5}	3J9	0.89	7.62×10^{-5}
3J1	1.74	1.14×10^{-4}	3J11	0.20	$(1.02 \times 10^{-5})^*$
3J1	3.26	1.91×10^{-4}	3J11	1.42	1.02×10^{-4}
3J2	0.18	$(6.86 \times 10^{-6})^*$	3J12	0.46	$(2.22 \times 10^{-5})^*$
3J2	1.47	2.29×10^{-4}	3J12	1.44	1.09×10^{-4}
3J2	0.20	$(1.35 \times 10^{-5})^*$	3J12	2.77	1.57×10^{-4}
3J2	0.58	7.62×10^{-5}	3J12	0.18	$(1.09 \times 10^{-5})^*$
3J2	1.68	1.02×10^{-4}	3J12	0.53	4.83×10^{-5}
3J2	3.26	2.16×10^{-4}	3J12	1.40	1.14×10^{-4}
3J4	0.20	$(1.35 \times 10^{-5})^*$	3J12	2.55	1.85×10^{-4}
3J4	0.64	4.57×10^{-5}	3J13	0.43	$(2.10 \times 10^{-5})^*$
3J4	1.08	4.32×10^{-5}	3J13	1.38	6.35×10^{-5}
3J4	1.64	5.08×10^{-5}	3J15	0.13	$(8.38 \times 10^{-6})^*$
3J4	0.36	$(1.78 \times 10^{-5})^*$	3J15	0.70	8.89×10^{-5}
3J4	1.04	6.60×10^{-5}	3J15	2.35	2.41×10^{-4}
3J4	1.75	8.64×10^{-5}	3J15	0.15	$(1.02 \times 10^{-5})^*$
3J7	0.18	$(9.53 \times 10^{-6})^*$	3J15	0.56	4.83×10^{-5}
3J7	0.76	7.62×10^{-5}	3J15	1.30	1.02×10^{-4}
3J7	1.63	9.65×10^{-5}	3J15	2.35	1.09×10^{-4}

* Calculation of $(\Delta a/\Delta N)_{av}$ disregarded cycles to crack initiation.

Table 14-4 Bay 4 Marker Band Based a_{av} and $(\Delta a/\Delta N)_{av}$ Results

Hole #	$(a)_{av}$ (mm)	$(\Delta a/\Delta N)_{av}$ (mm/cycle)	Hole #	$(a)_{av}$ (mm)	$(\Delta a/\Delta N)_{av}$ (mm/cycle)
4J2	0.25	$(1.27 \times 10^{-5})^*$	4J7	0.18	$(9.53 \times 10^{-6})^*$
4J2	1.14	6.35×10^{-5}	4J7	1.98	1.59×10^{-4}
4J2	0.38	$(1.91 \times 10^{-5})^*$	4J9	0.64	$(4.24 \times 10^{-5})^*$
4J2	1.09	6.60×10^{-5}	4J9	1.49	4.32×10^{-5}
4J2	1.89	9.40×10^{-5}	4J9	2.08	7.62×10^{-5}
4J1	0.25	$(1.70 \times 10^{-5})^*$	4J8	0.23	$(2.16 \times 10^{-5})^*$
4J1	0.86	7.11×10^{-5}	4J8	0.97	1.07×10^{-4}
4J1	1.92	6.99×10^{-5}	4J8	2.29	1.57×10^{-4}
4J5	0.31	$(1.96 \times 10^{-5})^*$	4J14	0.28	$(1.33 \times 10^{-5})^*$
4J5	0.84	6.86×10^{-5}	4J14	0.99	8.89×10^{-5}
4J5	1.91	1.27×10^{-4}	4J14	2.12	1.40×10^{-4}
4J5	3.87	2.67×10^{-4}	4J12	0.33	$(1.27 \times 10^{-5})^*$
4J4	0.20	$(1.02 \times 10^{-5})^*$	4J12	1.22	1.14×10^{-4}
4J4	0.81	8.38×10^{-5}	4J10	0.33	$(1.59 \times 10^{-5})^*$
4J4	1.88	1.27×10^{-4}	4J10	1.30	1.32×10^{-4}
4J3	0.13	$(8.38 \times 10^{-6})^*$	4J10	3.00	2.08×10^{-4}
4J3	1.14	5.84×10^{-5}	4J15	0.15	$(1.52 \times 10^{-5})^*$
4J6	0.38	$(1.52 \times 10^{-5})^*$	4J15	0.94	1.27×10^{-4}
4J6	1.68	1.83×10^{-4}	4J15	2.29	1.40×10^{-4}
4J6	0.13	$(8.38 \times 10^{-6})^*$	4J15	4.37	2.79×10^{-4}
4J6	0.61	6.86×10^{-5}	4J15	0.23	$(1.52 \times 10^{-5})^*$
4J6	1.58	1.27×10^{-4}	4J15	0.94	9.65×10^{-5}
4J6	3.16	1.91×10^{-4}	4J15	4.29	2.86×10^{-4}
4J5	0.33	$(2.21 \times 10^{-5})^*$	4J14	0.15	$(9.40 \times 10^{-6})^*$
4J5	1.12	9.14×10^{-5}	4J14	0.56	5.59×10^{-5}
4J5	3.51	1.93×10^{-4}	4J14	1.17	6.35×10^{-5}
			4J14	1.96	9.65×10^{-5}

*Calculation of $(\Delta a/\Delta N)_{av}$ disregarded cycles to crack initiation.

20 μm

a)

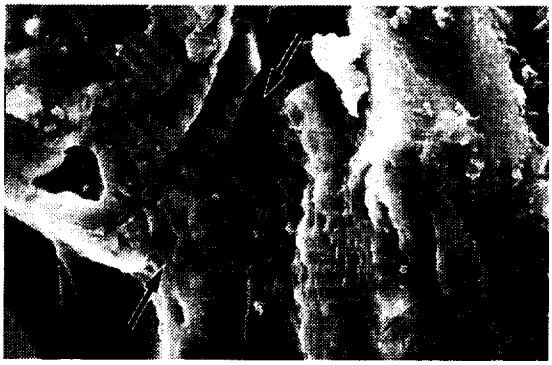

30 μm

b)

10 μm

c)

Figure. 14.1 SEM micrographs of: a) 6 marker bands between arrows comprising a 30 K set of marker bands. b) 10 marker bands between arrows comprising a 40 K set of marker bands. c) 4 marker bands between arrows comprising a 50 K set of marker bands.

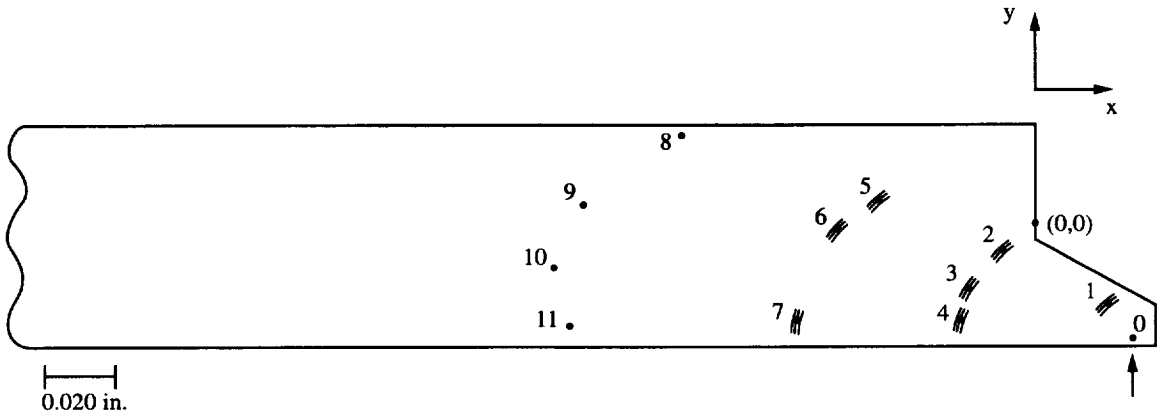

#	Coordinates (mm)	[in]	# of Bands (cycles)
0	(0.510, -0.646)	[0.025, -0.032]	Initiation
1	(0.55,-0.6)	[0.022,-0.024]	3(30K)
2	(-0.265,-0.2)	[-0.010,-0.008]	9(40K)
3	(-0.4875,-0.5)	[-0.019,-0.020]	9(40K)
4	(-0.5375,-0.6825)	[-0.021,-0.027]	9(40K)
5	(-1.13,0.2075)	[-0.051,0.008]	4(50K)
6	(-1.425,0.0)	[-0.056,0.000]	4(50K)
7	(-1.725,-0.655)	[-0.068,-0.026]	4(50K)
8	(-2.61,0.6225)	[-0.103,0.025]	Crack Front
9	(-3.3125,0.1583)	[-0.130,0.006]	Crack Front
10	(-3.53,-0.325)	[-0.139,-0.013]	Crack Front
11	(-3.63,-0.725)	[0.143,-0.028]	Crack Front

Figure 14.2 The schematic shows the initiation site, marker band and final crack front locations for the fatigue crack in rivet hole 3J1 that grew in the aft direction. Three sets of marker bands were found. The fatigue crack initiation region is marked with an arrow. The table summarizes the X-Y marker band coordinates relative to the origin (0,0), and the cycle count for each set of marker bands.

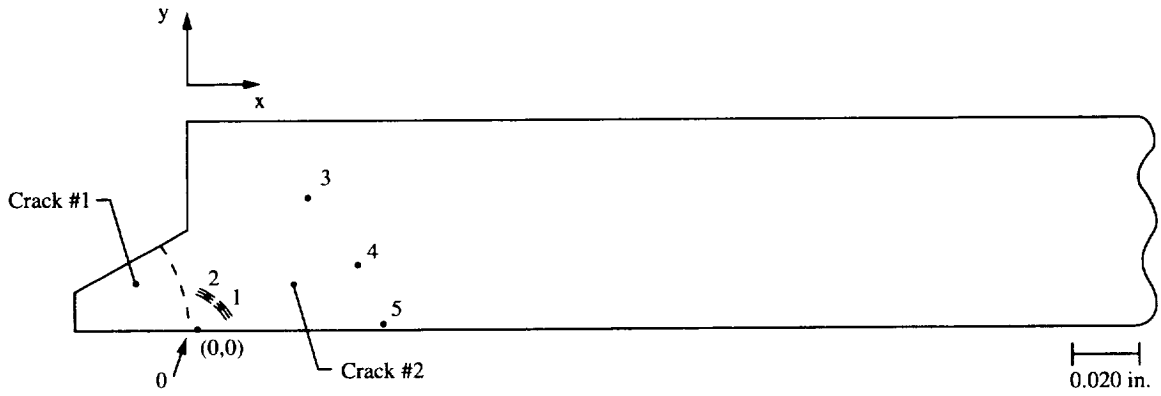

#	Coordinates (mm)	[in]	# of Bands (cycles)
0	(0.0, 0.0)	[0.0, 0.0]	Initiation
1	(0.2,0.15)	[0.008,0.006]	4(50K)
2	(0.0875,0.2625)	[0.014,0.041]	4(50K)
3	(0.85,1.0)	[0.033,0.039]	Crack Front
4	(1.2,0.5)	[0.047,0.020]	Crack Front
5	(1.45,0.0)	[0.057,0.000]	Crack Front

Figure 14.3 The schematic shows the initiation site, marker band and final crack front locations for the fatigue crack in rivet hole 3J1 that grew in the forward direction. This specimen contained two fatigue cracks. A set of marker bands was found radiating from the initiation region of crack #2. The fatigue crack initiation regions for cracks #1 and 2 are marked with a bracket and an arrow, respectively. The table summarizes the X-Y marker band coordinates relative to the origin (0,0), and the cycle count for each set of marker bands.

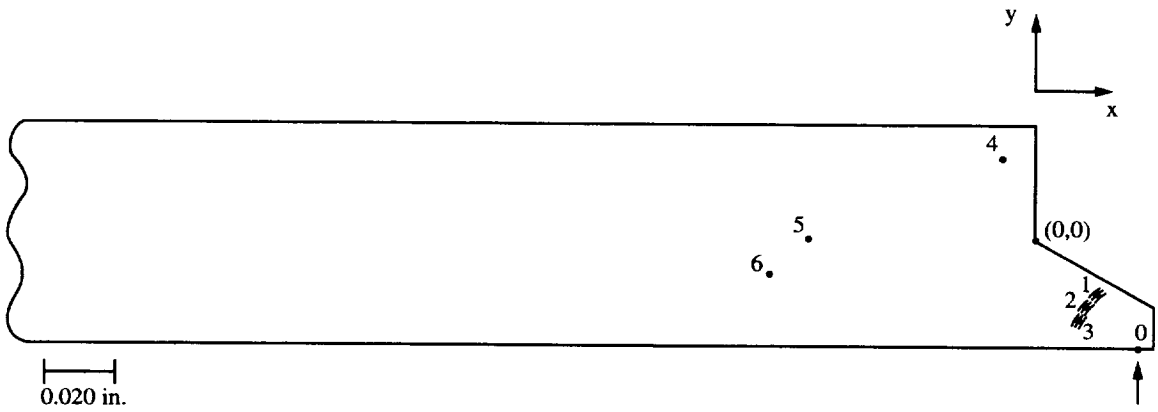

#	Coordinates (mm)	[in]	# of Bands (cycles)
0	(0.565, -0.616)	[0.028, -0.03]	Initiation
1	(0.4425,-0.3925)	[0.017,-0.015]	9(40K)
2	(0.35,-0.48)	[0.014,-0.019]	9(40K)
3	(0.3175,-0.5525)	[0.013,-0.022]	9(40K)
4	(-0.233,0.581)	[-0.009,0.023]	Crack Front
5	(-1.65,0.0)	[-0.065,0.000]	Crack Front
6	(-1.94,-0.271)	[-0.076,-0.011]	Crack Front

Figure 14.4 The schematic shows the initiation site, marker band and final crack front locations for the fatigue crack in rivet hole 3J2 that grew in the aft direction. One set of marker bands was found. The fatigue crack initiation region is marked with an arrow. The table summarizes the X-Y marker band coordinates relative to the origin (0,0), and the cycle count for each set of marker bands.

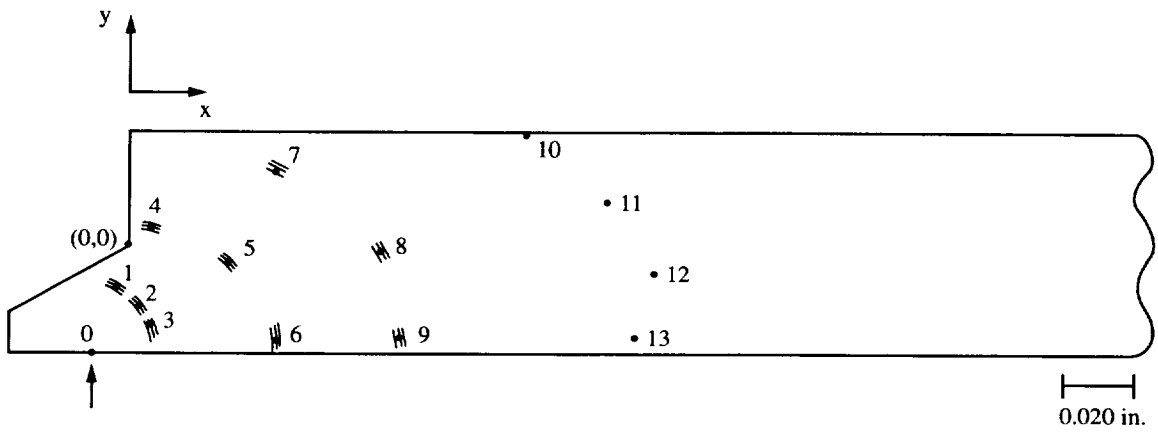

#	Coordinates (mm)	[in]	# of Bands (cycles)
0	(-0.210,-0.618)	[-0.010,-0.030]	Initiation
1	(-0.05,-0.3)	[-0.002,-0.012]	3(30K)
2	(0.1125,-0.4125)	[0.004,-0.016]	3(30K)
3	(0.2125,-0.525)	[0.008,-0.021]	3(30K)
4	(0.1625,0.125)	[0.006,0.005]	4(40K)
5	(0.75,-0.1325)	[0.030,-0.005]	4(40K)
6	(0.9875,-0.7125)	[0.039,-0.028]	4(40K)
7	(1.0875,0.5)	[0.043,0.020]	5(50K)
8	(1.8375,-0.05)	[0.072,-0.002]	5(50K)
9	(2.005,-0.625)	[0.079,-0.025]	5(50K)
10	(2.95,0.85)	[0.116,0.033]	Crack Front
11	(3.55,0.35)	[0.140,0.014]	Crack Front
12	(3.85,-0.24)	[0.152,-0.009]	Crack Front
13	(3.72,-0.6)	[0.146,-0.024]	Crack Front

Figure 14.5 The schematic shows the initiation site, marker band and final crack front locations for the fatigue crack in rivet hole 3J2 that grew in the forward direction. Three sets of marker bands were found. The fatigue crack initiation region is marked with a bracket. The table summarizes the X-Y marker band coordinates relative to the origin(0,0), and the cycle count for each set of marker bands.

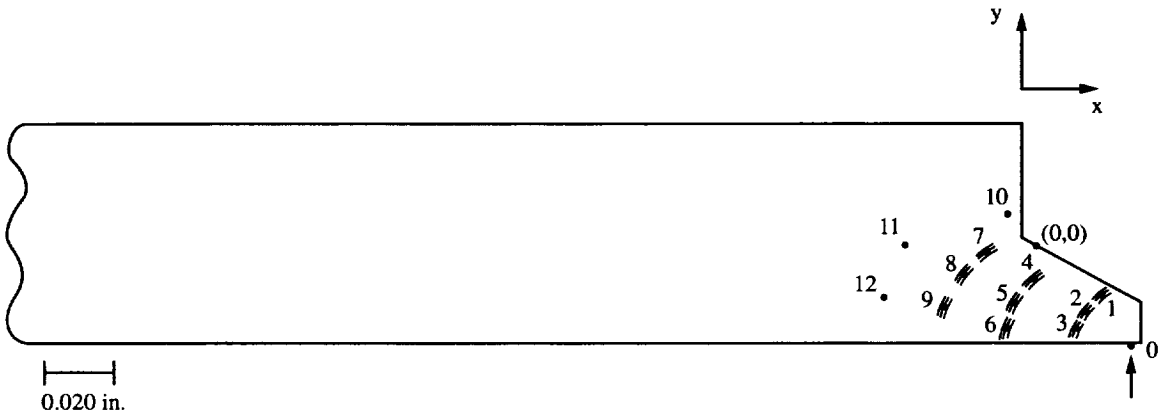

#	Coordinates (mm)	[in]	# of Bands (cycles)
0	(0.570,-0.586)	[0.028,-0.029]	Initiation
1	(0.45,-0.3875)	[0.018,-0.015]	6(30K)
2	(0.3125,-0.475)	[0.012,-0.019]	6(30K)
3	(0.2675,-0.5375)	[0.011,-0.021]	6(30K)
4	(-0.0125,-0.2375)	[-0.0005,-0.009]	9(40K)
5	(-0.1875,-0.425)	[-0.007,-0.017]	9(40K)
6	(-0.2,-0.5875)	[-0.008,-0.023]	9(40K)
7	(-0.375,-0.0625)	[-0.015,-0.002]	4(50K)
8	(-0.5625,-0.225)	[-0.022,-0.009]	4(50K)
9	(-0.65,-0.4)	[-0.026,-0.016]	4(50K)
10	(-0.225,0.25)	[-0.009,0.010]	Crack Front
11	(-1.0,0)	[-0.039,0.000]	Crack Front
12	(-1.135,-0.35)	[-0.045,-0.014]	Crack Front

Figure 14.6 The schematic shows the initiation site, marker band and final crack front locations for the fatigue crack in rivet hole 3J4 that grew in the aft direction. Three sets of marker bands were found. The fatigue crack initiation region is marked with an arrow. The table summarizes the X-Y marker band coordinates relative to the origin (0,0), and the cycle count for each set of marker bands.

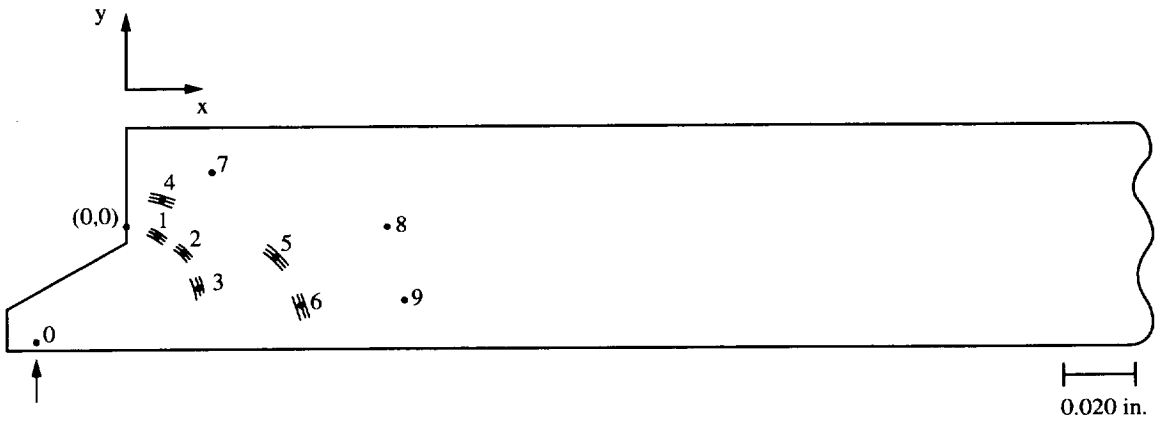

#	Coordinates (mm)	[in]	# of Bands (cycles)
0	(0.552-0.606,)	[0.027,-0.030]	Initiation
1	(0.2325,-0.025)	[0.009,-0.001]	9(40K)
2	(0.33,-0.17)	[0.013,-0.007]	9(40K)
3	(0.5125,-0.405)	[0.020,-0.016]	9(40K)
4	(0.2125,0.225)	[0.008,0.009]	4(50K)
5	(1.095,-0.175)	[0.043,-0.007]	4(50K)
6	(1.1625,-0.45)	[0.046,-0.018]	4(50K)
7	(0.4,0.595)	[0.016,0.024]	Crack Front
8	(1.95,0.0)	[0.077,0.000]	Crack Front
9	(2.005,-0.5)	[0.080,-0.020]	Crack Front

Figure 14.7 The schematic shows the initiation site, marker band and final crack front locations for the fatigue crack in rivet hole 3J4 that grew in the forward direction. Two sets of marker bands were found. The fatigue crack initiation region is marked with a bracket. The table summarizes the X-Y marker band coordinates relative to the origin (0,0), and the cycle count for each set of marker bands.

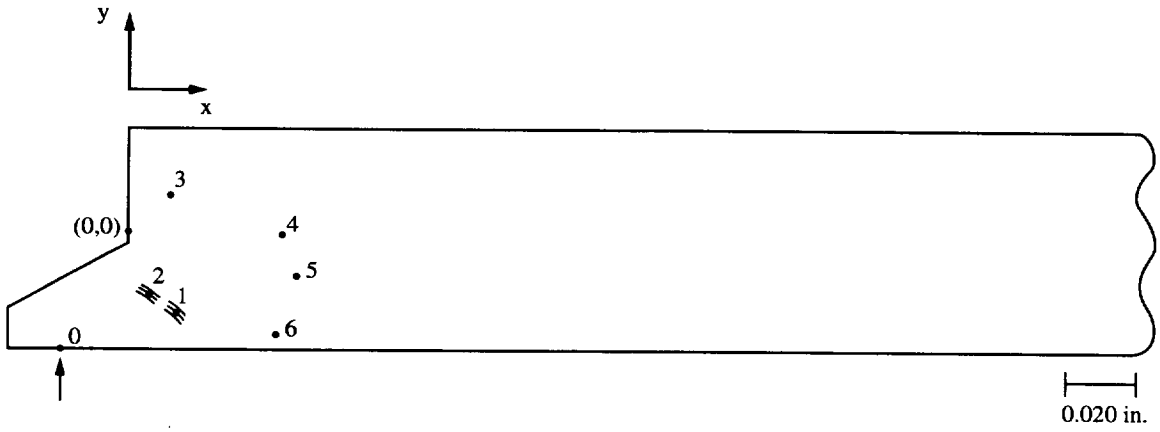

#	Coordinates (mm)	[in]	# of Bands (cycles)
0	(-0.405,-0.612)	[-0.020,-0.030]	Initiation
1	(0.4425,-0.425)	[0.017,-0.017]	4(50K)
2	(0.5125,-0.595)	[0.020,-0.023]	4(50K)
3	(0.25,0.225)	[0.010,0.009]	Crack Front
4	(0.95,0.0)	[0.037,0.000]	Crack Front
5	(1.225,-0.33)	[0.048,-0.013]	Crack Front
6	(1.04,-0.73)	[0.041,-0.029]	Crack Front

Figure 14.8 The schematic shows the initiation site, marker band and final crack front locations for the fatigue crack in rivet hole 3J5 that grew in the forward direction. One set of marker bands was found. The fatigue crack initiation region is marked with a bracket. The table summarizes the X-Y marker band coordinates relative to the origin (0,0), and the cycle count for each set of marker bands.

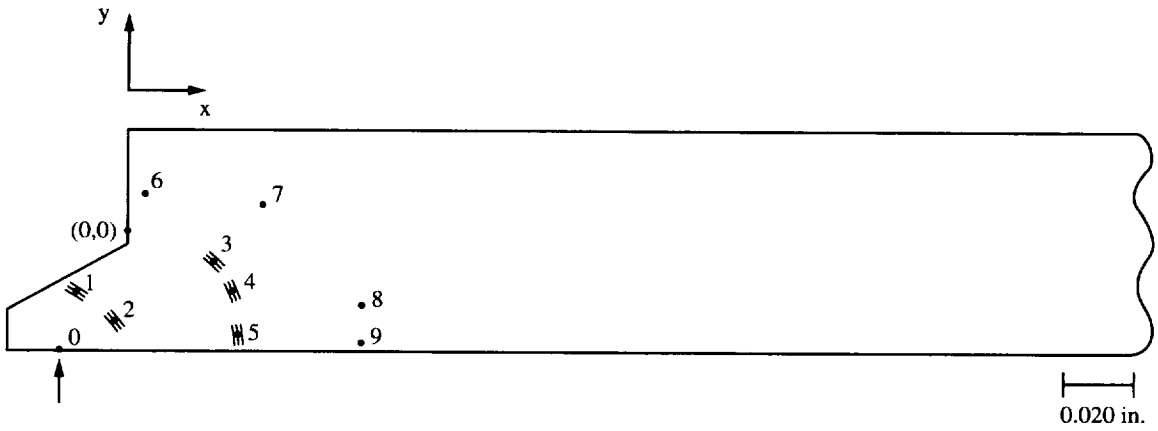

#	Coordinates (mm)	[in]	# of Bands (cycles)
0	(-0.390,-0.653)	[-0.019,-0.032]	Initiation
1	(-0.3125,-0.4125)	[-0.012,-0.016]	9(40K)
2	(-0.0625,-0.625)	[-0.002,-0.020]	9(40K)
3	(0.6175,-0.2125)	[0.024,-0.009]	4(50K)
4	(0.775,-0.4125)	[0.031,-0.016]	4(50K)
5	(0.825,-0.75)	[0.032,-0.030]	4(50K)
6	(0.12,0.29)	[0.005,0.011]	Crack Front
7	(1.0,0.24)	[0.039,0.009]	Crack Front
8	(1.75,-0.5)	[0.069,-0.020]	Crack Front
9	(1.71,-0.85)	[0.067,-0.033]	Crack Front

Figure 14.9 The schematic shows the initiation site, marker band and final crack front locations for the fatigue crack in rivet hole 3J7 that grew in the forward direction. Two sets of marker bands were found. The fatigue crack initiation region is marked with a bracket. The table summarizes the X-Y marker band coordinates relative to the origin (0,0), and the cycle count for each set of marker bands.

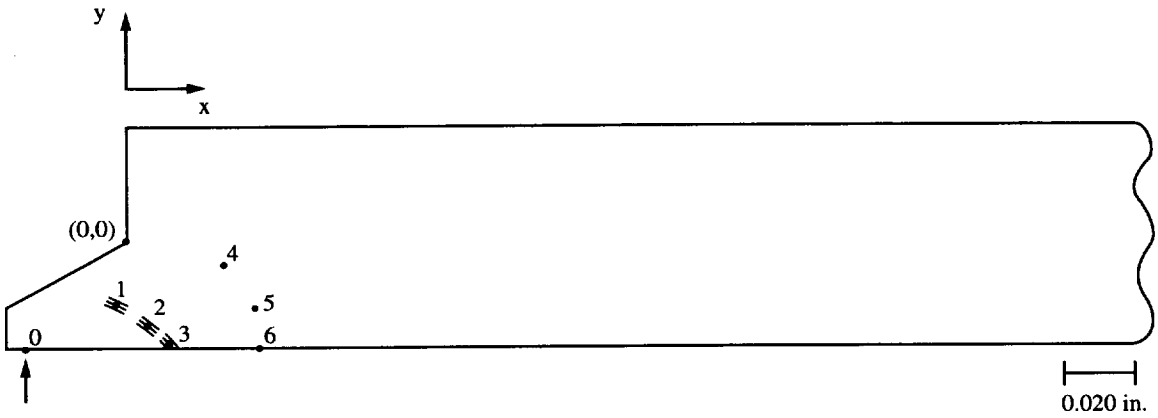

#	Coordinates (mm)	[in]	# of Bands (cycles)
0	(-0.513,-0.717)	[-0.025,-0.035]	Initiation
1	(-0.0875,-0.455)	[-0.003,-0.018]	4(50K)
2	(0.1625,-0.6025)	[0.006,-0.024]	4(50K)
3	(0.2725,-0.8125)	[0.011,-0.032]	4(50K)
4	(0.7,-0.2)	[0.028,-0.008]	Crack Front
5	(0.91,-0.5)	[0.036,-0.020]	Crack Front
6	(0.98,-0.91)	[0.039,-0.036]	Crack Front

Figure 14.10 The schematic shows the initiation site, marker band and final crack front locations for the fatigue crack in rivet hole 3J9 that grew in the aft direction. One set of marker bands was found. The fatigue crack initiation region is marked with a bracket. The table summarizes the X-Y marker band coordinates relative to the origin (0,0), and the cycle count for each set of marker bands.

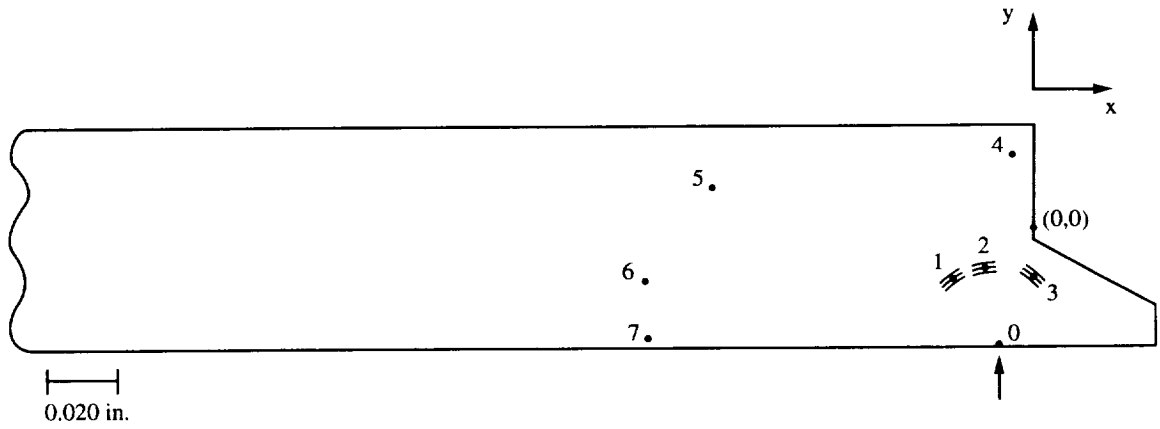

#	Coordinates (mm)	[in]	# of Bands (cycles)
0	(0.145,-0.650)	[0.007,-0.032]	Initiation
1	(-0.6075,-0.375)	[-0.024,-0.015]	9(40K)
2	(-0.33,-0.355)	[-0.013,-0.014]	9(40K)
3	(0.0,-0.4375)	[0.000,-0.017]	9(40K)
4	(-0.157,0.52)	[-0.006,0.020]	Crack Front
5	(-2.35,0.3)	[-0.092,0.012]	Crack Front
6	(-2.85,-0.4)	[-0.112,-0.016]	Crack Front
7	(-2.82,-0.8)	[-0.111,-0.031]	Crack Front

Figure 14.11 The schematic shows the initiation site, marker band and final crack front locations for the fatigue crack in rivet hole 3J11 that grew in the forward direction. One set of marker bands found. The fatigue crack initiation region is marked with a bracket. The table summarizes the X-Y marker band coordinates relative to the origin (0,0), and the cycle count for each set of marker bands.

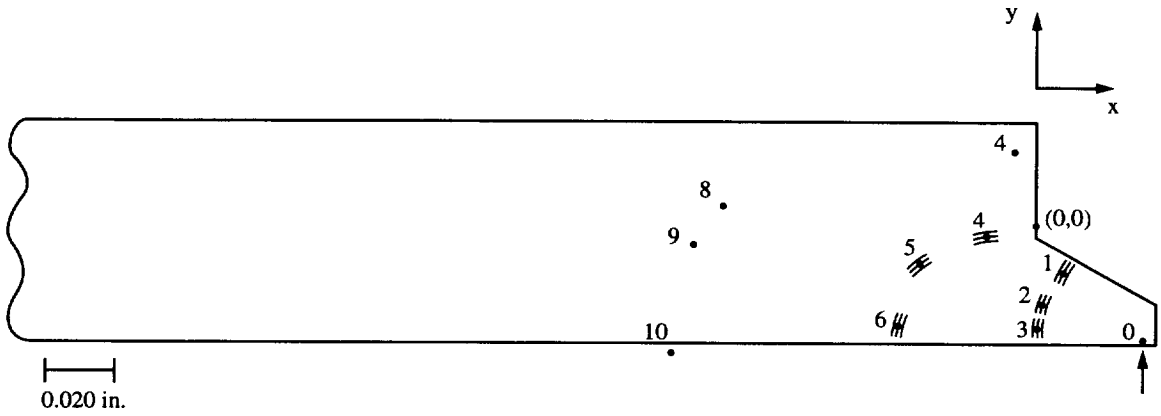

#	Coordinates (mm)	[in]	# of Bands (cycles)
0	(0.604,-0.588)	[0.030,-0.029]	Initiation
1	(0.0825,-0.1725)	[0.003,-0.007]	9(40K)
2	(-0.05,-0.3875)	[-0.002,-0.015]	9(40K)
3	(-0.05,-0.4875)	[-0.002,-0.019]	9(40K)
4	(-0.55,0.0375)	[-0.022,0.001]	4(50K)
5	(-1.0,-0.125)	[-0.039,-0.005]	4(50K)
6	(-1.1375,-0.6)	[-0.045,-0.024]	4(50K)
7	(-1.385,0.775)	[-0.055,0.031]	Crack Front
8	(-2.375,0.275)	[-0.094,0.011]	Crack Front
9	(-2.575,0.0)	[-0.101,0.000]	Crack Front
10	(-2.75,-0.775)	[-0.108,-0.031]	Crack Front

Figure 14.12 The schematic shows the initiation site, marker band and final crack front locations for the fatigue crack in rivet hole 3J12 that grew in the aft direction. Two sets of marker bands were found. The fatigue crack initiation region is marked with an arrow. The table summarizes the X-Y marker band coordinates relative to the origin (0,0), and the cycle count for each set of marker bands.

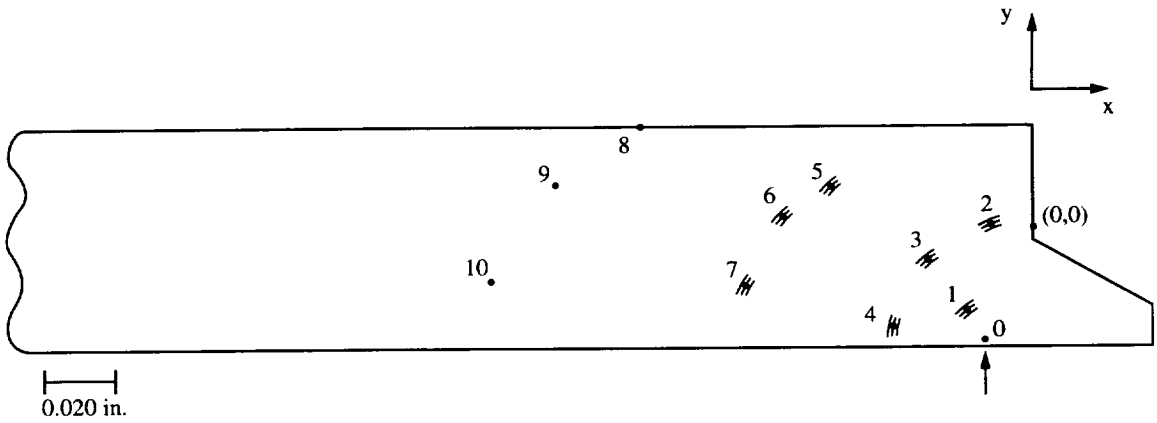

#	Coordinates (mm)	[in]	# of Bands (cycles)
0	(-0.339,-0.580)	[-0.017,-0.029]	Initiation
1	(-0.4325,-0.5675)	[-0.017,-0.022]	3(30K)
2	(-0.2625,0.0125)	[-0.010,0.0005]	9(40K)
3	(-0.75,-0.225)	[-0.030,-0.009]	9(40K)
4	(-0.995,-0.6625)	[-0.039,-0.026]	9(40K)
5	(-1.45,0.33)	[-0.057,0.013]	4(50K)
6	(-1.7875,0.125)	[-0.070,0.005]	4(50K)
7	(-2.1075,-0.4)	[-0.083,-0.016]	4(50K)
8	(-2.82,0.73)	[-0.111,0.029]	Crack Front
9	(-3.48,0.35)	[-0.137,0.014]	Crack Front
10	(-3.97,-0.38)	[-0.156,-0.015]	Crack Front

Figure 14.13 The schematic shows the initiation site, marker band and final crack front locations for the fatigue crack in rivet hole 3J12 that grew in the forward direction. Three sets of marker bands were found. The fatigue crack initiation region is marked with a bracket. The table summarizes the X-Y marker band coordinates relative to the origin(0,0), and the cycle count for each set of marker bands.

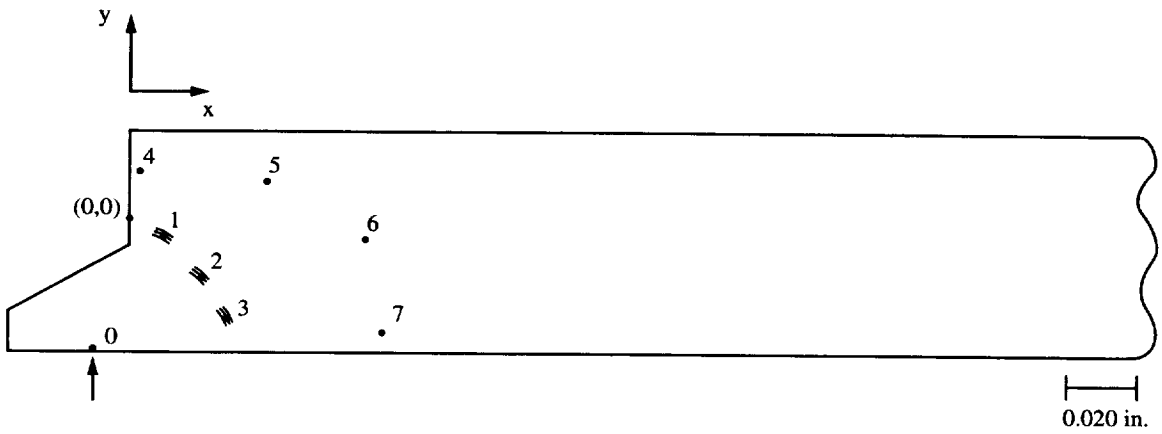

#	Coordinates (mm)	[in]	# of Bands (cycles)
0	(-0.274,-0.714)	[-0.013,-0.035]	Initiation
1	(0.25,-0.1175)	[0.01,-0.005]	9(40K)
2	(0.525,-0.3375)	[0.020,-0.013]	9(40K)
3	(0.7375,-0.675)	[0.029,-0.266]	9(40K)
4	(0.08,0.36)	[0.003,0.014]	Crack Front
5	(1.02,0.3)	[0.040,0.011]	Crack Front
6	(1.72,-0.2)	[0.068,-0.008]	Crack Front
7	(1.85,-0.78)	[0.073,-0.031]	Crack Front

Figure 14.14 The schematic shows the initiation site, marker band and final crack front locations for the fatigue crack in rivet hole 3J13 that grew in the forward direction. One set of marker bands was found. The fatigue crack initiation region is marked with a bracket. The table summarizes the X-Y marker band coordinates relative to the origin (0,0), and the cycle count for each set of marker bands.

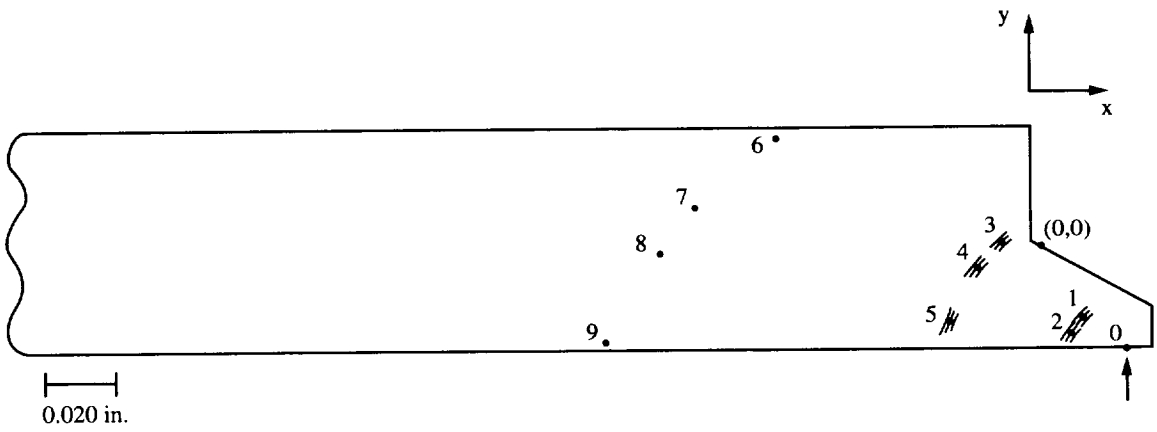

#	Coordinates (mm)	[in]	# of Bands (cycles)
0	(0.461,-0.589)	[0.023,-0.029]	Initiation
1	(0.2375,-0.5)	[0.009,-0.020]	3(30K)
2	(0.175,-0.64)	[0.007,-0.025]	3(30K)
3	(-0.325,0.0)	[-0.013,0.000]	9(40K)
4	(-0.525,-0.1625)	[-0.021,-0.006]	9(40K)
5	(-0.7125,-0.55)	[-0.028,-0.022]	9(40K)
6	(-1.95,0.79)	[-0.077,0.031]	Crack Front
7	(-2.55,0.28)	[-0.100,0.011]	Crack Front
8	(-2.84,-0.05)	[-0.112,-0.002]	Crack Front
9	(-3.2,-0.7)	[-0.126,-0.028]	Crack Front

Figure 14.15 The schematic shows the initiation site, marker band and final crack front locations for the fatigue crack in rivet hole 3J15 that grew in the aft direction. Two sets of marker bands were found. The fatigue crack initiation region is marked with a bracket. The table summarizes the X-Y marker band coordinates relative to the origin (0,0), and the cycle count for each set of marker bands.

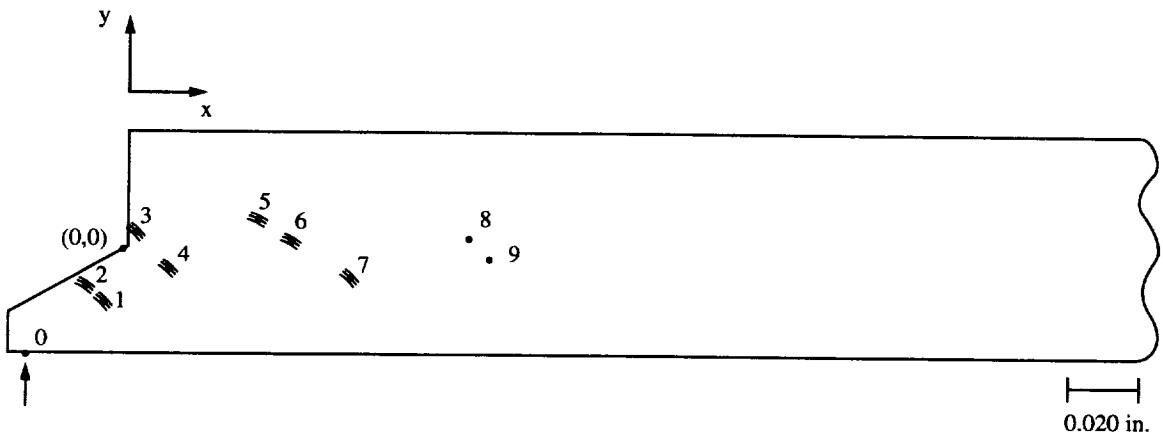

#	Coordinates (mm)	[in]	# of Bands (cycles)
0	(-0.542,-0.590)	[-0.027,-0.029]	Initiation
1	(-0.15,-0.37)	[-0.006,-0.015]	3(30K)
2	(-0.29,-0.2625)	[-0.011,-0.010]	3(30K)
3	(0.135,-0.0375)	[0.005,-0.001]	9(40K)
4	(0.3,-0.175)	[0.012,-0.007]	9(40K)
5	(0.9825,0.225)	[0.039,0.009]	4(50K)
6	(1.1875,0.095)	[0.047,0.004]	4(50K)
7	(1.625,-0.2325)	[0.064,-0.009]	4(50K)
8	(1.67,0.8)	[0.066,0.031]	Crack Front
9	(2.5,0.25)	[0.098,0.010]	Crack Front

Figure 14.16 The schematic shows the initiation site, marker band and final crack front locations for the fatigue crack in rivet hole 3J15 that grew in the forward direction. Three sets of marker bands were found. The fatigue crack initiation region is marked with a bracket. The table summarizes the X-Y marker band coordinates relative to the origin (0,0), and the cycle count for each set of marker bands.

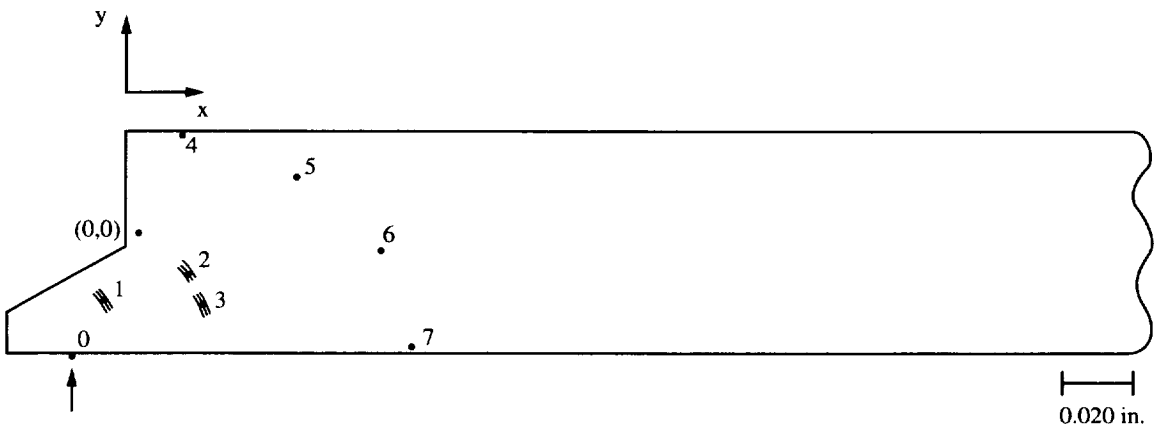

#	Coordinates (mm)	[in]	# of Bands (cycles)
0	(-0.432,-0.710)	[-0.021,-0.035]	Initiation
1	(-0.27,-0.463)	[-0.011,-0.018]	6(30K)
2	(0.35,-0.275)	[0.014,-0.011]	9(40K)
3	(0.45,-0.525)	[0.018,-0.021]	9(40K)
4	(0.3,0.65)	[0.012,0.026]	Crack Front
5	(1.13,0.39)	[0.044,0.015]	Crack Front
6	(1.8,-0.11)	[0.071,-0.004]	Crack Front
7	(1.97,-0.85)	[0.078,-0.033]	Crack Front

Figure 14.17 The schematic shows the initiation site, marker band and final crack front locations for the fatigue crack in rivet hole 4J1 that grew in the aft direction. Two sets of marker bands were found. The fatigue crack initiation region is marked with an arrow. The table summarizes the X-Y marker band coordinates relative to the origin (0,0), and the cycle count for each set of marker bands.

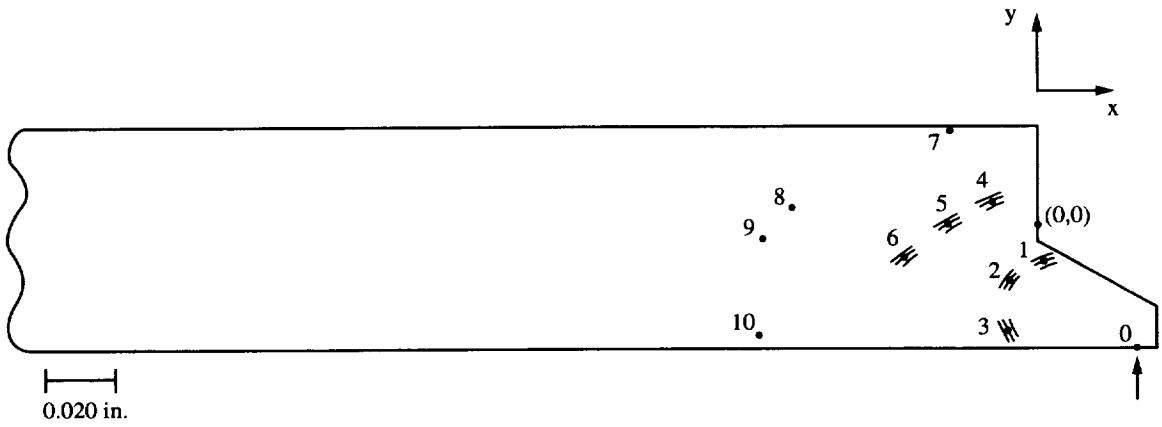

#	Coordinates (mm)	[in]	# of Bands (cycles)
0	(0.572,-0.670)	[0.028,-0.033]	Initiation
1	(0.090,-0.210)	[0.004,-0.008]	10(40K)
2	(-0.235,-0.45)	[-0.009,-0.018]	10(40K)
3	(-0.200,-0.8125)	[-0.008,-0.032]	10(40K)
4	(-0.330,0.170)	[-0.013,0.007]	4(50k)
5	(-0.6875,-0.075)	[-0.027,-0.003]	4(50k)
6	(-0.9625,-0.2625)	[-0.038,-0.010]	4(50k)
7	(-0.62,0.62)	[-0.024,0.024]	Crack Front
8	(-1.77,0.1)	[-0.070,0.004]	Crack Front
9	(-2.05,-0.15)	[-0.081,-0.006]	Crack Front
10	(-2.1,-0.92)	[-0.083,-0.036]	Crack Front

Figure 14.18 The schematic shows the initiation site, marker band and final crack front locations for the fatigue crack in rivet hole 4J2 that grew in the forward direction. Two sets of marker bands were found. The fatigue crack initiation region is marked with a bracket. The table summarizes the X-Y marker band coordinates relative to the origin (0,0), and the cycle count for each set of marker bands.

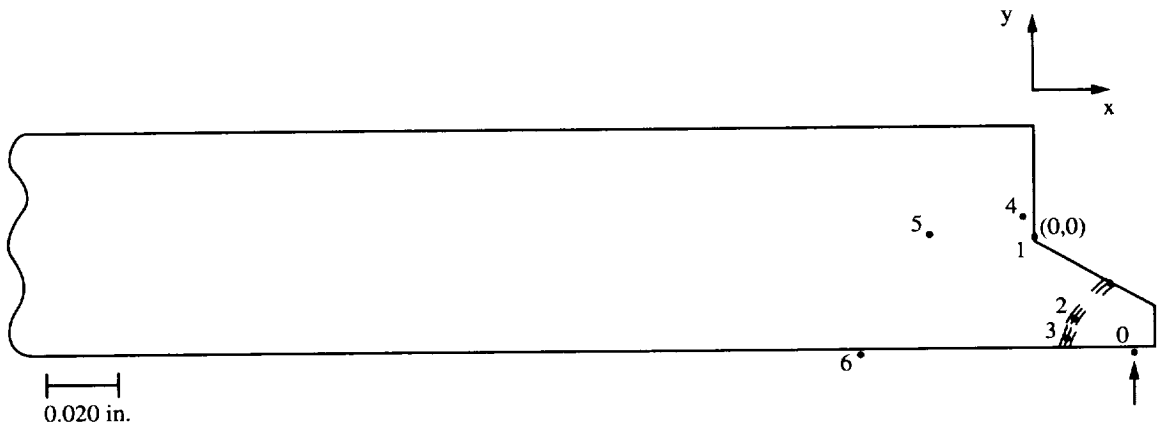

#	Coordinates (mm)	[in]	# of Bands (cycles)
0	(0.534,-0.650)	[0.026,-0.032]	Initiation
1	(0.5625,-0.3125)	[0.022,-0.012]	10(40K)
2	(0.300,-0.575)	[0.012,-0.023]	10(40K)
3	(0.255,-0.775)	[0.010,-0.031]	10(40K)
4	(-0.07,0.18)	[-0.003,0.007]	Crack Front
5	(-0.75,0.0)	[-0.029,0.000]	Crack Front
6	(-1.29,-0.85)	[-0.041,-0.033]	Crack Front

Figure 14.19 The schematic shows the initiation site, marker band and final crack frontlocations for the fatigue crack in rivet hole 4J2 that grew in the aft direction. One set ofmarker bands was found. The fatigue crack initiation region is marked with an arrow. The table summarizes the X-Y marker band coordinates relative to the origin (0,0), and the cycle count for each set of marker bands.

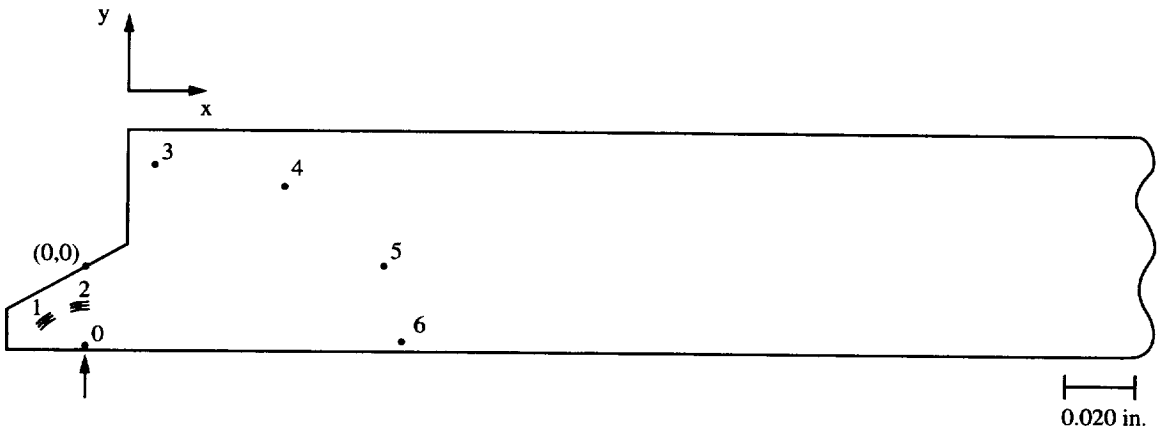

#	Coordinates (mm)	[in]	# of Bands (cycles)
0	(-0.016,-0.454)	[-0.001,-0.022]	Initiation
1	(-0.068,-0.275)	[-0.003,-0.011]	6(30K)
2	(-0.288,-0.323)	[-0.011,-0.013]	6(30K)
3	(0.47,0.72)	[0.019,0.028]	Crack Front
4	(1.43,0.6)	[0.056,0.024]	Crack Front
5	(1.95,0.0)	[0.077,0.000]	Crack Front
6	(2.08,-0.5)	[0.082,-0.020]	Crack Front

Figure 14.20 The schematic shows the initiation site, marker band and final crack front locations for the fatigue crack in rivet hole 4J3 that grew in the forward direction. One set of marker bands was found. The fatigue crack initiation region is marked with an arrow. The table summarizes the X-Y marker band coordinates relative to the origin (0,0), and the cycle count for each set of marker bands.

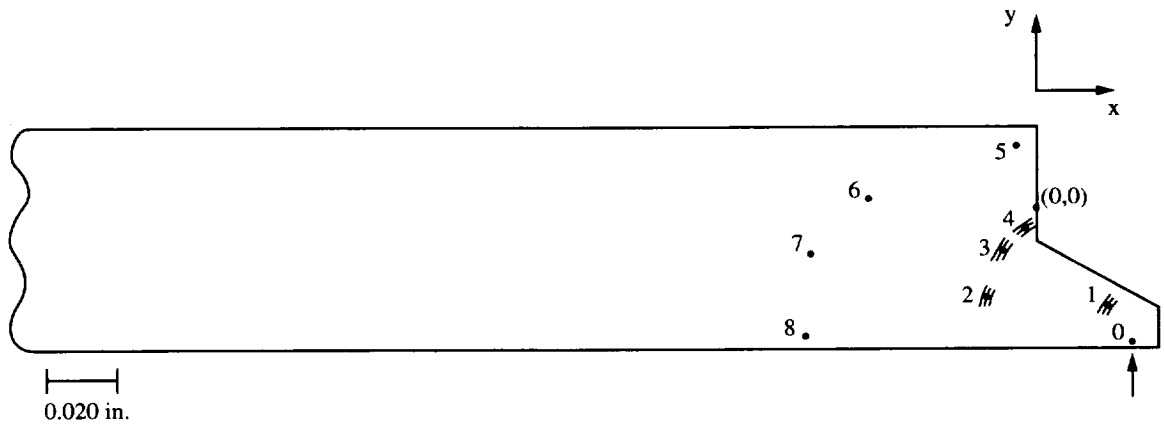

#	Coordinates (mm)	[in]	# of Bands (cycles)
0	(0.522,-0.658)	[0.026,-0.032]	Initiation
1	(0.525,-0.5675)	[0.021,-0.022]	10(40K)
2	(-0.3625,-0.500)	[-0.014,-0.020]	4(50K)
3	(-0.250,-0.1875)	[-0.010,-0.007]	4(50k)
4	(-0.0125,0.0125)	[-0.0004,0.0004]	4(50K)
5	(-0.15,0.58)	[-0.006,0.023]	Crack Front
6	(-1.21,0.2)	[-0.048,0.008]	Crack Front
7	(-1.65,-0.2)	[-0.065,-0.008]	Crack Front
8	(-1.72,-0.9)	[-0.068,-0.035]	Crack Front

Figure 14.21 The schematic shows the initiation site, marker band and final crack front locations for the fatigue crack in rivet hole 4J4 that grew in the forward direction. Two sets of marker bands were found. The fatigue crack initiation region is marked with a bracket. The table summarizes the X-Y marker band coordinates relative to the origin (0,0), and the cycle count for each set of marker bands.

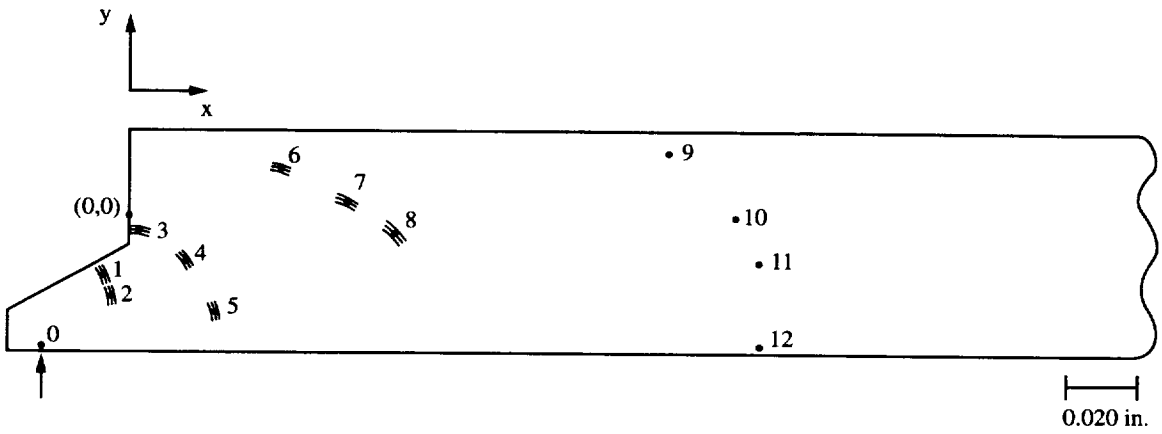

#	Coordinates (mm)	[in]	# of Bands (cycles)
0	(-0.468,-0.712)	[-0.023,-0.035]	Initiation
1	(-0.238,-0.413)	[-0.009,-0.016]	6(30K)
2	(-0.163,-0.5375)	[-0.006,-0.021]	6(30k)
3	(0.050,-0.075)	[0.002,-0.003]	9(40K)
4	(0.483,-0.260)	[0.019,-0.010]	9(40K)
5	(0.563,-0.663)	[0.022,-0.026]	9(40K)
6	(1.100,0.35)	[0.043,0.013]	4(50K)
7	(1.600,0.1375)	[0.063,0.005]	4(50K)
8	(1.950,-0.0875)	[0.077,-0.003]	4(50K)
9	(3.93,0.53)	[0.155,0.021]	Crack Front
10	(4.45,0.0)	[0.175,0.0]	Crack Front
11	(4.6,-0.3)	[0.181,-0.012]	Crack Front
12	(4.65,-0.9)	[0.183,-0.035]	Crack Front

Figure 14.22 The schematic shows the initiation site, marker band and final crack front locations for the fatigue crack in rivet hole 4J5 that grew in the aft direction. There were 3 sets of marker bands found. The fatigue crack initiation region is marked with a bracket. The table summarizes the X-Y marker band coordinates relative to the origin (0,0), and the cycle count for each set of marker bands.

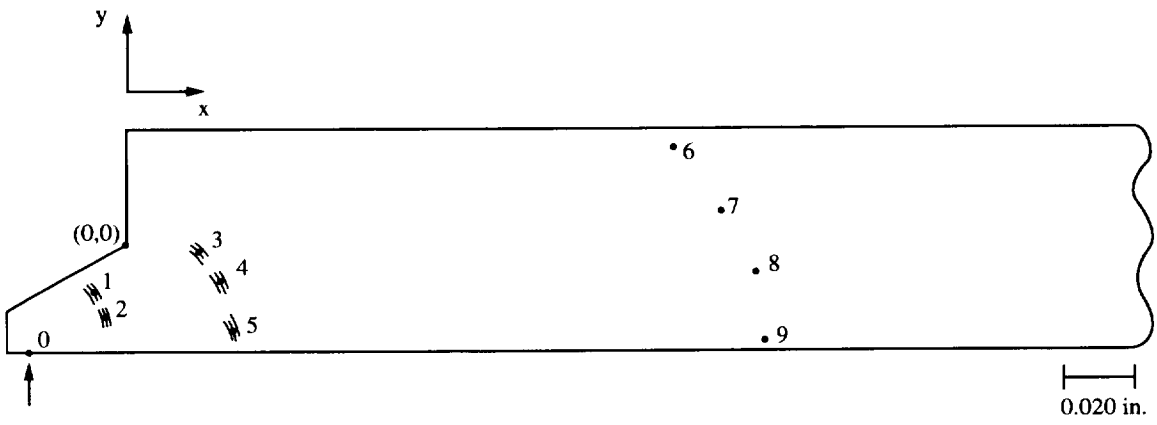

#	Coordinates (mm)	[in]	# of Bands (cycles)
0	(-0.533,-0.594)	[-0.026,-0.029]	Initiation
1	(-0.334,-0.217)	[-0.013,-0.009]	6(30K)
2	(-0.142,-0.493)	[-0.006,-0.019]	6(30K)
3	(0.509,-0.050)	[0.020,-0.002]	9(40K)
4	(0.676,-0.258)	[0.027,-0.010]	9(40K)
5	(0.793,-0.635)	[0.031,-0.025]	9(40K)
6	(4.0,0.77)	[0.157,0.030]	Crack Front
7	(4.4,0.2)	[0.173,0.008]	Crack Front
8	(4.6,-0.2)	[0.181,-0.008]	Crack Front
9	(4.6,-0.75)	[0.181,-0.029]	Crack Front

Figure 14.23 The schematic shows the initiation site, marker band and final crack front locations for the fatigue crack in rivet hole 4J5 that grew in the forward direction. There were 2 sets of marker bands found. The fatigue crack initiation region is marked with an arrow. The table summarizes the X-Y marker band coordinates relative to the origin (0,0), and the cycle count for each set of marker bands.

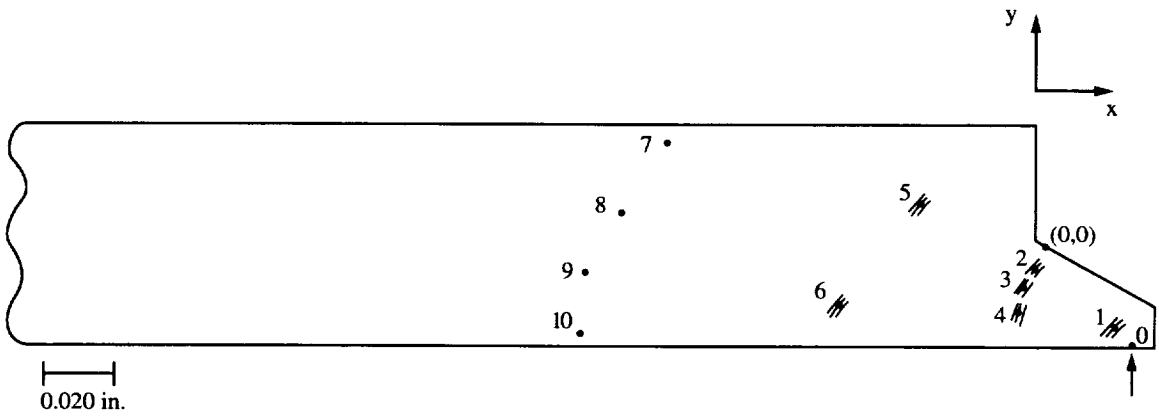

#	Coordinates (mm)	[in]	# of Bands (cycles)
0	(0.493,-0.551)	[0.024,-0.027]	Initiation
1	(0.550,-0.550)	[0.022,-0.022]	6(30K)
2	(-0.025,-0.175)	[-0.001,-0.007]	9(40K)
3	(-0.075,-0.250)	[-0.003,-0.010]	9(40K)
4	(-0.130,-0.4575)	[-0.005,-0.018]	9(40k)
5	(-0.875,0.2875)	[-0.034,0.011]	4(50K)
6	(-1.4375,-0.4375)	[-0.057,-0.017]	4(50K)
7	(-2.7,0.69)	[-0.106,0.027]	Crack Front
8	(-3.03,0.2)	[-0.119,0.008]	Crack Front
9	(-3.34,-0.2)	[-0.131,-0.008]	Crack Front
10	(-3.35,-0.8)	[-0.132,-0.031]	Crack Front

Figure 14.24 The schematic shows the initiation site, marker band and final crack front locations for the fatigue crack in rivet hole 4J6 that grew in the forward direction. There were 3 sets of marker bands found. The fatigue crack initiation region is marked with an arrow. The table summarizes the X-Y marker band coordinates relative to the origin (0,0), and the cycle count for each set of marker bands.

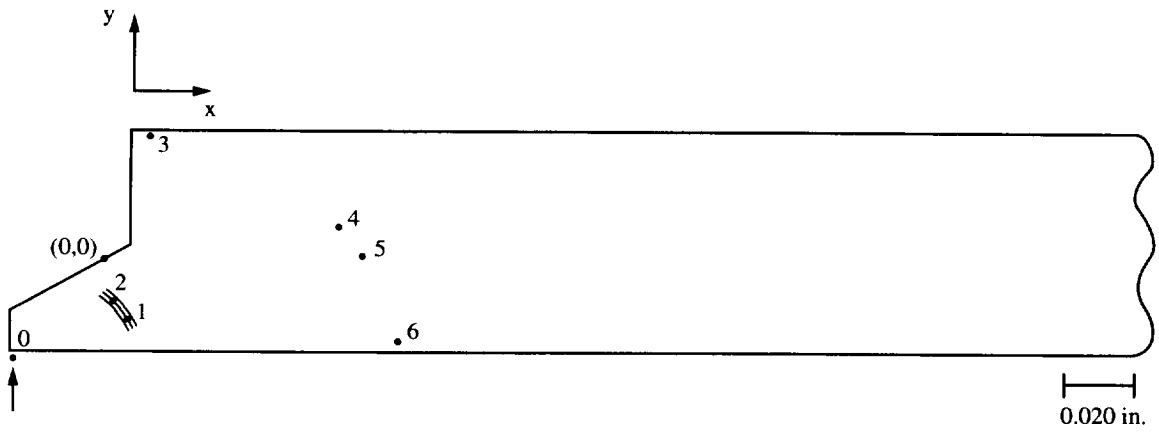

#	Coordinates (mm)	[in]	# of Bands (cycles)
0	(-0.479,-0.544)	[-0.024,-0.027]	Initiation
1	(0.095,-0.3625)	[0.004,-0.014]	4(50K)
2	(0.0175,-0.27)	[0.001,-0.010]	4(50K)
3	(0.25,0.83)	[0.010,0.033]	Crack Front
4	(1.7,0.2)	[0.067,0.008]	Crack Front
5	(1.91,0.0)	[0.075,0.0]	Crack Front
6	(2.1,-0.65)	[0.083,-0.026]	Crack Front

Figure 14.25 The schematic shows the initiation site, marker band and final crack front locations for the fatigue crack in rivet hole 4J6 that grew in the aft direction. Only one set of marker bands was found. The fatigue crack initiation region is marked with an arrow. The table summarizes the X-Y marker band coordinates relative to the origin (0,0), and the cycle count for each set of marker bands.

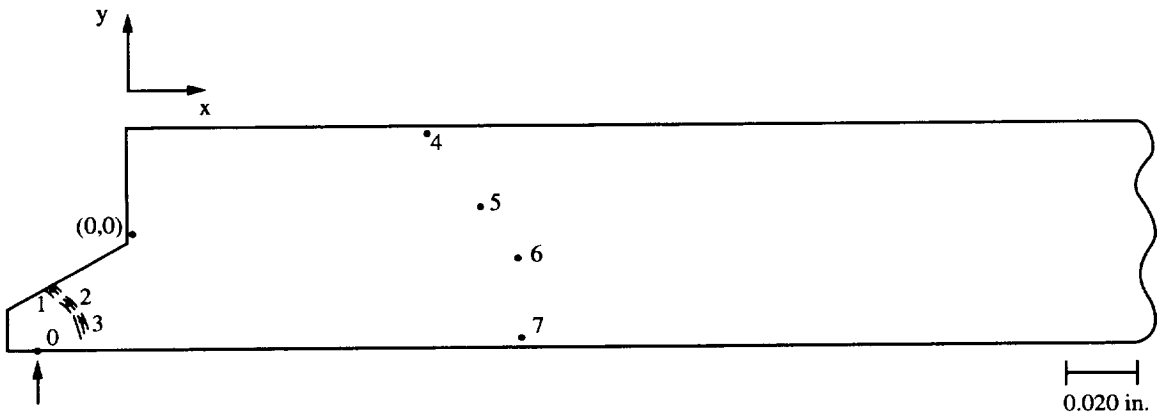

#	Coordinates (mm)	[in]	# of Bands (cycles)
0	(-0.533,-0.635)	[-0.026,-0.031]	Initiation
1	(-0.575,-0.4875)	[-0.023,-0.019]	9(40K)
2	(-0.4625,-0.5625)	[-0.018,-0.022]	9(40K)
3	(-0.325,-0.7125)	[-0.013,-0.028]	9(40K)
4	(2.2,0.72)	[0.087,0.028]	Crack Front
5	(2.5,0.2)	[0.098,0.008]	Crack Front
6	(2.85,-0.2)	[0.112,-0.008]	Crack Front
7	(2.86,-0.69)	[0.113,-0.027]	Crack Front

Figure 14.26 The schematic shows the initiation site, marker band and final crack front locations for the fatigue crack in rivet hole 4J7 that grew in the forward direction. Two sets of marker bands were found. The fatigue crack initiation region is marked with an arrow. The table summarizes the X-Y marker band coordinates relative to the origin (0,0), and the cycle count for each set of marker bands.

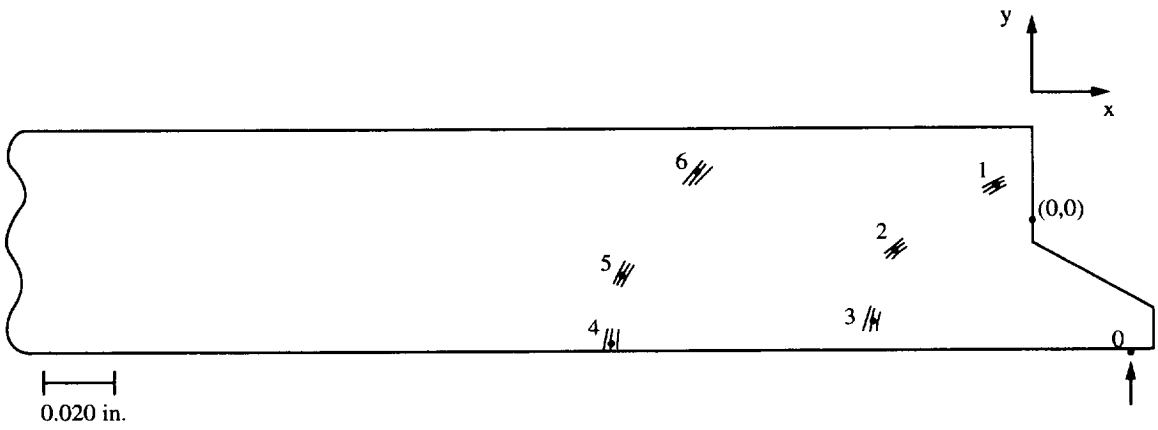

#	Coordinates (mm)	[in]	# of Bands (cycles)
0	(0.622,-0.711)	[0.031,-0.035]	Initiation
1	(-0.250,0.2375)	[-0.010,0.010]	6(30K)
2	(-1.000,-0.250)	[-0.039,-0.010]	6(30K)
3	(-1.1425,-0.925)	[-0.045,-0.036]	6(30k)
4	(-3.0625,-0.950)	[-0.121,-0.037]	9(40K)
5	(-2.9875,-0.425)	[-0.118,-0.017]	9(40K)
6	(-2.425,0.3375)	[-0.095,0.015]	9(40K)

• Crack front not available.

Figure 14.27 The schematic shows the marker band locations for the fatigue crack in rivet hole 4J8 that grew in the forward direction. Two sets of marker bands were found. The fatigue crack initiation region is marked with an arrow. The table summarizes the X-Y marker band coordinates relative to the origin (0,0), and the cycle count for each set of marker bands.

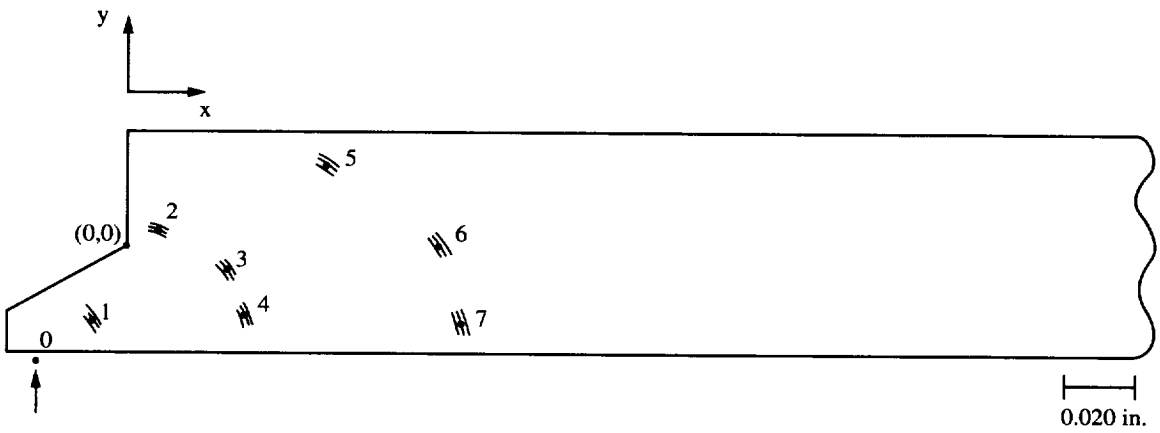

#	Coordinates (mm)	[in]	# of Bands (cycles)
0	(-0.507,-0.646)	[-0.025,-0.032]	Initiation
1	(-0.275,-0.5375)	[-0.011,-0.021]	3(20K)
2	(0.175,0.150)	[0.007,0.006]	6(30k)
3	(0.6875,-0.150)	[0.027,-0.006]	6(30k)
4	(0.820,-0.475)	[0.032,-0.019]	6(30k)
5	(1.3875,0.6125)	[0.054,0.024]	9(40K)
6	(2.2375,0.000)	[0.088,0.000]	9(40K)
7	(2.400,-0.525)	[0.097,-0.021]	9(40K)

- No crack front. Crack linked up with 4J9B.

Figure 14.28 The schematic shows the marker band locations for the fatigue crack in rivet hole 4J8 that grew in the aft direction. Three sets of marker bands were found. The fatigue crack initiation region is marked with an arrow. The table summarizes the X-Y marker band coordinates relative to the origin (0,0), and the cycle count for each set of marker bands.

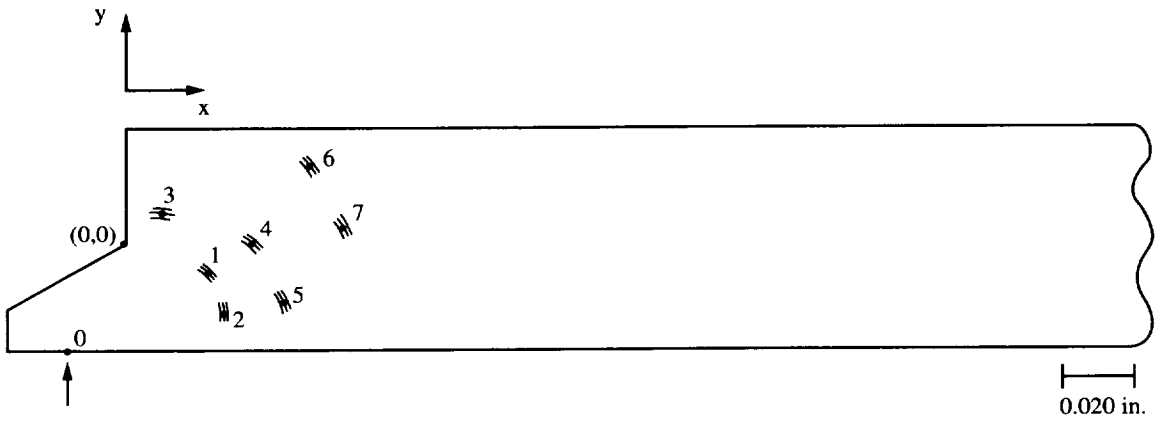

#	Coordinates (mm)	[in]	# of Bands (cycles)
0	(-0.290,-0.584)	[-0.014,-0.029]	Initiation
1	(0.5875,-0.1875)	[0.023,-0.007]	6(30K)
2	(0.695,-0.475)	[0.027,-0.019]	6(30K)
3	(0.2675,0.2425)	[0.010,0.010]	9(40K)
4	(0.8925,-0.0125)	[0.035,-0.0004]	9(40K)
5	(1.1125,-0.4125)	[0.044,-0.016]	9(40K)
6	(1.25,0.5875)	[0.049,0.023]	4(50K)
7	(1.570,0.125)	[0.062,0.005]	4(50K)

- No Crack front. Crack linked up with 4J8A.

Figure 14.29 The schematic shows the marker band locations for the fatigue crack in rivet hole 4J9 that grew in the forward direction. There were 3 sets of marker bands found. The fatigue crack initiation region is marked with an arrow. The table summarizes the X-Y marker band coordinates relative to the origin (0,0), and the cycle count for each set of marker bands.

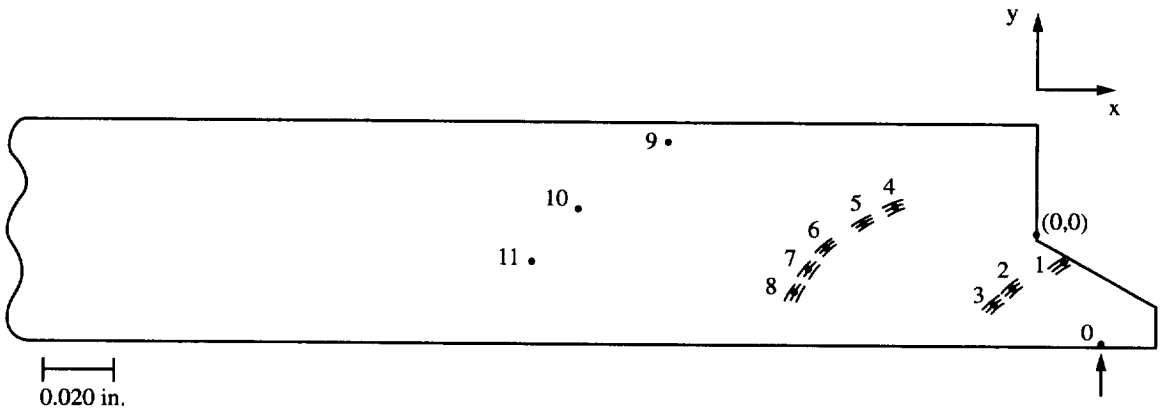

#	Coordinates (mm)	[in]	# of Bands (cycles)
0	(0.288,-0.581)	[0.014,-0.029]	Initiation
1	(0.2175,-0.175)	[0.009,-0.007]	9(40K)
2	(-0.1875,0.375)	[-0.007,0.015]	9(40K)
3	(-0.2875,-0.500)	[-0.011,-0.020]	9(40K)
4	(-1.7375,-0.4175)	[-0.068,-0.016]	4(50K)
5	(-1.6625,-0.275)	[-0.065,-0.011]	4(50K)
6	(-1.5125,-0.0875)	[-0.060,-0.003]	4(50K)
7	(-1.2375,0.080)	[-0.049,0.003]	4(50K)
8	(-1.000,0.200)	[-0.039,0.008]	4(50K)
9	(-2.65,0.67)	[-0.104,0.026]	Crack Front
10	(-3.28,0.2)	[-0.129,0.008]	Crack Front
11	(-3.68,-0.2)	[-0.145,-0.008]	Crack Front

Figure 14.30 The schematic shows the initiation site, marker band and final crack front locations for the fatigue crack in rivet hole 4J10 that grew in the aft direction. Two sets of marker bands were found. The fatigue crack initiation region is marked with a bracket. The table summarizes the X-Y marker band coordinates relative to the origin (0,0), and the cycle count for each set of marker bands.

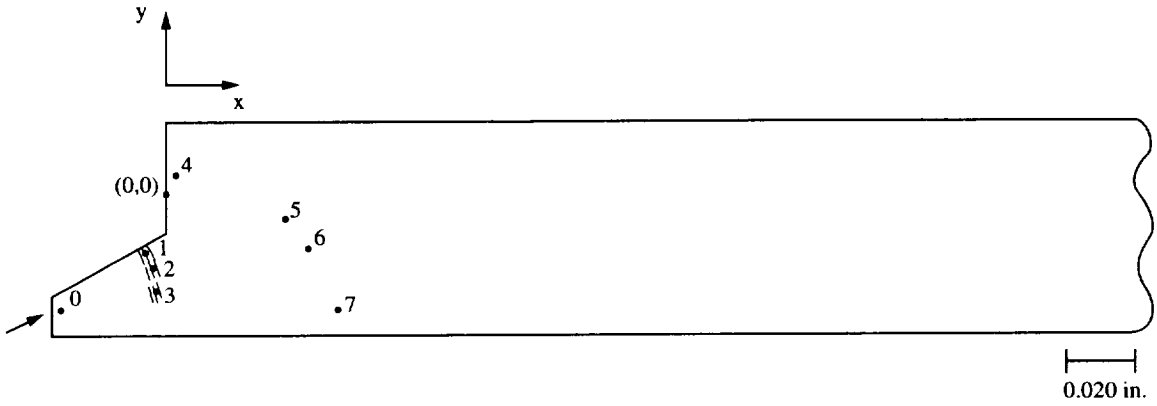

#	Coordinates (mm)	[in]	# of Bands (cycles)
0	(-0.636,-0.632)	[-0.031,-0.031]	Initiation
1	(-0.1625,-0.375)	[-0.006,-0.015]	4(50K)
2	(-0.1125,-0.500)	[-0.005,-0.020]	4(50K)
3	(-0.0875,-0.5625)	[-0.003,-0.022]	4(50K)
4	(0.04,0.14)	[0.002,0.006]	Crack Front
5	(0.89,-0.2)	[0.035,-0.008]	Crack Front
6	(1.05,-0.4)	[0.041,-0.016]	Crack Front
7	(1.24,-0.87)	[0.049,-0.034]	Crack Front

Figure 14.31 The schematic shows the initiation site, marker band and final crack front locations for the fatigue crack in rivet hole 4J12 that grew in the aft direction. One set of marker bands was found. The fatigue crack initiation region is marked with an arrow. The table summarizes the X-Y marker band coordinates relative to the origin (0,0), and the cycle count for each set of marker bands.

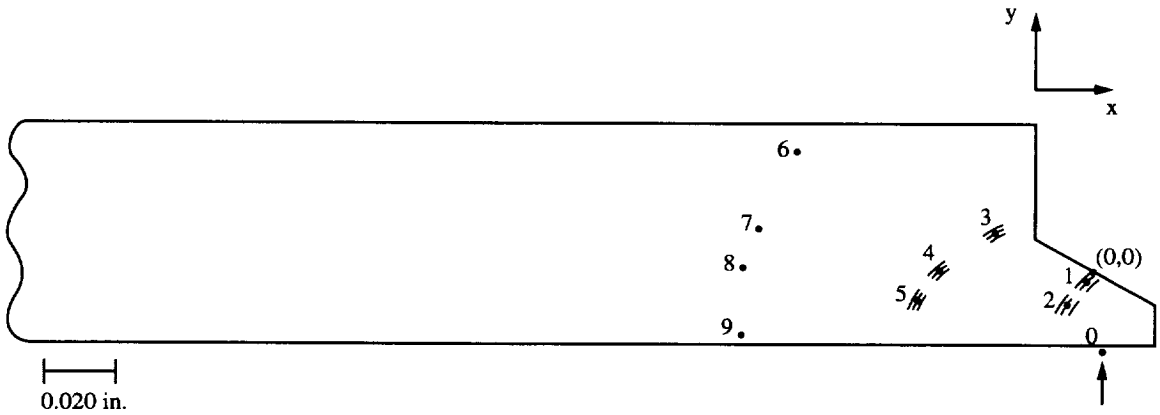

#	Coordinates (mm)	[in]	# of Bands (cycles)
0	(0.046,-0.448)	[0.002,-0.022]	Initiation
1	(0.000,-0.025)	[0.000,-0.001]	9(40K)
2	(-0.1625,-0.150)	[-0.006,-0.006]	9(40K)
3	(-0.6875,0.3025)	[-0.027,0.012]	4(50k)
4	(-1.1125,0.000)	[-0.044,0.000]	4(50K)
5	(-1.250,-0.2125)	[-0.049,-0.008]	4(50K)
6	(-2.15,0.85)	[-0.085,0.033]	Crack Front
7	(-2.45,0.3)	[-0.096,0.012]	Crack Front
8	(-2.59,0.0)	[-0.102,0.0]	Crack Front
9	(-2.66,-0.65)	[-0.105,-0.026]	Crack Front

Figure 14.32 The schematic shows the initiation site, marker band and final crack front locations for the fatigue crack in rivet hole 4J14 that grew in the aft direction. Two sets of marker bands were found. The fatigue crack initiation region is marked with a bracket. The table summarizes the X-Y marker band coordinates relative to the origin (0,0), and the cycle count for each set of marker bands.

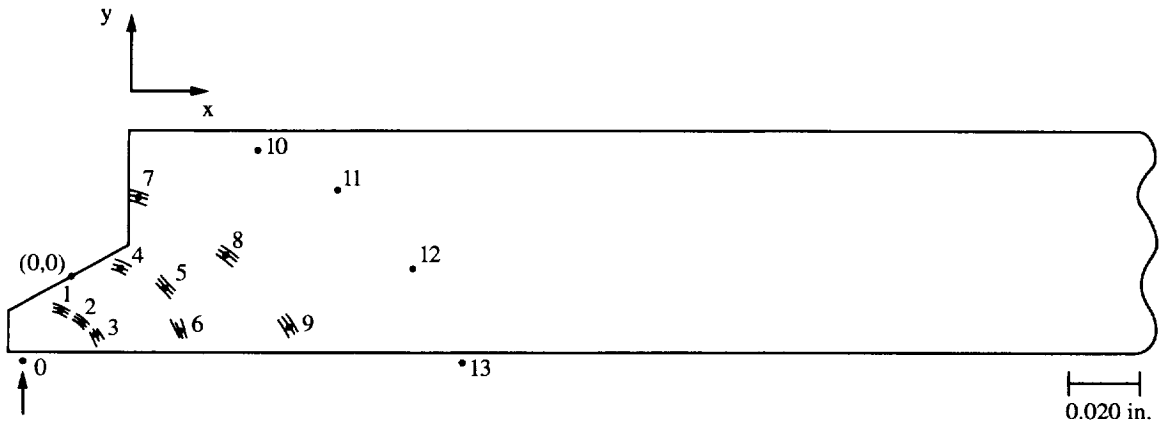

#	Coordinates (mm)	[in]	# of Bands (cycles)
0	(-0.244,-0.526)	[-0.012,-0.026]	Initiation
1	(-0.0625,-0.255)	[-0.002,-0.001]	6(30K)
2	(0.050,-0.2875)	[0.002,-0.011]	6(30K)
3	(0.160,-0.395)	[0.006,-0.016]	6(30K)
4	(0.325,-0.0625)	[0.013,-0.002]	9(40K)
5	(0.064,-0.150)	[0.025,-0.006]	9(40K)
6	(0.750,-0.350)	[0.030,-0.014]	9(40K)
7	(0.475,0.5325)	[0.019,0.021]	4(50K)
8	(1.125,0.125)	[0.044,0.005]	4(50K)
9	(1.550,-0.3125)	[0.061,-0.012]	4(50K)
10	(1.28,0.83)	[0.050,0.035]	Crack Front
11	(1.86,0.6)	[0.076,0.024]	Crack Front
12	(2.4,0.0)	[0.094,0.0]	Crack Front
13	(2.73,-0.7)	[0.107,-0.028]	Crack Front

Figure 14.33 The schematic shows the initiation site, marker band and final crack front locations for the fatigue crack in rivet hole 4J14 that grew in the forward direction. Three sets of marker bands were found. The fatigue crack initiation region is marked with an arrow. The table summarizes the X-Y marker band coordinates relative to the origin (0,0), and the cycle count for each set of marker bands.

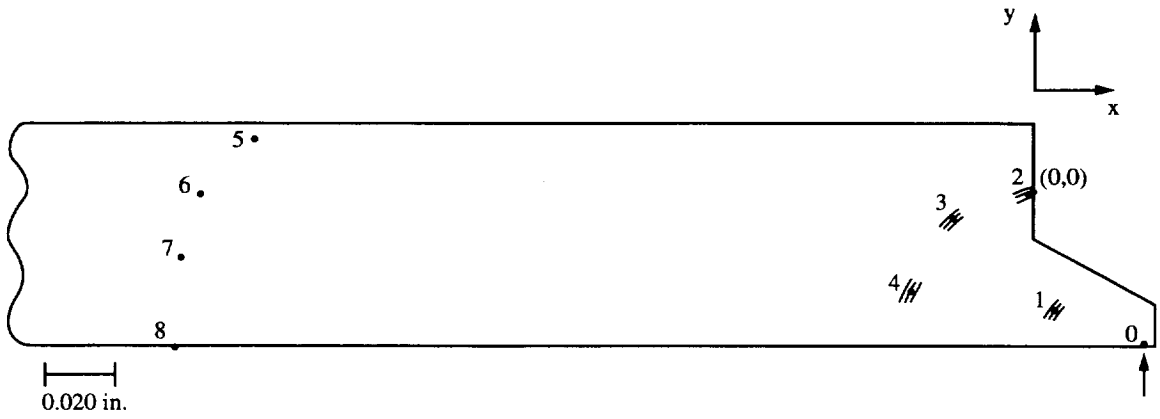

#	Coordinates (mm)	[in]	# of Bands (cycles)
0	(0.628,-0.852)	[0.031,-0.042]	Initiation
1	(0.153,-0.860)	[0.006,-0.034]	6(30K)
2	(0.000,0.000)	[0.000,0.000]	4(40K)
3	(-0.576,-0.200)	[-0.023,-0.008]	9(40K)
4	(-0.710,-0.835)	[-0.028,-0.033]	9(40k)
5	(-5.75,0.3)	[-0.226,0.012]	Crack Front
6	(-6.1,0.0)	[-0.240,0.000]	Crack Front
7	(-6.32,-0.5)	[-0.249,-0.020]	Crack Front
8	(-6.3,-1.15)	[-0.248,-0.045]	Crack Front

Figure 14.34 The schematic shows the initiation site, marker band and final crack front locations for the fatigue crack in rivet hole 4J15 that grew in the forward direction. Two sets of marker bands were found. The fatigue crack initiation region is marked with an arrow. The table summarizes the X-Y marker band coordinates relative to the origin (0,0), and the cycle count for each set of marker bands.

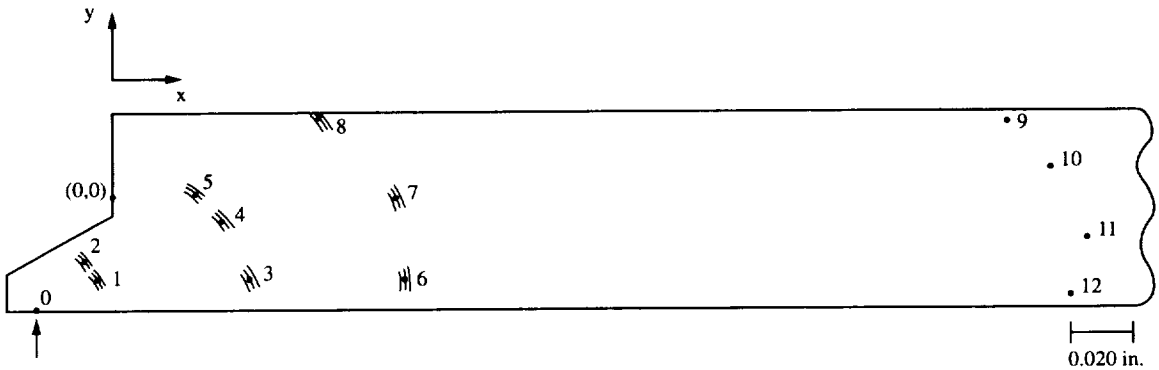

#	Coordinates (mm)	[in]	# of Bands (cycles)
0	(-0.463,-0.720)	[-0.023,-0.035]	Initiation
1	(-0.165,-0.650)	[-0.006,-0.026]	3(20K)
2	(-0.3125,-0.565)	[-0.012,-0.022]	3(20K)
3	(1.1375,-0.66)	[0.045,-0.026]	6(30K)
4	(0.9925,-0.200)	[0.039,-0.008]	6(30K)
5	(0.650,0.250)	[0.026,0.010]	6(30K)
6	(2.500,-0.7175)	[0.098,-0.028]	9(40K)
7	(2.375,-0.0625)	[0.093,-0.002]	9(40K)
8	(1.7125,0.6375)	[0.067,0.025]	9(40K)
9	(7.4,0.6)	[0.291,0.024]	Crack Front
10	(7.7,0.2)	[0.303,0.008]	Crack Front
11	(8.0,-0.2)	[0.315,-0.008]	Crack Front
12	(7.9,-0.82)	[0.311,-0.032]	Crack Front

Figure 14.35 The schematic shows the marker band locations for the fatigue crack in rivet hole 4J15 that grew in the aft direction. Three sets of marker bands were found. The fatigue crack initiation region is marked with a bracket. The table summarizes the X-Y marker band coordinates relative to the origin (0,0), and the cycle count for each set of marker bands.

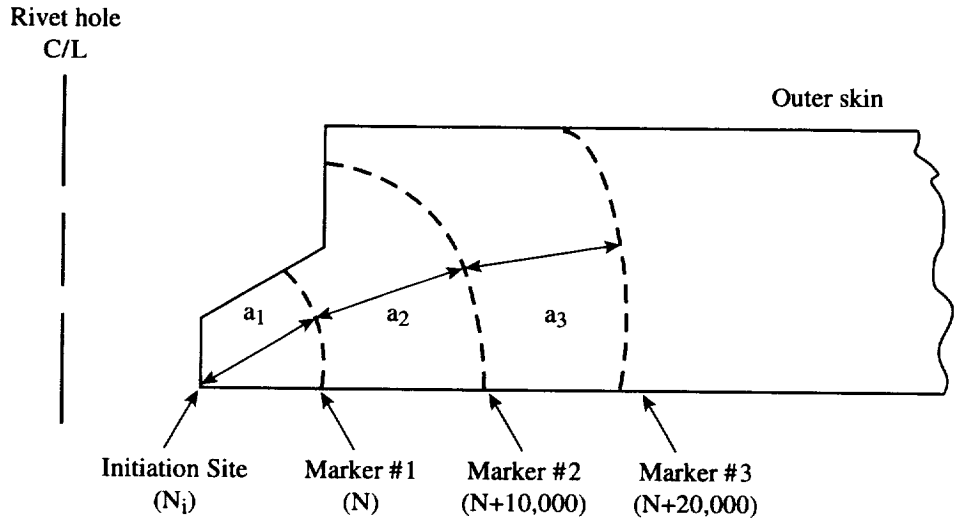

average crack length	average fatigue crack growth rate
$a_{av}\|_{1,2}=a_1+a_2/2$	$(\Delta a/\Delta N)_{av}\|_{1,2}=a_2/10{,}000$
$a_{av}\|_{2,3}=a_1+a_2+a_3/2$	$(\Delta a/\Delta N)_{av}\|_{2,3}=a_3/10{,}000$
$a_{av}\|_{1} =a_1/2$	$(\Delta a/\Delta N)_{av}\|_{1} =a_1/(N-N_i)$

Figure. 14.36 A schematic describing the method used to determine a_{av} and $(\Delta a/\Delta N)_{av}$ based on fatigue fracture surface marker band analysis.

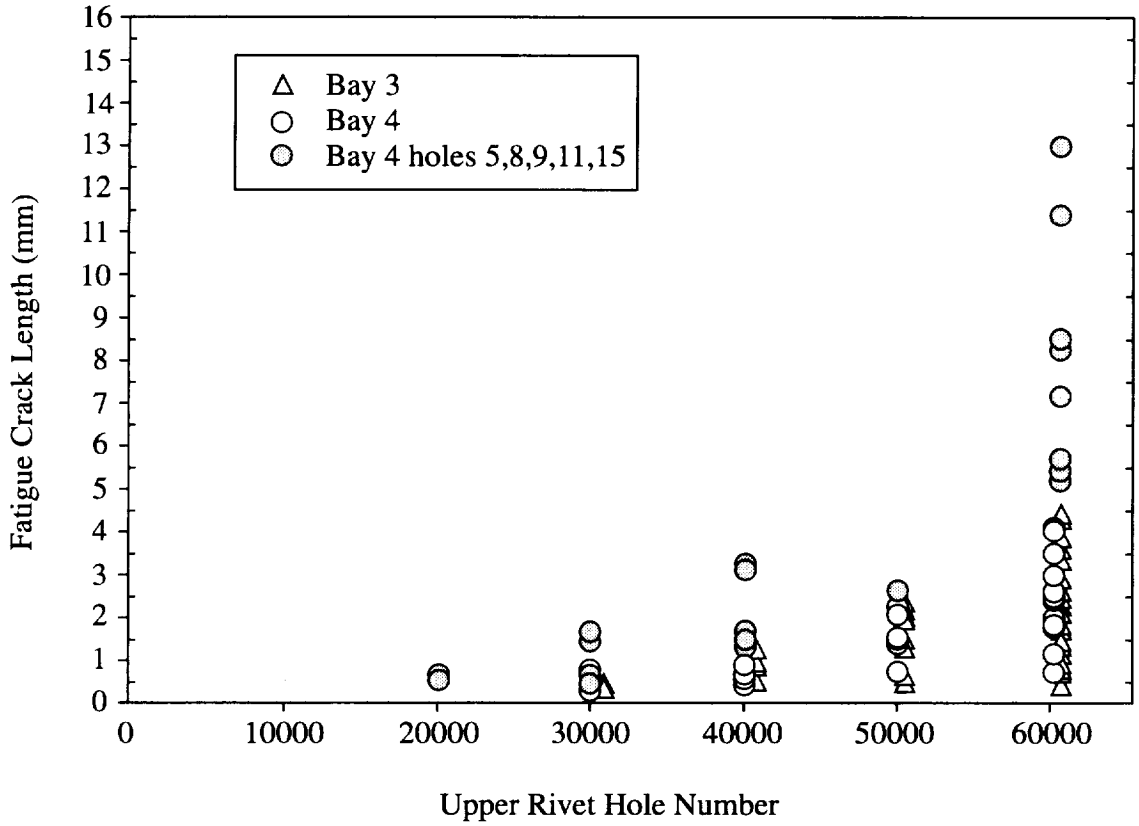

Figure 14.37 Bays 3 and 4 upper rivet row outer skin fatigue crack length history.

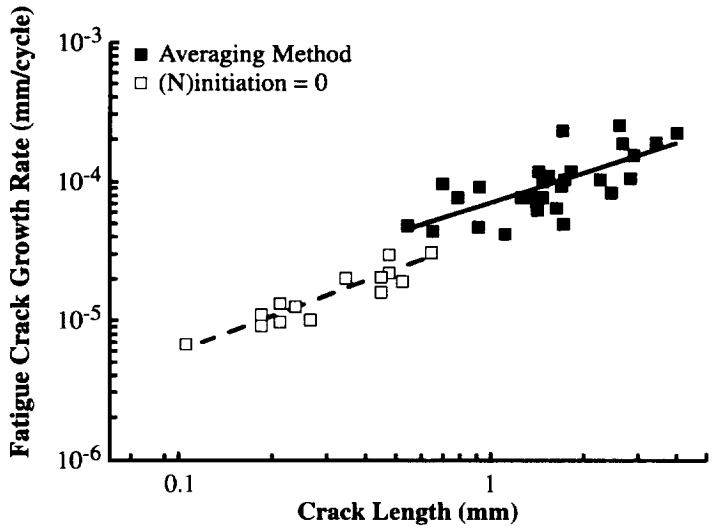

(a)

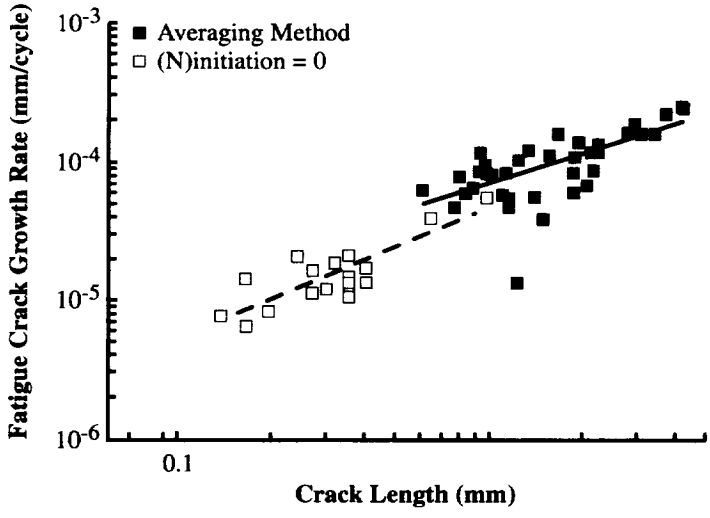

(b)

Figure 14.38 The growth characteristics of small fatigue cracks contained in the upper rivet row outer skin in a) bay 3 and b) bay 4.

15. Discussion

15.1 Characterization of MSD:

The complete characterization of fatigue cracks contained in the fuselage lap splice was achieved by a detailed teardown and fractographic characterization of the damaged regions. Figures 15.1 and 15.2 show the location of fuselage lap splice joint fatigue cracks as determined by NDE (visual and eddy current inspections) and Figure 15.3 shows the results of the destructive examinations. A comparison of the NDE results in Figures 15.1 and 15.2 show that (1) nearly all upper rivet row hole locations in bays 2, 3, and 4 contained evidence of cracking and (2) the majority of outer skin upper rivet row cracks found by within-hole eddy current inspection in bays 3 and 4 are subsurface and not detected by visual inspection. In addition, surface probe EC inspections revealed subsurface fatigue cracks in the bay 1 tear strap region, the 2/3 and 3/4 tear strap regions, and one indication along the second rivet row in bay 4. A comparison of Figures 15.1 and 15.2 with the destructive examination results shown in Figure 15.3 reveal that visual and EC methods detected cracks at approximately one-half of the rivet hole locations that contained fatigue cracks. Many of the fatigue cracks not detected by NDE were small (below the detection limit of surface probe EC), located under the rivet head, located along the faying surface, and/or contained in interior structure (inner skin, tear strap, or frame).

The results of the destructive examinations are summarized in Table 15.1. Forty-five percent of the rivet holes examined were found to contain fatigue cracks; a total of 281 rivet holes were examined and 126 holes were found to contain fatigue cracks. The bay 2 lap splice joint region contained the greatest number of fatigue cracks followed by bay 4 and bay 3. The bay 2/3 tear strap region contained a high number of fatigue cracks relative to the number of rivet hole examined; here, 83% of the rivet holes examined were found to contain cracks. Bay 1 and bay 3/4 tear strap regions contained similar amounts of cracking, 44% and 47%, respectively.

Table 15-1 Fatigue Crack Summary

Panel Location	No. of Rivet Holes Examined	No. and (%) of Rivet Holes Containing Fatigue Cracks
Bay #1-T.S.	25	11 (44%)
Bay #2	67	32 (48%)
Bay #2/3-T.S.	23	19 (83%)
Bay #3	66	23 (35%)
Bay #3/4 -T.S.	34	16 (47%)
Bay #4	66	25 (38%)
Totals	281	126 (45%)

The results of the destructive examination show that lap splice joint MSD is characterized by a wide distribution of crack sizes. Figures 15.4, 15.5, and 15.6 summarize the size distribution of fatigue cracks contained in the outer and inner skin of the bay 2, 3, and 4 lap splice joint. Outer skin fatigue cracks contained in bays 2 and 4 grew to a maximum length of approximately 14 mm (0.55 inch) prior to crack link-up. Inner skin fatigue cracks grew to a length of less than 5.6 mm (0.2 inch) in bay 2 and less than 1.3 mm (0.05 inch) in bays 3 and 4. Presumably, the formation of the long, 47.6 cm (18.75 inch), upper rivet row crack in the outer skin of bay 2 led to a redistribution of load to the inner skin which resulted in significantly more inner skin cracking in bay 2 compared to bays 3 and 4.

A summary of all fatigue cracks found in bays 2, 3, and 4 lap splice joints is shown in Figure 15.7. Noted in Figure 15.7a are the results of the visual and eddy current outer skin inspections. All outer skin fatigue cracks were detected by "within hole" eddy current inspection. Only outer skin cracks greater than 2.54 mm (0.10 inch) in length were detected by visual examination. The six fatigue cracks not detected by NDE, refer to Figure 15.7a, were located at "filled" hole rivet locations in the second rivet row (row I). Here, the sliding surface probe eddy current technique was unable to detect the presence of these outer skin fatigue cracks. The cracks not detected by surface EC probe ranged in size, four cracks having lengths ranging from 0 to 1.3 mm (0.05 inch), one crack of length ranging between 3.8 mm (0.15 inch) and 5.1 mm (0.20 inch), and one crack of length ranging between 5.1 mm (0.20 inch) and 6.4 mm (0.25 inch). Many of the inner skin cracks were small and were located in filled holes. Here, the within hole EC probe was not used and the surface probe was an inadequate technique to detect inner skin cracks.

The fatigue cracking in the 2/3 and 3/4 tear strap regions are summarized in Figure 15.8. Here, cracks are generally small, less than 1.3 mm (0.05 inch) in length. A total of eight fatigue cracks having lengths between 1.3 mm (0.05 inch) to 6.4 mm (0.25 inch) were noted in the outer skin, inner skin and tear strap. Tear 3/4 strap region was found to contain the greatest number of fatigue cracks.

15.2 Fatigue Crack Initiation:

The destructive examination revealed that fretting damage at each rivet hole was the primary mechanism for crack initiation along the upper rivet row. Table 15.2 ranks the different sources of fatigue crack initiation found in the fuselage lap splice joint.

Table 15-2 Sources of Fatigue Crack Initiation

	Location	Source of Crack Initiation
1.	Outer skin	a. Faying surface fretting adjacent to the rivet hole.
2.	Inner skin/ tear strap	a. Rivet hole surface fretting and high K_T regions(hole surface imperfections). b. High K_T regions (imperfections and burrs) at the rivet hole corner.

Results suggest that faying surface fretting fatigue can increase the likelihood of MSD in the lap splice outer skin. The characterization of lap splice faying surface in bays 2, 3, and 4, discussed in Section 13.0, revealed that the upper rivet row in bays 2, 3, and 4 exhibited the greatest evidence of fretting damage. Here, all outer skin upper rivet row fatigue cracks initiated along the faying surface as result of fretting fatigue damage in the aluminum clad layer. (The fuselage skin is constructed of Alclad 2024-T3 which is coated (clad) with a 1230 aluminum alloy. The 50 μm thick (nominal) clad layer is used for increased corrosion resistance.) The clad layer fretting fatigue damage was caused by the repeated relative movement of the inner and outer skin in the localized contact area around the rivet hole faying surface (See ref. 1-2). Research has shown that substantial reductions in fatigue life can result from this type of damage where displacement amplitudes are small compared to the contact size (See ref. 3). The surface degradation and debris zone around the inboard surface of the outer skin rivet hole, depicted in Figures 13.1-13.3, is characterized by a black aluminum oxide region (See ref.1-3). The location and shape of the debris zone

shown in Figures 13.1-13.3 is similar to that reported by Finney and Evans (See ref.2). They showed that fastener hole expansion and interference-fit fasteners can exacerbate faying surface fretting damage by displacing material into the faying surface contact region. Detailed examination of the crack initiation regions along the faying surface, refer to Figure 15.9, revealed that small regions of the ductile clad layer were plastically deformed creating a highly localized damage region characterized by superficial micro-cracking and particle formation similar to that reported by Blanchard et.al. (See ref.3). Figures 15.9a and 15.9b show the fatigue fracture surface and the fretting fatigue damage region along the faying surface adjacent to rivet hole location 3J3FWD. Figure 15.9c shows the typical fretting damage (micro-cracking) and debris in the region of fatigue crack initiation, region A in Figure 15.9b. At each upper rivet hole location, small fatigue cracks (refer to Figures 7.25-7.28 for typical examples) initiated in the clad layer fretting fatigue damaged region resulting in outer skin multiple site cracking.

Multiple site fatigue cracking in the lap splice inner skin and tear strap regions were primarily caused by damage at the rivet hole corner and along the rivet hole surface. Examples of corner cracks resulting from high K_T regions are shown in Figures 6.21 and 6.22, where cracks initiated at a corner burr, and Figure 7.34 is an example of a crack initiation from a corner imperfection. Examples of rivet hole fatigue cracking initiation by possible fretting between the rivet shank and the surface of the hole are shown in Figures 6.14-6.17, 6.20, 8.17. In each example, the surface of the hole exhibits a rough surface with microcracks (refer to Figures 6.14.b) in the region of fatigue crack initiation; this is an indication of possible fretting damage. Within hole fatigue crack initiation was also noted at surface imperfections as shown in Figures 8.14 and 8.32.

Knowing that all outer skin fatigue cracks grow at similar rates, refer to section 14.0 and paragraph 15.3, the crack length distribution shown in Figures 15.10 - 15.12 can be used to assess when, in relative terms, fatigue cracks initiated in bays 2, 3, and 4. The longer crack lengths in the mid bay region suggest that fatigue cracks generally initiated first in the mid-bay regions of bays 2 and 4 (Figures 15.10 and 15.12). The mid-bay region in bay 3 (Figure 15.11) exhibits a much shorter crack length distribution compared to bays 2 and 4, suggesting that fatigue cracks in bay 3 initiated later in life compared to bays 2 and 4. Even though each bay exhibits a distinct distribution of fatigue crack lengths, bay-to-bay and hole-to-hole random differences reveal the stochastic nature of each crack initiation event. For example, it is difficult to rationalize why cracks in adjacent bays (bay 3 versus bays 2 and 4) or adjacent rivet holes (4J8 versus 4J7) initiate at significantly different times within the life of the lap splice joint. The cause for the randomness of crack initiation is particularly difficult to rationalize when it is has been revealed that, (1) the same initiation mechanism (fretting) occurred at all outer skin rivet locations, and (2) all fatigue cracks grow at similar da/dN suggest that crack tip (local) stresses at each rivet hole are about the same. It is apparent that unknown local (micro) effects play an important role on fatigue crack initiation in the lap splice joint.

15.3 Fatigue Crack Propagation:

All outer skin fatigue cracks exhibit a similar elliptical crack front shape. Figure 12.1 reveals that outer skin fatigue cracks can grow to crack lengths, ranging from two to three skin thicknesses, before penetrating the outboard surface of the outer skin. Subsurface cracking may result from, (1) increased tensile stress along the outer skin inboard surface resulting from lap splice joint bending loads, and/or (2) compressive residual stress along the outer skin outboard surface resulting from rivet head expansion into the countersink region. Inner layer (inner skin, tear strap) fatigue crack front shapes vary; both, semi circular and elliptical crack front shapes were observed.

The outer skin fatigue crack growth characteristics of short cracks, 0.1 mm to 4 mm in length, contained in the upper rivet row were determined by marker band analysis. The results shown in Figure 14.38 reveal that all upper rivet cracks contained in bays 3 and 4 exhibit similar fatigue crack growth characteristics. The da/dN estimates shown in Figure 14.38 for crack lengths between 0.1 mm to 1 mm (open square symbols) are based on the position of a single marker band and the assumption that fatigue cracks initiated at the start of the pressure test ($N_{initiation} = 0$). A more reasonable estimate of $N_{initiation}$ can be made based on the crack length history plot shown in Figure 14.37. Extrapolating the crack length versus N plot suggests that the first crack initiation in bay 3 occurred between 10,000 and 15,000 pressure

cycles and bay 4 crack initiation occurred between 5,000 and 10,000 pressure cycles. Plotted in Figure 15.13 are the estimated short crack da/dN results (open triangles and diamonds) for extrapolated values of $N_{initiation}$. A comparison of the linear regression analysis lines for bays 3 and 4 ($N_{initiation}$= 15,000 and 10,000 cycles, respectively) with the long crack data (solid square symbols) strongly suggests that a single curve describes the growth behavior of upper rivet row fatigue cracks in each lap splice joint bay. A comparison of the fatigue crack growth characteristics for bays 3 and 4 is shown in Figure 15.14. Here, the linear regression analysis lines for bays 3 and 4 are in good agreement. This important result suggests that all outer skin fatigue cracks contained in the lap splice joint upper rivet row propagate at the same rate. The linear behavior of the log da/dN versus log a plot may suggest that complex local stresses, such as that resulting from rivet fit-up, have little effect on da/dN for fatigue cracks greater than 1 mm in length. If local stresses were significant, a non-linear da/dN versus a response would be expected as the crack grew out of a local stress environment into the remote stress dominated regime.

15.4 Fatigue Crack Link-up:

The long upper rivet row crack contained in bay 2 resulted from multiple crack link-up events. Crack link-up occurred due to rapid fracture of the remaining ligament between approaching fatigue cracks emanating from adjacent rivet holes. Each crack link-up event produced a fracture surface characterized by a ductile tearing morphology. Detailed fractographic examinations revealed that the size of the ductile tearing regions generally increased and fatigue crack lengths decreased as the main crack grew from the mid-bay region to the outer bay region. The crack link-up fracture morphology confirmed that, (1) initial crack link-up occurred at the mid-bay region, and (2) as the main crack grew in length, the driving force for crack propagation increased, thus increasing the critical length for crack link-up in the outer bay region.

The fracture surfaces adjacent to outer rivet hole locations 2J1 to 2J5 and 2J8 to 2J15 exhibited scratches normal to the direction of crack path, suggesting out-of-plane movement and Mode III loading. No evidence of fatigue crack surface scratches was observed in the region of initial crack link-up between rivet holes 2J5, 2J6, 2J7, and 2J8; here, the lack of scratches on the fracture surface suggest primarily a Mode I loading and small out-of-plane displacements during the initial crack link-up stage. The large out-of-plane displacements that would create fracture surface scratches normal to the direction of crack growth suggest that the rivet heads did not fasten the outer skin during the latter stage of crack link-up. As the bay 2 upper rivet row crack link-up process continued outward from the initial region of link-up (between holes 2J5 and 2J8), the local out-of-plane loads increased and substantial outer skin "pillowing" occurred. The pressure load was great enough to shear off the upper portion of the rivet heads at holes locations 2J2, 2J4, 2J5, 2J8, 2J10, 2J11, 2J12, and 2J14. Refer to Figures 3.4-3.6. Once the outer skin was no longer captured by the rivet heads, additional out-of-plane movement of the fracture surfaces resulted in scratches normal to the direction of crack growth. During this latter stage of crack link-up, it is likely that crack propagation was assisted by the addition of a local Mode III pressure load previously carried by the rivet (head).

Bays that exhibited crack link-up (bays 2 and 4) contain a similar distribution of fatigue crack lengths. Figures 15.10, 15.11, and 15.12 show the outer skin fatigue crack length at each upper rivet hole location in bays 2, 3, and 4, respectively. These figures represent the condition of each bay very near the end of the full scale fatigue test and immediately prior to crack link-up[1]. The bay 2 crack length data plotted in Figure 15.10 are based on *in situ* visual examinations conducted at fix pressure cycles; here, first link-up was observed between 58,040 and 58,200 pressure cycles and the remainder of the fatigue cracks linked between 58,200 and 58,500 pressure cycles. Figure 15.12 shows bay 4 fatigue crack lengths prior to crack link-up at 59,900 cycles. The fatigue crack distribution shown in Figure 15.11 for bay 3 at 60,000 pressure cycles

[1]Crack link-up occurred in bays 2 and 4. Because of fracture surface oxide debris, the exact location of the final fatigue crack front was not determined by fractography in bay 2. *In situ* visual crack length data are plotted in Figure 15.10. These results estimate the location of the crack front within 160 to 300 cycles prior to crack link-up (58,200 cycles). The fractographic based results for bay 4, shown in Figure 15.12, represent the condition of bay immediately prior to crack link-up (59,900 cycles). The fractographic based for bay 3 in Figure 15.11 represent the condition of the bay at the end of the pressure test (60,000 cycles).

is different than that observed for bays 2 and 4. Here, bay 3 exhibits a relatively flat crack length distribution compared to the adjacent bays (bays 2 and 4) that exhibited crack link-up.

15.5 References:

1. Schijve, J., Multiple-Site-Damage Fatigue of Riveted Joints, *Durability of Metal Aircraft Structures*, Atluri, S.N., Harris, C.E., Hoggard, A., Miller, N., and Sampath, S.N., eds., Atlanta Tech. Pub., Atlanta, GA, pp. 2-27, 1992.
2. Finney, J.M. and Evans, R.L., Extending the Fatigue Life of Multi-Layer Metal Joints, *Fatigue Fract. Engng. Mater. Struct.*, Vol. 18, No. 11, pp. 1231-1247, 1995.
3. Blanchard, P., Colombie, C., Pellerin, V., Fayeulle, S., and Vincent, L., Materials Effects in Fretting Wear: Application to Iron, Titanium, and Aluminum Alloys, *Met. Trans.*, Vol. 22A, pp. 1535 - 1544, 1991.

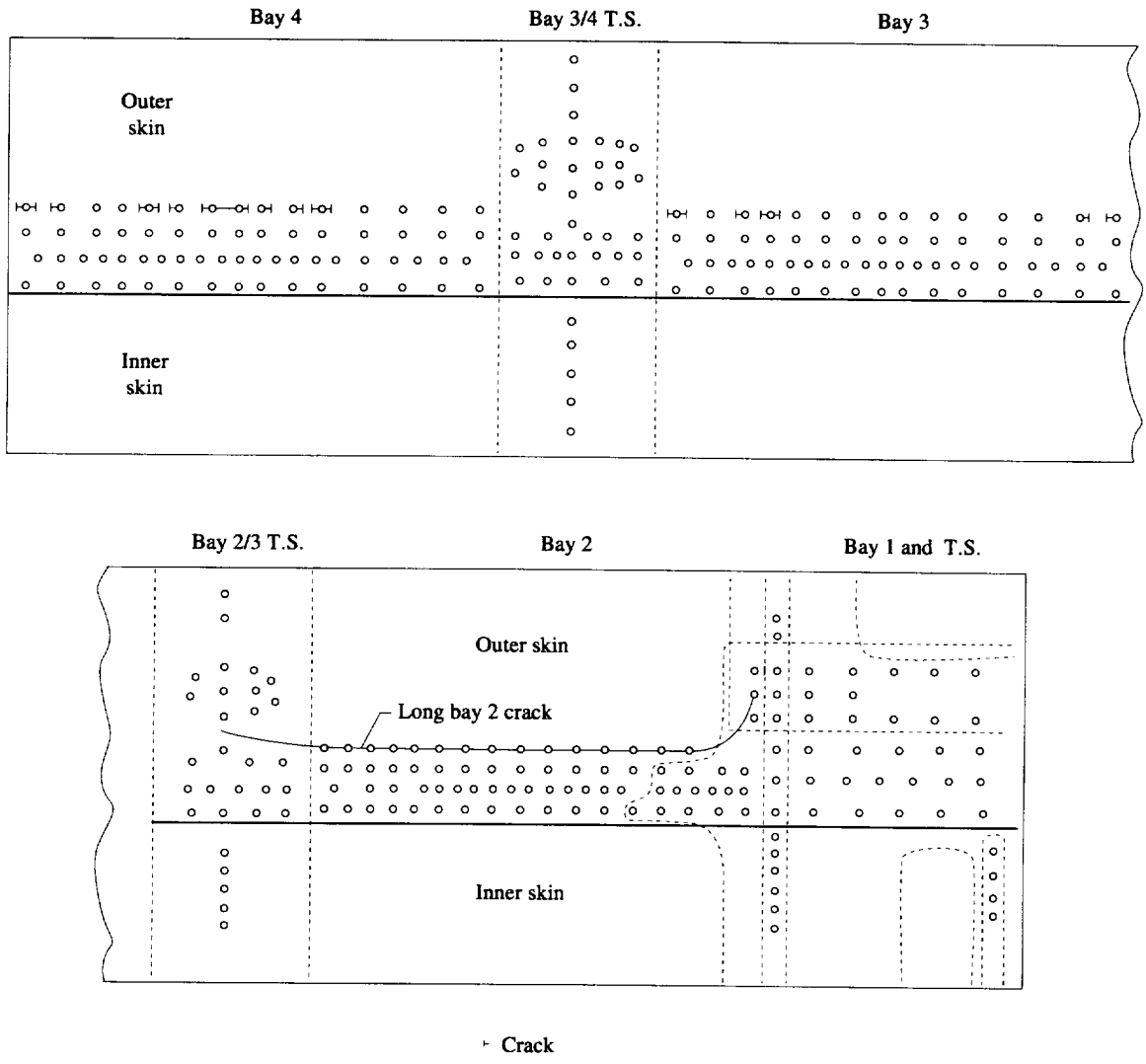

Figure 15.1 The results of the visual examination are shown for bays 2-4 and tear straps.

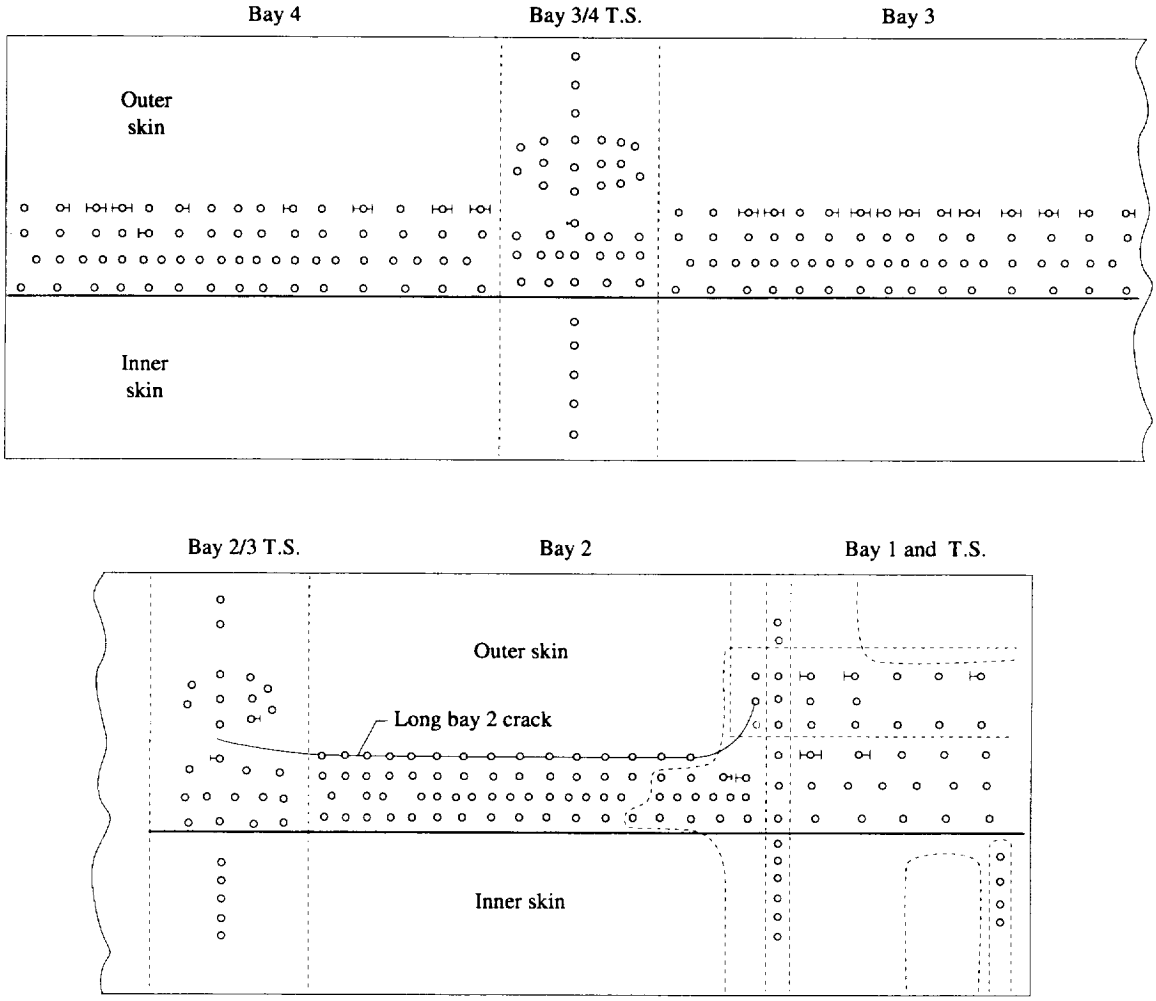

Figure 15.2 The results of the eddy current inspection are shown for bays 2-4 and tear straps. Shown are the locations of non-visible cracks detected by eddy current. All upper rivet holes contained in bays 2, 3, and 4 were examined using a "within" hole EC probe. All other locations were examined using a "sliding" surface EC probe.

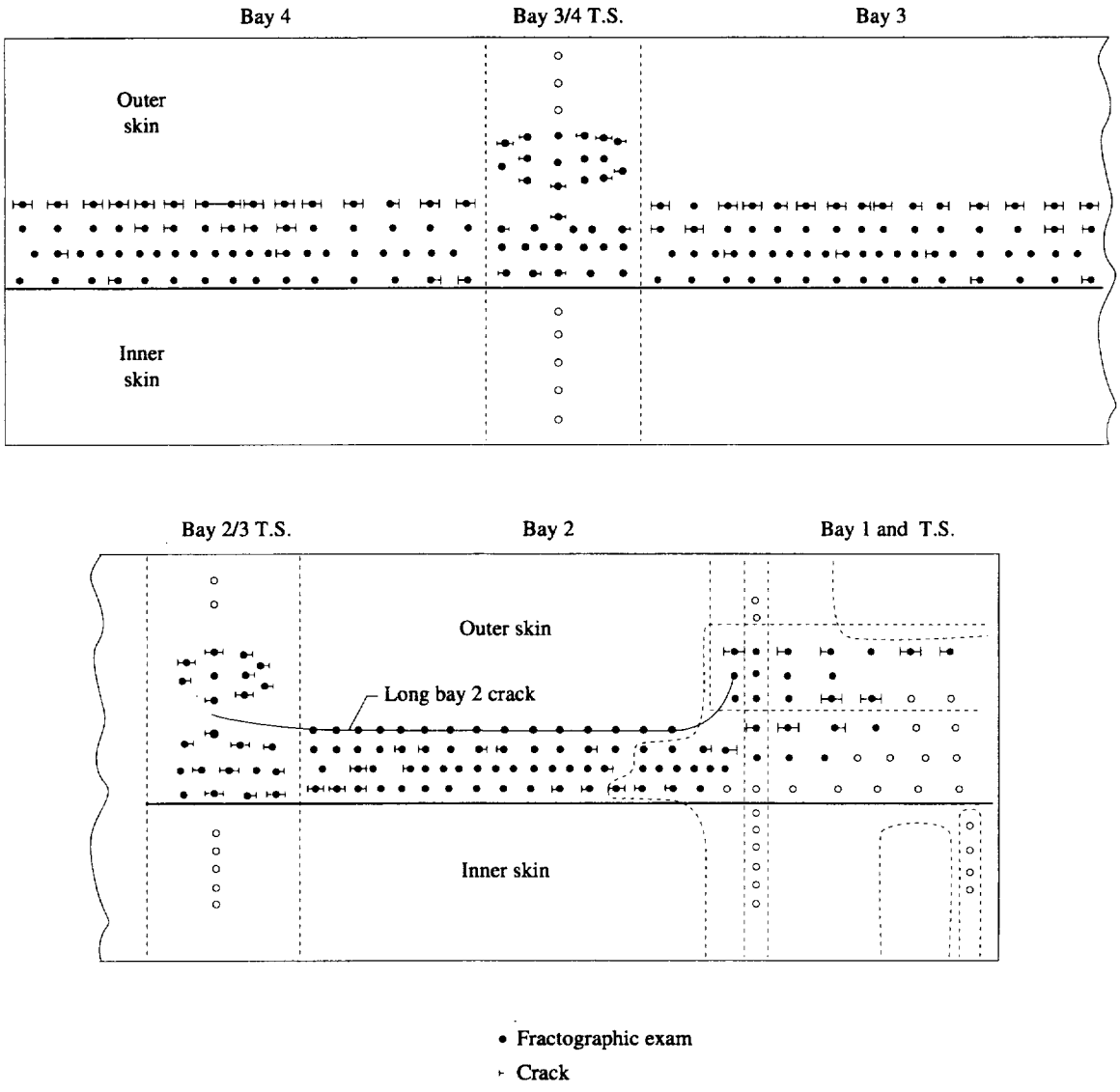

Figure 15.3 The results of the fractographic examination for bays 2-4 and tear straps. Solid rivet holes were destructively examined.

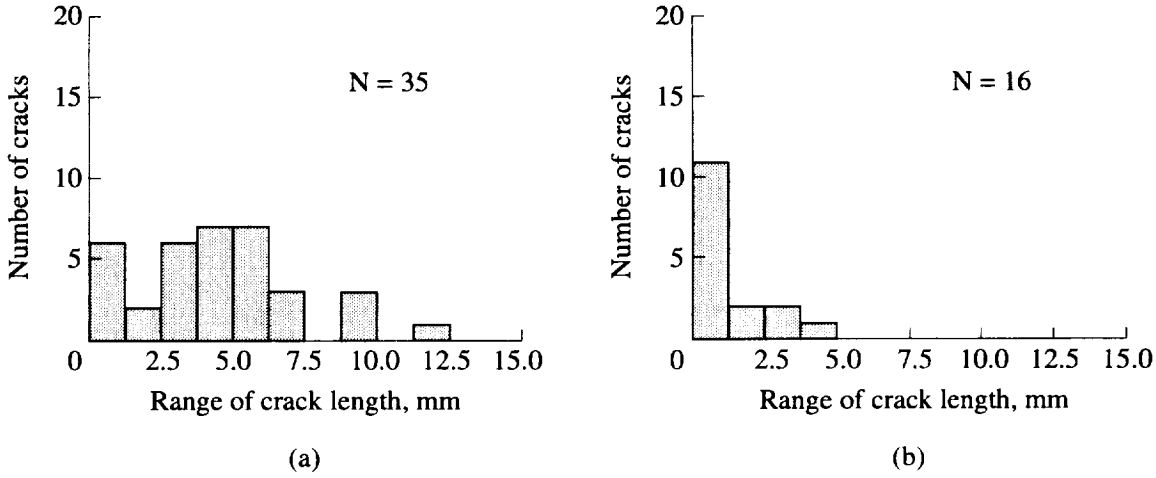

Figure 15.4 The fatigue crack size distribution is shown for bay 2 a) outer skin and b) inner skin.

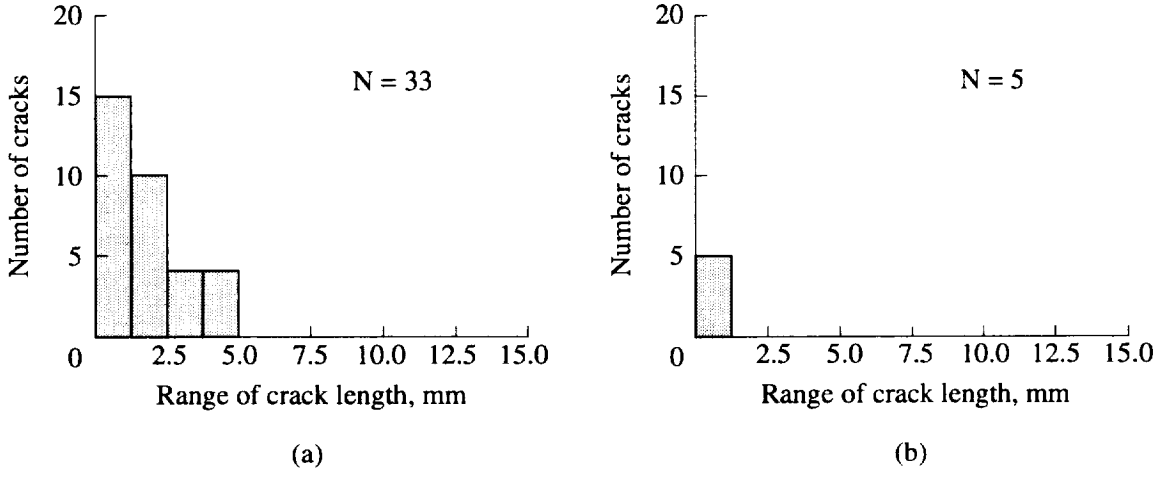

Figure 15.5 The fatigue crack size distribution is shown for bay 3 a) outer skin and b) inner skin.

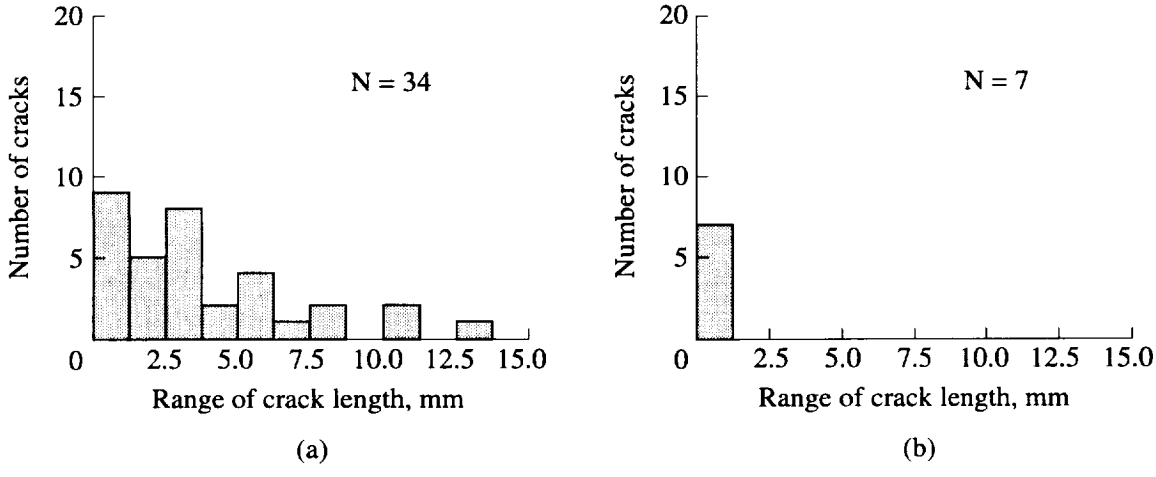

Figure 15.6 The fatigue crack size distribution is shown for bay 4 a) outer skin and b) inner skin.

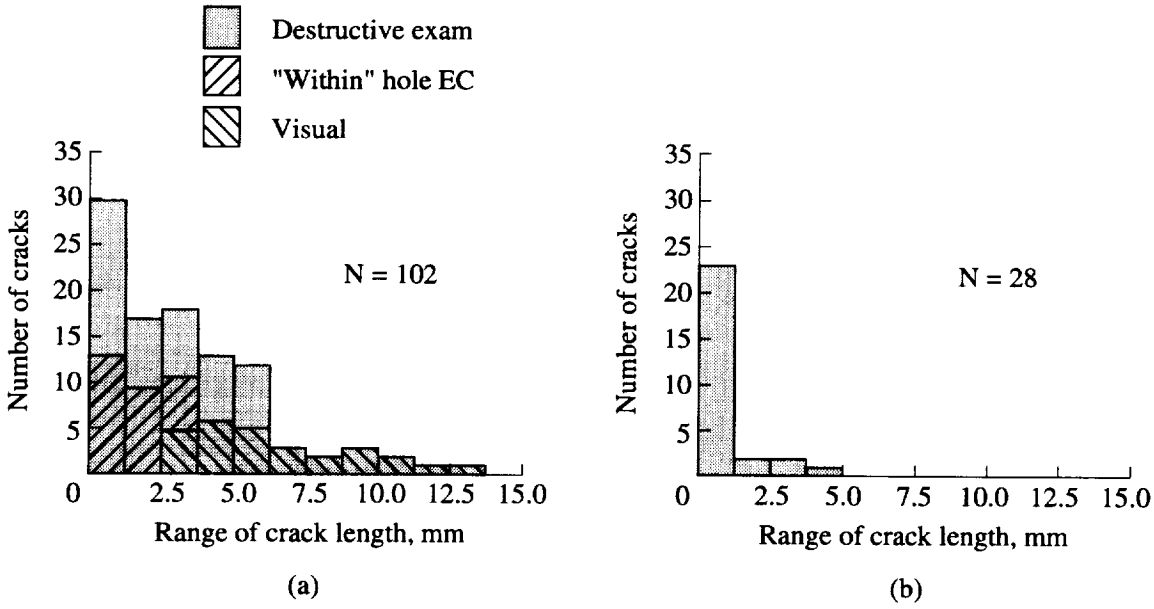

Figure 15.7 The total crack size distribution is shown for bays 2, 3, and 4 a) outer skin and b) inner skin.

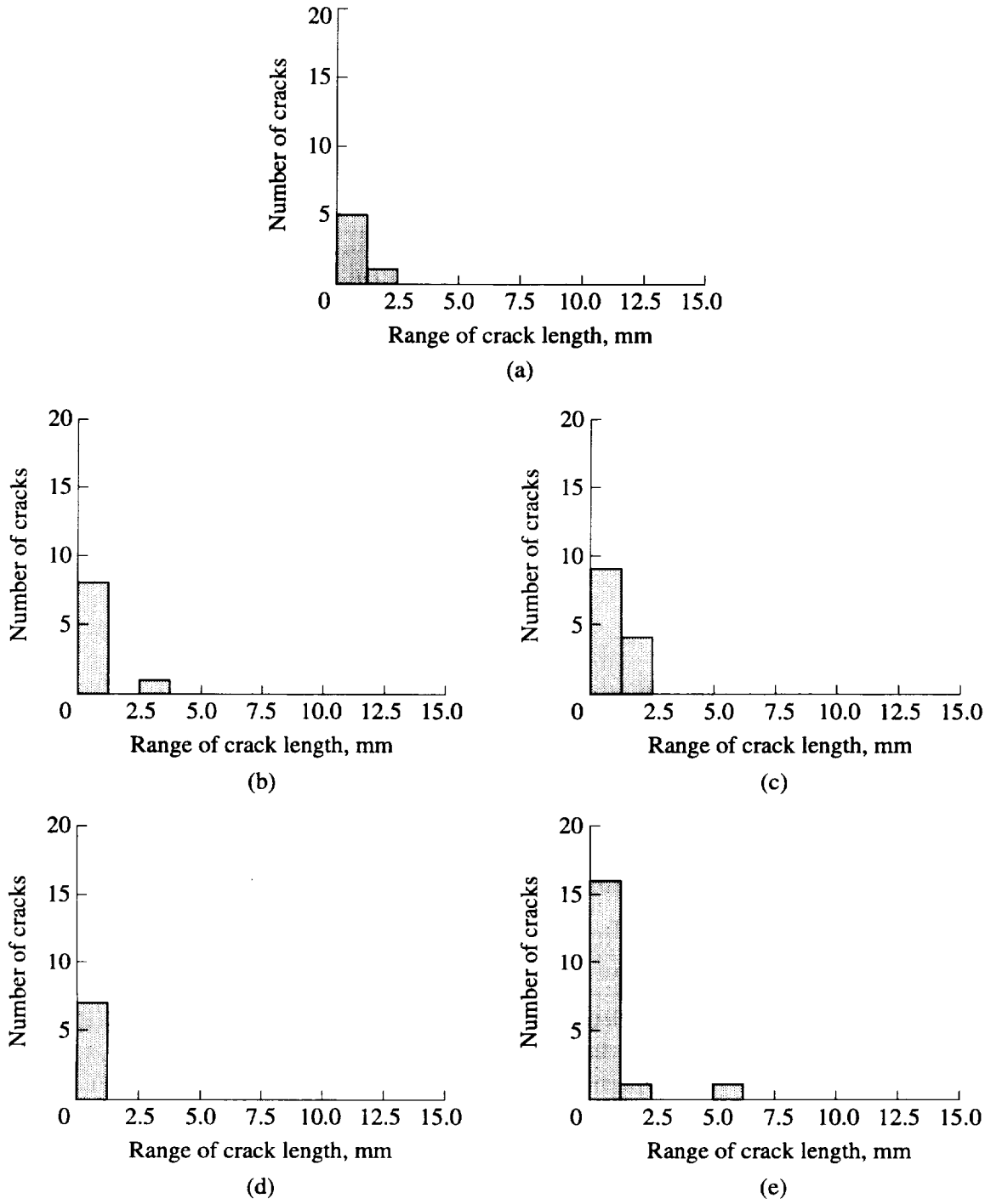

Figure 15.8 The crack size distribution is shown for the a) 2/3 TS outer skin, b) 2/3 TS inner skin, c) 2/3 upper and lower TS, d) 3/4 outer skin, and e) 3/4 upper and lower TS.

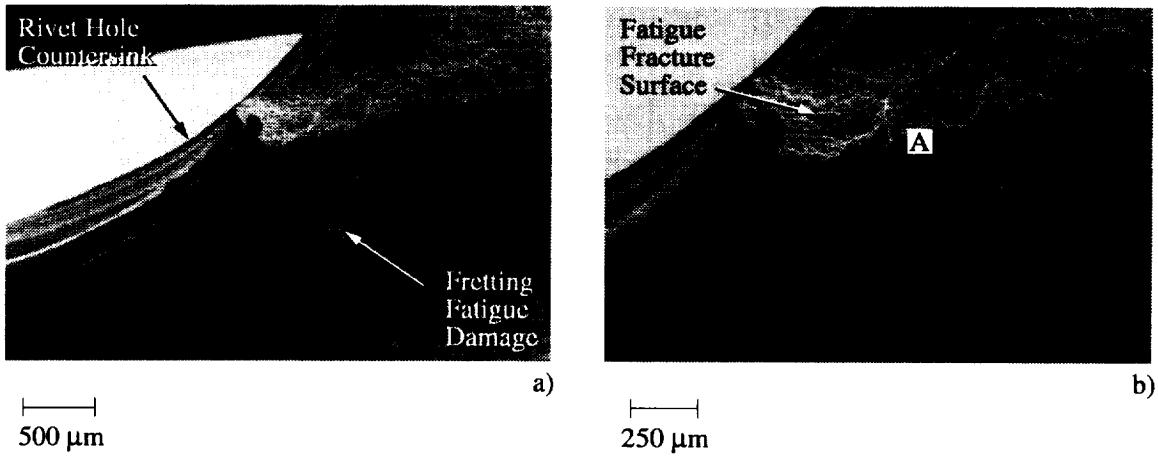

Figure 15.9 a) Scanning electron micrograph showing the location of faying surface fretting damage at rivet hole location 3J3 in the forward direction. b) SEM micrograph showing fretting damage at higher magnification. c) SEM micrograph showing microcracks and debris at location "A" in Figure 15.9b. The dashed line approximates the location of the fatigue fracture surface (above dashed line) and the faying surface edge (below dashed line).

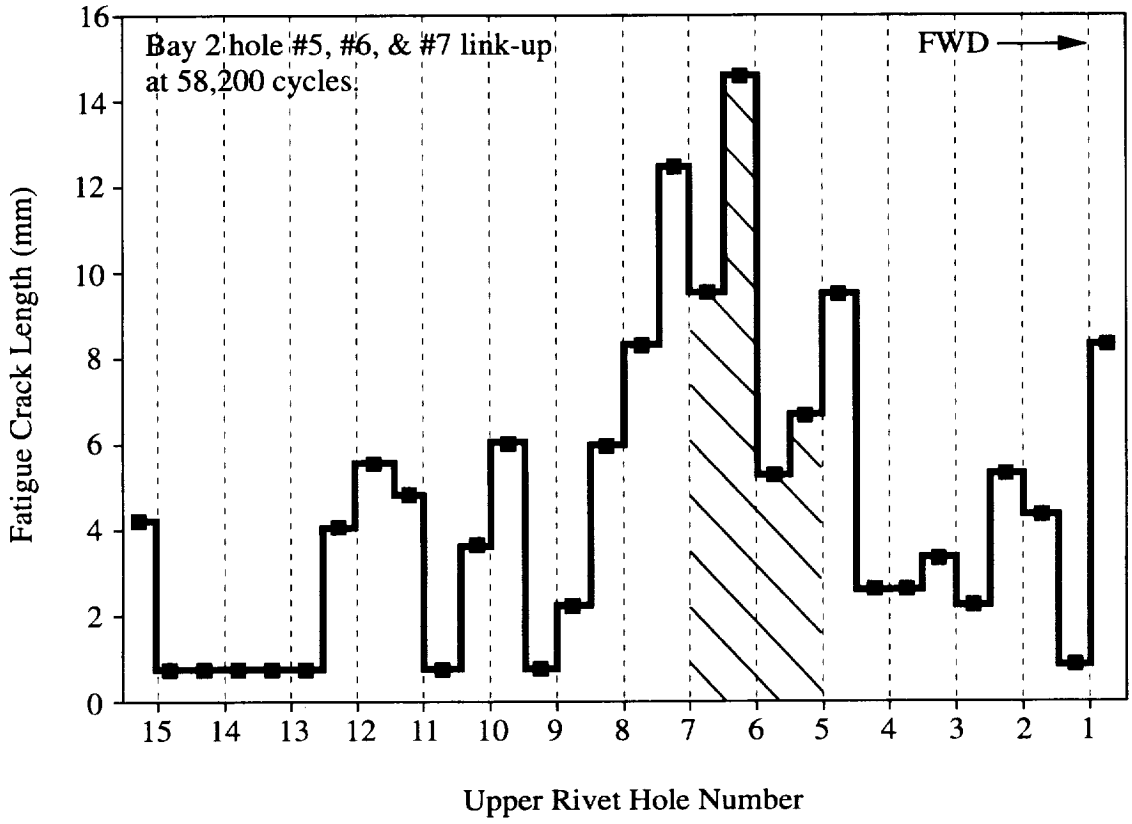

Figure 15.10 A plot of fatigue crack length prior to link-up for outer skin upper rivet row cracks contained in bay 2. Crack link-up occurred between rivet holes 5-7 (shaded region) between pressure cycles 55,500 and 58,000. Link-up occurred at other hole locations between pressure cycles 58,200 and 60,000.

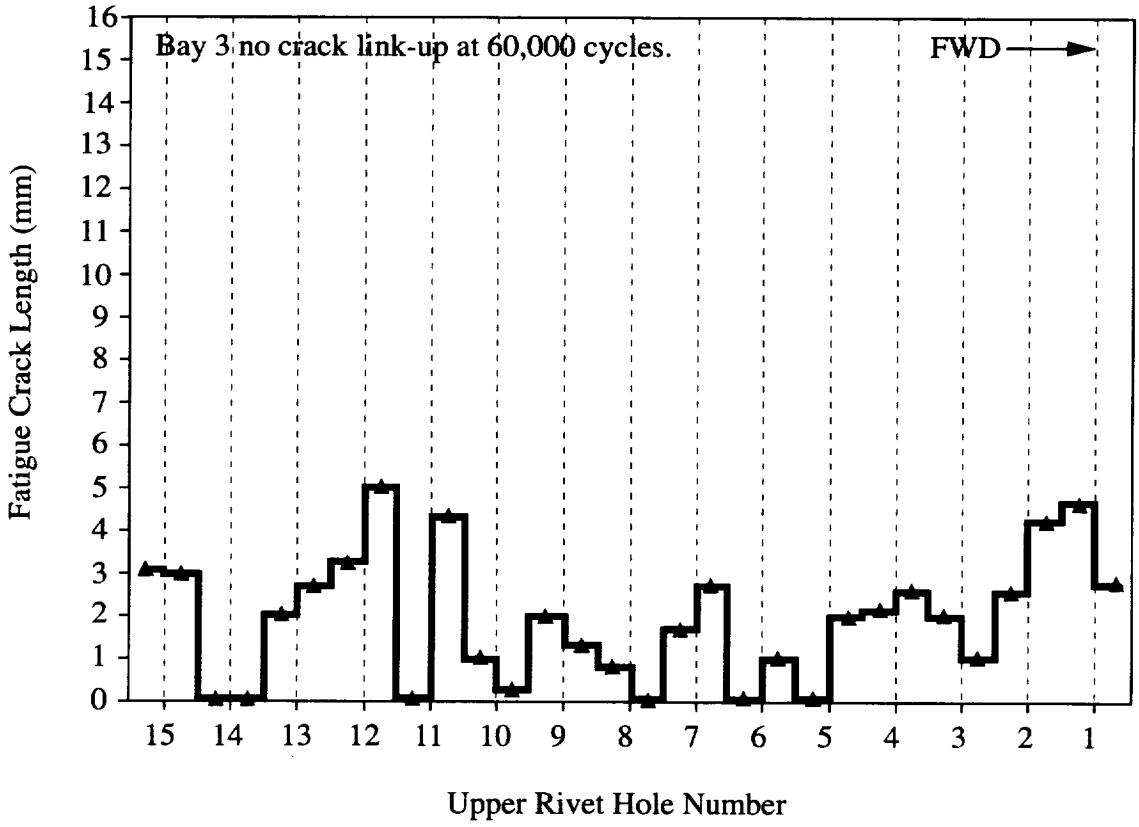

Figure 15.11 Shows bay 3 fatigue crack lengths at 60,000 cycles; no crack link-up occurred in bay 3.

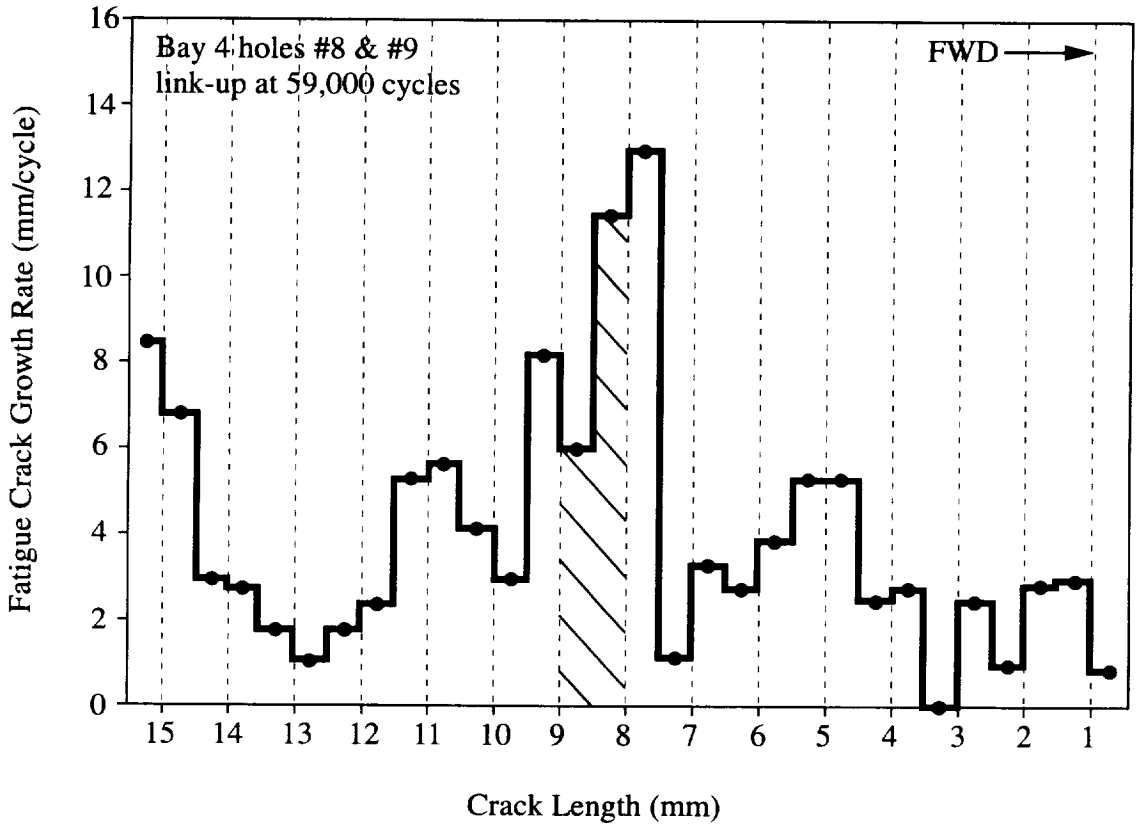

Figure 15.12 A plot of fatigue crack length prior to link-up for outer skin upper rivet row cracks contained in bay 4. Crack link-up occurred between rivet holes 8 and 9 (shaded region) at 59,900 pressure cycles

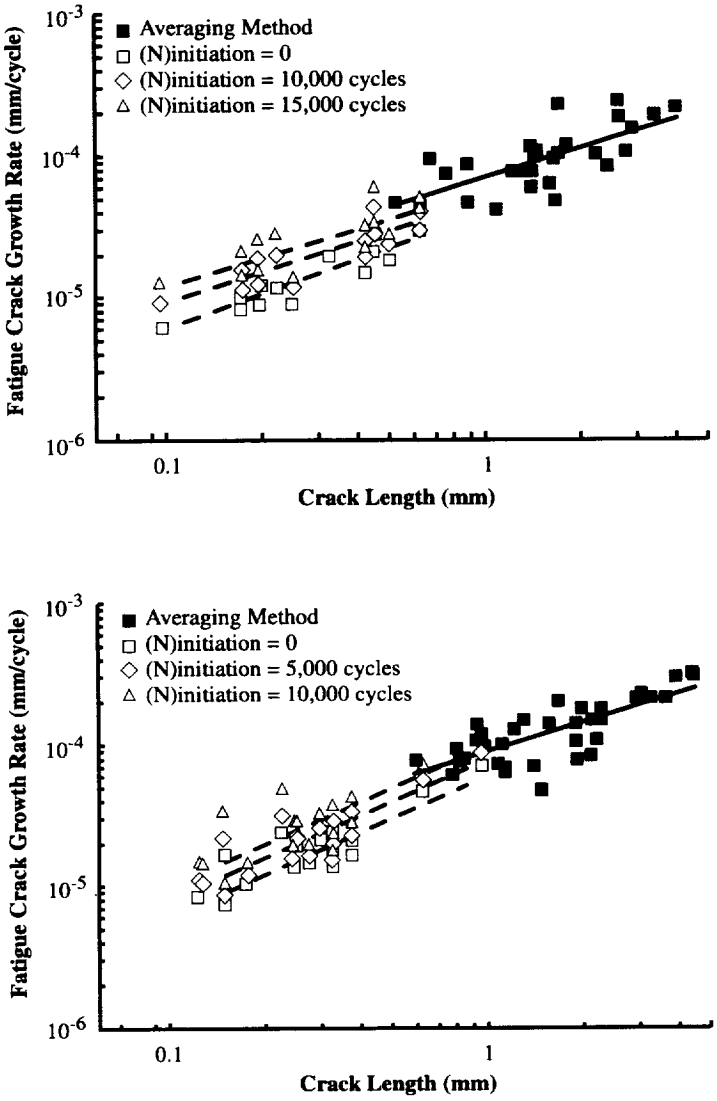

Figure 15.13 The growth characteristics of small fatigue cracks contained in the upper rivet row outer skin in a) bay 3 assuming N_i=0, N_i=10,000 cycles, and N_i=15,000 cycles and b) bay 4 assuming N_i=0, N_i=5,000 cycles and N_i=10,000 cycles.

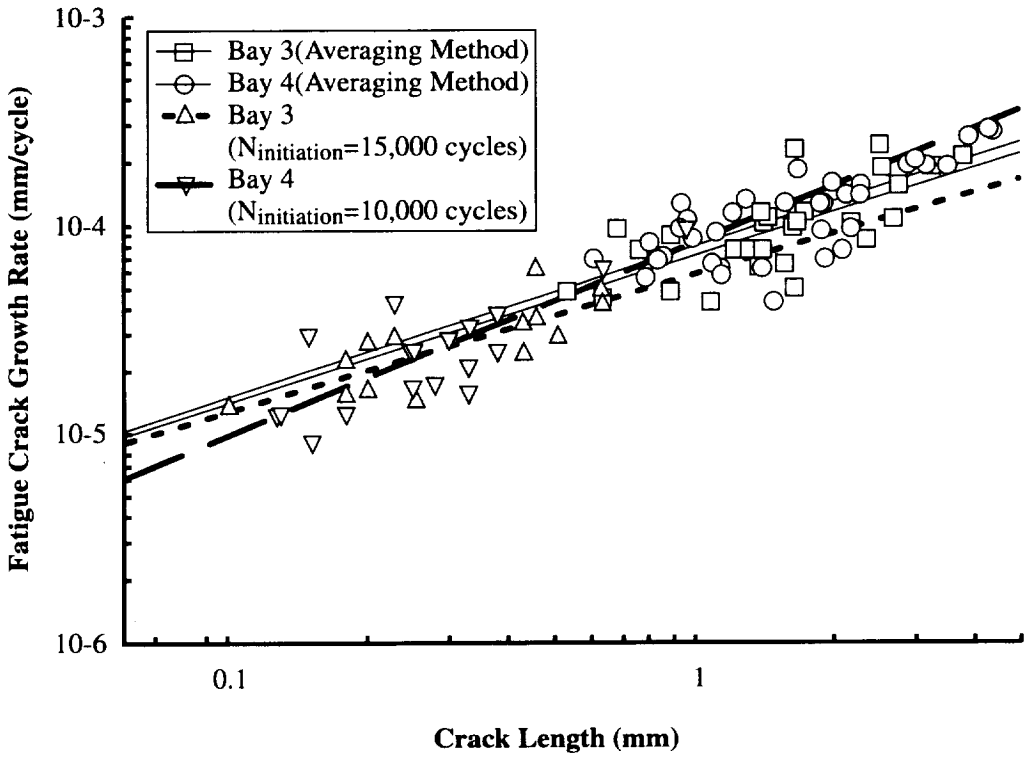

Figure 15.14 A comparison of the growth characteristics of outer skin fatigue cracks contained in bays 3 and 4 lap splice joint upper rivet row.

16. Summary

Full scale fuselage testing to 60,000 full pressure cycles has shown that MSD will occur in isolated regions of the fuselage lap splice joint. A section (panel) of the fuselage, containing four complete and two partial lap splice joint bays, that exhibited visible outer skin cracks along a single rivet row was removed from the full scale pressure test article for detailed examination. Destructive examination of a major portion of the panel (three full bays and one partial bay) has shown that MSD in the fuselage lap splice joint consists of rivet hole fatigue cracks contained in the outer skin, inner skin, and tear strap region. Multiple site damage in three adjacent fuselage lap splice joint bays is characterized by outer skin fatigue cracks at all upper row (row J) rivet holes and approximately 35% of second row (row I) rivet holes, inner skin fatigue cracks at approximately 18% of third row (row H) and 29% of fourth row (row G) rivet holes. The outer skin fatigue cracks along the upper row grew to critical crack lengths that resulted in crack link-up along the entire length of bay 2 and the link-up of two adjacent fatigue cracks in bay 4. The tear strap regions also contained a substantial number of fatigue cracks. The number of rivet holes that contained cracks varied with location; in the 2/3 T.S. region, 22% outer skin, 46% inner skin, 50% upper tear strap, and 26% lower tear strap rivet holes contained fatigue cracks, in the 3/4 T.S. region, 18% outer skin, 0% inner skin, 50% upper tear strap and 9% lower tear strap rivet holes contained fatigue cracks. No crack link-up was observed in the tear strap region.

Upper rivet row fatigue cracks initiated from fretting damage in the outer skin clad layer at a location adjacent to each rivet hole along the faying surface. Rivet hole crack initiation at inner layers (inner skin and tear straps) resulted from rivet hole imperfections (high K_T regions) and possible rivet shank/rivet hole fretting damage. Fatigue fracture surface marker band analysis results suggest that outer skin fretting induced crack initiation occurred between 5,000 and 15,000 pressure cycles.

Most outer skin fatigue cracks grew along the faying surface (elliptical shape) for substantial distances (two to three skin thicknesses) before penetrating the outboard surface of the outer skin. Crack growth rate determinations, based on detailed marker band analysis, revealed that all outer skin upper rivet row fatigue cracks grow at similar rates. Identical fatigue crack growth rate characteristics were observed for all cracks located in three adjacent lap splice bays and for crack lengths ranging in length from 0.1 mm to 4 mm. This important result suggests that fracture mechanics based methodology can be used to predict the growth of outer skin fatigue cracks in lap splice structure.

Multiple site fatigue damage can lead to crack link-up between adjacent structural elements and thereby reduce the residual strength of the fuselage structure. This damage process occurred in bays 2 and to a lesser extent in bay 4. The first indication of outer skin upper rivet row crack link-up was noted after 58,000 pressure cycles. Once the initial crack link-up occurred in the mid-bay region of bay 2, link-up of the remaining rivet hole cracks along the entire length of bay 2 occurred, within 460 pressure cycles. Fractographic results show that crack propagation during the link-up process is influenced by out-of-plane loading. Results suggest that mode III displacements increased as crack link-up continued to the outer regions of bay 2. After link-up occurred between the middle four or five rivet holes, the upper row rivets no longer captured the cracked portion of the outer skin, thus allowing additional out-of-plane loading of the propagating crack.

REPORT DOCUMENTATION PAGE

Form Approved
OMB No. 0704-0188

1. AGENCY USE ONLY (Leave blank)	2. REPORT DATE	3. REPORT TYPE AND DATES COVERED
	November 1997	Technical Publication

4. TITLE AND SUBTITLE
The Characteristics of Fatigue Damage in the Fuselage Riveted Lap Splice Joint

5. FUNDING NUMBERS
WU 538-02-10-01

6. AUTHOR(S)
R. S. Piascik and S. A. Willard*

7. PERFORMING ORGANIZATION NAME(S) AND ADDRESS(ES)
NASA Langley Research Center
Hampton, VA 23681-2199

8. PERFORMING ORGANIZATION REPORT NUMBER
L-17637

9. SPONSORING/MONITORING AGENCY NAME(S) AND ADDRESS(ES)
National Aeronautics and Space Administration
Washington, DC 20546-0001

10. SPONSORING/MONITORING AGENCY REPORT NUMBER
NASA/TP-97-206257

11. SUPPLEMENTARY NOTES
*Lockheed Martin Engineering and Sciences Co., Hampton, VA

12a. DISTRIBUTION/AVAILABILITY STATEMENT
Unclassified-Unlimited
Subject Category 24 Distribution: Standard
Availability: NASA CASI (301) 621-0390

12b. DISTRIBUTION CODE

13. ABSTRACT *(Maximum 200 words)*

An extensive data base has been developed to form the physical basis for new analytical methodology to predict the onset of widespread fatigue damage in the fuselage lap splice joint. The results of detailed destructive examinations have been cataloged to describe the physical nature of MSD in the lap splice joint. The catalog includes a detailed description, e.g., crack initiation, growth rates, size, location, and fracture morphology, of fatigue damage in the fuselage lap splice joint structure.

Detailed examinations were conducted on a lap splice joint panel removed from a full scale fuselage test article after completing a 60,000 cycle pressure test. The panel contained a four bay region that exhibited visible outer skin cracks and regions of crack link-up along the upper rivet row. Destructive examinations revealed undetected fatigue damage in the outer skin, inner skin, and tear strap regions. Outer skin fatigue cracks were found to initiate by fretting damage along the faying surface. The cracks grew along the faying surface to a length equivalent to two to three skin thicknesses before penetrating the outboard surface of the outer skin. Analysis of fracture surface marker bands produced during full scale testing revealed that all upper rivet row fatigue cracks contained in a three bay region grow at similar rates; this important result suggests that fracture mechanics based methods can be used to predict the growth of outer skin fatigue cracks in lap splice structure. Results are presented showing the affects of MSD and out-of-plane pressure loads on outer skin crack link-up.

14. SUBJECT TERMS
Multi site damage; Lap splice Joint; Fuselage structure; Fatigue cracking; Widespread fatigue damage; Tear down examination; Crack link-up

15. NUMBER OF PAGES
383

16. PRICE CODE
A17

17. SECURITY CLASSIFICATION OF REPORT	18. SECURITY CLASSIFICATION OF THIS PAGE	19. SECURITY CLASSIFICATION OF ABSTRACT	20. LIMITATION OF ABSTRACT
Unclassified	Unclassified	Unclassified	

NSN 7540-01-280-5500

Standard Form 298 (Rev. 2-89)
Prescribed by ANSI Std. Z-39-18
298-102